



Kent Academic Repository

Mayora Neto, Martin (2021) *Generation, Epitope swapping and stability studies of Filovirus pseudotypes and their utilisation in specific antibody assays*. Doctor of Philosophy (PhD) thesis, University of Kent,.

Downloaded from

<https://kar.kent.ac.uk/87603/> The University of Kent's Academic Repository KAR

The version of record is available from

<https://doi.org/10.22024/UniKent/01.02.87603>

This document version

UNSPECIFIED

DOI for this version

Licence for this version

CC BY (Attribution)

Additional information

Versions of research works

Versions of Record

If this version is the version of record, it is the same as the published version available on the publisher's web site. Cite as the published version.

Author Accepted Manuscripts

If this document is identified as the Author Accepted Manuscript it is the version after peer review but before type setting, copy editing or publisher branding. Cite as Surname, Initial. (Year) 'Title of article'. To be published in *Title of Journal*, Volume and issue numbers [peer-reviewed accepted version]. Available at: DOI or URL (Accessed: date).

Enquiries

If you have questions about this document contact ResearchSupport@kent.ac.uk. Please include the URL of the record in KAR. If you believe that your, or a third party's rights have been compromised through this document please see our [Take Down policy](https://www.kent.ac.uk/guides/kar-the-kent-academic-repository#policies) (available from <https://www.kent.ac.uk/guides/kar-the-kent-academic-repository#policies>).

**GENERATION, EPITOPE SWAPPING AND STABILITY
STUDIES OF FILOVIRUS PSEUDOTYPES AND THEIR
UTILISATION IN SPECIFIC ANTIBODY ASSAYS**

By

Martin Mayora Neto

A thesis submitted for
THE DEGREE OF DOCTOR OF PHILOSOPHY
IN THE SUBJECT OF PHARMACY

Medway School of Pharmacy
Universities of Kent and Greenwich at Medway
Central Avenue, Chatham, Kent, ME4 4TB

January 2021

Declaration

I hereby declare that this thesis and the work reported herein was composed by and originated entirely from me. Information derived from the published and unpublished work of others has been acknowledged in the text and references are given in the list of sources.

Print name:

Date:

Signature:

Acknowledgements

First of all, I would like to thank Simon for his mentorship during my PhD. Simon was always available for any help or support. Also to Nigel and Ed for their advice and helpful discussions throughout the project. Between the three of them, they have created an environment where students are not only encouraged to develop independence, present their work in Conferences and meetings, but also their interests and well-being are put first. Their mentorship extends to after students have left.

I would also like to thank all the past and present VPU members, especially George, Rebecca and Emma for mentoring me at the beginning of my PhD. Also Keith, Stuart and more recently Juggragarn, Cecilia, Hubert, Mariliza and Beth.

I would also like to thank our collaborators including Yasu, Giada and everyone at Intravacc.

To all my family for their constant support and understanding my absence.

Finally, I would to thank Gary and my friends for their support and understanding during the countless times I was unavailable to meet up due to work commitments.

Abstract

Filoviruses are single stranded negative sense RNA viruses belonging to the family *filoviridae*. Since their discovery in 1967, filoviruses have been responsible for sporadic outbreaks in humans with mortality rates of up to 90%. At least five species are known to be highly pathogenic, however some non-pathogenic species have also been found to infect humans. Other hitherto non-pathogenic species have been detected in bats in Africa, Asia and Europe. Recently, large Ebola virus (EBOV) outbreaks in Africa highlighted the need for improved therapeutics and/or an effective vaccine. However, research is hindered by the need of high containment facilities. Pseudotype viruses (PVs), chimeric non-replicative virions displaying glycoproteins of the virus of interest can be used as a surrogate to working with pathogenic viruses in low containment.

The main scope of the work presented in this thesis was to generate high titre filovirus PVs for use in antibody assays. A panel of filovirus PVs relevant to human and bat hosts was generated and utilised in neutralisation assays (PVNA) and ELISA to assess antibody responses against those viruses. EBOV PVs were shown to detect neutralising antibodies in convalescent serum from patients that recovered from EVD, as well as antibodies in ELISA when utilised as purified antigens. However, low-level cross-reactivity was detected against *marburgvirus* (RAVV) PVs. A chimeric RESTV GP was designed to display EBOV neutralising epitope KZ52 in lentiviral PVs (KZ52-RESTV PV), and was successfully neutralised by its corresponding monoclonal antibody using human and hamster target cell lines. The KZ52 monoclonal antibody also bound to KZ52-RESTV PVs in ELISA. This provides proof-of-concept evidence that filovirus GP can be mutated to have specific epitopes inserted within it, with the aim of incorporation into improved specificity antibody assays.

In addition, Filovirus PVs were found to be amenable to lyophilisation and storage at +4°C or less for up to two years, retaining infectivity after reconstitution. Lyophilised EBOV PVs also performed well in PVNAs after 1.5 years storage at +4°C. These could be used in future serological kits, making it more affordable by avoiding cold chain transportation. Finally, in a collaborative study with the University of Pecs, Lloviu virus (LLOV) PVs detected neutralising antibodies in bat sera from samples collected from dead and live animals in Hungary. This adds to the evidence of the circulation of those viruses in Europe, as well as highlighting the potential for LLOV or other filovirus PVs to be utilised in future serosurveillance studies.

Table of Contents

Declaration	II
Acknowledgements	III
Abstract.....	IV
Table of Contents.....	V
List of Figures.....	XII
List of Tables.....	XIX
Abbreviations	XXI
CHAPTER 1: Introduction	1
1.1 Filovirus classification and nomenclature.....	1
1.2 History of filovirus outbreaks.....	4
1.3 Filovirus genome organisation and protein functions	11
1.3.1 Nucleoprotein (NP).....	13
1.3.2 Viral Protein 35 (VP35)	14
1.3.3 Viral Protein 40 (VP40)	15
1.3.4 Surface Glycoprotein (GP)	16
1.3.4.1 <i>Ebolavirus</i> GP transcription strategies, protein synthesis and processing	19
1.3.4.2 <i>Marburgvirus</i> GP transcription strategies, protein synthesis and processing ..	21
1.3.5 Viral Protein 30 (VP30)	22
1.3.6 Viral Protein (VP24)	23
1.3.7 Viral Polymerase (L).....	24
1.4 Filovirus entry and tropism	25
1.5 Filovirus replication cycle.....	27
1.6 Viral budding.....	29
1.7 Filovirus pathogenesis and immune response.....	29
1.7.1 Clinical features.....	29
1.7.2 Specific role of filovirus GP in pathogenesis.....	31
1.7.3 Immune response against filoviruses and immune evasion mechanisms.....	33
1.7.3.1 Innate Immunity	33
1.7.3.2 Adaptive Immunity	34
1.7.3.3 Antibody-dependent enhancement (ADE)	35

1.8 Therapeutics	36
1.8.1 Virus entry as a target for therapeutics with monoclonal antibodies (mAb) or convalescent plasma.....	36
1.8.2 Targetting viral replication	38
1.8.3 Other therapies	39
1.9 Serology	39
1.9.1 ELISA.....	40
1.9.2 Functional assays.....	41
1.9.2.1 Plaque Reduction Neutralisation Test (PRNT)	41
1.9.2.2 Microneutralisation assays (MNA)	41
1.9.2.3 Pseudotype Virus Neutralisation Assay (PVNA).....	42
1.10 Pseudotype Viruses (PV)	42
1.10.1 Filovirus PVs in cell entry studies and GP characterisation	45
1.10.2 Antibody tests	46
1.10.3 Vaccine vectors and evaluation.....	46
1.10.4 Therapeutics and antivirals	49
1.10.5 PV generation.....	50
1.10.5.1 Titration methods.....	52
1.10.5.2 Pseudotype virus neutralisation assay (PVNA).....	53
1.10.5.2.1 Correlation between PVNAs and authentic EBOV neutralisation assays..	55
1.11 Aims and Objectives.....	56
CHAPTER 2: Materials and Methods.....	58
2.1 Molecular Biology	58
2.1.1 Plasmids	58
2.1.2 Restriction enzyme digestion	59
2.1.3 Agarose gel electrophoresis	60
2.1.4 DNA concentration	60
2.1.5 Ligation reactions	60
2.1.6 Transformation of competent <i>E. coli DH5α</i> cells.....	61
2.1.7 Glycerol stocks and Plasmid DNA purification.....	61
2.1.8 PCR – Polymerase Chain Reaction	62
2.1.9 Sanger Sequencing	63
2.2 Cell Culture	64
2.2.1 Cell lines and subculturing	64

2.2.2 Cell lines – frozen stocks	65
2.3 PV generation – Transfection with expression plasmids	65
2.3.1 Lentiviral core PVs	65
2.3.2 Vesicular Stomatitis Virus (VSV) core PVs	67
2.4 PV Titration	69
2.4.1 Infectivity assay	69
2.4.2 Determination of TCID ₅₀ /mL	70
2.5 Quality Control of PV production.....	71
2.5.1 Virion-associated p24 ELISA	71
2.5.2 SYBR-Green Product-Enhanced Reverse Transcriptase (SG-PERT) assay	73
2.6 Pseudotype Virus Neutralisation assay (PVNA)	75
2.7 ELISA using purified PVs as antigens	76
2.7.1 PV purification	76
2.7.2 Protein quantification assay	76
2.7.3 ELISA	77
2.7.3.1 Reagents	77
2.7.3.2 ELISA protocol.....	78
2.8 Data Analysis.....	78
CHAPTER 3: Generation and Optimisation of Filovirus Pseudotypes	79
3.1 Introduction	79
3.2 Materials and Methods.....	81
3.2.1 Gene constructs and plasmids	81
3.2.2 Cloning and Sanger sequencing	82
3.2.3 PV generation.....	82
3.2.3.1 Lentiviral (HIV-1) core	82
3.2.3.1.1 Luciferase reporter gene.....	82
3.2.3.1.2 eGFP reporter gene.....	83
3.2.3.2 Recombinant Vesicular Stomatitis Virus (luc) core.....	84
3.2.4 Quality control of Lentiviral PV production.....	84
3.2.5 Statistical analysis.....	84
3.3 Results.....	85
3.3.1 Cloning of MARV (Angola) and MARV (DRC)	85
3.3.2 Lentiviral (HIV-1) core PV generation – luciferase reporter	85

3.3.2.1 PV generation in different transfection reagents and cell culture vessels utilising established protocols	85
3.3.2.2 PV generation utilising HEK293T producer cells sourced from another laboratory	88
3.3.2.3 Optimising envelope input for PV generation	90
3.3.2.4 Upscaling PV production	93
3.3.2.5 Target cell lines for Filovirus PVs	94
3.3.2.6 TCID ₅₀ – 50% Tissue Culture Infective Dose assay	95
3.3.2.7 Quality control of Lentiviral PV production	95
3.3.2.7.1 p24 ELISA	95
3.3.2.7.2 SG-PERT.....	97
3.3.2.8 Filovirus PV stability after freeze-thawing cycles and Δ env signal	99
3.3.3 Lentiviral (HIV-1) core PV generation – eGFP reporter	99
3.3.4 Vesicular Stomatitis Virus (VSV) core PV generation – Luciferase reporter.....	101
3.3.4.1 Amplification of rVSV Δ G stocks	101
3.3.4.2 Generation of Filovirus VSV PVs	102
3.4 Discussion	105

CHAPTER 4: Application of Filovirus Pseudotypes for Neutralisation and Binding Assays

(ELISA)	112
4.1 Introduction	112
4.2 Materials and Methods.....	114
4.2.1 Viruses, sera and monoclonal antibodies.....	114
4.2.2 Antibody assays	115
4.3 Results.....	115
4.3.1 Pseudotype neutralisation assay (PVNA).....	115
4.3.1.1 Neutralising antibody responses against EBOV PVs using convalescent sera	115
4.3.1.2 Investigating consistency of PV input on PVNAs using both lentiviral and VSV cores	120
4.3.1.3 Neutralising antibody response and cross-reactivity	120
4.3.1.4 Neutralising responses of monoclonal antibodies against Filovirus PVs	122
4.3.2 PV ELISA	125
4.3.2.1 PV concentration and purification in a 20% sucrose cushion	125
4.3.2.2 PV ELISA optimisation	127
4.3.2.3 ELISA for detection of antibodies in convalescent sera	129

4.3.2.4 ELISA with monoclonal antibodies targetting EBOV GP.....	130
4.4 Discussion	131
CHAPTER 5: Epitope Modification of Filovirus Glycoproteins for Use in Pseudotype- based Neutralisation And Binding Assays (ELISA)	138
5.1 Introduction	138
5.2 Materials and Methods.....	142
5.2.1 Filovirus GP modelling	142
5.2.2 Plasmids and monoclonal antibodies	143
5.2.3 Primers	143
5.2.4 Reagents and equipment.....	143
5.2.5 Overlap Extension PCR protocol	144
5.2.5.1 1H3LLOV chimeric GP	146
5.2.5.2 KZ52LLOV chimeric GP	147
5.2.5.3 RAVV-LLOV chimeric GP	148
5.2.5.4 KZ52RESTV chimeric GP	148
5.2.5.5 4G7RESTV and 4G7/1H3RESTV chimeric GP	149
5.2.5.6 RAVV-RESTV chimeric GP	149
5.2.6 Cloning of synthesised genes.....	149
5.2.7 PV Generation and antibody assays	150
5.3 Results.....	150
5.3.1 Filovirus modelling.....	150
5.3.2 Mutagenesis	154
5.3.2.1 Mutagenesis of 1H3 epitope into LLOV GP	154
5.3.2.2 Mutagenesis of KZ52 epitope into LLOV GP	156
5.3.2.3 Mutagenesis to generate chimeric RAVV-LLOV GP.....	157
5.3.2.4 Mutagenesis of epitopes 4G7 and 1H3 into RESTV GP	158
5.3.2.5 Mutagenesis of epitope KZ52 into RESTV GP.....	158
5.3.3 PV production with chimeric GP	160
5.3.3.1 LLOV GP as scaffold for EBOV and RAVV epitopes.....	160
5.3.3.2 RESTV GP as scaffold for EBOV and RAVV epitopes.....	161
5.3.4 Antibody assays with chimeric GP PV	162
5.3.4.1 Neutralisation assays	162
5.3.4.1.1 LLOV GP as scaffold	162
5.3.4.1.2 RESTV GP as scaffold	164

5.3.4.2 ELISA.....	166
5.4 Discussion	168
CHAPTER 6: Application of <i>Cuevavirus</i> (LLOV) Pseudotypes to Serosurveillance of Bats in Hungary.....	174
6.1 Introduction	174
6.2 Materials and Methods.....	176
6.2.1 Plasmids and lentiviral LLOV PV generation.....	176
6.2.2 Bat serum samples and controls	177
6.2.3 Infectivity and TCID ₅₀ assays	177
6.2.4 Pseudotype Virus Neutralisation assay (PVNA).....	177
6.2.5 Statistical Analysis	178
6.3 Results.....	178
6.3.1 Generation of lentiviral Lloviu (LLOV) pseudotypes.....	178
6.3.2 Measuring neutralising antibody titre in pilot study of bat sera.....	179
6.3.3 Serological screening of bat serum panel.	181
6.3.3.1 Regimen 1 (1:40 start serum dilution in duplicate, 2 independent experiments)	
.....	182
6.3.3.2 Regimen 2 (1:40 start serum dilution in duplicate, 1 experiment).....	184
6.3.3.3 Regimen 3 (1:40 start serum dilution no duplicate, 1 experiment).....	185
6.3.3.4 Regimen 4 (1:100 start serum dilution no duplicate, 1 experiment).....	186
6.3.4 Determination of a positive cut-off point	187
6.4. Discussion	188
CHAPTER 7: Lyophilisation and Storage Stability of Filovirus Pseudotypes	193
7.1 Introduction	193
7.2 Materials and Methods.....	196
7.2.1 Viruses and cells	196
7.2.2 Reagents and equipment	196
7.2.3 Preparation of PV samples, lyophilisation and sample storage	197
7.2.4 Infectivity and neutralisation assays	199
7.3 Results.....	200
7.3.1 Generation of lentiviral PVs	200
7.3.2 Lyophilisation of filovirus PVs, evaluation of cryoprotection and choice of excipient	200

7.3.3 Long-term storage and stability of lyophilised <i>ebolavirus</i> PVs.....	203
7.3.4 Long-term storage and stability of lyophilised <i>cuevavirus</i> PVs	207
7.3.5 Long-term storage and stability of lyophilised <i>marburgvirus</i> PVs.....	208
7.3.6 Short-term storage and stability EBOV PVs lyophilised at Intravacc.....	211
7.3.7 Neutralisation assays (PVNA) with lyophilised PVs	213
7.3.8 Quality control of lentiviral particles present in samples stored at high temperatures – SG-PERT.....	215
7.4 Discussion	216
CHAPTER 8: Final Conclusions and Future work.....	222
8.1 Chapter 3.....	222
8.2 Chapter 4.....	223
8.3 Chapter 5.....	225
8.4 Chapter 6.....	226
8.5 Chapter 7.....	227
References:.....	229
Appendix I - Envelope glycoprotein nucleotide sequences (5' – 3').....	261
Appendix II - Mutagenesis strategies and PCR reactions.....	273

List of Figures

Figure 1.1. Filovirus virion diagram.	1
Figure 1.2. Phylogenetic tree based on genomic sequences.	3
Figure 1.3. Phylogenetic tree based on GP nucleotide sequences.	3
Figure 1.4. First electron micrograph of a MARV virion.	5
Figure 1.5. History of <i>Ebolavirus</i> outbreaks according to species and size.	6
Figure 1.6. Location of <i>marburgvirus</i> outbreaks.	9
Figure 1.7. Number of cumulative EBOV cases by country and prefecture during the 2013-2016 outbreak.	10
Figure 1.8. Cumulative cases during the 2018 - 2020 EBOV outbreak at the DRC.	11
Figure 1.9. 3D structure of filovirus virion.	12
Figure 1.10. Genome organisation of the main genera of filoviruses.	12
Figure 1.11. Cryo-EM Structure of EBOV NP RNA complex.	13
Figure 1.12. Structure of filovirus VP35.	14
Figure 1.13. Structure of EBOV VP40.	15
Figure 1.14. Structure of EBOV GP.	16
Figure 1.15. Crystal structure of EBOV GP in complex with a neutralising antibody.	17
Figure 1.16. EBOV GP ₁ and GP ₂ subunits.	18
Figure 1.17. Diagram of EBOV GP gene editing site.	19
Figure 1.18. <i>Ebolavirus</i> transcriptional editing model.	20
Figure 1.19. EBOV VP30 structure.	22
Figure 1.20. SUDV VP24 structure.	23
Figure 1.21. Diagram of viral polymerase (L) primary structure prediction.	24
Figure 1.22. Ribbon diagram of viral polymerase (L) structure prediction by Phyre2.	24
Figure 1.23. Model of filovirus GP and host cell fusion.	27
Figure 1.24. EBOV model of transcription and replication.	28

Figure 1.25. Infection cycle and cellular/tissue targets of EVD.	30
Figure 1.26. Pathogenesis of EVD/MVD.	32
Figure 1.27. Inhibition of interferon pathways during filovirus infection.	33
Figure 1.28. Filovirus virion, lentiviral and VSV PVs displaying filovirus GPs.	42
Figure 1.29. Lentiviral vectors for PV generation.	51
Figure 1.30. Infectivity assay.	53
Figure 1.31 Bioluminescence reaction catalysed by Firefly luciferase.	53
Figure 1.32. Pseudotype Virus Neutralisation Assay (PVNA).	54
Figure 2.1. Map of pCAGGS plasmid.	58
Figure 2.2. Diagram of 3-plasmid transfection to generate filovirus PVs with a luciferase reporter gene.	66
Figure 2.3. Schematic diagram of VSV core PV production.	69
Figure 2.4. Plate diagram of a TCID ₅₀ assay setup.	71
Figure 2.5. SG-PERT assay to quantify RT activity in lentiviral PV samples.	73
Figure 3.1. p1.18 expression vector.	81
Figure 3.2: Restriction digestion with <i>EcoRI</i> and <i>NheI</i> of miniprep of cloned MARV genes.	85
Figure 3.3. Generation of <i>ebolavirus</i> (EBOV, SUDV and BDBV) and <i>marburgvirus</i> (RAVV) PVs.	86
Figure 3.4. Generation of <i>ebolavirus</i> (EBOV, SUDV and BDBV) and <i>marburgvirus</i> (RAVV) PVs in 6-well plates.	87
Figure 3.5. Evaluation of transfection reagents in lentiviral core filovirus PV production.	87
Figure 3.6. Evaluation of FugeneHD and PEI in lentiviral core filovirus PV production.	88
Figure 3.7. Comparison of filovirus and influenza PVs in HEK293T cells originating from different VPU labs: Kent and Sussex.	90
Figure 3.8. Filovirus PV env optimisation.	91
Figure 3.9. Filovirus PV env optimisation in CHO-K1 target cells.	92

Figure 3.10. Filovirus PV upscaled production.	93
Figure 3.11. Filovirus PV functional titres in different target cell lines.	94
Figure 3.12. Filovirus TCID ₅₀ titres in HEK293T target cells.	95
Figure 3.13. Virion associated p24 ELISA.	96
Figure 3.14. Virion associated p24 ELISA in neat PV supernatants.	97
Figure 3.15. SG-PERT SYBR-Green Product Enhancement Reverse Transcriptase assay.	98
Figure 3.16. PV infectivity after freeze-thaw cycles.	99
Figure 3.17. Infectivity of filovirus PVs with an eGFP reporter.	100
Figure 3.18. Infectivity and TCID ₅₀ assays in BHK-21 target cells.	101
Figure 3.19. Generation of VSV core PVs in 6-well plates.	102
Figure 3.20. Generation of VSV core PVs in T25 flasks.	103
Figure 3.21. Generation of VSV core SUDV, BDBV, RESTV and MARV (Angola) PVs in T25 flasks.	104
Figure 3.22. Filovirus VSV PVs TCID ₅₀ and PFU titres in HEK293T target cells.	104
Figure 3.23. Infectivity of filovirus VSV PVs in CHO-K1 cells.	105
Figure 4.1. Neutralisation assay with anti-EBOV WHO NIBSC standards comparing target cell lines.	116
Figure 4.2. Neutralisation assay with anti-EBOV WHO NIBSC standard panel 16.344.	118
Figure 4.3. Neutralising titres of sera panel WHO NIBSC 16.344 against EBOV PVs.	119
Figure 4.4. Neutralisation assay with rabbit polyclonal anti-EBOV serum against lentiviral PVs bearing the EBOV (Makona C15) glycoprotein.	119
Figure 4.5. Neutralising titres of PVNAs with different filovirus PVs.	121
Figure 4.6. Neutralisation assay with anti-EBOV WHO NIBSC standards against lentiviral RAVV PVs.	121
Figure 4.7. Neutralisation assay with anti-EBOV WHO NIBSC 16.344 standard against lentiviral PVs.	122
Figure 4.8. Neutralising responses of monoclonal antibodies targetting the EBOV GP.	123

Figure 4.9. Neutralising responses of mAb MR78 targetting the Marburg virus GP.	125
Figure 4.10. Protein quantification with Pierce's BCA assay.	126
Figure 4.11. Infectivity assay of concentrated EBOV PVs for use in ELISA.	126
Figure 4.12. Indirect ELISA.	127
Figure 4.13. Indirect ELISA to assess secondary antibody input.	128
Figure 4.14. Indirect ELISA to screen convalescent sera.	129
Figure 4.15. Sandwich capture ELISA.	129
Figure 4.16. Indirect ELISA to assess cross-reactivity.	130
Figure 4.17. Indirect ELISA to screen monoclonal antibodies targetting the EBOV GP.	131
Figure 5.1. Structure of the EBOV GP trimer (orange) bound to the human antibody KZ52 (green).	140
Figure 5.2. Structure of RAVV GP trimer (orange) bound to the human antibody MR78 (green).	141
Figure 5.3. Overlap extension strategies.	146
Figure 5.4. Partial model of 1H3 (blue) and KZ52 (red) epitopes mutated into the LLOV GP.	150
Figure 5.5. Intensive model of LLOV GP containing 1H3 and KZ52 epitopes.	151
Figure 5.6. Partial model of LLOV GP containing MR78 epitope.	152
Figure 5.7. Intensive model of RAVV-LLOV GP containing MR78 epitope.	152
Figure 5.8. Intensive model of RESTV GP containing EBOV epitopes.	153
Figure 5.9. Intensive model of RAVV-RESTV GP containing MR78 epitope.	153
Figure 5.10. Gradient PCR of fragments AB and CD of chimeric GP containing 1H3 epitope.	154
Figure 5.11. Generation of final fragment AD of chimeric GP containing 1H3 epitope.	155
Figure 5.12. Colony PCR screen of cells transformed with 1H3LLOV-pCAGGS.	155
Figure 5.13. Sequence of 1H3 epitope (top blue annotation) flanked by LLOV sequence.	156

Figure 5.14. Gel extraction of final fragments of KZ52LLOV and KZ52/1H3LLOV chimeric GP.	156
Figure 5.15. Sequence analysis of chimeric LLOV GP constructs.	157
Figure 5.16. Gradient PCR to establish best annealing temperature.	158
Figure 5.17. Gradient PCR for generation of fragment KZ52RESTV GP.	159
Figure 5.18. Sequence analysis of KZ52RESTV GP construct.	160
Figure 5.19. Infectivity assay of lentiviral PVs bearing chimeric LLOV GPs.	161
Figure 5.20. Infectivity assay of lentiviral PVs bearing chimeric RESTV GPs.	162
Figure 5.21. Neutralisation assay with EBOV and LLOV PVs with murine derived mAbs.	163
Figure 5.22. Neutralisation assay with EBOV, LLOV and chimeric LLOV PVs.	163
Figure 5.23. Neutralisation assay with EBOV, RESTV and chimeric RESTV PVs.	164
Figure 5.24. Neutralisation assay with EBOV, RESTV and chimeric RESTV PVs with human mAb KZ52.	165
Figure 5.25. Neutralisation assay with anti-EBOV convalescent serum (WHO NIBSC 15.262) against EBOV, RESTV and chimeric RESTV PVs.	166
Figure 5.26. ELISA with chimeric LLOV PVs as antigens.	167
Figure 5.27. ELISA with chimeric RESTV PVs as antigens.	167
Figure 6.1. Genomic organisation of LLOV.	175
Figure 6.2. TEM of purified LLOV VLP produced in HEK293T cells.	176
Figure 6.3. Lentiviral LLOV PV titres.	178
Figure 6.4. Antibody neutralising response in bat serum samples.	181
Figure 6.5. Antibody neutralising response of 24 bat serum samples from the overall panel (n=71).	183
Figure 6.6. Antibody neutralising curves of bat serum samples.	183
Figure 6.7. Antibody neutralising response of an additional 21 low-volume bat serum samples.	185
Figure 6.8. Antibody neutralising response of a further 20 bat serum samples.	186
Figure 6.9. Antibody neutralising response of 6 bat serum samples.	187

Figure 6.10. Cut-off determination for positive samples.	187
Figure 7.1. Lyophilisation principles.	195
Figure 7.2. Labconco™ FreeZone™ 2.5L freeze drier.	197
Figure 7.3. Generation of Filovirus PVs displaying GPs of the three major genera: <i>ebolavirus</i> (EBOV, SUDV and BDBV); <i>cuevavirus</i> (LLOV); <i>marburgvirus</i> (RAVV, MARV-Angola and MARV-DRC).	200
Figure 7.4. Infectivity assay following a one-month storage of lyophilised filovirus PVs.	202
Figure 7.5. Infectivity assay following a six-month storage of lyophilised filovirus PVs.	203
Figure 7.6. Infectivity assay following long-term storage of lyophilised EBOV PVs.	205
Figure 7.7. Infectivity assay following short and long-term storage of lyophilised BDBV and SUDV PVs.	206
Figure 7.8. Infectivity assay following long-term storage of lyophilised LLOV PVs.	207
Figure 7.9. Infectivity assay following long-term storage of lyophilised RAVV PVs.	208
Figure 7.10. Infectivity assay following long-term storage of lyophilised MARV (Angola) PVs.	209
Figure 7.11. Infectivity following long-term storage of lyophilised MARV (DRC) PVs.	211
Figure 7.12. Infectivity assay following one-month and six-month storage of EBOV PVs lyophilised at Intravacc.	212
Figure 7.13. Neutralisation assay using reconstituted lyophilised EBOV PVs.	213
Figure 7.14. Neutralisation assay using reconstituted lyophilised EBOV PVs from Intravacc.	214
Figure 7.15. Reverse transcriptase assay (SG-PERT) of lyophilised samples.	215
Figure II.1. Position of epitope 1H3 within the LLOV GP.	273
Figure II.2. Position of epitope KZ52 within the LLOV GP.	274
Figure II.3. Strategy to generate chimeric RAVV-LLOV GP.	275
Figure II.4. Position of epitope 4G7 within the RESTV GP.	276

Figure II.5. Position of epitope KZ52 within the RESTV GP.	277
Figure II.6. Position of epitope 1H3 within the RESTV GP.	278
Figure II.7. Strategy to generate chimeric RAVV-RESTV GP.	279

List of Tables

Table 1.1. Genera and species of filoviruses identified to date.	2
Table 1.2. History of <i>ebolavirus</i> outbreaks.	8
Table 1.3. History of <i>marburgvirus</i> outbreaks.	10
Table 1.4 Filovirus vaccine trials.	48
Table 2.1. Fast digestion reactions.	59
Table 2.2. Restriction digestion reactions.	59
Table 2.3. PCR reaction setup for colony screening.	62
Table 2.4. List of internal primers for sequencing of filovirus GP gene constructs.	63
Table 2.5: Preparation of p24 antigen to generate a standard curve.	72
Table 2.6. MS2 primers for generation of MS2 cDNA.	74
Table 2.7. SG-PERT assay cycle conditions.	74
Table 4.1. End-point antibody neutralising titres in convalescent serum against EBOV PVs using HEK293T and CHO-K1 cell lines.	117
Table 4.2. PV input for EBOV, RESTV and RAVV VSV and lentiviral PVs.	120
Table 4.3 IC ₅₀ (µg/mL) values on PVNAs using mAbs against EBOV PVs in HEK293T target cells.	124
Table 5.1. Primers designed to insert EBOV epitopes KZ52, 1H3 into LLOV GP and generate chimeric RAVV-LLOV GP.	144
Table 5.2. Primers designed to insert EBOV epitopes KZ52, 1H3 and 4G7 into RESTV GP and generate the chimeric RAVV-RESTV GP.	145
Table 5.3. PCR program for gradient and mutagenesis PCRs.	147
Table 5.4. IC ₅₀ values of neutralisation assays with chimeric PVs.	164
Table 5.5: IC ₅₀ values (µg/mL) of neutralisation assays with KZ52RESTV chimeric GP.	166
Table 6.1. Neutralising antibody end-point titres from 7 bat serum samples.	179
Table 6.2. Antibody titres from bat serum samples.	182
Table 7.1. Excipient components and concentration.	198

Table 7.2. Lyophilisation protocol performed at Intravacc.	198
Table 7.3. Lyophilisation protocol – temperature monitoring.	199
Table 7.4 Percentage titre recovery of PV stored at ambient temperature for one month.	202
Table 7.5. Mean half maximum inhibitory concentration (IC_{50}) and 90% inhibitory concentration (IC_{90}) of Intravacc lyophilised samples in PVNAs.	214
Table II.1. PCR #1 generation of fragments AB and CD for mutating epitope 1H3 into LLOV GP.	280
Table II.2. PCR #2 generation of final gene fragment AD containing 1H3 epitope.	280
Table II.3. PCR #1 generation fragments 1,2 and 3 for mutating epitope KZ52 into RESTV GP.	281
Table II.4. PCR #2 generation of final gene fragment AD containing KZ52 epitope in RESTV GP.	281

Abbreviations

AAV	Adeno-associated virus
ADCC	Antibody-dependent cytotoxicity
ADE	Antibody-dependent enhancement
ASGP-R	Asialoglycoprotein receptor
BDBV	Bundibugyo virus
BOMV	Bombali virus
BSA	Bovine serum albumin
BSL	Biosafety level
catB	Cathepsin B
catL	Cathepsin L
CCHFV	Crimean-Congo haemorrhagic fever virus
CDC	Centers for Disease Control and Prevention
CFR	Case fatality rate
CMV	Cytomegalovirus
COVID-19	Coronavirus disease (caused by the SARS-CoV-2 virus)
CPE	Cytopathic effect
DC	Dendritic cell
DC-SIGN	DC-specific intercellular adhesion molecule-3-grabbing non-integrin
DMEM	Dulbecco's Modified Eagle's Medium
DMSO	Dimethyl sulfoxide
DNA	Deoxyribonucleic acid
DPBS	Dulbecco's Phosphate Buffered Saline
DRC	Democratic Republic of the Congo
EBOV	Ebola virus
EDTA	Ethylenediaminetetraacetic acid
ELISA	Enzyme-linked immunosorbent assay
ER	Endoplasmic reticulum
ERK	Extracellular signal-regulated kinase
EVD	Ebola virus disease
exNA	Exogenous neuraminidase
FBS	Fetal bovine serum
FGFR	Fibroblast growth factor receptor

FPV	Fowlpox virus
FR- α	Folate receptor α
GFP	Green fluorescent protein
GP	Glycoprotein
HA	Haemagglutinin
HR	Heptad region
HRP	Horseradish peroxidase
HUJV	Huangjiao virus
IC ₅₀	50% inhibitory concentration
IC ₉₀	90% inhibitory concentration
IFITM	Interferon-inducible transmembrane protein
IFL	Internal fusion loop
IFNAR	Interferon- α/β receptor
Ig	Immunoglobulin
IID	Interferon inhibitor domain
IL	Interleukin
INF	Interferon
IRF	Interferon regulatory factor
ISG	Interferon stimulating gene
lacZ	β -galactosidase
LASV	Lassa virus
LLOV	Lloviu virus
LB	Luria Bertani (broth)
L-SIGN	Liver/lymph node-specific intercellular adhesion molecule-3-grabbing integrin
LTR	Long terminal repeat
mAb	Monoclonal antibody
MAPK	Mitogen-activated protein kinase
MARV	Marburg virus
MEGA	Molecular evolutionary genetics analysis
MHC	Major histocompatibility complex
MIP	Macrophage inflammatory protein
MLD	Mucin-like domain
MLAV	Mengla virus

MLV	Murine leukemia virus
MNA	Microneutralisation assay
MOI	Multiplicity of infection
mRNA	Messenger RNA
MVA	Modified vaccinia virus Ankara
MVD	Marburg virus disease
NA	Neuraminidase
NHP	Non-human primate
NIBSC	National Institute for Biological Standards and Control
NK	Natural killer (cell)
NP	Nucleoprotein
NPC1	Niemann-Pick C1
NSP4	Nonstructural protein 4
NTP	Ribonucleoside triphosphate
OD	Optical density
PAMP	Pathogen-associated molecular pattern
PCR	Polymerase chain reaction
PEI	Polyethylenimine
PFU	Plaque forming unit
PHYRE2	Protein homology/analogy recognition engine v 2.0
PIM	Pressure rise test
PKR	Protein kinase R
PRNT	Plaque reduction neutralisation test
PV	Pseudotype virus
PVNA	Pseudotype virus neutralisation assay
qPCR	Quantitative polymerase chain reaction
RAVV	Ravn virus
RBS	Receptor-binding site
RdRp	RNA-dependent RNA polymerase
RESTV	Reston virus
RIG-I	Retinoic acid inducible gene I
RLU	Relative light units
RNA	Ribonucleic acid
RNP	Ribonucleoprotein

ROS	Reactive oxygen species
rpm	Revolutions per minute
RT	Room temperature
RT	Reverse transcriptase
RT-PCR	Reverse transcription polymerase chain reaction
SARS-CoV-2	Severe acute respiratory syndrome coronavirus 2
SEAP	Secreted embryonic alkaline phosphatase
SFFV	Spleen focus forming virus
SG-PERT	SYBR Green product-enhanced reverse transcriptase assay
siRNA	Small interfering RNA
sGP	Secreted glycoprotein
ssGP	Small secreted glycoprotein
STAT	Signal transducer and activator of transcription
SUDV	Sudan virus
SUMO	Small ubiquitin-like modifier
TAE	Tris-acetate-EDTA buffer
TACE	Tumor necrosis factor- α -converting enzyme
TAFV	Tai Forest virus
TCID ₅₀	50% tissue culture infectious dose
TMB	3,3',5,5'-Tetramethylbenzidine
TNF	Tumor necrosis factor
VLP	Virus-like particle
VP24	Viral protein 24
VP40	Viral protein 40
VP30	Viral protein 30
VP35	Viral protein 35
VP/mL	Virus particles per milliliter
VSV	Vesicular stomatitis virus
WHO	World Health Organisation
WPRE	Woodchuck hepatitis virus post-transcriptional regulatory element
XILV	Xilang virus

CHAPTER 1: Introduction

1.1 Filovirus classification and nomenclature

Filoviruses belong to the *filoviridae* family of the order mononegavirales, containing a single-stranded negative sense genome of approximately 19 kb, showing slight variations in size between genera and species. Virions are relatively pleomorphic, usually presenting as long filaments (Figure 1.1), sometimes branched, U-shaped, 6-shaped or circular forms. They have varying lengths of up to 14000 nm, but with a more constant 80 nm diameter (Geisbert and Jahrling 1995; Di Paola *et al.* 2020).

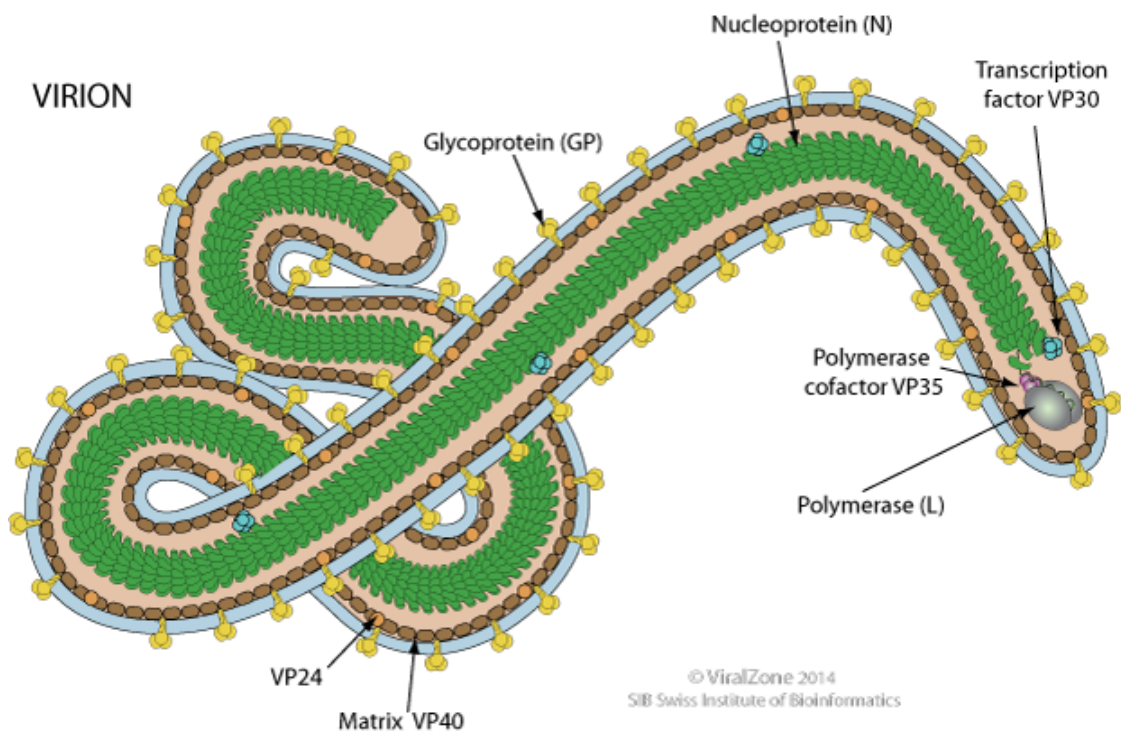


Figure 1.1. Filovirus virion diagram. Typical rod-like shape of filoviruses with their surface glycoprotein (yellow) embedded in the host derived lipid membrane. The nucleocapsid protein (green) encapsulates the negative sense single-stranded RNA genome, attached to the virus derived RNA-dependent polymerase (L). Matrix proteins VP24 and VP40, as well as VP30 and VP35 are also shown. Source: ViralZone.

Filoviruses are enveloped viruses containing a trimeric glycoprotein (GP) on their surface of approximately 5-10 nm length (Geisbert and Jahrling 1995), which is responsible for attachment and entry into host cells and it is the main target of neutralising antibodies.

To date, six genera of filoviruses have been identified: *ebolavirus*, *marburgvirus*, *cuevavirus*, *dianlovirus*, *striavirus* and *thamnovirus* (Table 1.1). *Ebolavirus* and

marburgvirus species have been associated with human disease apart from BOMV and RESTV (Table 1.1). BOMV and MLAV (Table 1.1) are putative species, yet to be confirmed as such (Kuhn *et al.* 2019; Amarasinghe *et al.* 2019).

Genus	Species	Virus	Abbreviation
<i>Ebolavirus</i>	<i>Zaire ebolavirus</i>	Ebola	EBOV
	<i>Sudan ebolavirus</i>	Sudan	SUDV
	<i>Bundibugyo ebolavirus</i>	Bundibugyo	BDBV
	<i>Reston ebolavirus</i>	Reston	RESTV
	<i>Tai Forest ebolavirus</i>	Tai Forest	TAFV
	<i>Bombali ebolavirus*</i>	Bombali	BOMV
<i>Marburgvirus</i>	<i>Marburg marburgvirus</i>	Marburg	MARV
		Ravn	RAVV
<i>Cuevavirus</i>	<i>Lloviu cuevavirus</i>	Lloviu	LLOV
<i>Dianlovirus*</i>	<i>Mengla dianlovirus*</i>	Mengla	MLAV
<i>Striavirus</i>	<i>Xilang striavirus</i>	Xilang	XILV
<i>Thamnovirus</i>	<i>Huangjiao thamnovirus</i>	Huangjiao	HUJV

Table 1.1. Genera and species of filoviruses identified to date. Pathogenic viruses in bold. *Putative species. Source: Kuhn *et al.* 2019.

BOMV RNA has been found in free-tailed bats in Sierra Leone, Kenya and Guinea (Goldstein *et al.* 2018; Forbes *et al.* 2019; Karan *et al.* 2019), whereas MLAV RNA was detected in bats in China (Yang *et al.* 2019). The transcriptional editing site present on *ebolaviruses* and *cuevaviruses* GP gene sequences, responsible for expression of the membrane-associated GP, is not present in MLAV, adding to the evidence of MLAV (Figure 1.2) having a closer evolutionary relationship with *marburgviruses* (Yang *et al.* 2019).

XILV and HUJV could be common ancestors of filoviruses (Figure 1.2). XILV RNA was isolated from gills of wenling frogfish and HUJV RNA isolated from greenfin horse-faced filefish in China. A sequence of approximately 17 Kb (out of 19 Kb) was recovered of XILV and found to have 42% amino acid similarity with BDBV (Shi *et al.* 2018).

However, the authors acknowledge the need for more sampling before confirming whether these viruses are indeed common ancestors of other filoviruses.

A phylogenetic tree was built based on GP nucleotide sequences (Figure 1.3), including those used in pseudotyping during this study (EBOV, SUDV, BDBV, RESTV, LLOV, RAVV, MARV (Angola) and MARV (DRC), as well as newly described *ebolavirus* (BOMV) and *dianlovirus* MLAV using the Neighbour-joining method (Saitou and Nei 1987). The evolutionary distances (number of base substitutions per site) were computed using the Maximum Composite Likelihood method (Tamura, Nei and Kumar 2004) and the tree built with Mega 7 software (Kumar, Stecher and Tamura 2016). Evolutionary relationship between species and genera based on the GP sequences used in this study (Figure 1.3) correlates to published phylogenetic analysis (Figure 1.2).

1.2 History of filovirus outbreaks

Filoviruses are amongst the deadliest pathogens identified to date. Since their discovery in 1967 in Marburg, Germany they have caused sporadic outbreaks (Figures 1.5 & 1.6) with mortality rates of up to 90% and varying numbers of people affected (Tables 1.2 & 1.3). In mid-August of 1967, 25 laboratory workers in Marburg, Germany and Belgrade, in the former Yugoslavia (now Serbia) fell ill with an unidentified disease with unusual symptoms not seen before (Martini 1969; Siegert 1972). All of them had been in contact with African green monkeys (*Cercopithecus aethiops*) imported from Uganda. In Marburg, they were imported to a poliomyelitis vaccine manufacturer to provide tissue for primary cell cultures (Ristanovic *et al.* 2020). New cases spread to healthcare workers and family members. A total of 31 cases were reported, out of which 7 died. Some were nosocomial infections in hospitalised patients. There was also an extra case confirmed retrospectively by serology (Feldmann, Slenczka and Klenk 1996).

It took a few months for the virus to be identified and characterised (Figure 1.4) due to the apparent virulence of the pathogen. Isolates obtained from patients were initially passaged in guinea pigs and non-human primates, then passaged in cell cultures. They were eventually identified through electron microscopy (Kissling *et al.* 1968; Ristanovic *et al.* 2020).

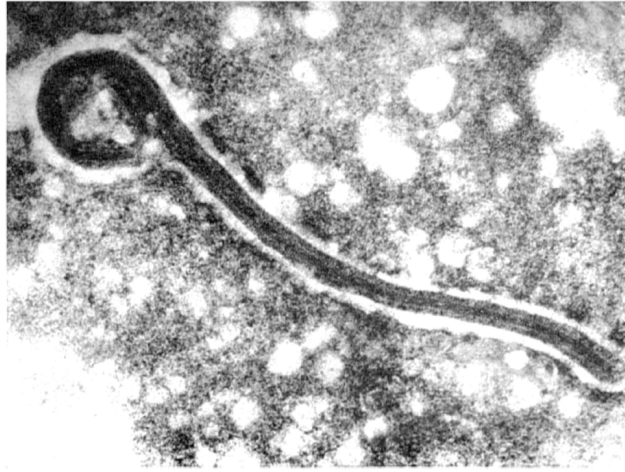


Figure 1.4. First electron micrograph of a MARV virion. Source: Brauburger *et al*, 2012. (original image provided by W. Slenczka).

In South Africa in 1975 a small MARV outbreak occurred after a man who had recently returned from Zimbabwe presented with symptoms. His travel companion also fell ill followed by a healthcare worker. The patient did not survive, however both the travel companion and healthcare worker did, after receiving supportive therapy (Gear *et al*. 1975).

Then in 1976, a similar haemorrhagic disease emerged in northern Zaire (now the Democratic Republic of Congo), affecting 318 people, of which 280 died (Case Fatality Rate - CFR = 88%). The virus was found to be a different filovirus species from the earlier outbreak of MARV and was named Ebola, after the river around 60 miles from Yambuko, the epicentre of the outbreak (Johnson *et al*. 1978). Concomitantly, another outbreak occurred in Sudan, which is thought to have started in a cotton factory affecting 284 people, of which 151 died (CFR = 53%). It was later found to be SUDV (Simpson *et al* 1978).

After several small outbreaks of EBOV and SUDV between 1976 and 1979, another outbreak of MARV occurred in Kenya (n=2, CFR = 50%). Next, RAVV emerged in Kenya again in 1987 in a 15 year-old Danish boy who had visited Kitum Cave in Mount Elgon National Park a few days before presenting with symptoms including headache, vomiting, malaise and fever. He died 11 days later despite receiving supportive therapy. The virus was isolated and partially characterised, exhibiting considerable sequence differences between previous strains Musoki and Popp; 72.3% nucleotide similarity with Musoki and 71% similarity with Popp (Musoki had 91.7% nucleotide similarity with Popp); similarly, RAVV had 72% amino acid similarity with Musoki and 67% similarity with Popp (Musoki had 93% amino acid similarity with Popp). Even though it was not classified as a new

species, it was named Ravn (RAVV) to differentiate from the current reference strains at the time (Johnson *et al.* 1996).

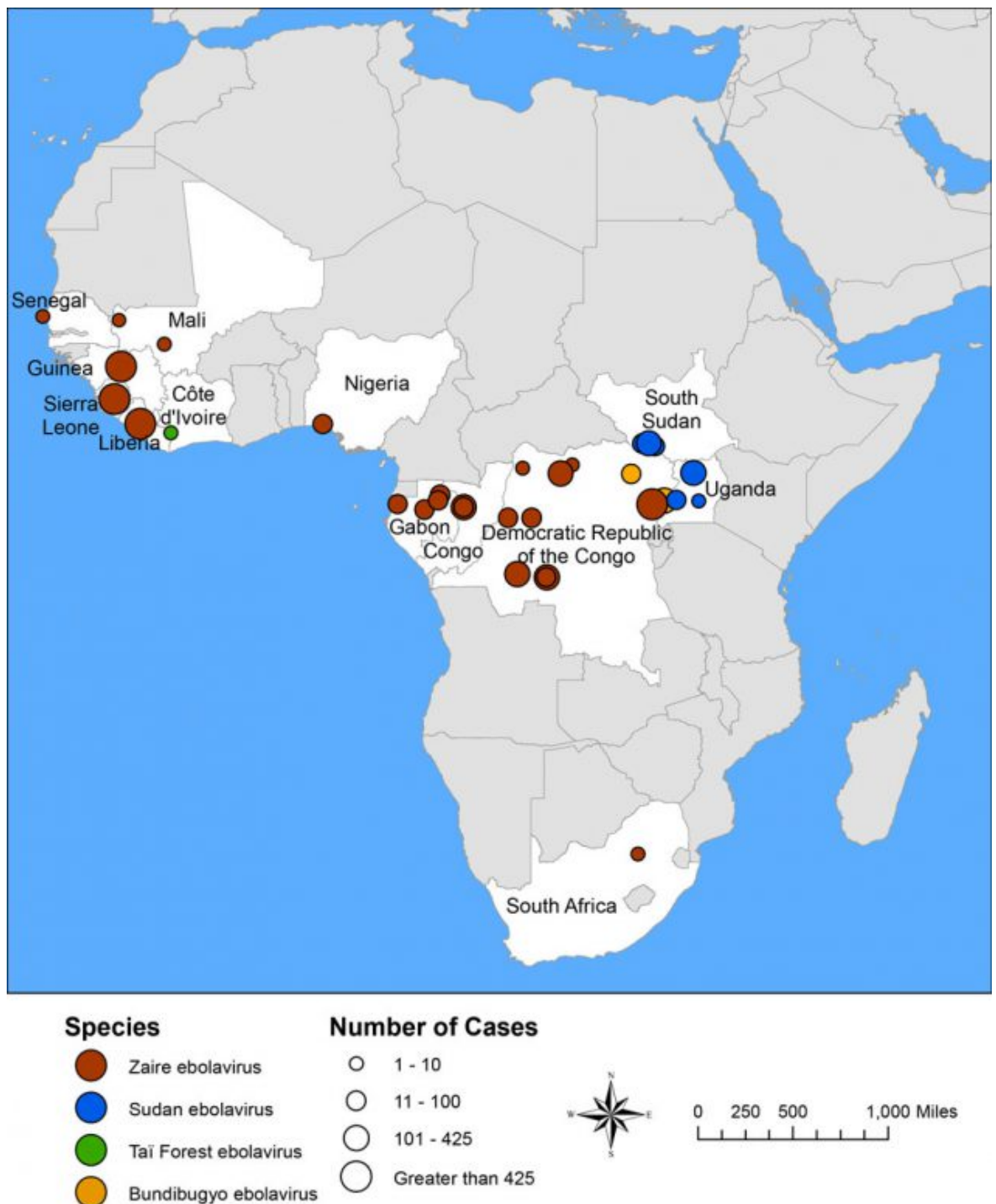


Figure 1.5. History of *Ebolavirus* outbreaks according to species and size. Note: the latest outbreak in the DRC declared in June 2020 is not shown here. Source: CDC, Centers for disease control and prevention.

In 1990 a laboratory worker in Russia was contaminated accidentally with MARV, then in 1998 a new outbreak, larger than usual, started in the DRC affecting 154 people with a high CFR of 83% (Bausch *et al.* 2006).

In 1989 the first filovirus that is not known to cause disease in humans was described after high mortality was observed in *Cynomolgus* macaques in a primate facility in the Philippines that exported animals to Virginia and Pennsylvania, USA. Three workers had antibodies detected but did not present any symptoms. The new species was named *Reston ebolavirus* (Miranda *et al.* 1987; Jahrling *et al.* 1990). The following year, four asymptomatic cases were detected in Virginia and Texas, USA in a quarantine facility. Since then, infected monkeys have been identified in a quarantine facility in Sienna, Italy in 1992; in a monkey export facility in the Philippines as well as a quarantine facility in Texas, USA in 1996. However, no human infections were detected (Table 1.2). In 2008, six workers in a pig farm in the Philippines developed antibodies against RESTV but did not present with symptoms. Detection of RESTV in pigs was achieved through microarray analysis, RT-PCR, immunohistochemistry and virus isolation in cell culture (Barrette *et al.* 2009).

A new *ebolavirus* species emerged in 1994 in the Ivory Coast (TAFV). High mortality events had been observed in a population of chimpanzees. Subsequently, a scientist fell ill, but was treated and recovered (Guenno *et al.* 1995). No further outbreaks of TAFV have been reported.

After some sporadic outbreaks of *ebolavirus* and *marburgvirus* (Tables 1.2 & 1.3), a new pathogenic ebolavirus species (BDBV) emerged in Uganda in the Bundibugyo district, affecting 131 people but with a much lower CFR (32%) than previously observed with EBOV or SUDV. Again, the time between initial cases and confirmation of the agent responsible for the disease allowed for infection to spread to a higher number of people (MacNeil *et al.* 2011). BDBV re-emerged in the DRC in 2012 affecting 31 people (CDC).

In 2014, the largest ever recorded outbreak of EBOV started in Guinea. It soon spread to neighbouring countries Liberia and Sierra Leone, affecting approximately 29000 people. Interestingly, it had a lower CFR (40%) than previously observed. It spread to a much wider geographic area (Figure 1.7), and affected a higher number of people than in previous outbreaks.

After a couple of smaller EBOV outbreaks in the DRC since, a new outbreak was declared in August 1st, 2018 in the North Kivu province in the DRC. In total, 3452 cases and 2262 deaths were reported, resulting in CFR = 66% (WHO).

year	Virus	Location	Number of cases	Deaths (CFR)
1976	EBOV	DRC	318	280 (88%)
1976	SUDV	Sudan	284	151 (53%)
1976	SUDV	UK**	1	0
1977	EBOV	DRC	1	1 (100%)
1979	SUDV	Sudan	34	22 (65%)
1989	RESTV	Philippines/USA§	3	0
1990	RESTV	USA§	4	0
1992	RESTV	Italy§	0	0
1994	TAFV	Ivory Coast	1	0
1995	EBOV	DRC	315	254 (81%)
1996	EBOV	Russia**	1	1 (100%)
1996	RESTV	Philippines/USA§	0	0
1996	EBOV	South Africa*	2	1 (50%)
1996	EBOV	Gabon	60	45 (75%)
1996	EBOV	Gabon	31	21 (68%)
2000	SUDV	Uganda	425	224 (53%)
2001	EBOV	Rep of the Congo	59	44 (75%)
2001	EBOV	Gabon	65	53 (82%)
2003	EBOV	Rep of the Congo	35	29 (83%)
2003	EBOV	Rep of the Congo	143	128 (90%)
2004	EBOV	Russia**	1	1 (100%)
2004	SUDV	Sudan	17	7 (41%)
2005	EBOV	Rep of the Congo	12	10 (83%)
2007	BDBV	Uganda	131	42 (32%)
2007	EBOV	DRC	264	187 (71%)
2008	EBOV	DRC	32	15 (47%)
2008	RESTV	Philippines	6	0
2011	SUDV	Uganda	1	1 (100%)
2012	SUDV	Uganda	6	3 (50%)
2012	BDBV	DRC	38	13 (34%)
2012	SUDV	Uganda	11	4 (36%)
2014	EBOV	DRC	69	49 (71%)
2014	EBOV	Guinea,Liberia, SL	28610	11308 (40%)
2014	EBOV	Italy*	1	0
2014	EBOV	Mali*	8	6 (75%)
2014	EBOV	Nigeria*	20	8 (40%)
2014	EBOV	Senegal*	1	0
2014	EBOV	Spain*	1	0
2014	EBOV	UK*	1	0
2014	EBOV	USA*	4	1 (25%)
2017	EBOV	DRC	8	4 (50%)
2018	EBOV	DRC	54	33 (61%)
2018	EBOV	DRC, Uganda	3470	2287 (66%)
2020	EBOV	DRC	130	55 (42%)

Table 1.2. History of *ebolavirus* outbreaks. Number of deaths (case fatality rates). DRC: Democratic Republic of Congo. SL: Sierra Leone. *imported cases. **laboratory accident. §imported infected non-human primates from The Philippines. Source: CDC, Centers for Disease Control and Prevention.



Figure 1.6. Location of *marburgvirus* outbreaks. African countries affect by MARV and RAVV outbreaks highlighted in blue. Map created with mapchart.net.

By June the following year, the DRC outbreak had spread to Uganda. Even though the number of new cases had decreased over time (Figure 1.8), the outbreak was not declared closed until a 42-day period of no recorded cases was observed in June, 25th 2020 (WHO Ebola Situation Report).

year	Virus	Location	Number of cases	Deaths (CFR)
1967	MARV	Germany, Yugoslavia¶	31	7 (23%)
1975	MARV	South Africa*	3	1 (33%)
1980	MARV	Kenya	2	1 (50%)
1987	RAVV	Kenya	1	1 (100%)
1990	MARV	Russia**	1	1 (100%)
1998	MARV, RAVV	DRC	154 (1 RAVV)	128 (83%)
2004	MARV	Angola	252	227 (90%)
2007	MARV, RAVV	Uganda	4 (3 RAVV)	1 (25%)
2008	MARV	USA*	1	0
2008	MARV	The Netherlands*	1	1 (100%)
2012	MARV	Uganda	15	4 (27%)
2014	MARV	Uganda	1	1 (100%)
2017	MARV	Uganda	3	3 (100%)

Table 1.3. History of *marburgvirus* outbreaks. Number of deaths (case fatality rate). *imported cases. **laboratory accident. ¶imported infected non-human primates from Uganda. Source: CDC, Centers for disease control and prevention.

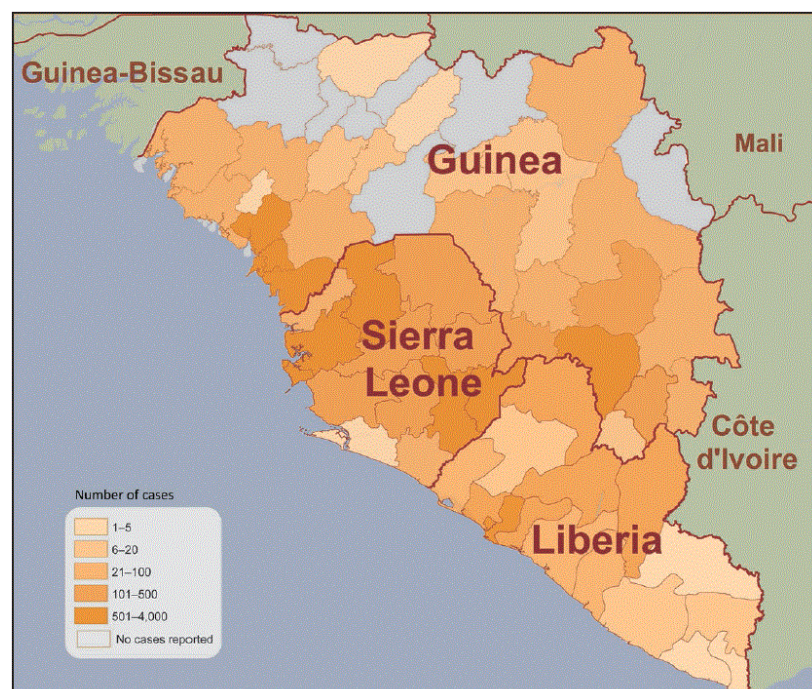


Figure 1.7. Number of cumulative EBOV cases by country and prefecture during the 2013-2016 outbreak. Source: WHO, Ebola Situation Reports.

The WHO recommended efforts to contain this outbreak were maintained despite dealing with the current COVID-19 outbreak (WHO). In a new development, a concomitant EBOV outbreak was declared on June, 1st 2020 in Mbandaka with 130 cases (55 deaths), declared over on November, 18th 2020 (WHO).

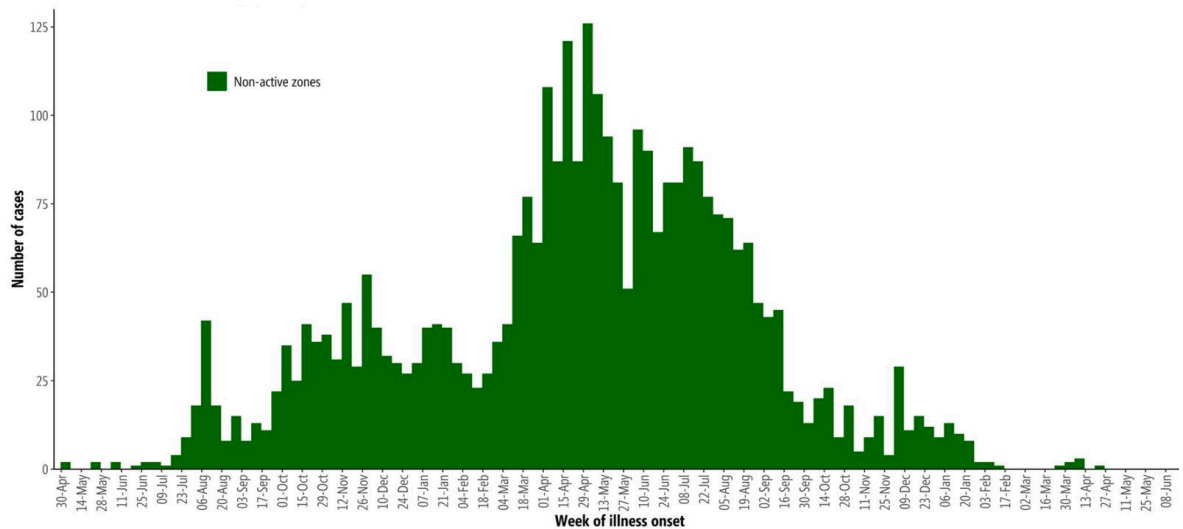


Figure 1.8. Cumulative cases during the 2018-2020 EBOV outbreak at the DRC. Source: WHO situation reports (July 2nd, 2019).

Newly described species (BOMV, LLOV, MLAV) have not caused disease in humans to date, but they could have the potential for zoonotic transmission (Negredo *et al.* 2011; Goldstein *et al.* 2018; Yang *et al.* 2019) and should be monitored.

1.3 Filovirus genome organisation and protein functions

Filovirus are filamentous particles with a negative sense single-stranded genome encapsulated by the nucleoprotein (Figure 1.9). The 19 kb genome is linear with seven genes encoding seven structural proteins (NP, VP35, VP40, GP, VP30, VP24, L) containing transcriptional start and termination signals. Transcription and replication are under the control of the viral polymerase and take place in the cytoplasm of the host cells. Replication occurs by generation of (positive sense) anti-genomes that serve as a template for genome synthesis (Feldmann *et al.* 1992; Feldmann, Klenk and Sanchez 1993; Dolnik, Kolesnikova and Becker 2008; Hume and Mühlberger 2019).

Early studies identified NP, VP35, VP30 and L proteins as part of the nucleocapsid complex (Figure 1.9) and associated with the virus genome (Elliott, Kiley and McCormick 1985), whereas matrix protein VP40 and VP24 are associated with the membrane and GP is a transmembrane glycoprotein (Feldmann, Klenk and Sanchez 1993).

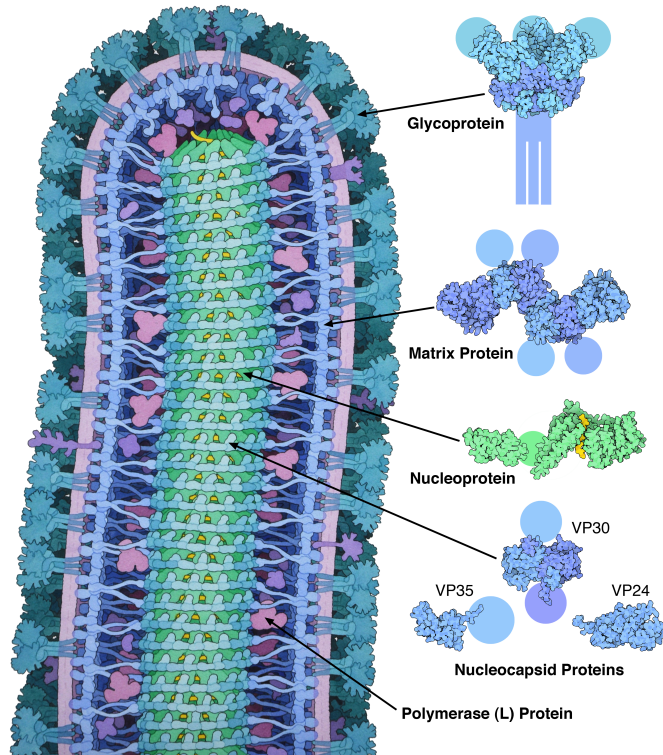
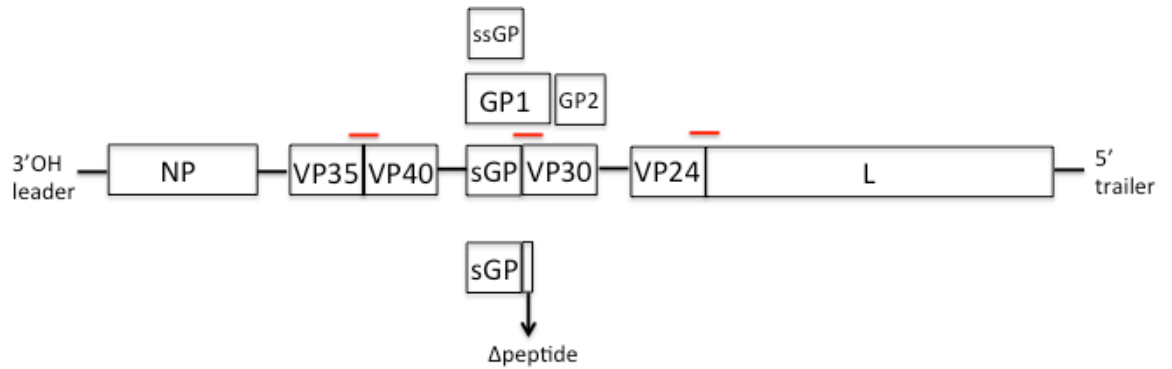


Figure 1.9. 3D structure of filovirus virion. Source: rcsb.org (Berman *et al*, 2000).

(a)



(b)



(c)

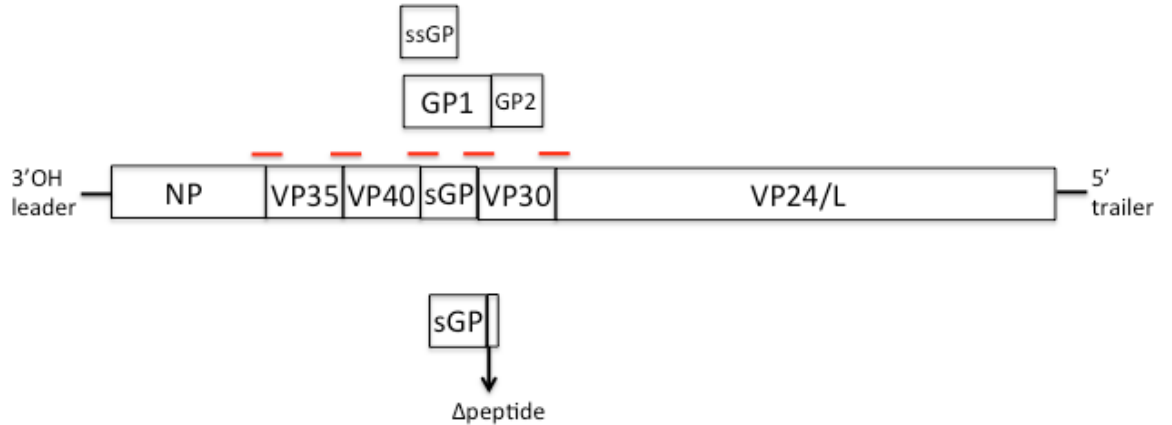


Figure 1.10. Genome organisation of the three main genera of filoviruses. (a) *ebolavirus*, (b) *marburgvirus* and (c) *cuevavirus* genome organisation. Overlapping open reading frames are highlighted red.

The three main genera have slight differences in genome organisation (Figure 1.10). *Ebolavirus* (Figure 1.10a) and *cuevavirus* (Figure 1.10c) primary transcripts encode a secreted truncated version of the GP, whereas *marburgvirus* primary transcripts encode the membrane associated GP (Figure 1.10b). There are differences in gene overlap between genera (Figure 1.10); and in *cuevavirus* the sixth transcript is bicistronic (Negredo *et al.* 2011), encoding both VP24 and L proteins (Figure 1.10c).

1.3.1 Nucleoprotein (NP)

The first viral protein to be transcribed is the nucleoprotein. It consists of 739 amino acids (Figure 1.11a). It has a hydrophobic N-terminus and a hydrophilic C-terminus. It is the main component of the ribonucleoprotein (RNP) complex (Figure 1.11b), with VP35, VP30, L, as well as the viral genome. It self assembles (Figure 1.11c), and forms VLPs when expressed with VP24 and VP35 (Sanchez *et al.* 1989; Mühlberger *et al.* 1999; Huang *et al.* 2002; Watanabe, Noda and Kawaoka 2006).

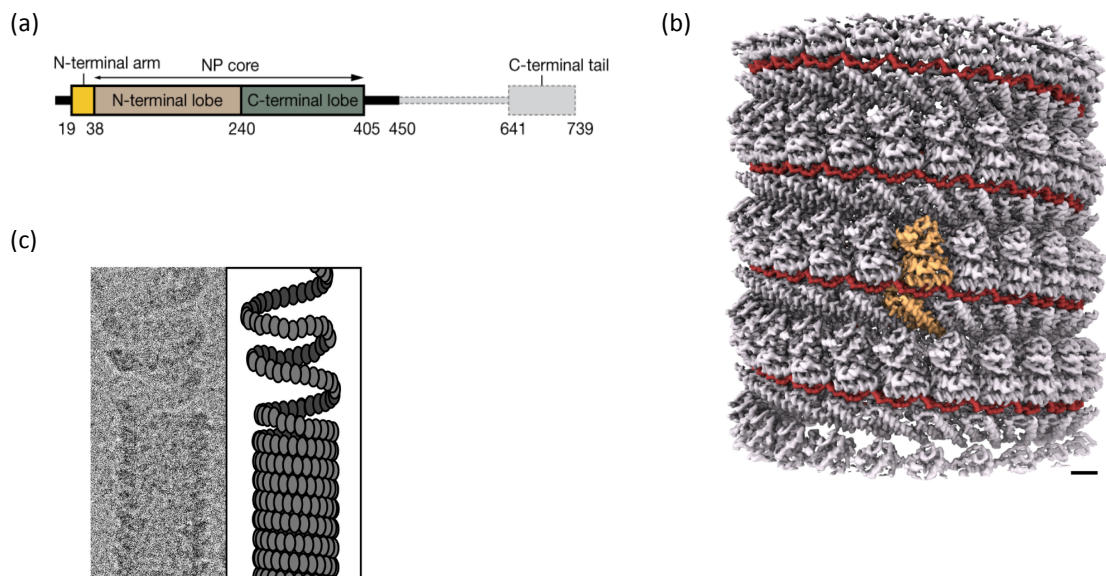


Figure 1.11. Cryo-EM Structure of EBOV NP-RNA complex. (a) diagram of NP primary structure; (b) iso-electron potential surface structure of NP-RNA complex. An NP subunit (orange) and RNA strand (red) are highlighted. Scale bar = 20 Å; and (c) digital micrograph of NP helices in amorphous ice. Scale bar = 50 Å Source: Sugita *et al.*, 2018.

NP has several important functions including regulation of RNA synthesis through interactions with VP30 and the viral genome. These interaction domains are highly conserved between different species of filoviruses. By modulating the affinity between

these interactions, the NP-VP30 complex regulates access of the genome to the viral polymerase (Kirchdoerfer *et al.* 2016).

More recently, interactions of NP with VP35 have been observed in SUDV keeping its NP free of RNA, playing a role on the regulation of transcription. It could be explored as a novel therapeutic target by disrupting this interaction, and therefore blocking transcription (Landeras-Bueno *et al.* 2019).

1.3.2 Viral Protein 35 (VP35)

VP35 is a co-factor of the L polymerase and forms part of the RNP complex (Möller *et al.* 2005; Prins *et al.* 2010). VP35 is a small protein with two domains: an oligomerisation domain and an interferon inhibitory domain (IID) or dsRNA-binding domain (Figure 1.12). Its interferon-antagonising functions include inhibiting IRF3 in the RIG-I signaling pathway or recognising other viral PAMPs, mainly through IID domain interactions (Prins, Cárdenas and Basler 2009; Leung *et al.* 2010; Zinzula *et al.* 2019). The oligomerisation domain seems to be responsible for structure stability and support during conformational changes when carrying out its functions (Zinzula *et al.* 2019). EBOV and MARV VP35 exhibit some differences with regards to PAMP recognition and mechanisms of inactivation (Ramanan *et al.* 2012). While EBOV can inhibit by recognising both dsRNA backbone or blunt ends, MARV VP35 only recognises dsRNA backbone (Leung *et al.* 2010; Ramanan *et al.* 2012).

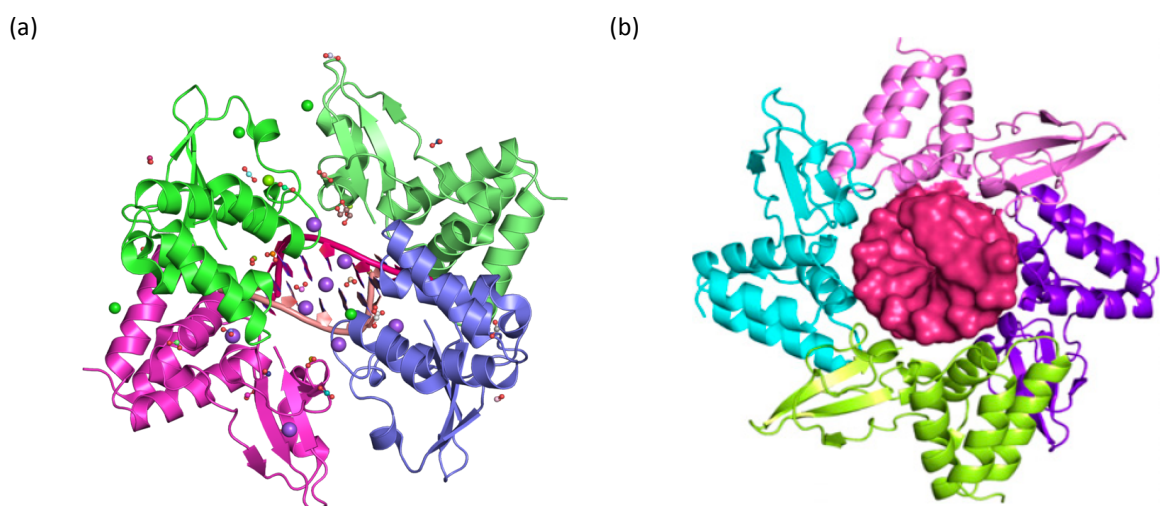


Figure 1.12. Structure of filovirus VP35. (a) EBOV and (b) MARV bound to dsRNA. In each structure there are four VP35 IID molecules in different colours. Source: Leung *et al.*, 2010 (EBOV) and Ramanan *et al.*, 2012 (MARV).

More recently, VP35 further involvement in replication in transcription has been described by newly identified helicase activity functions. VP35 was found to have a helicase activity despite not having helicase-like domains, by hydrolysing ribonucleotides triphosphates (NTPs), a function so far not observed with other proteins encoded by non-segmented single-stranded viral genomes (Shu *et al.* 2019). In addition, phosphorylation has been found to play an important role in viral replication, identifying a potential therapeutic target by modulating phosphorylation of VP35 (Zhu *et al.* 2020).

1.3.3 Viral Protein 40 (VP40)

VP40 is the main matrix component of filoviruses. It is the most abundant protein in the virion, comprising two domains and a 6 amino acid linker region over 326 amino acids (Figure 1.13). During virus assembly, it binds to the cellular membrane through a membrane-binding domain. This induces a conformational change resulting in oligomerisation and self-assembly (Scianimanico *et al.* 2000; Noda *et al.* 2002; Timmins *et al.* 2003; Wijesinghe *et al.* 2020).

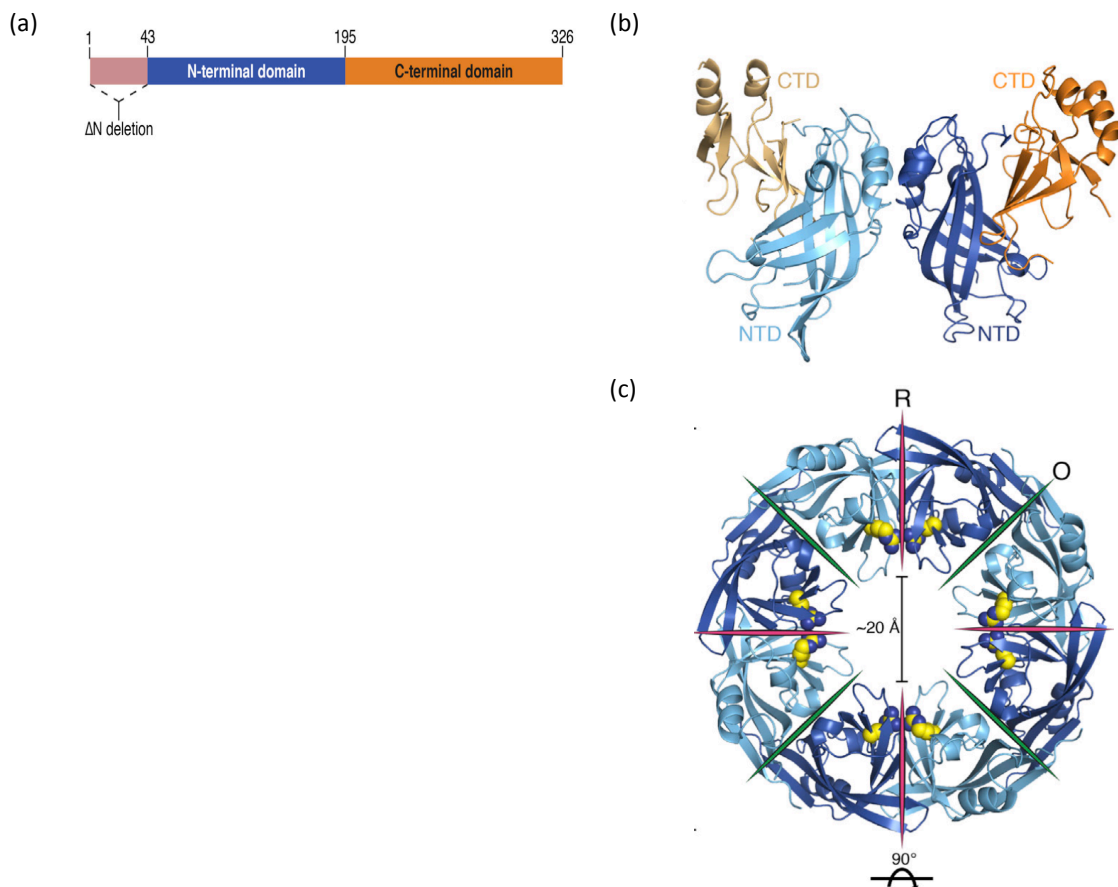


Figure 1.13. Structure of EBOV VP40. (a) diagram of VP40 primary structure (ΔN is a disorder region, whose deletion improves diffraction during the crystallisation process), (b) ribbon diagram of VP40 and (c) octameric ring structure. The RNA binding domain is in red. Source: Bornholdt *et al.*, 2013.

VP40 has been shown to be the main protein responsible for filovirus particle formation, probably aided by GP, as the GP enhances particle release when co-expressed with VP40 (Noda *et al.* 2002). It interacts with several host proteins regulating cargo transport from the Golgi apparatus, facilitating virion egress and binding to ribosomes as well as showing co-localisation with components of the cytoskeleton in confocal microscopy experiments (Harty *et al.* 2000; Panchal *et al.* 2003; Fan *et al.* 2020).

VP40 also plays a role in regulating transcription albeit through different mechanisms in EBOV and MARV. In EBOV, VP40 oligomers are directly involved in inhibition of transcription, whereas in MARV it disrupts the formation of inclusion bodies (Hoenen *et al.* 2010; Koehler *et al.* 2018).

1.3.4 Surface Glycoprotein (GP)

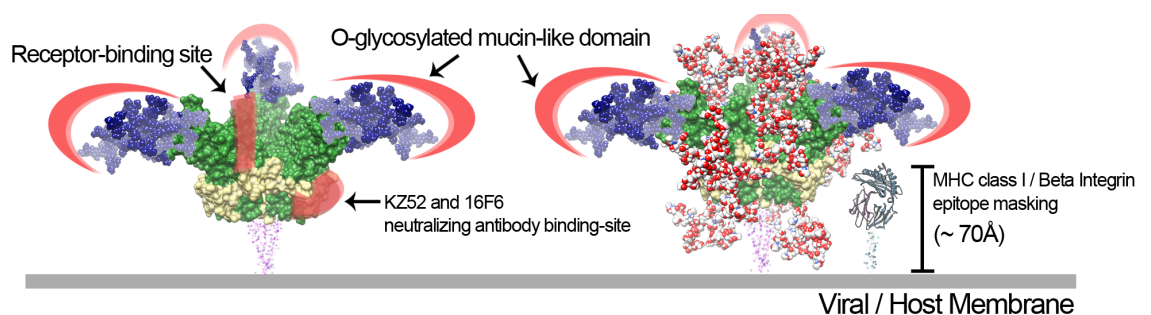


Figure 1.14. Structure of EBOV GP. GP₁ residues in green, GP₂ in yellow, N-linked glycans in red/white and O-linked glycans from MLD in blue. Epitope masking through steric shielding is shown. Source: Cook *et al.*, 2013.

The filovirus GP is the only surface protein embedded in the virus membrane and it is the main target of neutralising antibodies (Figure 1.14 & 1.15). It is highly glycosylated (Figure 1.14), displayed as trimer with each monomer containing two subunits, GP₁ and GP₂ (Figure 1.16), linked by disulphide bonds (S.Y. *et al.* 2000; Lee *et al.* 2008; Maruyama *et al.* 2014). The GP₁ trimer is described as in the shape of a “chalice”, seen from the top (Figure 1.15a-b), bottom (Figure 1.15c-d) and the side (Figure 1.15e-f) and it is involved in attachment to the host membrane (Lee *et al.* 2008).

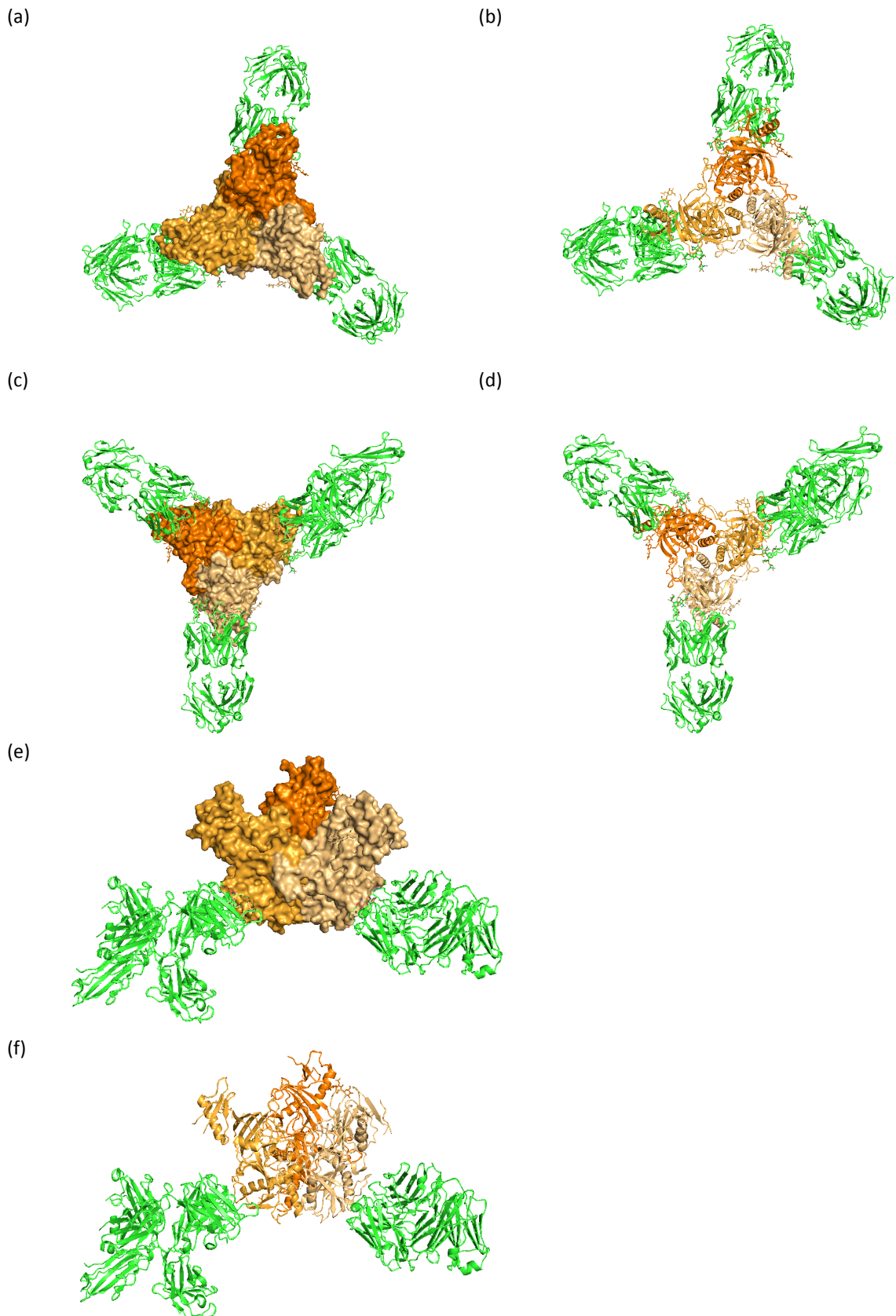


Figure 1.15. Crystal structure of EBOV GP in complex with a neutralising antibody. The GP trimer is composed of three monomers (in different shades of orange) forming a “chalice”. The Fab region of antibody KZ52 is shown in green. (a) surface top view; (b) ribbon top view; (c) surface bottom view; (d) ribbon bottom view; (e) surface side view and (f) ribbon side view. KZ52 antibody was isolated from a survivor of the 1995 Kikwit outbreak. 3D structure solved by Lee *et al*, 2008. PDB entry: 3CSY. Image created with PyMol v. 2.0.7.

The GP₂ is involved in fusion of the viral and host membranes (Figure 1.16). It contains the internal fusion loop (IFL) and two heptad regions (HR1 and HR2) that undergo conformational changes enabling fusion (Lee *et al.* 2008; Lee *et al.* 2010). Its pre-fusion conformation appears to be stabilised by a clamp formed at the base of GP₁ (Figure 1.16b), which prevents it from springing prematurely before membrane fusion (Lee *et al.* 2008).

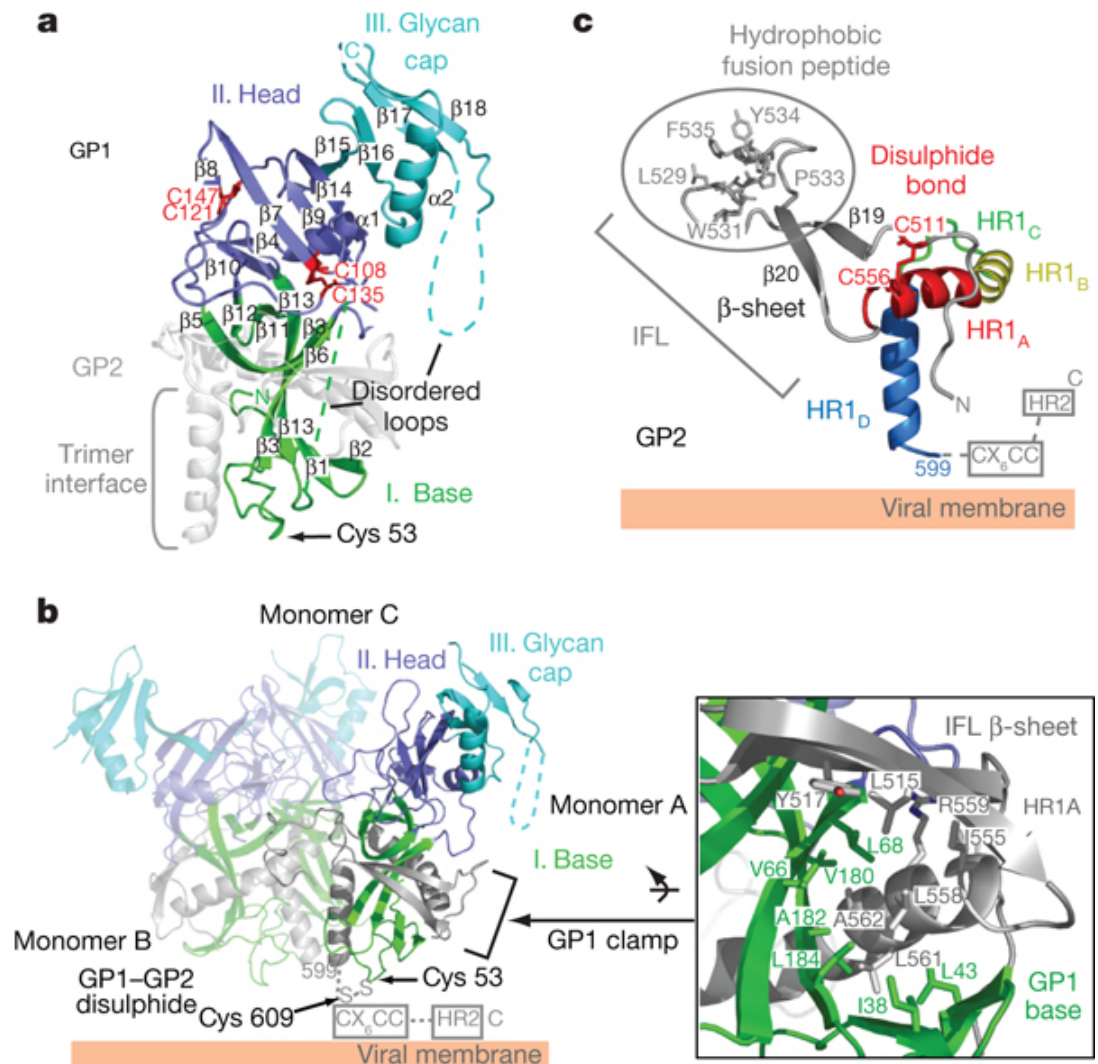


Figure 1.16. EBOV GP₁ and GP₂ subunits. (top left) ribbon diagram of GP₁ showing structural features of the (I) base, (II) head and (III) glycan cap. Disulphide bridges are highlighted red; (top right) ribbon diagram of pre-fusion GP₂ showing the IFL and HR regions and (bottom left) ribbon diagram of the GP trimer with the GP₁ in colour and the GP₂ in grey. The inset shows the stabilising clamp formed by the GP₁ into the GP₂ IFL and HR1A regions. Source: Lee *et al.*, 2008.

The GP is encoded by the fourth gene in all filovirus species, however transcription strategies are different between genera and will be described separately.

1.3.4.1 *Ebolavirus* GP transcription strategies, protein synthesis and processing

EBOV is the most studied representative of this genus, and indeed of all filoviruses. The GP gene has two overlapping open reading frames undergoing transcriptional editing during gene expression.

The gene primary reading frame encodes a shorter secreted version of the GP (sGP). The unedited mRNA happens in approximately 80% of mRNA transcripts (Volchkov *et al.* 1995). The editing site is a stretch of seven uridine residues on the genomic RNA and in about 20% of transcripts, the viral RNA-dependent RNA polymerase (L) adds an extra adenosine at the editing site (Figure 1.17). This changes the open reading frame, resulting in the membrane associated GP.

ssGP	AAAAAAAAA +2	266 amino acids
sGP	AAAAAAAA	292 amino acids
GP _{1,2}	AAAAAAAAA +1	676 amino acids

Figure 1.17. Diagram of EBOV GP gene editing site. The primary transcript encodes the sGP. The membrane bound GP transcript is generated through an addition of an adenosine residue at the editing site.

It is thought this site-specific transcriptional editing, which is also observed in the editing of the phosphoprotein gene of paramyxoviruses (Hausmann *et al.* 1999), is an evolutionary adaptation to maximise protein expression from their small genomes (Mehedi *et al.* 2011). The ssGP contains N-linked glycosylation sites, it is secreted as a homodimer (Mehedi *et al.* 2011), and found to occur in approximately 5% of transcripts. The editing of these transcripts was found to be GP specific, as other regions containing stretches of seven uridine residues such as one such region in the L gene, do not undergo transcriptional editing (Mehedi *et al.* 2013). The flanking regions of the editing site seem to be crucial as both upstream and downstream regions are important for successful editing (Figure 1.18), where the polymerase pauses when reaching the editing site, then stutters adding an additional adenosine (Figure 1.18). The RNA secondary structure on these flanking regions plays a role, as well as VP30 acting as a trans-acting factor overcoming a stem-loop secondary structure located upstream to the NP transcriptional start signal (Weik *et al.* 2002; Mehedi *et al.* 2013).

In some transcripts, either two adenosines are added or one is deleted, which shifts the open reading frame again (Figure 1.17), resulting in another secreted version (ssGP). This is secreted as a monomer (Volchkov *et al.* 1995; Volchkov *et al.* 1998).

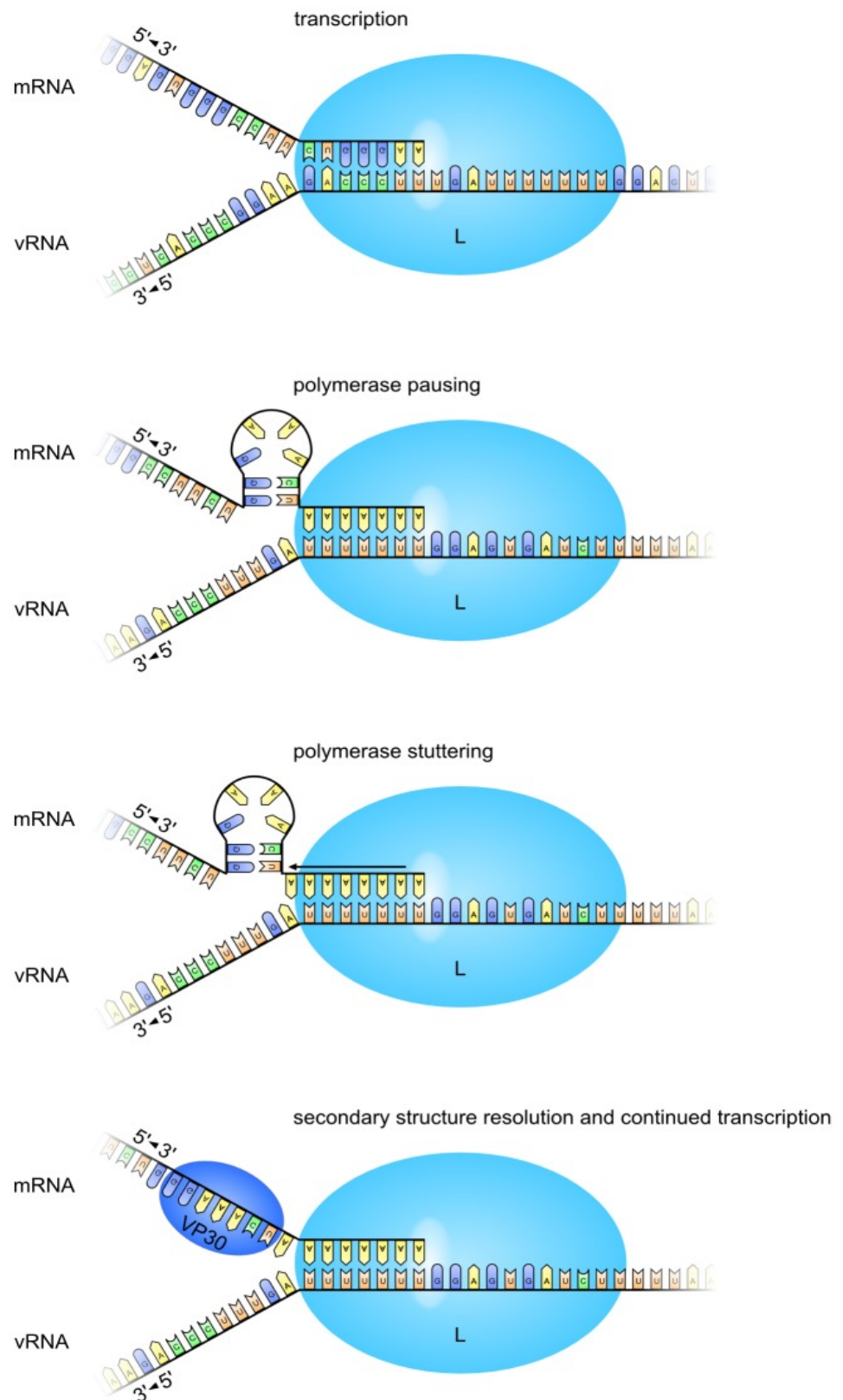


Figure 1.18. *Ebolavirus* transcriptional editing model. Proposed mechanism for polymerase pausing and stuttering adding the adenosine residue to generate a transcript encoding the membrane bound GP. Source: Mehedi *et al.*, 2013.

The sGP is a protein of 110 KDa and it is the primary product of the GP gene. Its precursor is the target of several post-translational modifications in the ER, where it also undergoes oligomerisation before being transported to the Golgi apparatus for further processing, including cleavage of the Δ -peptide by cellular furin. The sGP is secreted as a homodimer, with each monomer linked by two disulphide bridges, and in opposite orientation to each other (Volchkova *et al.* 1998; Sanchez *et al.* 1998; Volchkova, Klenk and Volchkov 1999). The sGP is thought to work as a decoy for circulating neutralising antibodies as these are reduced in the presence of sGP (Ito *et al.* 2001).

The membrane bound GP is a type-I transmembrane protein, which is processed through the ER and Golgi apparatus. From there the GP is transported to the plasma membrane where it is presented as a trimer; and as the virus buds, the GP is incorporated in the virion as part of the plasma membrane forming the viral envelope. It is responsible for attachment and entry into the host cells (Jeffers, Sanders and Sanchez 2002; Mohan *et al.* 2015). Once synthesised, the GP precursor protein is cleaved into GP₁ and GP₂. This cleavage is mediated by cellular furin, a protein convertase present in the cellular secretory pathways (Volchkov *et al.* 1998; Millet and Whittaker 2015).

Apart from the secreted GP versions described so far, the metalloprotease TACE (TNF- α converting enzyme), which releases TNF- α and other membrane proteins, cleaves the membrane anchor releasing another secreted version (GP_{1,2 Δ}) of the glycoprotein, which might also be involved in immune evasion (Dolnik *et al.* 2004; Escudero-Pérez *et al.* 2014; Escudero-Pérez *et al.* 2016). In addition, soluble GP₁ was also found in supernatant from infected HeLa cells *in vitro*, but thought to be the result of the disulphide bond with GP₂ not forming during processing in the ER (Volchkov *et al.* 1998; Volchkov *et al.* 1998).

1.3.4.2 *Marburgvirus* GP transcription strategies, protein synthesis and processing

The GP gene in *marburgvirus* strains encodes one open reading frame and it does not seem to undergo the transcriptional editing seen in *ebolavirus* species, however it does go through post-translational processing. Like *ebolavirus*, it is also cleaved by cellular furin into GP₁ and GP₂, which are linked by a disulphide bridge and presented as a trimer. While EBOV GP has 676 amino acids, MARV/RAVV has 681 amino acids. The furin recognition site is RRKR, cutting at position 501 on EBOV and 435 on MARV/RAVV (Sanchez *et al.* 1993; Will *et al.* 1993; Feldmann *et al.* 1999; Volchkov *et al.* 2000). It is not clear whether

TACE also sheds a GP_{1,2Δ} version as no studies assessing this could be found in the literature.

The genus *cuevavirus* (LLOV) has a genomic organisation similar to *ebolavirus*. It is predicted to have transcription strategies similar to and resulting in the secreted soluble GP versions seen in EBOV (Ng *et al.* 2014; Maruyama *et al.* 2014), whereas the recently described genus *dianlovirus* (MLAV) appears to be phylogenetically closer to *marburgviruses* from GP sequence analysis (Yang *et al.* 2019).

1.3.5 Viral Protein 30 (VP30)

EBOV VP30 is a 38 kDa protein of 288 amino acids including a zinc-binding domain and clustered phosphate acceptor sites (Figure 1.19). It appears to be crucial for activation of transcription in *ebolaviruses* but not for *marburgviruses* (Elliott, Kiley and McCormick 1985; Mühlberger *et al.* 1998).

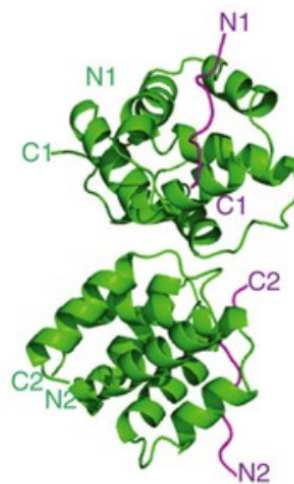


Figure 1.19. EBOV VP30 structure. Ribbon diagram of EBOV VP30. Interactions with NP are shown in purple. Source: Xu *et al.*, 2017.

Its zinc-binding domain is essential for binding RNA and initiating transcription. It regulates transcription through its phosphorylated and non-phosphorylated states. When non-phosphorylated, VP30 binds to RNA and VP35/L complexes, increasing affinity of the viral polymerase to RNA thereby increasing transcription (Weik *et al.* 2002; Modrof, Becker and Mühlberger 2003; John *et al.* 2007; Biedenkopf *et al.* 2016; Lier, Becker and Biedenkopf 2017).

1.3.6 Viral Protein (VP24)

VP24 is a monomer of 259 amino acids and its main function is antagonising interferon functions, blocking both interferon- α/β and interferon- γ pathways by inhibiting gene expression through inhibition of STAT1 (Reid *et al.* 2006; Zhang *et al.* 2012). Residues implicated in virus lethality in rodents have been identified, as well as karyopherin binding residues (Figure 1.20), which results in inhibition of transport of STAT-1 into the cell nucleus (Zhang *et al.* 2012).

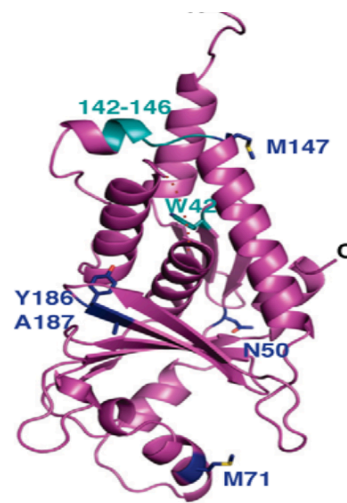


Figure 1.20. SUDV VP24 structure. Residues important for virulence are in dark blue whereas residues involved in binding to karyopherin are in light green. Source: Zhang *et al.*, 2012.

Analysis of the non-pathogenic RESTV has revealed approximately 30 different amino acid residues in VP24 (Zhang *et al.* 2012), including those sites conferring lethality in other *ebolaviruses*, which could contribute to the lack of pathogenicity of RESTV in humans.

VP24 is also involved in capsid formation (Huang *et al.* 2002), inhibition of transcription (Watanabe *et al.* 2007; Takamatsu *et al.* 2020) and budding (Han *et al.* 2003).

More recently, novel interactions of VP24 with cellular proteins involved in the interferon cascade have been identified such as the small ubiquitin-related modifier (SUMO), regulating inhibition of interferon (Vidal *et al.* 2019).

1.3.7 Viral Polymerase (L)

The viral RNA-dependent RNA polymerase (RdRp) is the largest protein (2,212 amino acids) in filoviruses, and it is involved in transcription, genome replication, mRNA capping, as well as methylation and polyadenylation (Pettini, Trezza and Spiga 2018). It has three functional domains (Figure 1.21), the RdRp catalytic site, the polyribonucleotidyl transferase domain and the mononegavirus-type SAM-dependent 2'-O-methyl transferase (MTase) domain.



Figure 1.21. Diagram of viral polymerase (L) primary structure prediction. Adapted from: Pettini *et al.*, 2019.

The RdRp catalytic site (aa 625-809) has a core with four channels to allow the RNA template to enter and exit, a transcript exit channel and one for NTP uptake (Pettini, Trezza and Spiga 2018). Modelling of the structure with Phyre2 (Kelley *et al.* 2015) revealed a 3D structure (Figure 1.22) formed of the RdRp catalytic site (light blue), capping (red) and MTase site (dark blue).

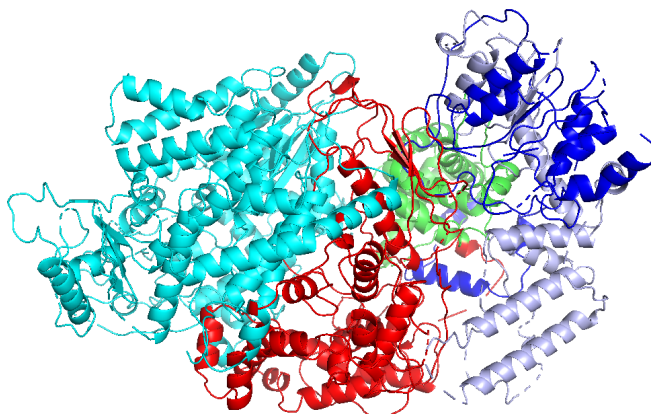


Figure 1.22. Ribbon diagram of viral polymerase (L) structure prediction by Phyre2. Modelling of viral polymerase based on homology of previously determined L structures.

More recently, a recombinant version of the L protein has been generated to be used in functional studies and antiviral screening (Tchesnokov *et al.* 2018).

1.4 Filovirus entry and tropism

Filoviruses have broad tropism infecting several cell types both *in vitro* and *in vivo*, including monocytes/macrophages, liver, epithelial, fibroblasts and several immortalised cell lines (Ito *et al.* 2001; Martines *et al.* 2015; Dahlmann *et al.* 2015; Brunton *et al.* 2019). Filovirus entry is mediated by the surface GP trimer. An initial interaction takes place between the GP and one of several host cell membrane molecules such as c-type lectins, β 1 integrins, folate receptor- α (FR- α), asialoglycoprotein receptor (ASGP-R), DC-SIGN, L-SIGN, tyrosine kinase receptor Axl and TIM-1, all of which have been identified as putative receptors for the initial virus-host interaction (Becker, Spiess and Klenk 1995; Yang *et al.* 1998; Takada *et al.* 2000; Chan *et al.* 2001; Alvarez *et al.* 2002; Younan *et al.* 2017; Brunton *et al.* 2019).

This receptor interaction with the GP triggers micropinocytosis of the virion and internalisation, going through the endocytic pathway into the late endosome. There, the GP₁ is cleaved by cellular proteases cathepsin B and L, removing the glycan cap and mucin-like domain (MLD), resulting in a metastable primed GP₁ with the RBS exposed, which then binds to the cellular receptor Niemann-Pick C1 (NPC1), a cholesterol transporter present in the endosomal lumen membrane (Ji *et al.* 2005; Ikeda and Kawaoka 2007; Schornberg *et al.* 2009; Kondratowicz *et al.* 2011; Hunt, Lennemann and Maury 2012; Lee *et al.* 2012; Kuroda *et al.* 2014; Jae and Brummelkamp 2015; Kuroda *et al.* 2015; Shimojima, Dahlmann *et al.* 2015; Zapatero-Belinchón *et al.* 2019). Binding to NPC1 receptor is essential for infection for all filoviruses studied so far, including newly discovered species BOMV and MLAV (Miller *et al.* 2012; Ng *et al.* 2014; Kuroda *et al.* 2015; Jae and Brummelkamp 2015; Gong *et al.* 2016; Bornholdt *et al.* 2016; Salata *et al.* 2019; Bortz *et al.* 2020). Primary cells from humans affected by Niemann-Pick disease, a neurological condition resulting in accumulation of cholesterol in lysosomes, were refractory to filovirus infection (Takadate *et al.* 2020).

Even though all filoviruses that have been characterised utilise the NPC1 as their cellular receptor and have similar infection entry mechanisms, differences in GP processing mean that some cellular factors required for infection may differ. GP cleavage by cellular proteases catB and catL are essential for *ebolavirus* infection but not for *marburgvirus*, for instance (Carette *et al.* 2011; Cote *et al.* 2012; Ng *et al.* 2014; Maruyama *et al.* 2014; Goldstein *et al.* 2018; Yang *et al.* 2019).

In bats, susceptibility to specific filoviruses seems to be determined by mutations in a particular region of the NPC1. Certain bat cell lines susceptible to EBOV but not MARV have a particular three amino acid substitution on loop 1 of NPC1, whereas another bat cell line susceptible to MARV but not EBOV had two amino acid substitutions on loop 2 of the NPC1. Rescuing NPC1 expression on these cell lines restored infectivity of those viruses (Kaletsky, Simmons and Bates 2007; Matsuno *et al.* 2010; Brecher *et al.* 2012).

It appears that this GP-NPC1 interaction alone is not sufficient to elicit fusion but the final details are yet to be elucidated (Miller *et al.* 2012; Simmons *et al.* 2016; Markosyan *et al.* 2016). It seems the low pH environment is required for cathepsin function rather than viral fusion with the host cell membrane (Markosyan *et al.* 2016), and traffic into a late endosome expressing NPC1 is key for fusion to occur (Mingo *et al.* 2015).

Two-pore calcium channels expressed in the late endosome also play a role in entry of filoviruses, as knock-out, siRNA or inhibiting experiments abrogate infectivity, including macrophages which are one the primary cells first infected (Sakurai *et al.* 2015).

The exact fusion mechanism of filoviruses and its triggers are not completely understood. It is thought a conformational change inserts the fusion peptide into the host membrane followed by the membranes fusing (Figure 1.23). Different cellular requirements seem to play a role. Cathepsins are dispensable for triggering fusion after NPC1 receptor binding but are necessary for fusion pore formation enabling genome delivery (Spence *et al.* 2016).

The structure of the GP₂ suggests a similar mechanism of fusion of other viral class I membrane proteins. A conformational change by a yet unknown trigger, causing a further change bringing the two membranes together with the GP₂ between them arranged in parallel, followed by a hemifusion state and fusion pore opening so the viral genome can be delivered into the cytoplasm (Chernomordik and Zimmerberg 1995; Weissenhorn *et al.* 1998; Watanabe *et al.* 2000; Rutten *et al.* 2020).

Most EBOV outbreaks have been zoonotic spillovers of relatively short duration. However, the large outbreak in West Africa (2013 to 2016) allowed for adaptations that could have resulted in improved infectivity and transmission between humans. The initial strain EBOV Makona C15, which was used in this study, evolved during the outbreak resulting in strains better adapted to human transmission. The mutation A82V, in a region of the RBS which interacts with the NPC1 receptor, increased infectivity in human cell

lines but not in bat cell lines (Urbanowicz *et al.* 2016). The same study identified mutations conferring positive epistatic effects, whereby two concurrent mutations result in increased viral fitness, more than it would be expected from two single mutations, and therefore enhancing human transmission (Urbanowicz *et al.* 2016). The A82V substitution was observed in approximately 90% of subsequent viral sequences obtained (Bedford and Malik 2016).

The same adaptation was found to increase infectivity in human and primate cell lines. However, it is not clear whether similar adaptations contributed to the increased size and duration of the outbreak, because other factors such as multiple reintroductions of the virus and increased movement of people between these geographical regions could have also played a role (Urbanowicz *et al.* 2016; Diehl *et al.* 2016).

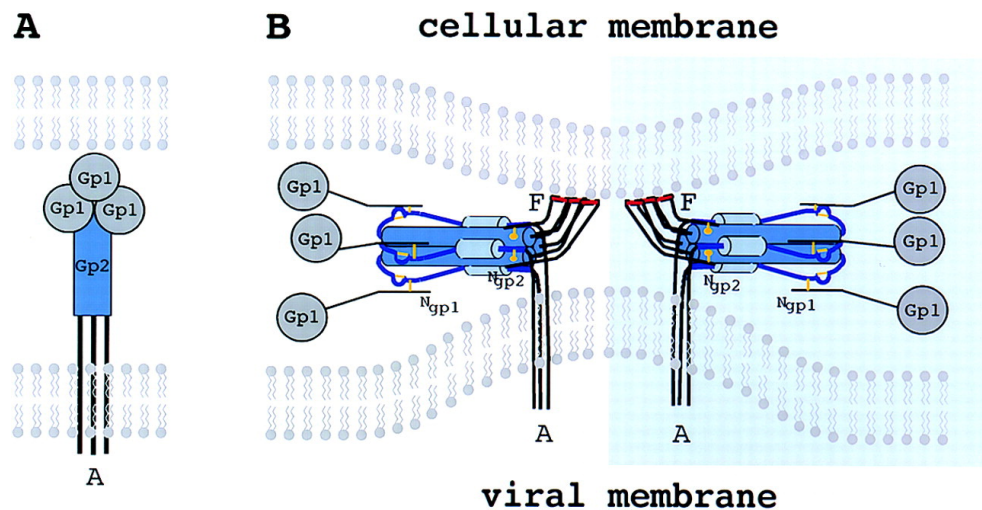


Figure 1.23. Model of filovirus GP and host cell fusion. (A) initial virus-host receptor interactions (B) those interactions trigger several conformational changes bringing the two membranes together resulting in fusion. Source: Weissenhorn *et al.*, 1998.

1.5 Filovirus replication cycle

After the genome is delivered to the host cell (Figure 1.24-1), primary transcription is initiated when VP35 binds to NP, redirecting L to the NP-RNA complex. Next, dephosphorylated VP30 binds to the VP35/L complex (Figure 1.24-2), presumably increasing affinity of the viral polymerase to the negative sense genome, starting at the 3'-leader sequence, resulting in a 5' triphosphate-leader mRNA which is capped and methylated (Mühlberger *et al.* 1999; Groseth *et al.* 2009; Kirchdoerfer *et al.* 2016). After

the stop signal, there is a stretch of uracil residues where the polymerase stutters, in a mechanism similar to the GP gene editing of *ebolaviruses*, creating the polyadenylation signal. As downstream genes are transcribed, a transcript gradient is formed (Figure 1.24-3) (Mühlberger 2007; Hume and Mühlberger 2019).

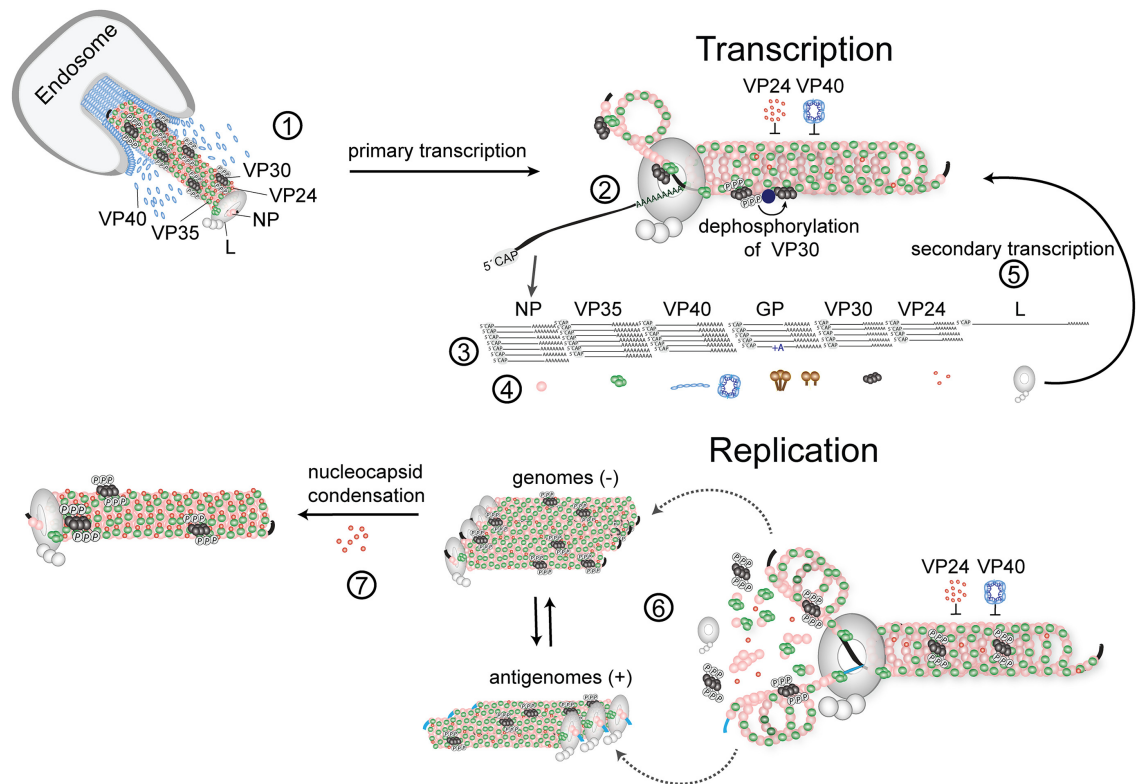


Figure 1.24. EBOV model of transcription and replication. The sequence of events is shown: (1) delivery of the genome, (2) VP30 binds to VP35/L complex, (3) transcription gradient is formed, (4) translation of viral mRNA, (5) further transcription, (6) downregulation of viral RNA and (7) nucleocapsid condensation. Source: Hume *et al*, 2019.

Translation of viral mRNA starts (Figure 1.24-4), which enables further transcription as the initial pool of viral proteins is depleted (Figure 1.24-5). As more viral proteins accumulate, VP30 is phosphorylated by cellular kinases decreasing transcription and switching to genome replication. VP40 and VP24 also downregulate viral RNA generation (Figure 1.24-6) (Hume and Mühlberger 2019). At this stage, inclusion bodies are formed, which are dynamic structures where viral proteins (NP, VP35, VP30, L) aggregate when viral replication takes place, visible through confocal microscopy, immunofluorescence and live-cell imaging studies (Hoenen *et al*. 2012).

Genome replication involves generation of positive sense complementary genomes that serve as templates for negative sense genome to be generated and packaged. VP24 supports NC oligomerisation and shifts the cycle to assembly of virions and budding

(Figure 1.24-7). NCs are transported to the membrane for budding by an actin-dependent mechanism (Schudt *et al.* 2013; Koehler *et al.* 2018; Hume and Mühlberger 2019).

1.6 Viral budding

Filovirus matrix proteins play a major role in viral egress and budding. VP40, the most abundant matrix protein (Jasenovsky and Kawaoka 2004; Liu and Harty 2010), appears to drive budding through viral domains (PPxY for example) interacting with host WW domains, present in proteins of the ubiquitin ligase family and proteins involved in signaling networks such as the Hippo pathway that regulates cell division and apoptosis in EBOV and MARV (Han *et al.* 2020; Han, Dash, *et al.* 2020). Angiomotin, a protein containing the PPXY motif involved in angiogenesis and cell motility, was found to regulate egress of virus-like particles (VLPs) and authentic EBOV through the interactions described above (Han *et al.* 2020). Other proteins have been identified, suggesting a multiple domain interaction, including host proteins such as the one encoded by the tumour susceptibility gene 101 (Tsg101), which also facilitates egress of HIV; and Nedd4, a membrane E3 ubiquitin ligase facilitating budding in EBOV and MARV (Liu and Harty 2010), as well as in LASV (Ziegler *et al.* 2019).

VP40 has been previously found to be able to induce release of VLPs in expression systems by localising to the cell membrane, along with the GP (Harty *et al.* 2000; Timmins *et al.* 2001).

1.7 Filovirus pathogenesis and immune response

1.7.1 Clinical features

Of all the pathogenic filovirus species, EBOV has been responsible for most outbreaks. It causes severe disease in humans and non-human primates (NHP). In the first reports of EVD the main signs and symptoms described were diarrhoea, bleeding, oral (throat lesions), vomiting, fever, headache and abdominal pain. In addition, conjunctivitis, cough, jaundice, edema, myalgia, nausea and arthritis were sometimes reported (Johnson *et al.* 1978). Bleeding was present in 78% of patients reported as melaena (blood in faeces),

haematemesis (vomiting blood), mouth/gingival bleeding and epistaxis (nose bleeding). EVD lasted approximately two weeks (Johnson *et al.* 1978).

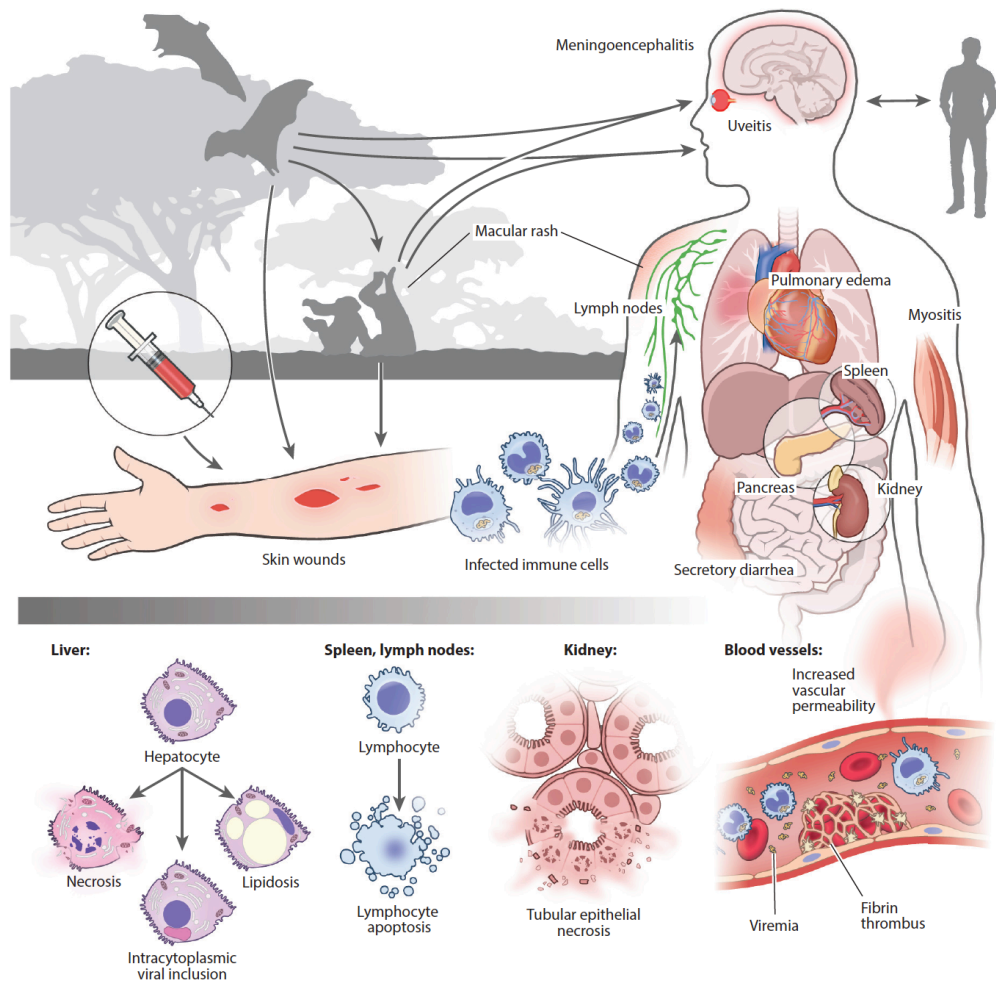


Figure 1.25. Infection cycle and cellular/tissue targets of EVD. Main forms of transmission of EBOV: zoonotic, person to person and nosocomial. The primary cells infected are monocytes/macrophages and dendritic cells. The initial viremia and dissemination affecting most organs cause tissue and vascular damage. Source: Baseler *et al.*, 2017.

In the first few days after infection through mucosal surfaces or skin, there is an exponential rise in viral load and systemic dissemination, as the virus infects several cell types, resulting in multiple organs affected (Figure 1.25). Viremia is varied between individuals and seems to be a determinant factor in survival (Edwards *et al.* 2015; Faye *et al.* 2015; Martines *et al.* 2015; Furuyama and Marzi 2019). Dendritic cells and macrophages are thought to be the first cells infected (Ströher *et al.* 2001; Hensley *et al.* 2002; Geisbert *et al.* 2003). Interestingly lymphocytes are refractory to infection (Martines *et al.* 2015).

The hallmarks of bleeding and other hematological manifestations are caused by damage to endothelial cells (Figure 1.26), affecting vascular integrity and homeostasis, along with a strong inflammatory response usually associated with high viral load. The GP and its secreted forms have been found to be cytotoxic and contribute to immune evasion during the course of infection. For instance, sGP was found to bind to neutrophils, inhibiting neutrophil activation by down regulation of 1-selectin (Martines *et al.* 2015).

Differential diagnosis is very challenging because the signs and symptoms are common to other diseases endemic in Africa such as malaria, leptospirosis, yellow fever, dengue, cholera as well as other haemorrhagic fevers such as lassa fever virus. Therefore, diagnosis should be made taking into account clinical signs and symptoms along with risk factors such as contact with patients or suspected cases, and confirmed by PCR when possible. The usual initial signs and symptoms are malaise, fatigue, myalgia and high temperature (Bwaka *et al.* 1999; Baseler *et al.* 2017).

As the disease progresses, severe diarrhoea is often observed, probably due not only because of damage to the intestinal epithelium, but also due to a secretory system, where disruption to ion and solute transporters leads to decrease in absorption and increase in secretion of fluids (Thiagarajah, Donowitz and Verkman 2015). If supportive therapy is not provided, severe dehydration can ensue, eventually leading to hypovolemic shock and multiple organ failure (Chertow *et al.* 2014; Chertow, Uyeki and Dupont 2015; Martines *et al.* 2015; Baseler *et al.* 2017).

1.7.2 Specific role of filovirus GP in pathogenesis

EBOV GP has been found to be cytotoxic to endothelial cells (Chan *et al.* 2000; Yang *et al.* 2000; Volchkov *et al.* 2001). The MAPK pathway has been identified as a major contributor to cytotoxicity through the inhibition of ERK2 resulting in loss of cell adhesion, increase in cell rounding and cell death (Zampieri *et al.* 2007; Cantoni and Rossman 2018). Cell death is thought to be via necrotic rather than apoptotic mechanisms (Olejnik *et al.* 2013), contributing further to tissue damage and inflammation.

The GP is involved in immune evasion via epitope masking and steric shielding (Figure 1.14), through their highly glycosylated motifs (Cook and Lee 2013).

The secreted sGP is thought to act as a decoy for neutralising antibodies. In mice, it induces a bias towards a neutralising antibody response that cross-reacts with GP epitopes, termed “antigenic subversion”, enabling recognition of anti-GP antibodies

(Mohan *et al.* 2012; Zhu *et al.* 2019). It is thought that because sGP is the more abundant protein, it drives the antibody response towards shared epitopes between GP and sGP.

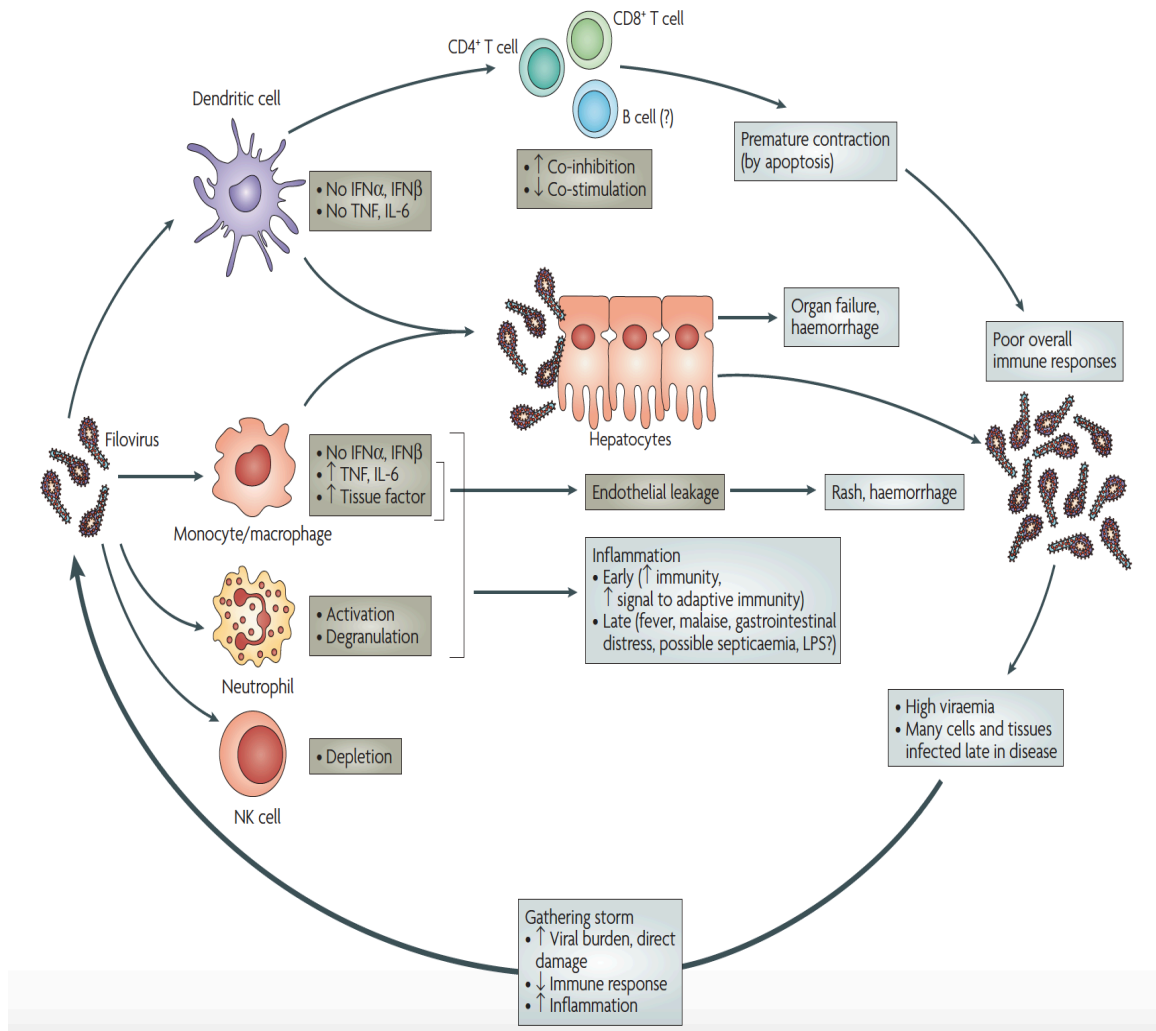


Figure 1.26. Pathogenesis of EVD/MVD. Inflammatory burden mechanisms during filovirus infection, eventually resulting in multi-organ failure. Source: Mohamadzadeh *et al.*, 2007.

Neither the sGP or Δ -peptide are involved in endothelial activation or a decrease in barrier function seen with EBOV GP (Wahl-Jensen *et al.* 2005). However, the Δ -peptide could work as a viroporin, increasing membrane permeabilisation and inducing several physiological changes that could contribute to pathogenesis. *Ebolavirus* and *cuevavirus* sequence analysis of their Δ -peptide revealed a conserved motif across other viroporins, such as the pore-forming NSP4 protein of rotaviruses. It is proposed the resulting permeabilisation results in enterotoxicity seen in most patients who present with severe diarrhoea for instance (Gallaher and Garry 2015; He *et al.* 2017).

1.7.3 Immune response against filoviruses and immune evasion mechanisms

1.7.3.1 Innate Immunity

EVD and MVD can present with a range of severe symptoms. Abnormalities in immune response contribute to the severity of symptoms in conjunction with the more direct effects in the different tissue types affected. The rapid course of the disease may contribute to the difficulties in controlling the infection.

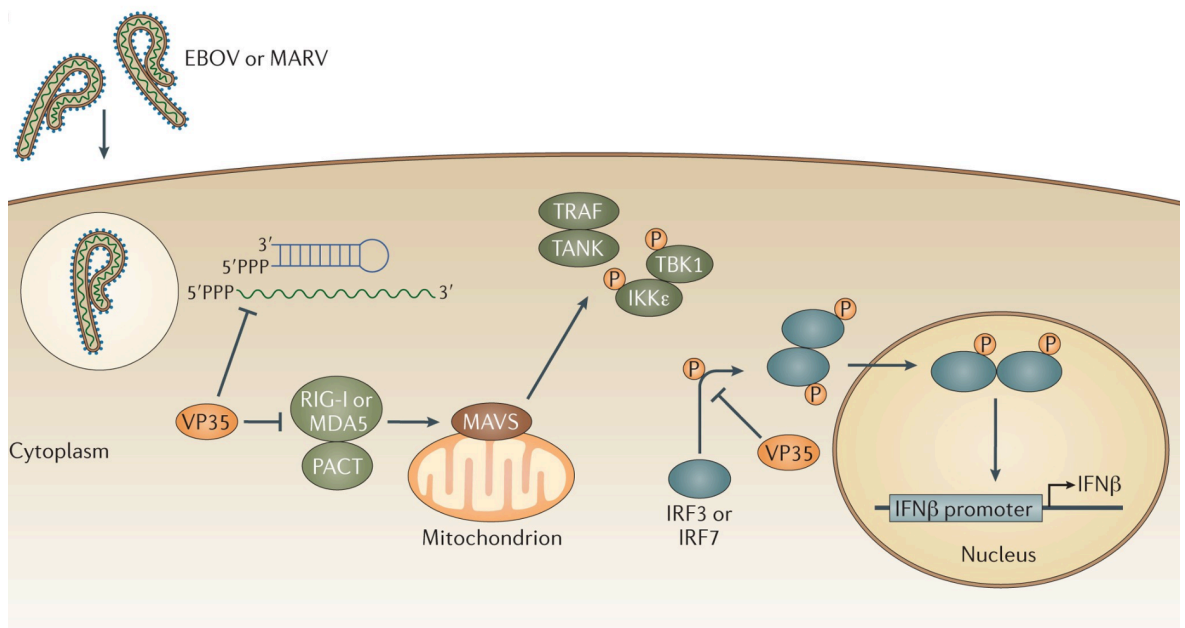


Figure 1.27. Inhibition of interferon pathways during filovirus infection. VP35 is involved in the inhibition of the host interferon response. Source: Messaoudi *et al*, 2015.

The inhibition of interferon signaling is one of the main mechanisms of pathogenesis and subversion of antiviral capabilities by the host. Type I interferon- α is released by infected monocytes whereas interferon- β is released by infected fibroblasts. They bind to specific receptors (IFNAR) on target cells increasing protein expression of inhibitors of viral replication. Viral proteins play a role inhibiting INF production. EBOV VP35 and VP24 both inhibit INF- α/β and INF- γ (Prins *et al.* 2009; Ramanan *et al.* 2012). VP35 blocks IRF 3 and IRF 7 pathways (Figure 1.27) whereas VP24 blocks STAT-1 and STAT-2 pathways, both resulting in downregulation of interferon stimulating genes (Basler *et al.* 2003; Wong, Kobinger and Qiu 2014; Basler 2015; Messaoudi, Amarasinghe and Basler 2015).

The disruption of interferon responses increases viral burden and immune deregulatory effects observed, such as the increase pro-inflammatory molecules such as TNF- α , IL-1 β ,

macrophage inflammatory protein (MIP-1 α), ROS and nitric radicals (Bray and Geisbert 2005; Wong, Kobinger and Qiu 2014).

A type I INF response is thought to be crucial for controlling the virus. Non-pathogenic RESTV infection of human cells line results in upregulation of ISGs (Kash *et al.* 2006; Wong, Kobinger and Qiu 2014). In mice, which are normally refractory to infection, knocking out STAT-1 or IFNAR genes makes them susceptible to EBOV infection (Bray 2001).

The INF-induced restriction factor tetherin prevents progeny virus release by effectively anchoring the virion to the host membrane. Viruses affected by it evolved evasion mechanisms to counteract this mechanism of restriction. HIV-1 accessory protein Vpu antagonises tetherin actions by co-localising with tetherin on the host cell membrane (Neil, Zang and Bieniasz 2008). In EBOV, the GP appears to be involved in antagonising tetherin antiviral effects. However, the exact mechanism(s) by which it counteracts tetherin are yet to be elucidated (Kaletsky *et al.* 2009; Brinkmann *et al.* 2016; González-Hernández *et al.* 2018).

The interferon-inducible transmembrane (IFITM) protein family are restriction factors that inhibit infectivity of a range of enveloped viruses such as influenza, coronaviruses and filoviruses (Huang *et al.* 2011; Diamond and Farzan 2013). IFITM1, 2 and 3 inhibit entry of EBOV and MARV PVs by interfering with endosomal trafficking; it also inhibited replication of authentic EBOV and MARV, which could be partly due to inhibition of viral entry (Huang *et al.* 2011).

1.7.3.2 Adaptive Immunity

It is important to note that even though innate immunity is triggered faster upon infection in contrast to adaptive responses, which take longer due to the need for antigen presentation and subsequent effects, the two are intertwined and highly dependent on each other through a myriad of interactions, but are presented here separately for clarity. T cells depend on three concomitant signals to be activated. First, antigen presenting cells such as macrophages and dendritic cells process viral antigens by cleaving them into peptides and presenting them on MHC-II and MHC-I molecules on their surfaces to CD4⁺ or CD8⁺ T cells. Next, co-stimulatory molecules are secreted and bind to their receptors on T cells. Then, cytokines provide the final signal necessary for a cytotoxic response by

CD8⁺ T cells for example. CD4⁺ T cells are involved in several processes including activating B cells to induce antibody production, for instance. Dendritic cells (DC) are important for T cell activation through antigen presentation and cytokine activation. Immature DCs need to mature to exert those antigen-presenting functions. Filovirus infection results in failure of maturation of DC cells or induction of co-stimulatory molecules for T cell activation (Mahanty *et al.* 2003; Wong, Kobinger and Qiu 2014). Depletion on CD8⁺ T and NK cells has been observed in humans and NHP, with Fas apoptosis markers detected, suggesting Fas-mediated apoptosis being induced in those cell populations (Baize *et al.* 1999; Reed *et al.* 2004).

Fatal outcomes are usually associated with impaired T cell response plus failure of stimulating appropriate antibody responses, with low levels of IgM and IgG detected (Baize *et al.* 1999). Apoptosis has been observed in lymphocytes from patients with fatal outcomes. As these cells are refractory to filovirus infection, it is thought that apoptosis is triggered through chemical mediators such as FasL or TNF- α secreted by infected macrophages (Geisbert *et al.* 2000).

1.7.3.3 Antibody-dependent enhancement (ADE)

Antibody-dependent enhancement of infection is the phenomenon of increased infectivity following the binding of antibodies to virus. ADE was detected when sera from immunised mice targetting the EBOV GP increased infectivity of EBOV pseudotypes *in vitro*. Interestingly, in mice immunised against the RESTV GP, which is less pathogenic in humans, a much weaker ADE was observed (Takada *et al.* 2001).

Fc receptor interaction with monocytic cells seems to play an important role in ADE *in vivo*. Antibodies of different specificities, neutralisation profile or subclasses can induce ADE (Suhrbier and La Linn 2003; Kuzmina *et al.* 2018), resulting in an anti-inflammatory state favouring secretion of IL-10 for instance, and general switch to Th-2 response hindering the generation of an efficient antiviral state (Suhrbier and La Linn 2003). ADE was observed for MARV using mouse antisera, also through Fc receptor interactions (Nakayama *et al.* 2011).

Convalescent serum from the Kikwit outbreak also enhanced infection *in vitro*. Two serum samples collected from patients in that outbreak significantly increased infectivity of VSV PVs and authentic EBOV (Takada *et al.* 2003).

1.8 Therapeutics

1.8.1 Virus entry as a target for therapeutics with monoclonal antibodies (mAbs) or convalescent plasma

Initial attempts at monotherapy with mAbs against GP in non-human primates were unsuccessful, even with potent neutralising antibodies such as KZ52 (Zeitlin *et al.* 2016). Antibody cocktails were then developed and tested in NHP. A combination of murine mAbs (ZMab) consisting of 1H3, 2G4 and 4G7, and a murine-human chimeric mAb combination (MB-003) consisting of 13C6, 13F6 and 6D8 resulted in varying degrees of protection (50% upwards) in NHP (Zeitlin *et al.* 2016; Mirza *et al.* 2019; Hoenen, Groseth and Feldmann 2019).

From those two combination therapy regimens, ZMapp was developed. It consisted of two neutralising antibodies (2G4 and 4G7) and a non-neutralising antibody (13C6) targeting the GP base and glycan cap, resulting in 100% protection of rhesus macaques even when therapy started 5 days post-infection (Qiu *et al.* 2014; Mirza *et al.* 2019; Hoenen, Groseth and Feldmann 2019). The non-neutralising antibody (13C6) was included due to its ability to induce antibody-dependent cell-mediated cytotoxicity (ADCC) (Olinger *et al.* 2012; Hoenen, Groseth and Feldmann 2019). Initial human trials found ZMapp to be 91.2% more beneficial for clinical outcomes in comparison to standard care alone (Davey *et al.* 2016).

More recently, monoclonal antibodies raised in humanised mice were isolated and tested as a cocktail (REGN-EB3) comprised of three neutralising antibodies: REGN 3470, 3471 and 3479 (Pascal *et al.* 2018), the first approved treatment for EVD (Inmazeb®) by the FDA (U.S Food and Drug Administration). They were selected for being the most potent neutralising mAbs as well as having FcγRIIIa functions such as triggering ADCC in NK cells (Yeap *et al.* 2016), and also protecting NHP against challenge in three independent experiments (Pascal *et al.* 2018).

A monoclonal antibody (mAb114) isolated from a human survival patient, which targets the receptor-binding site and had been shown to fully protect NHP from EBOV challenge, was well tolerated in a phase-I trial, albeit being a small cohort (Corti *et al.* 2016; Misasi *et al.* 2016; Gaudinski *et al.* 2019). It was also used compassionately as a single use intravenous infusion in the North Kivu (DRC) outbreak in 2018.

In a recent randomised controlled trial of 681 patients positive for EBOV (Ituri) by RT-PCR from one of the latest outbreaks in the DRC, four treatment groups were assessed: ZMapp (control), Remdesivir, mAb 14 and REGN-EB3. The latter two were found to have better outcomes than Remdesivir or ZMapp, with mortalities of 35.1% and 33.5% for mAb 114 and REGN-EB3 treatment cohorts respectively (Mulangu *et al.* 2019). All patients had received standard care for EVD as well as one the treatment groups. In addition, patients who had been vaccinated with the rVSVΔG-ZEBOV vaccine recently approved by the FDA had mortality rates of 27.1% in comparison with 48.4% with patients who had not been vaccinated. A decrease in viral load as well as improved kidney and liver functions were associated with better outcomes across all treatments (Mulangu *et al.* 2019).

Neutralising antibodies rEBOV 520 and rEBOV 548 reduced EVD in NHP with 100% of survival in the treatment group. They act by binding to the glycan cap and a conformational epitope spanning the GP₁ and the GP₂ IFL (internal fusion loop). The antibody cocktail also conferred some protection (50%) in mice challenged with SUDV (Gilchuk *et al.* 2020). Even though neutralisation through Fab interactions are correlated to protection, it seems that both neutralisation and immune effector (Fc) functions are necessary to achieve effective protection (Saphire *et al.* 2018; Hoenen, Groseth and Feldmann 2019).

A nonrandomised comparative study (n=99) was conducted in Guinea to assess administration of convalescent plasma to treat EVD. A regimen of two transfusions on the day (or +2 days) of diagnosis was tested. Even though there were not serious adverse effects, they only found a slight reduction on the risk of death (31% compared to 38% in the control group). This difference was reduced by -3% when adjusted for age and Ct values (van Griensven *et al.* 2016). The level of neutralising antibodies present in the different donor's plasma was not known.

Ebola viral proteins with more conserved regions such as VP35, VP40, VP30 and VP24 might be better targets for antivirals (Grifoni *et al.* 2016), and several compounds being tested target those proteins.

1.8.2 Targetting viral replication

Viral replication can be targeted by directly disturbing the viral polymerase after binding or indirectly by targetting cell host factors. At the moment, there are no licensed antivirals in the USA (CDC) or in the UK (NHS) to treat EVD.

Nucleoside analogues such as remdesivir stop viral replication by acting as delayed chain terminators, inhibiting RNA synthesis downstream of where the terminator was incorporated (Tchesnokov *et al.* 2019). They showed promise in protecting animal models (Warren *et al.* 2016), but that did not translate to humans. After promising results *in vitro* (Ko *et al.* 2020), remdesivir was recently trialed in COVID-19 patients (n=236) but resulted in no statistically significant difference in clinical improvement, even though patients in the treatment group had quicker recovery time than the placebo group receiving standard care (Wang *et al.* 2020).

Other nucleoside analogues such as favipiravir (T-705) have shown promise in animal models (Oestereich *et al.* 2014; Smither *et al.* 2014; Bixler *et al.* 2018). A human trial was attempted but yielded non-conclusive results as it was not randomised (Sissoko *et al.* 2016; Cardile *et al.* 2016).

Indirect approaches targetting host factors to inhibit viral replication are more likely to induce adverse effects, considering these host factors are usually involved in other physiological processes, therefore this avenue has not been explored extensively. The cancer drug irinotecan (CPT-11) was found to inhibit viral replication by blocking the host topoisomerase-1 (TOP1) interaction with the L polymerase (Takahashi *et al.* 2013), which could be explored for EVD/MVD. However, cancer chemotherapy is often associated with toxicity (Chen *et al.* 2013), and that would have to be monitored carefully.

The approved drug nitazoxanide (NTZ) used to treat diarrhoea caused by certain bacterial infections was found to inhibit viral replication *in vitro* by upregulating RIG-I and PKR pathways leading to enhancement of type-I INF responses, counteracting the effects of VP35 (Jasenosky *et al.* 2019). The mechanisms of upregulation are unknown, but it could also be explored as a new therapy for EVD/MVD.

Some small molecules had also shown promising results *in vitro*, including a broad-spectrum compound (FGI-106) with inhibitory activity against ebola, Rift Valley and dengue fever viruses, suggesting they target a common pathway utilised by these viruses (Aman *et al.* 2009).

1.8.3 Other therapies

Therapeutic strategies targetting pathological characteristics resulting from viral infection have been explored to alleviate haemorrhagic symptoms for instance. Disruption of the coagulation cascade is one of the hallmarks of EVD and MVD. The TF/fVIIa complex is involved in homeostasis of the coagulatory pathway and its overexpression leads to systemic intravascular coagulation and organ failure (Geisbert *et al.* 2003; Geisbert *et al.* 2003).

Using an EBOV NHP model, the TF/fVIIa inhibitor recombinant NAPc2 (rNAPc2) was given to macaques either 10 min or 24h after challenge with EBOV. Survival increased by 33% in comparison to untreated animals in both treatment regimens. This approach could be explored for treatment in humans as rNAPc2 has a good safety profile (Geisbert *et al.* 2003). This would be an example of a therapy strategy targetting the disease itself rather than the virus and its replicative mechanisms.

One of the hallmarks of EVD and MVD pathogenesis is the cytokine storm often observed in non-survivors, where the sustained release of cytokines eventually leads to multiple organ failure, as previously discussed (Misasi and Sullivan 2014; Falasca *et al.* 2015; Younan *et al.* 2017). This is a feature seen in other pathogenic viruses such as SARS-CoV-2 (Zhang *et al.* 2020). Immunotherapy with tocilizumab, a recombinant humanised mAb targetting the IL-6 receptor, has been explored for counteracting the damaging effects of severe symptoms resulting from the cytokine storm caused by SARS-CoV-2 with promising results, with a decrease in O₂ administration necessary in 75% of patients, remission of lung lesions in 91% of patients, as well as improvements in several blood tests including liver functions tests. In addition, no adverse effects were reported (Xu *et al.* 2020). However, the sample was very small (n=20) and a control group did not seem to be included, making it an observational study. A randomised controlled trial would have to be conducted to draw any conclusions, but if successful it could be utilised for treatment of EVD or MVD.

1.9 Serology

EVD and MVD are zoonotic diseases with high morbidity and mortality rates, therefore serological data on distribution and spread of these viruses is crucial to inform

preventative measures and rapid public health responses as new outbreaks arise. These can be challenging as co-morbidities are often present, such as measles and SARS-CoV-2 outbreaks concomitant with the EBOV outbreak in the DRC (WHO). Large serological surveys are needed to better understand the distribution of these viruses, including possible asymptomatic cases (Gonzalez *et al.* 2000; Becquart *et al.* 2010; Glynn *et al.* 2017; Bower and Glynn 2017; Mulangu *et al.* 2018).

Initial filovirus serological investigations relied on immunofluorescence methods, but subsequent studies have been based on ELISA (Formella and Gatherer 2016).

1.9.1 ELISA

Binding assays detect antibody bound to a specific antigen. The most common being enzyme-linked immunosorbent assay (ELISA), used extensively in filovirus research for detection, quantification or subclass identification of antibodies, in serological studies as well as vaccine evaluation (Broadhurst, Brooks and Pollock 2016; Lambe, Bowyer and Ewer 2017).

ELISA can be performed using purified recombinant filovirus proteins or inactivated whole virions and it can be modified to suit different requirements. For instance, detection of specific antibody classes such as IgM can be achieved by using a sandwich capture platform using monoclonal antibodies targetting IgM. Human serum from vaccinated individuals is then added, followed by recombinant EBOV GP. Next, anti-GP polyclonal antibodies and conjugated secondary antibodies are added to finalise the setup (Atre *et al.* 2019). IgG subclasses can also be detected using a similar approach so the antibody response can be better characterised (Davis *et al.* 2019).

ELISAs targetting the GP have been used in several vaccine evaluation studies (Lambe, Bowyer and Ewer 2017), as well as evaluation of antibody responses in survivors (Krähling *et al.* 2016; Dean *et al.* 2020).

1.9.2 Functional assays

1.9.2.1 Plaque Reduction Neutralisation Test (PRNT)

The PRNT is an antibody neutralisation assay where live virus is incubated with serial dilutions of serum or antibodies. Next, cells are added to allow any virus not neutralised by the serum to infect them. An overlay is then added and plates are incubated for approximately 7-8 days to allow plaque formation caused by viral CPE. The overlay is removed and cells are fixed with 0.2% crystal violet and 10% formalin to aid plaque visualisation. Finally, the plaques are counted and PFU (plaque-forming units) calculated for each well ($\text{PFU/mL} = \text{average } n \text{ of plaques} / (\text{dilution} * \text{volume})$). The PRNT₅₀ is reported as the first dilution with 50% fewer plaques than the average of virus-only wells (Baer and Kehn-Hall 2014; Rimoin *et al.* 2018).

Slightly variations in protocols are utilised, with different kinds of solid and liquid overlays. The latter are reported to be more user friendly, being easier to apply and remove (Baer and Kehn-Hall 2014). Other dyes such as neutral red can be used instead of crystal violet (Maruyama *et al.* 1999).

PRNT for filoviruses is considered the gold standard for detection of antibodies (Broadhurst, Brooks and Pollock 2016). However, they have to be conducted in BSL-4 facilities, therefore limiting the number of laboratories that can carry them out. In addition, they can be laborious and take at least one week to generate results for many viruses.

1.9.2.2 Microneutralisation assays (MNA)

The MNA is similar to PRNT, except no overlay is added and infected cells (rather than plaques) can be assessed 48h later through fixation and incubation with monoclonal antibodies targetting the virus, as well as a tagged secondary antibody. Results (MNA₅₀) are reported and the highest dilution at which 50% of viruses are neutralised (Brown *et al.* 2018). Even though they are quicker than PRNT to yield results, they also require high containment facilities.

1.9.2.3 Pseudotype Virus Neutralisation Assay (PVNA)

PVNA utilise non-replicative chimeric virus particles as surrogates for the native pathogen and thus can be handled in low containment facilities. Their usage will be described in detail next.

1.10 Pseudotype Viruses (PV)

Research on filoviruses and other highly pathogenic viruses is hindered by the need for high containment (BSL-4) facilities, which are scarce, especially in countries affected by EVD and MVD. One strategy to address this issue is the use of pseudotype viruses (PVs), as safer surrogates to the natural pathogens, which can be handled at BSL-1/2. Although certain aspects of filovirus life cycle can only be studied with authentic viruses, PVs can be used to study basic aspects of pathogenesis and help develop much-needed novel therapeutics such as vaccines and antivirals.

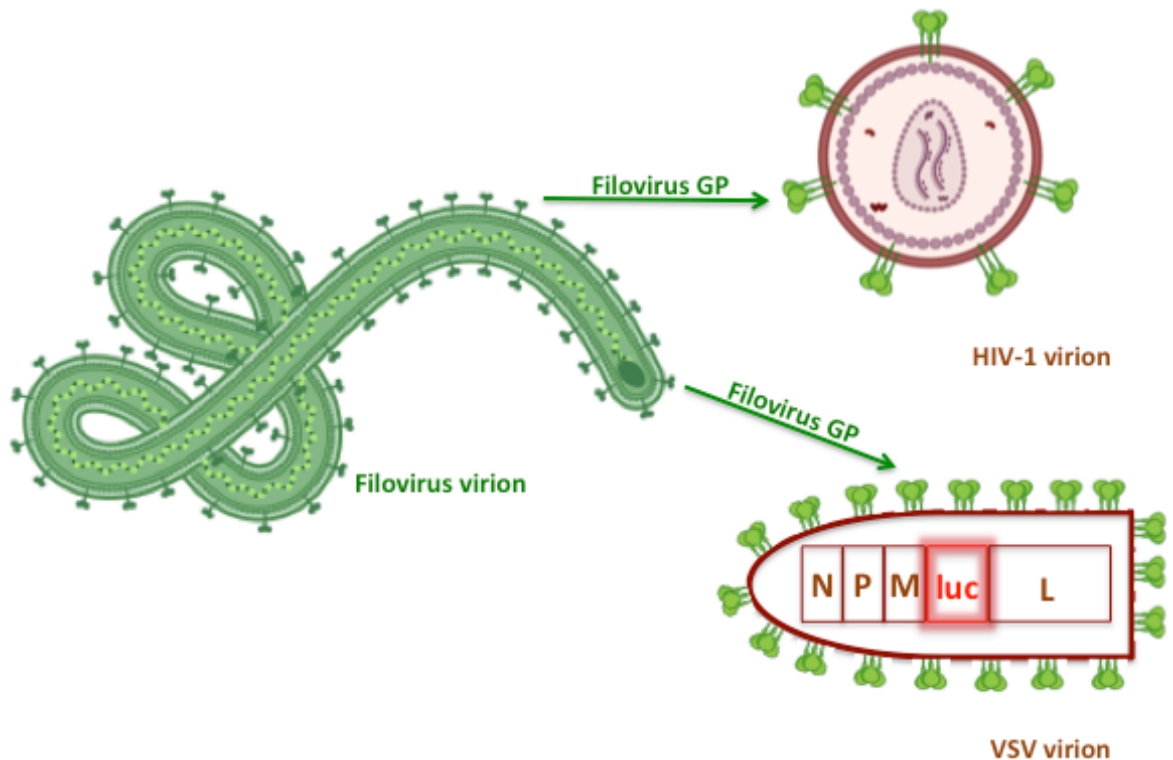


Figure 1.28. Filovirus virion, lentiviral and VSV PVs displaying filovirus GPs. The HIV-1 core PV has its genome replaced by a lentiviral vector encoding the reporter gene, whereas the VSV core PV has the G gene replaced by the reporter gene. Diagram created with Biorender and PowerPoint for Mac 2011.

Pseudotype viruses (also known as pseudotyped particles or pseudotypes) possess chimeric virions containing the core of one virus displaying heterologous glycoproteins in its lipid membrane (Figure 1.28). These are the proteins that permit attachment and entry into host cells, by interacting with cellular receptors. The core is usually a gammaretrovirus (e.g. murine leukaemia virus; MLV), lentivirus (e.g. human immunodeficiency virus 1; HIV-1) or a rhabdovirus (e.g. vesicular stomatitis virus; VSV) where most or some of the genome is replaced by a reporter gene encoding firefly luciferase or green fluorescent protein for example (Carette *et al.* 2011; Scott *et al.* 2012; Temperton, Wright and Scott 2015; Carnell *et al.* 2015; King *et al.* 2016; Ferrara and Temperton 2018). This renders the PVs replication-deficient, and is the fundamental reason why they can be handled in low biological containment facilities. Due to their pathogenicity, filoviruses are classified as BSL-4 agents and thus require commensurate handling. PVs obviate this issue, permitting important aspects of filovirus research to be conducted under standard BSL-2 laboratory conditions, thus alleviating a research bottleneck.

The terms pseudotypes, pseudovirions and pseudotyped viruses can be used interchangeably as the production of viruses *in vitro* through transfection of appropriate plasmids in producer cells resulting in virus containing the core of one virus (VSV, MLV or HIV for instance) and a heterologous envelope glycoprotein. Historically however, studies initially described pseudotyping or phenotypic mixing as the natural phenomenon of viruses displaying their own membrane glycoproteins as well as a GP from another virus when there is co-infection (Zavada 1982; Pickl, Pimentel-muiños and Seed 2001), rather than an artificial system employed in research. Retroviral core PVs have their genome replaced by a lentiviral vector encoding a reporter gene (Figure 1.28), whereas VSV core PVs harbour their own genome where the glycoprotein gene (G) is replaced by a reporter gene (Figure 1.28). Some would consider the VSV system as a chimeric virus, even though they have to be pseudotyped with a heterologous GP *in trans* to become infectious (Illyikh *et al.* 2016; Ndungo *et al.* 2016). These chimeric viruses, which are often referred as pseudotypes, form the basis for the only approved vaccine against EVD to date (see section 1.10.3).

The first few studies using PVs in filovirus research were conducted in the late 1990s. Takada *et al* utilised a VSV core PV with a GFP reporter displaying RESTV GP to infect a

variety of cell lines including monkey (Vero, COS-1), human (293T), hamster (BHK, CHO), dog (MDCK) and bat (Tb1Lu). It infected all of them apart from an insect cell line (C6/36), establishing the broad tropism of RESTV (Takada *et al.* 1997). It also determined the requirement of a low pH environment for infection, as the addition of ammonium chloride (NH₄Cl), neutralising the acidic pH of the endosomes, decreased infectivity in a dose-dependent manner (Takada *et al.* 1997).

Next, Wool-Lewis and Bates utilised a murine leukemia virus (MLV) core PV with a β -galactosidase reporter gene to generate PVs bearing the EBOV GP to characterise cell tropism and performance in neutralisation assays (Wool-Lewis and Bates 1998). It confirmed EBOV broad tropism seen with RESTV previously, and the requirement for a low pH for infection. In addition, they observed three different human B-cell lines (Nalm-6, Daudi, WEHI) and three human T-cell lines (HUT-78, CEM(E), IF-1) were refractory to infection with EBOV MLV PVs while being permissive to VSV-G MLV PVs, making these cells ideal targets for receptor identification studies, as they could be transfected with candidate receptor genes and assayed for an increase in infectivity. Lastly, EBOV MLV PVs performed well in neutralisation assays against polyclonal serum raised in rabbits, with a maximum neutralisation of 80% at the lower dilution of 1:50 (Wool-Lewis and Bates 1998).

Other surrogate systems have been recently developed to work with pathogenic viruses in low containment. S-FLU uses a non-replicative influenza virus created by suppressing the hemagglutinin (HA) signal sequence and thus reducing packaging of viral RNA, pseudotyped with the HA of another strain, inducing a heterosubtypic response and protecting mice from challenge with a highly pathogenic influenza virus and a heterologous H3N2, indicating the system could be used for vaccine delivery with broad coverage (Powell *et al.* 2012). The S-FLU platform was then adapted for filoviruses creating E-S-FLU displaying the EBOV GP. It was found to depend on NPC1 receptor interaction for infection. Next, it was used in neutralisation assays against the monoclonal antibody KZ52, which targets the EBOV GP; as well as in a drug screening throughput assay where 228 molecules out of 1280 were found to inhibit E-S-FLU, some of which also inhibited EBOV PVs and authentic EBOV (Xiao *et al.* 2018). S-FLU has been expanded to display other filovirus GP (SUDV, BDBV) and used in neutralisation assays to help identify possible therapeutic monoclonal antibodies (Rijal *et al.* 2019).

1.10.1 Filovirus PVs in cell entry studies and GP characterisation

Filovirus PVs have been utilised to investigate the role of GP in virus entry in several cell types. They were used to identify the initial binding receptors before internalisation, such as TIM-1 (Kondratowicz *et al.* 2011), then providing evidence that the NPC1 cholesterol transporter is the universal receptor for filoviruses so far identified following internalisation (Carette *et al.* 2011; Cote *et al.* 2012; Maruyama *et al.* 2014; Goldstein *et al.* 2018; Yang *et al.* 2019). More recently, the new species of *ebolavirus*, Bombali virus (BOMV) and the newly described genus *dianlovirus*, comprising solely of the bat Mengla virus (MLAV), whose RNA was found in Rousettus bats in China, both utilise the NPC1 receptor for entry. In both species studied, VSV pseudotyped with the corresponding GP can only infect cell lines expressing the NPC1, whereas in knock-out cell lines, infectivity was greatly decreased (Goldstein *et al.* 2018; Yang *et al.* 2019).

Characterisation of GP processing during infection was also achieved with PVs. The highly glycosylated mucin-like domain (MLD) of GP₁ acts as a shield to neutralising antibodies, exposing the GP to such antibodies when deleted, and consequently allowing increased infectivity. In neutralisation assays, anti-EBOV serum against recombinant VSV pseudotyped with either EBOV GP, EBOV GP lacking the MLD, and EBOV GP with the MLD from Crimean-Congo haemorrhagic fever virus, had a moderate increase of approximately 2 to 2.5 fold in neutralising titres when PVs with the GP lacking the MLD were used (Martinez *et al.* 2011).

PVs have also been employed to characterise how the level of GP expression affects infectivity. Using a HIV-1 core expressing EBOV, SUDV, LLOV and MARV GPs, Mohan *et al.* showed that higher levels of GP expression determined by western blot reduced infectivity of target cells in contrast to HIV-1 env. They proposed a model where overexpression of GP results in steric shielding of domains involved in GP attachment to receptors and interferes with endosomal processing before infection, which could contribute to the impairment of viral production and infectivity (Mohan *et al.* 2015).

They corroborated those findings using VLPs in place of PVs, and proposed the RNA editing mechanism seen for EBOV transcripts is a way of regulating GP expression and facilitate infection by ensuring the amount of GP expression is optimum to avoid toxicity, as well as an immune evasion strategy. However, MARV does not exhibit this editing mechanism and nevertheless retains the ability to efficiently infect cells. In fact, MARV exhibits higher infectivity *in vitro* compared to other filoviruses when pseudotyped

(Chapter 3). MARV GP is also synthesised as a precursor, which is then cleaved by cellular furin into GP₁ and GP₂, however no secreted GP variant is produced. In addition, it does not seem to depend on cathepsin proteolysis to expose the NPC1 receptor-binding site like *ebolaviruses* do (Gnirß *et al.* 2012).

1.10.2 Antibody tests

Current diagnostics employ RT-PCR methods for detection of viral RNA during active infection. ELISA can be used during early (IgM) or late (IgG) infection stages, however less reliably (Broadhurst, Brooks and Pollock 2016; Semper *et al.* 2016). Most serological studies rely on ELISA (Broadhurst, Brooks and Pollock 2016; Mulangu *et al.* 2018), but having alternative diagnostic tests would be advantageous to conduct serological surveys to get a better understanding of how these viruses spread and circulate in animal populations. PVs have been used to detect neutralising antibodies for a number of viruses including influenza (Scott *et al.* 2012), lyssaviruses (Wright *et al.* 2008) and filoviruses (Flyak *et al.* 2016), amongst many others (Li *et al.* 2018). As previously discussed PVs are non-replicative viruses with a genome encoding a reporter gene. They can be handled in BSL 1/2 facilities (Temperton, Wright and Scott 2015), and therefore could be used in a serology kit that would provide a tool to distinguish between different genera and species of filoviruses. One of the issues with such a kit may be avoiding the cold chain, especially for low-resource countries where filoviruses are prevalent. As PVs are usually maintained at temperatures of minus 70/80°C, transportation would be expensive as well as relying on recipient field and laboratory centres having such freezers, which might not be the case. Lyophilisation could offer a solution to this problem if PVs can be freeze-dried, stored appropriately, then reconstituted and used without its GP or capsid being compromised during the process or storage. Lyophilisation of PVs will be explored in detail in Chapter 7.

1.10.3 Vaccine vectors and evaluation

Candidate vaccines have been in development for prophylaxis as well as to contain any outbreaks that may arise, especially since the large EBOV outbreak in the DRC in 2013-2016. Even though most vaccines did not cause major side effects and were immunogenic

in animal models, neutralising antibody responses appear to wane over time, therefore it is crucial to determine correlates of protection for long lasting immunity. In survivors, levels of neutralising antibodies (IgG) lasted for over two years (Davis *et al.* 2019). A few platforms at different stages of development use viral vectors as a way of antigen delivery, including the rVSVΔG-ZEBOV (Table 1.4) used compassionately in a recent outbreak in the DRC, before it had been approved for clinical use (Dhama *et al.* 2018). This vaccine was first evaluated in various animal models, including NHP (Geisbert *et al.* 2008). Consequently it was used in a human open-label, cluster-randomised ring vaccination trial strategy (Ebola ça suffit! trial) in Guinea. It was reported to have 100% vaccine efficacy as no further infections were observed, although this figure was later questioned (Metzger and Vivas-Martínez 2018); with few side effects, except for two serious vaccine related reactions, where both individuals recovered (Henao-Restrepo *et al.* 2015; Henao-Restrepo *et al.* 2017). In the recent outbreak in the DRC the rVSVΔG-ZEBOV vaccine was found to have 88.1% to 97.5% efficacy, depending on whether the analysis included onset of EVD symptoms throughout or only 10 days after vaccination (Kalenga *et al.* 2019). The rVSVΔG-ZEBOV vaccine has been found to elicit a strong neutralising antibody response associated with protection (Ehrhardt *et al.* 2019).

PVs have been used to evaluate experimental vaccines in low containment facilities (Table 1.4), as levels of neutralising antibodies are a good indication of immunogenicity. A phase-I study consisting of a single dose ChAd3-EBOV (Mayinga strain), with or without a booster consisting of MVA (Modified Vaccinia Ankara strain), plus the GPs of MARV and SUDV, and the nucleoprotein (NP) of TAFV was conducted. The immune response was evaluated after vaccination using authentic EBOV as well as lentiviral EBOV PVs, which were found to correlate in ELISA and neutralising antibody assays (Ewer *et al.* 2016). This single dose ChAd3-EBOV elicited a similar response to the rVSVΔG-ZEBOV used in the ring vaccination study described previously, but when the MVA boost was given antibody titres increased by a factor of 9. Similarly, there was a significant increase in IC₅₀ values after MVA boosts using the PV system (Ewer *et al.* 2016). This is a perfect example where viral vectors can be employed as vaccine antigen delivery systems as well as evaluation tools measuring neutralising antibodies. Although a significant increase in neutralising antibodies does not necessarily indicate a protective response (Oswald *et al.* 2007), in the context of vaccination it might be a useful indication of protection when considered in conjunction with the cellular response (Ledgerwood *et al.* 2011; Ewer *et al.* 2016; Ledgerwood *et al.* 2017).

Vaccine type	Vaccine	Trial identification	Start date	n	ref
DNA	VRC-EBODNA012-00-VP-DNA: 3-plasmid (transmembrane-deleted EBOV GP, SUDV GP, nucleoprotein)	NCT00072605	Nov 2003	27	Martin <i>et al</i> , 2016
Viral vector-based*	rAdHu5 EBOV and SUDV GP with single point mutation in GP (asp- > glu at position 71)	NCT00374309	Sep 2006	31	Ledgerwood <i>et al</i> , 2010
DNA	VRC-EBODNA023-00-VP 2 plasmids—SUDV and EBOV GPs with a Marburg DNA vaccine (full-length WT GP)	NCT00605514	Jan 2008	20	Sawar <i>et al</i> , 2015
DNA	VRC-EBODNA023-00-VP 2 plasmids—SUDV and EBOV GPs with a Marburg DNA vaccine (full-length WT GP)	NCT00997607	Nov 2009	108	Kibuuka <i>et al</i> , 2015
Viral vector-based*	Mixture of ChAd3 EBOV and SUDV GP	NCT02231866	Sep 2014	20	Ledgerwood <i>et al</i> , 2014
Viral vector-based*	ChAd3 EBOV GP	NCT02240875	Sep 2014	60	Ewer <i>et al</i> , 2016
Viral vector-based*	ChAd3 EBOV GP and MVA-BN Filo	NCT02240875	Sep 2014	30	Ewer <i>et al</i> , 2016
Viral vector-based*	rVSV-ZEBOV	NCT02269423NCT02280408	Oct 2014	52	Regules <i>et al</i> , 2015
Viral vector-based*	ChAd3 EBOV GP	NCT02289027	Oct 2014	120	De Santis <i>et al</i> , 2016 Ewer <i>et al</i> , 2016
Viral vector-based*	ChAd3 EBOV GP	NCT02267109	Oct 2014	91	Tapia <i>et al</i> , 2016
Viral vector-based**	rVSV-ZEBOV	NCT02296983NCT02283099NCT02287480	Nov 2014	158	Agnandji <i>et al</i> , 2015
Viral vector-based*	AdHu26 EBOV GP and MVA-BN Filo	NCT02313077	Dec 2014	87	Milligan <i>et al</i> , 2016
Viral vector-based*	rAdHu5 encoding EBOV GP from 2014 outbreak strain	NCT02326194	Dec 2014	120	Zhu <i>et al</i> , 2015
Viral vector-based**	rVSV-ZEBOV	NCT02287480	Jan 2015	56	Huttner <i>et al</i> , 2015

Table 1.4 Filovirus vaccine trials. *Replication-deficient viral vectors. ** live replicating (VSV) viral vaccine. n=number of participants. Adapted from Lambe *et al*, 2017.

Hence, filovirus PVs have been a very useful tool to evaluate vaccination programs in low containment settings. In addition, a baculovirus system for expressing nanoparticles containing the EBOV GP (Makona strain) was used to vaccinate mice with or without the potent adjuvant Matrix-M, which contains the natural product saponin. The neutralising antibody response was then evaluated using EBOV VSV PVs (Mayinga strain). Mice given GP (Makona strain) with the adjuvant were found to have a 32-fold higher neutralising antibody titre than mice given GP alone (Bengtsson *et al.* 2016).

Overall it seems adjuvants, chemicals such as aluminium salts used in vaccines to enhance immunogenicity, are crucial to elicit strong cellular and humoral responses after vaccination, both of which are desirable for protection (Meyer *et al.* 2019), as the GP alone is not as immunogenic.

1.10.4 Therapeutics and antivirals

Effective therapeutics are urgently needed for future filovirus outbreaks. So far, therapies were mainly supportive, apart from compassionate use of vaccines and monoclonal antibodies.

In antibody therapeutics being explored at the moment, the aim is primarily to develop antibodies conferring broad protection against different species and strains. In a small cohort of 15 survivors of an EBOV outbreak in the DRC in 2014, 5 survivors were identified by ELISA to have a pan-filovirus response with reactivity to most *ebolavirus* species and some even to *marburgvirus*. Those 5 survivors were then assessed in a VSV based PV neutralisation assay, in which all but one neutralised EBOV PVs, two of them had a broad response neutralising TAFV, SUDV and BDBV; and two neutralised MARV PVs (Bramble *et al.* 2018). Despite being a small cohort, results were encouraging with regards to a pan-filovirus therapeutic strategy.

Studies assessing newly characterised monoclonal antibodies conferring protection in animal models utilised PVs to map epitopes through site-directed mutagenesis, generating mutated GPs to assess performance in neutralisation assays, determining amino acid residues important for binding, as well as mapping which steps during virus entry are targeted by particular monoclonal antibodies (Zhang *et al.* 2016).

Even though outbreaks of MARV/RAVV are rarer than EBOV, with fewer people infected, appropriate therapeutics are also needed. The recently isolated mAb MR191 neutralises

MARV PVs by recognising conserved residues on the RBS of the GP, competing with the NPC1 receptor (Fusco, *et al.* 2018).

A panel of mAbs was purified from the plasma of a patient who recovered from MARV infection in Uganda. Amongst these mAbs, several neutralising antibodies were identified, all of which targeted the RBS in GP. Their neutralisation capabilities were assessed comparing authentic virus and VSV PVs. Nine mAbs were deemed high-potency neutralising antibodies in PVNAs and are good candidate for a future therapeutic cocktail (Flyak *et al.* 2015). However, they were less potent in PRNT with authentic MARV. The structural basis for neutralisation and epitope characterisation of the MR series of mAbs were confirmed by solving the crystal structure of the GP bound to the MR78 mAb (Hashiguchi *et al.* 2015).

Other mAbs raised and purified from mice, which provided protection in murine models, were found to target a structural motif unique to Marburg viruses and could be used in the future as part of an antibody cocktail similar to ZMapp (Fusco *et al.* 2015). It is important to note that murine models are not as reliable as NHP, and possibly in-field human studies in a compassionate setting would have to be performed, as disease prevention in mice may not translate to humans.

1.10.5 PV generation

PV generation will be described in detail in Chapter 2. In the current study, both lentiviral and VSV core PVs were produced bearing heterologous filovirus GPs.

Lentiviral vectors have been developed historically for gene therapy studies and are now also used in PV generation, both for expression of lentiviral core proteins to assemble the virion, as well as a lentiviral vector encoding the reporter gene to be packaged as the PV genome (Figure 1.29).

For generation of HIV-1 particles, the pCMVΔR8.91 plasmid (Figure 1.29a) was used (Zufferey *et al.* 1997). It contains the gag and pol genes necessary for the HIV-1 core proteins and the enzymes necessary for reverse transcription (reverse transcriptase), virion maturation (protease) and integration (integrase), as well as tat and rev responsible for transcription activation and nuclear transport. All the accessory protein genes (vif, vpr, vpu, nef), which are involved in several aspects of HIV-1 pathogenesis, as well as the HIV-1 envelope gene (env) are deleted. The packaging signal sequence (ψ) is also deleted,

preventing packaging of genome encoding core proteins into new virions and ultimately further replication (Naldini *et al.* 1996; Zufferey *et al.* 1997).

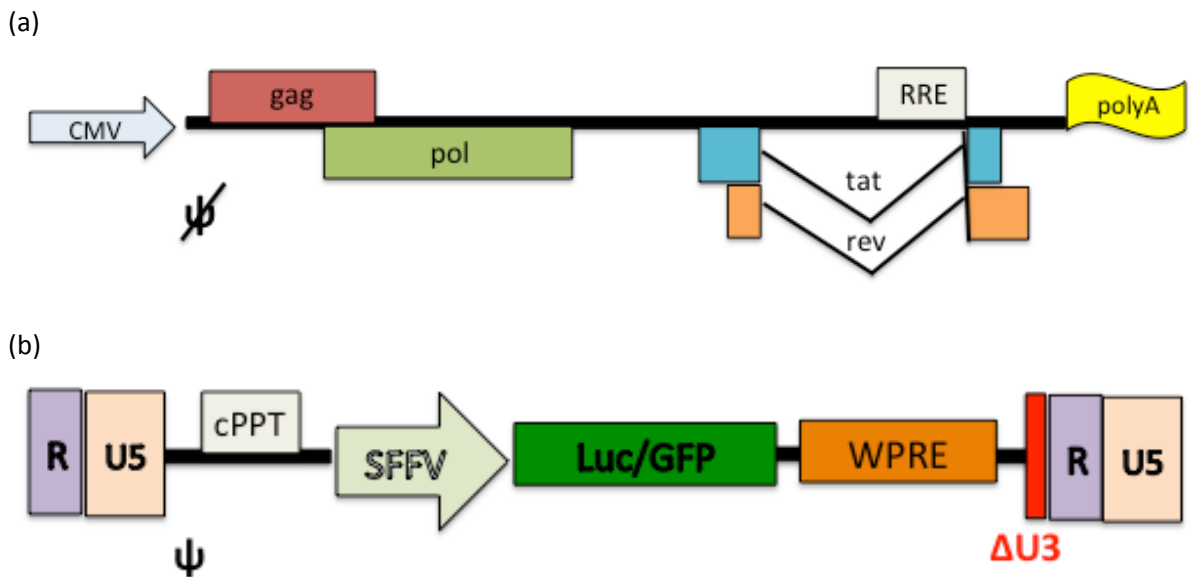


Figure 1.29. Lentiviral vectors for PV generation. Diagram of (a) p8.91 plasmid for HIV-1 expression of core proteins (*gag*) and *pol* genes for expression of polymerase, protease and integrase, and (b) lentiviral vector coding for luciferase or GFP reporter genes to packaged into PVs. Diagram constructed in PowerPoint for Mac 2011. Adapted from: Demaison *et al.* 2002 and Zufferey *et al.* 1997.

The reporter genes used in this study were encoded by a self-inactivating second-generation lentiviral vector (Figure 1.29b), containing a packaging signal sequence (ψ) that directs the incorporation of the lentiviral vector into the PV core as its genome. The vector was originally designed with the GFP reporter gene (pCSGW) for PVs expressing GFP (Demaison *et al.* 2002). Replacing the GFP with the luciferase gene (pCSFLW) enabled use of the same vector for luciferase expression. Reporter gene expression is under the spleen focus-forming virus promoter (SFFV) and enhanced by the Woodchuck hepatitis post-transcriptional regulatory element (WPRE), which increases transgene expression by an unknown mechanism (Higashimoto *et al.* 2007). The deletion of the LTR U3 region prevents it from replication due to the deletion of sequences involved in transcription. When the RNA is retrotranscribed by the reverse transcriptase enzyme the 3' LTR region becomes the 5' LTR region of the pro-viral DNA. This reduces the chances of generation of full length vector in the target cells, which forms the basis of its self-inactivating characteristic (Zufferey *et al.* 1998).

HIV-1 particles are produced containing two copies of the positive stranded RNA produced by transcription of the lentiviral vector (pCSeGW or pCSFLW), which bud out of the cell. HEK293T are ideal producer cells as expression of HIV restriction factors is down-regulated, resulting in high titre PVs (Ferreira *et al.* 2020). The supernatant can then be harvested and titrated by an appropriate method.

VSV core PVs are generated through production of a recombinant VSV where the glycoprotein (G) gene is replaced with the reporter gene. These are then used to infect transiently transfected cells with the GP of interest. This is also explained in detail in Chapter 2 (Figure 2.3).

1.10.5.1 Titration methods

Infectivity assays measure indirectly the amount of functional PV present in the harvested supernatant. For successful transduction of target cells, a virus GP and cell receptor interaction must occur, resulting in virion entry followed by reverse transcription of its genome and finally integration into the target cell genome (Wu 2004).

The assay is performed by serially diluting PV supernatants followed by addition of permissive target cells (Figure 1.30). Once gene expression occurs, either luciferase or GFP is produced and the appropriate read out can be made. Other reporter genes such as β -galactosidase (lacZ) or secreted embryonic alkaline phosphatase (SEAP) can be used depending on cost, laboratory expertise or equipment available (Wright *et al.* 2009).

For GFP PVs, the read out generated by looking at expression of GFP via fluorescence microscopy, then counting the number of green cells.

Luciferase PVs used in this study encode the firefly luciferase gene. Once expressed in the target cells, the assay can be read approximately 48h post-infection. The substrate, which will contain a detergent to denature the cell membranes as well as beetle luciferin, is added causing the cells to break open exposing the luciferase produced, catalysing the oxidation of beetle luciferin into oxyluciferin, emitting light (Figure 1.31) that can be measured in a luminometer.

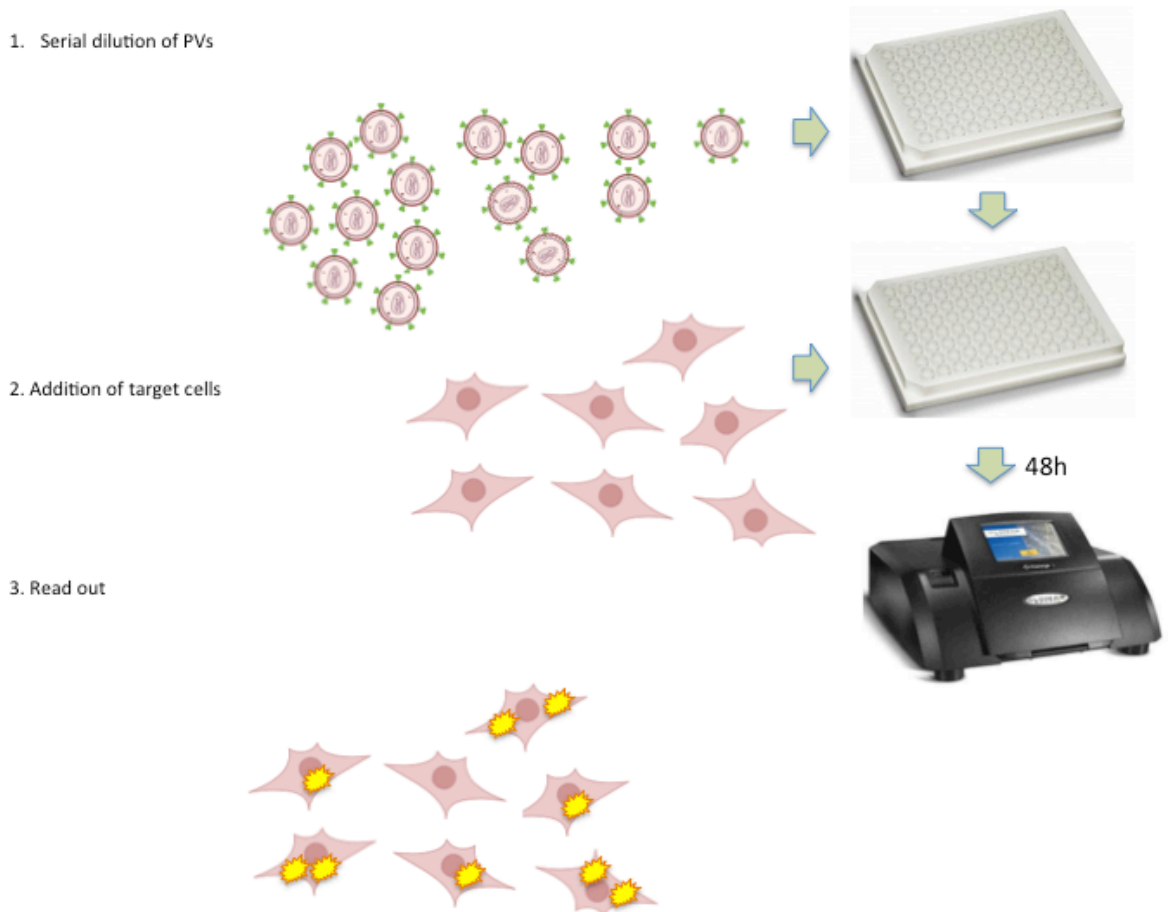


Figure 1.30. Infectivity assay. Indirect quantification of PVs by target cell transduction. Incubation of PV serial dilution with target cells. Luciferase expression can be quantified in relative light units (RLU) or a modified protocol for determination of TCID₅₀. Figure created with Biorender and PowerPoint for Mac 2011.

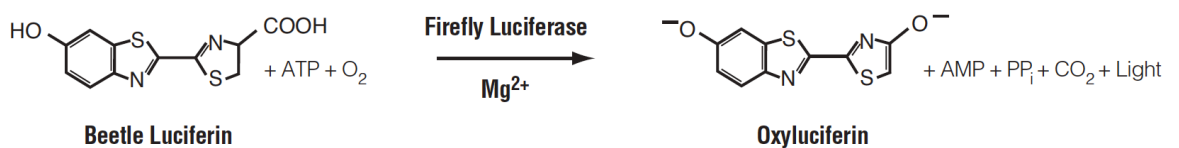


Figure 1.31 Bioluminescence reaction catalysed by Firefly luciferase. The conversion of luciferin to oxyluciferin catalysed by luciferase generates light. Source: Promega.

1.10.5.2 Pseudotype virus neutralisation assay (PVNA)

PVNAs (Figure 1.32) have been used extensively for the study of a wide range of viruses in low containment settings (Li *et al.* 2018), including influenza (Temperton *et al.* 2007; Scott *et al.* 2012; Carnell *et al.* 2015; Giotis *et al.* 2019), rabies (Wright *et al.* 2009; Wright *et al.*

2010) and filoviruses. It is typically less time consuming than classical virus neutralisation tests.

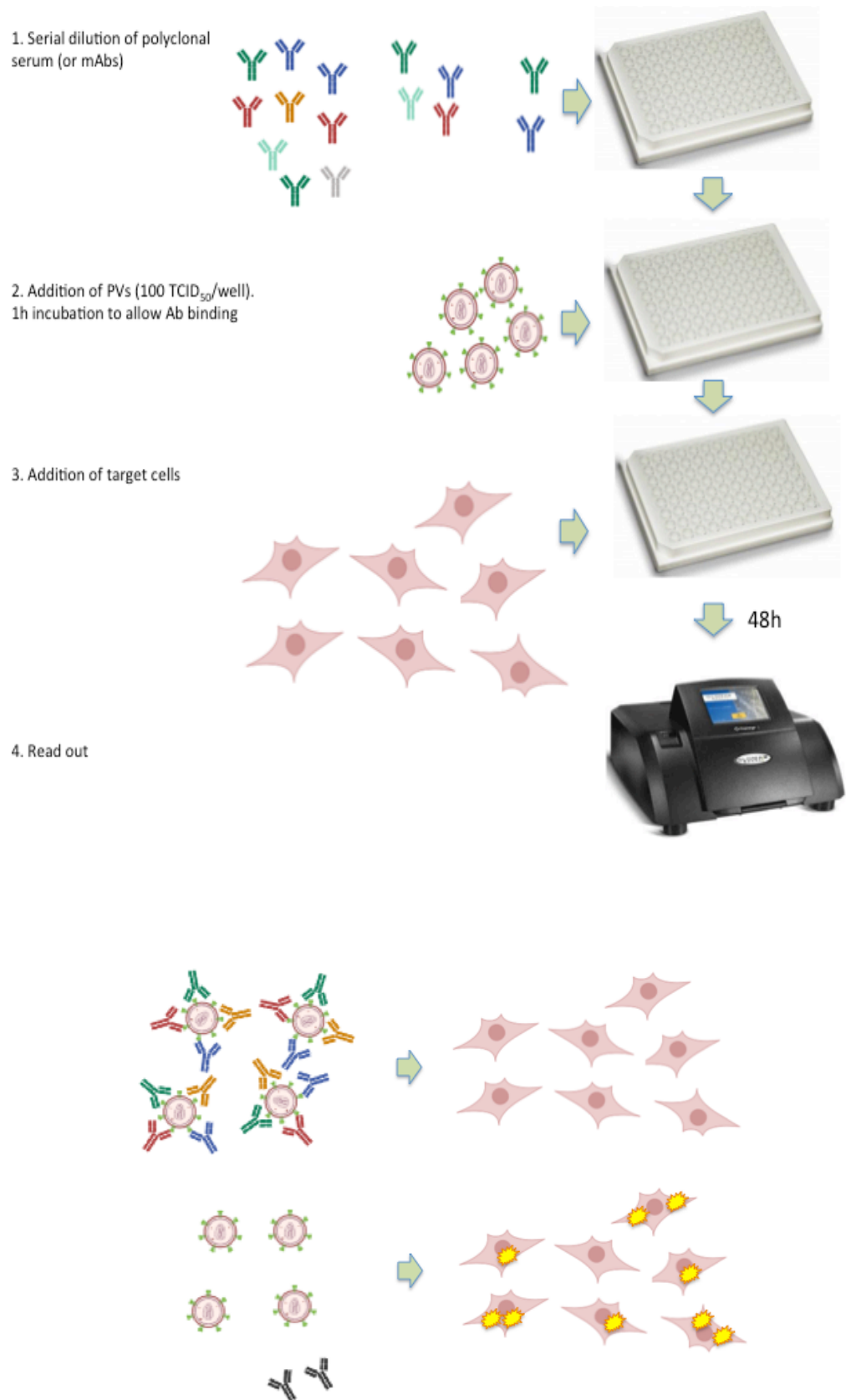


Figure 1.32. Pseudotype Virus Neutralisation Assay (PVNA). Detection of neutralising antibodies targetting the GP resulting in a decrease in reporter gene expression. Figure created with Biorender and PowerPoint for Mac 2011.

First, a serial dilution of the serum or monoclonal antibodies to be assayed is performed (Figure 1.32-1). Next, a fixed amount of PVs (100 TCID₅₀ or ~10⁵ RLU) is added to the sample wells on the assay plate and incubated for 1h at 37°C to allow for antibody binding to the GP (Figure 1.32-2). Finally, target cells are added and incubated for 24-48h (Figure 1.32-3) to allow infection of cells if the serum or mAbs have not neutralised PVs. For luciferase reporter assays, the plates are read in a luminometer (Figure 1.32-4). The end-point titre is reported as the reciprocal of the dilution at which 50% of PVs are neutralised by the serum, as evidenced by 50% reduction in luminometer readings. For mAbs, the neutralisation titre is reported as the concentration at which 50% of PVs are neutralised.

1.10.5.2.1 Correlation between PVNAs and authentic EBOV neutralisation assays

PVs are often found to be more sensitive than authentic virus in neutralisation assays (Scott *et al.* 2012; Wilkinson *et al.* 2017). Lentiviral particles are notably smaller (HIV-1 ~120 nm) than filoviruses (80 nm diameter to up to 14000 nm length), and therefore might be easier to be neutralised due to size or having higher density of GP on their surface, maximising GP-receptor interactions (Zhang *et al.* 2016; Wec *et al.* 2017).

Ilinykh *et al.* argued PVs might not be the best model for antibody characterisation as they do not seem to represent an accurate picture of what occurs *in vivo*. They found VSV pseudotyped with EBOV, BDBV and MARV GP were neutralised more efficiently by mAbs than authentic viruses (Ilinykh *et al.* 2016). However, as they correctly point out, some mAbs such as KZ52, which was isolated from a human EVD survivor, neutralise both PVs and authentic EBOV. Therefore, PVs can be useful for antibody screening and vaccine evaluation, for instance. Also, studies using authentic virus were found to require much higher concentration of antibody to achieve 50% neutralisation than lentiviral or VSV PVs, in some cases ~40 µg/mL for authentic EBOV instead of 0.78 µg/mL for EBOV PVs (Zhang *et al.* 2016), or ~93 µg/mL for authentic MARV instead of 5 µg/mL for MARV VSV PVs (Flyak *et al.* 2015), highlighting the higher sensitivity of PV based assays.

Initial reports found a poor correlation of neutralising titres between PVNA and PRNTs, but with VSV PVs performing better than lentiviral PVs in PVNAs (Wilkinson *et al.* 2017). However, it was a small study and some of the labs involved reported technical difficulties. More recently, VSV PVs bearing EBOV GPs containing a GFP reporter gene used in fluorescence reduction neutralisation test (FRNT) were found to correlate ($R^2 =$

0.96) to authentic EBOV used in plaque reduction neutralisation tests (Konduru *et al.* 2018).

1.11 Aims and Objectives

The main aim of the work presented in this thesis was to generate a panel of high titre filovirus PVs for use in antibody assays, improve specificity in antibody detection (binding and neutralisation) to differentiate between species, and evaluate their performance after lyophilisation and long-term storage in different conditions.

Initial objectives were to improve titres of previously generated *ebolavirus* lentiviral PVs to low titres (Ewer *et al.* 2016), by investigating and altering a series of different parameters such as cell culture vessels, transfection reagents and varying amounts of envelope glycoprotein expression plasmid input in transfection experiments. PVs of other filovirus genera were also generated including *cuevavirus* and *marburgvirus*. For comparison, a panel of filovirus PVs with a VSV core were also produced and optimised, by varying amounts of envelope glycoprotein expression plasmid input in transfection experiments.

EBOV PVs were then used in pseudotype virus neutralisation assays and ELISA for standardised detection of antibodies in convalescent serum. Next, a panel of chimeric LLOV and RESTV PVs were generated displaying heterologous epitopes to be utilised in PVNAs in an attempt to improve specificity. Monoclonal antibodies were utilised in proof-of-concept experiments to establish whether such epitopes were displayed correctly.

In addition, long-term studies of lyophilised PVs were conducted to assess functional stability in various storage conditions, different temperatures and humidity levels. The aim was to determine which conditions could be used for storage (and shipping) of future PV-based serological kits that could differentiate between genera and species of filoviruses, for human or animal serological surveys.

Finally, we conducted a serological survey of bats from caves in the Bukk mountains in Hungary after LLOV genomic RNA had been detected in those animals, as part of a collaborative study with the University of Pecs, Hungary. This study aimed to identify a potential reservoir of that (and possibly other filovirus) species, with future aims to further investigate filovirus distribution in bat populations within Europe.

In summary, the main objectives of this study were:

- Generation of high titre filovirus lentiviral and VSV core PVs;
- Assess antibody response against filovirus utilising PVs in PVNAs and ELISA;
- Generation of artificial antigens (chimeric GP with heterologous epitopes) for improving specificity in antibody assays;
- Storage and stability studies of lyophilised PVs;
- LLOV serological survey of bats in Hungary

CHAPTER 2: Materials and Methods

2.1 Molecular Biology

2.1.1 Plasmids

All Filovirus envelope GP gene constructs used in this study were cloned into the pCAGGS expression vector (Figure 2.1), under the control of a chicken β -actin promoter (Niwa *et al.* 1991), which were kindly donated by Dr Graham Simmons (Vitalant Research Institute – USA). Chimeric LLOV and RESTV GP containing EBOV epitopes, produced during this study, were also cloned into pCAGGS.

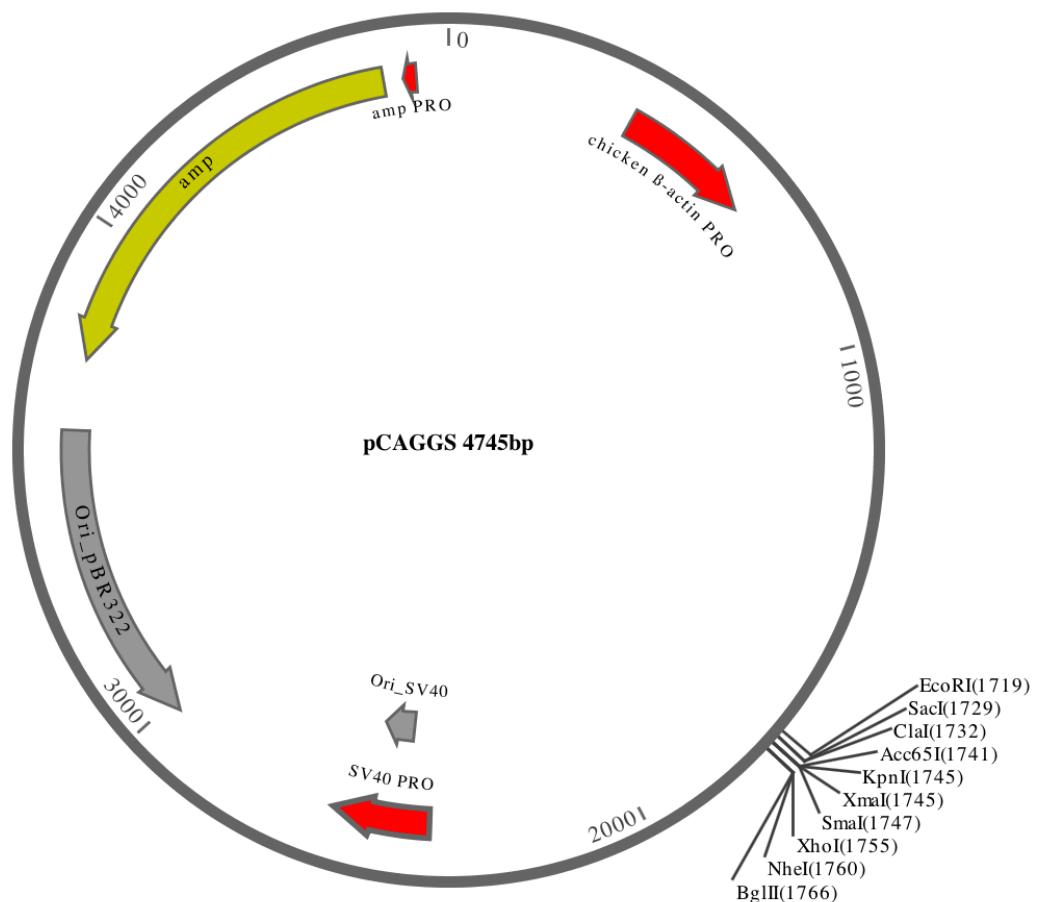


Figure 2.1. Map of pCAGGS plasmid. The multiple cloning site is displayed as well as some of its features including an ampicillin resistance gene, origin of replication for selection and replication in bacteria, and the chicken β -actin promoter for GP expression in mammalian cells. (Created with DNA Dynamo v. 1.546 – Blue Tractor Software).

For lentiviral PV production, the necessary HIV-1 genes gag and pol were encoded in the plasmid p8.91 provided by Prof Greg Towers (University College London) under control of a CMV promoter. Accessory genes (vpr, vpu, nef, vif) and a packaging signal (ψ) are deleted in this construct (Zufferey *et al.* 1997). The firefly luciferase (pCSFLW) and enhanced green fluorescent protein (pCSeGW) plasmids were provided by Dr Nigel Temperton (University of Kent). These are self-inactivating lentiviral vectors, modified from the original pCSGW vector, containing a packaging signal. The reporter gene is under the control of a SFFV promoter (Demaison *et al.* 2002).

2.1.2 Restriction enzyme digestion

All restriction enzymes and ‘Fast Digestion’ (FD) enzymes utilised for cloning and diagnostic digests to ensure the correct gene size in plasmids were obtained from Thermo Fisher Scientific. Typical restriction digestion reactions with FD enzymes for diagnostic analysis were set up as follows:

Reagent/DNA	Quantity
10X Fast Digest Green Buffer	2 μ L
DNA	(~1 μ g)
FD Enzyme #1	1 μ L (1 μ L/ μ g)
FD Enzyme #2	1 μ L (1 μ L/ μ g)
ddH ₂ O	to 20 μ L

Table 2.1. Fast digestion reactions. Incubated for 15-30 min at 37°C.

Standard (non FD) restriction digestions for cloning were set up in a total of 30 μ L and incubated for 2h at 37°C, as follows:

Reagent/DNA	Quantity
10X Tango buffer	3 μ L
DNA	(~1 μ g)
Enzyme #1	1 μ L (10 U/ μ L)
Enzyme #2	1 μ L (10 U/ μ L)
ddH ₂ O	to 30 μ L

Table 2.2. Restriction digestion reactions. Incubated for 2h at 37°C.

Universal 'Tango' buffer was used for all restriction digestions reactions. For enzymes requiring different buffer concentrations such as *Clal* and *XhoI*, sequential reactions were set up with an initial 2h incubation at 1X Tango buffer for *Clal*; then subsequently 3.75 μ L Tango buffer and 1 μ L of *XhoI* were added to make a 2X Tango reaction, then incubated for another 2h at 37°C.

2.1.3 Agarose gel electrophoresis

DNA visualisation was achieved by running 1% (v/v) agarose gels for diagnostic analysis (Fisher) or gel extraction (Sigma A9539-500G) in 1X Tris Acetate EDTA buffer (50X TAE Scientific Laboratory Supplies NAT1222). When loading dye was not present in the reaction buffer, 6x loading dye (Thermo Fisher Scientific R0611) was added. Gels were stained with ethidium bromide (Sigma-Aldrich 46067), Nancy-520 (Sigma 01494) or SYBR Safe (Thermo Fisher Scientific S33102), run at 80-100V via a Consort EV231 power supply and images acquired in a G:Box gel imager Syngene ChemiXT Imaging System with the GeneSnap Software.

2.1.4 DNA concentration

DNA concentration and purity were determined using a Nanodrop 2000 Spectrophotometer (Thermo Fisher Scientific) according to the manufacturer's instructions. As nucleic acids absorb at 260 nm, ratios 260/280 around 1.8 were considered pure for purified plasmid DNA preps, regarding contaminants that absorb near 280 nm such as proteins; and ratios 260/230 around 2.0-2.2 were considered free of contaminants that absorb near 230 nm such as carbohydrates

2.1.5 Ligation reactions

Reactions were performed to ligate digested GP DNA to digested (open) pCAGGS plasmid through their complementary 5' and 3' overhangs using 5U/ μ L T4 DNA ligase (Thermo

Fisher Scientific EL0014). Once DNA concentrations were determined (section 2.1.4), various molar ratio for vector to insert were calculated according to the formula:

$$\text{Mass of insert (ng)} = (\text{insert length/vector length}) * \text{mass of vector (ng)}$$

Reactions were set up at 1:1, 1:3 and 1:6 molar ratios of vector to insert in a total volume of 10 μL and 2.5U of T4 DNA ligase per reaction. Two control reactions were set up: one containing no insert, and another with no insert or T4 ligase to assess the presence of any self-ligated vector. Reactions were incubated 24-48hr at room temperature. The resulting ligation reaction was used to transform competent *E.coli DH5 α* cells.

2.1.6 Transformation of competent *E. coli DH5 α* cells

Subcloning Efficiency™ *DH5 α* ™ cells (ThermoFisher Scientific 18265017) were aliquoted in a dry ice/ethanol bath containing 12.5 μL or 25 μL of cells and kept at -80°C . For each transformation, a cell vial was transferred to wet ice and thawed for 5 min before adding 10% (v/v) of DNA (1.25 μL or 2.5 μL) with gentle mixing and incubated for 30 min on ice. Cells were then heat shocked at 42°C for 30 s and put back on ice for 5 min. Following heat shock, 200 μL of SOC medium (Scientific Laboratory Supplies Ltd S1797-10X5ML) was added to the cells and incubated for 1h on a 37°C orbital shaker at 225 rpm. Finally, 50-75 μL was plated on LB agar plates containing a final concentration of 100 $\mu\text{g}/\text{mL}$ ampicillin (ThermoFisher Scientific BP1760), and incubated overnight at 37°C . Colonies were subsequently screened for the plasmid containing the insert by restriction digest or polymerase chain reaction (PCR). Any positive colonies were then picked with a pipette tip, placed in 5 mL LB broth (ThermoFisher Scientific BP1426) containing a final concentration of 100 $\mu\text{g}/\text{L}$ of ampicillin and incubated overnight on a 37°C shaker at 225 rpm to enable the preparation of glycerol stocks and purification of plasmid DNA with a Qiagen or Monarch miniprep kit.

2.1.7 Glycerol stocks and Plasmid DNA purification

To isolate and purify plasmids for subsequent use in virus production a miniprep kit was used following manufacturer's instructions (Qiaprep from QIAGEN or Monarch from New England Biolabs). Before the plasmid purification process, 800 μL of bacterial culture was mixed with 200 μL of 80% (v/v) glycerol to make a 16% stock to be frozen and kept at

minus 80°C for future use. The remaining culture was used for miniprep purification of plasmid DNA.

2.1.8 PCR – Polymerase Chain Reaction

Following cloning experiments, a colony PCR screen was routinely performed to identify those that had taken up the plasmid containing the GP gene, with a DreamTaq Green PCR 2X Master Mix (Thermo Fisher Scientific K1081). Primers (Invitrogen) recognise sequences on either side of the multiple cloning site (Figure 2.1) of the pCAGGS expression vector:

pCAGGS FWD primer: 5'-TTC TCC ATC TCC AGC CTC GGG-3'

pCAGGS REV primer: 5'-CCC ATA TGT CCT TCC GAG TGA-3'

According to the number of colonies present in negative control plates, a representative number of colonies were picked with a pipette tip, streaked on ampicillin LB agar plate and placed at 37°C, the tip then placed in a thin-walled 0.2ml PCR tube (Greiner Bio-One 683201) with 10 µL ddH₂O for a few minutes before heating to 95°C for 5 min in a Mastercycler Ep Gradient (Eppendorf) thermocycler to disrupt the bacterial cell walls and release cell contents. This was then used as the plasmid DNA source for each reaction as follows:

Reagent/DNA	Quantity
Dream Taq Green MM	12.5 µL
DNA	5 µL
pCAGGS FWD	0.5 µL (5 pmol/µL)
pCAGGS REV	0.5 µL (5 pmol/µL)
ddH ₂ O	1.5 µL

Table 2.3. PCR reaction setup for colony screening. A Master mix was prepared according to the number of colonies picked to avoid pipetting errors.

The PCR programme used was: 94°C for 2 min, 25 x (94°C for 1 min, 51°C for 1 min, 72°C for 2 min), 72°C for 5 min. The reactions were loaded onto 1% (v/v) agarose gels (see section 2.1.3). Filovirus GP size is ~2 kb including chimeric GPs. Positive colonies were then picked from streaked plates described above, inoculated in 5 mL LB broth containing

100 µg/mL ampicillin and incubated overnight at 37°C, 225 rpm in an orbital shaker for about 16-18h before plasmid DNA purification.

2.1.9 Sanger Sequencing

To assess the fidelity of GP gene sequences after cloning and plasmid purification, DNA was sent to GATC (Eurofins Genomics Ltd) mixed with appropriate primers for LIGHTrun™ analysis according to their instructions: 5 µL of DNA at 100 ng/µL and 5 µL of primer at 5 pmol/µL. For all Filovirus GP constructs, three reactions were usually set up: pCAGGS FWD, pCAGGS REV and an internal primer to cover the full length of the 2 kb GP gene (Table 2.4). Sequencing results were then available to download and analysed using SnapGene® Viewer 5.0.5 and DNA Dynamo Software v 1.556. Internal sequencing primers were designed for all Filovirus GP as well as a LASV control GP. Likewise, for LLOV and RESTV GPs a series of internal primers were utilised, designed to cover the gene when mutations were introduced to create the chimeric GP for the epitope modification studies (Chapter 5):

Primer	Sequence (5' to 3')
ZEBOV_OptInt_FWD¹	GAACGCCACAGAAGATCC
SEBOV_Int_FWD²	AAACGTTCTTCAATCACC
BEBOV_Int_FWD³	TTTCAGAAGGTGTTGTGG
RESTV_Int720_FWD	TGTGCAACTAGATCGTCCACA
RESTV_Int1500_REV	ACCGATCGCCTTTGTTTCCT
MARV_ConInt_FWD⁴	AAGGTCAAACCCTCATGC
LLOV_Int440_FWD	ATGCCGCTATGTCCACAGAG
LLOV_Int560_FWD	GTAACCTTTACGGAAGGCAC
LLOV_Int1160_FWD	TACAAGCCGTACATCCAGGC
LLOV_Int1402_FWD	ACAACACAACGCCAAACCATG
LLOV_Int1640_REV	GTTTTGCATCCTTGTTTGC
LLOV_Int1810_REV	GGGCTTTAGTAGTGGTGTTCGC
LASV_Int493_FWD	AGTACAACCTGAGCCACAGC

Table 2.4. List of internal primers for sequencing of filovirus GP gene constructs. ¹ZEBOV_OptInt_FWD targets the sequence of codon optimised EBOV (Makona C15) GP. ²SEBOV_Int_FWD targets the sequence of SUDV. ³BEBOV_Int_FWD targets the sequence of BDBV and ⁴MARV_ConInt_FWD targets a conserved sequence in RAVV and MARV (DRC and Angola strains).

2.2 Cell Culture

All cell culture, virus generation, titration and neutralisation assays were performed at the Viral Pseudotype Unit in an MSC-Advantage™ Class II Biological Safety Cabinet (Thermo Fisher Scientific). All cells were incubated at 37°C with 5% CO₂ in a Heracell™ 150i humidified incubator (Thermo Fisher Scientific).

2.2.1 Cell lines and subculturing

Human Embryonic Kidney (HEK293T/17) cells (ATCC CRL-11268), Human hepatocellular carcinoma (Huh-7) cells and Green monkey kidney (Vero) cells (ATCC CCL-81) were subcultured regularly when reaching ~90% confluence in Dulbecco Modified Eagle Medium (DMEM with: 4.5 g/l Glucose, stab. Glutamine, Sodium pyruvate, 3.7 g/l NaHCO₃, Pan Biotech UK Ltd P04-04510).

Chinese hamster ovary (CHO-K1) cells (ATCC CCL-61) were subcultured in Ham's F-12 medium (Gibco™ - Fisher Scientific 15172529) and were a kind gift from Dr Giada Mattiuzzo – National Institute for Biological Standards and Control, UK.

All media were supplemented with 10% (v/v) Foetal Bovine Serum (FBS, EU approved, filtrated bovine serum, virus and mycoplasma tested, heat inactivated, PanBiotech UK Ltd P40-37500HI) and 1% (v/v) Penicillin/Streptomycin (PanBiotech UK Ltd P06-07100) to make “complete medium”, and pre-warmed before subculturing.

Cells were maintained and passaged in 10 cm dishes (Nunclon™ - Thermo Fisher Scientific 150350). When subculturing, cells were washed with 2 mL Dulbecco's phosphate-buffered saline (DPBS w/o: Ca⁺⁺ and Mg⁺⁺ - Pan Biotech UK Ltd P04-36500), treated with 2 mL Trypsin (0.05 % EDTA 4 Na 0,02 % in HBSS, w: phenol red - Pan Biotech UK Ltd P10-040100) at 37°C, 5% CO₂ until complete cell detachment from the dish (usually ~5 min), followed by inactivation of trypsin with 6 mL of complete medium, thorough resuspension and appropriate seeding into a new dish according to the cell line growth characteristics and planning of future experiments.

2.2.2 Cell lines – frozen stocks

To maintain stocks of each cell line, 10 cm dishes were seeded to achieve 70-80% confluence the following day. Cells were trypsinised as described above, the resulting 8 mL resuspension transferred into a 15 mL Falcon tube and centrifuged at 400 rpm (~21 g) for 5 min. The medium was discarded and the cell pellet resuspended in 1 mL 'Freezing' media (complete media supplemented with 5% dimethyl sulfoxide - DMSO - VWR International Ltd 282164K), transferred into a 2 mL cryotube (Corning – Fisher Scientific 10546243) and placed in a Mr Frosty™ container (Thermo Fisher Scientific 5100-0001) containing isopropanol to ensure gradual freezing.

Cell line stocks were kept at -80°C and renewed regularly. When thawing cells, a 10 cm dish containing 8 mL of complete medium was placed in the incubator to adjust temperature and pH for about 30 min. Then, a cryotube of frozen cells was thawed and the whole content added to a 10 cm dish, rocked gently and returned to the incubator. The following day, the medium was replaced with 8 mL of complete medium to remove any residual DMSO. The cells were subcultured when confluence was higher than 90%. They were then passaged at least twice before being used in any experiments. Cells were checked under the microscope daily and a PV titration with PV supernatant of known titre was performed to assess performance in the titration. Cell viability was checked by counting the number of live cells, as it will be described in section 2.3.1

2.3 PV generation – Transfection with expression plasmids

2.3.1 Lentiviral core PVs

The transfection protocol used in this study is an optimised version of the standard transfection protocol used for influenza PV generation in the Viral Pseudotype Unit. As filoviruses have only one GP on their surface, a 3-plasmid transfection on HEK293T/17 producer cells was used to generate PVs bearing filovirus GP on their surface (Figure 2).

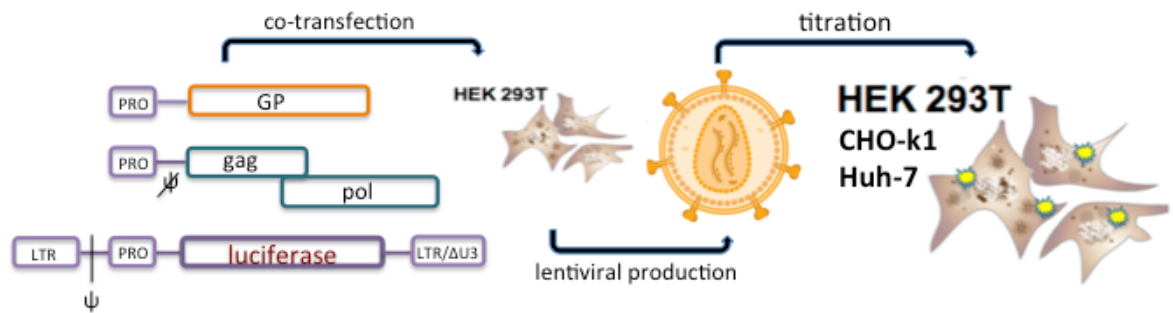


Figure 2.2. Diagram of a 3-plasmid transfection to generate filovirus PVs with a luciferase reporter gene. The luciferase gene can be replaced by GFP or any other choice of reporter. HEK293T cells are the best producer cells for lentiviral core PVs. Different target cells with the appropriate GP can be used in transduction experiments, as indicated.

The plasmids used were described in section 2.1.1: the envelope GP of interest in a pCAGGS expression vector; the HIV-1 core p8.91 expressing gag and pol proteins, and either pCSFLW or pCSeGW lentiviral vectors expressing firefly luciferase or enhanced green fluorescent protein reporter genes.

On day 1, a confluent 10 cm dish containing HEK293T cells was subcultured to seed 1×10^6 cells in a T25 flask (Thermo Fisher Scientific 156340) containing 4 mL complete DMEM.

To count cells, 10 μ L of resuspended cells was mixed with 10 μ L of Trypan blue 0.4% solution (Bio Rad 1450021), 10 μ L of the mixture loaded onto a cell counting slide (Bio Rad 1450015) and inserted in a TC20™ Automated Cell Counter (Bio Rad 145-0101). The amount of cells to be seeded can be calculated according to the amount of live cells present in addition to assessing cell viability concomitantly.

On day 2, a DNA mix containing 1:1.6:1 (700 ng, 1.1 μ g, 700 ng) envelope GP: reporter gene: HIV-1 gag-pol plasmids was prepared in 120 μ L of optiMEM (Gibco – Thermo Fisher Scientific 51985034). In a separate tube, 20 μ L of 1 mg/mL Polyethylenimine (Sigma-Aldrich 408727-100ML) was added to 120 μ L optiMEM, just under the surface avoiding touching the sides of the tube; gently tapping the tube to mix and incubated for 5 min at RT. The PEI/optiMEM mix was then added to the DNA mix and incubated for 20 min at RT with frequent mixing by gently tapping the tube during the incubation, to allow complex formation between the DNA and PEI molecules.

During the incubation the medium was replaced in the T25 flasks with 4 mL of complete DMEM and the DNA/PEI/optiMEM mix added dropwise to the flask followed by a gentle

rock up and down, side to side motion to disperse the mixture throughout the flask, and incubated at 37°C, 5% CO₂.

On day 3, the medium was replaced with 4 mL complete DMEM, and incubated at 37°C, 5% CO₂.

On day 4, the supernatant was harvested, filtered through a 0.45 µm sterile cellulose acetate filter (Fisher Scientific 10460031 or Starlab UK E4780-1453) to remove cell debris, aliquoted and stored at -80°C until titration. Sometimes media was replaced with 4 mL complete DMEM and an additional harvest performed on day 5 as described above.

For upscaled production of PVs, 3 x 10⁶ cells were seeded in a T75 flask (Thermo Fisher Scientific 156499) with 8 mL complete medium on day 1. The same protocol for production in T25 flasks was followed, except the ratio was 1:1.5:1 (1 µg, 1.5 µg, 1µg) for envelope GP: reporter gene: HIV-1 gag-pol plasmids and 35 µL of 1 mg/mL PEI was added to prepare the DNA/PEI/optiMEM mix.

2.3.2 Vesicular Stomatitis Virus (VSV) core PVs

VSV has been used extensively as a core for pseudotyping filovirus GP. However, it is much more laborious to generate and maintain PV stocks than using lentiviral core PVs in our hands. VSV pseudotyping technology was introduced in our lab just before this study was due to finish therefore there was very limited time to optimise a protocol for neutralisation assays. However, VSV pseudotyping was included in our study as a comparison of PV titres and controls in other assays such as SG-PERT, as this assay measure reverse transcriptase activity in lentiviral PVs.

In contrast to lentiviral PVs produced in a single 3-plasmid transfection, VSV core PVs are produced in three different stages (Figure 2.3). Firstly recombinant VSV (rVSVΔG), where the glycoprotein G gene was replaced with the firefly luciferase gene, was generated and recovered from BHK cells (Kerafast Inc.). Viral gene expression is under the bacteriophage T7 RNA polymerase promoter. This was carried out by Dr Mariliza Derveni in Dr Edward Wright's lab at the University of Sussex adapted from a previously optimised protocol (Whitt 2010). Some of these recovered rVSVΔG stocks, as well as BHK and BHK-cocal cells were kindly donated to us. Briefly, the protocol involved infection of BHK cells with the recombinant fowlpox helper virus (FPV-T7), to express the T7 RNA polymerase, at an MOI of 3 in 6-well plates. The inoculum was removed after 2h, cells thoroughly washed and an

optiMEM/DNA/TransIT2020 transfection mix (500 μ L) containing support plasmids N ϕ T (3 μ g/well), P ϕ T (5 μ g/well), G ϕ T (8 μ g/well), L ϕ T (1 μ g/well), pVSV Δ G-luc (5 μ g/well) was added and incubated for 2h at 37°C before 1.5 mL of medium was added (supplemented with 5% FBS). The support plasmids N, P, G, L encode the viral proteins, and the pVSV Δ G-luc is the genome containing the luciferase reporter gene. The following day, the medium was replaced to remove the transfection mix. Recombinant VSV Δ G was harvested 48h after transfection and filtered with a 0.45 μ m filter to remove any cell debris (Derveni *et al.* 2019). Stocks were subject to infectivity assays and TCID₅₀ calculations (Section 2.4). Titres in PFU/mL can be estimated by multiplying TCID₅₀/mL by 0.7 based on the Poisson distribution. Dr Derveni provided 1 mL of rVSV Δ G supernatant with a reported titre of 5.5x10⁵ PFU/ml, which was then used to amplify our own stocks (Figure 2.3).

The second stage is amplification of rVSV Δ G stocks in BHK cells stably expressing the coccal glycoprotein (G), which is a vesiculoviral species related to the VSV Indiana species (VSV-G) used widely in PV production, and results in high titre PVs (Derveni *et al.* 2019). Briefly, 3 x 10⁶ coccal G-expressing BHK cells (BHK-cocal) were seeded into 10 cm tissue culture plates (100 x 17mm Dish, Nunclon™ Delta – Thermo Fisher Scientific 150350) and incubated overnight at 37°C, 5% CO₂. The following day, the medium was replaced with 8 mL DMEM (5% FBS) and the cells infected with rVSV Δ G at an MOI of 0.1 for 2h at 37°C, 5% CO₂; inoculum was removed, cells were washed 3 x with 3 mL DPBS and medium replaced with 8 mL DMEM (5% FBS) before being incubated overnight at 37°C, 5% CO₂. Supernatant was harvested at 24h and 48h post-infection as described above. Aliquots were stored at -80°C.

Once rVSV Δ G stocks have been subjected to infectivity assays and TCID₅₀ calculations, VSV PVs bearing foreign GP can be generated. On day 1, 4 x 10⁵ HEK293T cells were seeded in either 6-well plates or T25 flasks in 2 mL and 4 mL complete medium and incubated overnight at 37°C, 5% CO₂. On day 2, medium was replaced and cells transfected with the filovirus GP of interest at different amounts (100 ng, 700 ng and 1500 ng) using the PEI method as described in section 2.3.1. It is important to note the only plasmid used is the pCAGGS-GP. On day 3, the medium was replaced and cells were infected with the previously amplified rVSV Δ G at an MOI of 0.5 for 2h. Finally, VSV PVs were harvested at 24h and 48h post-infection. PVs were then characterised as described in the following section (2.4).

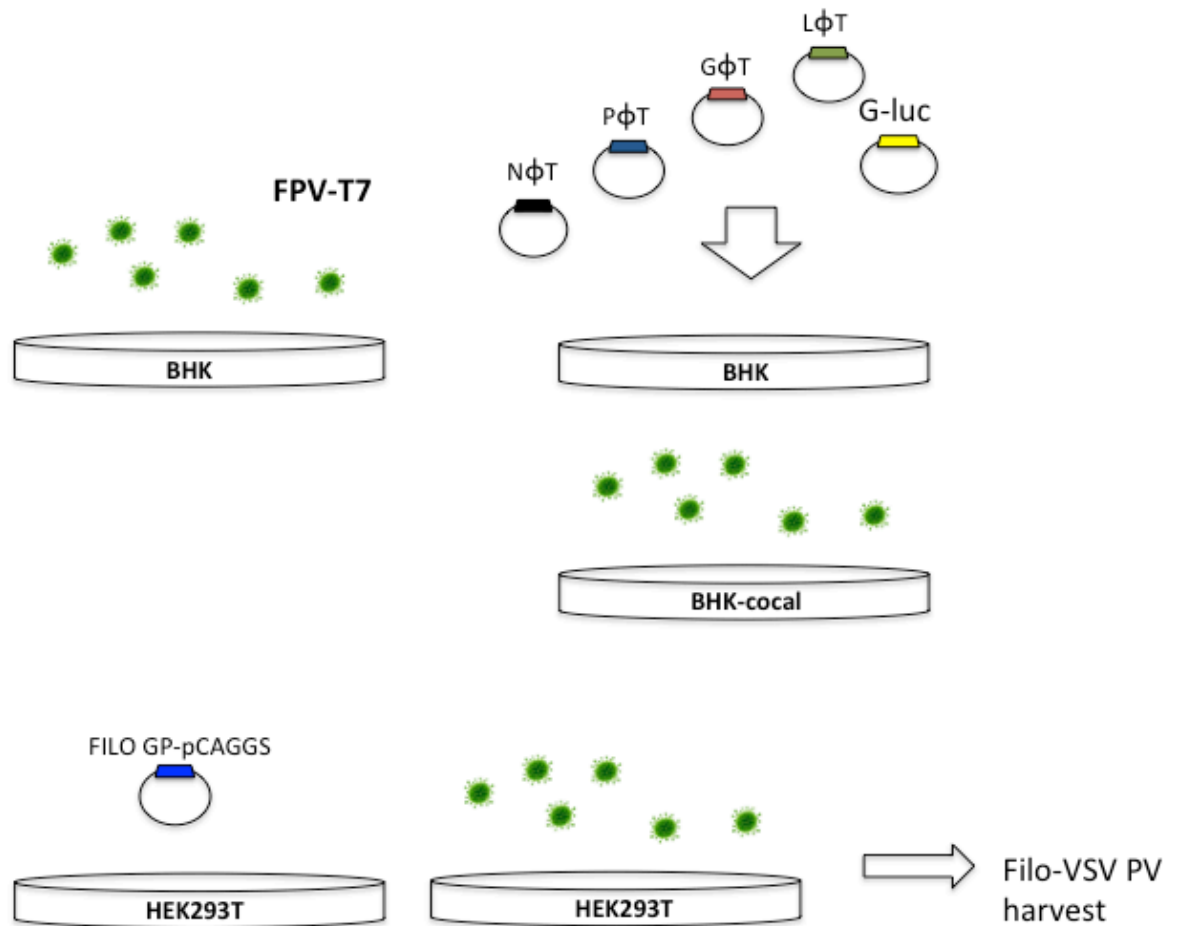


Figure 2.3. Schematic diagram of VSV core PV production. BHK cells are initially infected with recombinant FPV-T7 for expression of the T7 RNA polymerase, followed by support plasmids for generation of core VSV particles and the viral genome (G-luc) with the luciferase gene replacing the (G) gene, which is provided *in trans* (GφT). Rescued recombinant virus is then amplified by infecting BHK cells stably expressing the cocl G. Resulting rVSVΔG particles displaying the cocl G are used to generate VSV PVs bearing filovirus GP previously transfected in HEK293T producer cells.

2.4 PV Titration

2.4.1 Infectivity assay

For PVs containing a luciferase reporter, viral supernatant was added (100 μ L/well) to a white, flat-bottom, sterile Nunc 96-well microplate (Thermo Scientific 10072151) and serially diluted 2-fold, discarding the last 50 μ L. Controls (i.e. any PV of known titre as well as a column of wells with only cells - no PV) were added to ensure the assay performed as expected and to discount any background luminescence detected in the cell only wells.

Target cells (2×10^4 cells/well in 50 μ L) were added and incubated for 48h at 37°C, 5% CO₂. After 48h, the media was removed and discarded; Bright-Glo™ reagent (Promega)

was added to the plate (25 μ L of Bright-Glo™ : DPBS 1:1) and incubated at room temperature for 5 min before measuring luminescence on a GloMax 96 luminometer (Promega) to ultimately determine the relative light units (RLU) per mL, an indirect measure of PV titre.

The output given by the luminometer is a measure of RLU for each well. These values were then exported to Microsoft Excel for Mac 2011 to determine the RLU/mL value for each dilution and obtain an average final RLU/mL titre. These values were finally exported to Prism version 8 for statistical analysis and graphical depiction.

For PVs containing an enhanced GFP reporter, viral supernatant was added (100 μ L/well) to a transparent, flat-bottom, sterile Nunc 96-well microplate (Thermo Scientific 269787) and serially diluted 2-fold, discarding the last 50 μ L. Target cells (2×10^4 cells/well in 50 μ L) were added and incubated for 48h at 37°C, 5% CO₂. After 48h, the cells were visualised by fluorescence microscopy for detection of any green GFP-expressing cells.

2.4.2 Determination of TCID₅₀/mL

The 50% tissue culture infective dose per mL can be used as a standard measure of viral titre and allows standardisation of PV input. It indicates the dilution at which 50% of cells challenged with the PV supernatant will become infected. It was used in this study as an extra tool to compare titres of PVs containing the firefly luciferase reporter genes and PV input in neutralisation assays.

In a white, flat-bottom, sterile Nunc 96-well microplate 25 μ L of PV supernatant was added in quadruplicates (A1,B1,C1,D1 or E1,F1,G1,H1). Next, 100 μ L of complete medium was added to all wells and a 5-fold dilution series was performed from columns 1 to 11. Column 12 is left as a negative control containing only cells (no PV). The plate was centrifuged (ELMI CM-6MT centrifuge) for 3 s at 400 rpm (~21 g) and target cells (2×10^4 /well in 100 μ L) were added making the start dilution 1:10, and incubated for 48h at 37°C, 5% CO₂. After 48h, the media was removed and discarded; Bright-Glo™ reagent was added to the plate (25 μ L of Bright-Glo™ : DPBS 1:1) and incubated at room temperature for 5 min before measuring luminescence on the luminometer (Figure 2.4).

For high titre PVs such as RAVV, MARV, LASV, VSV-G the initial input is 5 μ L PV supernatant + 20 μ L complete medium, following the rest of the protocol, making the initial dilution 1:50 instead of 1:10. The luminescence values were used to calculate the

PV titre (TCID₅₀/mL) using the Reed-Muench method (Reed and Muench 1938). The cumulative number of positive and negative wells for PV infection at each dilution was determined and the percentage calculated for each. The threshold value for a positive well was set at 2.5 x the average luminescence value of the cell only negative controls.

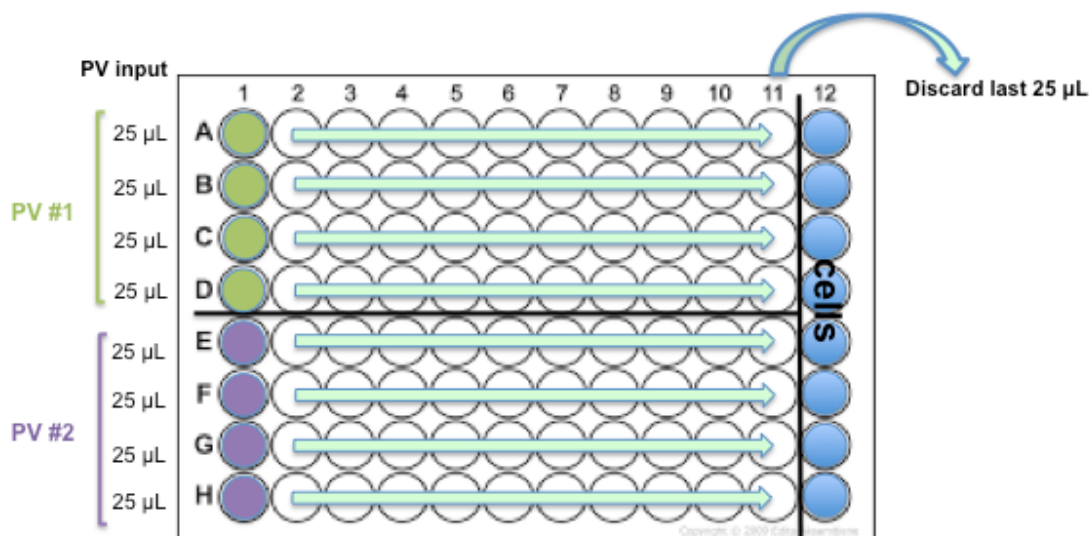


Figure 2.4. Plate diagram of a TCID₅₀ assay setup. A 5-fold PV dilution is performed in quadruplicates. Target cells are added and luminescence read after 48h.

2.5 Quality Control of PV production

To ensure consistency and monitor lentiviral PV production two different assays were used in this study to establish the number of PV particles in each batch produced. An ELISA measuring the amount of virion associated p24 protein and an RT-PCR based assay (SG-PERT) measuring reverse transcriptase activity were performed in conjunction during PV production.

2.5.1 Virion-associated p24 ELISA

The QuickTiter™ Lentivirus Titer Kit (Lentivirus-Associated HIV p24) ELISA (Cell Biolabs, Inc. VPK-107) was developed to detect virion associated HIV-1 p24 core protein only, eliminating free p24 generated during transient transfection of HEK293T, therefore increasing accuracy.

Their ViraBind™ reagent (undisclosed formula) forms complexes with virions whilst the free p24 remains in the supernatant that is later discarded. From the total amount of p24 in the sample the number of particles can be deducted, considering there are approximately 2000 p24 molecules per virion (Cell Biolabs Inc.).

The ELISA was performed according to the manufacturer’s instructions. Briefly, a dilution series of recombinant HIV-1 p24 antigen was prepared to achieve a range of 0 to 100 ng/mL of recombinant p24 in sample diluent and produce a standard curve (Table 2.5). The tubes were vortexed briefly and incubated at 37°C for 30 min.

Standard #	p24 standard (µL)	Sample diluent (µL)	p24 (ng/mL)
1	10	990	100
2	500 of tube #1	500	50
3	500 of tube #2	500	25
4	500 of tube #3	500	12.5
5	500 of tube #4	500	6.25
6	500 of tube #5	500	3.125
7	500 of tube #6	500	1.5625
8	0	500	0

Table 2.5: Preparation of p24 antigen to generate a standard curve.

To prepare and inactivate the lentiviral samples, dilutions of PV supernatant were included: neat (not diluted), 1:10, 1:100 and 1:1000 diluted in complete medium keeping the final volume at 1 mL, as well as a cell culture medium only negative control. 10 µL of ViraBind™ reagent A was added to each sample and mixed by inverting. Next, 10 µL of ViraBind™ reagent B was added to each sample and mixed by inverting followed by a 30 min incubation at 37°C. Samples were centrifuged at 17000 g for 5 min, the supernatant discarded and the pellet resuspended in 250 µL of sample diluent, vortexed briefly and incubated at 37°C for 30 min to inactivate PVs.

In the anti-p24 antibody coated plate provided in the kit, 100 µL of standards and inactivated PV samples were loaded in duplicates, a plate cover applied and stored overnight at 4°C.

The following day, samples were removed and the plate was washed 3x with 1x wash buffer, 100 µL of 1:1000 diluted FITC-conjugated anti-p24 monoclonal antibody was

added to each well, the plate covered and incubated at RT for 1h. The plate was washed 3x with 1x wash buffer, 100 μ L of 1:1000 diluted HRP-conjugated anti-FITC monoclonal antibody was added to each well, the plate covered and incubated at RT for 1h. The plate was washed 3x with 1x wash buffer, 100 μ L of substrate solution previously warmed to RT was added to each well and incubated at RT for approximately 15 min. 100 μ L of stop solution was added to each well and read at 450 nm in a Tecan Infinite[®] PRO plate reader. The standard curve was plotted and unknown values interpolated. The lentivirus associated p24 amount (p24 titre) in each sample was: p24 (ng/mL) x Dilution Factor x 0.25 mL/1.0 mL.

Considering there are approximately 2000 p24 molecules per PV particle:

$2000 \times 24 \times 10^3 / (6 \times 10^{23})$ g of p24 = 8×10^{-17} g or 8×10^{-8} ng of p24 in 1PV, therefore 1 ng of p24 will contain 1.25×10^7 PVs. This is a physical titre, the infectious titre depends on the transduction and analysis methods used, target cell lines etc.

2.5.2 SYBR-Green Product-Enhanced Reverse Transcriptase (SG-PERT) assay

The reverse transcriptase (RT) activity was quantified by RT-PCR with an assay developed by Pizzato *et al*, 2009 and subsequently updated by Vermeire *et al*, 2012 (Figure 2.5).

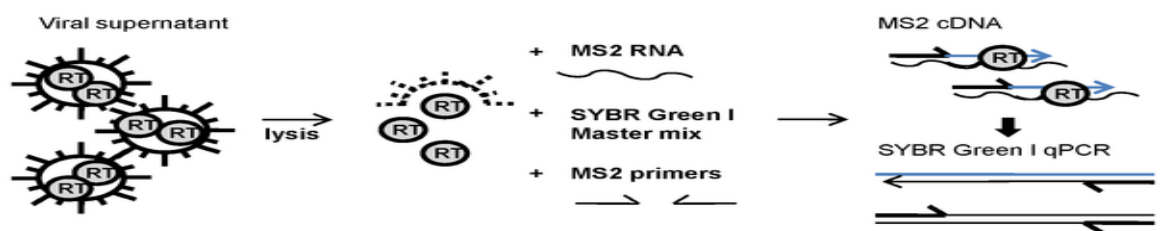


Figure 2.5. SG-PERT assay to quantify RT activity in lentiviral PV samples. PV supernatant is lysed to allow its RT to generate cDNA copies of the exogenous RNA so it can be quantified in the qPCR step. Source: Vermeire *et al*, 2012.

Supernatant containing PVs is lysed, an exogenous RNA (phage MS2) and its primers are introduced to generate MS2 cDNA which is then quantified in a SYBR Green I qPCR (Figure 2.5). A standard curve from recombinant HIV-1 RT is generated at the same time that enables interpolation of unknown values in each sample.

To generate the standard curve, recombinant HIV-1 RT (Merck-Millipore 382129-500U) was diluted to 10 mU/ μ L (1×10^{10} pU/ μ L) in PCR grade water before each assay. A 10-fold

series dilution was prepared in PCR grade water to achieve 0.5×10^9 pU/ μ L to 0.5×10^3 pU/ μ L to add 2 μ L per reaction.

PV samples were lysed by adding 5 μ L of PV supernatant or control to 5 μ L of 2 x lysis buffer (100 mM TrisHCl, 50 mM KCl, 0.25% Triton X-100, 40% glycerol) supplemented with 0.8 U/ μ L Ribolock RNase inhibitor (Thermo Fisher Scientific EO 0381) before each assay for a final concentration of 0.4 U/ μ L per reaction, incubated at RT for 10 min, 90 μ L of PCR graded water added, mixed and centrifuged briefly.

Primer	Sequence
MS2 Fwd	5'-TCCTGCTCAACTTCCTGTGCGAG-3'
MS2 Rev	5'-CACAGGTCAAACCTCCTAGGAATG-3'

Table 2.6. MS2 primers for generation of MS2 cDNA.

A master mix was prepared according to the number of samples for a total of 25 μ L per reaction containing Lightcycler® 480 SYBR Green I Master Mix (Roche 04707516001), 0.5 μ M of MS2 Fwd and Rev primers (Eurofins – Table 2.6), 3.5 pmol/mL MS2 RNA (Sigma-Aldrich 10165948001), 0.02 U/ μ L Ribolock RNase inhibitor.

Step	Time	Temp (°C)
Reverse transcription	20 min	42
Taq Fast start	5 min	95
3-step cycling (40 cycles):		
Denaturation	5 s	95
Annealing	5 s	60
Extension	15 s	72

Table 2.7. SG-PERT assay cycle conditions. Fluorescence acquisition was at the end of extension phase. Melting curve analysis was calculated automatically according to the machine default settings.

The assay was set up in 96-well white LightCycler® 480 Multiwell plates (Roche 04729692001) by adding 13 μ L of master mix in each well in duplicates, 12 μ L of PV lysate or controls. For the remaining RT standards, 10 μ L of PCR grade water was added per reaction to the master mix and 23 μ L aliquoted in each well in duplicates, 2 μ L per well of each standard added (except the first standard 1×10^{10} pU/ μ L where 1 μ L of 10 mU/ μ L HIV-1 RT and 1 μ L of PCR grade water were added in each well in duplicate). The plate

was sealed and centrifuged briefly. The SG-PERT was run in a LightCycler® 480 Instrument (Roche) with cycle conditions (Table 2.7) as described (Vermeire *et al.* 2012).

Data was analysed with the LightCycler® 480 Software v 1.5.0 and Microsoft Excel for Mac 2011. Results can be reported as enzyme activity (pU/μL) or the number of PVs estimated considering each PV has ~300 pU/μL of RT activity (Pizzato *et al.* 2009; Vermeire *et al.* 2012).

2.6 Pseudotype Virus Neutralisation assay (PVNA)

PVs containing the firefly luciferase reporter gene were used to assess and quantify the amount of antibodies in serum samples, or known concentrations of monoclonal antibodies (mAb), which recognise neutralising epitopes in the GP, were used to characterise the neutralising antibody response of generated PVs.

A 2-fold serial dilution of serum (or mAbs) was set up in duplicate or triplicate, depending on the amount of serum (or mAbs) available, in white, flat-bottom, sterile Nunc 96-well microplates, at a starting dilution of 1:20 (160 μg/mL of mAb) in 50 μL. PV was then diluted in complete medium to add ~ 1×10^5 RLU or ~100 TCID₅₀ in 50 μL per well, except in the cell control wells (100% neutralisation) where 50 μL of complete medium (no PV) was added. A PV only control (0% neutralisation) with no serum (or mAb) was also set up. These controls establish the 100% and 0% neutralisation values that will be used to normalise the RLU readings in the assay. A negative serum containing no antibodies specific to the GP of interest was included in every assay. After the addition of PVs the final starting dilution was 1:40 (or 80 μg/mL of mAb). The plate was centrifuged for 1 min at 400 rpm (~21 g) then incubated at 37°C, 5% CO₂ for 1h to allow the antibodies to bind to the GP. Target cells (2×10^4 /well in 50 μL) were added and incubated for 48h at 37°C, 5% CO₂. After 48h, the media was removed and discarded; Bright-Glo™ reagent was added to the plate (25 μL of Bright-Glo™ : DPBS 1:1) and incubated at room temperature for 5 min before measuring luminescence. The data was normalised to the percentage reduction in luminescence according to the average RLU of the cell only (100% neutralisation) and PV only (0% neutralisation) controls and fitted into a non-linear regression model (log [inhibitor] vs. normalised response – variable slope) to interpolate the inhibitory concentrations at 50% (IC₅₀) and 90% (IC₉₀), that is, the reciprocal of the dilution at which 50% or 90% of PVs were inhibited, respectively. When using mAbs, the

interpolated concentrations of antibodies to achieve such reductions in RLU were reported.

2.7 ELISA using purified PVs as antigens

An in-house ELISA was developed and optimised using purified PVs as antigens to assess antibody binding, including binding of non-neutralising antibodies to the GP. An indirect ELISA with or without a capture antibody was optimised with monoclonal antibodies targeting the GP or convalescent serum as primary antibodies, followed by either an anti-mouse IgG for murine mAbs or an anti-human IgG for human mAbs or convalescent serum, conjugated with horseradish peroxidase. The protocol used was adapted from Dr Giada Mattiuzzo (NIBSC) who kindly advised on the method as well as the best secondary antibodies to avoid background signal. It is a standard ELISA protocol (Krähling *et al.* 2016) with a few adaptations detailed in 2.7.3.2.

2.7.1 PV purification

Purification of PV supernatant was performed on a 20% Sucrose cushion. A sterile 20% (v/v) Sucrose (Sigma) – DPBS solution was prepared and filtered. On the day of purification, 24 aliquots of 400 µL 20% Sucrose-DPBS were prepared in a cell culture cabinet. Next, 900 µL of PV supernatant were added to each 1.5 mL eppendorf tubes. Usually, 8 to 16 tubes were set up for each PV. They were placed in a previously cooled 4°C benchtop centrifuge (Micro Star 17R 521-1647BTU) for at least 2h at 17000 g. After centrifugation the supernatant and cushion were carefully removed leaving ~10 µL in each tube, then 35 µL of DPBS was added per tube. Finally, each resuspended purified PV was pooled and stored at -80°C for analysis.

2.7.2 Protein quantification assay

The Pierce™ BCA Protein Assay Kit (Thermo Scientific 23227) was used to quantify the amount of protein antigen present in each pooled purified PV. It is based on the reduction

of Cu^{2+} to Cu^+ by the presence of protein followed by the colorimetric detection of Cu^+ using bicinchoninic acid (BCA). Protein concentration was determined against a bovine serum albumin dilution series from 2000 $\mu\text{g}/\text{mL}$ to 0 $\mu\text{g}/\text{mL}$ according to the manufacturer's instructions. Briefly, a dilution series of BSA was prepared in DPBS to achieve final BSA concentrations of: 2000, 1500, 1000, 750, 500, 250, 125, 25 and 0 $\mu\text{g}/\text{mL}$. The BCA working reagent was prepared according to their instructions depending on the number of samples to be assayed:

$(\# \text{ standards} + \# \text{ unknowns}) \times (\# \text{ replicates}) \times (\text{vol of working reagent per sample}) = \text{total vol required.}$

In a flat bottom, transparent 96-well plate (Thermo Fisher Scientific), 25 μL of each standard or unknown sample was added in duplicates. Next, 200 μL of working reagent was added to each well and the plate rocked gently to mix. The cover was replaced and the plate incubated at 37°C for 30 min.

Whenever protein was present, the colour developed from green into purple. After 30 min, the plate was cooled to RT and read at 562 nm on a plate reader (Tecan Infinite® PRO). The standard curve was plotted and the unknown samples interpolated via a quadratic curve fit model as advised by the manufacturer for more accurate results.

2.7.3 ELISA

2.7.3.1 Reagents

Primary 1H3 and 4G7 murine monoclonal antibodies were donated by Dr Xiangguo Qiu (Public Health Agency, Winnipeg, Canada); KZ52 was donated by Dr Erica Saphire (Scripps Institute, Los Angeles, USA); CA45, FVM04 and FVM09 were donated by Prof Jonathan Heeney, University of Cambridge. EBOV convalescent serum was purchased from the National Institute for Biological Standards and Control (Potters Bar, UK).

Goat Anti-mouse HRP-conjugated IgG H+L (Stratech Scientific Ltd 115-035-146-JIR) and rabbit anti-human HRP-conjugated IgG H+L (Stratech Scientific Ltd 309-035-082-JIR) were used as secondary antibodies.

Negative human serum (Merck- Millipore H4522-20ML), collected from healthy humans tested negative for HIV-1/2, HIV-Ag, HCV and HBsAg, was used as a negative control serum.

2.7.3.2 ELISA protocol

On day 1, a Nunc MaxiSorp™ plate (Thermo Fisher Scientific 44-2404-21) was coated with 50 µg/mL PV per well or DPBS as a control (No PV) in 100 µL/well. When adding a capture antibody, a 1:400 dilution (~2.5 µg/mL) of 1 mg/mL antibody was prepared in coat buffer (DPBS), added 100 µL/well and incubated for 2h at RT, the plate washed twice with DPBS and PVs added at 50 µg/mL per well as described above. The plate was sealed and stored overnight at 4°C.

On day 2, the plate was washed twice with 300 µL/well of DPBS, blocked with 200 µL/well 2% (v/v) fish gelatin (Merck- Millipore G7765-250ML) in DPBS for 1h at RT. The plate was washed twice with 300 µL DPBS-Tween 0.05% (v/v) per well, 100 µL/well samples in diluent buffer (DPBS-10% v/v FBS) were added and incubated for 2h at RT. The plate was washed twice with DPBS-Tween as described and 100 µL/well of secondary antibody was added (1:5000 to 1:100000) in diluent buffer and incubated for 1h at RT. The plate was then washed twice with DPBS-Tween as described and 100 µL/well of TMB (1-Step™ Ultra TMB-ELISA Substrate Solution, Thermo Fisher Scientific 34028) previously warmed to RT was added and let it develop for ~15 min before stopping with 1M H₂SO₄ solution and read at 450 nm (Tecan Infinite® PRO).

2.8 Data Analysis

Data was analysed with Excel for Mac 2011 and Prism 8, including all graphs, standard curves, non-linear regression and quadratic fit model analysis.

Methods that are more specific to particular studies are described in detail in the appropriate chapters.

CHAPTER 3: Generation and Optimisation of Filovirus Pseudotypes

3.1 Introduction

Filoviruses are members of the *Filoviridae* family and possess non-segmented negative strand RNA genomes. Some filovirus species are highly pathogenic and have been responsible for several sporadic, and more recently, sustained outbreaks of Ebola virus disease (EVD) with high case fatalities rates in West Africa (Mbala-Kingebeni *et al.* 2019; Languon and Quaye 2019), and the DRC between 2018-2020 (WHO). Marburg virus strains are also highly pathogenic but have caused less frequent outbreaks (Languon and Quaye 2019; Amman *et al.* 2020); and two new genera have been described after filoviral RNA was found in bats in Europe and Asia, but have thus far not been reported to cause disease in humans (Negredo *et al.* 2011; Yuan *et al.* 2012; Kemenesi *et al.* 2018; Yang *et al.* 2019).

Research efforts have been hindered by the need of high-containment facilities, therefore any means of circumventing this would be highly beneficial. As a result, pseudotype viruses (PVs) have been applied to research of these pathogens, as they are a safe alternative to using authentic viruses. PVs consist of the core of one virus bearing the surface glycoprotein(s) (GP) of the virus of interest, usually with part or most of the genome replaced by a transgene (Carnell *et al.* 2015). There is a range of reporter genes that can be selected according to budget and ease of use. For serological studies, pseudotype-based neutralisation assays have high sensitivity and are amenable to multiplexing (Wool-Lewis and Bates 1998; Sinn *et al.* 2003; Wright *et al.* 2009; Molesti *et al.* 2014; Carnell *et al.* 2015; Ferrara and Temperton 2018). More specifically, PVs have been used in filovirus research for receptor usage and tropism studies (Maruyama *et al.* 2014; Mohan *et al.* 2015; Ng *et al.* 2015; Goldstein *et al.* 2018; Yang *et al.* 2019; Takadate *et al.* 2020); vaccine delivery and evaluation of immunogenicity (Ewer *et al.* 2016; Collier *et al.* 2017; Venkatraman *et al.* 2018); antiviral screening (Barrientos *et al.* 2004) and serological studies (Steffen *et al.* 2020).

In this study, a range of PVs from the *Filoviridae* family have been generated and optimised for use in antibody assays, with representatives from three genera of filoviruses: *ebolavirus* (EBOV, SUDV, BDBV and RESTV); *marburgvirus* (RAVV, MARV –

Angola and MARV – DRC) and *cuevavirus* (LLOV). In addition, control PVs from the *arenaviridae* family: *mammarenavirus* (LASV) and *orthomyxoviridae* family - *alphainfluenzavirus* (H3 subtype) were generated.

LASV PVs were generated using the 3-plasmid protocol described for filovirus PVs in Chapter 2. Influenza PVs however, require neuraminidase activity to release virions after budding, either as a co-transfected plasmid, or added exogenously post-transfection, as well as a HA-cleaving protease necessary for infectivity. The neuraminidase (NA) is responsible for cleaving sialic acids, releasing virions as they bud out of the producer cell membrane, while the protease is responsible for cleaving the hemagglutinin (HA) precursor (HA0) into the fusion competent HA1 and HA2 subunits (Bottcher-Friebertshauer *et al.* 2010; Carnell *et al.* 2015; Ferrara and Temperton 2018).

For the majority of the study, including all antibody assays described in this thesis, a lentiviral (HIV-1) core was used for PV production with a firefly luciferase reporter gene lentiviral vector. Green fluorescent protein was also used as a reporter gene for validation of PV production by microscopy and analysis of the dynamics of a viral particle devoid of glycoprotein (Δ env), used as a negative control in infectivity assays. Additional quality control checks for PV production was achieved using a commercial ELISA kit and an RT-PCR based reverse transcriptase assay (SG-PERT) for lentiviral core PVs (described in Chapter 2).

PV production was based on previously described protocols for influenza virus (Temperton *et al.* 2007; Scott *et al.* 2012; Carnell *et al.* 2015; Ferrara and Temperton 2018). Optimisation was performed with varying amounts of GP expressing plasmids in transfection experiments, as it has been reported to be an important aspect in filovirus PV generation (Mohan *et al.* 2015). A range of cell culture vessels and transfection reagents were evaluated in order to examine impact on production titres, as well as producer cells (HEK293T) that had been cultured in different laboratories, possibly generating different clones. Also, production was upscaled to larger culture vessels to maintain PV single batch consistency in downstream experiments.

Filovirus PVs were also produced using vesicular stomatitis virus (VSV) as a core. Initial recombinant VSV (rVSV Δ G) stocks bearing the coccal glycoprotein were generated by Dr Mariliza Derveni at the University of Sussex, some of which were kindly donated to us. Here, rVSV Δ G-cocal stocks were amplified and used to infect HEK293T cells displaying filovirus and LASV glycoprotein complex to generate rVSV-GP PVs, as described in Chapter 2, for comparison to lentiviral core PVs.

3.2 Materials and Methods

3.2.1 Gene constructs and plasmids

Filovirus GP genes (Appendix I) were described in Chapter 2. LASV GPC (glycoprotein complex) gene construct was a gift from Dr Edward Wright (University of Sussex); influenza HA and NA gene constructs were provided by Dr Simon Scott and Dr Nigel Temperton (University of Kent). All filovirus and LASV genes were provided or cloned into pCAGGS expression vector; and influenza HA and NA genes were provided in the pI.18 expression vector (Figure 3.1). One unit of exogenous NA (Sigma N2876) was also utilised to generate influenza PVs that harboured HA only. The human airway trypsin-like protease (HAT) was provided in the pCAGGS expression vector by Eva Böttcher-Friebertshäuser, Institute of Virology, Philipps University, Marburg, Germany.

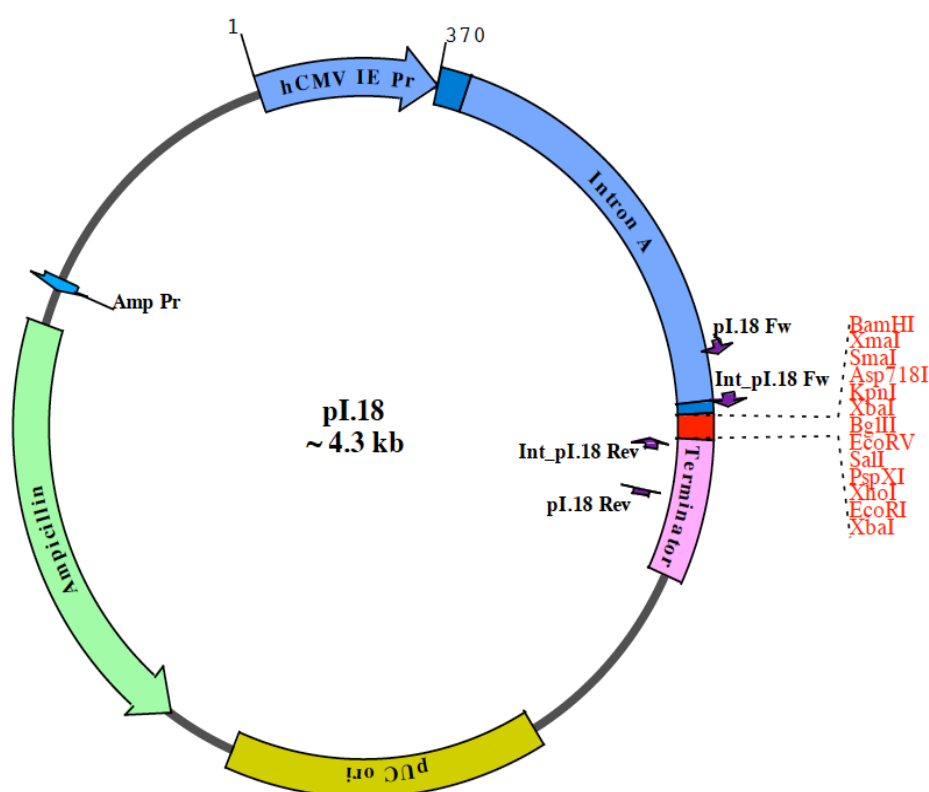


Figure 3.1. pI.18 expression vector. Gene expression is under the CMV promoter (blue arrow). The ampicillin resistance gene (green arrow) allows selection in cloning experiments. Multiple cloning site (MCS) is shown in red. Sequencing primer sites are indicated as well. The plasmid was developed by I. Tarpey and N. Greenwood (US patent number US6187759 B1). Source: Viral Pseudotype Unit.

3.2.2 Cloning and Sanger sequencing

Cloning of MARV (Angola) and MARV (DRC) genes (gBlocks® - Integrated DNA Technologies) and LightRun Sanger sequencing was performed as described in Chapter 2 in Dr. Edward Wright's lab. All other envelope glycoproteins had already been cloned into pCAGGS. Transformation of competent *E. coli* DH5 α cells, overnight cultures, glycerol stocks and plasmid preparations were performed as described in Chapter 2. After transformation correct sequences were confirmed with LightRun Sanger sequencing.

3.2.3 PV generation

3.2.3.1 Lentiviral (HIV-1) core

3.2.3.1.1 Luciferase reporter gene

The generation of filovirus PVs in T25 and T75 flasks using PEI transfection reagent was described in detail in Chapter 2. PV production was also attempted in 5-cm dishes (Thermo) using the same conditions, and in 6-well plates (Thermo) using an influenza PV production protocol with 500 ng env, 500 ng p8.91 (gag-pol) and 750 ng pCSFLW (luciferase reporter). Further optimisation was attempted in T25 flasks with varying degrees of env input: 100 ng, 300 ng, 500 ng, 700 ng, 900 ng, 1.1 μ g and 1.5 μ g for EBOV, LLOV and RAVV PVs.

Different transfection reagents were also tested (in T25 flasks): Transfectin™ (Bio Rad), Superfect® (Qiagen), Viafect™ (Promega), Fugene® HD (Promega), and PEI. All transfections were performed according to the manufacturer's protocol.

Seeding of HEK293T cells and subsequent media change before transfection was performed as described in Chapter 2. The amount of plasmid DNA was constant for all transfections: 0.7 μ g env, 0.7 μ g p8.91 and 1.1 μ g pCSFLW, prepared in opti-MEM to improve complex formation.

Briefly, for Transfectin™ the DNA mix was prepared in 500 μ L opti-MEM. In a separate tube, 20 μ L of Transfectin™ reagent was gently mixed in 500 μ L optiMEM by tapping before being added to the DNA mix and incubated for 20 min at RT. The reagent-DNA mix

was then added to the T25 flask and rocked gently to disperse evenly. The following day the medium was replaced with 4 mL complete medium and incubated at 37°C, 5% CO₂ for 48h before being harvested.

For Superfect® the DNA mix was prepared in 150 µL optiMEM. Next, 30 µL of Superfect® was added directly in the DNA mix and pipetted up and down 5 times, before being incubated for 10 min at RT. Next, 600 µL complete medium was added to the reagent-DNA mix, pipetted up and down twice, added immediately to the T25 flask and rocked gently. It was incubated for 3h at 37°C, 5% CO₂ then washed with 1 mL DPBS and 4 mL complete medium added. Finally it was incubated at 37°C, 5% CO₂ for 48h then harvested. A modified protocol was attempted leaving the reagent-DNA mix incubated overnight with medium being replaced the following day, as described in other reagent protocols, when PV titres were low after following the manufacturer's protocol.

For Viafect™ the DNA mix was prepared in 250 µL optiMEM. In a separate tube, 20 µL of Viafect™ reagent was gently mixed in 250 µL optiMEM before being added to the DNA mix and incubated for no longer than 20 min at RT. The reagent-DNA mix was then added to the T25 flask and rocked gently. The following day the medium was replaced with 4 mL complete medium and incubated at 37°C, 5% CO₂ for 48h before being harvested.

For Fugene® HD the DNA mix was prepared in 250 µL optiMEM. In a separate tube, 20 µL of Fugene® HD reagent was gently mixed in 250 µL optiMEM by tapping before being added to the DNA mix and incubated for 15 min at RT. The reagent-DNA mix was then added to the T25 flask and rocked gently. The following day the medium was replaced with 4 mL complete medium and incubated at 37°C, 5% CO₂ for 48h before being harvested.

In order to assess whether producer HEK293T cells that had been sub-cultured in a different laboratory would have an impact on PV titre, stocks obtained from Dr Edward Wright were sent to us. After four passages in our lab, those HEK293T cells were used for PV production in T25 flasks using PEI as described. EBOV, RAVV and Influenza H3N9 PVs were generated as well as virions bearing no envelope GP (Δ env) for comparison.

3.2.3.1.2 eGFP reporter gene

PV production with eGFP was performed in 6-well plates. 8×10^5 HEK293T cells were seeded in each well the day before transfection. Next, transfection was set up using PEI as

described with 500 ng env, 500 ng p8.91 (gag-pol) and 750 ng pCSeGW (eGFP). LASV was used as a control.

Harvested PVs were used to transduce target cells seeded in 6-well plates. PV dilutions (10-fold) were prepared with 10 µg/mL polybrene. In the no infection control well (“mock”), complete medium and polybrene were added (No PV). Cells were incubated at 37°C, 5% CO₂ for at least 48h.

3.2.3.2 Recombinant Vesicular Stomatitis Virus (luc) core

Generation of VSV core PVs has been described in detail in Chapter 2.

3.2.4 Quality control of Lentiviral PV production

A virion-associated p24 ELISA (QuickTiter™ Lentivirus Titer Kit) and RT-PCR based assay (SG-PERT) measuring reverse transcriptase activity using a recombinant HIV-1 reverse transcriptase (Merck-Millipore 382129-500U) were utilised as quality controls in PV production. They have been described in detail in Chapter 2.

3.2.5 Statistical analysis

Infectivity assay data was analysed with Excel for Mac 2011 to normalise luminescence results to relative light units per mL (RLU/mL) and presented as log (RLU/mL). Infectivity graphs were plotted in Prism 8 as the mean log (RLU/mL) ± standard deviation of at least two independent experiments.

TCID₅₀ graphs were also plotted in Prism 8 after titre calculated in Excel.

In infectivity assays, the Mann-Whitney test was used to determine statistical significance in comparison to Δenv PVs assuming a non-parametric distribution of titre values.

To compare differences in titres between different producer and target cell lines, the Kruskal-Wallis test was used, a non-parametric test to compare two or more independent groups.

3.3 Results

3.3.1 Cloning of MARV (Angola) and MARV (DRC)

Synthesised MARV genes (Angola and DRC strains) were digested with *EcoRI* and *NheI* along with pCAGGS; ligation reactions set; competent bacterial cells transformed, glycerol stocks and plasmid preparation performed as described in Chapter 2.

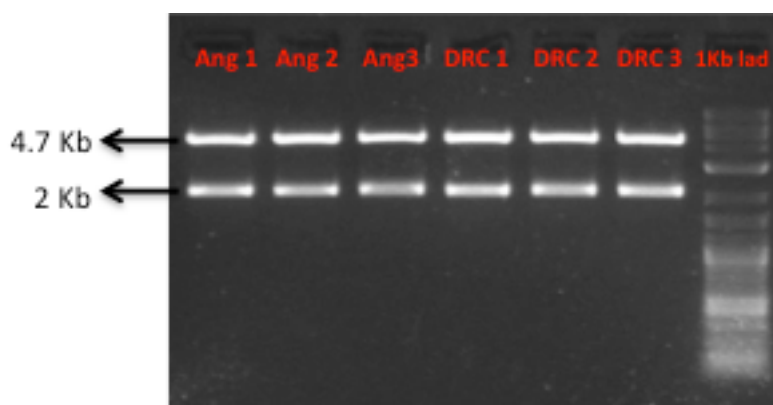


Figure 3.2: Restriction digestion with *EcoRI* and *NheI* of miniprep of cloned MARV genes. Three colonies were picked from each transformation. MARV (Angola): Ang 1, Ang 2 and Ang3; and MARV (DRC): DRC 1, DRC 2 and DRC 3. The 2 Kb band from each gene and the 4.7 Kb pCAGGS bands are shown next to the Quick-Load® Purple 1 kb Plus DNA Ladder – New England Biolabs.

Three clones from each gene were picked and a diagnostic fast digestion with *EcoRI* and *NheI* was performed (Figure 3.2) to check the 2 kb gene and the 4.7 kb plasmid could be identified separately. Clones used for PV generation were confirmed by sequencing before transfection as previously described.

3.3.2 Lentiviral (HIV-1) core PV generation – luciferase reporter

3.3.2.1 PV generation in different transfection reagents and cell culture vessels utilising established protocols

Initial PV production was attempted for EBOV, SUDV, BDBV and RAVV in T25 flasks and 5-cm dishes, utilising a previously optimised transfection protocol for production of influenza PVs with PEI as the transfection reagent. Resulting production titres were high ranging from approximately 1×10^8 RLU/mL for *ebolavirus* PVs EBOV, SUDV and BDBV and 1×10^{10} RLU/mL for *marburgvirus* RAVV PVs harvested 48h post-transfection, either in T25 flasks (Figure 3.3a) or 5-cm dishes (Figure 3.3c). PVs harvested 72h post-transfection had

production titres approximately 10-fold lower than 48h post-transfection PVs, either in T25 flasks (Figure 3.3b) or 5-cm dishes (Figure 3.3d).

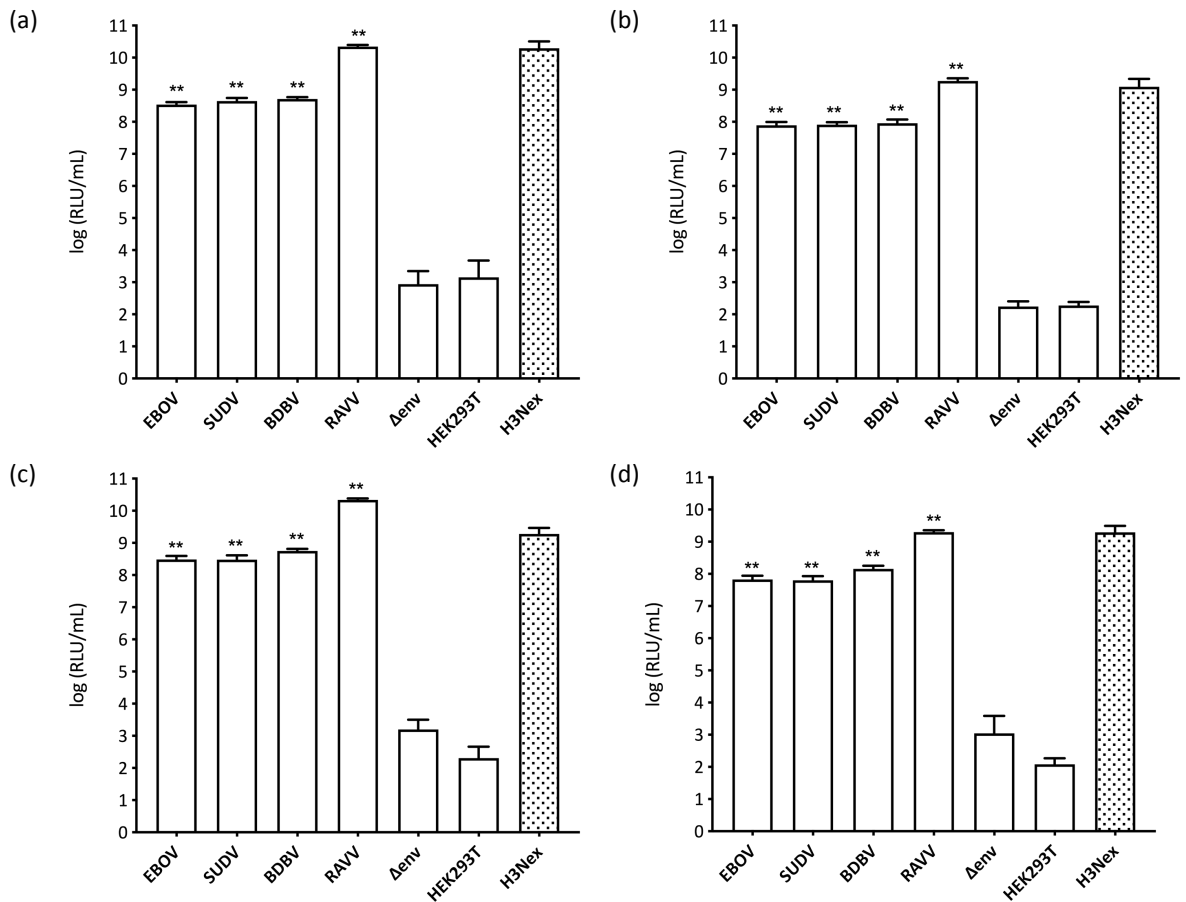


Figure 3.3. Generation of *ebolavirus* (EBOV, SUDV and BDBV) and *marburgvirus* (RAVV) PVs. PVs were produced in: (a) T25 flask, 48h harvest; (b) T25 flask, 72h harvest; (c) 5-cm dish, 48h harvest and (d) 5-cm dish, 72h harvest. Transduction titres are expressed as the mean \pm s.d log (RLU/mL) values of at least three independent experiments. H3Nex is a previously titrated canine influenza (subtype H3) PV where budding was achieved with the addition of exogenous NA (Nex). Titre from lentiviral particles bearing no GP (Δ env) and background luminescence from uninfected cells (HEK293T) is also shown. Graph and statistical significance (** $p < 0.001$ Mann-Whitney test) in comparison to Δ env determined with Prism 8.

Considering influenza PVs had been produced successfully with high titres in 6-well plates previously, an attempt was made with filovirus PVs. Functional PV titres were observed, however these were approximately 10 to 100-fold lower than filovirus PVs generated in T25 flasks (Figure 3.3), either after a 48h harvest (Figure 3.4a) or a 72h harvest (Figure 3.4b).

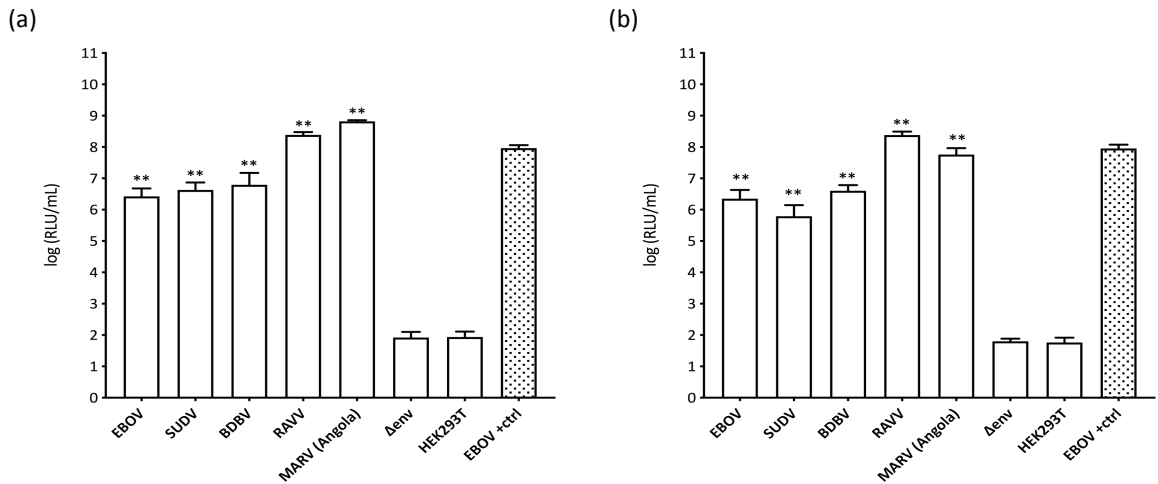


Figure 3.4. Generation of *ebolavirus* (EBOV, SUDV and BDBV) and *marburgvirus* (RAVV) PVs in 6-well plates. PVs were harvested at (a) 48h and (b) 72h post-transfection. Transduction titres are expressed as the mean \pm s.d log (RLU/mL) values of two independent experiments. EBOV +ctrl is a previously titrated PV. Titre from lentiviral particles bearing no GP (Δ env) and background luminescence from uninfected cells (HEK293T) is also shown. Graph and statistical significance (** $p < 0.001$ Mann-Whitney test) in comparison to Δ env determined with Prism 8.

Finally, different transfection reagents were used for PV production: Transfectin, Superfect, Viafect and Fugene HD, as well as PEI. Two *ebolavirus* species (EBOV and SUDV) PVs were compared. Fugene HD and PEI yielded the highest titres (Figure 3.5). For SUDV PVs, functional titres were significantly higher ($p = 0.004$) when transfections were carried out with FugeneHD (Figure 3.5). No significant difference in titres was observed between most transfection reagents.

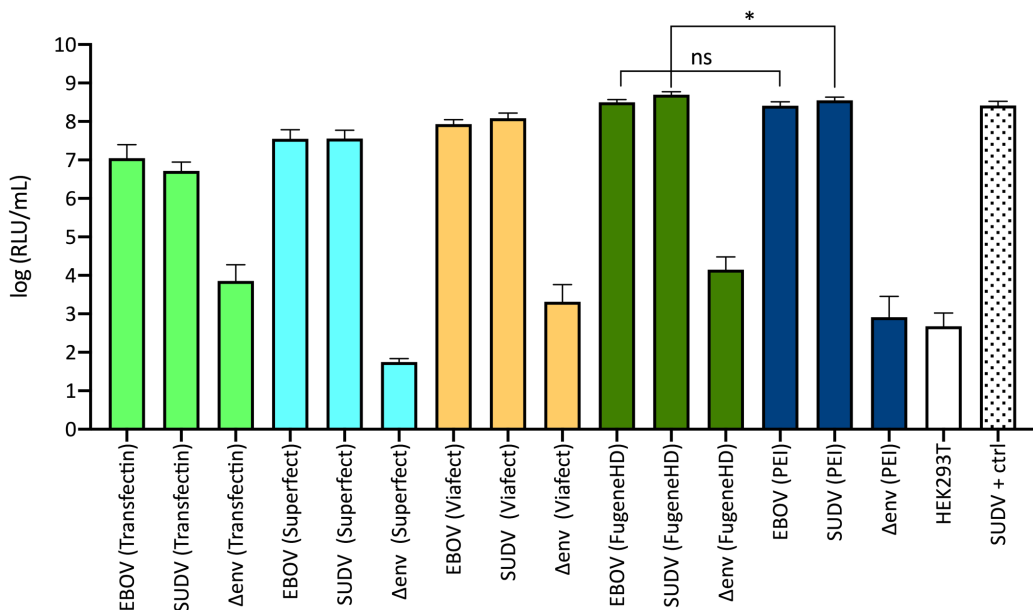


Figure 3.5. Evaluation of transfection reagents in lentiviral core filovirus PV production. SUDV +ctrl is a previously generated PV of known titre. Titre from lentiviral particles bearing no GP (Δ env) and background luminescence from uninfected cells (HEK293T) is also shown. Graph and statistical significance (* $p < 0.05$ Mann-Whitney test) calculated with Prism 8.

Transfectin yielded the lowest titres of approximately 1×10^7 RLU/mL (Figure 3.5). Superfect yielded high titres (Figure 3.5) once the manufacturer's protocol was modified to include an overnight incubation with the transfection mix.

To further evaluate those differences and understand the reasons SUDV yielded significantly higher titres when generated with FugeneHD but not EBOV, individual titre points are shown (Figure 3.6) in a linear scale to make those differences more apparent. SUDV indeed has a higher titre with FugeneHD than PEI, in comparison to EBOV (Figure 3.6).

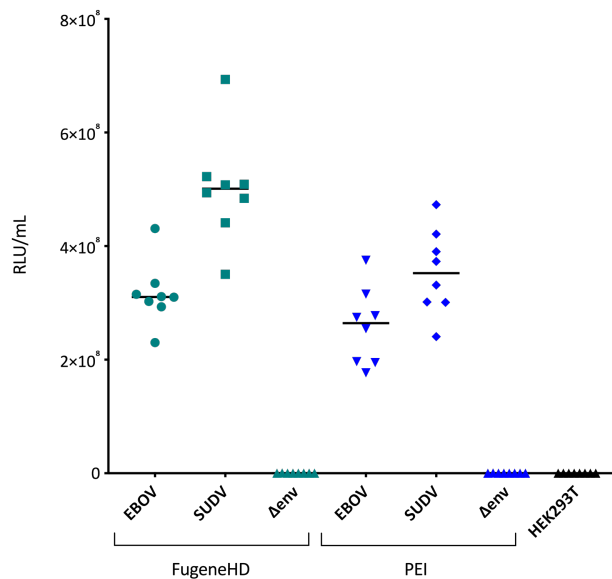


Figure 3.6. Evaluation of FugeneHD and PEI in lentiviral core filovirus PV production. Functional titre expressed in a linear scale showing variation in transduction titres. Titre from lentiviral particles bearing no GP (Δenv) and background luminescence from uninfected cells (HEK293T) is also shown. Graph and statistical significance ($*p < 0.05$ Mann-Whitney test) calculated with Prism 8.

3.3.2.2 PV generation utilising HEK293T producer cells sourced from another laboratory

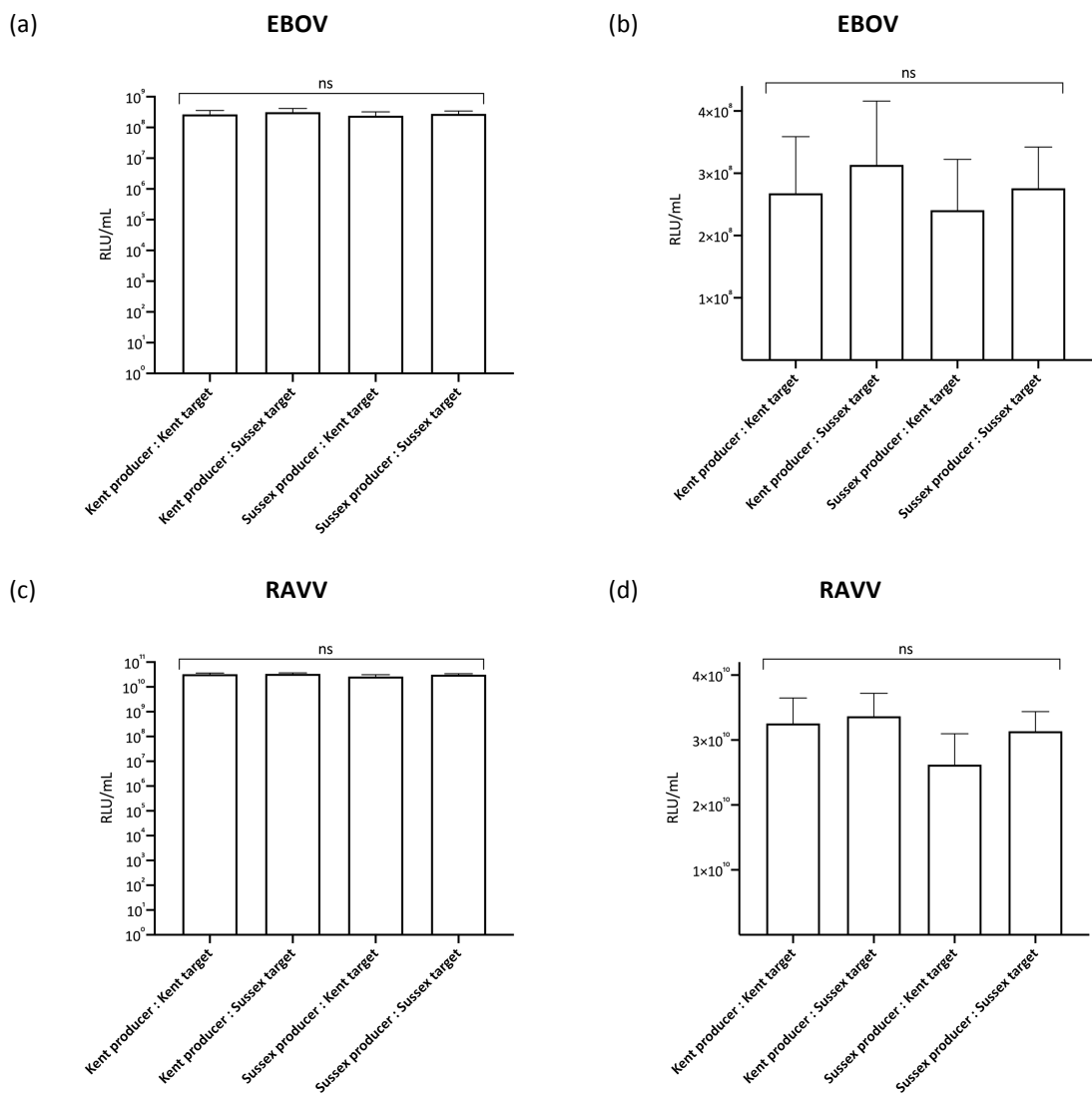
Lentiviral PV generation has been successful in HEK293T producer cells as their innate immune response does not affect lentiviral titres, through dampening of interferon and cytokine secretion (Ferreira *et al.* 2020). They have been utilised extensively in PV production.

We hypothesised that cells that were being passaged in different labs for lengthy periods might result in phenotypic differences affecting PV titre. Thus, we obtained HEK293T cells from Dr Edward Wright's lab at the University of Sussex, subcultured them separately

from Kent stocks, and used these to generate EBOV, RAVV and Influenza H3N9 PVs to assess any differences in PV production resulting from these cells.

EBOV, RAVV and H3N9 PVs were generated in T25 flasks as described on Chapter 2 using HEK293T producer cells originating from the Viral Pseudotype Unit in Kent or Sussex Universities. Then, transductions were performed using these cells as targets resulting in PVs generated in Kent HEK293T producer cells being tested in either Kent or Sussex HEK293T target cells; and PVs generated in Sussex HEK293T producer cells also being tested in either Kent or Sussex HEK293T target cells.

Functional titres were consistent with previously produced PV in T25 flasks (Figure 3.3). In addition, titres were consistent within the different permutations between the different producer and target cells. To further evaluate differences in functional titres from each producer cell, PVs were grouped by species for ease of comparison (Figure 3.7).



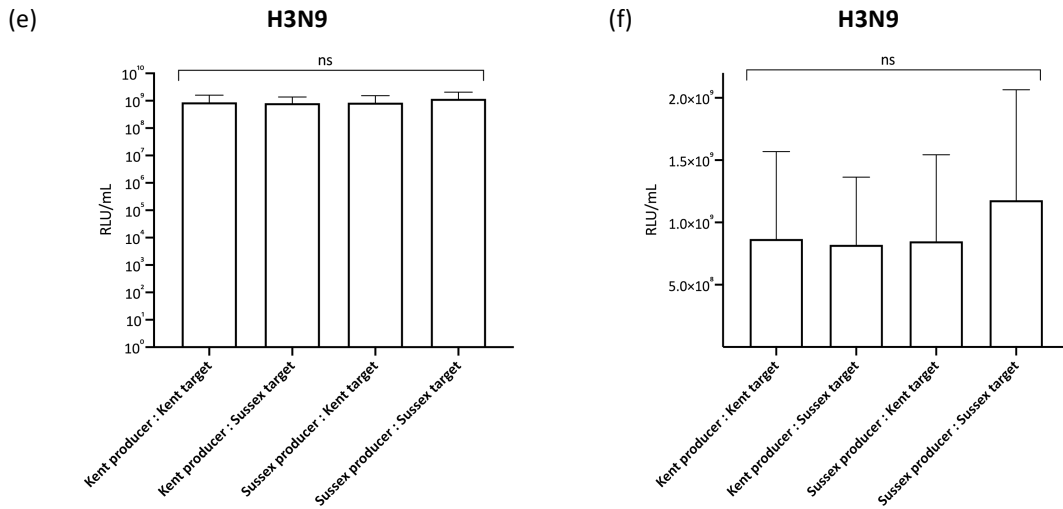


Figure 3.7. Comparison of filovirus and influenza PVs in HEK293T cells originating from different VPU labs: Kent and Sussex. Titres are expressed in log and linear scales for (a-b) EBOV, (c-d) RAVV and (e-f) H3N9 PVs, as the mean \pm s.d RLU/mL values of two independent experiments. Graphs and statistical significance (Kruskal-Wallis test comparing the four independent groups; ns = not significant) calculated with Prism 8.

EBOV PVs yielded titres of approximately 1×10^8 RLU/mL regardless of which producer or target cell line (Figure 3.7a and 3.7b), with ~ 0.5 -fold variation in a linear scale (Figure 3.7b); RAVV PVs yielded titres of approximately 1×10^{10} RLU/mL regardless of which producer or target cell line (Figure 3.7c and 3.7d), with ~ 0.5 -fold variation in a linear scale (Figure 3.7d) and H3N9 PVs yielded titres of approximately 1×10^9 RLU/mL regardless of which producer or target cell line (Figure 3.7e and 3.7f), with ~ 0.5 -fold variation in a linear scale (Figure 3.7f). Differences between the groups were not statistically significant ($p > 0.05$).

3.3.2.3 Optimising envelope input for PV generation

Further optimisation was attempted by varying amounts of envelope glycoprotein expressing plasmids for PV generation in T25 flasks, with one species from each genus.

In HEK293T target cells, EBOV PV titres were inversely proportional to the amount of envelope GP and the optimal amount of EBOV env was 300 ng, varying from 5.4×10^6 RLU/mL with 1500 ng of env and 4.1×10^8 RLU/mL with 300 ng of env (Figure 3.8a). LLOV PV titres decreased slightly as amount of env increased (Figure 3.8b) and RAVV PV titres remained constant as the amount of env increased (Figure 3.8c). For EBOV and LLOV, PVs generated with 100 ng of envelope had statistically significant higher titres ($p < 0.0002$)

than PVs generated with 1500 ng envelope input. For RAVV, there were no statistically significant differences in titres.

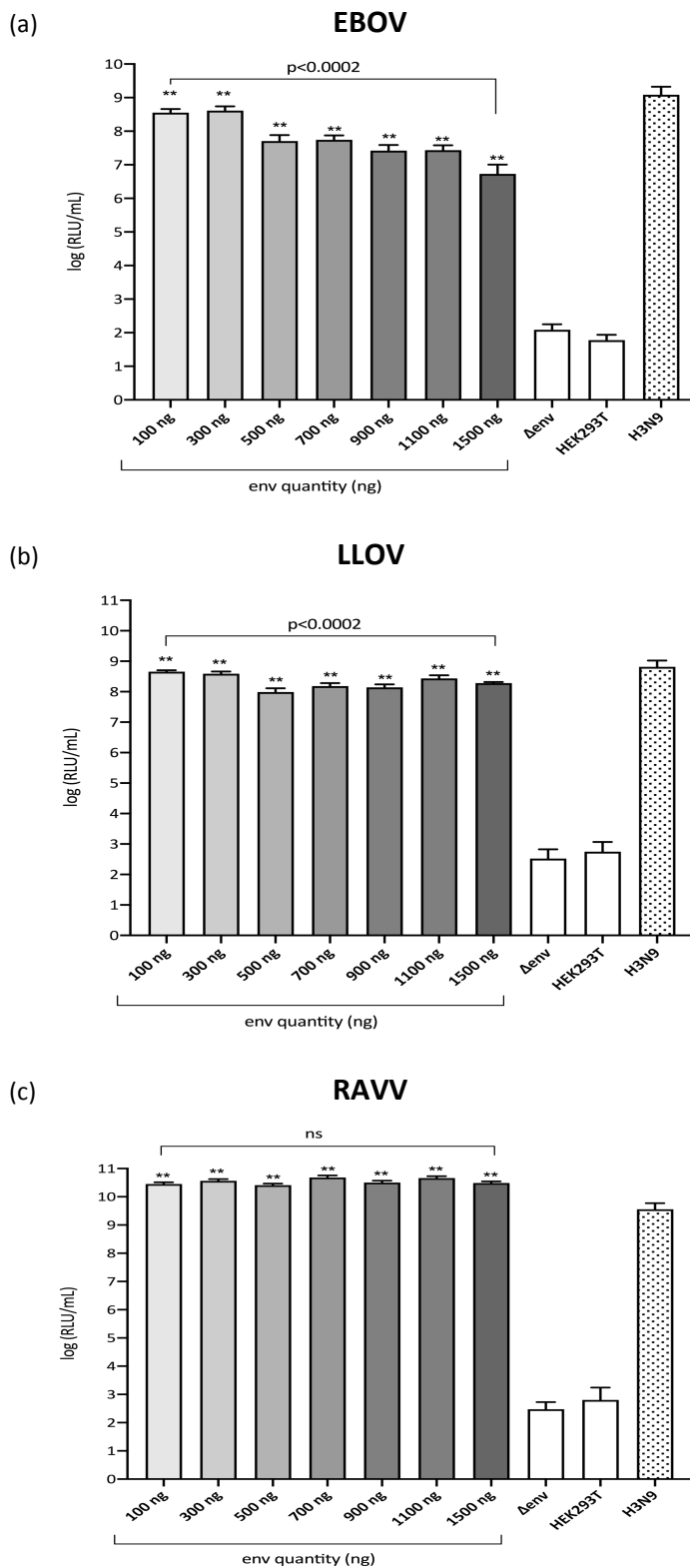


Figure 3.8. Filovirus PV env optimisation. (a) EBOV, (b) LLOV and (c) RAVV PVs in HEK293T target cells. Transduction titres are expressed as the mean \pm s.d log (RLU/mL) values of two independent experiments. Titre from lentiviral particles bearing no GP (Δ env) and background luminescence from uninfected (HEK293T) are also shown. Statistical significance (** $p < 0.001$ Mann-Whitney test) in comparison to Δ env for PV production, as well as between PVs generated with 100 ng or 1500 ng envelop input ($p < 0.0002$ Mann-Whitney test; ns: not significant) are shown. Graphs and statistics calculated with Prism 8.

In CHO-K1 target cells, which were found to be a good cell target for EBOV PVNAs (Bentley *et al.* 2016), a similar trend in titre decrease was observed.

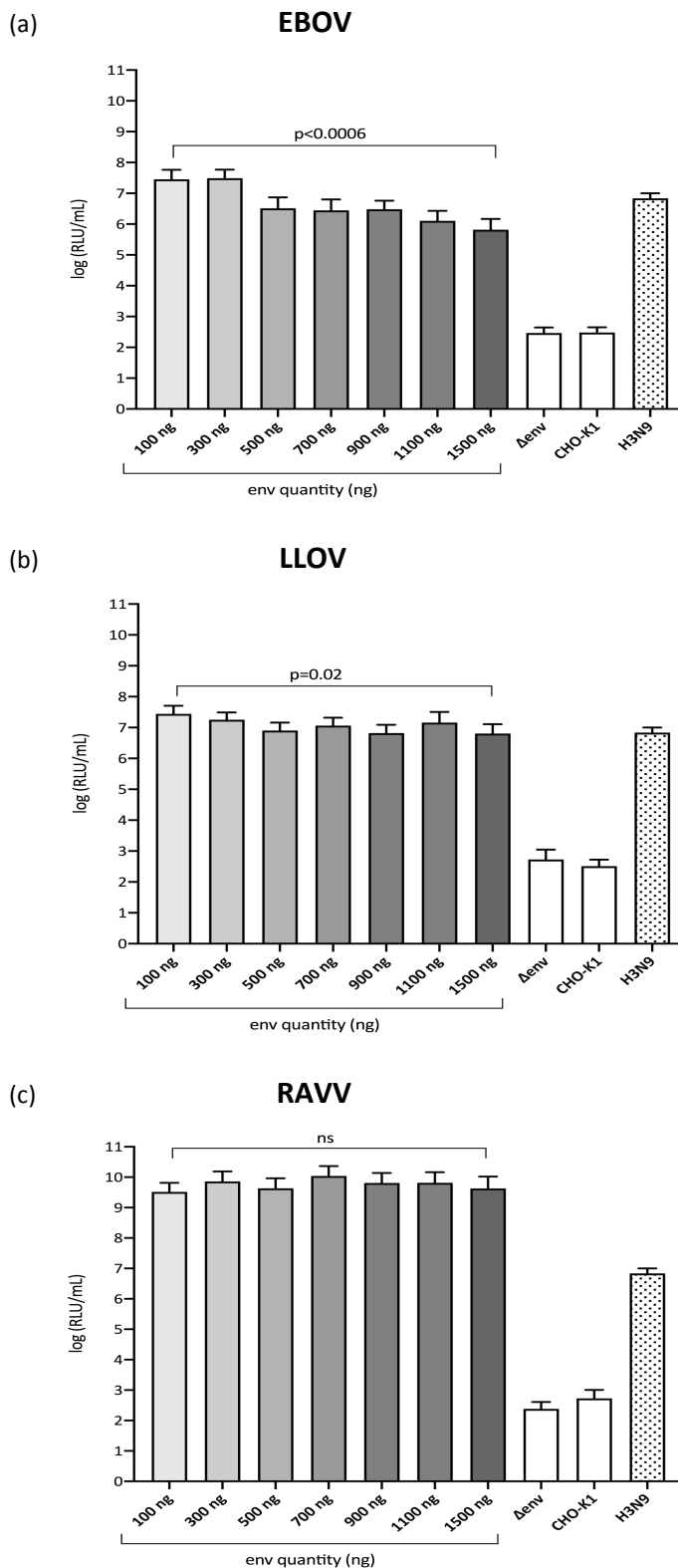


Figure 3.9. Filovirus PV env optimisation in CHO-K1 target cells. (a) EBOV, (b) LLOV and (c) RAVV PVs in CHO-K1 target cells. Transduction titres are expressed as the mean \pm s.d log (RLU/mL) values of two independent experiments. Titre from lentiviral particles bearing no GP (Δ env) and background luminescence from uninfected (CHO-K1) are also shown. Statistical significance between PVs generated with 100 ng or 1500 ng envelope input (Mann-Whitney test; ns: not significant) is shown. Graphs and statistics calculated with Prism 8.

EBOV PV titres were inversely proportional to the amount of envelope GP and the optimal amount of EBOV env was 300 ng, varying from 6.5×10^5 RLU/mL with 1500 ng of env and 3.1×10^7 RLU/mL with 300 ng of env (Figure 3.9a). LLOV PV titre differences (Figure 3.9b) were also more subtle than EBOV; and in RAVV PVs (Figure 3.9c) there was no statistically significant differences in titres between the lower and higher envelope input.

3.3.2.4 Upscaling PV production

Upscaling filovirus PV production to larger flasks was attempted to decrease the number of transfection experiments necessary as well as minimising variation and improving consistency in PV production, especially for future lyophilisation experiments as using PV from the same batch would decrease the number of variables in subsequent tests. Consequently, transfections to generate filovirus PVs previously carried out in T25 flasks were upscaled to T75 flasks (Chapter 2). Also included were newly acquired env GPs for RESTV, LLOV, MARV (Angola) and MARV (DRC), as well as LASV PV to be used as controls (Figure 3.10). *Ebolavirus* and *cuevavirus* PVs yielded usual T25 titres of approximately 1×10^8 RLU/mL and *marburgvirus* PVs yielded titres of approximately $1 \times 10^9 - 1 \times 10^{10}$ RLU/mL (Figure 3.10).

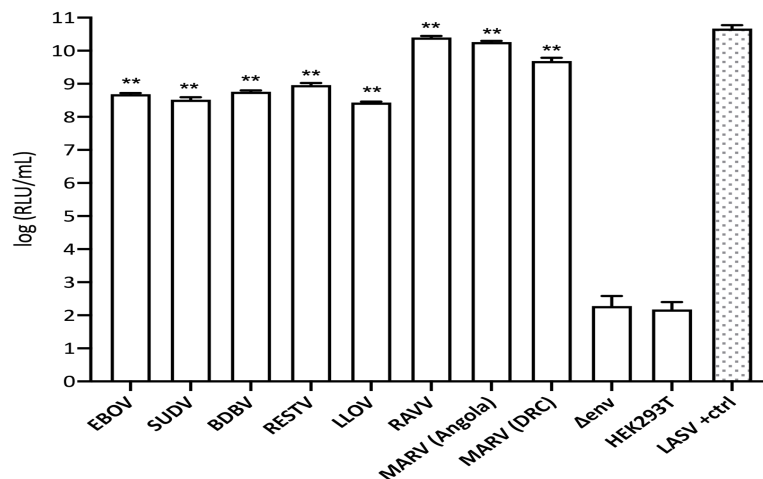


Figure 3.10. Filovirus PV upscaled production. Transduction titres are expressed as the mean \pm s.d log (RLU/mL) values of two independent experiments. Titre from lentiviral particles bearing no GP (Δ env) and background luminescence from uninfected cells (HEK293T) is also shown. Graph and statistical significance (** $p < 0.001$ Mann-Whitney test) in comparison to Δ env determined with Prism 8.

3.3.2.5 Target cell lines for Filovirus PVs

Filovirus PVs were used to transduce different cell lines to assess transduction efficiency. Human cell lines such as Huh-7 were permissive (Figure 3.11a), albeit to approximately 10-fold lower titres in comparison to HEK293T. MDCK-II cells, used as targets for certain influenza PVs, had titres comparable to HEK293T cells (Figure 3.11b). Vero cells, used for propagating authentic filoviruses, had titres 1000-fold lower than HEK293T and the influenza control did not transduce these cells (Figure 3.11c), as these cells restrict HIV-1. A more extensive panel of PVs was tested in CHO-K1 cells (Figure 3.11d); yielding titres approximately 10-fold lower than observed in HEK293T cells.

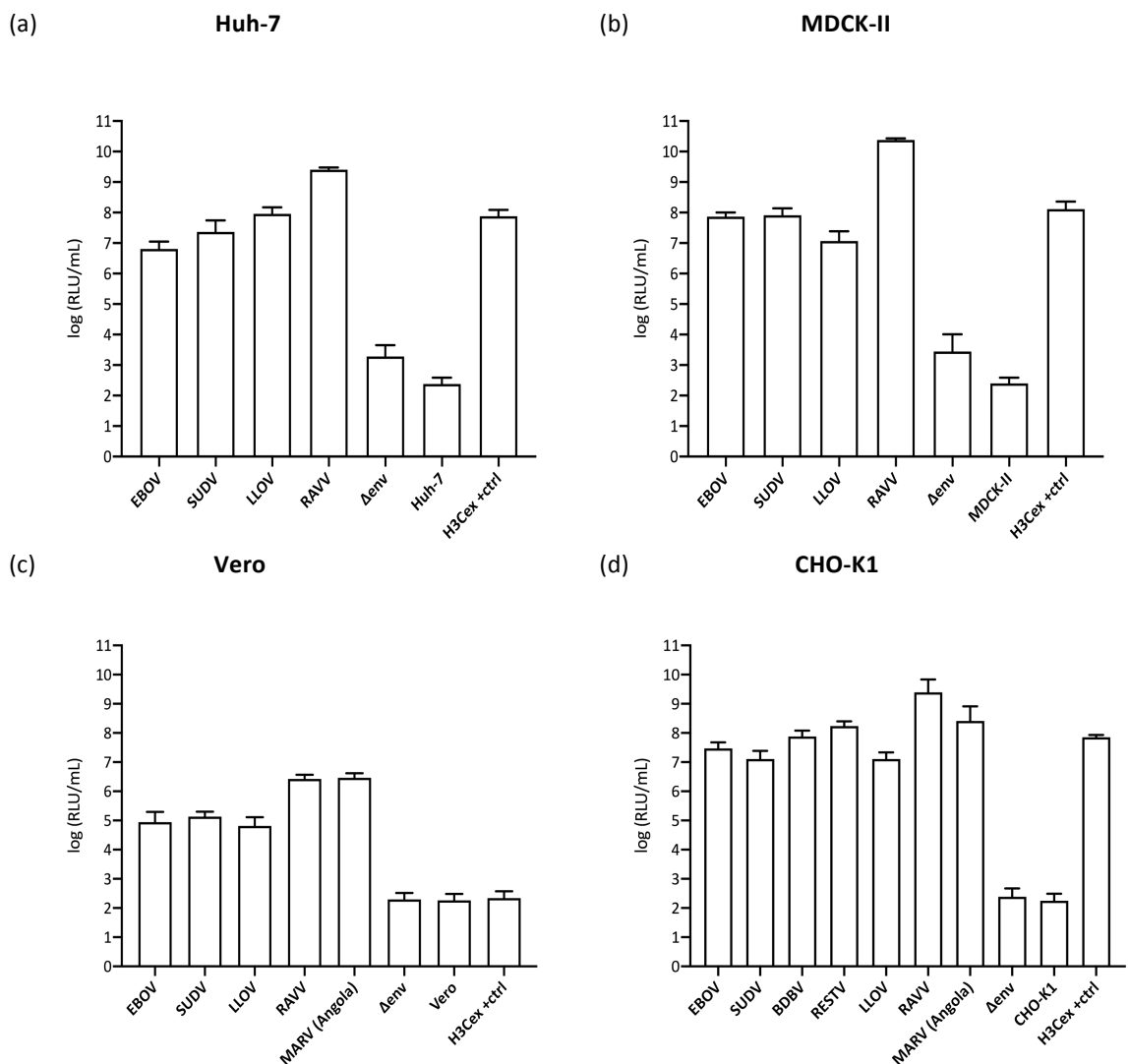


Figure 3.11: Filovirus PV functional titres in different target cell lines. (a) Huh-7, (b) MDCK-II, (c) Vero and (d) CHO-K1 target cells. Transduction titres are expressed as the mean \pm s.d log (RLU/mL) values of two independent experiments. Titre from lentiviral particles bearing no GP (Δ env) and background luminescence from uninfected cells (HEK293T) is also shown. Graphs generated with Prism 8.

3.3.2.6 TCID₅₀ – 50% Tissue Culture Infective Dose assay

A TCID₅₀ assay was performed to standardise virus input and produce comparable titres to the literature (Fields, Knipe and Howley 2013; Hoffmann *et al.* 2019).

Ebolavirus (EBOV, SUDV and RESTV) and *cuevavirus* (LLOV) PVs all yielded titres of approximately 1×10^4 TCID₅₀/mL (Figure 3.12), whereas *marburgvirus* (RAVV) and LASV PVs yielded titres of approximately 1×10^6 TCID₅₀/mL (Figure 3.12). These titres were used to standardise PV input in neutralisation assays (100 TCID₅₀/well - $\sim 10^5$ RLU/well).

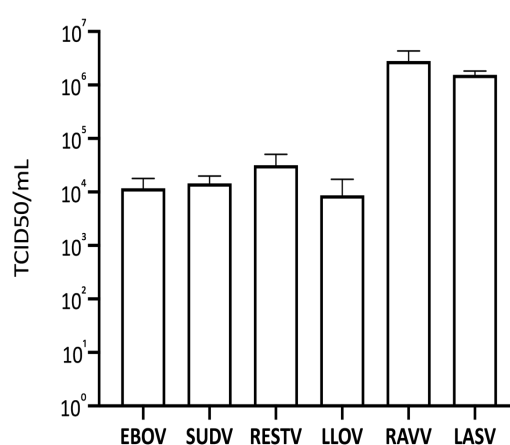


Figure 3.12. Filovirus TCID₅₀ titres in HEK293T target cells. Transduction titres are expressed as the mean \pm s.d TCID₅₀/mL values of two independent experiments. Graphs generated with Prism 8.

3.3.2.7 Quality control of Lentiviral PV production

3.3.2.7.1 p24 ELISA

To determine the number of viral particles in harvested supernatant from producer HEK293T cells the Virion-associated QuickTiter™ Lentivirus Titer Kit was used.

An initial optimisation was performed (Figure 3.13) to ascertain the amount of PV input necessary for the assay, as the kit reports a sensitivity of 1 ng/mL of p24. Even though a 1:10 PV supernatant dilution yielded a slightly higher titre than neat for most PVs (Figure 3.13c), neat supernatant was used to measure the amount of virion associated p24 capsid protein in a subsequent test, yielding between 11 – 15 ng/mL or approximately 1×10^8 VP/mL for most PVs tested, except MARV (DRC) PVs yielding approximately 2 ng/mL or

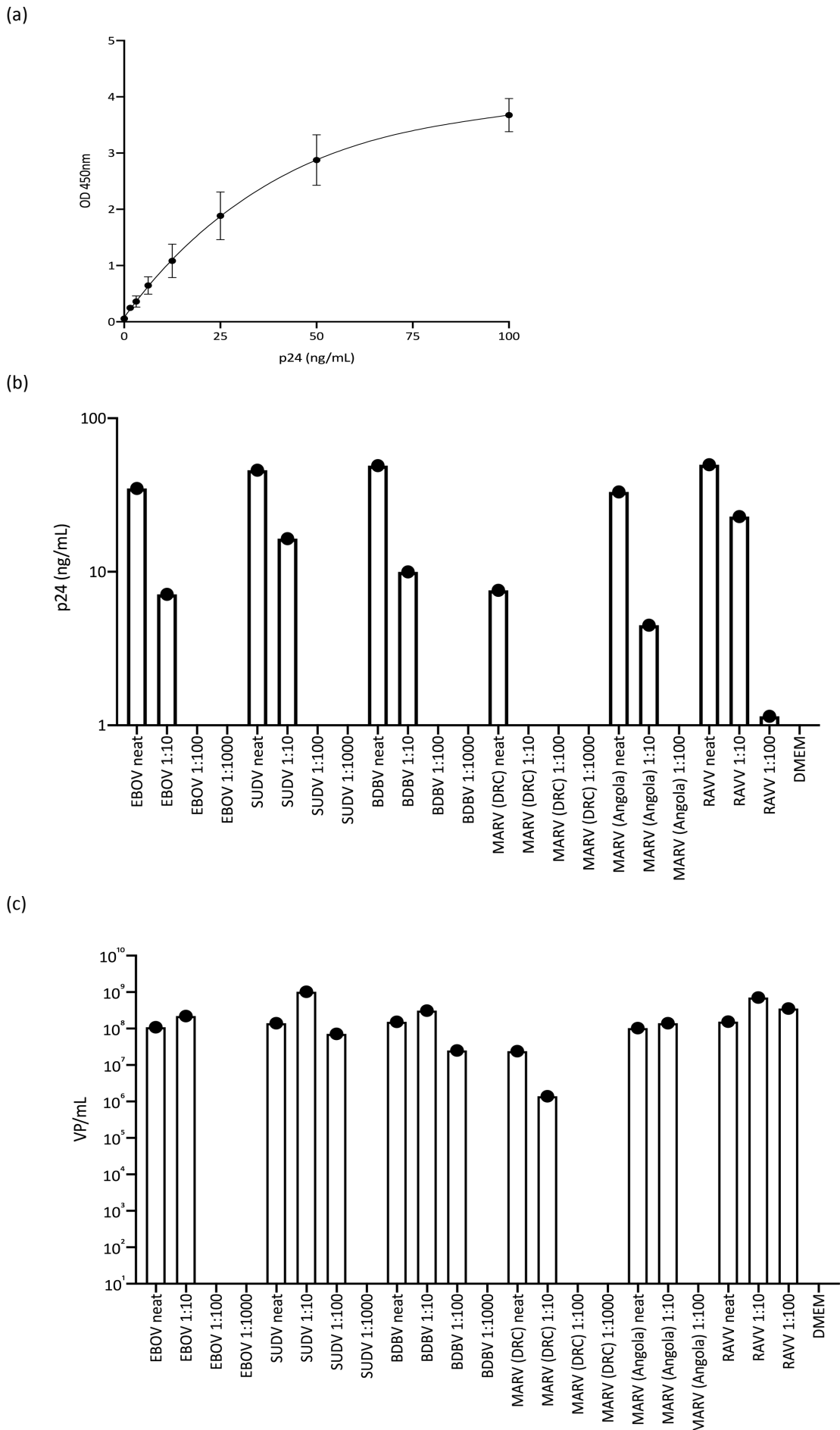


Figure 3.13. Virion associated p24 ELISA. An initial optimisation of PV input was performed. (a) Standard curve (smooth curve – fit spline function) was generated using a recombinant HIV-1 p24 standard as well as

(b) different dilutions of PVs: neat, 1:10, 1:100 and 1:1000 with p24 amounts interpolated from the curve. From the amount of p24 present, (c) the number of viral particles per mL (VP/mL) could be estimated. Graphs generated with Prism 8.

1×10^7 VP/mL (Figure 3.14). It is important to note this assay could detect non-functional virus particles devoid of genome.

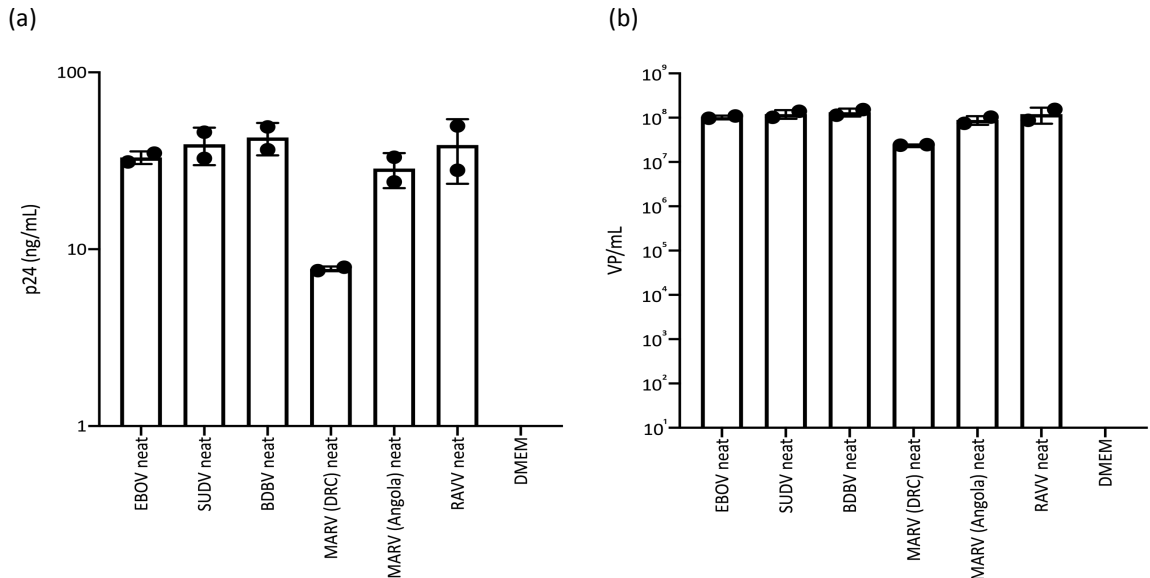


Figure 3.14. Virion associated p24 ELISA in neat PV supernatants. (a) The amount of virion-associated p24 was determined from PV supernatants. From the amount of p24 present, (b) the number of viral particles per mL (VP/mL) could be estimated. Graphs generated with Prism 8.

3.3.2.7.2 SG-PERT

An alternative, cheaper method to characterise PVs generated was utilised, which measures reverse transcriptase activity. Similarly to the p24 ELISA, the amount of viral particles per mL can be estimated, assuming one HIV-1 virion generates 300 pU/mL RT activity based on prior studies summarised in Vermeire *et al*, 2012.

A commercially available recombinant HIV-1 RT was used to generate a standard curve of known RT activity (Figure 3.15a). RT activity in PV supernatant could then be extrapolated. A range of 14 to 670 mU/mL was found for all PVs tested (Figure 3.15b) including PVs devoid of GP (Δ env), corresponding to a range of $\sim 1 \times 10^7$ to 1×10^9 VP/mL (Figure 3.15c). The number of virus particles had no correlation to the functional titre. As expected, high titre PVs such as RAVV had approximately the same number of particles per mL as virions (Δ env) devoid of GP (Figure 3.15c).

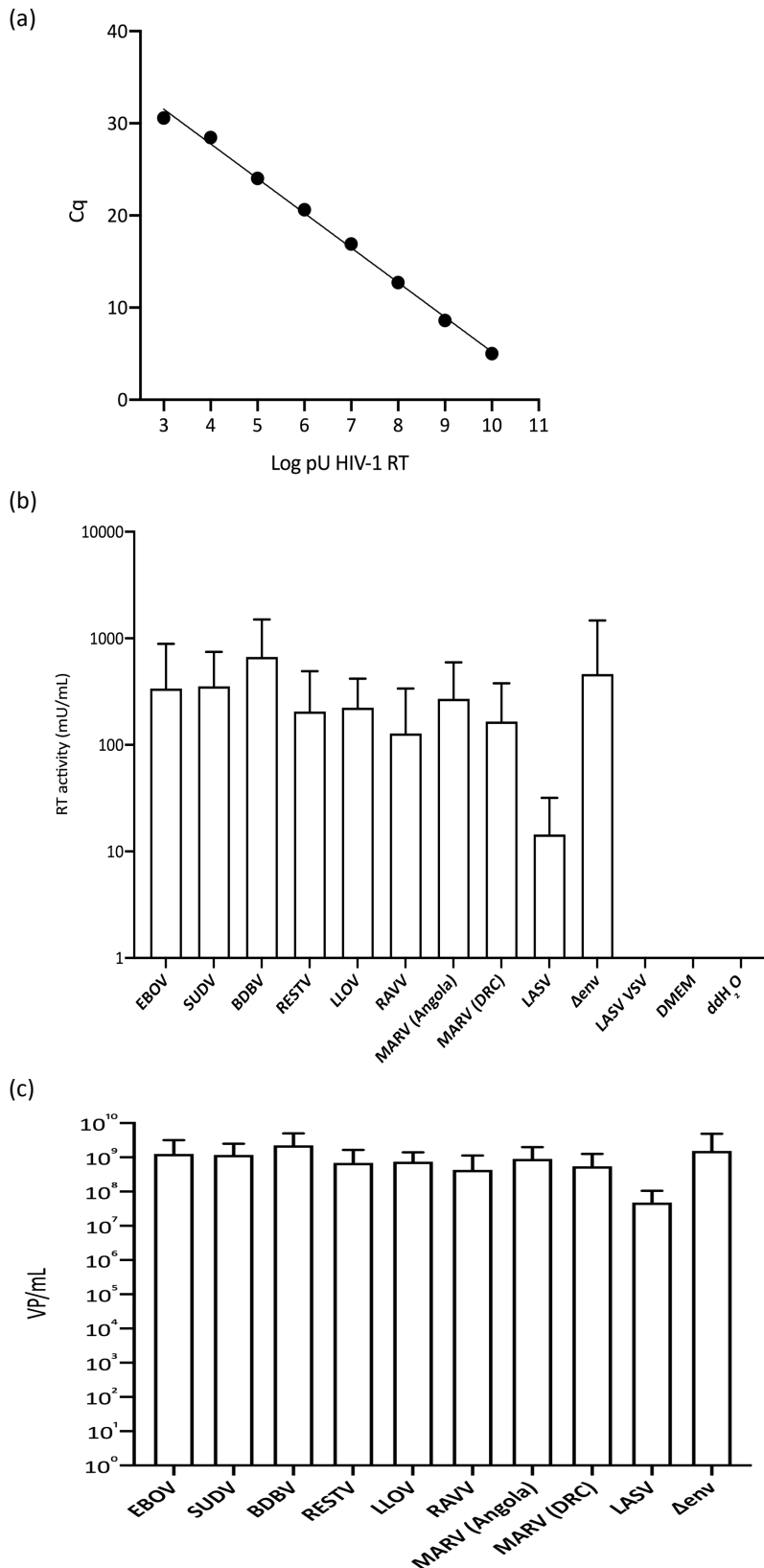


Figure 3.15. SG-PERT SYBR-Green Product Enhancement Reverse Transcriptase assay. A (a) standard curve was generated (linear regression) using a recombinant HIV-1 RT to (b) measure reverse transcriptase activity. From the RT activity levels, (c) the number of viral particles per mL could be estimated. A LASV VSV core PV was included in the negative controls. Graphs generated with Prism 8.

3.3.2.8 Filovirus PV stability after freeze-thawing cycles and Δenv signal

We hypothesised that repeated freeze-thaw cycles would impact on functional PV titres. Also, we wanted to establish whether the luminescence signal observed in particles devoid of GP (Δenv), but still containing the luciferase coding genome, was due to non-specific endocytosis of virus particles or simply background cellular luminescence. Therefore, a small-scale experiment was performed to test these two hypotheses. EBOV PVs retained their functional titre for up to three full freeze-thaw cycles (Figure 3.16). In addition, PV supernatant added to wells without any target cells present yielded similar luminescence readings (Figure 3.16) to cell only wells (HEK293T). To further test the latter, PVs carrying the green fluorescent protein gene were generated.

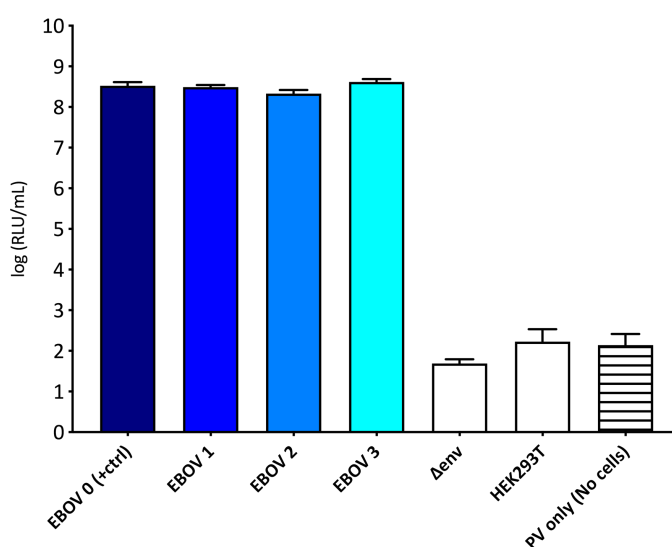


Figure 3.16. PV infectivity after freeze-thaw cycles. Three freeze-thaw cycles were performed (EBOV 1 to 3). Transduction titres are expressed as the mean \pm s.d log (RLU/mL) values of two independent experiments. Titre from lentiviral particles bearing no GP (Δenv), background luminescence from uninfected cells (HEK293T) and PVs without any cells added is also shown. Graph plotted with Prism 8.

3.3.3 Lentiviral (HIV-1) core PV generation – eGFP reporter

Filovirus PVs containing the eGFP reporter gene transduced target cells and distinct green cells were observed 48h pi. The number of green cells approximately corresponded to PV titres in the luciferase assay. *Marburgvirus* and LASV PVs resulted in a higher number of green cells than *ebolavirus* and *cuevavirus* PVs. Within the *ebolavirus* genus, RESTV and BDBV produced a higher number of green cells than EBOV or SUDV (Figure 3.17).

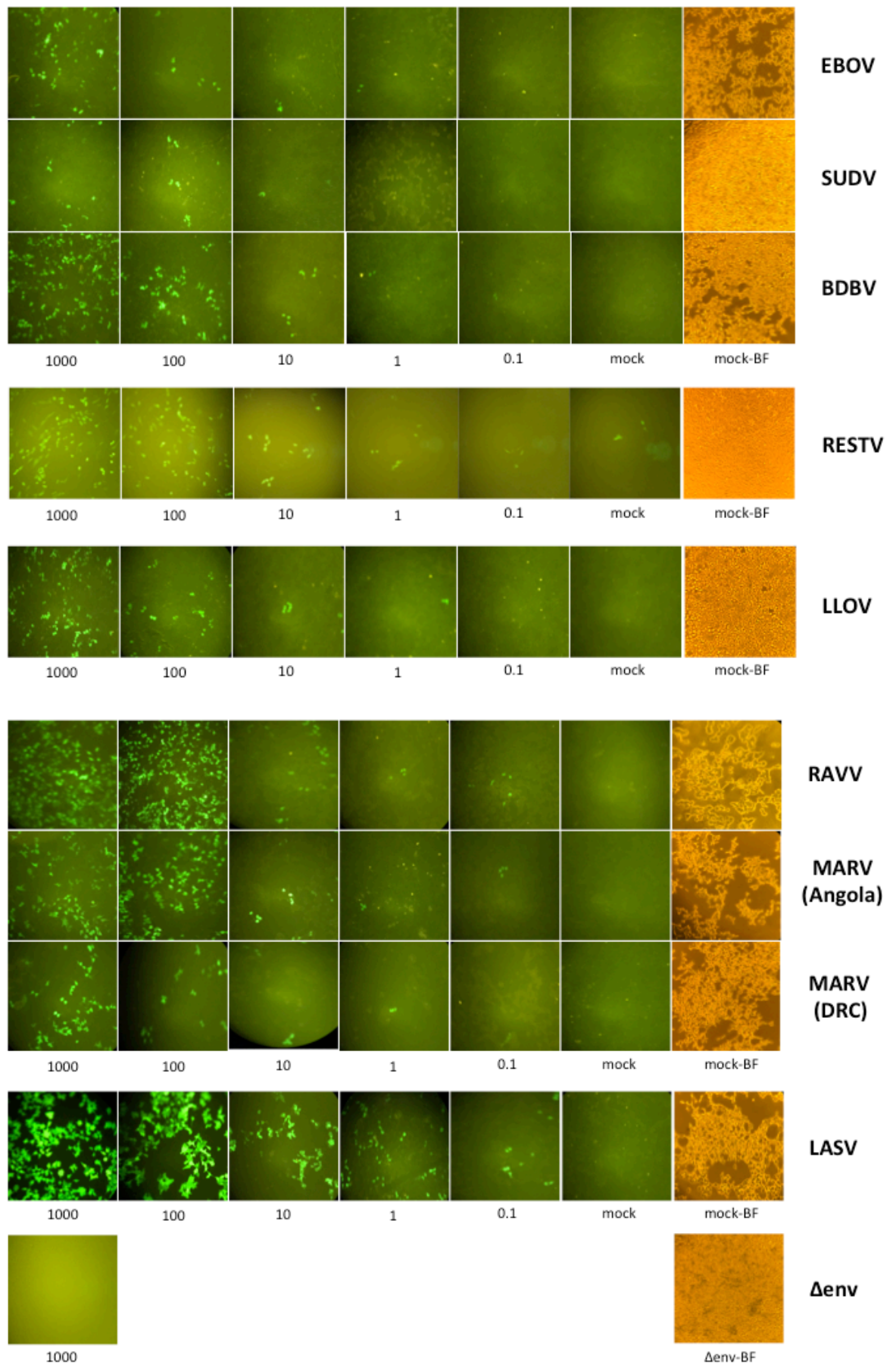


Figure 3.17. Infectivity of filovirus PVs with an eGFP reporter. Transduction of HEK293T cells was carried out in 6-well plates, except for RESTV where CHO-K1 cells were used. Images (20X) representative of results of one from at least two independent experiments. A 10-fold serial dilution of PV supernatant starting at 1000 μ L was performed. Mock: cells “mock” infected with DMEM-polybrene only. BF=bright field.

Within the *marburgvirus* genus, MARV (DRC) PVs resulted in fewer green cells in comparison to RAVV or MARV (Angola) (Figure 3.17).

Infection of cells with Δ env PVs did not result in any observable green cells (Figure 3.17).

3.3.4 Vesicular Stomatitis Virus (VSV) core PV generation – luciferase reporter

Filovirus PV with a VSV core were generated as described in Chapter 2: rVSV Δ G stocks were first amplified, then used to infect HEK293T cells expressing the GP of interest, following pre-transfection with GP plasmid.

3.3.4.1 Amplification of rVSV Δ G stocks

BHK-21 cells stably expressing the coccal VSV-G (BHK-21 coccal) were infected with rVSV Δ G virus at an MOI of 0.1.

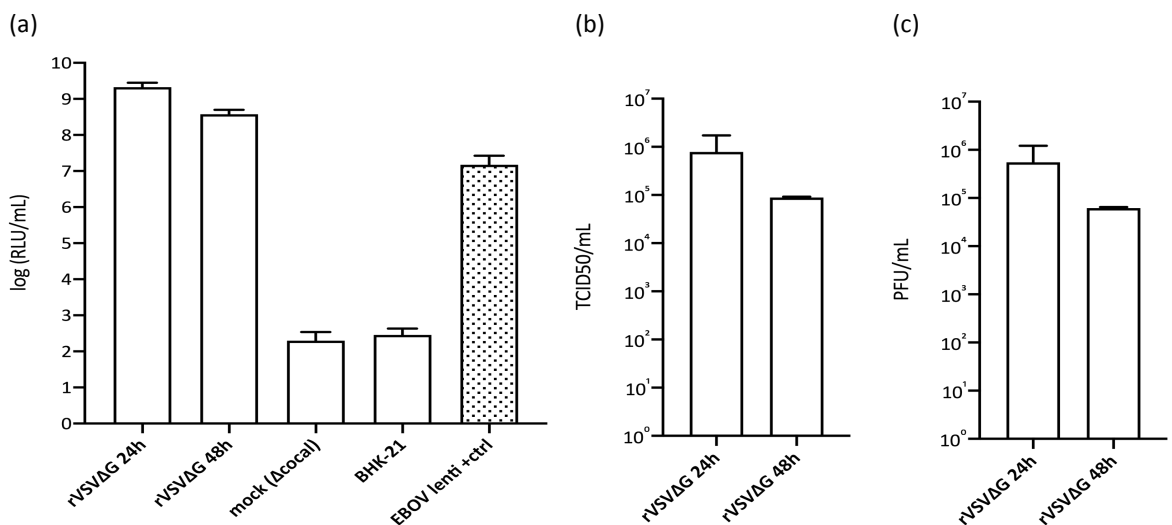


Figure 3.18. Infectivity and TCID₅₀ assays in BHK-21 target cells. Transduction titres are expressed as the mean \pm s.d log (RLU/mL) values of two independent experiments, as well as TCID₅₀/mL and PFU/mL at 24h and 48 pi. Titre from a mock infection (rVSV Δ G infecting BHK-21 not expressing the coccal VSV-G) – mock (Δ coccal) and background luminescence from uninfected cells (BHK-21) are also shown. Graph plotted with Prism 8.

Titres at 24h pi were slightly higher in both assays (Figure 3.18). rVSV Δ G virus did not generate functional PVs when infecting BHK-21 cells not expressing the coccal VSV-G (Figure 3.18a). Titres at 24h pi were slightly higher ($\sim 1 \times 10^6$ TCID₅₀/mL) than PVs harvested at 48pi (Figure 3.18b and 3.18c). Amplified rVSV Δ G stocks were then used to infect HEK293T cells transfected with the GP of interest to generate VSV PVs.

3.3.4.2 Generation of Filovirus VSV PVs

Producer HEK293T were transfected with different GP expressing plasmids with increasing amounts of env. The following day, they were infected with rVSVΔG at an MOI of 0.5.

PV generation in 6-well plates yielded titres of approximately 1×10^6 to 1×10^7 RLU/mL for EBOV (Figure 3.19a) and LLOV (Figure 3.19b) either at 24h or 48h pi; 1×10^9 to 1×10^{10} RLU/mL for RAVV (Figure 3.19c) and 1×10^9 to 1×10^{11} RLU/mL for LASV VSV PVs.

Upscaling VSV PV generation was attempted in T25 flasks. EBOV VSV PVs yielded more comparable titres around 1×10^8 RLU/mL (Figure 3.20a), starting to decrease when the env amount was increased to 3000 ng (Figure 3.20a).

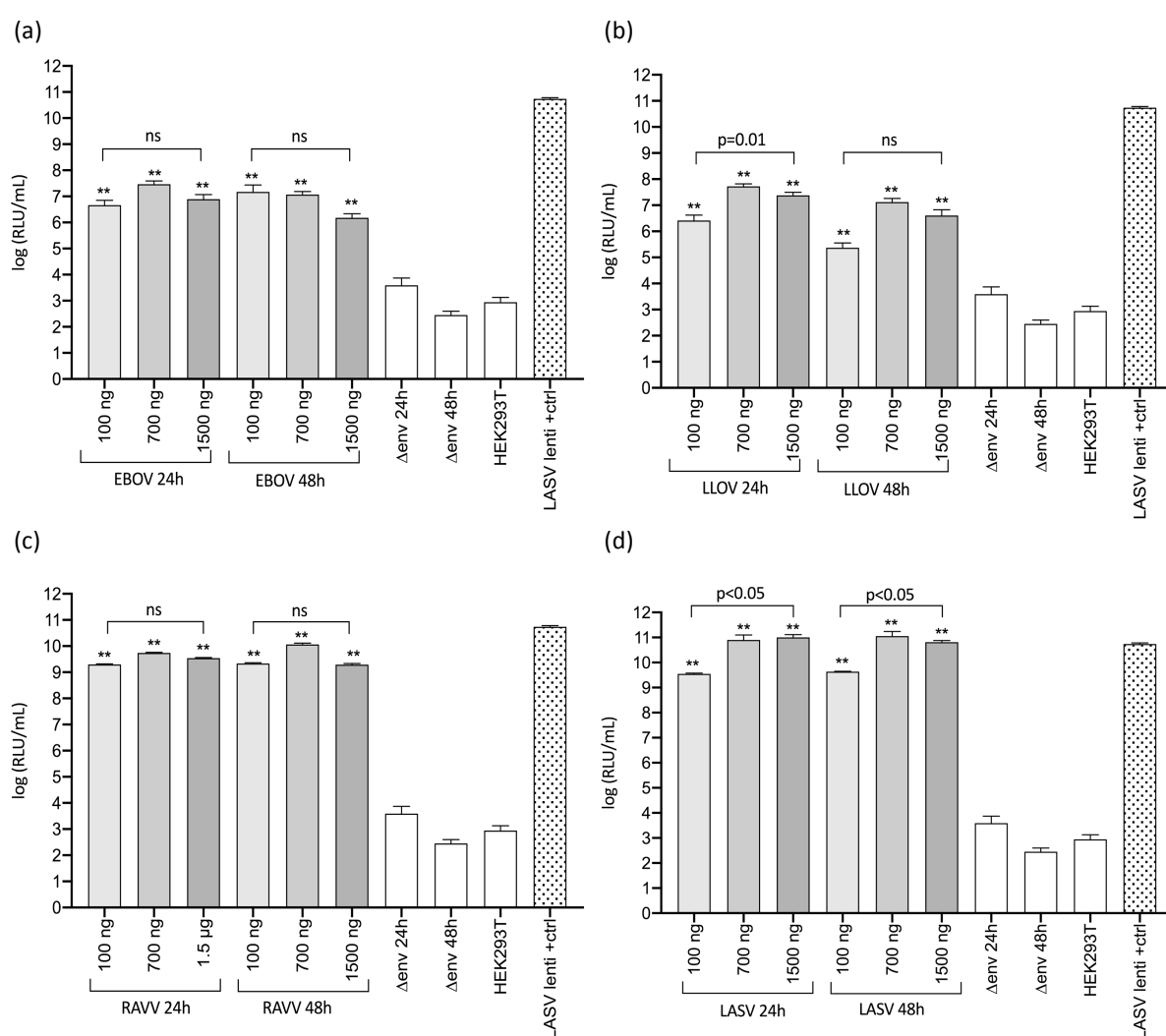


Figure 3.19. Generation of VSV core PVs in 6-well plates. (a) EBOV, (b) LLOV, (c) RAVV and (d) LASV VSV PVs in 6-well plates with varying amounts of env (100 ng to 1.5 µg), harvested at 24h and 48h post-infection. Transduction titres are expressed as the mean \pm s.d log (RLU/mL) values of two independent experiments. Titre from a VSV particle bearing no GP (Δ env) and background luminescence from uninfected (HEK293T) is also shown. Graph and statistical significance (**p<0.001 Mann-Whitney test) in comparison to Δ env, or between treatment groups as indicated, determined with Prism 8. ns = not significant.

LLOV VSV PV titres increased slightly to around 1×10^8 RLU/mL when env amount was 700 ng harvested at 24h pi (Figure 3.20b). RAVV and LASV VSV PV titres were consistent at 1×10^{10} RLU/mL (Figure 3.20c) and 1×10^{11} RLU/mL (Figure 3.20d) respectively.

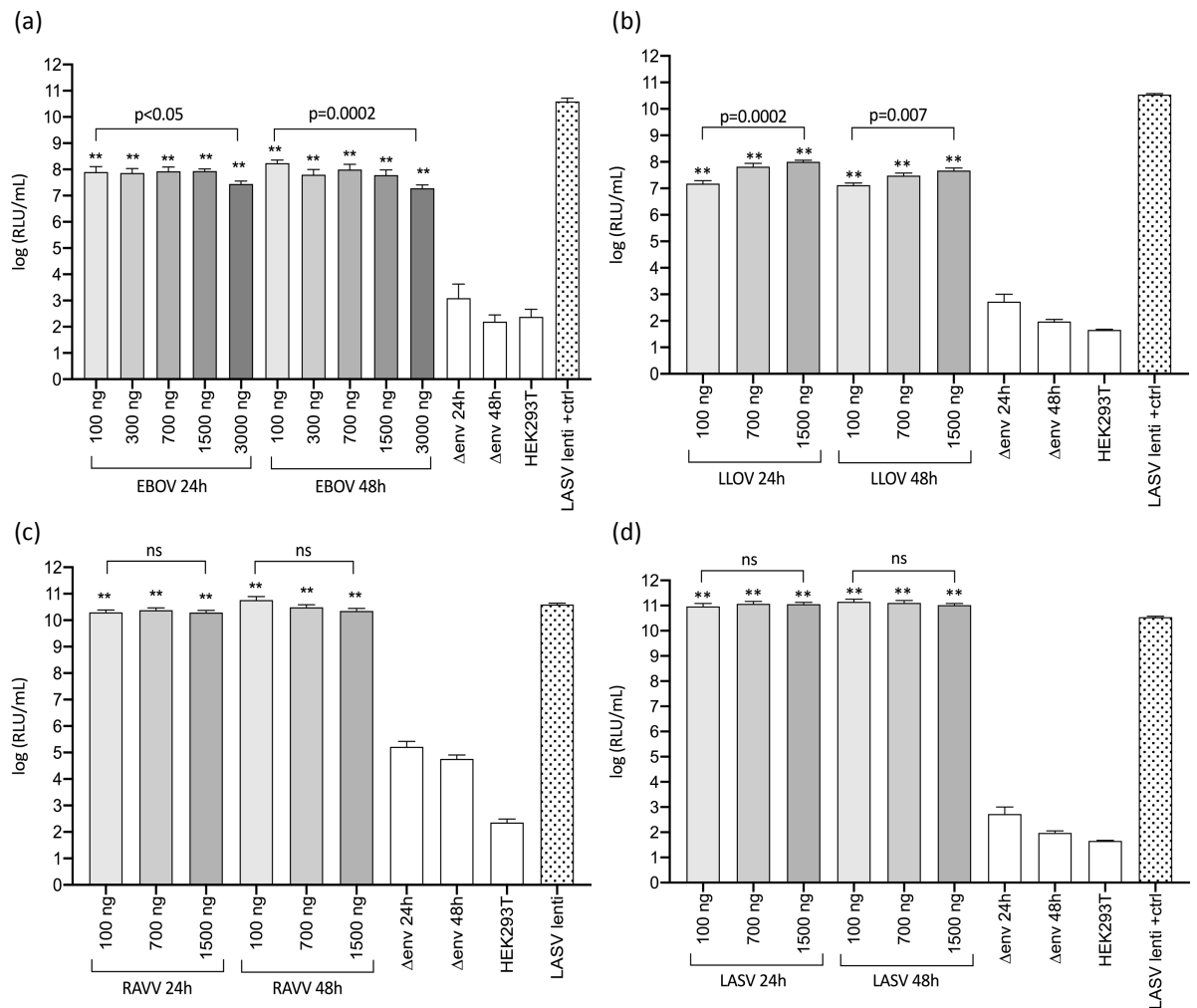


Figure 3.20. Generation of VSV core PVs in T25 flasks. (a) EBOV, (b) LLOV, (c) RAVV and (d) LASV in T25 flasks, harvested at 24h and 48h post-infection. Transduction titres are expressed as the mean \pm s.d. log (RLU/mL) values of two independent experiments. Titre from a VSV particle bearing no GP (Δ env) and background luminescence from uninfected (HEK293T) is also shown. Graph and statistical significance (**p<0.001 Mann-Whitney test) in comparison to Δ env, or between treatment groups as indicated, determined with Prism 8. ns = not significant.

Further VSV PVs were generated with 700 ng of env as previously described (Chapter 2). SUDV and BDBV titres were slightly lower, especially at 48h pi (Figure 3.21), however RESTV and MARV (Angola) titres were approximately 1×10^8 RLU/mL and 1×10^{10} RLU/mL respectively (Figure 3.21). A TCID₅₀ assay in HEK293T target cells yielded titres of approximately 5×10^3 TCID₅₀/mL (3×10^3 PFU/mL) for EBOV VSV PV and 2×10^6 TCID₅₀/mL (1.6×10^6 PFU/mL) for RAVV VSV PVs (Figure 3.22).

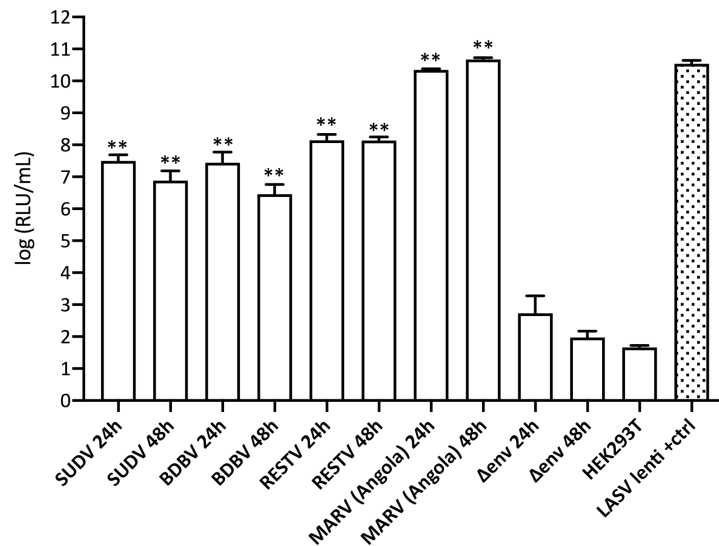


Figure 3.21. Generation of VSV core SUDV, BDBV, RESTV and MARV (Angola) PVs in T25 flasks. PVs were harvested at 24h and 48h post-infection. Transduction titres are expressed as the mean \pm s.d log (RLU/mL) values of two independent experiments. Titre from a VSV particle bearing no GP (Δ env) and background luminescence from uninfected (HEK293T) is also shown. Graph and statistical significance (** $p < 0.001$ Mann-Whitney test) in comparison to Δ env determined with Prism 8.

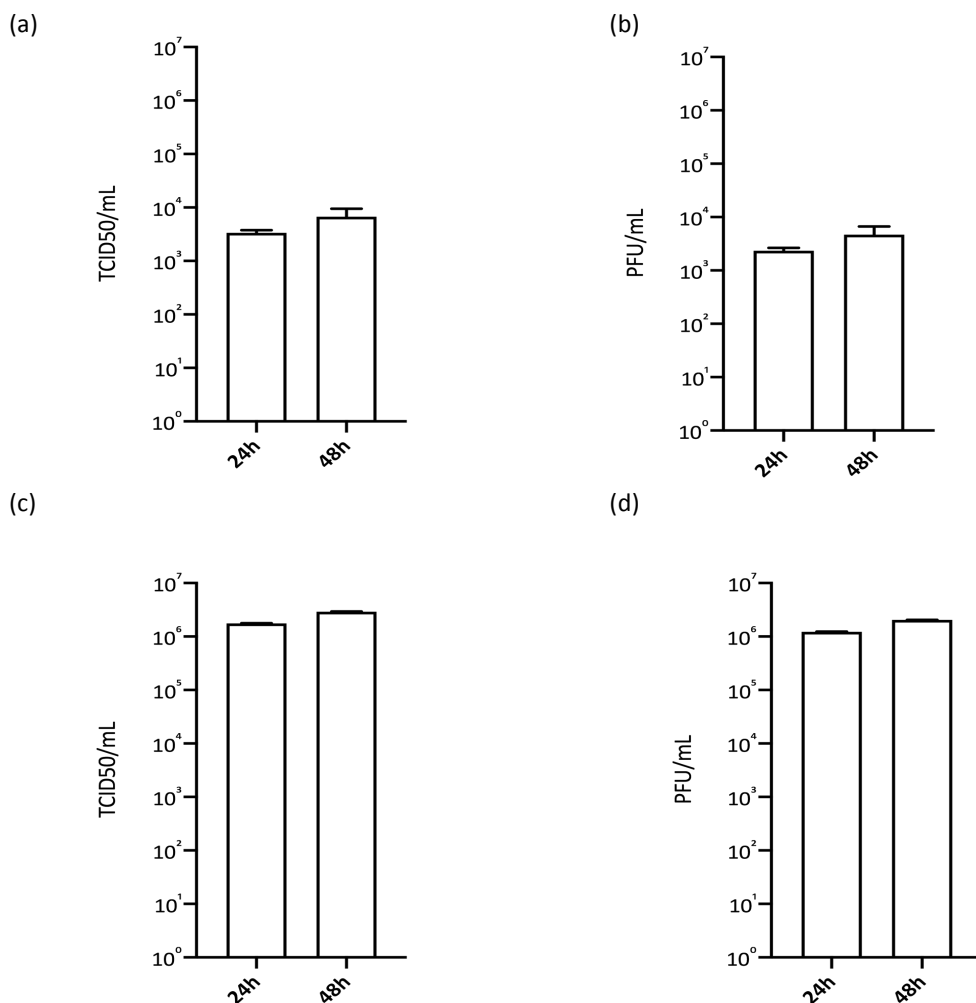


Figure 3.22. Filovirus VSV PVs TCID₅₀ and PFU titres in HEK293T target cells. (a-b) EBOV and (c-d) RAVV VSV PVs. Transduction titres are expressed as the mean \pm s.d TCID₅₀/mL or PFU/mL values of two independent experiments. Graphs generated with Prism 8.

Finally, permissiveness of another cell line was tested. CHO-K1 cells were infected with Filovirus VSV PVs. Functional titres were between 1×10^6 and 1×10^7 RLU/mL for EBOV, RESTV and LLOV VSV PVs (Figure 3.23).

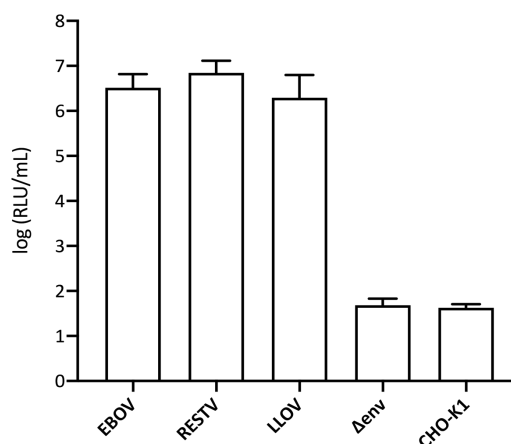


Figure 3.23. Infectivity of filovirus VSV PVs in CHO-K1 cells. Transduction titres are expressed as the mean \pm s.d log (RLU/mL) values of two independent experiments. Titre from a VSV particle bearing no GP (Δ env) and background luminescence from uninfected (CHO-K1) is also shown. Graph plotted with Prism 8.

3.4 Discussion

Since the large outbreak of Ebola virus (EBOV) in West Africa in 2013-2016, pseudotypes have been used extensively in entry studies, vaccine delivery and evaluation, amongst others. Pseudotype-based serological assays are sensitive and amenable to multiplexing and can be handled at low containment (Temperton, Wright, and Scott 2015).

Previous vaccine evaluation studies utilised lentiviral core EBOV PVs successfully (Ewer *et al.* 2016). However, improving PV production titres would be advantageous to avoid concentration of PVs prior to assay setup, as well as reducing batch variables. In this study, we aimed to generate EBOV and other filovirus PVs to high titre for use in future antibody assays. In addition, filovirus PVs with a VSV core were generated for comparison, as they are widely used in filovirus research (Matsuno *et al.* 2010; Qiu *et al.* 2011; Maruyama *et al.* 2014; Wilkinson *et al.* 2017; Suder *et al.* 2018; Salata *et al.* 2019).

An initial attempt using existing VPU protocols for influenza yielded high titres observed for previously generated RAVV PVs (Mather *et al.* 2014) of approximately 1×10^{10} RLU/mL (Figure 3.3), but also resulted in high titre of approximately 1×10^8 RLU/mL for EBOV, SUDV and BDBV (Figure 3.3).

Different culture vessels were used for PV production: T25 flasks (Figure 3.3a-b) and 5-cm dishes (Figure 3.3c-d); and harvested at 48h (Figure 3.3a and 3.3c) and 72h (Figure 3.3b and 3.3d) post-infection. Titres were comparable between producer cell culture vessels, with PVs harvested 72h pi having a 10-fold lower titre in comparison to PVs harvested 48h pi (Figure 3.3).

Considering influenza PVs have been previously generated in 6-well plates successfully to high titres, this approach was attempted for filovirus PVs, with plasmid amount scaled to vessel surface area. However, titres were approximately 10-fold lower (Figure 3.4) in comparison to T25 flasks and 5-cm dishes, either at 48h or 72h harvest. However, these titres were comparable to previously reported EBOV PV titres (Bentley *et al.* 2016; Wool-Lewis and Bates 1998).

A range of transfection reagents was also tested for generation of EBOV and SUDV PVs. FugeneHD and PEI yielded the highest titres at approximately 1×10^8 RLU/mL each. For SUDV PVs, functional titres were significantly higher ($p=0.004$) when produced with FugeneHD, whereas for EBOV PVs this difference ($p>0.05$) was not statistically significant (Figure 3.5). To attempt to establish why this discrepancy in results occurred, individual titre points were plotted in a liner scale (Figure 3.6), showing a larger difference in titre for SUDV generated with FugeneHD, which could explain the statistical significance. Regardless of SUDV PV titre being higher when generated with FugeneHD, PVs titres of 1×10^8 RLU/mL obtained with PEI make this transfection reagent a much more attractive option, especially for laboratories located within low-resource settings, as PEI is a significantly cheaper transfection reagent than FugeneHD.

For PVs generated with a lentiviral core, including various virus families such as filoviruses, orthomyxoviruses, rhabdoviruses and coronaviruses, HEK293T cells are the best producer cells identified thus far, as the inflammatory response occurs with a decrease in cytokine production, inhibiting HIV-1 restriction (Scott *et al.* 2012; Carnell *et al.* 2015; Ferreira *et al.* 2020).

When evaluating whether producer HEK293T cells being cultured in different labs would have an impact on PV titre, EBOV, RAVV and H3N9 PVs were generated using our in-house HEK293T producer cells and the same cell line from Dr Edward Wright's lab at the University of Sussex. We assessed these cells as producers as well as targets, resulting in four combinations of producer and target cells. PV titres were constant whether PVs were generated with HEK293T cells from Kent, with either Kent HEK293T cells or Sussex HEK293T cells as targets. Similarly, PVs produced with HEK293T cells from Sussex resulted

in similar titres, with either Kent HEK293T cells or Sussex HEK293T cells as targets (Figure 3.7).

By grouping the PVs produced by species (Figure 3.7), there were no significant differences in PV titres, therefore the HEK293T cell lines being cultured in different labs did not seem to affect PV titres. Long-term studies might be needed to investigate this matter further. There would be other factors to take into account when evaluating reproducibility such as different users and protocols, different reagents and equipment. Sharing of cell lines without characterisation is often discouraged (Freedman *et al.* 2015). Finally, optimisation of the amount of envelope glycoprotein plasmid used for transfection was attempted utilising a representative from each genus: EBOV, LLOV and RAVV. For EBOV, titres were inversely proportional to the amount of env (Figure 3.8a) as previously described (Mohan *et al.* 2015). However, the amount of env could have been increased further to notice a more prominent drop in functional titre. Marburg (RAVV) PVs did not seem to be affected by the amount of env plasmid (Figure 3.8c), whereas LLOV titre drop might have been more prominent if the amount of env was further increased (Figure 3.8b). Differences in the way *marburgvirus* GPs are processed and displayed after being synthesised such as having one single ORF, a different furin cleavage site, no gene editing site or secreted GP versions, and the fact the *ebolavirus* GP has been implicated in cytotoxicity (Sullivan *et al.* 2005), might explain why RAVV PVs are not affected by the amount of env. Similarly, LLOV and EBOV GPs are processed and displayed in a similar way as well as being more closely related phylogenetically (Hunt, Lennemann and Maury 2012; Gnirß *et al.* 2012; Ng *et al.* 2014; Kemenesi *et al.* 2018). When the same PVs were used to transduce CHO-K1 cells, the same pattern of either titre decrease in EBOV (Figure 3.9a) and LLOV (Figure 3.9b), or titre consistency in RAVV (Figure 3.9c) was observed.

Filovirus PVs were upscaled successfully to T75 flasks producing comparable titres of approximately 1×10^8 RLU/mL for *ebolavirus* and *cuevavirus* PVs and 1×10^{10} RLU/mL for *marburgvirus* PVs (Figure 3.10). This enabled the use of the same batch of PVs for several experiments, and was particularly useful in lyophilisation studies (Chapter 7), eliminating an extra variable.

Filovirus PVs were tested in different target cell lines. Human cell line Huh-7 (Figure 3.11a) yielded titres approximately 10-fold lower than in HEK293T. MDCK-II cells (Figure 3.11b) yielded comparable titres to HEK293T. CHO-K1 cells (Figure 3.11d) also yielded titres approximately 10-fold lower than in HEK293T, but these cells had performed well in

neutralisation assays (Dr Emma Bentley – personal communication), therefore they were used in PVNAs along with HEK293T cells for comparison (Chapter 4). The differences in neutralisation between these cell lines could be due to differences in receptor expression (Ooi *et al.* 2016; Malm *et al.* 2020). These can be sometimes observed between different clones of the same cell line (Haines *et al.* 2012).

Even though titres are mainly reported in relative light units per mL for most infectivity and neutralising assays using this system, it is difficult to compare with titres reported elsewhere in the literature. Therefore, a 50% Tissue Culture Infective Dose (TCID₅₀) assay was performed according to the Reed-Muench method (Reed and Muench 1938), except here any luminescence value 2.5x higher than the background cell control was considered positive for cytopathic effect. *Ebolavirus* and *cuevavirus* PVs were found to have titres of approximately 1×10^4 TCID₅₀/mL whereas RAVV and LASV PVs were found to have titres of approximately 1×10^6 RLU/mL (Figure 3.12a), comparable to the 100-fold difference in RLU titres. Even though PVs do not form plaques, to estimate titres in plaque forming units (Figure 3.13b), values were multiplied by 0.7 (Reed and Muench 1938). This is particularly useful not only for consistency and reproducibility but also in experiments where the multiplicity of infection (MOI) is an important factor to consider, for instance when generating VSV PVs (Whitt 2010).

Quality control of lentiviral PV production was done with two different assays to estimate the number of lentiviral particles per mL of harvested supernatant.

One commercially available ELISA kit that measures amount of virion-associated HIV-1 capsid protein (p24) in samples. The amount of viral particles can then be estimated according to the amount of p24. An initial optimisation of PV input established undiluted supernatant to give the better signal in the p24 ELISA (Figure 3.13). The amount of viral particles per mL was estimated to be 1×10^7 VP/mL for MARV (DRC) PVs and 1×10^8 VP/mL for EBOV, SUDV, BDBV, RAVV and MARV – Angola (Figure 3.14).

The other assay, which is more affordable, is a qPCR-based reverse transcription assay, measuring RT activity by introducing an exogenous RNA (MS2 phage), using lysed PVs as a source of RT, and producing and amplifying cDNA in a qPCR step, subsequently quantifying RT activity with a standard curve generated by a recombinant HIV-1 RT. It is estimated that one virion results in approximately 300 pU/μL of RT activity (Sears, Repaske and Khan 1999; Ma and Khan 2009; Vermeire *et al.* 2012). Therefore, the amount of viral particles can be estimated according to the RT activity in a PV sample. Both ELISA (Ao *et al.* 2008; Kutner, Zhang and Reiser 2009) and SG-PERT (Ruscic *et al.*

2019; Ferreira *et al.* 2020) can estimate the amount of viral particles, however SG-PERT detects particles that carry the genome. Whether these are functional or not will be determined by the presence of GP and receptor interaction. The level of RT activity found in lentiviral filovirus PVs was comparable to other lentiviral PVs (Munis *et al.* 2018).

For all PVs assessed, reverse transcriptase activity was found to be between 10^2 and 10^3 mU/mL (Figure 3.15b), except for LASV (10^1 to 10^2 mU/mL); and the number of viral particles estimated to be between 10^8 and 10^9 VP/mL (Figure 3.15c). This is in agreement with p24 ELISA titres. Determining genome copies is also possible, but it is important to note not all integrated genomes in transduced cells will result in reporter gene expression (Geraerts *et al.* 2006), therefore affecting functional titres, as well as the presence of GP. Also, transgene-associated toxicity in producer and target cells can affect titre (Lizée *et al.* 2003). Indeed, the number of viral particles in a sample did not correspond to functional titres. LASV, RAVV and MARV PVs have consistently higher functional titres of approximately 1×10^{10} to 1×10^{11} RLU/mL or 1×10^6 TCID₅₀/mL (Figures 3.3, 3.8, 3.10 and 3.12a), however they were estimated to have approximately the same number of virions as *ebolavirus* and *cuevavirus* PVs (Figure 3.14b). These virions exhibited RT activity (Figure 3.15c), therefore were not empty cores. This difference in functional titres might be explained the fact these GP have different processing requirements and infectivity dynamics such as a more accessible receptor-binding site. *Ebolavirus* and *cuevavirus* GPs have secreted versions of their GP for example, which may affect infectivity. Also, *marburgvirus* GP appear to infect cells regardless of cleavage by cathepsins L or B, which could perhaps improve infectivity *in vitro* at least (Simmons and Bates 2007; Schornberg *et al.* 2009; Lee, Road and Jolla 2010; Matsuno *et al.* 2010; Kaletsky, Marzi, Reinheckel and Feldmann 2012; Brecher *et al.* 2012; Maruyama *et al.* 2014; Mohan *et al.* 2015), although there appears to be differences in cathepsin requirements within the same genus, with EBOV and TAFV being dependent on cathepsin B cleavage but not SUDV or RESTV for example (Misasi *et al.* 2012). In addition, EBOV receptor-binding site is hidden within the 3D structure, becoming exposed after cathepsin cleavage, whereas in MARV the receptor-binding site was found to be accessible, and it is of the main targets of neutralising antibodies (Hashiguchi *et al.* 2015; Flyak *et al.* 2015).

In order to confirm these findings, lentiviral PVs were generated with a GFP reporter gene. The number of green cells appeared to correspond to the difference in functional titres observed between PVs with a luciferase reporter gene. LASV, RAVV and MARV PVs resulted in a higher number of green cells after infection in comparison to *ebolavirus* or

cuevavirus PVs (Figure 3.17). Small differences in titres between EBOV and SUDV compared with RESTV for example were also observed, as well as differences between RAVV and MARV (Angola) compared with MARV (DRC) (Figure 3.17).

Infectivity or lack of, with particles devoid of GP (Δenv) was also confirmed with eGFP PVs, as no green cells were observed after several attempts at infection (Figure 3.17). Therefore, care should be taken not to overinflate Δenv titres when normalising raw luminescence values to RLU/mL.

Finally, lentiviral PVs were shown to retain their infectivity after repeated freeze-thaw cycles (Figure 3.16), which would be beneficial in any future use of filovirus PVs for diagnostic assays. However, other studies previously found lentiviral PVs not only to be sensitive to repeated freeze-thaw cycles, but also GP specific possibly due to differences in protein stability assuming the lipid-envelope remained intact after the freeze-thaw cycles (Watson *et al.* 2002; Molesti *et al.* 2014).

Considering most of the literature on filovirus report the use of VSV core PVs, we attempted to create a panel of VSV PVs for comparison. Generation of VSV core PVs is slightly different and more laborious than lentiviral core PVs. Lentiviral core PVs can be generated utilising a simple 3-plasmid transfection system (Figure 2.2), whereas VSV core PVs require production of a recombinant VSV where the G gene, which normally codes for its viral envelope protein, is replaced with a reporter gene. The G protein has to be provided *in trans* (Whitt 2010) by transfection of producer cells with a G plasmid (cocal). The resulting recombinant virus (rVSV Δ G) is used to infect cells, which have been transiently transfected with the GP of interest (Figure 2.3). VSV PVs can be then harvested at 24h and 48h after this infection.

Amplification of rVSV Δ G stocks bearing the cocal G resulted in titres of approximately 1×10^6 TCID₅₀/mL (Figure 3.18b) in BHK-21 target cells, for rVSV Δ G viruses harvested 24h pi. Harvest at 48h resulted in approximately 10-fold lower titres (Figure 3.18). Amplified rVSV Δ G stocks were then used to infect HEK293T cells transiently expressing the GP of interest.

Generation of VSV PVs in 6-well plates (Figure 3.19) according to existing protocols from the University of Sussex resulted in titres comparable to lentiviral PVs produced in 6-well plates; whereas generation of VSV PVs in T25 flasks resulted in higher titres (Figure 3.20), also comparable to lentiviral PV titres. It may be that scaling up PV production improved titres, therefore controlled experiments assessing cell density and other parameters such

as plasmid amount would have to be performed to establish why this difference in titres was observed.

The inverse correlation of env amount and titre observed in EBOV PVs was less prominent in VSV core PVs than for lentiviral PVs (Figure 3.8a and 3.9a), however there was a more noticeable decrease in titre when the amount of env was increased to 3 µg (Figure 3.20a). Large amounts of EBOV env plasmids have been associated with a decrease in titres as previously discussed (Mohan *et al.* 2015).

Other filovirus VSV PVs (SUDV, BDBV, RESTV and MARV – Angola) were generated using 700 ng of env. Titres at 24h (Figure 3.21) were comparable to previously produced VSV PVs. TCID₅₀ assays for EBOV and RAVV yielded titres of approximately 1×10^3 – 1×10^4 and 1×10^6 TCID₅₀/mL respectively (Figure 3.22). Finally, CHO-K1 cells were found to be permissive to VSV PVs (Figure 3.23), therefore they could also be used in PVNAs.

Reported titres can vary depending on the core. In this study we managed to increase titres for HIV-1 core EBOV PVs than previously reported (Chan *et al.* 2000; Ewer *et al.* 2016; Zapatero-Belinchón *et al.* 2019). For VSV, some more established protocols reported higher titres for EBOV and MARV VSV PVs (Garbutt *et al.* 2004). Even though we managed to generate functional VSV core PVs, it will certainly require further optimisation. Lentiviral core PVs were easier to generate and optimise in this study. In addition, certain GPs do not pseudotype with certain cores, therefore having different cores available can be advantageous.

Filovirus GP have been shown to be amenable to pseudotyping with all species tested in this study, generating functional PVs which in turn could be used in future neutralisation assays, or any other tests where PVs can offer a safe alternative to authentic virus. High titre PVs generated in larger cell culture vessels minimise any possible batch variation in studies, ensuring consistency and eliminating variables.

CHAPTER 4: Application of Filovirus Pseudotypes for Neutralisation and Binding Assays (ELISA)

4.1 Introduction

Emerging viruses cause sporadic outbreaks with potentially severe economic and healthcare burdens, especially in low-resource countries. Filoviruses have been responsible for several outbreaks with case fatality rates of up to 90% since they have been discovered (Languon and Quaye 2019). The large EBOV outbreak in West Africa, the 2018-2020 EBOV outbreak at the DRC as well as the current SARS-CoV-2 outbreak highlight the importance of serosurveillance in aiding containment of emerging diseases and dictating future healthcare policy measures.

Control measures and diagnostics for filoviruses are essential, as well as serological assays that can detect previous infections, to aid public health policies to better manage and control any future outbreaks. In addition, establishing and monitoring animal reservoirs would help track spread and identify any risk areas should an unknown outbreak occur.

The gold standard for diagnosis of filoviruses is RT-PCR based, including some portable methods being tested requiring less technical expertise and facilities (Raftery *et al.* 2018; Makiala *et al.* 2019; Murphy 2019). Most serological studies of filoviruses are ELISA based using purified antigens to detect serum antibodies. Serosurveillance of filoviruses initially utilised immunofluorescence methods (IF), then mainly ELISA thereafter. It has been speculated that failure to identify emerging diseases early in outbreaks was a possible cause of the size of the West Africa EBOV outbreak, due to its unusual geographical location (Formella and Gatherer 2016), highlighting yet again the importance of continuous serosurveillance in animal and human populations.

In addition, as current evidence suggests, filoviruses appear to be more prevalent and within a wider geographical distribution than previously thought, either in unidentified species with milder symptoms, asymptomatic cases such as RESTV infection (Becker *et al.* 1992; Cantoni *et al.* 2016), or species circulating in bats and other animals with the potential for future zoonotic transmission (Yang *et al.* 2019; Forbes *et al.* 2019). Sequencing platforms were utilised to study EBOV persistence, which has been reported in semen of patients who recovered from EVD, being able to transmit the virus to different partners after approximately 500 days after infection where viral RNA was

detected in semen by RT-PCR (Diallo *et al.* 2016). Therefore, monitoring and surveillance is crucial for infection control.

Working with authentic filoviruses is problematic due to the fact they require high containment facilities, restricting the number of laboratories able to perform such studies. ELISA can be performed in low containment using recombinant proteins as antigens, which could explain why the majority of studies utilise this method. Neutralising antibody assays are useful to assess levels of functional antibodies against these viruses, as well as being a good indication of potential protective responses, therefore they can be more informative than binding assays (Carnell *et al.* 2015; Mire *et al.* 2015; Ewer *et al.* 2016; King *et al.* 2018). It is important to point out neutralising antibodies do not always confer protection against infection (Escudero-Pérez *et al.* 2016; Zhang *et al.* 2016).

Pseudotype viruses are a safe alternative to working with authentic viruses as they can be handled in low containment and exhibit high sensitivity when used in neutralisation assays, as the GP is the main target of neutralising antibodies (Mather *et al.* 2013; Ewer *et al.* 2014; Rimoin *et al.* 2017). They have been utilised extensively in influenza research (Ao *et al.* 2008; Scott *et al.* 2012; Powell *et al.* 2012; Carnell *et al.* 2015; Ferrara and Temperton 2018; Giotis *et al.* 2019), but for filovirus serological studies, ELISA is more widely reported (Formella and Gatherer 2016). However, pseudotype neutralisation assays are sometimes utilised in serosurveillance studies (Ito *et al.* 2001; Steffen *et al.* 2019), and they appear to correlate well with neutralisation assays utilising authentic viruses (Ewer *et al.* 2016; Konduru *et al.* 2018).

With any serological testing, sensitivity and specificity are important to ensure the correct viruses are being identified. Specificity is an issue in many tests. Filovirus cross-reactivity has been reported previously in convalescent serum in ELISA. A strong IgG response against heterologous antigens from EBOV, SUDV, BDBV and RESTV was found in convalescent serum from outbreaks in Kikwit, DRC (EBOV), Gulu, Uganda (SUDV), Bundibugyo, Uganda (BDBV) and the Philippines (RESTV) (Nakayama *et al.* 2010; MacNeil, Reed and Rollin 2011), as well as in monoclonal antibodies (Hashiguchi *et al.* 2015; Flyak *et al.* 2016). Cross-reactivity would be detrimental if you were trying to establish which species was responsible for the infection. However it is important to point out that for therapeutics, using less specific monoclonal antibodies would be highly desirable, being able to treat different species with a single mAb or a “cocktail” of two or three mAbs as a “universal” or “pan-filo” therapy (Qiu *et al.* 2014; Furuyama *et al.* 2016; Qiu *et al.* 2016).

In this study, a panel of filovirus PVs was generated for use in antibody assays – PVNA and ELISA. The lack of convalescent serum against other species under study meant only EBOV PVs could be assessed in PVNAs. Convalescent sera from patients who had recovered from EVD were acquired from NIBSC. Three sets of sera were available, single patients and pooled, as described below. Monoclonal antibodies against *ebolavirus* and *marburgvirus* were also utilised as a proof-of-concept in PVNAs and ELISA, to assess feasibility of using such PVs in future assays, establishing whether they target unique specific epitopes suitable for serological diagnostics or cross-reactive “pan-filo” epitopes more suitable for therapeutics.

4.2 Materials and Methods

4.2.1 Viruses, sera and monoclonal antibodies

Cell lines, plasmids and PVs used in this study, have been described extensively in Chapters 2 and 3.

EBOV convalescent sera used in this study was purchased from the National Institute for Biological Standards and Control (NIBSC), Potters Bar, United Kingdom. These were the following WHO reference reagents:

- anti-EBOV plasma, human NIBSC 15.220*[^]
- anti-EBOV convalescent plasma pool – Sierra Leone, NIBSC 15.262*[¶]
- anti-EBOV convalescent plasma panel, NIBSC 16.344*[§]

*tested negative for HBsAg, anti-HIV and HCV RNA. PCR-negative for Ebola virus. Solvent-detergent treated.

[^]also known as EBOV Ab sample 79

[¶]pooled convalescent plasma obtained from six Sierra Leone patients who recovered from Ebola virus disease (EVD).

[§]individual panel members are NIBSC 15.280 (ARC), 15.282 (NHSBT), 15.284 (NOR), 15.286 (INMI), 15.288 (negative human plasma). “It is intended that the panel is used in the assessment of factors that affect variability of assays used in detection and quantification of EBOV antibodies”.

Rabbit anti-EBOV GP, an affinity purified rabbit polyclonal antibody, was a kind gift from IBT Bioservices (catalogue #0301-015) that had been previously tested by western blot and ELISA.

The other negative sera used in this study were negative human serum (Merck-Millipore H4522-20ML), and a horse serum kindly provided by Dr Simon Scott. The horse had been previously vaccinated against several subtypes of equine influenza and equine herpes virus (Dr Simon Scott – personal communication). Monoclonal antibodies used in this study were gifts from: Dr Xianguo Qiu (4G7 and 1H3), Dr Erica Sapphire (KZ52), and Prof Jonathan Heeney (FVM04, FVM09 and CA45) targetting EBOV; and Dr James Crowe (MR78) targetting MARV/RAVV.

4.2.2 Antibody assays

Pseudotype virus neutralisation assay (PVNA) and ELISA have been described in Chapter 2. A 50 mM carbonate-bicarbonate buffer pH9.6 was also tested to compare to DPBS as a coating buffer in ELISA. It was prepared with sodium carbonate anhydrous 500 g (Fisher Scientific 10264540) and sodium bicarbonate 500 g (Fisher Scientific 10583381).

Statistical analysis was performed as described in Chapter 2.

4.3 Results

4.3.1 Pseudotype neutralisation assay (PVNA)

4.3.1.1 Neutralising antibody responses against EBOV PVs using convalescent sera

All Ebola convalescent sera tested in this study exhibited some level of neutralising antibodies detected by PVNA. Initially, two different convalescent sera were tested for neutralising antibodies targetting the EBOV GP using a lentiviral EBOV PV.

Neutralising responses were moderate (Figure 4.1), with IC_{50} values (reciprocal of serum dilution) ranging from 84 to 805 (Figure 4.5b) when using NIBSC 15.220 in PVNAs, whereas NIBSC 15.262 IC_{50} ranged from 71 to 691 (Figure 4.5a) in PVNAs. A modest decrease (10-100 fold) in transduction efficiency (decrease in luminescence in target cells) was observed both for NIBSC 15.220 and 15.262 standards (Figure 4.1) in comparison to the negative human serum. The choice of target cell lines appears to have an effect in neutralisation response detection.

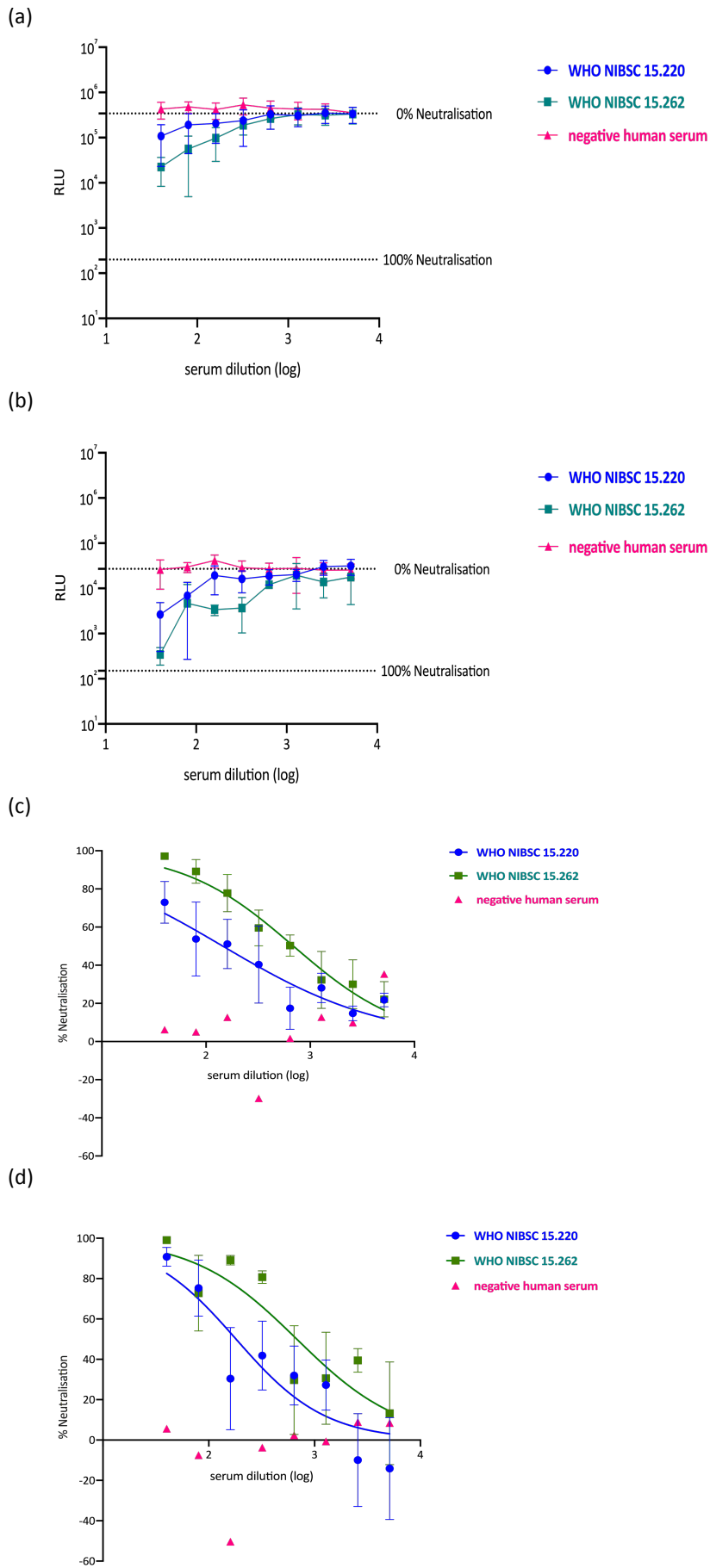


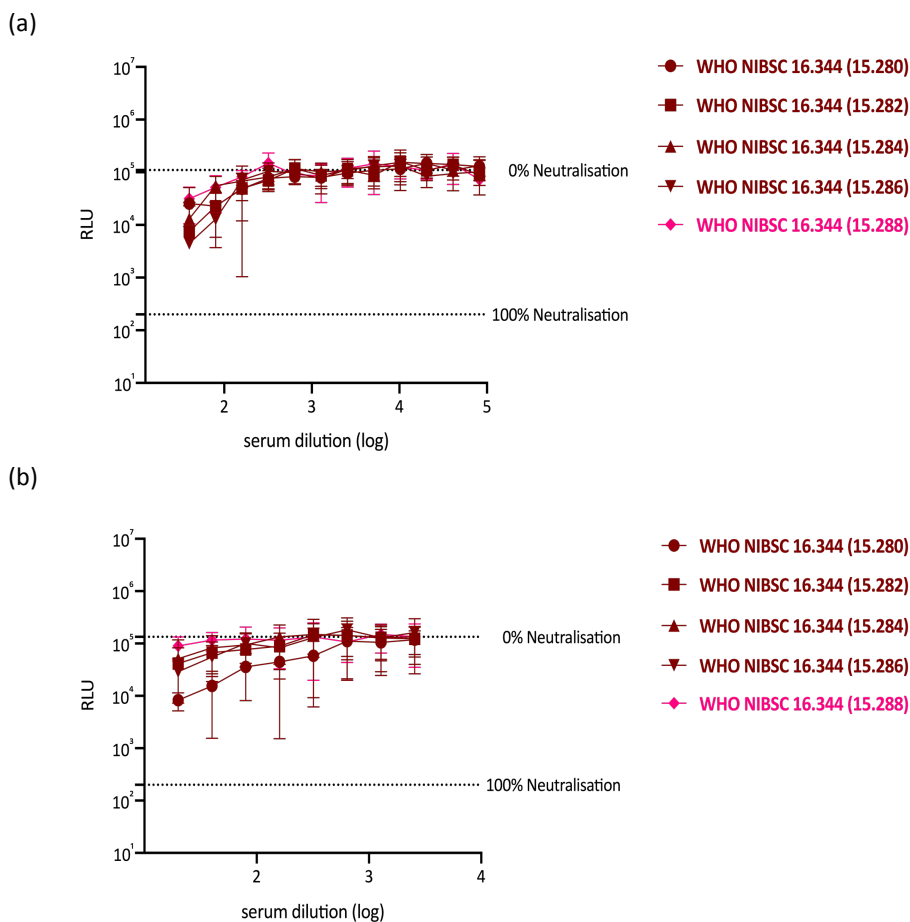
Figure 4.1. Neutralisation assay with anti-EBOV WHO NIBSC standards comparing target cell lines. Lentiviral PVs bearing the EBOV (Makona C15) glycoprotein were used in PVNAs to compare HEK293T and CHO-K1 target cells. For each serum assessed (a-b) a reduction in luminescence at lower dilutions and 0% and 100% neutralisation values, as well as neutralising curves showing the inverse relationship between

increase in dilution and a decrease in neutralisation when antibodies are present in (c) HEK293T target (15.220 $r^2 = 0.5$, 15.262 $r^2 = 0.8$) and (d) CHO-K1 target (15.220 $r^2 = 0.5$, 15.262 $r^2 = 0.5$). Results from at least two independent experiments. Graphs and non-linear regression curves (log [inhibitor] vs normalised response; constraint: hill slope <0) generated with Prism 8.

The antibody-mediated decrease in cell transduction (RLU) by PVs was more pronounced in CHO-K1 target cells. The input was also lower in these cells (Figure 4.1b) than in HEK293T (Figure 4.1a). The antibody neutralising titres were generally higher in CHO-K1 cells (Table 4.1).

	HEK293T	CHO-K1
NIBSC 15.220	145	181
NIBSC 15.262 (pooled)	380	677
Negative human serum	NN	NN

Table 4.1. End-point antibody neutralising titres in convalescent serum against EBOV PVs using HEK293T and CHO-K1 cell lines. IC₅₀ values reported as the mean for at least two independent experiments. NN = not neutralised. Non-regression analysis performed with Prism 8.



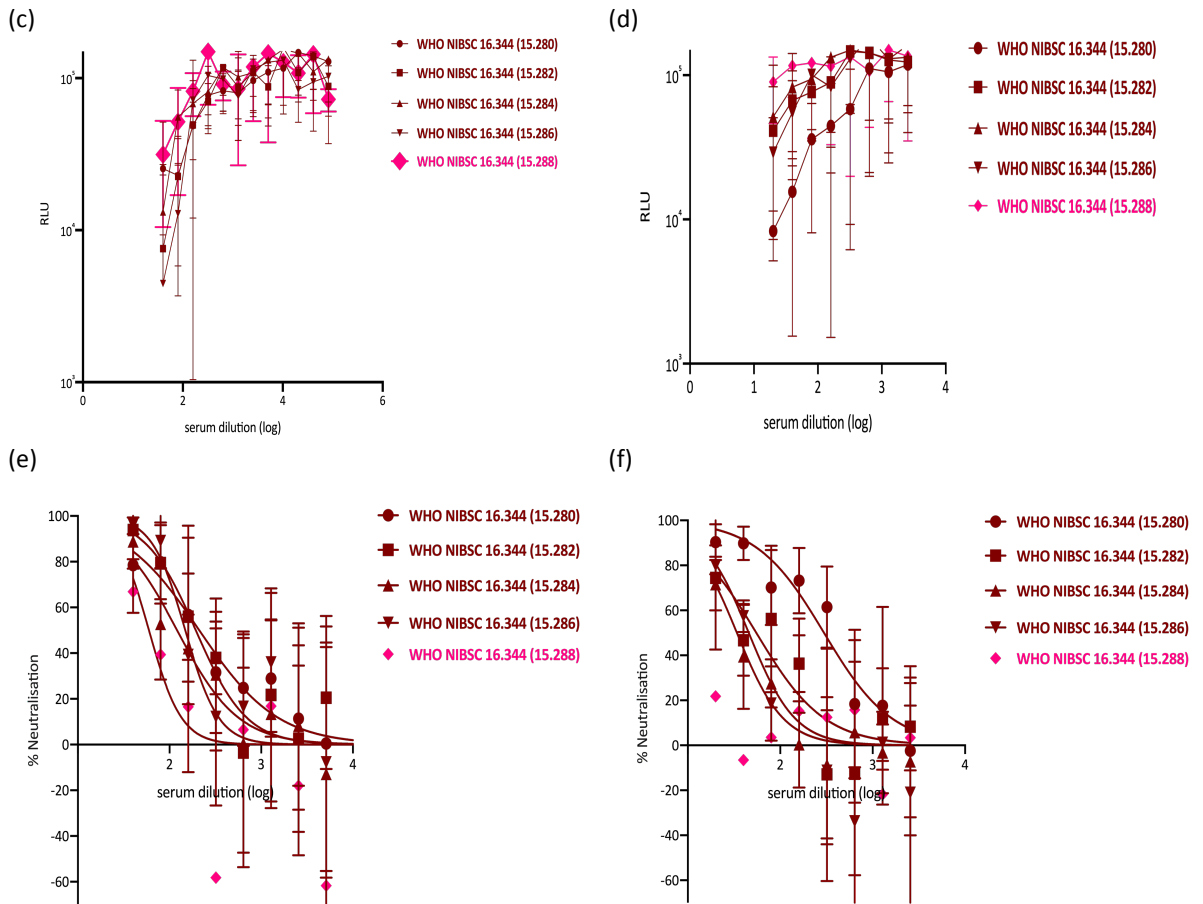


Figure 4.2. Neutralisation assay with anti-EBOV WHO NIBSC standard panel 16.344. lentiviral PVs bearing the EBOV (Makona C15) glycoprotein were used in PVNAs to compare (a,c,e) HEK293T and (b,d,f) CHO-K1 target cells. For each sera assessed (a-d) a decrease in transduction (RLU) at lower dilutions and 0% and 100% neutralisation values, as well as (c-d) shorter range on the y-axis, as well as neutralising curves showing the inverse relationship between increase in dilution and a decrease in neutralisation when antibodies are present in (e) HEK293T (15.280 $r^2 = 0.4$, 15.282 $r^2 = 0.4$, 15.284 $r^2 = 0.3$, 15.286 $r^2 = 0.3$, 15.288 $r^2 = 0.06$) and (f) CHO-K1 (15.280 $r^2 = 0.6$, 15.282 $r^2 = 0.5$, 15.284 $r^2 = 0.5$, 15.286 $r^2 = 0.6$, 15.288 $r^2 = 0.01$). Results from four independent experiments. Graphs and non-linear regression curves (log [inhibitor] vs normalised response; constraint: hill slope <0) generated with Prism 8.

The panel of sera from four patients (NIBSC 16.344) who recovered from EVD (15.280, 15.282, 15.284 and 15.286) and a negative control serum (15.288) performed similarly in PVNAs with either with HEK293T (Figure 4.2 a,c & e) or CHO-K1 (Figure 4.2 b,d & f) as target cell lines. In HEK293T target, the decrease in transduction was less accentuated (Figure 4.2a) in comparison to the negative control serum (NIBSC 15.288), in contrast to the CHO-K1 cell line (Figure 4.2b), where there was a greater antibody-mediated reduction in transduction. In CHO-K1 target cells, there was less variability between replicates (higher r^2) and the regression model fitted the observations better (Figure 4.1f) than in HEK293T target cells lines (Figure 4.1e).

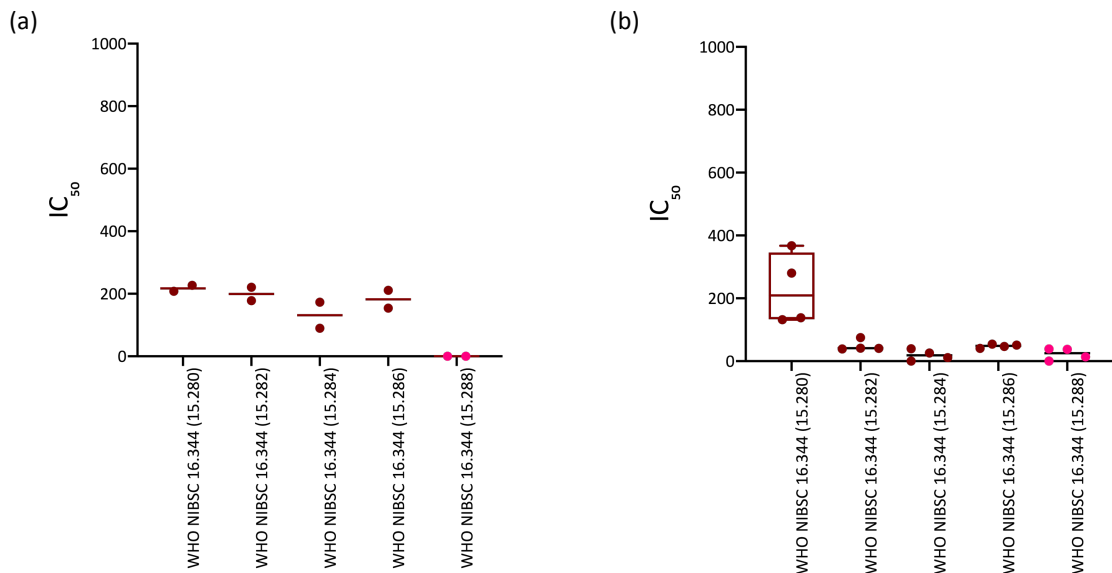


Figure 4.3. Neutralising titres of sera panel WHO NIBSC 16.344 against EBOV PVs. Either (a) HEK293T or (b) CHO-K1 target cells were used in PVNAs. IC₅₀ values are reported as the reciprocal of the dilution in which 50% of PVs were neutralised by the serum. Graphs and non-linear regression titres (log [inhibitor] vs normalised response; constraint: hill slope <0) generated with Prism 8.

When plotting a shorter range, the decrease in transduction is more evident, especially for NIBSC 15.280 in HEK293T (Figure 4.2c), and even more pronounced in CHO-K1 cell line (Figure 4.2d).

Finally, an affinity purified rabbit anti-EBOV GP polyclonal antibody was also tested against EBOV PVs, which had been validated for ELISA and western blot. No neutralising response was observed in the assay, with no detectable decrease in transduction (Figure 4.4).

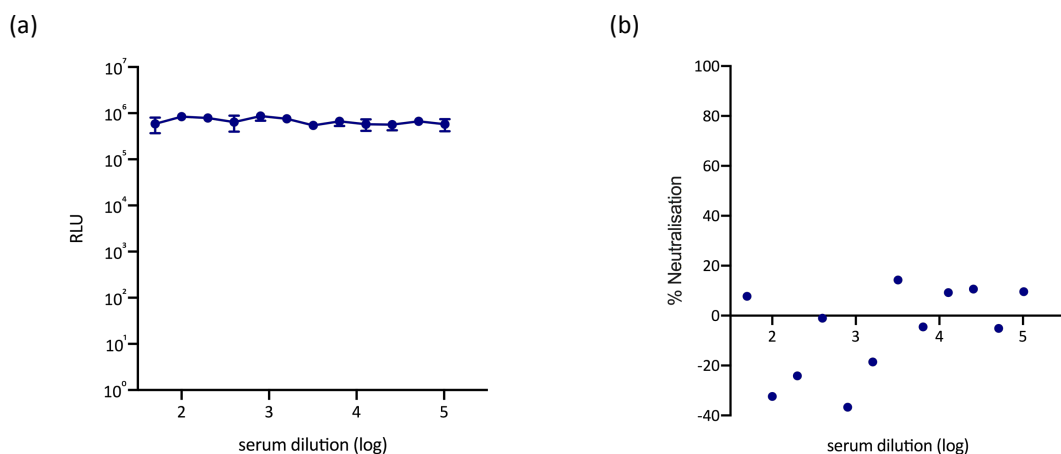


Figure 4.4. Neutralisation assay with rabbit polyclonal anti-EBOV serum against lentiviral PVs bearing the EBOV (Makona C15) glycoprotein. A (a) luminescence detected as well as (b) non-linear regression analysis Results from two independent experiments. Graphs generated with Prism 8.

4.3.1.2 Investigating consistency of PV input on PVNAs using both lentiviral and VSV cores

Lentiviral PVs showed consistent RLU values in all experiments in at least 8 wells for each virus only control (Table 4.2).

PVs with a VSV core were generated successfully (Chapter 3) for all filovirus GPs available as well as LASV. However, when PVNAs were attempted, the VSV core PV input was not consistent, especially for EBOV or RESTV (Table 4.2), after repeated attempts.

PV	EBOV VSV	EBOV lenti	RESTV VSV	RESTV lenti	RAVV VSV	RAVV lenti
Lowest read	7.8×10^1	2.5×10^5	6.2×10^2	1.9×10^5	2.7×10^5	1.4×10^5
Highest read	2.2×10^5	5.5×10^5	3.5×10^5	3.5×10^5	1.3×10^6	5×10^5
Mean luminescence (RLU/well)	4.3×10^4	3.9×10^5	1.4×10^5	2.9×10^5	7.5×10^5	2.4×10^5

Table 4.2. PV input for EBOV, RESTV and RAVV VSV and lentiviral PVs. Each PV input was aimed at 1×10^5 RLU/well (~ 100 TCID₅₀/well) in at least eight replicates. RLU values shown are the raw data from the luminometer. This is a representative example from numerous attempts. Table created with Excel for Mac 2011.

While RAVV VSV PVs were very consistent with most values within the 10^5 RLU range, RESTV and EBOV were not sufficiently consistent to perform well in PVNAs, with EBOV VSV PVs ranging from 10^1 to 10^5 RLU/well (Table 4.2).

4.3.1.3 Neutralising antibody response and cross-reactivity

Antibody neutralising responses against lentiviral EBOV PVs were variable ranging from 71 to 691 IC₅₀ (median = 192) with NIBSC 15.262 convalescent serum (Figure 4.5a), and 84 to 805 (median = 157) with NIBSC 15.220 convalescent serum (Figure 4.5b).

The two negative controls, human (Figure 4.5c) and horse (Figure 4.5d) negative serum, showed no neutralising response against any of the PVs tested. In the pooled serum NIBSC 15.262, low-level cross-reactivity was observed against RAVV PVs (Figure 4.5a). In the NIBSC 15.220 convalescent serum from a single patient, cross-reactivity was more apparent, with RAVV PVs cross-reacting the most (Figure 4.5b). Both convalescent sera were less reactive against LLOV or RESTV PVs (Figure 4.5a-b).

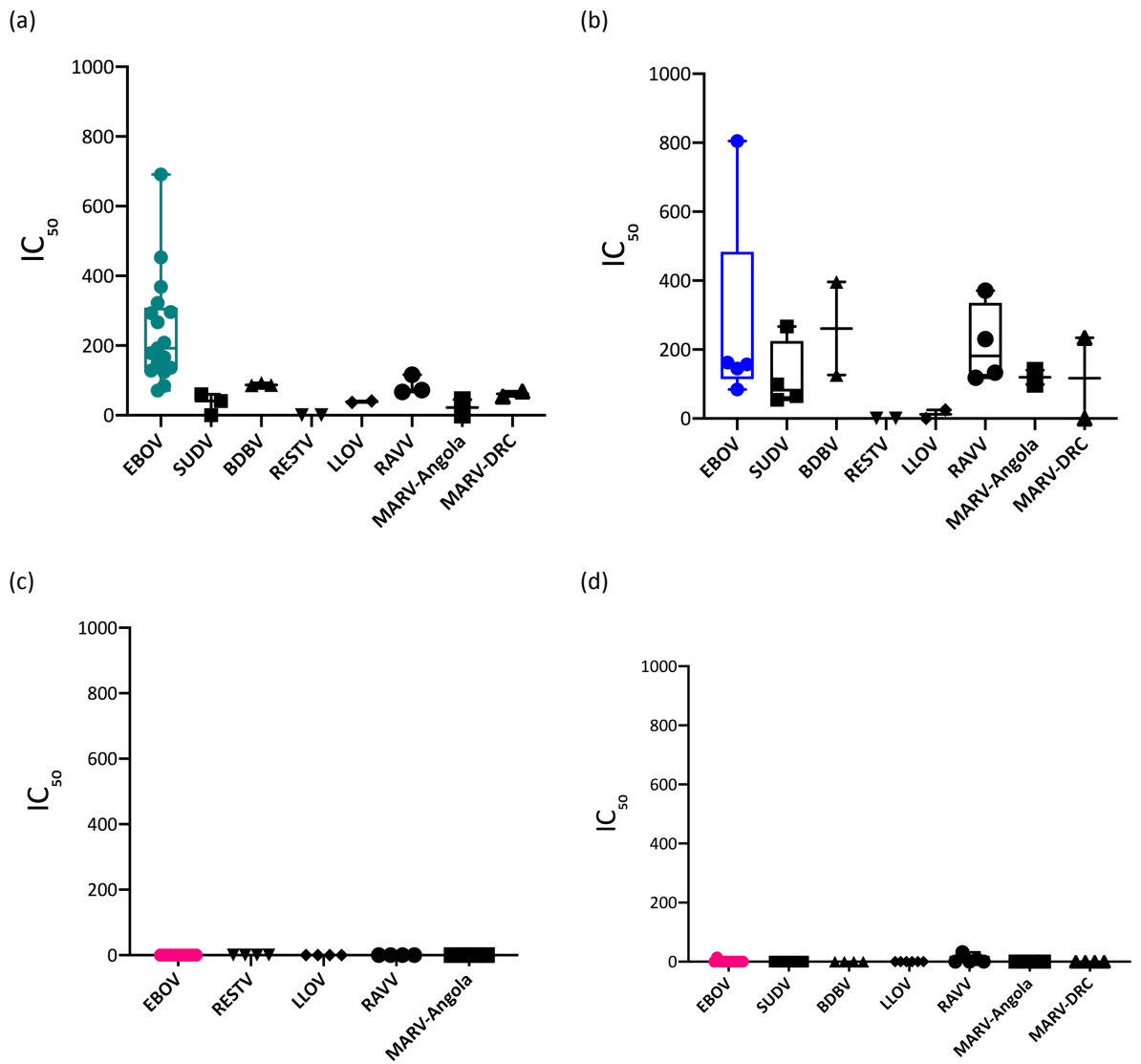


Figure 4.5. Neutralising titres of PVNAs with different filovirus PVs. Serum samples: (a) WHO NIBSC 15.262, (b) WHO NIBSC 15.220, (c) negative human serum and (d) negative horse serum. IC_{50} values are reported as the reciprocal of the dilution in which 50% of PVs were neutralised by the serum. Graphs and non-linear regression titres (log [inhibitor] vs normalised response; constraint: hill slope <0) generated with Prism 8.

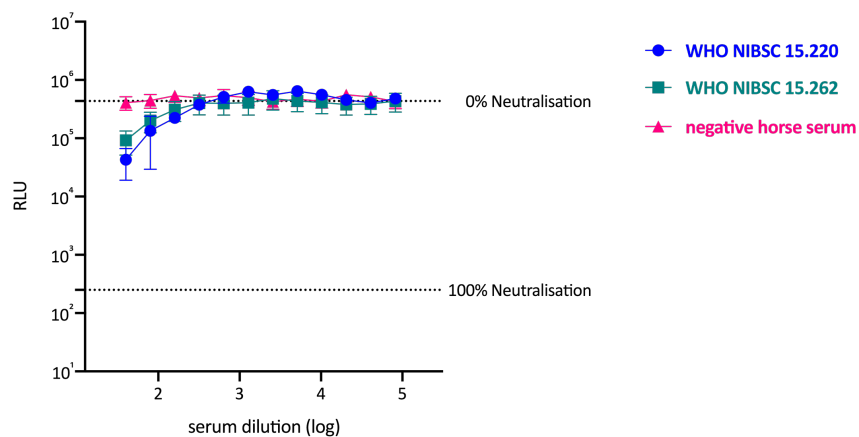


Figure 4.6. Neutralisation assay with anti-EBOV WHO NIBSC standards against lentiviral RAVV PVs. The decrease in transduction (RLU) is shown for each standard, as well as 0% and 100% neutralisation values. Results from at least two independent experiments. Graph generated with Prism 8.

In general, EBOV convalescent sera appeared to cross-react the most against RAVV PVs as the reduction in luminescence observed was comparable to EBOV (Figure 4.6).

The panel NIBSC 16.344 was also tested for cross-reactivity against LLOV and MARV PVs. While the NIBSC serum panel 16.344 did not cross-react against LLOV PVs (Figure 4.7a), it cross-reacted slightly against MARV (Angola) PVs, especially against NIBSC 15.286 (Figure 4.7b).

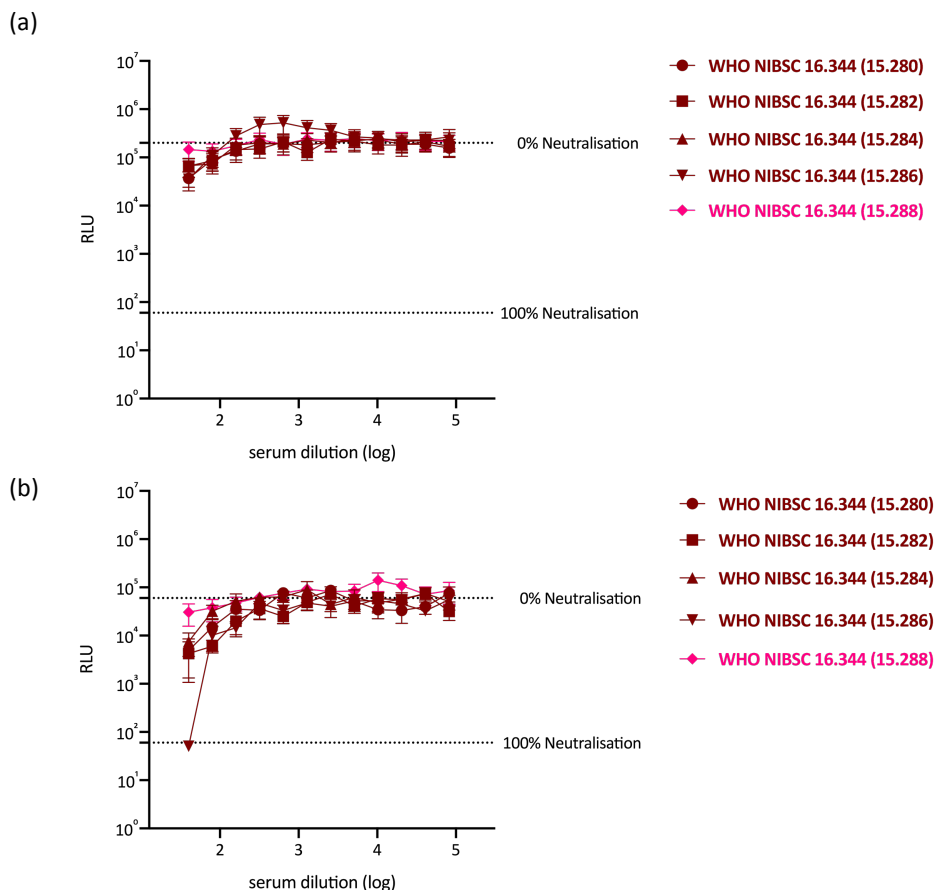


Figure 4.7. Neutralisation assay with anti-EBOV WHO NIBSC 16.344 standard against lentiviral PVs. PVs bearing the (a) LLOV and (B) MARV (Angola) glycoproteins were used. The decrease in transduction (RLU) and 0% and 100% neutralisation values are shown. Results from at least two independent experiments. Graph generated with Prism 8.

4.3.1.4 Neutralising responses of monoclonal antibodies against Filovirus PVs

The neutralising antibody response against EBOV PVs, including cross-reactivity against other species and genera, will also be discussed in Chapter 5 using anti-EBOV mAbs 4G7, 1H3 and KZ52 as examples. A further panel of mAbs targetting the EBOV GP – FVM04, FVM09 and CA45 were tested in PVNAs against EBOV PVs here. In addition, a monoclonal

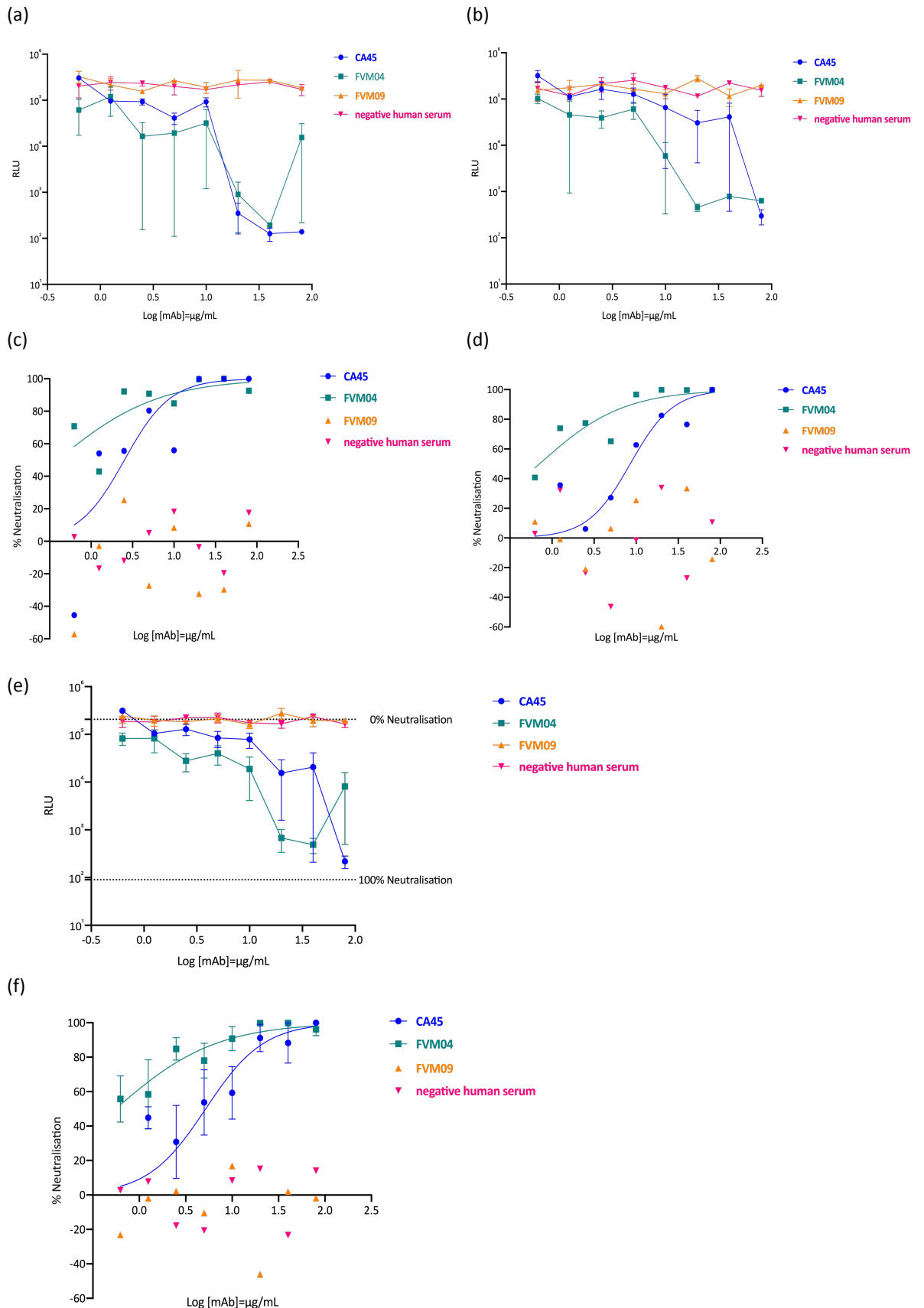


Figure 4.8. Neutralising responses of monoclonal antibodies targetting the EBOV GP. (a-b) RLU decrease of two independent tests and (c-d) neutralisation curves of each test (CA45 $r^2 = 0.6$ & 0.5 , FVM04 $r^2 = 0.3$ & 0.6 , FVM09 $r^2 = 0.07$ & 0.004 , negative serum $r^2 = 0.04$ & 0.004). Combined (e) transduction decrease including 0% and 100% neutralisation values and (f) neutralisation curves (CA45 $r^2 = 0.5$, FVM04 $r^2 = 0.4$, FVM09 $r^2 = 0.03$, negative serum $r^2 = 0.01$) of two independent tests. Graphs and non-linear regression curves (log [inhibitor] vs normalised response; constraint: hill slope >0) generated with Prism 8.

antibody targeting the RAVV GP – MR78 was tested in PVNAs against RAVV and MARV PVs.

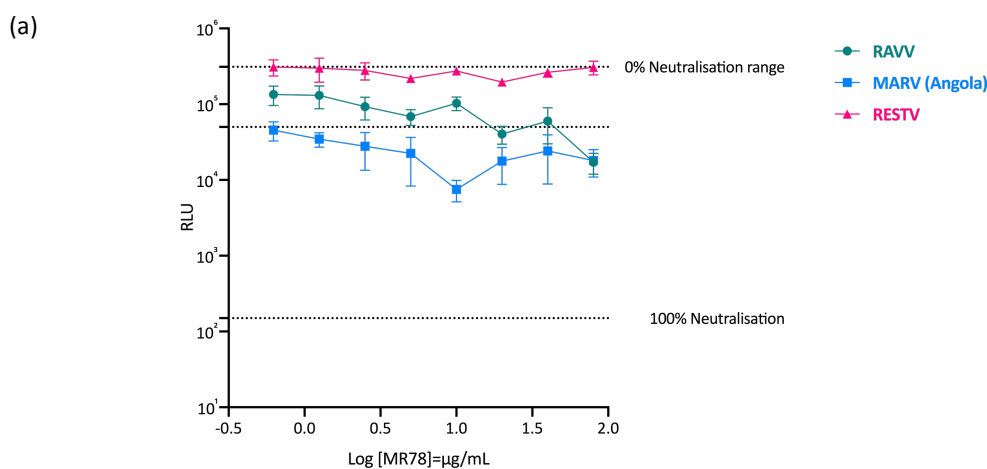
A strong neutralising response was observed in the PVNA with mAb FVM04, with a decrease in cell transduction evident by the decrease in luminescence (Figure 4.8e). The assay was reproducible, both in terms of transduction decrease (Figure 4.8a & b) and IC₅₀ values, with a mean IC₅₀ of 0.6 µg/mL (Table 4.3).

Monoclonal antibody CA45 had a more moderate neutralising response, with a decrease in transduction (Figure 4.8e) and a mean IC₅₀ of 5.2 µg/mL (Table 4.3), whereas mAb FVM09 did not neutralise EBOV PVs in this study (Figure 4.8 and Table 4.3), as expected.

	CA45	FVM04	FVM09	Neg human serum
PVNA#1	2.5	0.4	NN	NN
PVNA#2	8.5	0.7	NN	NN
n=2	5.2	0.6	NN	NN

Table 4.3 IC₅₀ (µg/mL) values on PVNAs using mAbs against EBOV PVs in HEK293T target cells. NN = not neutralised. Non-linear regression analysis performed with Prism 8.

Monoclonal antibody MR78 isolated from a patient who recovered from MVD had a weak neutralising response against RAVV and MARV (Angola) with IC₅₀ values of 19.3 µg/mL and 24.8 µg/mL respectively.



(b)

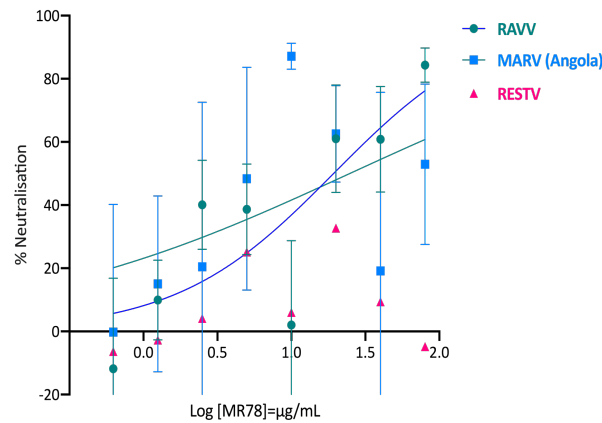


Figure 4.9. Neutralising responses of mAb MR78 targetting the Marburg virus GP. (a) RLU reduction including 0% and 100% neutralisation values, (b) neutralisation curve (RAVV vs MR78 $r^2 = 0.2$, MARV (Angola) vs MR78 $r^2 = 0.02$ RESTV vs MR78 $r^2 = 0.01$). Graphs and non-linear regression curves (log [inhibitor] vs normalised response; constraint: hill slope >0) generated with Prism 8.

The transduction decrease with MR78 mAb was fairly moderate against MARV or RAVV PVs (Figure 4.9). MR78 did not cross-react with RESTV PVs in this study and were used as a negative control (Figure 4.9).

4.3.2 PV ELISA

The use of PVs as antigens in ELISA will be further discussed in Chapter 5. Here, a preliminary optimisation of the ELISA protocol was attempted using purified PVs as antigens for detection of antibodies targetting the GP on the surface of virions. Convalescent sera and monoclonal antibodies were used as the primary antibody, either in an indirect or a sandwich ELISA platform.

4.3.2.1 PV concentration and purification in a 20% sucrose cushion

Filovirus PVs were concentrated and purified in a 20% Sucrose cushion to provide enough antigen for the assay, as described in Chapter 2. The amount of protein present was quantified according to the Pierce's BCA (bicinchoninic acid) assay kit.

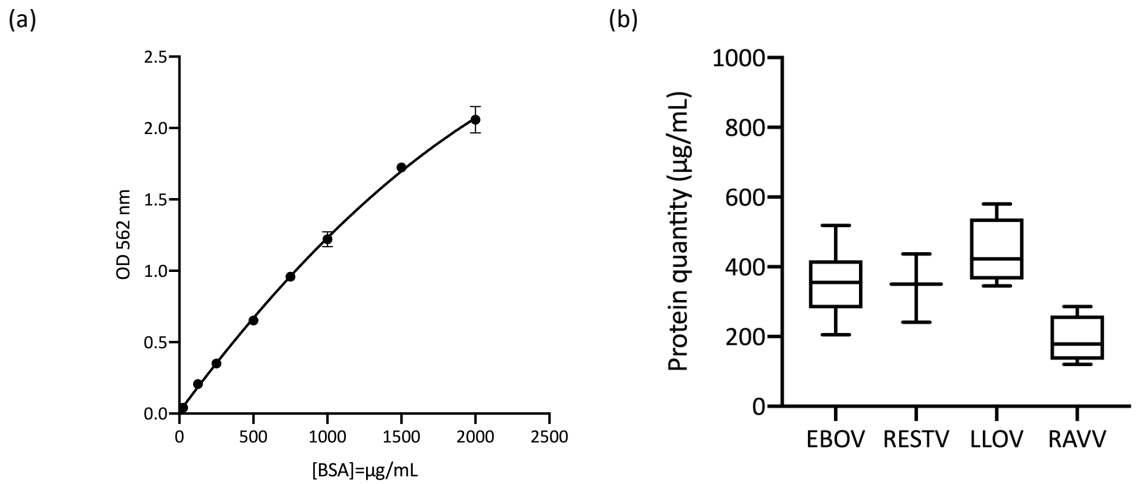


Figure 4.10. Protein quantification with Pierce's BCA assay. A (a) standard curve with known amounts of bovine serum albumin and (b) amount of protein found in samples. Standard curve and box-and-whisker plot generated with Prism 8.

For each assay, a bovine serum albumin (BSA) standard curve was generated (Figure 4.10a), and the unknown values from each purified PV sample (Figure 4.10b) were extrapolated using quadratic regression, as suggested by the manufacturer. Protein quantity values ranged from approximately 200 to 580 µg/mL per sample (Figure 4.10b). Concentrated EBOV PVs purified on a 20% sucrose cushion were titrated in an infectivity assay as described in Chapters 2 and 3. Purified PVs retained their functional titre (Figure 4.11) and were used as antigens in ELISA for detection of antibodies against EBOV in convalescent serum, as well as monoclonal antibodies targetting the EBOV GP.

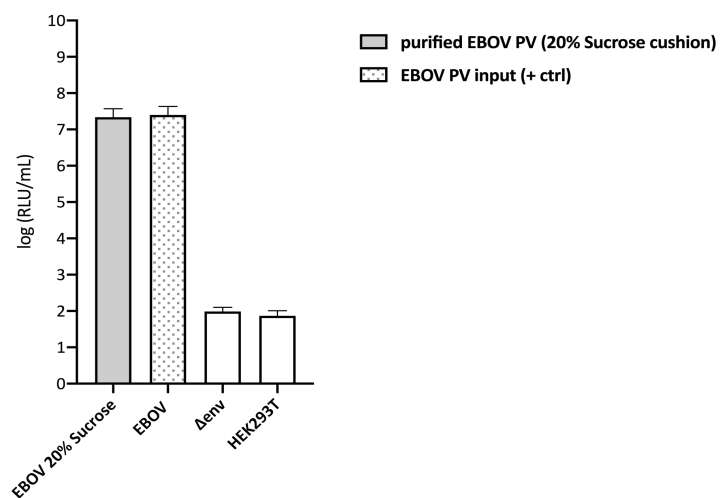


Figure 4.11. Infectivity assay of concentrated EBOV PVs for use in ELISA. Original, unpurified EBOV PV was used as a positive control for the assay. PV particles devoid of GP (Δ env) and uninfected cells (HEK293T) were negative controls. PV titres and graph generated with Prism 8.

4.3.2.2 PV ELISA optimisation

An indirect ELISA was attempted using NIBSC 15.262 pooled convalescent serum as the primary antibody to assess whether a carbonate-bicarbonate buffer would perform better than DPBS as an appropriate coat buffer in ELISA.

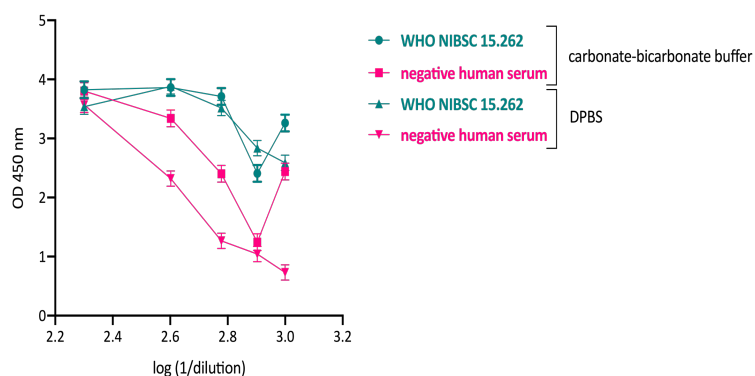
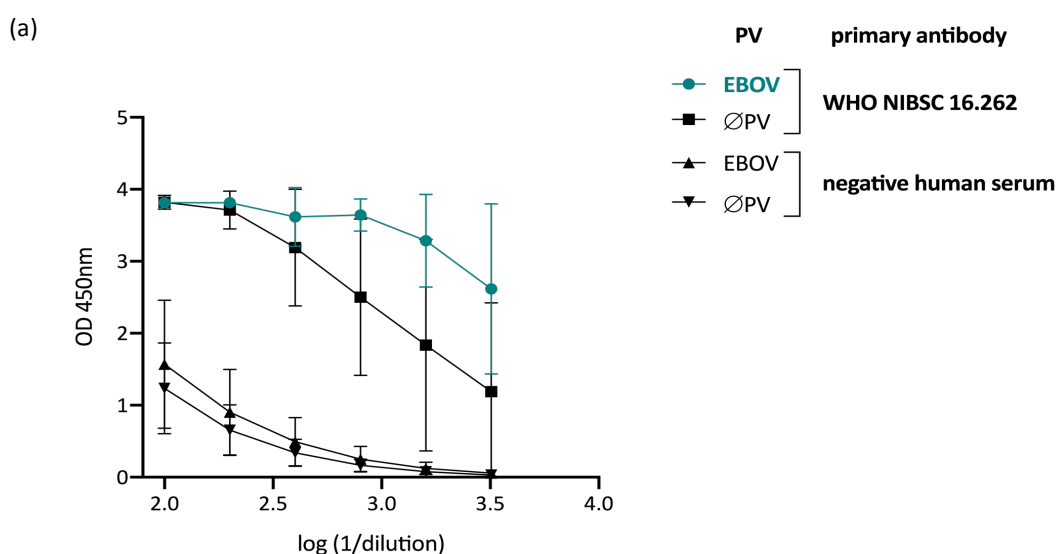


Figure 4.12. Indirect ELISA. EBOV PVs were used to coat the plate at 50 µg/mL in either carbonate-bicarbonate buffer or DPBS. WHO NIBSC 15.262 pooled convalescent serum was used as the primary antibody and an anti-human IgG (1:5000) as the secondary antibody. Results from at least two independent experiments. Graph generated with Prism 8.

The signal from EBOV coated wells was equivalent when carbonate-bicarbonate or DPBS were used as buffers (Figure 4.12). However, the background signal from the negative human serum appeared to be lower when DPBS was used as a buffer (Figure 4.12), therefore DPBS was used in subsequent ELISAs.



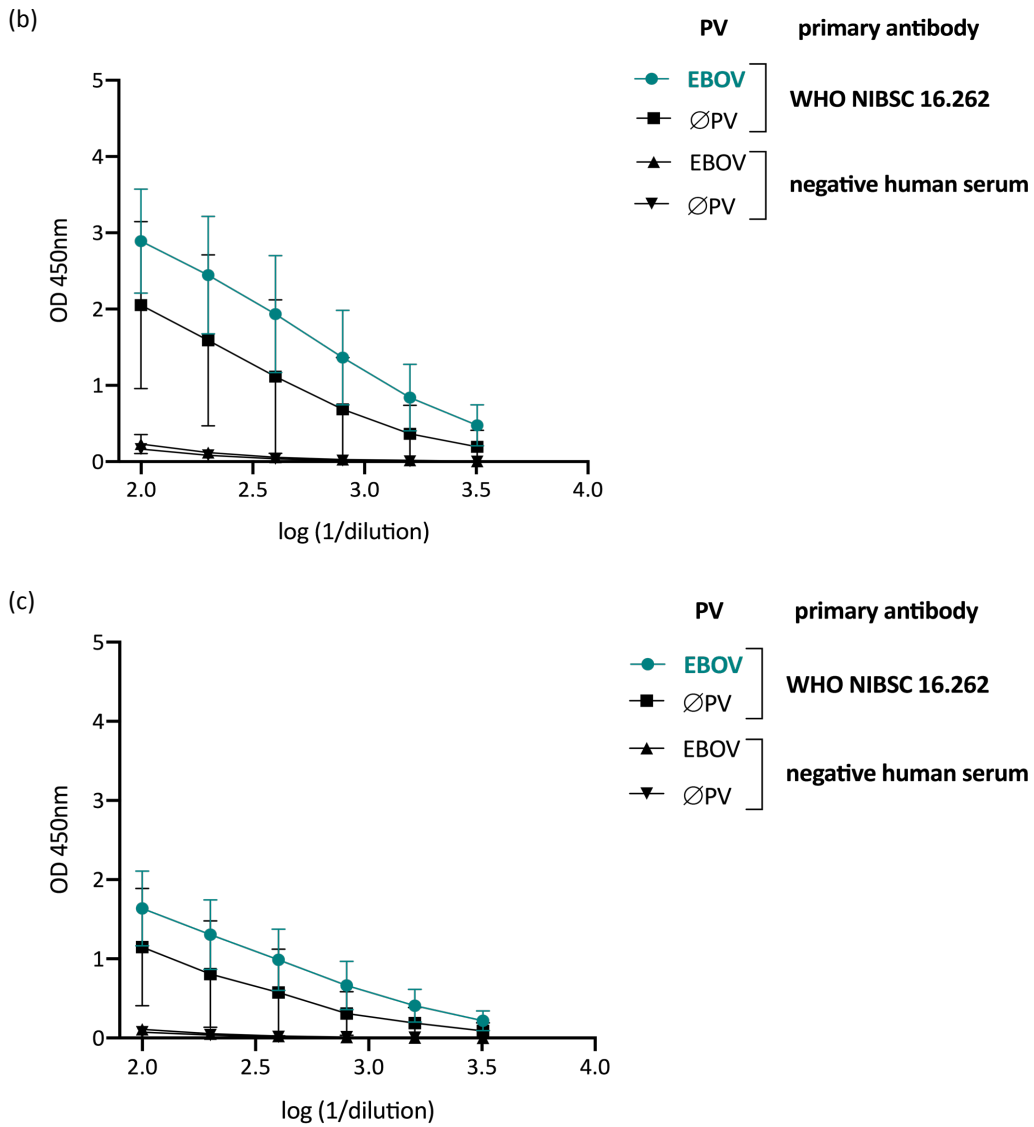


Figure 4.13. Indirect ELISA to assess secondary antibody input. EBOV PVs were used to coat the plate at 50 $\mu\text{g}/\text{mL}$ in DPBS. ΦPV are wells coated with DPBS only. WHO NIBSC 15.262 pooled convalescent serum was used as the primary antibody and an anti-human IgG as the secondary antibody at (a) 1:5000, (b) 1:50000 and (c) 1:100000 dilutions. Results from at least two independent experiments. Graph generated with Prism 8.

The signal was still higher than expected therefore optimisation of the secondary anti-human IgG antibody was attempted by assessing various dilutions; 1:5000, 1:50000 and 1:100000.

As expected, the signal from the convalescent serum NIBSC 15.262 binding to EBOV PVs was higher at the 1:5000 dilution (Figure 4.13a), decreasing at lower dilutions (Figure 4.13b-c). The background signal from wells that had not been coated with EBOV PVs was high in all conditions (Figure 4.13), however there seemed to be a greater difference between EBOV coated wells and buffer only wells at lower primary antibody dilution when the secondary antibody dilution was 1:5000 (Figure 4.13a), therefore the 1:5000 dilution of anti-human IgG secondary antibody was utilised thereafter.

4.3.2.3 ELISA for detection of antibodies in convalescent sera

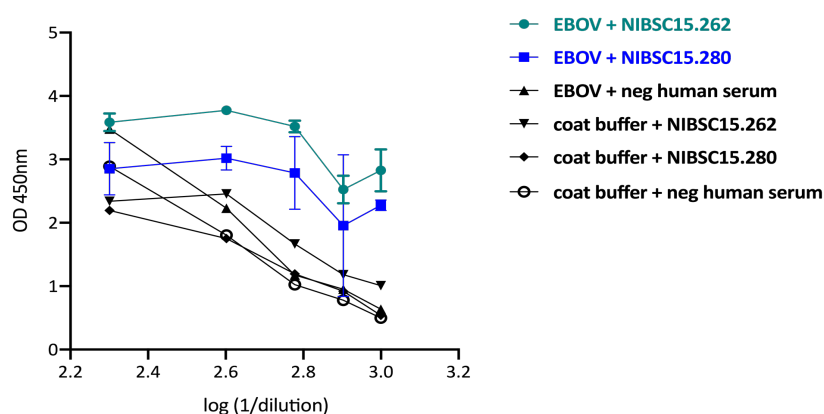


Figure 4.14. Indirect ELISA to screen convalescent sera. EBOV PVs were used to coat the plate at 50 µg/mL in DPBS. WHO NIBSC 15.262 and NIBSC 15.280 (NIBSC 16.344) were used as the primary antibody and an anti-human IgG as the secondary antibody at a 1:5000 dilution. Results from at least two independent experiments. Graph generated with Prism 8.

EBOV convalescent serum NIBSC 15.262 resulted in higher binding to the EBOV PV antigen target than NIBSC 15.280 (Figure 4.14), as well having a higher neutralising antibody titres in PVNAs (Figure 4.5). Background signal from negative human serum and wells not coated with EBOV PVs (coat buffer) was still high (Figure 4.14), especially at lower dilutions.

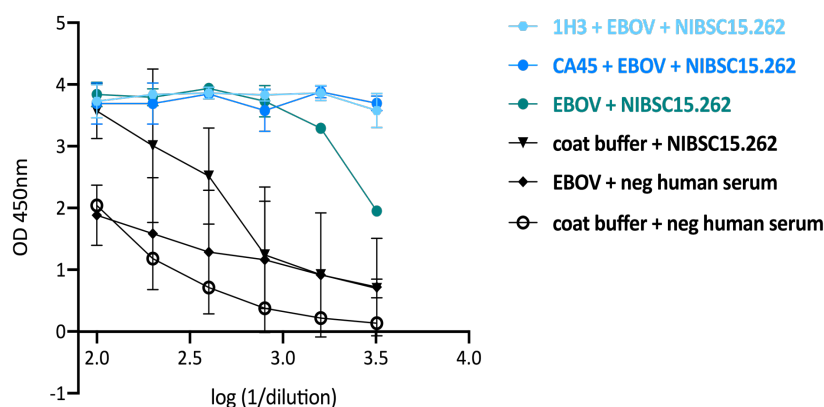


Figure 4.15. Sandwich capture ELISA. Plate was coated with monoclonal antibodies 1H3 and CA45 targetting EBOV GP before purified EBOV PVs were added to set up the assay. Results from at least two independent experiments. Graph generated with Prism 8.

A sandwich capture ELISA using monoclonal antibodies 1H3 and CA45 targeting the EBOV GP was used to attempt to increase specificity. Binding using these antibodies was similar whether a capture (Figure 4.15-light and dark blue) or indirect (Figure 4.15-green) ELISA was used. The background signal was high as in previous indirect ELISA experiments.

Cross-reactivity of convalescent serum was also explored using ELISA.

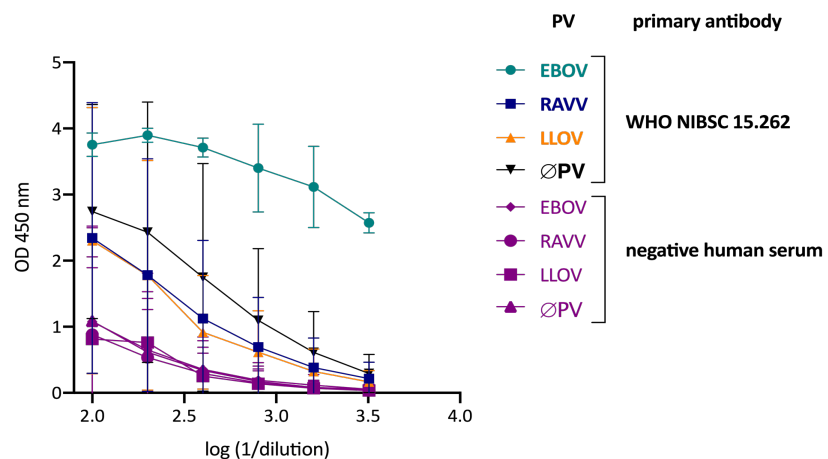


Figure 4.16. Indirect ELISA to assess cross-reactivity. EBOV, RAVV and LLOV PVs were used to coat the plate at 50 µg/mL in DPBS. WHO NIBSC 15.262 was used as the primary antibody and an anti-human IgG as the secondary antibody at a 1:5000 dilution. Results from at least two independent experiments. Graph generated with Prism 8.

NIBSC 15.262 did not cross-react with RAVV or LLOV PVs (Figure 4.16). Both were within the range of the background signal from the negative controls (Figure 4.16). Background from convalescent serum in wells not coated with EBOV PVs was higher than negative human serum (Figure 4.16).

4.3.2.4 ELISA with monoclonal antibodies targeting EBOV GP

When monoclonal antibodies targeting the EBOV GP were used as primary antibodies in an indirect ELISA, all the three mAbs tested bound to EBOV PVs. The mAb KZ52, isolated from a human patient during the EBOV Kikwit (DRC) outbreak of 1995 bound the strongest (Figure 4.17).

Monoclonal antibodies 4G7 and 1H3 isolated from GP immunised mice bound less strongly than KZ52 (Figure 4.17). Background signal from uncoated wells was negligible for the mAbs tested (Figure 4.17)

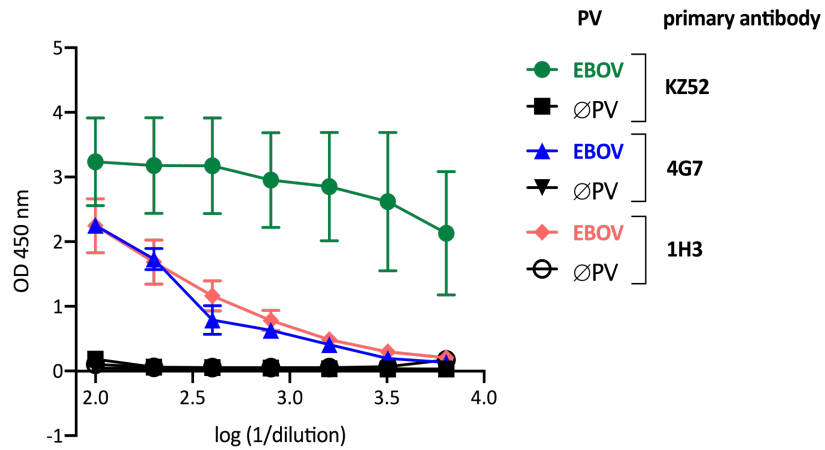


Figure 4.17. Indirect ELISA to screen monoclonal antibodies targetting the EBOV GP. EBOV PVs were used to coat the plate at 50 µg/mL in DPBS. Monoclonal antibodies KZ52, 4G7 and 1H3 were used as the primary antibody, an anti-human IgG (for KZ52) and anti-mouse IgG (for 4G7 & 1H3) as the secondary antibody at a 1:5000 dilution. Results from at least two independent experiments. Graph generated with Prism 8.

4.4 Discussion

Serological assays are very important to inform healthcare policy with regards to emerging diseases, as the current SARS-CoV-2 pandemic highlights. The need for sensitive and specific testing is paramount to managing such outbreaks.

The lack of extensive serological studies in the African continent has been implicated as one of the reasons the large EBOV outbreak in West Africa in 2013-6 became so widespread, because that particular geographical area was not previously associated with the virus (Formella and Gatherer 2016).

During outbreaks, diagnostic tests that are cheaper, simple to use and provide quick results are highly desirable (Clark *et al.* 2018). However, there is often a slight compromise in sensitivity or specificity in some of the rapid field tests available (Broadhurst *et al.* 2015; Phan *et al.* 2016).

Expanding the range of serosurveillance studies would be highly beneficial for management and control of future filovirus outbreaks in Africa. Even though the majority of outbreaks are caused by EBOV, other known pathogenic species of *ebolavirus* (SUDV, BDBV and TAFV) and *marburgvirus* (MARV, RAVV) have caused sporadic outbreaks with high mortality rates (Languon and Quaye 2019). Even though until recently there was not a licenced therapeutic approach to treat EVD or MVD, apart from support care and “compassionate” use of monoclonal antibodies and the rVSVΔG-ZEBOV vaccine (Murin *et al.* 2014; Mendoza, Qiu and Kobinger 2016; Mendoza, Racine and Kobinger 2017; Dhama

et al. 2018), having a test that could differentiate between species and genera of filoviruses would help monitor outbreaks and viral distribution. Also, it could dictate therapeutic strategies should more suitable treatments be available in the future, especially if treatment is specific to a particular species or genus.

Pseudotype based assays are excellent candidates for conducting such studies in low containment research facilities. They produce more rapid results than the traditional plaque reduction neutralisation assay. Initially, PVNAs were not thought to correlate well with authentic virus neutralisation assays (Wilkinson *et al.* 2017), however only a few labs were involved in this study and some technical issues were reported. More recently, PVNAs have been found to better correlate with live virus assays than previously thought (Ewer *et al.* 2016; Lambe, Bowyer and Ewer 2017; Konduru *et al.* 2018).

In this study, we utilised filovirus PVs to assess their suitability in detecting previous infection using convalescent serum available commercially from NIBSC; as well as monoclonal antibodies targetting Ebola (EBOV) and Marburg (RAVV, MARV) GP. All PVs used for PVNAs had a lentiviral core. Three convalescent sera were available, all from patients that had recovered from EVD, including a pooled serum from six patients (NIBSC 15.262) and a panel of five (NIBSC 16.344).

The neutralising antibody response was moderate (Figure 4.1). A decrease in transduction equating to a decrease in luminescence, was observed for both NIBSC 15.220 and NIBSC 15.262 (Figure 4.1). Neutralising titres ranged from 84 to 805 (Figure 4.5b) for NIBSC 15.220, whereas for NIBSC 15.262 they ranged from 71 to 691 (Figure 4.5a). The antibody neutralising titres found for NIBSC 15.220 corresponded to the initial assessment of this sample by NIBSC. According to their report, the convalescent plasma was collected approximately 3 months post-infection (Wilkinson *et al.* 2015). Their reported titres for PVNA using lentiviral EBOV PVs ranged from <20 to 180, with a reported median of 164, while VSV PVs had reported titres of up to 427. Authentic EBOV yielded titres between 20 and 180 (Wilkinson *et al.* 2015). The median from our PVNAs with lentiviral PVs was 157 from a total of 5 independent experiments (Figure 4.5b). The pooled sera NIBSC 15.262 had more consistent neutralising antibody titres (Figure 4.5a), with a slightly higher median of 192.

The panel of convalescent sera NIBSC 16.344 neutralising titres was comparable to those of 15.220 and 15.262 at approximately 200 (Figure 4.3a), using HEK293T target cells. The decrease in transduction was very similar to the negative control serum 15.288 (Figure

4.2a). A shorter range did not help in discerning those differences (Figure 4.2c), but the increase in transduction in the positive sera was inversely proportional to the serum dilution (Figure 4.2e).

The choice of target cell line is important because the assay depends on any antibodies in the test serum blocking transduction of target cells. The human derived HEK293T cell line would be a good candidate as a target cell, shown to be permissive to filovirus infection *in vitro*. However, the Chinese hamster CHO-K1 cell line had been previously tested in EBOV PVNAs and been found to produce clearer neutralising curves (Bentley *et al.* 2016). The decrease in transduction was more apparent when CHO-K1 cells were used as targets for all 4 sera (NIBSC 15.280, 15.282, 15.284 and 15.286), especially for 15.280 (Figure 4.2d) in comparison to the negative control serum NIBSC 15.288 (Figure 4.2b). Neutralising curves (Figure 4.2f) were similar to curves produced in HEK293T target (Figure 4.2e), however neutralising antibody titres for NIBSC 15.282, 15.284 and 15.286 were higher in HEK293T (Figure 4.3a) than in CHO-K1 target cells (Figure 4.3b). It is tempting to speculate whether a lower neutralising response might have gone undetected. NIBSC 15.280 resulted in consistently higher titres, whether in HEK293T or CHO-K1 target cells (Figure 4.3).

For NIBSC 15.220 and 15.262, the decrease in transduction was much more apparent in CHO-K1 target cells (Figure 4.2b), making it a superior target for detection of antibodies targetting filoviruses in PVNAs.

We also tested a polyclonal sera generated in rabbits immunised with EBOV GP, and validated for western blots and ELISA. It had been used in immunohistochemistry studies targetting the GP (Perry *et al.* 2018), and it could have been used as positive control in our study if a strong neutralising response was detected. However, no neutralisation was observed against EBOV PVs (Figure 4.4).

To compare VSV core PVs with our lentiviral PV panel, EBOV PVs with a VSV core were generated (Chapter 3). However, a consistent VSV core input was difficult to achieve. After titre was calculated, a dilution containing 2×10^6 RLU/mL (1×10^5 RLU/50 μ L) was made and pipetted in a plate with the appropriate number of cells. After incubation, the RLU readings were very inconsistent (Table 4.6), especially for EBOV VSV PVs, with titres ranging from 10^1 to 10^5 RLU/well. RAVV VSV PV however had more consistent RLU readings (Table 5.6). RESTV VSV PV exhibited more wells with the target 10^5 RLU/well but was also inconsistent with titres as low as 10^2 RLU/well, in contrast to lentiviral PVs which produced consistent luminescence readings between replicates (Table 5.6). Therefore, EBOV VSV PVs could not be used in PVNAs until further optimisation to resolve the input

inconsistency issue. VSV has been reported to caused cytotoxicity resulting in characteristic cell rounding which was observed at lower dilutions of VSV core PVs (Kopecky and Lyles 2003), therefore shorter incubation periods could have been attempted.

It is not clear why *marburgvirus* VSV PVs were more consistent in the infectivity assay, except for a possible synergistic effect with cytotoxicity caused by VSV and the EBOV GP (Yang *et al.* 2000). The issue of MARV/RAVV PVs resulting in higher titres has been discussed in Chapter 3. Several differences are observed in *marburgviruses* with regards to GP expression such as lack of sGP, different location of protease cleavage site and route of infection (Volchkov *et al.* 2000; Hunt, Lennemann and Maury 2012).

In any serological study, sensitivity and specificity are crucial for accurate results. As one of the aims of this project was to produce a pseudotype based assay that can distinguish between genera and species of filoviruses, we tested our panel of lentiviral PVs displaying filovirus GPs across the three main genera: EBOV, SUDV, BDBV, RESTV, LLOV, RAVV and MARV. Some cross-reactivity was detected against certain PVs. The NIBSC 15.220 standard cross-reacted mainly with RAVV PVs and to a less extent with SUDV (Figure 4.5b). The pooled sera NIBSC 15.262 also cross-reacted with RAVV PVs (Figure 4.5a), albeit to a less extent than 15.220.

The NIBSC 16.344 panel was tested for cross-reactivity with LLOV and MARV (Angola) PVs. No apparent transduction decrease was observed against LLOV PVs (Figure 4.7a), however the panel reacted slightly against MARV (Angola) PVs, particularly serum 15.286 (Figure 4.7b).

Initially, the negative serum available was a horse serum of UK origin. The horse was immunised against different subtypes of equine influenza as well as equine herpesvirus (Dr Simon Scott – personal communication), and it would not have ever been exposed to filovirus infection. As expected, the horse serum did not neutralise any of filovirus PVs tested (Figure 4.5d). A human negative serum became available later on and was used in subsequent assays as a more suitable negative control.

In an indirect ELISA, which does not rely in neutralisation but rather antibody binding to the target antigen, convalescent serum NIBSC 15.262 bound to EBOV PVs but not to RAVV PVs (Figure 4.16). Serum NIBSC 15.220 was not tested in ELISA.

It is not clear why cross-reactivity was observed in neutralisation assays but not in ELISA. However, ELISA relies on antibodies binding to specific epitopes on the GP whereas neutralisation can be achieved through different mechanisms such as blocking of receptor

binding or capsid binding in case of non-enveloped viruses, blocking endocytosis, intercalation of antibodies between the virus-cell fusion membranes, conformational changes in the GP induced by antibody binding. Also, high antibody affinity is not always required for successful neutralisation (Klasse and Sattentau 2002; Nelson *et al.* 2007; Marasco and Sui 2007; King *et al.* 2018; Schuh *et al.* 2019). It would be reasonable to assume cross-reactivity in polyclonal serum if antibodies are targetting conserved amino acid sequences. On the other hand, ELISA relies on specific binding and could be used along with PVNA to rule out cross-reactivity. ELISA also has the advantage of not requiring cell culture facilities or high containment as recombinant proteins could be used instead of viruses (Wilkinson *et al.* 2017).

Monoclonal antibodies (mAbs) targetting the EBOV GP were used in PVNAs: mAbs 4G7, 1H3 and KZ52 will be discussed in detail in Chapter 5 where attempts were made to improve specificity in PVNAs. Here, neutralising mAbs CA45 and FVM04, as well as non-neutralising mAb FVM09 were used in PVNAs (Figure 4.8). As expected, CA45 and FVM04 neutralised EBOV PVs successfully (Figure 4.9e-f) with IC_{50} of 5.2 and 0.6 $\mu\text{g}/\text{mL}$ respectively (Table 4.3).

CA45 is a macaque derived mAb and has been shown to neutralise EBOV, SUDV, BDBV and RESTV VSV PVs *in vitro*. IC_{50} values for EBOV VSV PVs were 1.2 $\mu\text{g}/\text{mL}$ for CA45 and 0.4 $\mu\text{g}/\text{mL}$ for KZ52 (Zhao *et al.* 2017). CA45 was also found to be protective in mice and guinea pigs against challenge with EBOV or SUDV; and in ferrets against BDBV (Zhao *et al.* 2017). Therefore, it could be explored for therapeutics as a pan-ebolavirus protective mAb.

FVM04 is also macaque derived and it was found to neutralise EBOV VSV PVs by blocking the receptor interaction, with an IC_{50} of 0.8 $\mu\text{g}/\text{mL}$ (Howell *et al.* 2016). It cross-reacted with SUDV and BDBV VSV PVs and protected mice and guinea pigs against experimental EBOV and SUDV infection (Howell *et al.* 2016).

In the current study, it neutralised lentiviral EBOV PVs with a similar IC_{50} of 0.6 $\mu\text{g}/\text{mL}$ (Table 4.3). Cross-reactivity with other PVs was not tested.

FVM09, another macaque derived mAb, is non-neutralising as reproduced here against EBOV PVs (Figure 4.8 and Table 4.3), however it had been found to enhance neutralisation (in a dose-dependent manner) to mAbs 2G4 and ADI15946, but not to KZ52 (West *et al.* 2019). It also provided partial protection against EBOV challenge in mice (Keck *et al.* 2016).

MR78 targets the receptor-binding site of *marburgviruses*. As the RBS is a conserved region amongst filoviruses, it has been reported to bind to EBOV GP lacking the mucin-like domain, which normally shields the RBS. M78 neutralises authentic MARV, however it does not neutralise authentic EBOV (Hashiguchi *et al.* 2015), and it did not cross-react with RESTV PVs in this study (Figure 4.9).

Neutralisation of MARV and RAVV was very mild (Figure 4.9) with IC_{50} values of 24.8 $\mu\text{g}/\text{mL}$ and 19.3 $\mu\text{g}/\text{mL}$ respectively. MARV (Uganda) VSV PVs were neutralised ($IC_{50} = 5 \mu\text{g}/\text{mL}$) by MR78, whereas authentic MARV (Uganda) were moderately neutralised at 93 $\mu\text{g}/\text{mL}$ (Flyak *et al.* 2015).

A PV ELISA using purified PVs was used to assess binding of polyclonal sera (NIBSC standards) as well as monoclonal antibodies to various filovirus GPs. PVs were purified on a 20% sucrose cushion (Figure 4.10) and remained viable in subsequent infectivity assays (Figure 4.11), suggesting its GP and virion had no integrity issues.

NIBSC 15.262 pooled serum standard bound to EBOV PVs in ELISA. Initially, two different coating buffers were used: carbonate-bicarbonate and DPBS. Binding of polyclonal antibodies to EBOV PVs was not affected by the choice of buffer, however background signal from the negative human serum was slightly lower when DPBS was used (Figure 4.12). Therefore, DPBS was selected as a buffer to coat plates with purified PVs.

The secondary antibody dilution was optimised in an indirect ELISA with 1:5000 (Figure 4.13a), 1:50000 (Figure 4.13b) and 1:100000 (Figure 4.13c) dilutions, however the difference in background and signal from the polyclonal serum was the same between the dilutions. The lowest dilution still had the better signal (Figure 4.13a).

Antibody neutralising titres seemed to correlate to higher binding, as seen with EBOV convalescent serum NIBSC 15.262 having a higher signal in ELISA than NIBSC 15.280 (Figure 4.14), as well having a higher neutralising antibody titre (Figures 4.5a). Background signal from negative human serum and wells not coated with EBOV PVs (coat buffer only) was still high (Figure 4.14), especially at lower dilutions. It is likely the anti-human secondary antibody is recognising the negative human serum, as non-specific binding to serum is one of the issues reported in ELISA (Güven *et al.* 2014; Terato *et al.* 2016; Moritz *et al.* 2019). In addition, the amount of antigen coated on the plates could have been optimised, as 50 $\mu\text{g}/\text{mL}$ is higher than reported in most studies (El-Duah *et al.* 2019; Atre *et al.* 2019; Bortz *et al.* 2020). In addition, it would have been interesting to test VSV core PVs in ELISA to assess performance against lentiviral PVs.

A capture ELISA using non-neutralising mAb 1H3 and neutralising mAb CA45 did not improve signal (Figure 4.15). However, background signal was lower than previous experiments (Figure 4.14 & 4.15).

Monoclonal antibodies performed much better in ELISA as primary antibodies than polyclonal sera. Neutralising mAbs KZ52 and 4G7 and non-neutralising mAb 1H3 were tested in an indirect ELISA. KZ52 had a higher mean OD than 4G7 and 1H3 (Figure 4.17). It is interesting to note KZ52 is a more potent neutralising mAb than 4G7 (Chapter 5), and it bound more strongly than 4G7 in ELISA (Figure 4.18). Furthermore, background was practically undetected (Figure 4.17).

In order to use filovirus PVs in PVNAs in future screening tests, further optimisation and validation will be required. But most importantly, cross-reactivity has to be addressed to improve specificity. This issue is explored in the next chapter utilising chimeric GPs.

CHAPTER 5: Epitope Modification of Filovirus Glycoproteins for Use in Pseudotype-based Neutralisation And Binding Assays (ELISA)

5.1 Introduction

Filoviruses are enveloped viruses with a 19 Kb single-stranded, non-segmented negative sense RNA genome that require handling in high containment (BSL-4). *Ebolavirus* and *marburgvirus* pathogenic species can cause mortality rates of up to 90% and the majority of infections occur in resource-limited regions, therefore improved diagnostics and therapeutics are warranted (Mühlberger 2007; Gire *et al.* 2014; Clark *et al.* 2018). Its glycoprotein (GP) is the only viral protein present on the surface of the virion and is the main target of neutralising antibodies. It is expressed in the cell-derived viral membrane as a trimer where each monomer consists of fragments GP₁ and GP₂ linked by disulphide bridges forming the shape of a “chalice” (Figure 5.1), with a base and a trans-membrane domain (Martin *et al.* 2016; Beniac and Timothy 2017; Gilchuk *et al.* 2018).

Pseudotyped viruses (PV) are a safe alternative for the study of BSL 3-4 viruses for entry, serological, antiviral screening and vaccine evaluation studies (Wright *et al.* 2008; Wright *et al.* 2010; Mather *et al.* 2013; Temperton, Wright and Scott 2015). Filovirus PVs have been used in neutralisation assays to characterise the antibody response against these viruses and evaluate their performance in a low containment setting (Chapter 4). EBOV PVs have been shown to correlate to live EBOV in neutralisation assays (Konduru *et al.* 2018) despite initial doubts about the correlation between the different platforms (Wilkinson *et al.* 2017). The convalescent serum available to us was derived from EBOV infection, responsible for most filovirus outbreaks, including the one in West Africa in 2013-2016 (Holmes *et al.* 2016; Malvy *et al.* 2019). These sera were WHO standards produced by NIBSC from patients that recovered from ebola virus disease (EVD). In the previous chapter, PVs bearing the EBOV GP were neutralised by the different WHO standards tested, as well as monoclonal antibodies targetting EBOV and RAVV. However, low-level cross-reactivity was detected when WHO standards were tested against different filovirus PVs (Chapter 4, Figs 4.5 - 4.7). To address this issue, we aimed to create a chimeric GP containing EBOV and RAVV epitopes in a neutral GP scaffold that could be used in future screening with improved specificity. The scaffold would be a filovirus GP that is not neutralised by heterologous sera. We selected LLOV and RESTV GPs as

scaffolds, as no cross-reactivity was observed when these were tested against the anti-EBOV WHO standards (Chapter 4).

Most EBOV neutralising antibodies target the base of the GP (Mohan *et al.* 2015; Davis *et al.* 2019). Neutralising epitopes 4G7 and KZ52 (Figure 5.1) and non-neutralising epitope 1H3 (Figure 5.1a-d) (Qiu *et al.* 2011; Zhang *et al.* 2016; Pallesen *et al.* 2016), as well as RAVV neutralising epitope MR78 (Figure 5.2) were selected for this study (Hashiguchi *et al.* 2015). EBOV epitopes not located within the receptor-binding site (RBS) were chosen whenever possible to avoid problems in generating PVs, as neutralisation assays are dependent on functional GP-receptor interactions.

To attempt a similar approach utilising *marburgvirus* neutralising epitopes, the monoclonal antibody MR78 was selected. However, most neutralising antibodies against MARV/RAVV (Figure 5.2) isolated so far target the RBS (Hashiguchi *et al.* 2015; Fusco *et al.* 2015), therefore two different approaches were used. Firstly, synthesising the LLOV GP gene with the multi-locus MR78 epitope. Secondly, creating a chimeric GP containing RAVV GP₁ RBS and the remainder of either LLOV or RESTV GP₁ and GP₂, in case introducing mutations in the RBS resulted in PVs not being able to transduce target cells, which is crucial in infectivity or neutralisation assays. There are neutralising antibodies against MARV that target the base of the GP that would have been more suitable than mutating epitopes in the RBS, however they have weaker neutralising activity when compared to MR78 (Fusco *et al.* 2015).

MR78 is part of a series of monoclonal antibodies targetting the RBS of MARV with varying degrees of neutralisation of both authentic virus or VSV core PVs. MR78 has strong neutralising activity against VSV PVs bearing MARV GP (Flyak *et al.* 2015). However, this neutralisation was only moderate when compared to the human mAb KZ52 against EBOV PVs (Zhang *et al.* 2016).

KZ52 is a potent EBOV neutralising monoclonal antibody (Figure 5.1e-h) isolated from a human survivor of the 1995 Kikwit EBOV outbreak. The epitope has two regions at the base of GP₂ and a two amino acid residue region at the N-terminus of GP₁ (Lee *et al.* 2008; Zhang *et al.* 2016).

EBOV neutralising epitope 4G7 and non-neutralising epitope 1H3 are murine derived and were part of ZMab along with 2G4, tested as potential therapeutics for EVD (Qiu *et al.* 2011; Audet *et al.* 2015), later developed into ZMapp comprised of 13C6, 2G4 and 4G7 (Qiu *et al.* 2014).

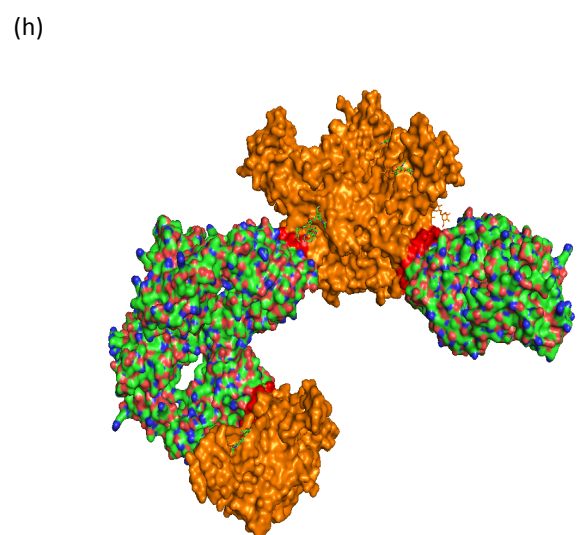
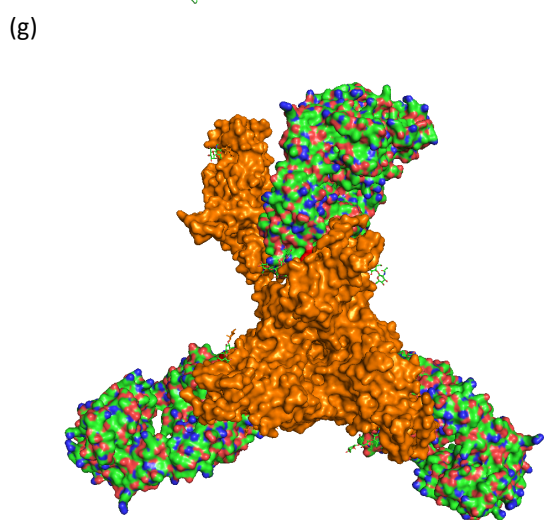
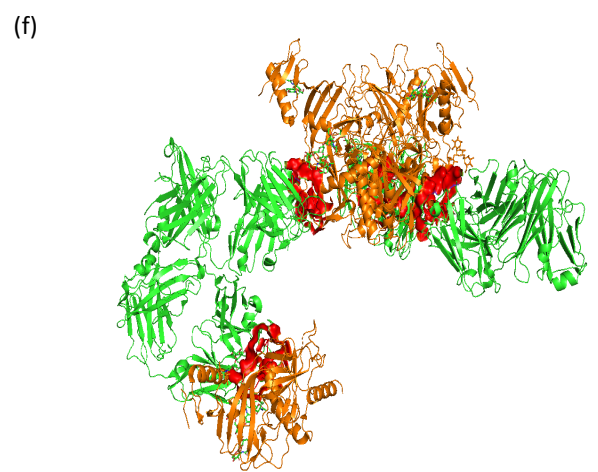
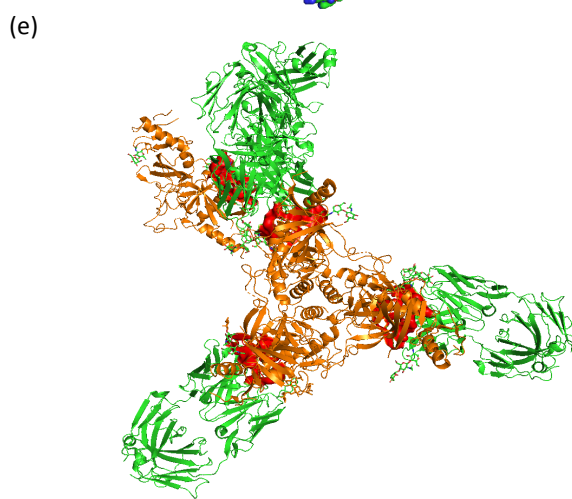
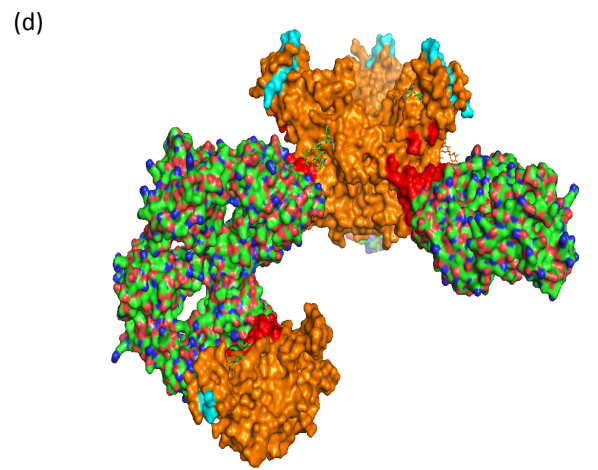
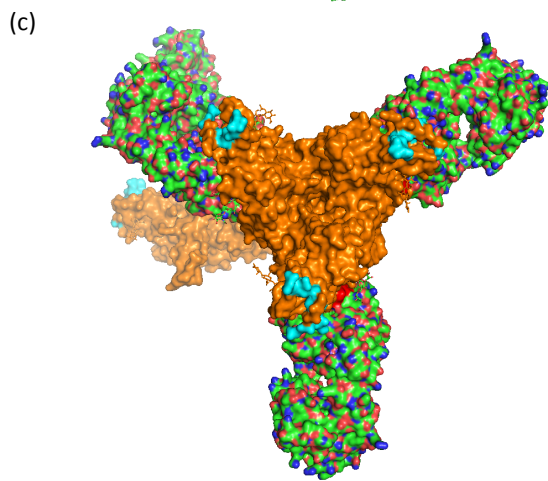
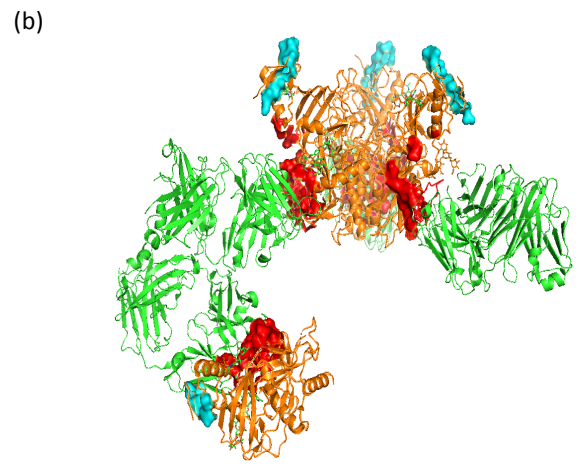
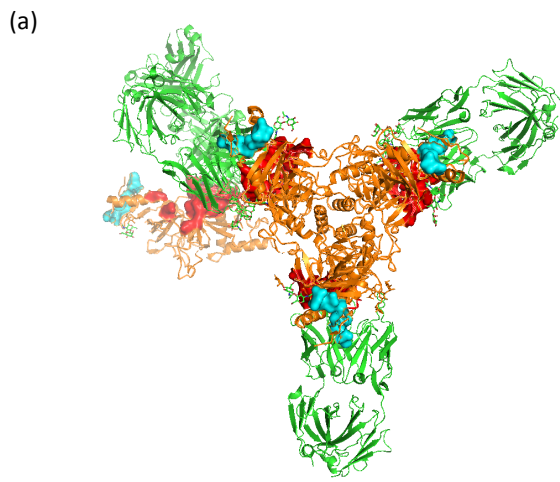


Figure 5.1. Structure of the EBOV GP trimer (orange) bound to the human antibody KZ52 (green). Ribbon display (a) top and (b) side views of the GP trimer with epitopes 1H3 (blue surface) on the top of the 'chalice' and 4G7 (red surface) at the base of the trimer. A monomer can be seen clearly in (b) bound to the second Fab fragment of KZ52. Surface display (c) top and (d) side views of the GP with epitopes 1H3 and 4G7. Ribbon display (e) top and (f) side views of the GP trimer with epitope KZ52 (red surface) at the base. Surface display (g) top and (h) side views with KZ52 bound to the GP. Note that epitopes 4G7 and KZ52 contain residues in GP₁ and GP₂ and overlap at several points. On surface antibody display: carbon = green; nitrogen = blue and oxygen = red. The KZ52 bound to the GP structure was solved by Lee *et al*, Nature 2008. pdb entry: 3CSY. Figure generated with PyMOL.

The 4G7 epitope (Figure 1a-d) is comprised of several residues at GP₁ and base of GP₂ (Pallesen *et al.* 2016). The 1H3 epitope (Figure 1a-d) is in one continuous region within the GP₁ but it is predicted to be conformational as it is detected in ELISA but not in western blots (Qiu *et al.* 2011; Audet *et al.* 2015).

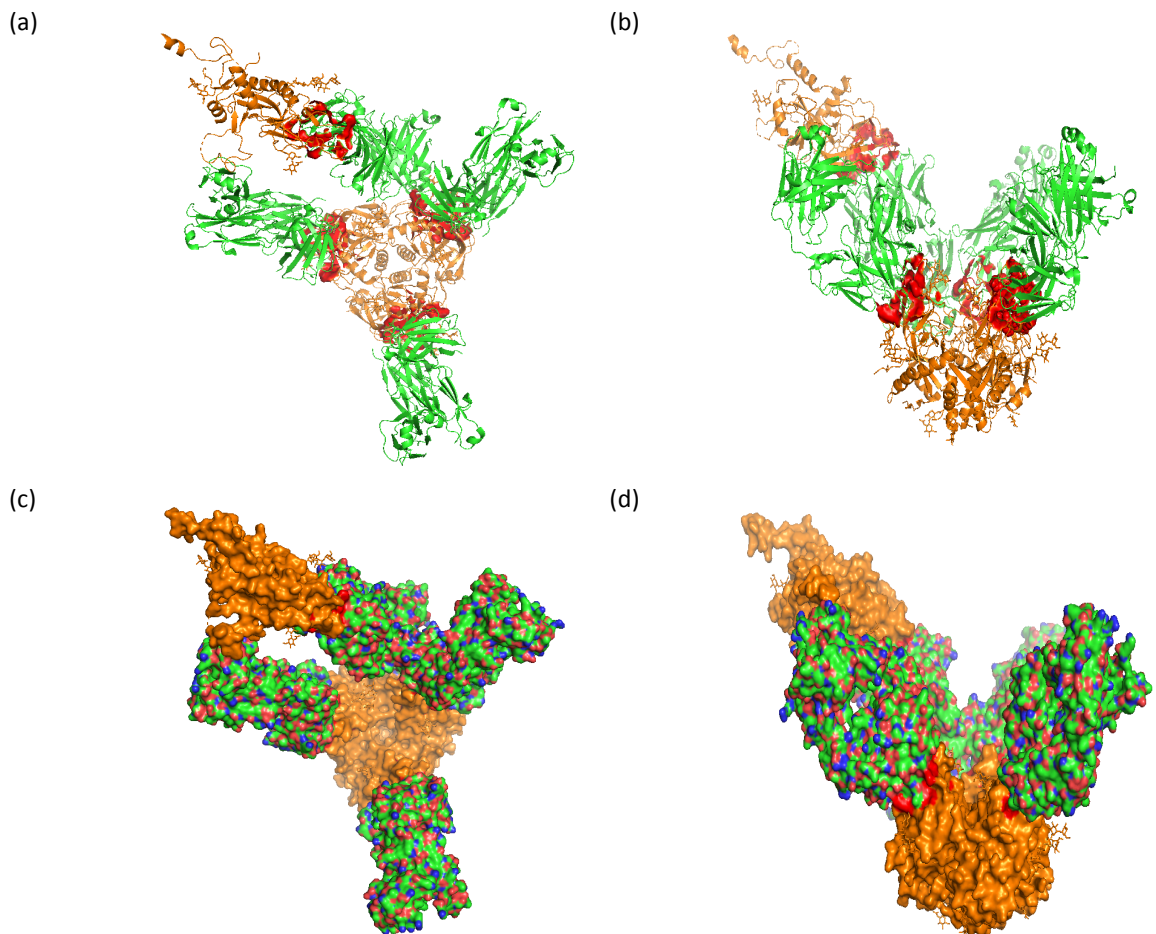


Figure 5.2. Structure of RAVV GP trimer (orange) bound to the human antibody MR78 (green). Ribbon display (a) top and (b) side views of the GP trimer with epitope MR78 (red surface) at the RBS. Surface display (c) top and (d) side views of the GP trimer. A monomer can be seen in both structures bound to a second Fab fragment of MR78. On surface antibody display: carbon = green; nitrogen = blue and oxygen = red. The GP structure was solved by Hashiguchi *et al*, Cell 2015. pdb entry: 5UQY. Figure generated with PyMOL.

The introduction of epitopes into LLOV or RESTV GP backbones was achieved through either gene synthesis for those epitopes with several different loci (4G7 or MR78 into LLOV GP), or through overlap extension PCR (4G7, 1H3 and KZ52 into RESTV GP and chimeric RAVV-LLOV and RESTV-LLOV) when mutagenesis was feasible.

Overlap extension PCR (Heckman and Pease 2007) was adapted for this study. It is a straightforward technique suitable for site-directed mutagenesis and gene splicing with a success rate of >90%, by creating overlapping PCR fragments containing the mutation, insertion or deletion of interest, which are then used as templates for a second PCR reaction to join the fragments to generate the final full length product incorporating the desired mutation. This is then ligated into an expression plasmid of choice. Primer design is key to successfully achieve the desired outcome.

The main objective of this study was to generate PVs bearing chimeric GPs to improve specificity in neutralisation assays. Given their lack of cross-reactivity, LLOV and RESTV GP were used as a scaffold GP to display neutralising epitopes from EBOV and MARV. Successfully generated PVs were tested against monoclonal antibodies targeting those particular epitopes in PVNAs, and against convalescent serum (anti-EBOV) when available.

5.2 Materials and Methods

5.2.1 Filovirus GP modelling

To predict whether epitopes would be displayed correctly on each of the scaffold GPs, a modelling strategy based on published GP structures was attempted with a **Protein Homology/analogY Recognition Engine (PHYRE2)** V 2.0 software program developed at the Structural Bioinformatics group at Imperial College, London (Kelley *et al.* 2015); accessed at <http://www.sbg.bio.ic.ac.uk/phyre2>. Our modelling study was a collaborative effort with Dr Mark Wass and Prof Martin Michaelis at the University of Kent in Canterbury who provided guidance in the initial stages. The different tools available in PHYRE2 enable you to predict protein structure and function when amino acid changes are introduced. However, because it is based on protein homology, modelling will not be successful if homology is not detected. Therefore, having a published 3D structure is crucial for success using this strategy.

Once the predicted GP structures were generated, they were analysed and annotated using PyMOL Molecular Graphics System software v 2.0.7, which is a “user-sponsored

molecular visualisation system”, enabling protein structures to be annotated to highlight important features or particular regions.

5.2.2 Plasmids and monoclonal antibodies

The *cuevavirus* (LLOV) GP gene (Gene Bank accession n: JF828358.1) and *ebolavirus* (RESTV) GP gene (Gene Bank accession n: AY769362.1) cloned into pCAGGS were used as backbones for mutagenesis and chimeric GP generation.

The monoclonal antibody KZ52 was a gift from Dr Erica Saphire (Scripps Institute, Los Angeles, USA); 4G7 and 1H3 were gifts from Dr Xiangguo Qiu (Public Health Agency, Winnipeg, Canada)

Gene synthesis (4G7LLOV and MR78LLOV GP) was ordered from Invitrogen Gene Strings™ (Thermo Fisher Scientific).

5.2.3 Primers

All primers were manually designed, ordered through Eurofins Genomics Ltd and HPLC purified.

When LLOV GP was used as the scaffold, primers were designed to insert EBOV epitopes KZ52 and 1H3 as well as generating a chimeric GP containing the receptor-binding site of RAVV followed by the remainder of LLOV GP (Table 5.1).

When RESTV GP was used as the scaffold GP, primers were designed to insert EBOV epitopes KZ52, 4G7 and 1H3 as well as generating a chimeric GP containing the receptor-binding site of RAVV followed by the remainder of RESTV GP (Table 5.2).

5.2.4 Reagents and equipment

A Dream Taq Green PCR mix (2X) (Thermo Scientific K1081) and a high-fidelity Platinum Superfi PCR mix (2X) (Invitrogen 12358010) were used for gradient PCR and mutagenesis PCR, respectively. Gel extractions were performed using a Qiagen Gel Extraction kit (28704 and 28706) and DNA concentration was determined with a Nanodrop 2000 spectrophotometer (ThermoFisher Scientific) according to the manufacturer’ instructions. Ligation reactions were incubated overnight at RT with T4 ligase (ThermoFisher Scientific

primer	Sequence (5' to 3')
LLOV_ClaI_FWD_A	GAGTCATCGATAGCCAC
LLOV_XhoI_REV_D	TGCTAGCTCGAGCTATCA
KZ52 epitope:	
KZ52LLOV_42-43_REV_B	GTTTGGGTCAGGGTGTGTTTC
KZ52LLOV_42-43_FWD_C	GAAACAACACCCTGACCCAAAC
4G7LLOV_REV_B	GCTGGGCGTTCACGATCACTTCCCGGGATGTCTTGCTAACTGTG
4G7LLOV_FWD_C	TCGTGAACGCCAGCCCAAGTGAATCCCAACCTTAGATA
KZ52LLOV_549-556_REV_B	ATCAGGCCGTCCTGGTTGTGCATTATCCCGTCTGTGATCC
KZ52LLOV_549-556_FWD_C	CCAGGACGGCCTGATCTGCCAGTTACGGGAGCTCGCGAAC
1H3 epitope:	
1H3LLOV_REV_B	TTTCAGATCAGCTTGCCGGTGGTGTGCTATCTCCGGTAAGATTAGCCAATCT TTCTTG
1H3LLOV_FWD_C	AAGCTGATCTGGAAAGTGAACCCCGAGATCACATTGGAGCTCGGTGATTGGTC CGGTTGG
RAVV-LLOV chimeric GP:	
NtermRAVV-ClaI_FWD_A	GAGTCATCGATAGCCACCATGAAGACCATATATT
IntRAVV-LLOV_REV_B	GCTCTAGATTTGCTGGAGGAAGAGATGGAGGGCATGTTTG
IntRAVV-LLOV_FWD_C	CATGCCCTCCATCTCTCTCCAGCAAATCTAGAGC

Table 5.1. Primers designed to insert EBOV epitopes KZ52, 1H3 into LLOV GP and generate chimeric RAVV-LLOV GP. 4G7 and MR78 epitopes were found to contain too many fragments to be inserted by mutagenesis therefore the genes were synthesised.

EL0016) in a total of 10 μ L, followed by transformation of *DH5 α* competent cells (ThermoFisher Scientific 18265017), and plating in LB-agar plates containing ampicillin (100 μ g/mL). Colonies were PCR screened and positive clones selected for plasmid purification using a Monarch miniprep kit (New England Biolabs T1010L).

5.2.5 Overlap Extension PCR protocol

For each scaffold GP, LLOV and RESTV, flanking primers (A and D) were designed with the aim of generating a final product (Figure 5.3) to be ligated into the pCAGGS expression vector. For site-directed mutagenesis, internal mutagenesis primers (C and B) were designed to contain the desired nucleotide substitutions with an overlapping region of \sim 15 nt between the primer pairs (Figure 5.3a). In the first PCR using LLOV or RESTV GP as

primer	sequence (5' to 3')
RESTV_EcoRI_FWD_A	TGGCAAAGAATTCGCCAC
RESTV_XhoI_REV_D	ATCTGCTAGCTCGAGTCA
KZ52 epitope:	
KZ52RESTV_504-14_REV_B	GCATTTGGGTTGAGCATTGACAATAACCGATCGCCTTTGTTTCCTG
KZ52RESTV_504-14_FWD_C	GCTCAACCCAAATGCAACCCCAATCTTTACTATTGGACAGCTGTTGAT
KZ52RESTV_N553D_REV_B	GCCCGCAAATAAGCCCATCCTGATTATGCATTAC
KZ52RESTV_N553D_FWD_C	GTAATGCATAATCAGGATGGGCTTATTTGCGGGC
1H3 epitope	
1H3RESTV_REV_B	CTTCAAATTAGTTTTCCCGTGGTGTGCTAAGGCGATTATTTCTTCG
1H3RESTV_FWD_C	AAACTAATTTGGAAGGTCAACCCCGAAATTGAACCAGATGTTGGTGAGTGGGC
4G7 epitope	
4G7RESTV_Y517H_REV_B	ATCAACAGCTGTCCAATAATGAAGATTGGGGTTGC
4G7RESTV_Y517H_FWD_C	GCAACCCCAATCTTCATTATTGGACAGCTGTTGAT
4G7RESTV_V548L_REV_B	GCCCATCCTGATTATGCATTAGACCCTCAATGTAGATGC
4G7RESTV_V548L_FWD_C	GCATCTACATTGAGGGTCTAATGCATAATCAGGATGGGC
RAVV-RESTV chimeric GP	
NtermRAVV-ClaI_FWD_A	GAGCTCATCGATAGCCACCATGAAGACCATATATT
RAVV-RESTV_GP_REV_B	GCGGAGTGTGTGGACGATCAAGAGATGGAGGGCATGTTTG
RAVV-RESTV_GP_FWD_C	CAAACATGCCCTCCATCTCTTGATCGTCCACACTCCGC

Table 5.2. Primers designed to insert EBOV epitopes KZ52, 1H3 and 4G7 into RESTV GP and generate the chimeric RAVV-RESTV GP.

templates, two reactions were set up: one with primers A and B and another with primers C and D, generating two fragments containing the desired mutation within the overlapping region to be used as templates in a second reaction with primers A and D to generate the final fragment. This was digested with the appropriate restriction enzymes to be ligated into pCAGGS. For non-linear epitopes such as 4G7 and KZ52, two or three sets of internal primers were designed to cover all mutations.

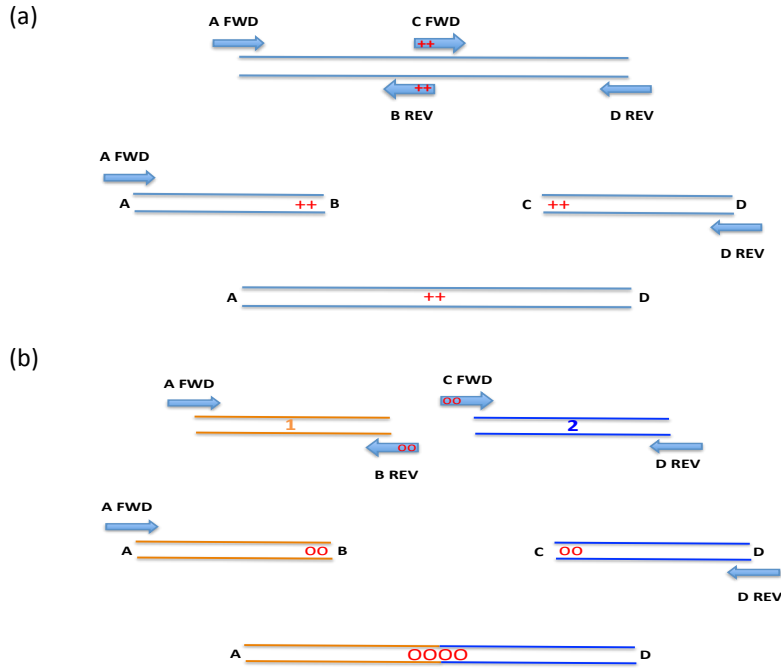


Figure 5.3. Overlap extension strategies. For site-directed mutagenesis (a) overlapping fragments generated with internal primers containing the mutations to introduce the desired substitutions, insertions or deletions, which are used as templates in a final PCR with flanking primers A and D generating the final chimeric gene. For chimeric gene generation (b) fragments containing the N-terminal RAVV GP₁ RBS gene segment (orange) and the remainder of RESTV GP (or LLOV) gene (blue) are generated with internal primers containing overlapping 5' regions, which are used as templates in a final PCR with flanking primers A and D generating the final chimeric gene.

When generating the chimeric RAVV-LLOV and RAVV-RESTV GPs, a flanking primer (A) was designed to amplify the N-terminal RAVV GP gene, and internal primers (C and B) with an overlapping region (Figure 5.3b) to join RAVV GP₁ RBS region to either LLOV or RESTV GP using the appropriate flanking primer (D) for LLOV or RESTV.

Once ligated into the pCAGGS expression vector all constructs were sent for sequencing prior to PVs being produced.

5.2.5.1 1H3LLOV chimeric GP

As 1H3 is a continuous epitope (Appendix II – Figure II.1) the protocol was followed as described (Figure 5.3a). Before attempting to generate the intermediate fragments to be used as templates for the final gene product, a gradient PCR was performed to assess the optimal annealing temperature.

Using LLOV GP as a template for PCR #1, reactions were set up to assess different annealing temperatures (Table 5.3) with ~90 ng (50 to 125 ng) of template DNA and 50 pmol of each primer to introduce epitope 1H3 (Appendix II – Table II.1). Once the optimal annealing temperature was established, the same reaction conditions using a high fidelity Superfi PCR mix in a total of 50 µL was prepared, running the same PCR program (Table 5.3) for 30 cycles. After addition of 6x loading dye (Thermo Fisher Scientific R0611) samples were loaded in a 1% (v/v) high-purity agarose gel and run for an hour, bands visualised on a Mini UVivue Transilluminator – Uvitec (254 mm wavelength) at a 70% setting to minimise DNA damage when excising bands for purification. The band was excised carefully with a scalpel; DNA extracted using the Qiagen gel extraction kit and DNA concentration determined on a Nanodrop 2000.

To generate fragment AD the same strategy described above was used with fragments AB and CD as templates (Appendix II – Table II.2), with flanking primers A and D (Table 5.1). The 1H3LLOV GP gene and pCAGGS were then digested with restriction enzymes *ClaI* and *XhoI* as described (Chapter 2). Ligation reactions were set up overnight with vector to insert ratios of 1:1, 1:3 and 1:6.

To generate the 4G7/1H3LLOV chimeric GP the strategy described above was used with the synthesised 4G7LLOV gene as a template. The PCR program (Eppendorf Mastercycler EP S Thermal Cycler) for gradient and mutagenesis PCR was as follows:

Initial denature	94°C for 3 min
Cycles 1 to 25 (or 1 to 30)	denature 94°C for 1 min
	annealing 50° - 60°C for 1 min
	extension 72°C for 2 min
Final extension	72°C for 7 min
hold	4°C ∞

Table 5.3. PCR program for gradient and mutagenesis PCRs.

5.2.5.2 KZ52LLOV chimeric GP

To insert epitope KZ52 into LLOV (Appendix II – Figure II.2), the final gene was generated in two stages: first a gene containing the shared GP₂ proximal region with 4G7 using primers 4G7LLOV_REV_B and 4G7LLOV_FWD_C and flanking primers LLOV_ClaI_FWD_A

and LLOV_XhoI_REV_D (Table 5.1). Then a further round was performed generating three overlapping fragments with the remainder of the primers before a final PCR with three templates and flanking primers A and D to generate the full chimeric gene.

5.2.5.3 RAVV-LLOV chimeric GP

To generate the chimeric RAVV-LLOV (Appendix II – Figure II.3), an extra flanking primer (A) was designed to cover the RAVV-pCAGGS N-terminal region, and internal overlapping primer C to generate the RAVV GP₁, as well as primers C and D to generate LLOV GP₁-GP₂ regions (Table 5.1), before a final PCR reaction with the two fragments as templates with flanking primers A and D to assemble the final chimeric gene.

5.2.5.4 KZ52RESTV chimeric GP

RESTV has more conserved amino acid sequences with EBOV in comparison to LLOV requiring fewer primers (Appendix II – Figure II.5). Therefore using RESTV GP as a template for the reaction, three PCR reactions were set up for each annealing temperature assessed (50°C, 53°C and 60°C) with 50-125 ng of template DNA and 50 pmol of each primer (Appendix II – Table II.3). While the program was running, a 1% (v/v) agarose gel was prepared in TAE buffer with SYBR Safe dye according to manufacturer's instructions. The Dream Taq Green PCR mix has its own loading dye therefore the samples were loaded and run for an hour at 80V before being visualised as described.

Once the optimal annealing temperature was established, the same reaction conditions using the high fidelity Superfi PCR mix in a total of 50 µL was prepared, running the PCR program for 30 cycles (Table 5.3). DNA was gel purified as described (section 5.2.5.1). To generate the final gene product (fragment AD) the same conditions for previous reactions were followed (Appendix II – Table II.4).

When this strategy (from Heckman and Pease, 2007) was not successful, the amount of template was adjusted to take it into account their size, molecular weight and number of molecules:

$$\text{No. of copies} = (\text{ng} \times 6.022 \times 10^{23}) / (\text{length} \times 1 \times 10^9 \times 650),$$

where: ng = nanograms of fragment; 6.022×10^{23} is the Avogadro number or number of molecules per mole; length of fragment in bp; 1×10^9 = conversion to ng and 650 = average weight of a base pair (bp).

The number of copies of each fragment was then kept constant in order to improve the PCR yield. Once the optimal annealing temperature was established, the same reaction conditions using the high fidelity PCR mix in a total of 50 μ L was prepared for 30 cycles (Table 5.3). DNA was gel purified as described (section 5.2.5.1). The chimeric gene and pCAGGS were then digested with the appropriate restriction enzymes. Ligation reactions were set up as described (section 5.2.5.1).

5.2.5.5 4G7RESTV and 4G7/1H3RESTV chimeric GP

To generate 4G7RESTV chimeric GP (Appendix II – Figure II.4), two sets of internal primers (Table 5.2) were used to substitute amino acids Y517H and V548L, creating three fragments of ~1.5 kb, ~100 bp and ~400 bp. The final gene fragment AD was assembled with an annealing temperature of 57°C and the three initial fragments used as templates. The rest of the cloning strategy was performed as previously described. The 1H3 (Appendix II – Figure II.6) mutagenesis primers (Table 5.2) were then used with 4G7RESTV as template to assemble the 4G7/1H3RESTV construct, and with RESTV to assemble the 1H3RESTV construct.

5.2.5.6 RAVV-RESTV chimeric GP

To generate the chimeric RAVV-RESTV GP (Appendix II – Figure II.7), the strategy described in section 5.2.5.3 was used.

5.2.6 Cloning of synthesised genes

Synthesised gene strings 4G7LLOV and MR78LLOV GP were cloned into pCAGGS as described in section 5.2.5.

5.2.7 PV Generation and antibody assays

Once plasmids were all checked by Sanger Sequencing (Chapter 2), PVs were generated in T75 flasks, titrated and used in neutralisation assays and ELISA as previously described (Chapter 2).

5.3 Results

5.3.1 Filovirus modelling

Modelling of the chimeric GP structures was attempted in order to establish where the epitopes would sit within the GP and whether the structure might be compromised.

Modelling was challenging because the PHYRE2 software/program relies on protein homology. Therefore, due to the lack of published GP structures for LLOV and RESTV scaffold GPs, only partial modelling was achieved.

The model of 1H3LLOV GP resulted in a partial structure from N-terminal amino acid 42 to C-terminal amino acid 316, which covered the region containing the epitope. However it was predicted to be disordered (Figure 5.4a in blue), which makes it difficult to ascertain whether the epitope was going to be displayed properly. Disorder regions lack a fixed 3D structure, sometimes alternating between structured and unstructured states, due to low content of hydrophobic amino acids. They often present as loops or flexible linkers (Jones and Cozzetto 2014).

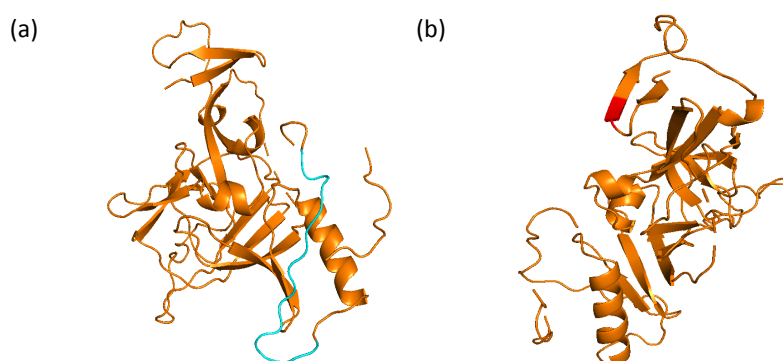


Figure 5.4. Partial model of 1H3 (blue) and KZ52 (red) epitopes mutated into the LLOV GP.

The KZ52LLOV model also resulted in a partial structure, predicting the epitope region on the GP₁ (EBOV amino acids 42-43) would present as part of a β -strand (Figure 5.4b in red). The rest of the epitope could not be predicted as the model stopped at amino acid 316. An 'intensive mode' to model protein regions without detectable homology was run to attempt to model the full GP (Figure 5.5).

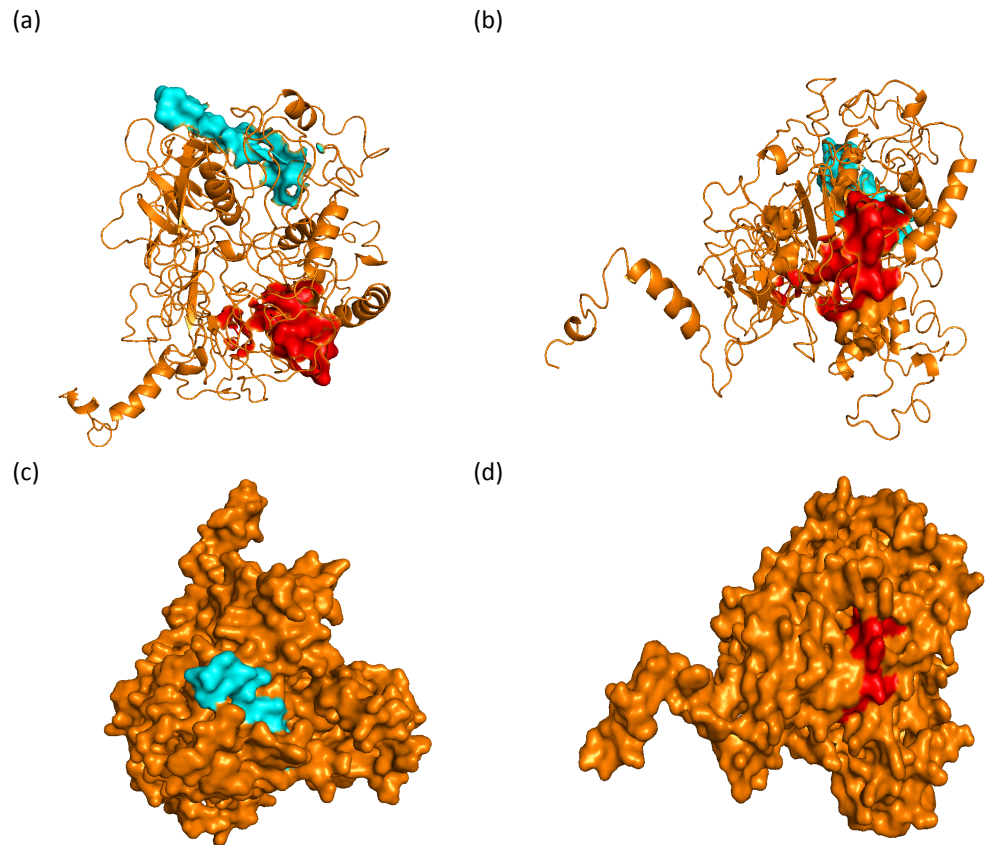


Figure 5.5. Intensive model of LLOV GP containing 1H3 and KZ52 epitopes. Ribbon display (a) top and (b) bottom view of 1H3 (blue surface) and KZ52 (red surface) epitopes. Surface display (c) top and (d) bottom views showing epitopes partly hidden within the structure.

Epitope 1H3 (blue surface) is seen on the top of GP (Figure 5.5a and 5.5c) and KZ52 (red surface) is seen in separated regions and partially hidden (Figure 5.5b and 5.5d), which indicates it might not be displayed correctly.

The MR78LLOV GP was predicted more successfully, as the whole epitope fell within the GP₁ with regions within α -helices, β -strands and some disordered regions (Figure 5.6).

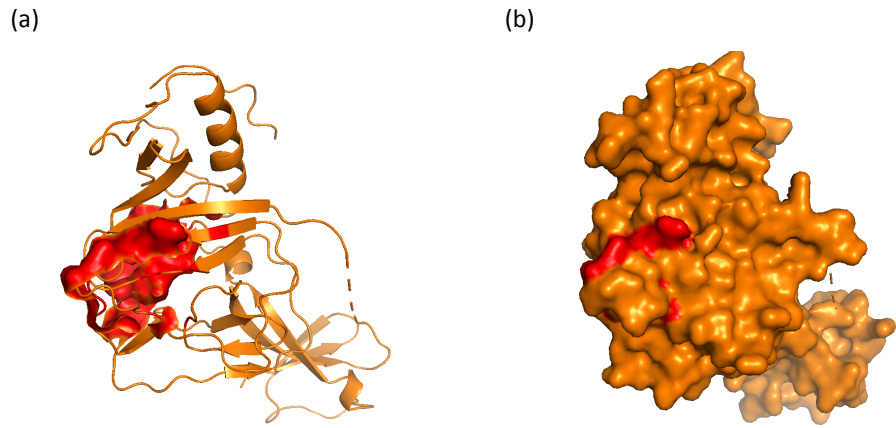


Figure 5.6. Partial model of LLOV GP containing MR78 epitope. Ribbon display (a) top view with MR78 (red surface) and (b) surface display of MR78LLOV GP.

The RAVV-LLOV chimeric GP intensive mode model resulted in mainly disordered regions where the epitope appears partly hidden within the structure (Figure 5.7).

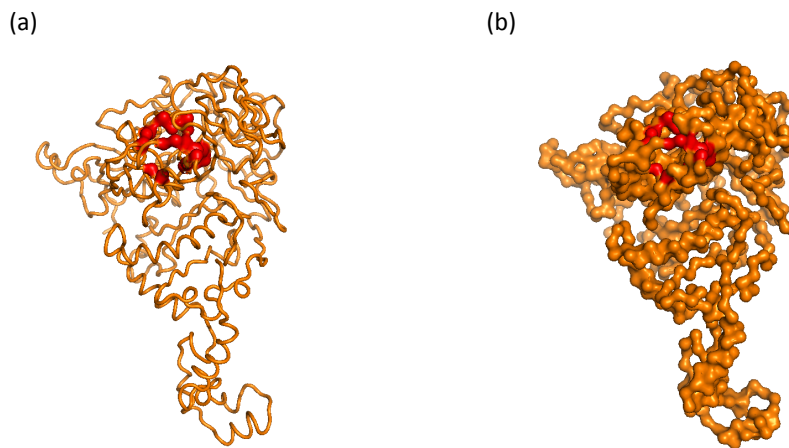
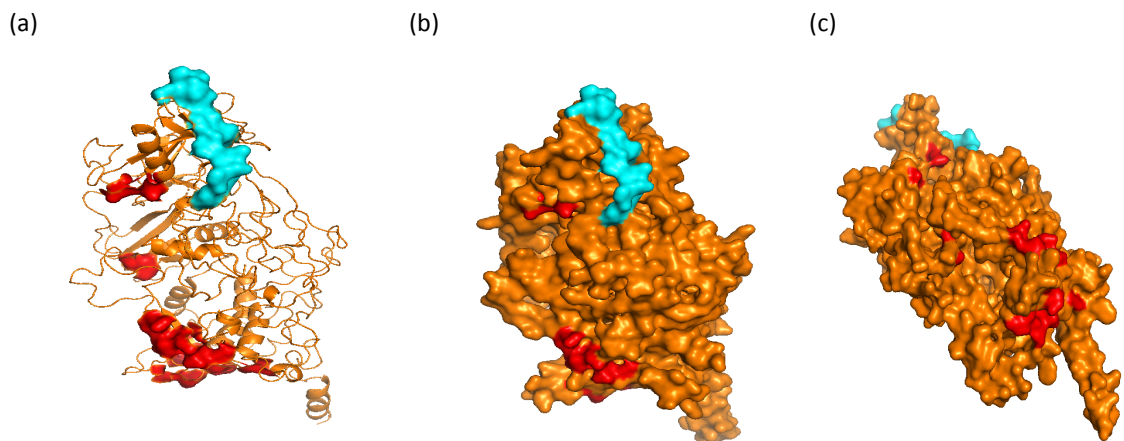


Figure 5.7. Intensive model of RAVV-LLOV GP containing MR78 epitope. Ribbon display (a) top view with MR78 (red surface) and (b) surface display of RAVV-LLOV GP.



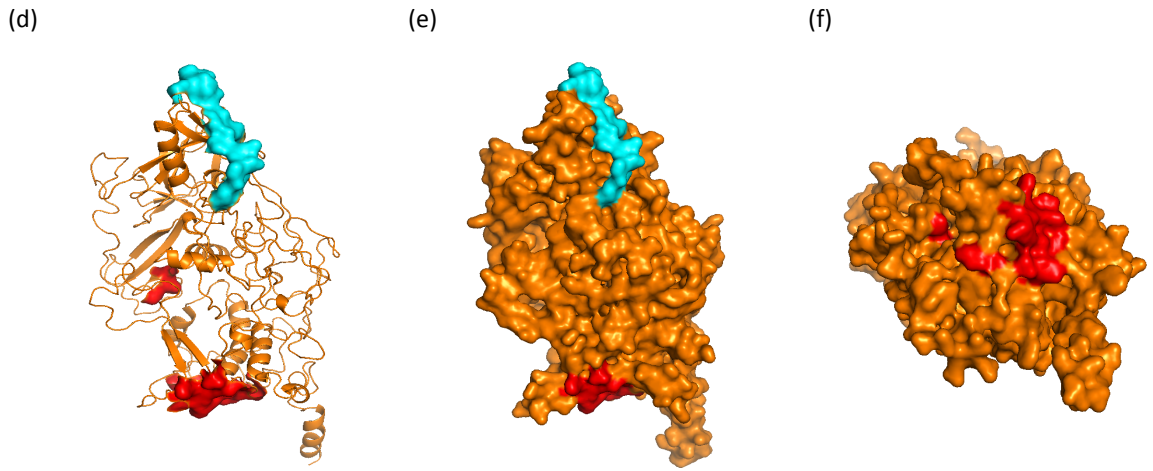


Figure 5.8. Intensive model of RESTV GP containing EBOV epitopes. 1H3 (blue); 4G7 (red - a to c) and KZ52 (red - d to f). (a,d) side view ribbon; (b,e) side view surface and (c,f) bottom view surface display.

Modelling of chimeric RESTV GP was more successful. GP₁ epitope 1H3 was presented on the surface (Figure 5.8). Overlapping epitopes 4G7 (Figure 5.8 a-c) and KZ52 (Figure 5.8 d-f) were presented in separate regions but more exposed than in the LLOV model (Figure 5.5). Several disordered regions were predicted throughout the protein.

The RAVV-RESTV chimeric GP intensive mode model resulted in mainly disordered regions where the epitope appears partly hidden within the structure (Figure 5.9), as seen with RAVV-LLOV (Figure 5.7).

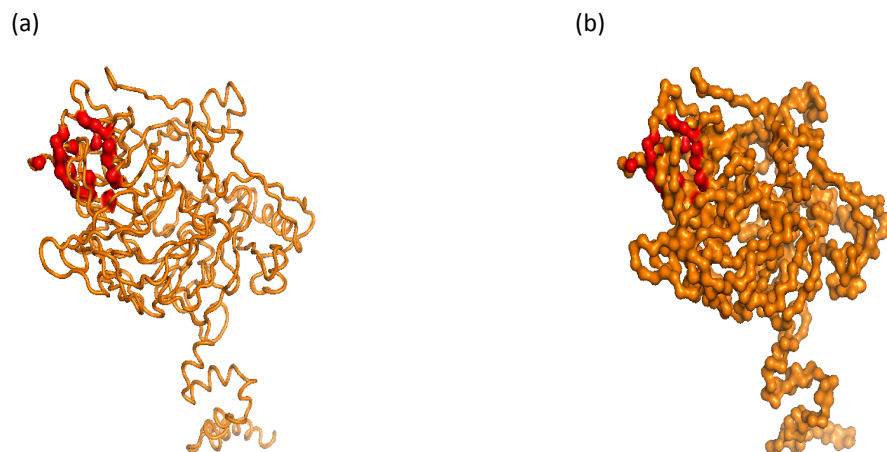


Figure 5.9. Intensive model of RAVV-RESTV GP containing MR78 epitope. Ribbon display (a) top view with MR78 (red) and (b) surface display of RAVV-RESTV GP.

5.3.2 Mutagenesis

5.3.2.1 Mutagenesis of 1H3 epitope into LLOV GP

To establish the best annealing temperature for generation of fragments AB and CD (Figure 5.3a), a gradient PCR was set up with a Green Dream Taq Green Master Mix. Fragment AB was expected to be ~800 bp and fragment CD ~1200 bp.

All annealing temperatures tested generated appropriate sized fragments. Both AB and CD fragments (Figure 5.10) were clearly visible for every temperature tested without any evidence of non-specific binding.

The same reaction was subsequently run using the Superfi high fidelity mix and an annealing temperature of 60°C. The resulting fragments were run in a 1% (v/v) agarose gel and the bands excised. The DNA fragments extracted were used as templates for the second PCR with flanking primers A and D (Table 5.1).

Again, a gradient PCR was run as described above to verify the best annealing temperature (Figure 5.11a), followed by a PCR with the Superfi high fidelity mix and an annealing temperature of 53°C. Next, the final fragment AD was also run in a 1% (v/v) agarose gel, the bands excised and gel extracted (Figure 5.11b).

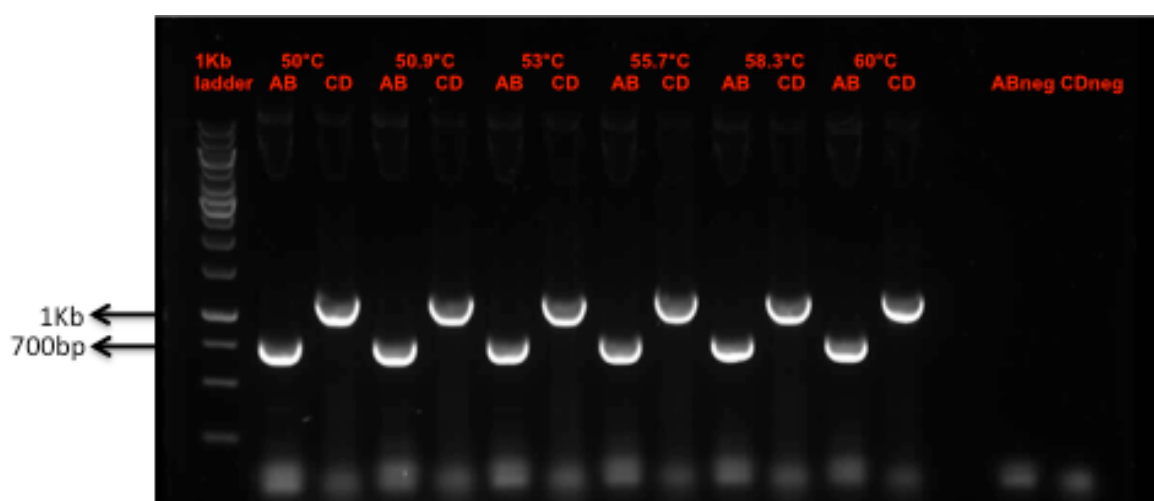


Figure 5.10. Gradient PCR of fragments AB and CD of chimeric GP containing 1H3 epitope. The sizes indicated on the left correspond to the 1Kb Gene Ruler ladder.

Once purified, fragment AD of LLOV GP containing 1H3 epitope (1H3LLOV) and the pCAGGS expression vector were digested with *Clal* and *XhoI*, ligated then transformed into *DH5α* cells, resulting in five to ten colonies per plate (no colonies on negative control plates).

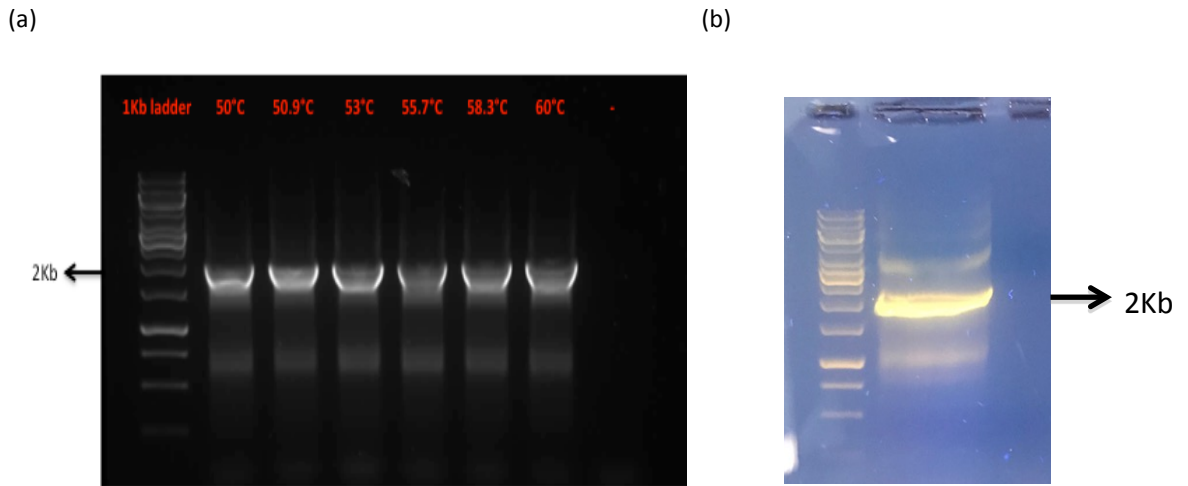


Figure 5.11. Generation of final fragment AD of chimeric GP containing 1H3 epitope. (a) gradient PCR to establish best annealing temperature. (b) PCR #2 with high fidelity Superfi mix for gel extraction.

A total of 13 colonies were picked from the plates and a colony PCR diagnostic test run (Figure 5.12) with primers LLOV_Int440FWD and pCAGGS REV. Most of the 13 colonies were positive for 1H3LLOV-pCAGGS (Figure 5.12). Three colonies were picked (1,7,11) and plasmid DNA extracted as described. DNA from one purified plasmid clone (colony #1) was sent for Sanger sequencing, which revealed that the epitope had been successfully mutated (Figure 5.13). The rest of the sequence matched the original LLOV GP gene.

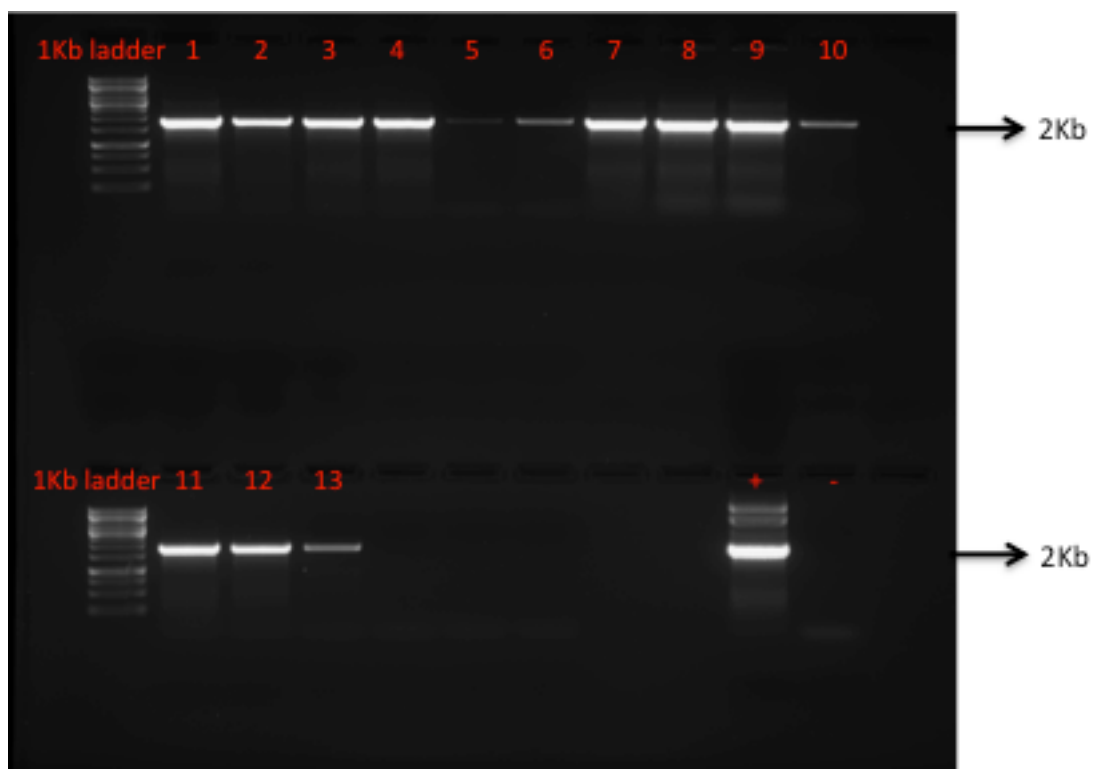


Figure 5.12. Colony PCR screen of *DH5α* cells transformed with 1H3LLOV-pCAGGS. Positive control was a positive colony from a previously transformed LLOV-pCAGGS clone; negative control = no DNA in PCR reaction.

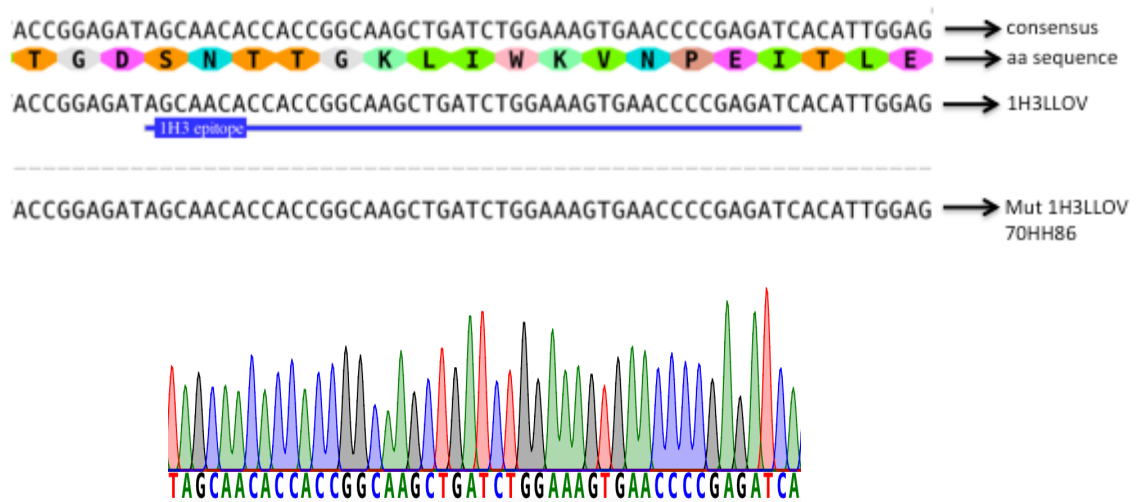


Figure 5.13. Sequence of 1H3 epitope (top blue annotation) flanked by LLOV sequence. Bottom chromatogram from LightRun Sanger sequencing. Remainder of LLOV sequence matched the original construct.

5.3.2.2 Mutagenesis of KZ52 epitope into LLOV GP

Mutagenesis to introduce the KZ52 epitope into LLOV GP was done sequentially. Next, a mutagenesis strategy to insert 1H3 (section 5.2.5.1) was performed to insert 1H3 into the KZ52LLOV GP to create another chimeric LLOV GP containing both 1H3 and KZ52 epitopes.

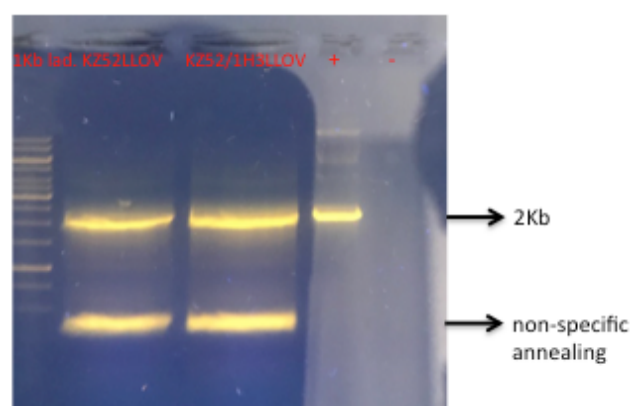


Figure 5.14. Gel extraction of final fragments of KZ52LLOV and KZ52/1H3LLOV chimeric GP. Positive control = LLOV-pCAGGS and negative control = no DNA in PCR reaction.

The final AD fragments (Figure 5.14) were digested with the appropriate restriction enzymes, purified, cloned into pCAGGS and sent for Sanger sequencing (Figure 5.15) as described previously.

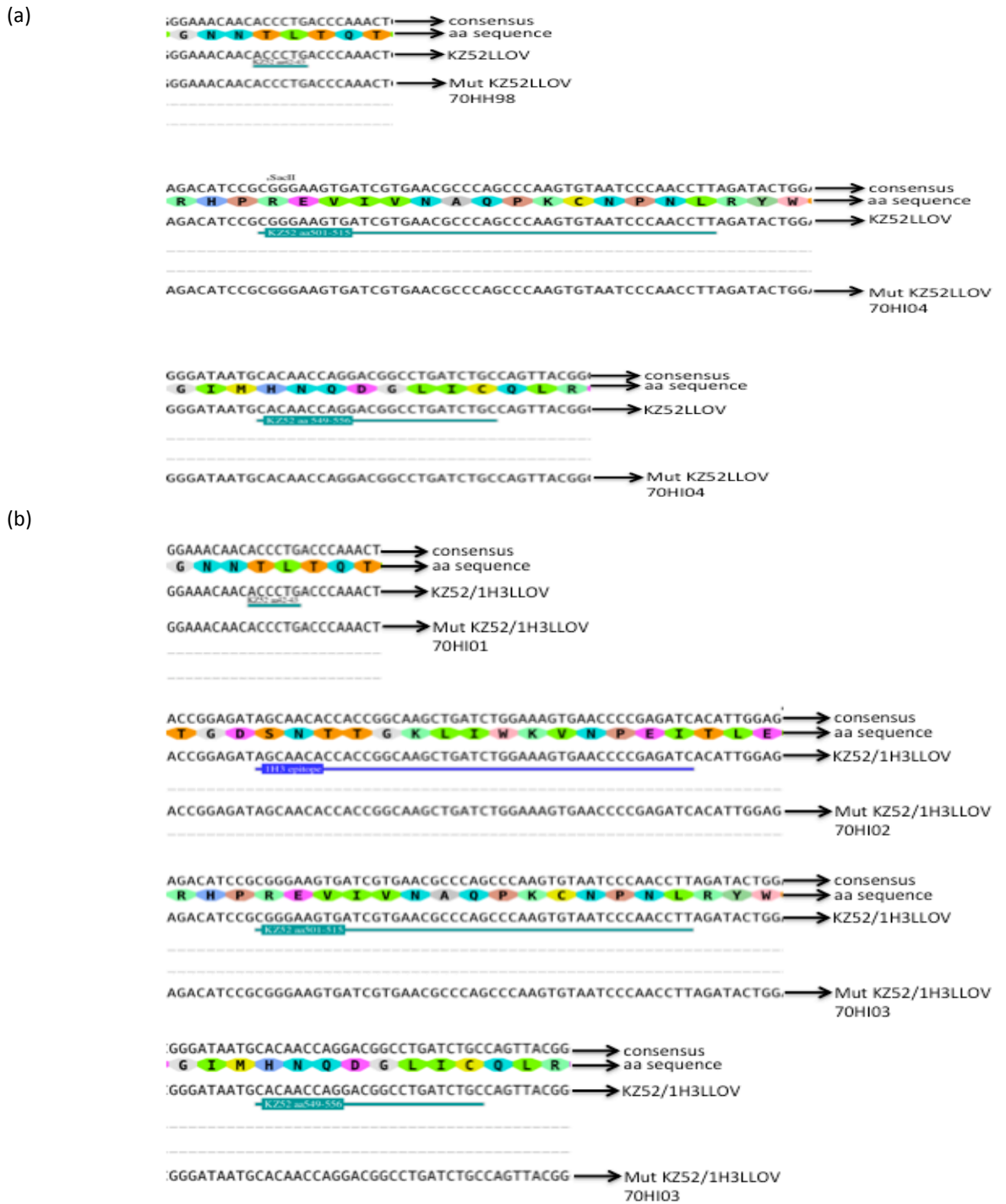


Figure 5.15. Sequence analysis of chimeric LLOV GP constructs. (a) KZ52LLOV and (b) KZ52/1H3LLOV GP constructs sequence analysis. All chromatograms were carefully checked for fidelity. No undesirable mutations were found.

5.3.2.3 Mutagenesis to generate chimeric RAVV-LLOV GP

To create a chimeric RAVV-LLOV GP the same PCR conditions and cloning strategy described for 1H3LLOV GP were used (data not shown).

5.3.2.4 Mutagenesis of epitopes 4G7 and 1H3 into RESTV GP

To generate 4G7RESTV chimeric GP, two sets of internal primers (Table 5.2) were used to substitute amino acids Y517H and V548L, creating three fragments of ~1.5 kb, ~100 bp and ~400 bp (Figure 5.16). To generate the final fragment AD an annealing temperature of 57°C was selected (Figure 5.16), and the three fragments used as templates for the final PCR reaction.

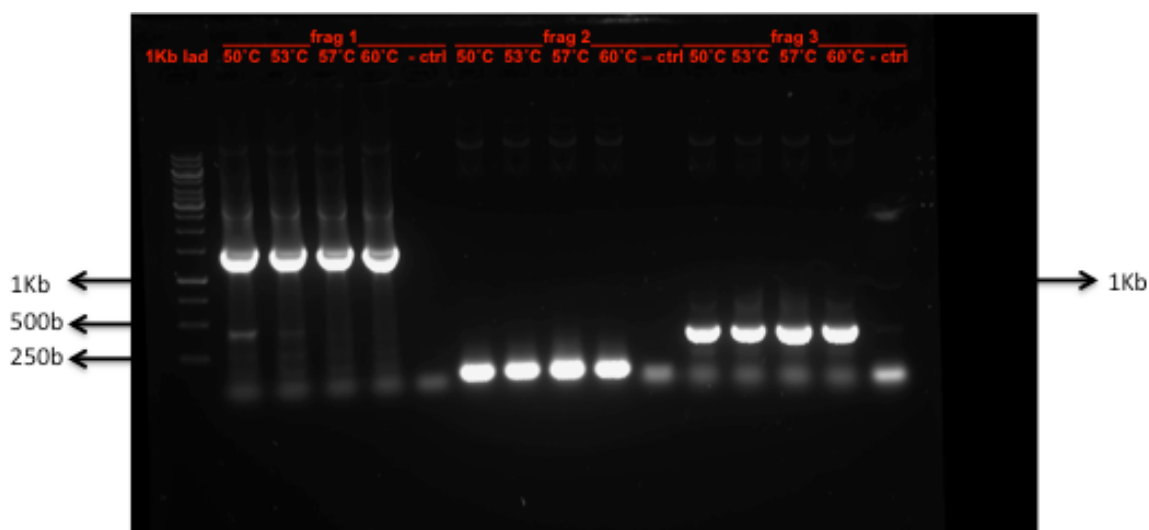


Figure 5.16. Gradient PCR to establish best annealing temperature. PCR conditions for generation of fragments 1,2 and 3 before PCR assembly of 4G7RESTV GP construct. The indicated sizes correspond to the 1Kb Gene Ruler ladder.

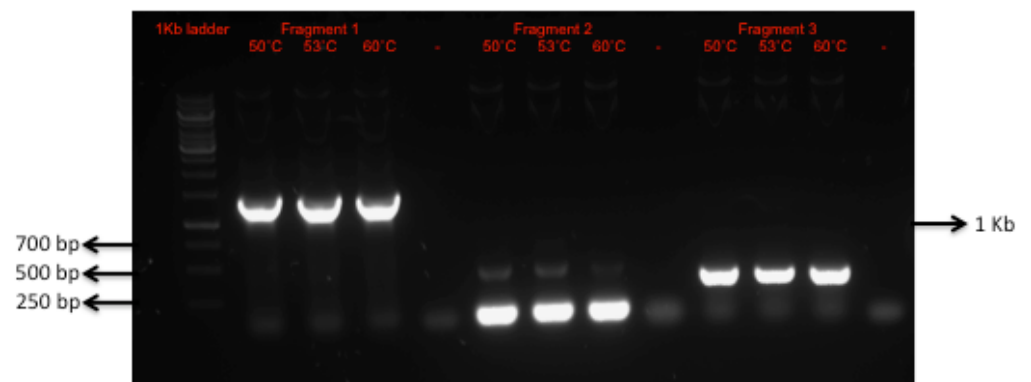
The resulting 4G7RESTV was used as a template to generate 4G7/1H3RESTV; and RESTV as a template to generate 1H3RESTV (data not shown). The rest of the cloning strategy was performed as previously described (section 5.2.5).

5.3.2.5 Mutagenesis of epitope KZ52 into RESTV GP

The KZ52 neutralising epitope was mapped to EBOV GP amino-acid residues 42-43 on GP₁, 504-514 and 549-553 on GP₂ (Pallesen *et al.* 2016). A sequence alignment between RESTV and EBOV GPs was performed with Clustal W. The GP₁ region (RESTV aa 43-44) did not need to be mutated (Appendix II – Figure II.5), therefore the primers were designed to substitute the amino acids at the two highlighted regions in the GP₂ (Figure 5.18). A gradient PCR was set up (Appendix II – Table II.3) to determine the ideal annealing temperature generating 3 fragments: ~1600 bp, ~115 bp and ~400 bp (Figure 5.17a) that

were used as templates in a second PCR reaction with flanking primers A and D (Table 5.2), to assemble the whole gene. The initial gradient PCR for the final gene assembly produced an unreliable result without a clear 2Kb band (Figure 5.17b). It seems the recommended amount of template (50-125 ng) only works when there are only two fragments of similar size. In this case, the amount of template in PCR #2 was changed to include the same number of DNA copies (see section 6.2.5.4) of each fragment as templates, with a gradient of 50°C, 53°C, 57° and 60°C. An annealing temperature of 57°C yielded a clear 2 kb band (data not shown). The PCR was subsequently run with the high fidelity Superfi mix and the resulting band was gel extracted and cloned into pCAGGS as described previously (section 5.2.5).

(a)



(b)

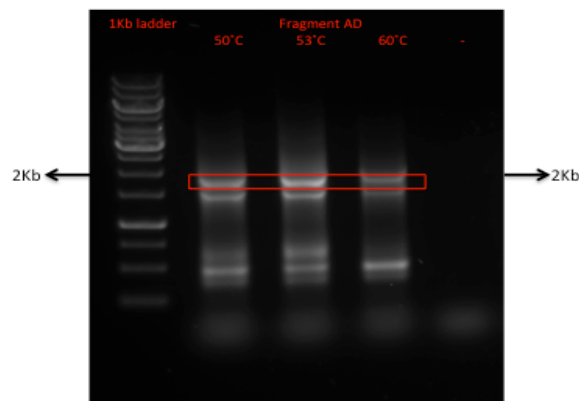


Figure 5.17. Gradient PCR for generation of fragment KZ52RESTV GP. (a) PCR #1 for fragments #1, #2 and #3. (b) PCR #2 for final fragment AD. The amount of recommended template (50-125 ng) was used in both reactions.

Once purified the chimeric GP plasmids were sent for Sanger sequencing (Figure 5.18).

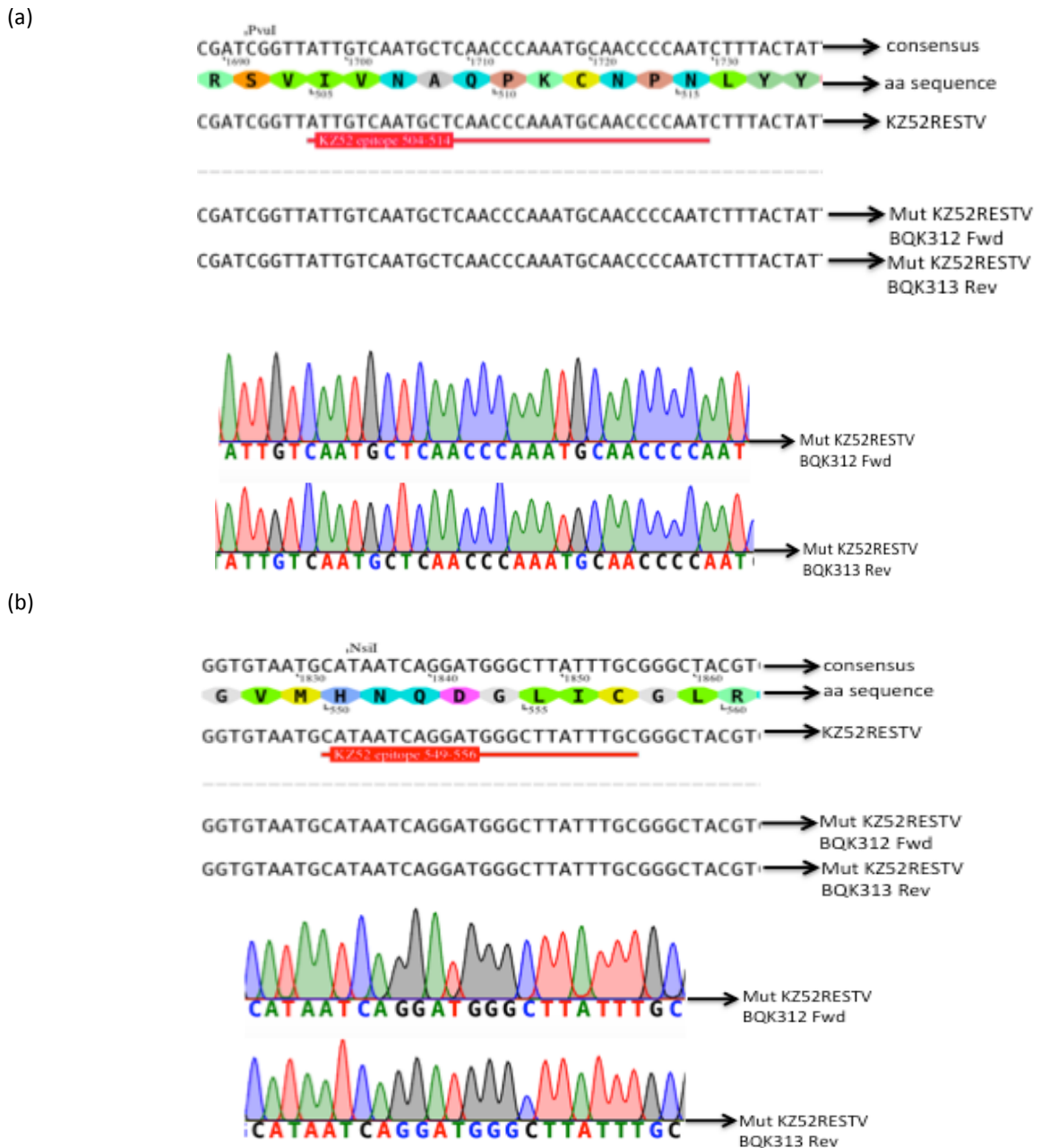


Figure 5.18. Sequence analysis of KZ52RESTV GP construct. The (a) proximal and (b) distal GP₂ regions mutated were sequenced with both Forward and Reverse primers to check the correct mutations had been introduced, as well as any accidental mutations.

5.3.3 PV production with chimeric GP

5.3.3.1 LLOV GP as scaffold for EBOV and RAVV epitopes

PVs bearing the chimeric LLOV GP were generated in T75 flasks as described (Chapter 2). The synthesised 4G7LLOV GP gene did not generate functional PVs, and neither did the chimeric GP containing both 4G7 and 1H3 epitopes (Figure 5.19a).

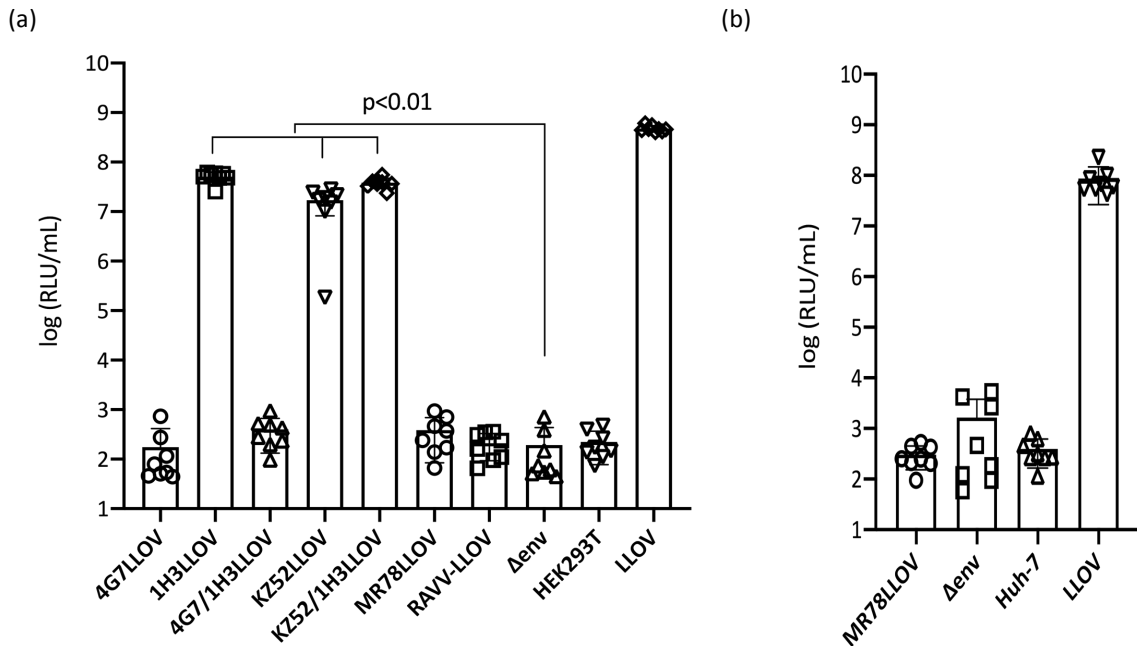


Figure 5.19. Infectivity assay of lentiviral PVs bearing chimeric LLOV GPs. Transduction titres in (a) HEK293T and (b) Huh-7 target cells. Statistical analysis comparing each PV titre to virions devoid of GP (Δ env). Mann-Whitney test ($p < 0.01$). Wild-type LLOV PVs were used as positive controls.

Also, synthesised GP gene containing Marburg virus epitope MR78 (MR78LLOV) or chimeric RAVV-LLOV GP gene did not generate functional PVs (Figure 5.19a) on HEK293T target cells.

The human cell line Huh-7 was also used as a target to check for functional MR78LLOV PVs unsuccessfully (Figure 5.19b). However, 1H3LLOV, KZ52LLOV and KZ52/1H3LLOV GP were all incorporated in lentiviral particles generating functional PVs, albeit with slightly lower titres than wild-type LLOV PVs (Figure 5.19a).

5.3.3.2 RESTV GP as scaffold for EBOV and RAVV epitopes

RESTV GP retained infectivity when mutated to display EBOV epitopes 4G7, 1H3 and KZ52 (Figure 5.20a) resulting in high titre PVs $\sim 1 \times 10^9$ RLU/mL comparable to the parental scaffold GP RESTV. No decrease in titres was observed such as seen with the chimeric GPs using LLOV as a scaffold (Figure 5.19a).

To attempt to generate RAVV-RESTV PVs, two clones (#6 and #7) were used. However, the chimeric RAVV-RESTV GP did not generate functional PVs (Figure 5.20).

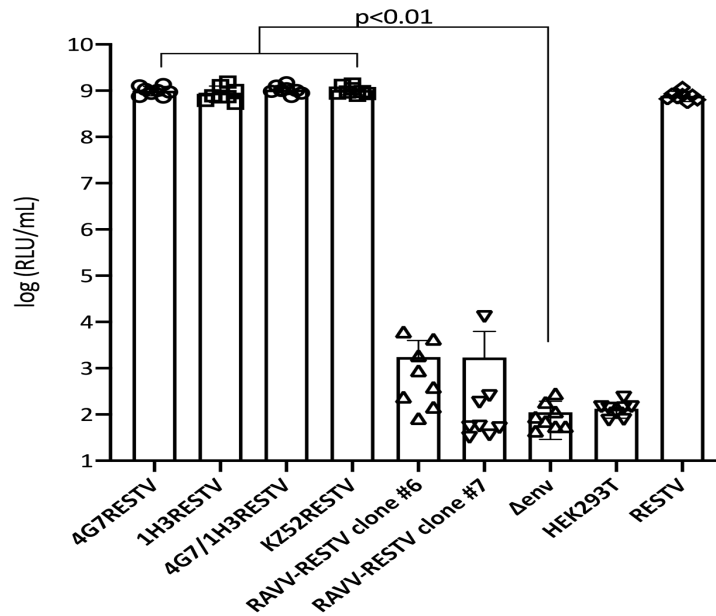


Figure 5.20. Infectivity assay of lentiviral PVs bearing chimeric RESTV GPs. Transduction titres in HEK293T target cells. Statistical analysis comparing each PV titre to virions devoid of GP (Δenv). Mann-Whitney test ($p < 0.01$). Wild-type RESTV PVs were used as positive controls.

5.3.4 Antibody assays with chimeric GP PVs

5.3.4.1 Neutralisation assays

5.3.4.1.1 LLOV GP as scaffold

Neutralisation assays were performed to assess whether inserting EBOV epitopes into a LLOV GP scaffold would result in neutralisation by its respective monoclonal antibody and subsequently by convalescent serum.

The gene containing the 4G7 epitope within the LLOV GP scaffold was synthesised, as there were too many residues to be introduced by mutagenesis. However, PV production was not successful (Figure 5.19a). There are two extra residues that do not overlap with the KZ52 epitope: R136 and Q251, the first is located within the receptor-binding site the latter within the glycan cap (Gregory *et al.* 2011; Pallesen *et al.* 2016). These differences might have resulted in abrogation of infectivity. The 4G7 monoclonal antibody would have been a good candidate for neutralising LLOV PVs containing the 4G7 epitope if PV

production had been successful as it neutralises EBOV PVs (Figure 5.21a). Monoclonal antibody 1H3 did not neutralise EBOV PVs (Figure 5.21b), even at double the initial concentration (160 $\mu\text{g}/\text{mL}$) normally set up for 4G7 and KZ52 mAbs, however they were included in the chimeric GP in case of any cooperativity with neutralising mAbs.

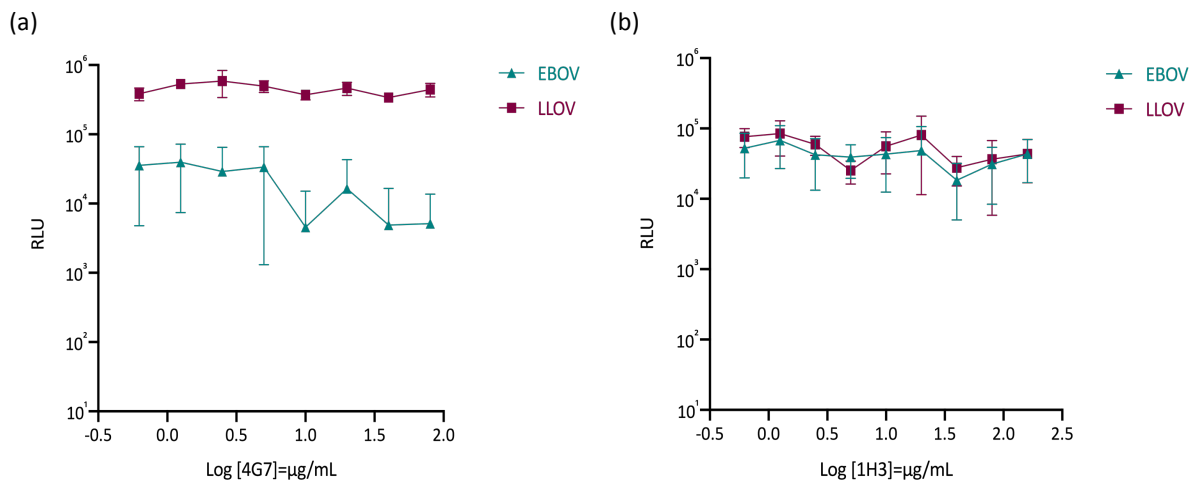


Figure 5.21. Neutralisation assay with EBOV and LLOV PVs with murine derived mAbs. (a) 4G7 at a maximum of 80 $\mu\text{g}/\text{mL}$ and (b) 1H3 at a maximum of 160 $\mu\text{g}/\text{mL}$. Overall PV input in (b) was lower. Results from at least two independent experiments.

LLOV GP was mutated to contain the EBOV KZ52 neutralising epitope. PVs generated with the chimeric GP were not neutralised by its respective mAb (Figure 5.22), unlike the wild-type EBOV PVs

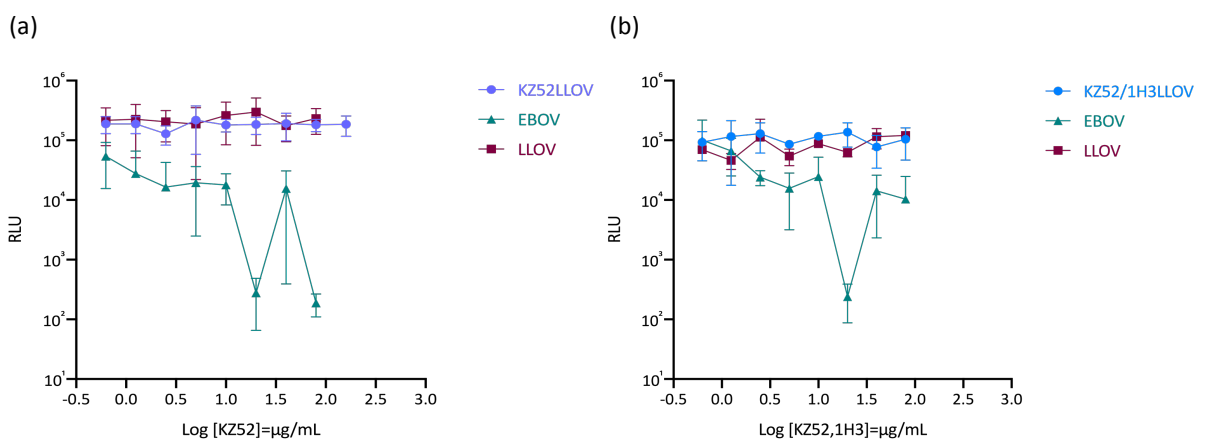


Figure 5.22. Neutralisation assay with EBOV, LLOV and chimeric LLOV PVs. (a) with human mAb KZ52 and (b) combined human and murine mAbs KZ52 and 1H3. Results from at least two independent experiments.

Cooperativity is a synergistic effect sometimes observed in neutralisation assays with more than one mAb. Nevertheless, cooperativity between KZ52 and 1H3 epitopes was not observed (Figure 5.22b).

None of the chimeric LLOV GPs bound to their respective monoclonal antibodies in ELISA using purified PVs as antigens (Figure 5.26).

5.3.4.1.2 RESTV GP as scaffold

Neutralisation assays were performed to assess whether inserting EBOV epitopes into RESTV GP would result in neutralisation by their respective monoclonal antibody and subsequently convalescent serum.

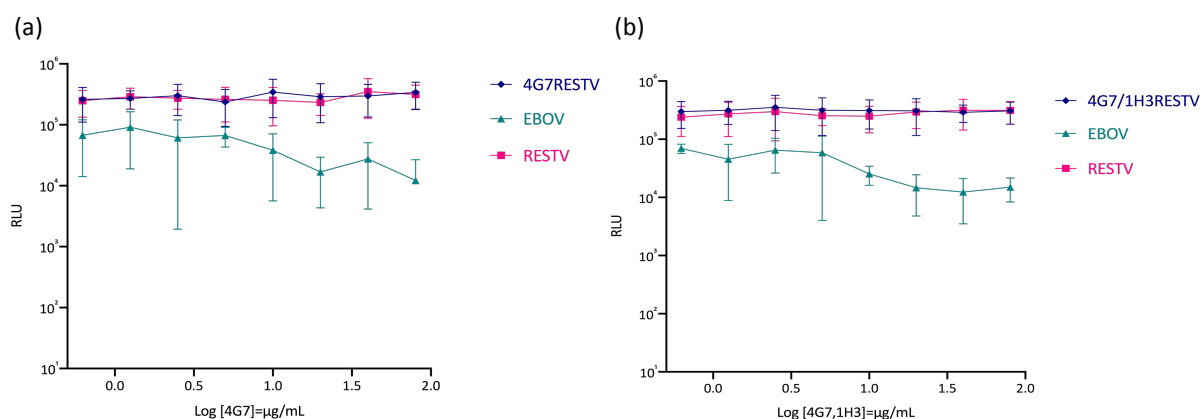


Figure 5.23. Neutralisation assay with EBOV, RESTV and chimeric RESTV PVs. (a) murine mAb 4G7 and (b) combined murine mAbs 4G7 and 1H3. Results from at least two independent experiments.

PVs with the chimeric RESTV GP bearing EBOV 4G7 epitope were not neutralised by the monoclonal antibody 4G7 (Figure 5.23, Table 5.4). A degree of cooperativity has been reported when combining non-neutralising or weakly neutralising mAbs, however RESTV GP bearing both 4G7 and 1H3 epitopes were not neutralised by their combined mAbs, each at a starting concentration of 80 µg/mL (Figure 5.23b, Table 5.4).

	4G7			4G7 + 1H3		
	#1	#2	Mean IC ₅₀	#1	#2	Mean IC ₅₀
EBOV	10.55	7.50	9.03	7.75	9.77	8.76
RESTV	NN	NN	NN	NN	NN	NN
4G7RESTV	NN	NN	NN	NT	NT	NT
4G7/1H3RESTV	NT	NT	NT	NN	NN	NN

Table 5.4. IC₅₀ values of neutralisation assays with chimeric PVs. NT = not tested. NN = not neutralised.

However, in PVs displaying chimeric RESTV GP containing EBOV epitope KZ52 were indeed neutralised by the KZ52 monoclonal antibody in two different target cell lines. Five neutralisation assays were performed: three using HEK293T cells as target (Figure 5.24a and 5.24c) and two using CHO-K1 cells (Figure 5.24b and 5.24d). In all assays, it was evident that PVs bearing the chimeric RESTV GP containing EBOV KZ52 epitope were neutralised by mAb KZ52 (Figure 5.24). The wild-type RESTV GP was not neutralised by the mAb KZ52, as luminescence remained constant at every dilution (Figure 5.24a-b).

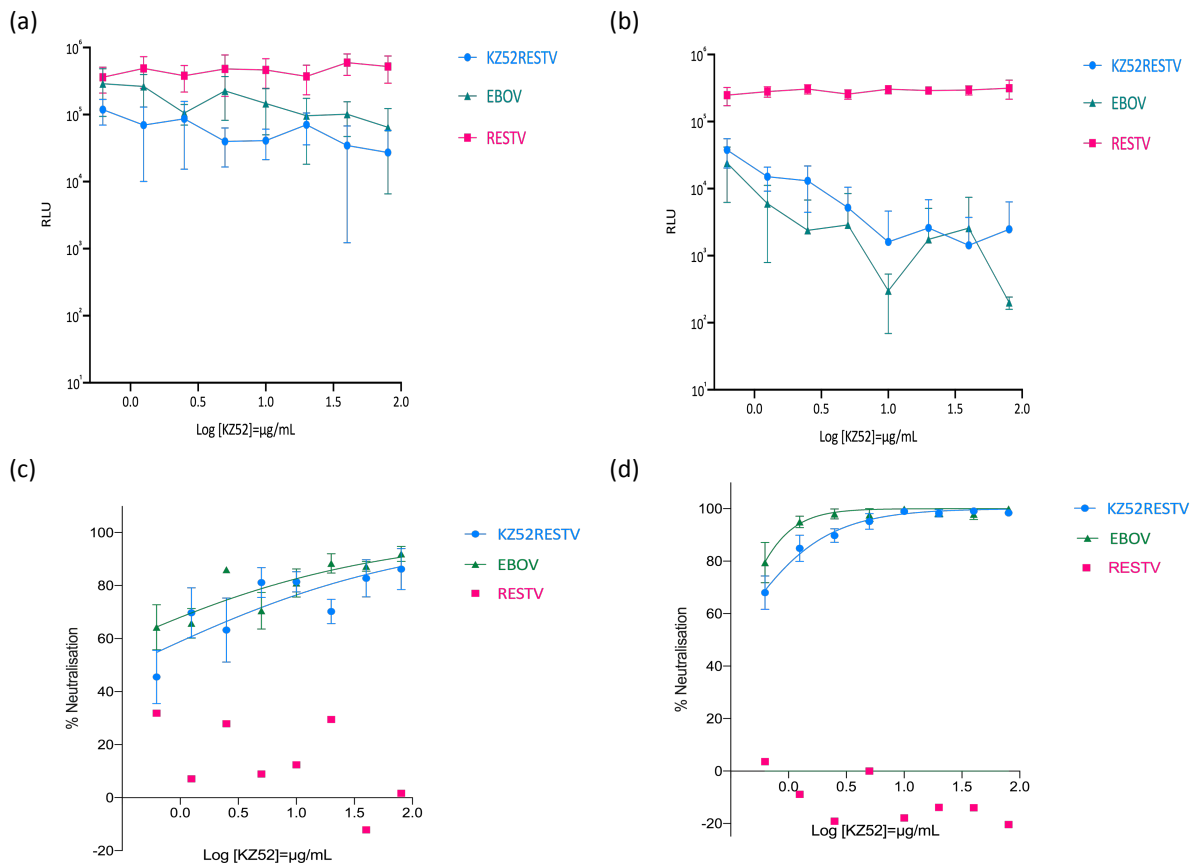


Figure 5.24. Neutralisation assay with EBOV, RESTV and chimeric RESTV PVs with human mAb KZ52. Decrease in luminescence in (a) HEK293T (n=3) and (b) CHO-K1 (n=2) target cells. Non-linear regression analysis in (c) HEK293T (KZ52RESTV $r^2 = 0.2$, EBOV $r^2 = 0.3$) and (d) CHO-K1 (KZ52RESTV $r^2 = 0.7$, EBOV $r^2 = 0.6$) target cells. Analysis from at least two independent experiments. Graphs and non-linear regression curves (log [inhibitor] vs normalised response; constraint: hill slope >0) generated with Prism 8.

Even though mean IC_{50} titres were similar (Table 5.5), CHO-K1 cells would probably be the best choice of target cells for PVNA using filovirus PVs. The neutralising response was clearer (Figure 5.24d) and the reduction in RLU values more accentuated (Figure 5.24b) in assays using CHO-K1 cells as targets than in HEK293T target cells (Figure 5.24a and 5.24c).

	HEK293T target				CHO-K1 target		
	#1	#2	#3	Mean IC ₅₀	#1	#2	Mean IC ₅₀
EBOV	0.28	0.1	0.04	0.14	0.49	0.09	0.29
RESTV	NN	NN	NN	-	NN	NN	-
KZ52RESTV	0.07	0.6	0.84	0.5	0.32	0.33	0.33

Table 5.5. IC₅₀ values (µg/mL) of neutralisation assays with KZ52RESTV chimeric GP. NN = not neutralised.

The concentration of mAbs (0 to 80 µg/mL) and PV input (~1 x 10⁵ RLU or ~100 TCID₅₀) were kept constant in all assays.

Neutralisation assays using pooled convalescent serum (NIBSC 15.262) did not show PV neutralisation via the chimeric KZ52RESTV epitope (Figure 5.25). Polyclonal serum seems to be less potent than monoclonal antibodies in PVNAs therefore a single neutralising epitope might not be sufficient for neutralisation if it is not immunodominant within the GP.

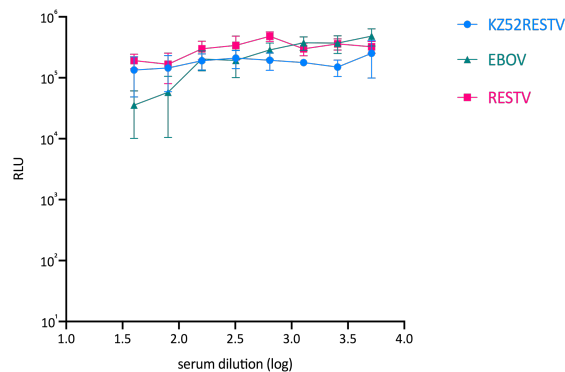


Figure 5.25. Neutralisation assay with anti-EBOV convalescent serum (WHO NIBSC 15.262) against EBOV, RESTV and chimeric RESTV PVs. Decrease in luminescence in HEK293T target cells. Analysis from at least two independent experiments performed with Prism 8.

5.3.4.2 ELISA

In ELISA assays, mAbs did not bind to their respective chimeric LLOV GP bearing EBOV epitopes (Figure 5.26).

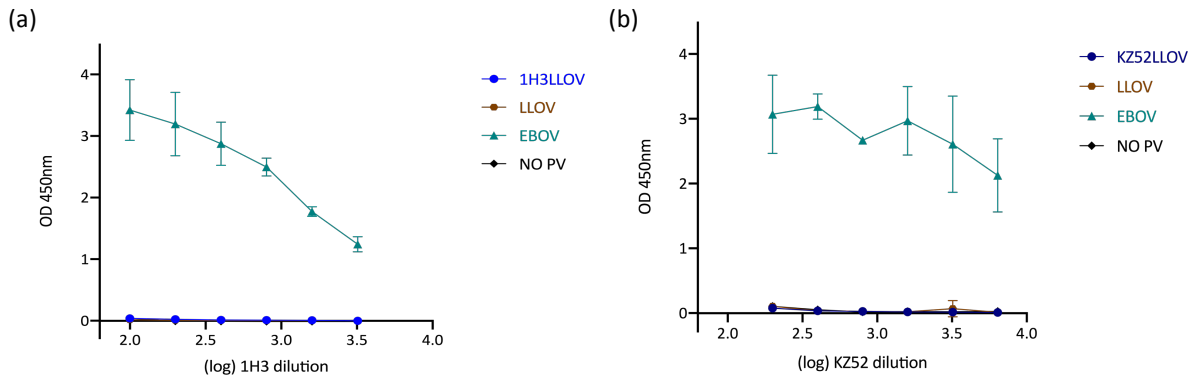


Figure 5.26. ELISA with chimeric LLOV PVs as antigens. Indirect ELISA with mAbs (a) 1H3 and (b) KZ52 as primary antibodies. EBOV PVs were included as positive control and well coated with buffer only (NO PV) were included as negative controls. Data from at least two independent experiments analysed with Prism 8.

Monoclonal antibodies 4G7 and 1H3 did not bind to their respective chimeric RESTV GP bearing EBOV epitopes 4G7 (Figure 5.27a) or 1H3 (Figure 5.27b) that were used as antigens in ELISA. However, monoclonal antibody KZ52 bound to the chimeric KZ52RESTV GP in ELISA (Figure 5.27c), as well as neutralising PVs bearing the KZ52RESTV GP in PVNAs (Figure 5.24), suggesting epitope modification is possible if the particular epitope is maintained when mutated into a new GP scaffold.

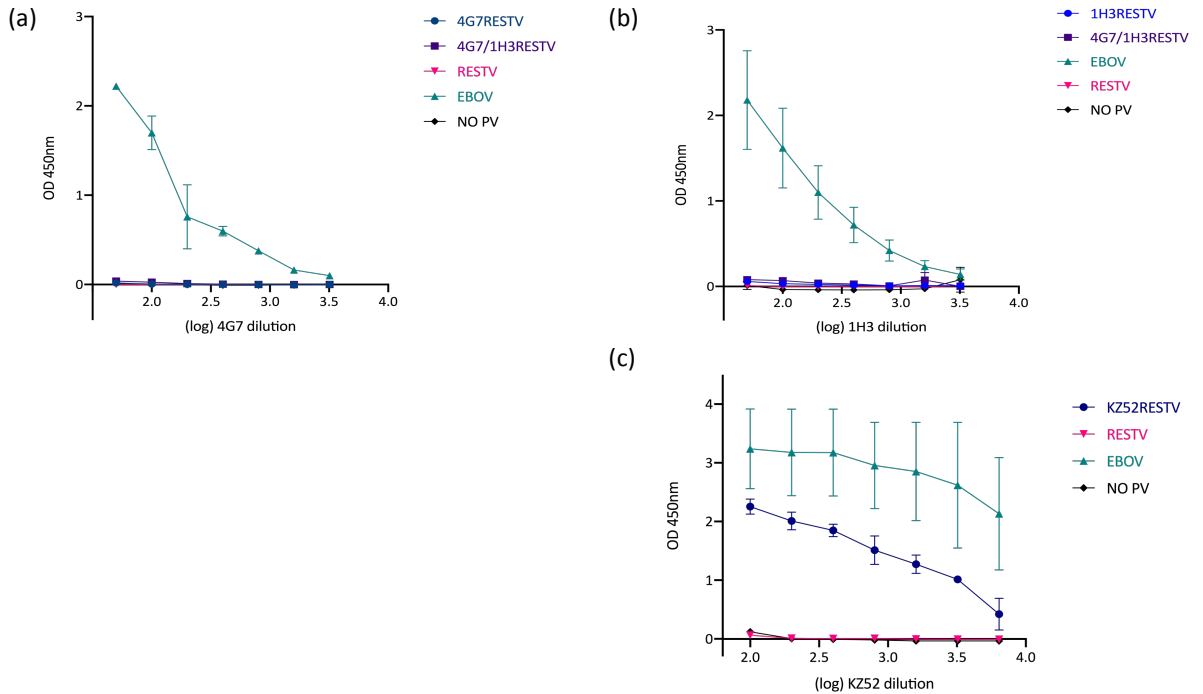


Figure 5.27. ELISA with chimeric RESTV PVs as antigens. Indirect ELISA with mAbs (a) 4G7, (b) 1H3 and (c) KZ52 as primary antibodies. EBOV PVs were included as positive control and well coated with buffer only (NO PV) were included as negative controls. Data from at least two independent experiments analysed with Prism8.

5.4 Discussion

Identifying the correct viral species responsible for a particular outbreak is important to inform appropriate public health responses. In addition, it helps epidemiological studies to determine geographical spread, susceptibility and exposure within a population. Improved filovirus screening would benefit such studies in countries affected, even retrospectively if serum samples are available for testing. Even though most filovirus outbreaks are caused by EBOV (formerly known as Zaire or ZEBOV), other *ebolavirus* species such as SUDV and BDBV have also caused short sporadic outbreaks. *Marburgvirus* species are also highly pathogenic but have caused fewer and smaller outbreaks than *ebolavirus* (Languon and Quaye 2019).

Lloviu virus (LLOV), a potentially zoonotic filovirus, has been detected in bats in different locations in Europe (Negredo *et al.* 2011; Kemenesi *et al.* 2018; De Arellano *et al.* 2019), therefore prompt identification of those different genera and species would be highly advantageous in studies regarding animal reservoirs, or indeed in future human outbreaks.

We attempted to create a filovirus PV screening tool for detection of neutralising antibodies directed to its glycoprotein (GP) that could differentiate between genera and species. EBOV neutralising antibodies can be detected using commercially available convalescent serum (NIBSC). However, cross-reactivity against RAVV PVs was observed (Chapter 4). To address this issue, chimeric GPs bearing EBOV epitopes displayed in a neutral GP scaffold (LLOV or RESTV) were generated to improve specificity.

Firstly, modelling the 3D structure of the proposed chimeric GPs was conducted (utilising the PHYRE2 software program) to assess whether the epitopes would be displayed correctly (Kelley *et al.* 2015). However, as there are no LLOV or RESTV GP structural studies available yet, modelling was challenging due to the lack of published structures. When using LLOV as scaffold, EBOV epitope 1H3 was predicted to be located in a disordered region, or a lack of a fixed 3D structure (Figure 5.4a). In addition, the intensive mode model showed the 1H3 epitope 'buried' on top of the GP (Figure 5.5c), which could explain why it did not bind in ELISA (Figure 5.26a) if part of the epitope was hidden within the structure.

The KZ52 GP₁ region was predicted to be part of a β -sheet (Figure 5.4b), but predicting the full GP was not possible. The intensive mode model also showed KZ52 only partially

exhibited on the outside of the structure (Figure 5.5d), and it did not bind in ELISA either (Figure 5.26b).

Marburg virus epitope MR78 resulted in a somewhat more successful model with some regions as α -helices and β -sheets, as well as disordered regions (Figure 5.6b). However, the intensive model also showed the MR78 epitope only partially exhibited on the outside of the structure (Figure 5.7).

Modelling of filovirus epitopes displayed on RESTV GP scaffold was more successful. EBOV epitope 1H3 is shown on the GP surface; and epitopes 4G7 and KZ52 appear more exposed (Figure 5.8) than in the LLOV GP model. Overall, modelling using PHYRE2 might have been more helpful if there had been published GP structures of the chosen scaffolds.

Apart from 4G7LLOV and MR78LLOV GPs, all chimeric constructs were generated via overlap extension PCR (Heckman and Pease 2007). Careful primer design was crucial, taking into account the overlapping regions have to be long enough for annealing during gene assembly, as well as making sure no internal sites of the cloning enzymes are introduced during chimeric primer design. However, other factors such as GC content and hairpin structures were more difficult to avoid because the location of the primers was determined by where the desired substitution was, and therefore only primer length could be adjusted. Nevertheless, all chimeric constructs that did not require gene synthesis were successfully generated using this method. Overlap extension PCR cloning can be tailored and adapted according to the type of mutations needed.

PV production of chimeric GP constructs 1H3LLOV, KZ52LLOV and KZ52/1H3LLOV was successful with titres of $\sim 1 \times 10^7$ RLU/mL, slightly lower than wild-type LLOV PVs (Figure 5.19a). However, 4G7LLOV, 4G7/1H3LLOV and MR78LLOV GP gene constructs did not generate functional PVs (Figure 5.19a). Considering the RBS is absolutely essential for infectivity and neutralisation assays (Kuhn *et al.* 2006; Temperton, Wright and Scott 2015), mutations that disrupt the GP structure, particularly the RBS, could compromise downstream assays. Substitutions N50S, S51T and A261Q in LLOV GP to insert 4G7 epitope might have been sufficient to disrupt the GP structure and prevent generation of functional PVs. However, substitution S51T was introduced as part of the KZ52 epitope into LLOV, resulting in functional PVs (Figure 5.19).

Most of identified neutralising antibodies against MARV/RAVV so far target the RBS, except the G series of mAbs, which target the base of the GP. However, these are comparatively less potent in neutralisation assays (Flyak *et al.* 2015; Hashiguchi *et al.*

2015; Fusco *et al.* 2015), therefore they might not be suitable for epitope modification strategies. The extensive mutation of the RBS to insert epitope MR78 into LLOV impaired PV production (Figure 5.19a). The permissive human cell line Huh-7 was used as a target in an attempt to detect a functional titre for MR78LLOV PVs unsuccessfully (Figure 5.19b). It is worth noting that not all mutations in the RBS are detrimental. Some adaptations in the RBS such as the substitution A82V in EBOV (C15 Makona) can actually increase infectivity in certain cell lines, including human Huh-7 (Urbanowicz *et al.* 2016). This is seen in other RNA viruses such as influenza, where this type of adaptation enables transmission from avian to human hosts (Yamada *et al.* 2006), or the SARS-CoV-2 virus containing mutations in its spike to increase affinity to the human ACE2 receptor (Andersen *et al.* 2020; Wan *et al.* 2020).

Chimeric RAVV-LLOV and RAVV-RESTV GPs did not generate functional PVs (Figure 5.19-5.20). It is possible that the GP structure was severely compromised by the large domain swaps undertaken. Replacing the whole GP₁ might have been a more feasible approach, as it has been done with influenza successfully whereby the globular head of one strain was linked to the stalk of another (Krammer *et al.* 2013). However, specificity could still be an issue if the whole of RAVV GP₁ was included in the chimeric GP.

PV titres where RESTV was the GP scaffold bearing EBOV epitopes was more consistent, with 100% titre retention in all chimeric PVs (Figure 4.20a), in comparison to using LLOV as a scaffold GP (Figure 5.19a).

Functional PVs bearing chimeric GPs were tested in neutralisation assays. When LLOV GP was a scaffold for EBOV epitopes, none of the chimeric PVs were neutralised by their respective monoclonal antibodies. 4G7 mAb was previously shown to neutralise (IC₅₀= 9 µg/mL) wild-type EBOV PVs (Figure 5.21a, Table 5.4), however functional LLOV PVs bearing the 4G7 epitope were not successfully produced (Figure 5.19a). The 1H3 epitope is continuous and part of the GP₁, thought to have a conformational presentation. Monoclonal antibody 1H3 had been reported to weakly neutralise EBOV VSV PVs and a laboratory variant EBOV (Mayinga) expressing eGFP, produced by reverse genetics with the eGFP gene inserted between the NP and VP35 ORFs (Qiu *et al.* 2011; Audet *et al.* 2015), however 1H3 did not neutralise EBOV PVs (Figure 5.21b), even after the mAb concentration was increased (to 160 µg/mL).

The neutralising mAb KZ52 was probably the best candidate as it strongly neutralises EBOV PVs (IC₅₀ ~0.1 µg/mL), more potently than mAb 4G7. However, KZ52 did not neutralise KZ52LLOV PVs (Figure 5.22a). Cooperativity with 1H3 was hypothesised as non-

neutralising epitopes are reported to have a synergistic effect in neutralising assays such as mAb FVM09, which in itself is non-neutralising, but when combined with weakly neutralising m8C4 a synergistic effect was observed in neutralisation assays with EBOV VSV PVs (Howell *et al.* 2017). They propose a mechanism by which binding of FVM09 causes a conformational change whereby a particular region, the β 17- β 18 loop that is normally “hidden” within the 3D structure, becomes exposed allowing binding of mAb m8C4 (Howell *et al.* 2017).

A similar effect was observed with mAbs FVM09 and ADI-15946 against EBOV VSV PVs and authentic EBOV (West *et al.* 2019). However, that was not observed when mAbs 4G7 and 1H3 were tested against wild-type EBOV PVs (Table 5.4), or when mAbs KZ52 and 1H3 were tested against wild-type EBOV PVs or chimeric KZ52/1H3LLOV PVs (Figure 5.22).

Some of those synergistic effects *in vitro* have translated in increased protection in animal models when compared with a single mAb treatment (Howell *et al.* 2017). However, enhanced protection *in vivo* do not always correlate to increased neutralisation *in vitro* (Rijal *et al.* 2019).

None of the monoclonal antibodies bound to the chimeric LLOV PVs in ELISA using purified PVs as antigens (Figure 5.26) corroborating the neutralising data (Figure 5.22). It is reasonable to hypothesise that the epitopes were not displayed correctly after mutations were introduced, even though functional PVs were generated successfully in some cases. None the EBOV epitopes (1H3, 4G7 and KZ52) are located within the RBS, making PV production more feasible, as opposed to the MR series of epitopes within the RBS of *marburgviruses*, which includes MR78.

RESTV GP was selected as an alternative GP scaffold to LLOV due to being of similar size to EBOV GP, therefore easier to align (Appendix II). In addition, EBOV convalescent sera did not cross-react against RESTV PVs. We reasoned it might be more likely to display the epitopes correctly.

Monoclonal antibodies 4G7 and 1H3 did not neutralise 4G7RESTV or 4G7/1H3RESTV PVs (Figure 5.23, Table 5.4), or bind in ELISA (Figure 5.27a-b). However, mAb KZ52 did neutralise KZ52RESTV PVs using either HEK293T (Figure 5.24a and 5.24c) or CHO-K1 (Figure 5.24b and 5.24d) target cell lines, in a total of five independent experiments. In addition, mAb KZ52 bound to KZ52RESTV PVs in ELISA (Figure 5.27c), albeit more weakly than to wild-type EBOV PVs. This suggests the KZ52 epitope was correctly displayed in the chimeric RESTV GP.

It is not clear why 4G7 did not neutralise 4G7RESTV PVs. In this study, 4G7 was not as potent as KZ52 in neutralisation assays against wild-type EBOV PVs (Tables 5.4 and 5.5). This is consistent with the neutralising profile in other studies (Saphire *et al.* 2018; Gilchuk *et al.* 2018). 4G7 has also been shown to have less binding affinity to EBOV GP in ELISA (Davidson *et al.* 2015), which was also observed in our in-house PV ELISA (Figure 5.27). 4G7 and KZ52 were also found to have a similar neutralisation profile in a reverse genetic system (expressing the eGFP reporter) of EBOV (Makona C15) as well as EBOV (Ituri), one of the strains involved in the recent outbreak in the Democratic Republic of Congo (McMullan *et al.* 2019).

This study suggests the chimeric PV approach is feasible if the right epitopes and scaffold GP are chosen. Having a published structure of the scaffold GP would help considerably in modelling the epitope modification strategy in advance. It could be a useful tool not only to address specificity issues in serological tests, but also to improve immunogenicity in vaccine design, as well as a possible universal filovirus vaccine if inserting epitopes from different species is successful.

Similar epitope swapping approaches have been used in gene therapy studies of adeno-associated virus (AAV) vectors, where epitopes with low affinities for the resin column used for purifications were substituted for a high affinity epitope to improve purification methods, as well as enabling a universal protocol for different serotypes (Wang *et al.* 2015); and to differentiate between transgene and endogenous FGFR1 (fibroblast growth factor receptor type I) by inserting a FLAG epitope disrupting another known epitope (M17A3) in functional physiological studies, where the distinction between the recombinant protein and the endogenous equivalent is crucial (Zheng and Yan 2000). This is achieved with mAbs targeting FLAG or M17A3. In vaccine research, directing the antibody response by epitope grafting is being attempted for several pathogens, including influenza and respiratory syncytial virus for instance (McLellan *et al.* 2011; Dormitzer, Grandi and Rappuoli 2012; Grimm and Ackerman 2013). In addition, epitope prediction tools could aid vaccine design by identifying conserved epitopes across species and genera (Jain and Baranwal 2019).

Pooled EBOV convalescent serum (WHO standard NIBSC 15.262) did not neutralise chimeric KZ52RESTV PVs (Figure 5.25), indicating a single epitope might not be sufficient in a screening test that can differentiate between species, therefore adding extra epitopes will be necessary in future attempts. In addition, polyclonal serum is less potent than monoclonal antibodies in PVNAs (Chapter 4). Studies using PVs expressing EBOV GP

lacking the glycan cap and mucin-like domain (EBOV GP_{CL}) are neutralised more efficiently than PVs exhibiting the native GP (Luczkowiak *et al.* 2018). Therefore generating a chimeric RESTV GP_{CL} containing the KZ52 epitope, and possibly several neutralising epitopes might result in neutralisation by convalescent serum.

Epitopes targeted by IgM antibodies identified by ELISA and surface plasma resonance may also be considered as they have been found to contribute to the neutralising response in the early stages of infection (Khurana *et al.* 2016). Furthermore, antibody-dependent enhancement (ADE) of infectivity should also be taken into account. Although this has not been tested in this study, ADE might affect *in vitro* assays. Considering most of ADE epitopes are within the glycan cap and MLD (Takada *et al.* 2003; Takada *et al.* 2007; Kuzmina *et al.* 2018), it could be one of the reasons why EBOV GP_{CL} results in increased neutralising responses. ADE is also observed in *marburgvirus* species to different degrees (Nakayama *et al.* 2011). A chimeric MARV GP_{CL} might also be useful, considering the location of most ADE epitopes.

Other chimeric strategies have also been used for screening of antibodies to develop therapeutic mAbs using reverse genetic systems (Ilinykh *et al.* 2018), which are desperately needed considering the recent EBOV outbreaks in the DRC.

PVs can be employed not only for working with highly pathogenic viruses in low containment, but also as vaccine delivery systems and high-throughput antiviral screening. Insertion or swapping epitopes can potentially be utilised in improving specificity in current serological assays or vaccine platforms.

CHAPTER 6: Application of *Cuevavirus* (LLOV) Pseudotypes to Serosurveillance of Bats in Hungary

6.1 Introduction

Bats have been identified as the animal reservoir for many zoonotic viruses such as lyssaviruses, coronaviruses, henipaviruses, influenza H17N10 and H18N11 and possibly picornaviruses (Li *et al.* 2005; Wright *et al.* 2010; Halpin *et al.* 2011; Tong *et al.* 2012; Tong *et al.* 2013; Kemenesi *et al.* 2015; Yinda *et al.* 2017; Brook *et al.* 2019; Giotis *et al.* 2019). They are the most obvious candidates for being the animal reservoir of filoviruses. Ebola and Marburg virus RNA has been previously detected in bats. Antibodies against *marburgviruses* were found in apparently healthy animals (Swanepoel *et al.* 2007; Towner *et al.* 2009). In addition, active infection was detected and virus isolation from some of these animals was successfully achieved, providing evidence that Egyptian rousette bats are the animal reservoir for *marburgvirus* (Towner *et al.* 2009; Amman *et al.* 2020).

Since the largest outbreak of Ebola virus (EBOV) in West Africa in 2013-2016, research efforts to identify the animal reservoir for EBOV and other filoviruses were increased but have so far proved elusive. Establishing the reservoir would not only improve understanding of disease transmission but also help prevention of future outbreaks by educating local human populations to avoid contact with possible sources, such as on dangers of hunting for bush meat or being in close contact with infected people. In addition, serosurveillance will help us understand transmission patterns and the geographical distribution of those pathogens.

For decades, only two genera of filoviruses (*marburgviruses* and *ebolaviruses*) had been described since their respective discoveries in 1967 and 1976. However in 2002, mortality events were observed in colonies of *Miniopterus schreibersii* (Schreiber's bats) in caves in Spain. Thirty-four bat carcasses were collected from Cueva del Lloviu in Asturias for analysis, and filovirus sequences were detected in five animals by RT-PCR, however virus isolation was not successful. Nevertheless, high-throughput sequencing yielded enough reads to characterise almost a full genome. Genome phylogenetic analysis demonstrated a distinct genetic lineage classified as a new genus – *cuevaviruses*. Only one virus species has been described to date; Lloviu virus or LLOV (Negredo *et al.* 2011). This study indicated that filoviruses have a wider geographical distribution than previously thought.

More recently, filovirus RNA has also been detected in fruit bats in China and a fourth genus, *Dianlovirus* – Mengla virus (MLAV) has been described, more closely related to MARV. Like other filoviruses, MLAV utilises the NPC-1 receptor for entry and has a broad cell tropism. The virus has not been isolated yet, however VSV PVs bearing the MLAV GP were able to transduce three human, five bat, a hamster and two monkey cell lines (Yuan *et al.* 2012; Yang *et al.* 2017; Yang *et al.* 2019).

Characterisation of the LLOV genome revealed similarities to *ebolaviruses* such as secreted versions of the surface glycoprotein (GP), which *marburgviruses* and *dianloviruses* lack. Seven viral proteins expressed by LLOV are encoded by only six genes. Here, the VP30/L gene produces a bicistronic mRNA (Figure 6.1). LLOV has sequence identities at the genomic level of 48% with *ebolaviruses* and 45% with *marburgviruses* (Negredo *et al.* 2011; Burk *et al.* 2016; Yang *et al.* 2019).

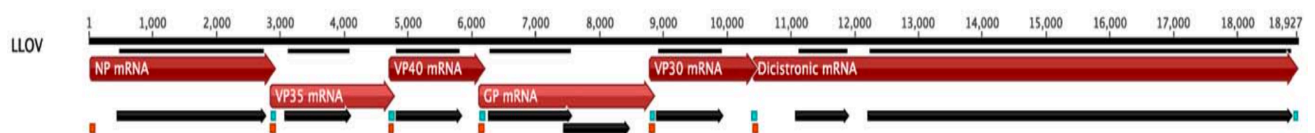


Figure 6.1. Genomic organisation of LLOV. Black bars correspond to the open reading frames (ORFs), red arrows are predicted mRNA transcripts and start (blue box) and termination (red box) signals for each transcript are indicated. (Figure source: Negredo *et al.*, 2011).

Characterisation of the glycoprotein (GP) gene identified a putative editing site used by the viral RNA-polymerase (L) for expression of the membrane bound GP as seen on *ebolaviruses*; as well as identifying C-type lectins as one of the initial attachment factors for cellular entry (Maruyama *et al.* 2014). Finally, requirement of NPC-1 receptor for entry once internalised into the endosome (Ng *et al.* 2014). In addition, LLOV virus-like particles (VLPs) generated through the expression of matrix proteins VP40, NP and the desired GP, were found to be morphologically similar to other filoviruses in transmission electron microscopy (Figure 6.2), with filaments of different lengths and diameters consistent with other VLP systems (Maruyama *et al.* 2014).

LLOV also emerged in 2016 in Hungary after mortality events were observed in caves in the Bukk Mountains and other sites. Initially, the carcasses collected were too old for genomic detection analysis but showed signs of respiratory hemorrhaging. Later, fresh carcasses were collected and a nested RT-PCR developed targetting the RNA-dependent polymerase (L gene), which revealed LLOV RNA in one lung sample. In addition, a nested RT-PCR targetting the nucleoprotein (NP gene) was also developed and results showed

98% and 99% homology with the Spanish LLOV for L and NP genes respectively (Kemenesi *et al.* 2018). Isolation of infectious particles has not yet been achieved.

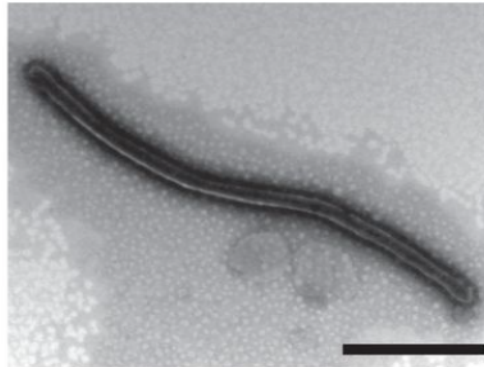


Figure 6.2. TEM of purified LLOV VLP produced in HEK293T cells. Scale bar=500 nm. (Picture adapted from Maruyama *et al.*, 2014).

Since then, LLOV PVs were generated for use in a serological survey of wild bat populations, a collaborative study with the University of Pecs in Hungary. Initially, seven samples were sent to the Viral Pseudotype Unit, three of which had tested positive for LLOV RNA by researchers in Pecs. Following successful PV testing, a further 71 samples were sent for screening.

The aim of this study was to screen bat samples for neutralising antibodies against LLOV to determine whether these animals had already been exposed to infection, gaining insight on the geographical distribution of those viruses; as well as establishing whether these bats are the natural reservoir for the virus, should isolating LLOV infectious particles be successful.

6.2 Materials and Methods

6.2.1 Plasmids and lentiviral LLOV PV generation

The Lloviu virus glycoprotein gene (GenBank JF828358.1 – Appendix I) inserted into pCAGGS was used for PV generation. The plasmid encoding firefly luciferase (pCSFLW) was provided by Dr Nigel Temperton (Viral Pseudotype Unit) and HIV-1 gag-pol core proteins (pCMV- Δ R8.91) was provided by Prof Greg Towers (University College London). LLOV lentiviral pseudotypes containing the firefly luciferase gene were generated based on a plasmid co-transfection method previously described (Chapter 2).

6.2.2 Bat serum samples and controls

Heat inactivated bat sera were sent by Dr Jakab Ferenc and Dr Gabor Kemenesi (University of Pecs, Hungary). Initially, seven samples were sent for a pilot study to compare with prior PCR results conducted in Hungary. Later, a further 71 serum samples were sent for analysis, mainly from live bats that had been caught in caves in Hungary where mortality events had been previously observed (Dr Gabor Kemenesi - personal communication).

Convalescent serum from EVD patients (WHO NIBSC 15.262 and NIBSC 15.282) against EBOV PVs were used as a control for the assay, as a positive LLOV control serum was not available.

6.2.3 Infectivity and TCID₅₀ assays

Infectivity and TCID₅₀ assays have been described in Chapter 2.

6.2.4 Pseudotype Virus Neutralisation assay (PVNA)

PVNAs were performed as previously described (Chapter 2), however a few adaptations were made in the initial serum dilution due to the amount of serum available. Briefly, serially diluted bat sera (1:40 to 1:5120; 1:100 to 1:12800 or 1:200 to 1:25600) were incubated with LLOV PVs ($\sim 1 \times 10^5$ RLU/well or ~ 100 TCID₅₀/well, calculated according to the titration results) for 1h at 37°C, 5% CO₂ to allow for binding of any antibodies to the PVs. Additionally an infection-only control (PVs, no serum) and a cell only control (no PVs or serum) were included to determine 0% and 100% neutralisation respectively. Next, 2×10^4 HEK293T/17 cells per well were added and incubated at 37°C, 5% CO₂ for 48h, before luminescence read. IC₅₀ antibody titres are given as the reciprocal of the dilution at which 50% of pseudotypes were neutralised by the serum and calculated using non-linear regression analysis (Prism 8 software). Average values of two independent experiments are reported unless stated otherwise.

6.2.5 Statistical Analysis

Statistical analysis of PV generation and PVNA titres was performed with Prism 8 as described in Chapter 2.

6.3 Results

6.3.1 Generation of lentiviral Lloviu (LLOV) pseudotypes

LLOV PVs were successfully generated yielding high titres of approximately 1×10^8 RLU/mL or 1×10^4 TCID₅₀/mL (Figure 6.3) for subsequent use in PVNAs. An EBOV PV of known titre (1×10^8 RLU/mL) was used as a positive control. Cell only (HEK293T/17) and Δ env (PV particle devoid of GP) were used as negative controls. The same PV batch was used for all experiments.

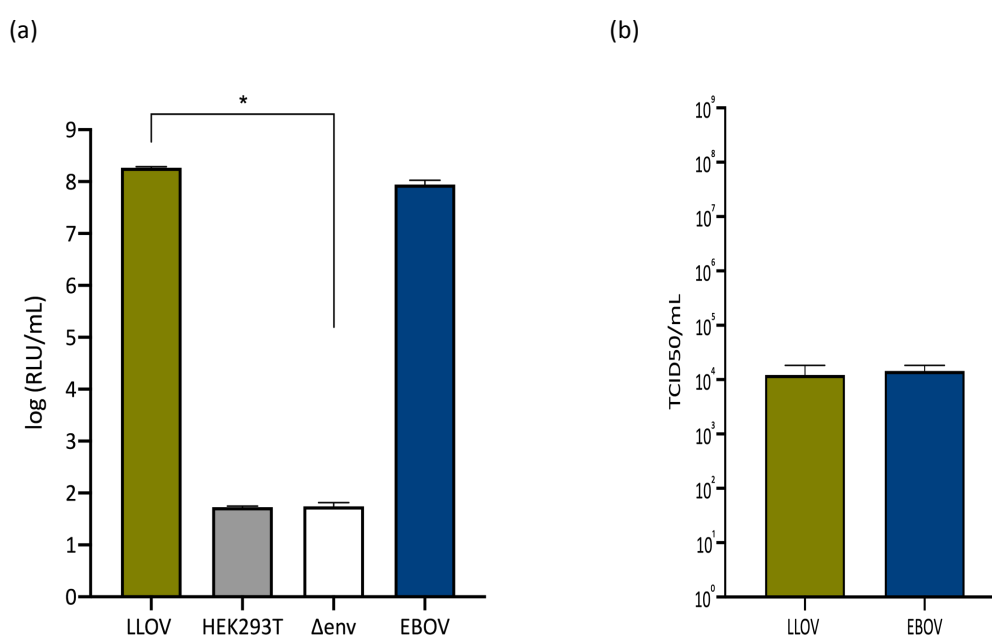


Figure 6.3. Lentiviral LLOV PV titres. An *ebolavirus* PV (EBOV) generated and titrated previously was included as a positive control in (a) infectivity and (b) TCID₅₀ assays. Uninfected cells (HEK293T) and particles devoid of GP (Δ env) were included as negative controls. Average titre of at least three independent experiments reported. The error bars indicate the standard deviation. Statistical significance (* $p < 0.05$ Mann-Whitney test) in comparison to Δ env determined with Prism 8 software.

6.3.2 Measuring neutralising antibody titre in pilot study of bat sera

Initially seven serum samples were sent to us for analysis. These samples had already been characterised by RT-PCR by our collaborators at the University of Pecs (Table 6.1). To evaluate their antibody titres against LLOV PVNAs were performed. All bats that tested positive in RT-PCR had neutralising antibodies detected against LLOV (Table 6.1).

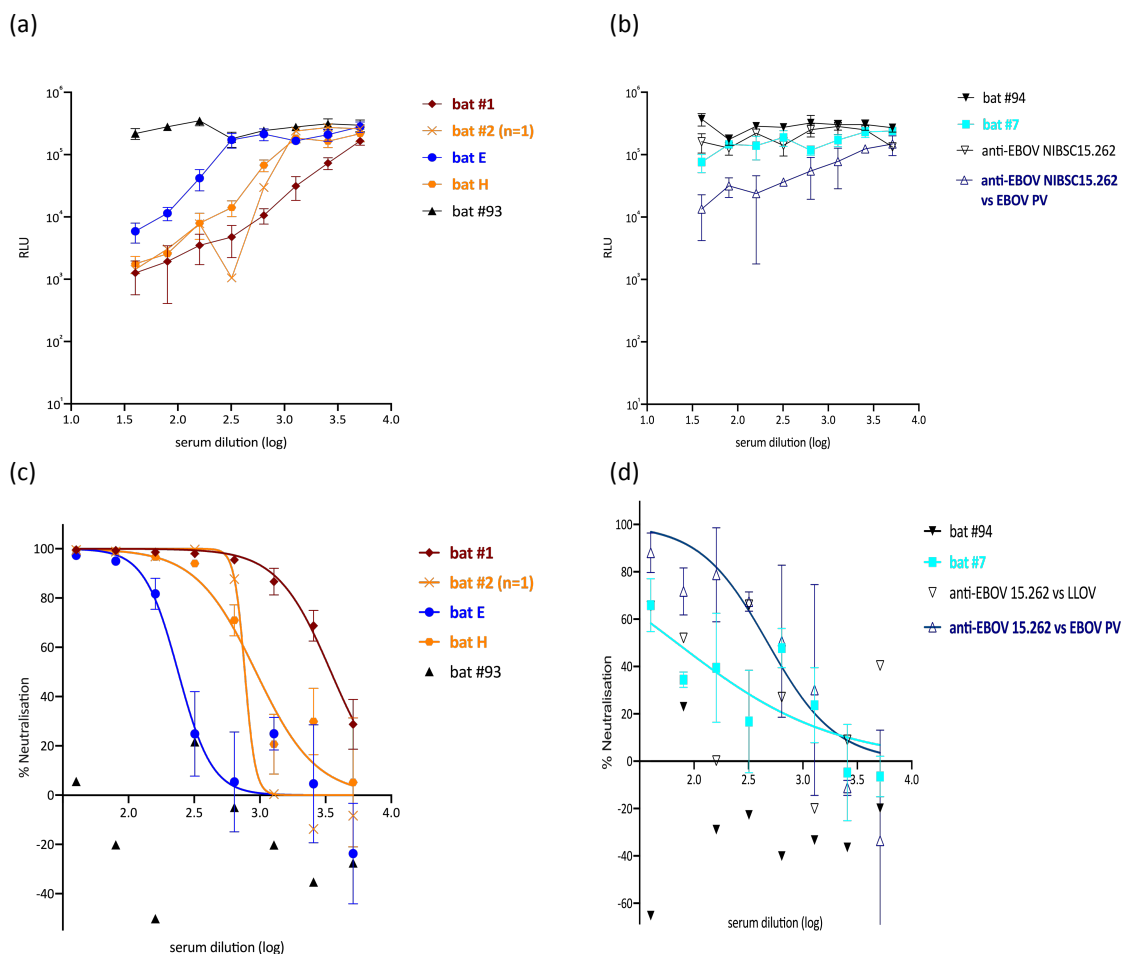
Bat	Characteristics	PVNA #1 IC ₅₀	PVNA #2 IC ₅₀	Mean IC ₅₀
<i>Miniopterus schreibersii</i> animal 1 2016/Mád	PCR positive	2999	3972	3486
<i>Miniopterus schreibersii</i> animal 2 2016/Mád	PCR positive	768	-*	768
<i>Miniopterus schreibersii</i> animal E 2019/Mád	PCR positive	172	337	255
<i>Miniopterus schreibersii</i> animal H 2019/Mád	PCR negative	757	1136	947
<i>Myotis myotis</i> animal 93 2018/Szársomlyó	PCR negative	NN	21	21
<i>Miniopterus schreibersii</i> animal 94 2018/Szársomlyó	PCR negative	NN	NN	NN
<i>Miniopterus schreibersii</i> animal 7 2016/Mád	Heart lavage with PBS from bat #2	53	110	82

Table 6.1. Neutralising antibody end-point titres from 7 bat serum samples. Titres reported as the reciprocal of the dilution in which 50% of PVs were neutralised. The bat species is followed by the animal identification name/place in Hungary where captured. *PVNA not performed due to lack of serum for a repeat experiment. NN = not neutralised.

Bat #1 had a strong neutralising response (IC_{50} range of 2560 to 5120) in both tests, higher than normally observed in PVNAs with EBOV convalescent serum against EBOV PVs. Also, PCR positive bat E had antibody titres in the range of 160 to 320 (Table 6.1).

PCR positive bat #2 had antibody titres in the range of 640-1280 but could only be tested once, as there was not enough serum available for a repeat run (Table 6.1). When neutralising antibodies specific to the LLOV GP were present, the RLU increased as the serum was diluted (Figure 6.4a) in a dose-dependent manner.

Bats #93 and #94 were PCR negative and had no detectable LLOV-specific neutralising antibodies, however bat H was also PCR negative but did have neutralising antibodies in the range of 640 to 1280 (Table 6.1), showing a decrease in transduction in a dose-dependent manner (Figure 6.4a), indicating prior LLOV infection. Neutralisation curves showed a strong neutralising response for bat #1 followed by bat #2, H and E (Figure 6.4c). Bat #94 was PCR negative (Table 6.1) and no decrease in transduction was observed (Figure 6.4b), and finally bat #7, which is a heart lavage sample from bat #2, might have caused a subtle decrease in transduction at the lower dilution (Figure 4.6b), with a weak neutralising response (Figure 6.4d).



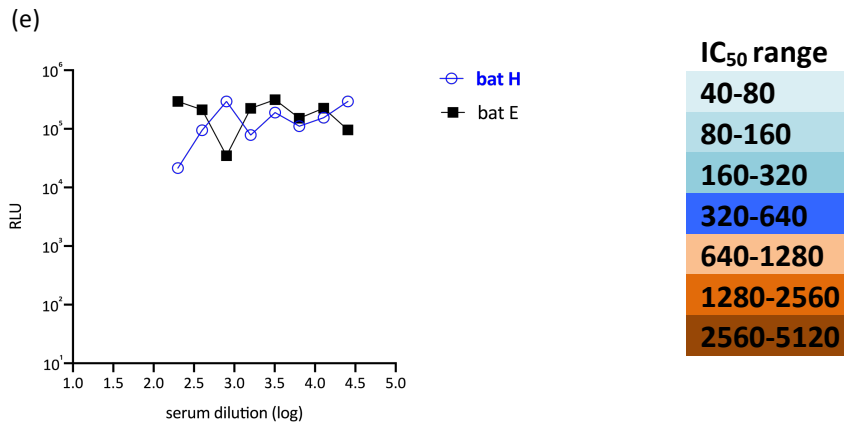


Figure 6.4. Antibody neutralising response in bat serum samples. The bat identification numbers were kept the same as provided by the University of Pecs in Hungary (see Table 1). Samples were tested against LLOV PVs except the PVNA positive control (anti-EBOV convalescent sera WHO NIBSC 15.262) against EBOV PVs. IC₅₀ responses were colour-coded following a gradient from weak (light blue) to strong (dark red). Reduction in transduction from (a) bats #1, #2, E, H, #93 and (b) bats #94, #7, and controls; neutralisation curves from (c) bats #1 ($r^2 = 0.9$), #2 ($r^2 = 0.9$), E ($r^2 = 0.7$), H ($r^2 = 0.7$), #93 and (d) bats #94 ($r^2 = 0.3$), #7 ($r^2 = 0.3$), and controls (NIBSC 15.262 vs EBOV PV $r^2 = 0.6$); and (e) cross-reactivity test against EBOV PVs. The error bars represent s.d (standard deviation of the mean) from duplicates of two independent experiments, except (a) bat #2 and (e) cross-reactivity test, where not enough serum was available. Graphs and non-linear regression curves (log [inhibitor] vs normalised response; constraint: hill slope <0) generated with Prism 8.

Notably anti-EBOV convalescent serum NIBSC 15.262 did not cross-react with LLOV PVs as no reduction in transduction was observed (Figure 6.4b), however bat H might have shown some cross-reaction with EBOV PVs, as a subtle reduction in transduction was observed at the lower serum dilution (Figure 6.4e). A positive control serum against LLOV was not available therefore the anti-EBOV convalescent serum NIBSC 15.262 against EBOV PVs was used as a control for the assay (Figure 6.4b).

6.3.3 Serological screening of bat serum panel.

Following initial screening of 7 samples, a panel of 71 serum samples taken from bats caught alive were sent for analysis: bats were numbered 95-150, 153-160 and 162-168. Serum samples had varying volumes from 2 μ L to 30 μ L, therefore it was not always possible to perform a repeat experiment with duplicates, which requires 20 μ L in total. Hence, depending on available serum volume, the testing regimen had to be adjusted regarding start dilution, number of duplicates within each test and number of independent tests; therefore results are presented in sections according to experimental regimen. Whenever possible, each sample was tested in duplicates followed by a repeat

independent PVNA, with a starting dilution of 1:40. For some samples, duplicates or repeats were not possible and/or the starting dilution was adjusted to 1:100 or 1:200.

Bat	PVNA #1	PVNA #2	Mean
	IC₅₀	IC₅₀	IC₅₀
#99	156	174	165
#115	143	197	170
#130	177	59	118
#102	132	-*	132
#138	83	*	83
#98	211	-*	211
#110	64	-*	64**
#118	155	-*	155
#143	90	-*	90

Table 6.2. Antibody titres from bat serum samples. *PVNA not performed due to lack of serum for a repeat experiment. **Under the cut-off point for what would be considered a positive value (see section 6.3.4).

Measurable antibody titres against LLOV PVs ranged from weak to moderate responses in 11.3% of animals tested (Table 6.2).

6.3.3.1 Regimen 1 (1:40 start serum dilution in duplicate, 2 independent experiments)

In 24 samples there was enough serum to perform two independent tests containing duplicates of each sample with a starting dilution of 1:40. Of those, bat #99 and bat #115 had moderate neutralising antibody titres in the range of 160-320 (Table 6.2) and a decrease in transduction in a dose-dependent manner was observed (Figure 6.5a); bat #130 had a weak titre in the range of 80-160 (Table 6.2), with a corresponding modest decrease in transduction (Figure 6.5b). All other samples in that group were negative, with no decrease in transduction observed (Figure 6.5). A control serum for LLOV was not available therefore an anti-EBOV convalescent serum (NIBSC 15.282) was used against EBOV PVs as a control for the assay (Figure 6.5d). There was not enough serum to test for cross-reactivity against EBOV PVs.

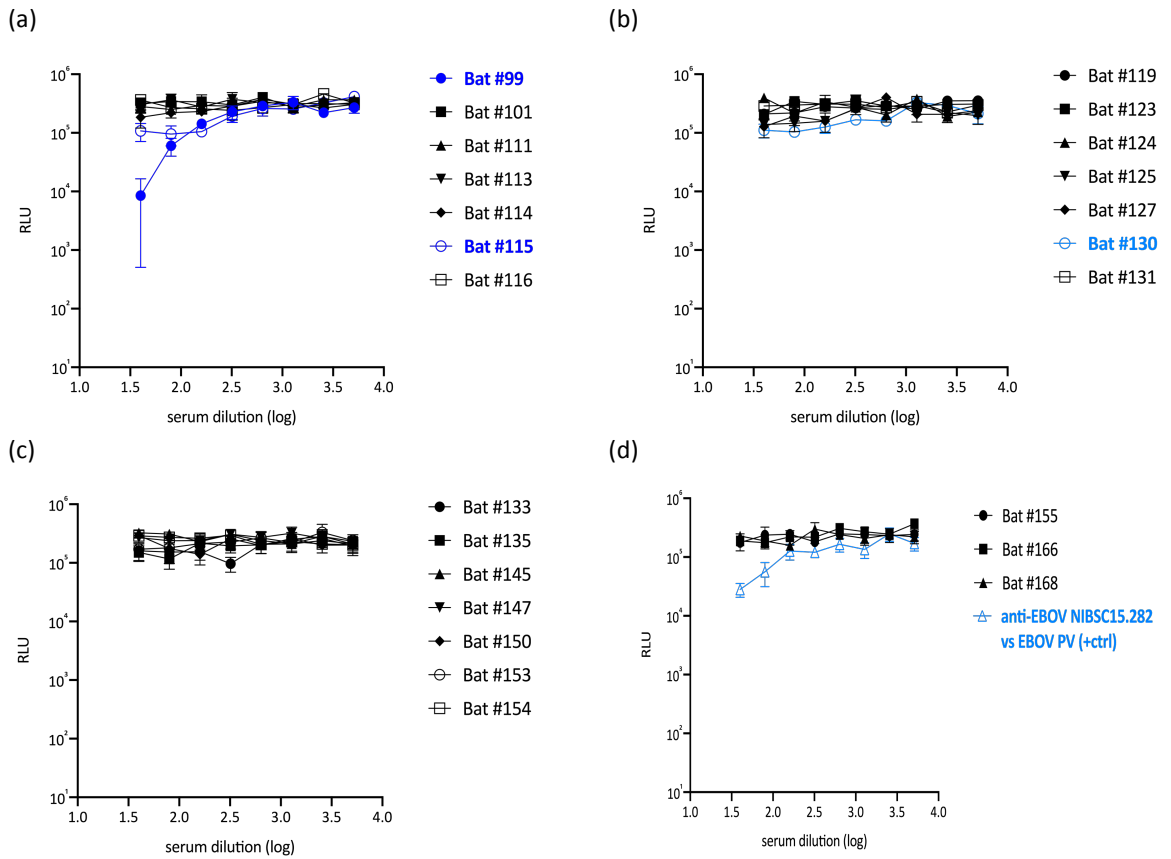


Figure 6.5. Antibody neutralising response of 24 bat serum samples from the overall panel (n=71). The sample numbers were kept the same as provided by the University of Pecs in Hungary. Samples were tested against LLOV PVs except the PVNA control (anti-EBOV convalescent sera WHO NIBSC 15.282) against EBOV PVs. IC₅₀ gradient was colour coded according to Figure 6.4. The error bars represent s.d (standard deviation of the mean) from duplicates in two independent experiments, except bat #2 where not enough serum was available, calculated using Prism 8.

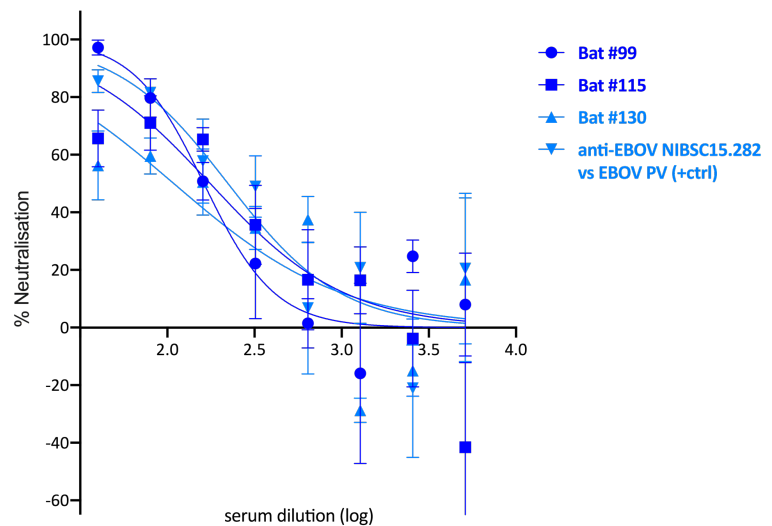


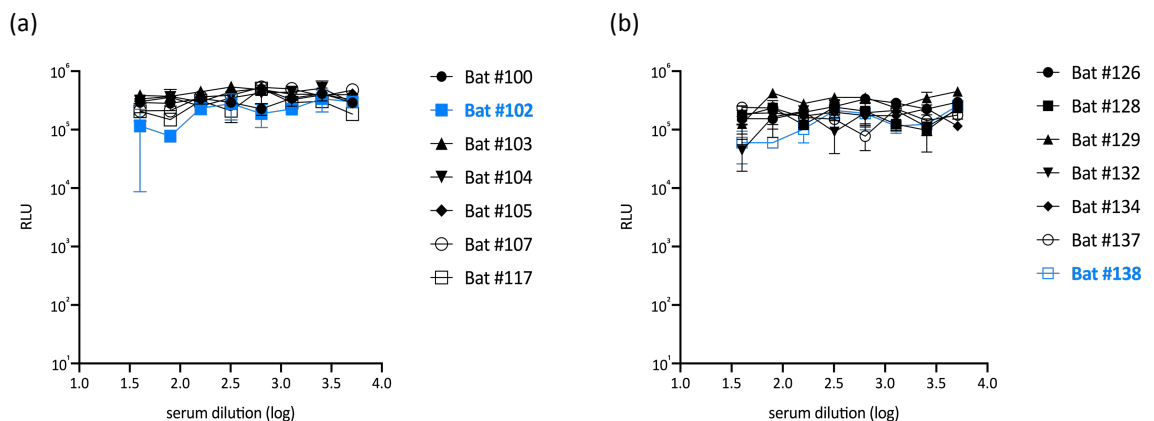
Figure 6.6. Antibody neutralising curves of bat serum samples. Bat #99 ($r^2 = 0.6$), bat #115 ($r^2 = 0.5$), bat #130 ($r^2 = 0.4$) and NIBSC 15.282 ($r^2 = 0.5$). The error bars represent s.d (standard deviation of the mean) from duplicates in two independent experiments. Graphs and non-linear regression curves (log [inhibitor] vs normalised response; constraint: hill slope <0) generated with Prism 8.

Neutralisation curves of the positive samples show the increase in neutralisation as the concentration of antibodies against the LLOV GP increases. Strongest bat sera #99 and #115 neutralised up to ~90-100% and ~70-80% of LLOV PVs respectively (Figure 6.6).

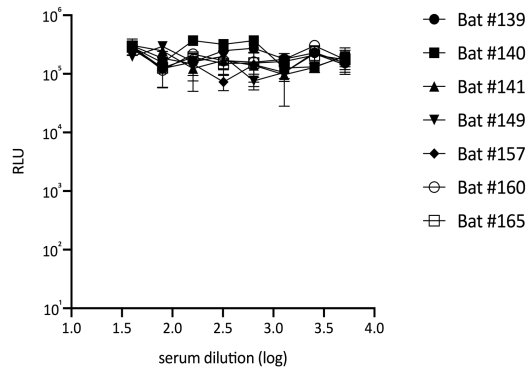
6.3.3.2 Regimen 2 (1:40 start serum dilution in duplicate, 1 experiment)

An additional 21 samples contained enough sera for one test with a starting dilution of 1:40 in duplicate. From those, bats #100, #134 and #139 had enough sera for an extra test. Bat #102 and #138 had a weak neutralising antibody titre in the range of 80-160 (Table 6.2). A modest reduction in transduction at the lower dilutions was observed for bat #102 (Figure 6.7a) and bat #138 (Figure 6.7b). All other samples were negative, with no evidence of a dose-dependent transduction decrease (Figure 6.7).

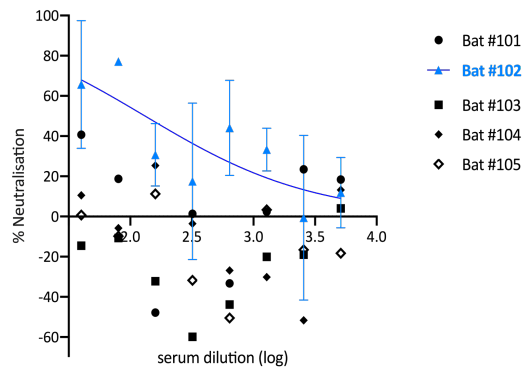
Neutralisation curves were not very clear showing modest neutralisation of up to approximately 60-70% for bat #102 (Figure 6.7d) and bat #138 (Figure 6.7e). Not having enough sera to include duplicates and repeat experiments made analysis difficult.



(c)



(d)



(e)

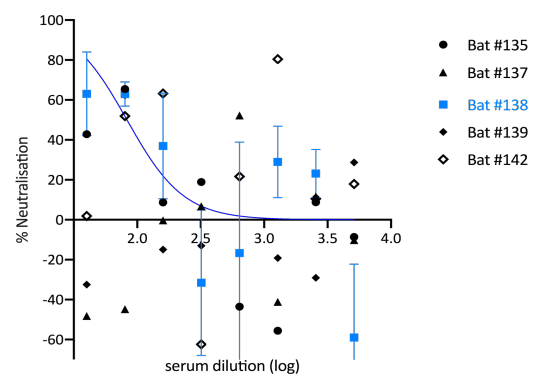


Figure 6.7. Antibody neutralising response of an additional 21 low-volume bat serum samples. IC₅₀ gradient was colour coded according to Figure 6.4. (a-c) transduction reduction and (d-e) neutralisation curves (bat #102 and bat #138 $r^2 = 0.3$). The error bars represent s.d (standard deviation of the mean) from a duplicate in one independent experiment. Except Bats #100, #134 and #139 where n=2. Graphs and non-linear regression curves (log [inhibitor] vs normalised response; constraint: hill slope <0) generated with Prism 8.

6.3.3.3 Regimen 3 (1:40 start serum dilution no duplicate, 1 experiment)

Next, a further 20 samples were tested once at a starting dilution of 1:40, no duplicates, except for bats #97, #106, #108, #112, #118, #163 where a duplicate was possible at a starting dilution of 1:100 and bats #120, #121, #122 at 1:200.

Bat #98 had a moderate titre of 211 (Table 6.2) and bat #110 a weak titre of 64 (Table 6.2), under the cut-off value for a positive sample, with a modest decrease in transduction and antibody concentration increases (Figure 6.8a). Bat # 118 had a weak titre of 155 (Table 6.2), and 84 in the replicate at 1:100 start dilution.

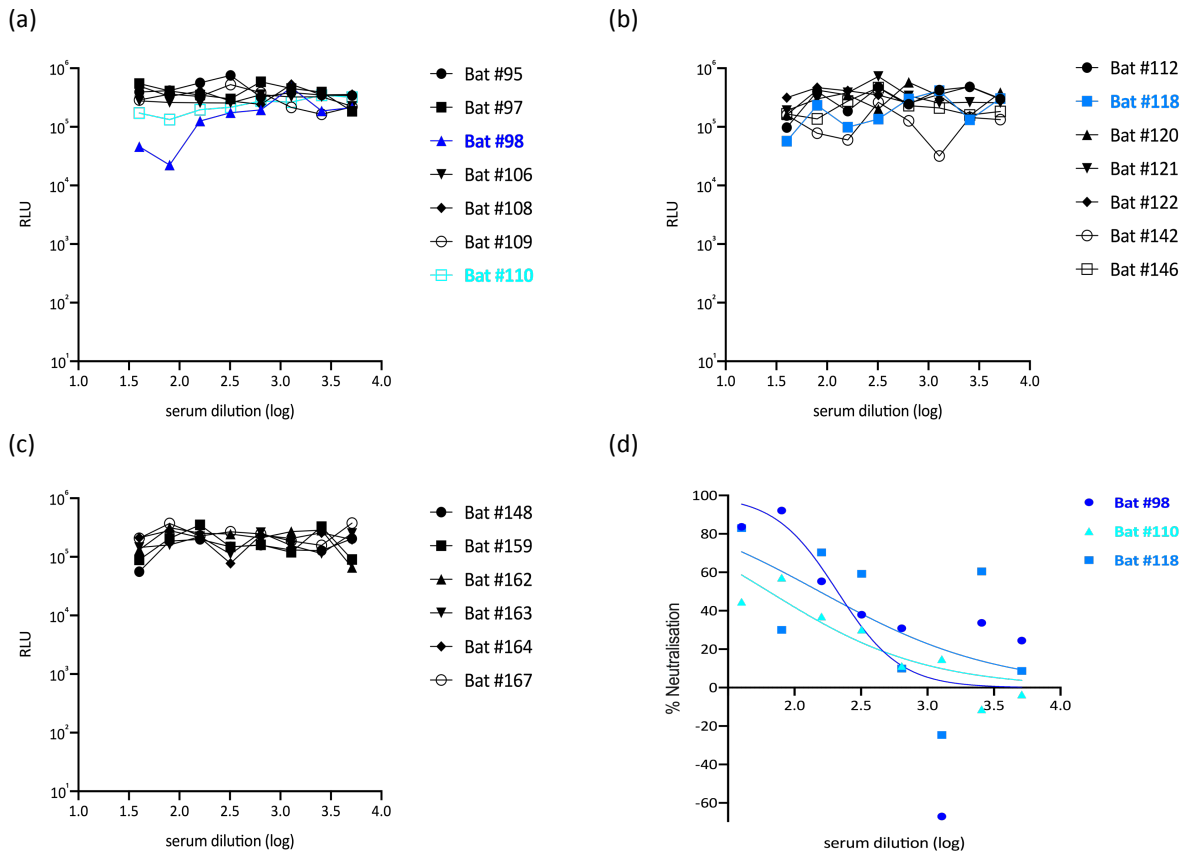


Figure 6.8. Antibody neutralising response of a further 20 bat serum samples. (a-c) transduction decrease and (d) neutralising curve of positive samples (bat #98 $r^2 = 0.6$, bat #110 $r^2 = 0.8$, bat #118 $r^2 = 0.3$). IC_{50} gradient was colour coded according to Figure 6.4. $n=1$. Graphs and non-linear regression curves (log [inhibitor] vs normalised response; constraint: hill slope <0) generated with Prism 8.

Neutralising curves were not clear, except for bat #98 (Figure 6.8d). All other bats were negative (Figure 6.8).

6.3.3.4 Regimen 4 (1:100 start serum dilution no duplicate, 1 experiment)

The final six samples were of such small volume that this enabled testing only once, with no duplicates, at a starting serum dilution of 1:100. Bat #143 had a weak response (Table 6.2) following non-linear regression analysis. The rest of the samples were negative (Figure 6.9).

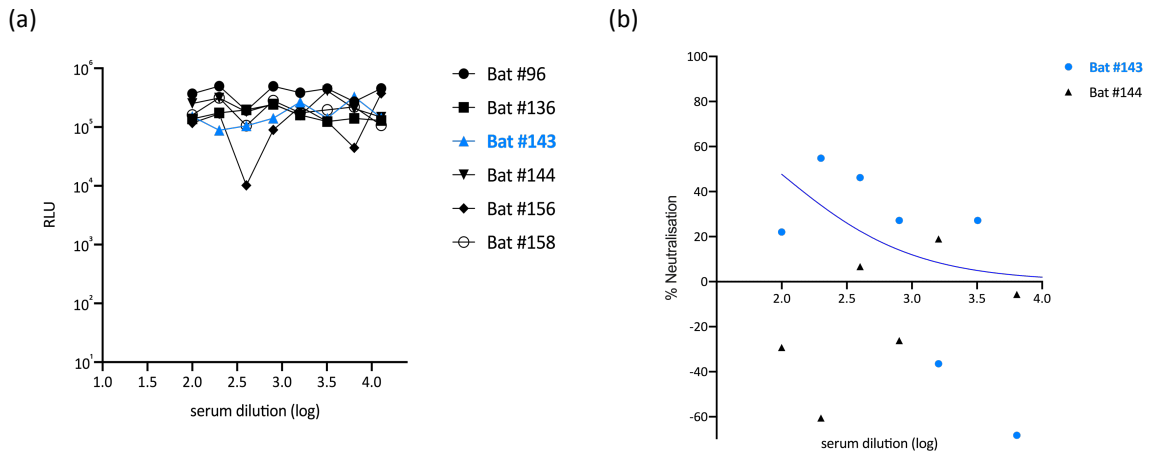


Figure 6.9. Antibody neutralising response of 6 bat serum samples. (a) transduction decrease and (b) neutralisation curve (bat #143 $r^2 = 0.2$). IC_{50} gradient was colour coded according to Figure 6.4. $n=1$. Graphs and non-linear regression curves (log [inhibitor] vs normalised response; constraint: hill slope <0) generated with Prism 8.

6.3.4 Determination of a positive cut-off point

To determine a cut-off point for positive samples, IC_{50} values from animals where the total reduction in RLU was less than 20% of the PV/no serum control (0% neutralisation value); or when neutralisation of less than 70% was achieved, were collected (Figure 6.10), its mean calculated and a cut-off point stipulated as any value higher than the mean + 3 standard deviations (Jacobson 1998; Lester *et al.* 2019; Nie *et al.* 2020).

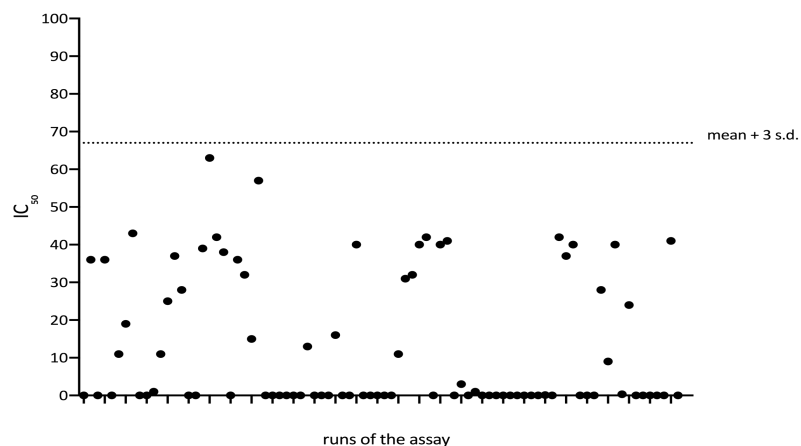


Figure 6.10. Cut-off determination for positive samples. Samples included had shown no significant reduction in transduction compared to PV only samples (no serum). 46 tests had an IC_{50} of zero. The remaining 40 tests were found to have a low range of IC_{50} titres, but showed no significant reduction in luminescence and therefore were included in the analysis. Mean, standard deviation (s.d.) and cut-off point calculated by Prism 8. $n=86$.

6.4. Discussion

Serosurveillance of bat populations will help us monitor viral prevalence and geographical distribution, identify putative reservoirs for zoonotic pathogens and facilitate the implementation of preventative measures to avoid spillover causing epidemics or pandemics (Swanepoel *et al.* 2007; Wright *et al.* 2009; Laing *et al.* 2018; Yang *et al.* 2017; Yang *et al.* 2019). The use of pseudotype viruses (PV) offers a safer, and thus more accessible, alternative to screen serum samples in low containment settings, which is highly desirable especially for filoviruses or any other BSL-4 pathogens.

Since being first described in 2011, the genus *cuevavirus* has so far not been responsible for any human infections, but it has since been detected in Hungary in 2016 (Kemenesi *et al.* 2018). In this instance, LLOV RNA was detected in bat populations roosting in caves at different mountain regions, reinforcing the idea that filoviruses are more diverse and widespread than previously thought. So far filoviruses had been found mainly in the African continent, except when people and monkeys had travelled back or were transported to other Continents, but filovirus RNA has also been detected in Europe and Asia in bats (Yang *et al.* 2017; Yang *et al.* 2019). Serological evidence has also emerged of RESTV infection humans working on a pig farm. In addition, virus has been isolated from pigs in the Philippines (Barrette *et al.* 2009).

The broad cell tropism seen in filoviruses (Takada 2012; Maruyama *et al.* 2014) could possibly increase the risk of transmission between different species, therefore better characterisation of interspecies transmission will be crucial in the future. Schreiber's bat cells have already been shown to be permissive to transduction by LLOV as well as EBOV, RESTV and MARV *in vitro* utilising a VSV core pseudotype system. Cells from the Indian flying fox (*Pteropus giganteus*) were also found to be permissive to infection by LLOV PVs (Maruyama *et al.* 2014), making it another suitable candidate for a reservoir, assuming the virus could be circulating in other bat species.

Transmission of filoviruses between bat populations is still poorly understood. Evidence from experimental infection of bats with authentic EBOV or MARV can be contradictory. In some studies, shedding of virus was not observed in infected animals (Paweska *et al.* 2016), whereas in other studies EBOV was successfully isolated from experimentally infected animals (Swanepoel *et al.* 1996). It is important to point out that no isolation of EBOV has been achieved from healthy bat populations yet (Leroy *et al.* 2005; Kock *et al.* 2019).

In this study we used LLOV PVs to screen Schreiber's bat and the Greater mouse-eared bat serum samples from Hungary in a collaborative work with the University of Pecs, following their recent findings where LLOV RNA was recovered from bat carcasses (Kemenesi *et al.* 2018).

An initial 7 serum samples were sent, which had been characterised by RT-PCR in Hungary, to ascertain whether PVNA results correlated. Bats samples #1 and #2 had a strong neutralising antibody titre and bat E showed a moderate response (Table 6.1), in accordance with RT-PCR results. However, bat H was negative on RT-PCR but had a strong antibody titre (mean $IC_{50} = 947$), possibly indicating the animal had a LLOV infection prior to being sampled for RT-PCR testing. PCR would only detect an acute infection, whereas specific antibodies would be present following recovery. If this animal has managed to clear a LLOV infection it could provide some evidence these bats act as a reservoir. Cross-reactivity with other filoviruses has not been tested for most samples due to the lack of sufficient sera available, nevertheless EBOV convalescent serum did not cross-react with LLOV PVs (Figure 6.1). However, there was serum left (1 μ L) from bats E and H that had been found to have neutralising antibodies against LLOV. These were tested against EBOV PVs at a starting dilution of 1:200, in one experiment with no duplicates. Bat H showed a slight decrease in luminescence but an IC_{50} could not be determined (Figure 6.4e), therefore any conclusions would have to be confirmed with additional tests. It is possible that bat H serum either cross-reacted mildly with EBOV PVs, as LLOV GP has 35% identity to EBOV GP at the amino acid level (Maruyama *et al.* 2014), and might share the same ancestors (Negredo *et al.* 2011); or it had been previously infected with EBOV. The latter might be less likely considering it was an animal found in Europe, and intercontinental bat migration is unlikely to happen (Fleming 2019). However, it cannot be completely dismissed without further investigation because co-infection is plausible. Yang *et al.* found sequences of yet unidentified bat filoviruses in China in apparently healthy bats. One animal was found to contain RNA from four distinct strains of filoviruses with high divergence from other known filoviruses, possibly belonging to a new species or genus (Yang *et al.* 2017). Therefore, one must be cautious about making assumptions based on geographical distribution. It is worth noting that none of the EBOV convalescent sera available to us (NIBSC 15.220, 15.262 and 16.344) cross-reacted with LLOV PVs (Chapter 4).

Following the pilot study, further samples were obtained from 71 live bats in the same site in Hungary (Kemenesi *et al.* 2018). A total of eight samples (plus an inconclusive one) had detectable LLOV GP-specific neutralising antibodies (Table 6.2).

Ideally these tests would be carried out at least twice with duplicates within each test. This was only possible with 24 out of 71 samples sent to us (Regimen 1). From this experimental regimen, three animals had neutralising antibodies detected: bat #99 (mean IC_{50} =165), bat #115 (mean IC_{50} =170) and bat #130 (mean IC_{50} =118). This was the most robust regimen considering samples were tested in duplicates in two independent experiments. Other animals from this group had no neutralising antibodies detected (Figure 6.5). Neutralisation curves from the positive serum sample showed neutralisation of 70% and above (Figure 6.6).

Due to the amount of serum available, different experimental regimens had to be applied. Samples in Regimen 2 (n=21) were only tested once, in duplicates and with a starting serum dilution of 1:40. Two samples had neutralising antibodies detected: bat #102 (IC_{50} =132) and bat #138 (IC_{50} =83). Neutralisation curves showed neutralisation of 60% of LLOV PVs and above for bat #102 (Figure 6.7d) and bat #138 (Figure 6.7e). Samples in Regimen 3 (n=20), which were also only tested once at starting dilution of 1:40 but without duplicates, had neutralising antibodies detected in two bats: #98 (IC_{50} =211) and #118 (IC_{50} =155). Bat #110 had an antibody titre very close to the positive cut-off point (Table 6.2) and the result was inconclusive.

Finally, samples in Regimen 4 (n=6) were tested once at a starting serum dilution of 1:100 without duplicates. Bat #143 had neutralising antibodies detected (IC_{50} =90). Neutralising antibody curves from Regimen 3 (Figure 6.8d) and Regimen 4 (Figure 6.9b) were not clear, most likely due to the fact no duplicates or repeat experiments could be performed (Ferrara and Temperton 2018).

Determining a cut-off for positive values was challenging. Based on previous studies, bat serum samples that resulted in less than 20% reduction in RLU of the PV input, or resulting in low level neutralisation (<70% of PVs) were included in the analysis (Jacobson 1998; Lester *et al.* 2019; Nie *et al.* 2020). A stringent mean +/- 3 standard deviation was chosen resulting in a cut-off of 67 (Figure 6.10). As discussed above, one animal (bat #110) had an end-point antibody titre of 64 (Table 6.2), making it inconclusive without repeating the PVNA. In addition, results from experimental regimes other than Regimen 1 need to be interpreted with caution, especially Regimens 3 and 4, which includes bat #110.

We will have a clearer picture regarding active or previous infection once PCR and sequencing data is available. Our collaborators at the University of Pecs are conducting this work. However, it seems likely these animals have previously been infected with LLOV if the virus circulates in bat populations (Kemenesi *et al.* 2018). Longitudinal studies showing how long antibody titres last after infection and recovery would also be useful to elucidate the humoral response against LLOV.

In humans, survivors of EBOV infection appear to have a long-lasting antibody response in some cases (Fuentes *et al.* 2020). In bats however, different species of bats seem to have different levels of antibodies against EBOV for instance (Nys *et al.* 2018). In addition, the neutralising response is often weak but highly specific, thought to be because of their evolutionary adaptations to support infection of otherwise highly pathogenic viruses (Baker, Tachedjian and Wang 2010). Here, antibody neutralising response in bats sampled was varied, from weak (Table 6.2) to strong neutralising responses, particularly bat #1 in the pilot study (Table 6.1).

It should be noted the LLOV GP sequence of PVs used in this study was from the Spanish strain. At the moment, the Hungarian GP sequence has not been determined. It will be interesting to compare sequence data between these European isolates, however considering the high homology at the nucleotide level between the L (98%) and NP genes (99%) between the Hungarian and Spanish strains of LLOV (Kemenesi *et al.* 2018), it is likely the GP gene would follow the same trend. Our neutralisation data matched the RT-PCR data from the pilot study, apart from bat H (Table 6.1).

Initially LLOV was thought to be pathogenic in bats (Negredo *et al.* 2011), which would make them unlikely as a putative reservoir for LLOV, being able to harbour the virus without disease so the virus can be maintained and transmitted (Haydon *et al.* 2002). However, a recent study of Schreiber's bats caught alive from the same caves as the 2002 mortality events in Spain where LLOV was first described, found ~36.5% of bats to be previously exposed to LLOV (De Arellano *et al.* 2019). They used an immunoblot assay with the C-terminal domain of LLOV GP₂ as the antigen surveying 60 Schreiber's bats, plus 10 common serotine bats and 22 humans as controls, assuming they were negative for LLOV infection. The animals were also tested for LLOV RNA in faecal samples which were all negative (De Arellano *et al.* 2019). This adds to the evidence of circulating pre-exposed bats without mortality events or chronic shedding of the virus, although more tissue

samples would have to be tested to have a clearer picture, in case viral shedding can be detected in tissue but not faecal samples for instance.

Our study found 11.3% of captured live bats to contain neutralising antibodies against LLOV, indicating that bats have been infected with LLOV then recovered. Monitoring animals for signs of infection in capture-release experiments and increasing the sample size would be useful. If LLOV isolation were achieved from these animals it would add strong evidence that Schreibers's bats are one of the reservoirs for LLOV.

Even though LLOV has not yet been found to infect humans, there is always a possibility that a spillover could happen in the future, considering it is able to infect human cell lines such as kidney HEK293T (Figure 6.1), liver Huh-7 (Chapter 3) and the leukemia cell line K562 (Maruyama *et al.* 2014). However, there would be less chance of spillover through bushmeat consumption in Europe for instance, but it could arise in cave exploration endeavors or tourism, if anyone comes in close contact with those bats or its droppings. Transmission to humans seems to occur by direct contact with bats through consumption, bites or contact with droppings directly or indirectly in foodstuffs such as fruit or other contaminated objects (Swanepoel *et al.* 1996; Leroy *et al.* 2005; Amman *et al.* 2015; Markotter *et al.* 2020).

There could still be other filoviruses circulating to be discovered, as some individuals are asymptomatic (Glynn *et al.* 2017; Mulangu *et al.* 2018). Antibodies against different species of filoviruses have been detected in bats and bat hunters in India (Dovih *et al.* 2019), as well as RESTV in humans in South East Asia (Barrette *et al.* 2009), raising the possibility of antigenically similar viruses in asymptomatic humans.

Further serosurveillance studies of LLOV and other filoviruses are warranted, not only to increase our knowledge of transmission of those pathogens between reservoir and hosts but also to help monitor possible spillover events.

CHAPTER 7: Lyophilisation and Storage Stability of Filovirus Pseudotypes

7.1 Introduction

Emerging viruses routinely affect resource-limited countries with high population densities, usually imposing challenges for implementing healthcare measures as well as appropriate diagnostics. Filoviruses have been implicated in outbreaks affecting a large number of people in Africa, including the recent EBOV outbreak in the Democratic Republic of Congo and the 2013-16 outbreak in West Africa; in contrast with previous, smaller outbreaks (Languon and Quaye 2019), which highlights the need for improved containment measures as well as diagnostics, treatment and vaccines.

Screening tests that are affordable would be highly advantageous. One of the major costs associated with reagents and certain vaccines, including the rVSVΔG-ZEBOV vaccine for instance, is the requirement of cold-chain transportation. Therefore, vaccines or reagents that can be transported at room temperature are very desirable (Broadhurst, Brooks and Pollock 2016; Murphy 2019).

The gold standard in diagnostics for filoviruses is viral RNA detection using RT-PCR based platforms. Several approaches for their use in point-of-care situations are being evaluated (Weidmann, Mühlberger and Hufert 2004; Cherpillod *et al.* 2016; Semper *et al.* 2016; Magro *et al.* 2017; Raftery *et al.* 2018; Clark *et al.* 2018). RT-PCR has high sensitivity and specificity (Weidmann, Mühlberger and Hufert 2004; Cherpillod *et al.* 2016; Broadhurst, Brooks and Pollock 2016), however it requires expertise and expensive equipment. Some of these point-of-care platforms such as RT-PCR based GeneXpert (Cepheid, Sunnyvale, CA, USA) require minimal training and no sample pre-treatment (Semper *et al.* 2016; Vuren *et al.* 2016; Raftery *et al.* 2018). However, the equipment itself costs ~\$17,000 plus running costs of ~\$50 per sample, on top of maintenance expenses.

Portable lateral flow devices for antigen detection are also being evaluated as a more affordable option. They present varying degrees of sensitivity, which would have to be addressed before being rolled out for point-of-care diagnostics (Phan *et al.* 2016; Wonderly *et al.* 2019; Makiala *et al.* 2019).

More recently, genomic approaches including next-generation sequencing platforms have been employed for diagnostics, as well as monitoring geographical spread and adaptations as an epidemic progresses (Gire *et al.* 2014; Gardy and Loman 2018; Deng *et al.*

al. 2020). They have the advantages of detecting as yet unidentified pathogens; and avoiding “signature-erosion”, where mutations occur in primer targets resulting in false negative or positive results (Sozhamannan *et al.* 2015; Deng *et al.* 2020).

Serological evaluation complements diagnostic efforts by identifying genera and species responsible for specific outbreaks to help implement appropriate healthcare measures, such as identifying workers who have been exposed or are immune as the current COVID-19 outbreak highlighted. ELISA and PVNAs are often used in conjunction to map geographical distributions and spread. Recently, individuals with antibodies against Marburg virus have been found in locations in West and Central Africa with no previous history of Marburg virus outbreaks (Steffen *et al.* 2020).

Ebola virus serological surveys have been conducted more frequently due to the fact most of the human outbreaks are caused by EBOV rather than other filoviruses (Mulangu *et al.* 2018; Brook *et al.* 2019). Sero-surveillance of bats is equally important considering they are potential reservoirs for EBOV, raising the possibility of zoonotic spillover events (Nys *et al.* 2018; Laing *et al.* 2018). More recently, antibodies against filoviruses have been detected in bats in Europe. These were classified as a new genus, *cuevavirus*, and monitoring those viruses is crucial as they also pose the potential for a future human spillover, having re-emerged recently in bats in Hungary and shown to be able to infect human cells *in vitro* (Negredo *et al.* 2011; Maruyama *et al.* 2014; Kemenesi *et al.* 2018; Ram *et al.* 2019). A serological study utilising LLOV PVs to screen bats from Hungary was described in Chapter 6.

Pseudotypes have several advantages when researching highly pathogenic viruses as they can be handled in low-containment facilities, often yield high titres permitting upscaled use, can be multiplexed for assaying different viruses and can be adapted for high-throughput screening. In addition, there are a range of reporter genes that can be incorporated, and they are highly sensitive in PVNAs (Wright *et al.* 2008; Mather *et al.* 2013; Temperton, Wright and Scott 2015; Long *et al.* 2015; Ferrara and Temperton 2018). Most of the assays and methods described so far require high-power (-70/80°C) freezers and expensive transportation requirements to maintain a cold chain. Therefore vaccines or reagents that can be transported at room temperature would be very desirable, as previously mentioned. One possible solution to reduce those costs would be to lyophilise reagents whenever possible, especially if these are to be used or sent to resource-limited countries, often in tropical regions with high temperature and humidity.

Lyophilisation or freeze-drying has been used in production of pharmaceutical products and vaccines to avoid cold-chain transportation and increase shelf life of reagents (Kraan *et al.* 2014). It usually consists of two steps: freezing of the sample followed by drying in a low-pressure environment, whereby the frozen water in the sample sublimates (Figure 7.1). However, some residual moisture will still be present. In industrial freeze-drying facilities, a secondary drying step is performed at a higher temperature (~25.5°C) to eliminate residual moisture (Wang 2000; Nireesha *et al.* 2013; Kraan *et al.* 2014). For most of the current proof-of-concept study described here, only the primary step was performed, as our freeze-drier was not equipped to perform a secondary drying step. Therefore, we conducted a small study utilising industrial facilities to account for residual moisture.

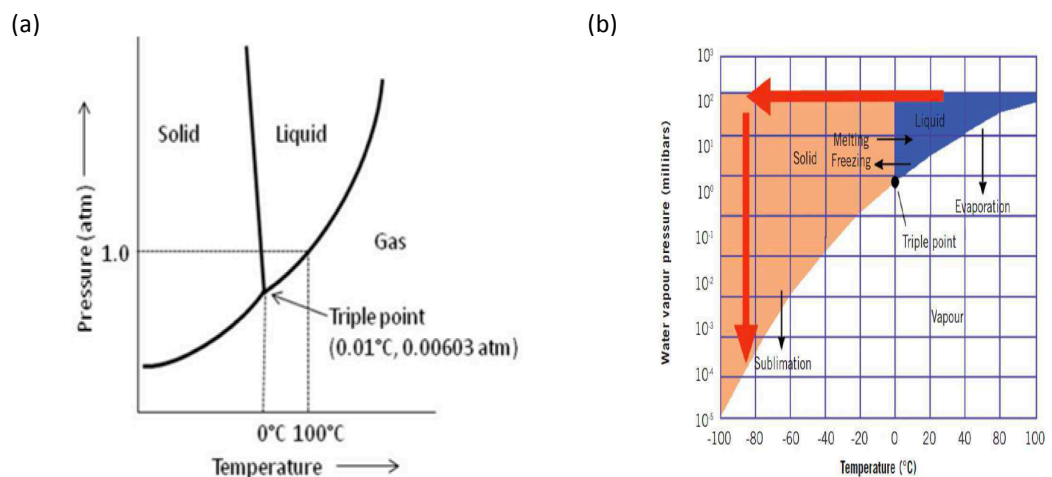


Figure 7.1. Lyophilisation principles. Diagrams: (a) showing the different physical properties of water. Lyophilisation exploits those properties by going from the solid to the gas phase, bypassing the liquid phase (sublimation); and (b) showing the steps of Lyophilisation. The sample is frozen (top red arrow), then put in a vacuum chamber where the pressure is lowered (down red arrow) resulting in sublimation of the water content. Source: Nireesha *et al.*, 2013.

Cryoprotectants are added in order to protect the structure of the substance being lyophilised. Excipients are often prepared with sugars such as sucrose, trehalose and sorbitol to prevent damage. They are commonly used as cryoprotectants in solution with a choice of buffer (Wang 2000) for lyophilisation of viruses, including recombinant adenovirus and lentiviral PVs (Shin, Salvay and Shea 2010). Sucrose has also been previously assessed as a cryoprotectant in lyophilised PVs stored for up to one month at different temperatures and humidity conditions.

Influenza, rabies and Marburg virus pseudotypes have been lyophilised and tested after short-term storage in different temperatures and conditions. PV titres were maintained in

infectivity assays after resuspension. Marburg virus PV titre recovery was near 100% in temperatures up to +20°C after one-month storage. In addition, reconstituting the dry pellets with DMEM or ddH₂O made no difference in infectivity assays. Influenza and rabies PVs also performed well in neutralisation assays. Marburg PVs were not tested due to lack of convalescent serum (Mather *et al.* 2014).

The current study aimed to assess long-term storage and stability of lyophilised filovirus PVs, as well as performance in neutralisation assays for future use in an antibody detection kit. We also assessed performance of PVs lyophilised via industrial equipment in collaboration with Intravacc (Bilthoven, The Netherlands), where a full lyophilisation protocol (including a secondary drying step) was performed. This was done to assess whether eliminating residual moisture would have a positive impact in titre retention at higher storage temperatures, as well as impact of air transport of samples.

7.2 Materials and Methods

7.2.1 Viruses and cells

EBOV, SUDV, BDBV, LLOV, RAVV, MARV (Angola), MARV (DRC) PVs and target cells used for titration (HEK293T) and neutralisation assays (HEK293T and CHO-K1) were described in detail in Chapter 2 (Materials and Methods).

7.2.2 Reagents and equipment

Sucrose (Sigma Aldrich S0389-500G) and Sorbitol (D-Sorbitol – Sigma Aldrich S1876-500G) were used as cryoprotectants during lyophilisation. They were prepared as stock solutions to the desired final concentration in Dulbecco's Phosphate-Buffered Saline (Pan Biotech) or Tris buffer (pH 7.4).

Low surface-tension polypropylene 1.5 mL tubes (Simport, Canada T330-7LST) were used to prepare and lyophilise PV samples.

All lyophilisation was carried out in a FreeZone 2.5 L (Figure 7.2) freeze-dryer (Labconco – USA), connected to a vacuum pump (Rotary Vane 7739402), except the additional EBOV

samples, which were prepared in Sucrose-DPBS cryoprotectant in Kent, frozen and shipped on dry ice to Intravacc (Bilthoven, The Netherlands) for lyophilisation in their industrial facility. This was used as a comparison to our simpler lyophilisation process.



Figure 7.2. Labconco™ FreeZone™ 2.5L freeze drier. The machine is comprised of a freezer lowering the temperature in the top chamber, and an attached pump (left) that creates a vacuum in the top chamber lowering the pressure. Inside the chamber there is a stack of 88 PV samples being freeze dried.

7.2.3 Preparation of PV samples, lyophilisation and sample storage

Previously titrated PV supernatant (Chapter 3) was mixed with cryoprotectant and buffer solution (Table 7.1) in a total of 200 μL at a 1:1 (v/v) ratio in a low-surface tension tube, vortexed to mix contents, centrifuged briefly and placed in -80°C overnight. A pierced lid was placed on top of each tube before freeze-drying to let air escape when pressure changed during the lyophilisation process. The lyophilisation cycle was run overnight at -40°C to -50°C with pressure dropping to < 0.033 mBar (3.3 Pa).

After lyophilisation the pierced lid was discarded and the low-surface tension tube's own lid was closed before the freeze-dried samples were placed in storage.

Experimental storage conditions were: -20°C , $+4^{\circ}\text{C}$, ambient temperature $\sim +22.5^{\circ}\text{C}$, $+37^{\circ}\text{C}$ (20% humidity) and $+37^{\circ}\text{C}$ (90% humidity). Temperature and humidity were monitored regularly in the different storage containers with a Fisherbrand™ Traceable™ Jumbo Thermo-Humidity Meter (Fisher Scientific 11536973).

Reconstitution of lyophilised pellets was done in 100 μL of complete medium before titration or neutralisation assays.

For the lyophilisation performed at Intravacc, EBOV PV supernatant was mixed with 1M Sucrose – DPBS solution 1:1 (v/v) for a final concentration of 0.5M Sucrose in a total of 8

mL, frozen overnight and shipped on dry ice via courier. The samples were reported to have arrived the following day still frozen. Lyophilised EBOV samples at the Viral Pseudotype Unit were also sent in the same shipment box, kept in -80°C at Intravacc, then sent back with the newly lyophilised samples to assess whether the journey would have an impact on titre retention.

Excipient	Final concentration (per sample)
1M Sucrose - DPBS	0.5M
1M Sucrose - Tris	0.5M
1M Sorbitol - DPBS	0.5M (10%)
1M Sorbitol - Tris	0.5M (10%)
0.5M Sorbitol - DPBS	0.25M (5%)
0.5M Sorbitol - Tris	0.25M (5%)

Table 7.1. Excipient components and concentration.

The materials used by Intravacc were as follows: Glass vials (APG Packaging 1003201), autoclaved in-house before use; Rubber stoppers (APG Packaging 1008739), in-house dried overnight at 105°C. Intravacc description of the initial procedure was: “The sample was thawed at RT. Forty glass vials were filled with 200 µl of sample and half stoppered before loading the freeze dryer. The sample vials were surrounded with empty vials in a metal fork.”

Lyophilisation protocol:

Freezing		Primary drying			Secondary drying		
Temperature (°C)	Time (hours)	Temperature (°C)	Time (hours)	Pressure (µbar)	Temperature (°C)	Time (hours)	Pressure (µbar)
-50	- *	-45	0.5	20	25.5	24	20
-50	2	-45**	96	20	25.5	24	20
		-45**	2	20	4	0.5	20
					4	99 ***	20

Table 7.2. Lyophilisation protocol performed at Intravacc.

* Shelf preparation, prior to loading of the vials

** Pressure rise test (PIM):

Max loops: 10

Extra drying time: 2 hours

Allowed pressure rise: 5 µbar

Test time: 60 seconds

*** Storage of the vials at 4°C until the freeze dryer was stopped manually

Freeze drying was done in a Telstar Lyobeta freeze dryer.

Temperature sensors were placed on the following vials and locations in the freeze dryer:

Sensor	Vial	Location
1	Shelf	NA
2	Sample vial	left
3	Sample vial	right
4	NA	NA

Table 7.3. Lyophilisation protocol – temperature monitoring.

End time of primary drying, second step: 96 hour

End time of primary drying, third step: 2 hours

PIM second primary drying step: 20.492 μ bar

PIM third primary drying step: 20.2832 μ bar

“After freeze drying, the vials were fully stoppered in the freeze dryer, still under a pressure of 20 μ bar. Subsequently, the vials were capped with an aluminium cap”.

A summary of the lyophilisation cycle was provided (Table 7.2) including the monitoring of temperatures during the cycle (Table 7.3).

Samples were transported back by air at ambient temperature to the UK along with the lyophilised EBOV samples that undertook the return journey. Intravacc EBOV samples were then stored at -20°C, +4°C, +22.5°C, +37°C (20%) and +37°C (90%) for an initial 1 month period, and some for 6 months, at +22.5°C and +37°C (20%) to assess if there was an improvement in titre retention when lyophilisation was performed with industrial equipment used for commercial purposes such as vaccine manufacturing.

7.2.4 Infectivity and neutralisation assays

Infectivity and neutralisation assays were performed as described (Chapter 2). Analysis of infectivity assays has to take into account that cryoprotectants such as sucrose or sorbitol are cytotoxic at higher concentrations, therefore the corresponding lower dilution results (neat to 1:8) are removed from titration analysis. In PVNAs, the reconstituted pellets containing cryoprotectant are diluted before being pipetted uniformly down the plate, therefore cytotoxicity was not an issue.

Titre recovery of lyophilised PVs was calculated in comparison to their unlyophilised counterparts. Generally, titres of $> 1 \times 10^7$ RLU/mL are sufficient for PVNAs to achieve 100 TCID₅₀ per well. Serum samples were described previously (Chapter 4).

7.3 Results

7.3.1 Generation of lentiviral PVs

The generation and optimisation of lentiviral PVs has been previously described (Chapter 3). PVs were produced in T75 flasks and their infectivity measured (Figure 7.3).

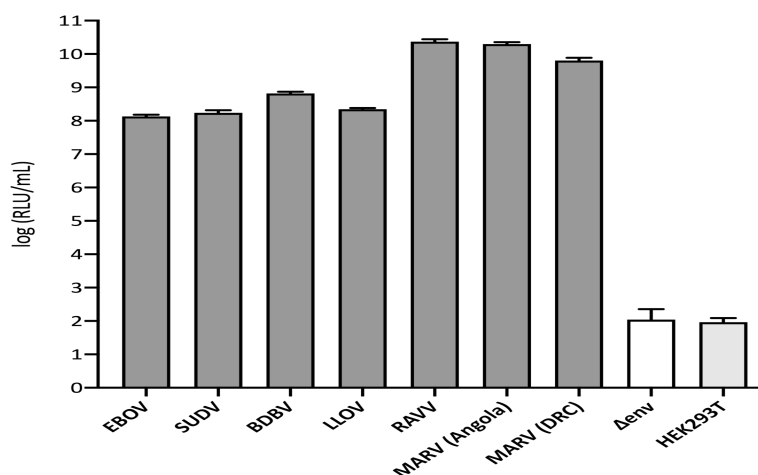


Figure 7.3. Generation of Filovirus PVs displaying GPs of the three major genera: *ebolavirus* (EBOV, SUDV and BDBV); *cuevavirus* (LLOV); *marburgvirus* (RAVV, MARV-Angola and MARV-DRC). Transduction titres are expressed as the mean \pm s.d log (RLU/mL) values of at least three independent experiments. The titre of lentiviral particles bearing no GP (Δ env) and background luminescence from uninfected cells (HEK293T) are also shown. Graph generated with Prism 8.

Typical titres of $\sim 1 \times 10^8$ RLU/mL were observed for *ebolavirus* and *cuevavirus* PVs, and $\sim 1 \times 10^{10}$ RLU/mL for *marburgvirus* PVs (Figure 7.3). These PVs were lyophilised and the remainder PV stock used as positive controls, as well as a comparison to calculate titre retention in further experiments.

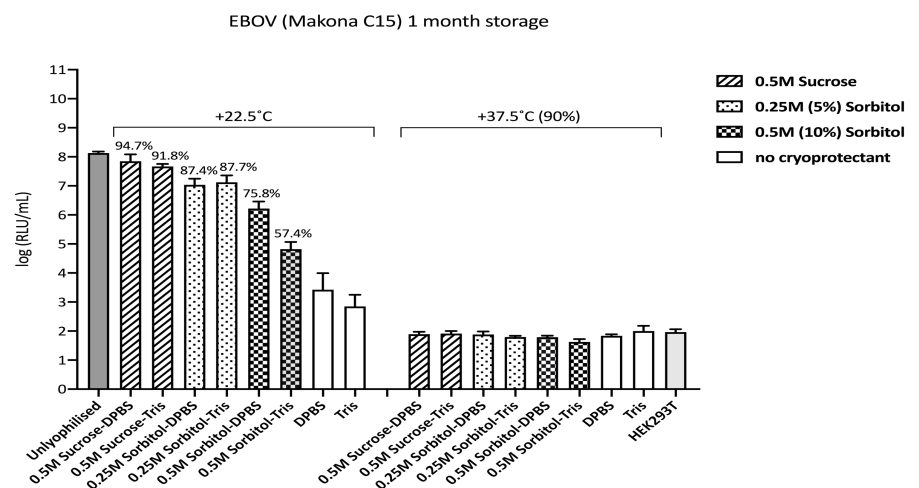
7.3.2 Lyophilisation of filovirus PVs, evaluation of cryoprotection and choice of excipient

Two representatives of *ebolavirus* (EBOV and SUDV) and two representatives of *marburgvirus* (RAVV and MARV) genera were lyophilised with different excipients containing a cryoprotectant (Table 7.1) to assess optimal conditions for long-term storage studies. They were stored for one month at $+22.5^\circ\text{C}$ and $+37^\circ\text{C}$ (90% humidity) before being reconstituted in 100 μL complete medium to assess infectivity. These higher temperatures were chosen to better assess any titre decrease.

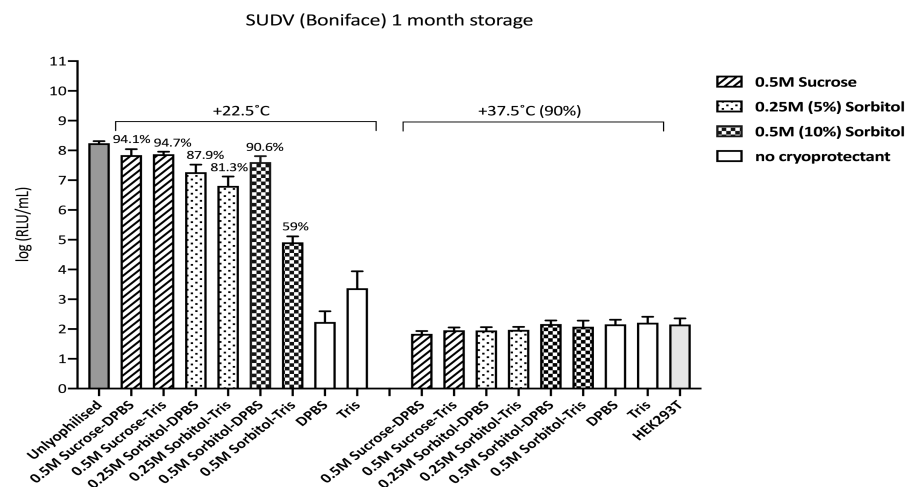
Samples stored at +22.5°C retained a functional titre after one month (Figure 7.4). All lyophilised PVs retained a higher titre when using sucrose as a cryoprotectant. No significant difference was observed between DPBS and Tris buffer containing excipients, except for EBOV lyophilised in 0.5M Sorbitol-DPBS, which retained 75.8% and 0.5M Sorbitol-Tris retaining 57.4% ($p=0.002$) of their initial titres respectively (Figure 7.4a, Table 7.4); and SUDV lyophilised in 0.5M Sorbitol-DPBS retaining 90.6% and 0.5M Sorbitol-Tris retaining 59% ($p=0.002$) of their titres (Figure 7.4b, Table 7.4). RAVV (Figure 7.4c) and MARV (Figure 7.4d) had statistically significant higher titres ($p\leq 0.005$) in 0.5M Sorbitol-DPBS than in 0.5M Sorbitol-Tris (Table 7.4).

A lower concentration of Sorbitol (0.25M) retained slightly higher percentage titres overall at ambient temperature (Table 7.4), and at +37°C (90% humidity) none of the samples produced a functional titre (Figure 7.4).

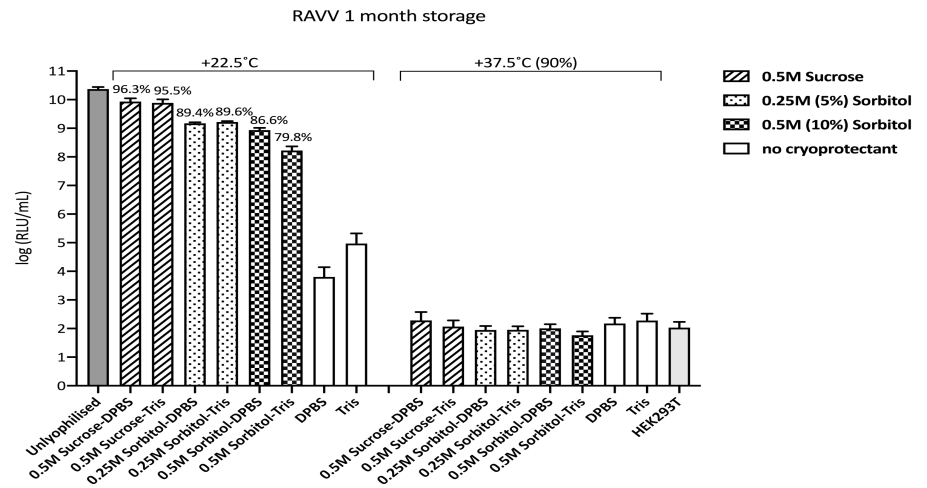
(a)



(b)



(c)



(d)

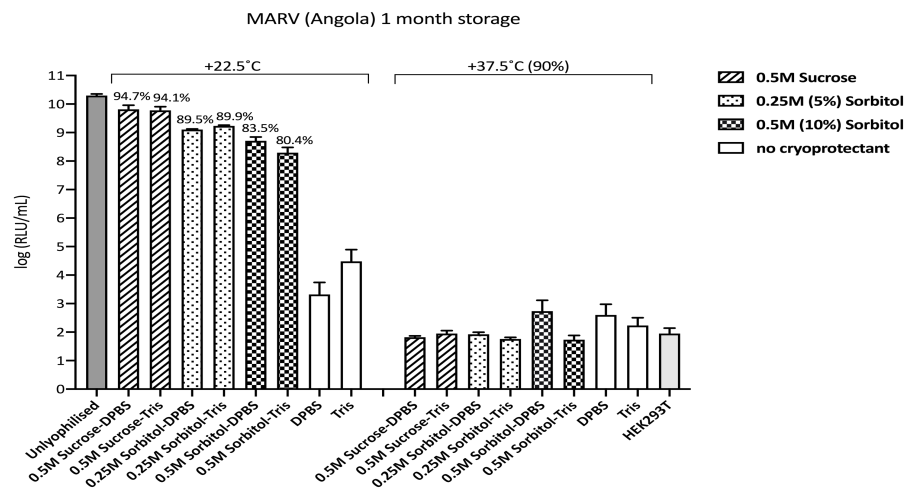


Figure 7.4. Infectivity assay following a one-month storage of lyophilised Filovirus PVs. (a) EBOV, (b) SUDV, (c) RAVV and (d) MARV (Angola). PVs were lyophilised at 0.5M Sucrose and 0.25M or 0.5M Sorbitol and kept at +22.5°C and +37°C (90% humidity). Dulbecco's Phosphate-Buffered Saline and Tris buffer (pH 7.4) were used to prepare the cryoprotectant solutions. Unlyophilised PVs were positive controls for the assay, as well as a parameter for comparison to calculate titre retention after lyophilisation, storage and reconstitution. Transduction titres are expressed as the mean (log) RLU/mL \pm s.d from at least two independent experiments. Storage temperature [and (humidity)] is shown on top of each graphs and % titre retention is displayed on top of each bar. Background luminescence in uninfected cells (HEK293T) is also shown. Graphs generated with Prism 8.

As reconstituted PVs retained the highest titre percentage when lyophilised in 0.5M Sucrose-DPBS, reproducing results from Mather *et al*, 2014, long-term studies were conducted with this excipient.

Excipient	EBOV	SUDV	RAVV	MARV
0.5M Sucrose-DPBS	94.7%	94.1%	96.3%	94.7%
0.5M Sucrose-Tris	91.8%	94.7%	95.5%	94.1%
0.25M Sorbitol-DPBS	87.4%	87.9%	89.4%	89.5%
0.25M Sorbitol-Tris	87.7%	81.3%	89.6%	89.9%
0.5M Sorbitol-DPBS	75.8%	90.6%	86.6%	83.5%
0.5M Sorbitol-Tris	57.4%	59%	79.8%	80.4%

Table 7.4 Percentage titre recovery of PV stored at ambient temperature for one month.

After 6 months, *ebolavirus* representatives EBOV (Figure 7.5a) and SUDV (Figure 7.5b) both had significant titre decreases to background levels of luminescence seen in cell only controls (HEK293T).

Marburgvirus representatives RAVV (Figure 7.5c) and MARV – Angola (Figure 7.5d) retained 69.5% and 55.8% of titre respectively when lyophilised with 0.5M Sucrose – DPBS and stored at ambient temperature (+22.5°C) for six months. All other samples had titre decreases to background level as described above (Figure 7.5).

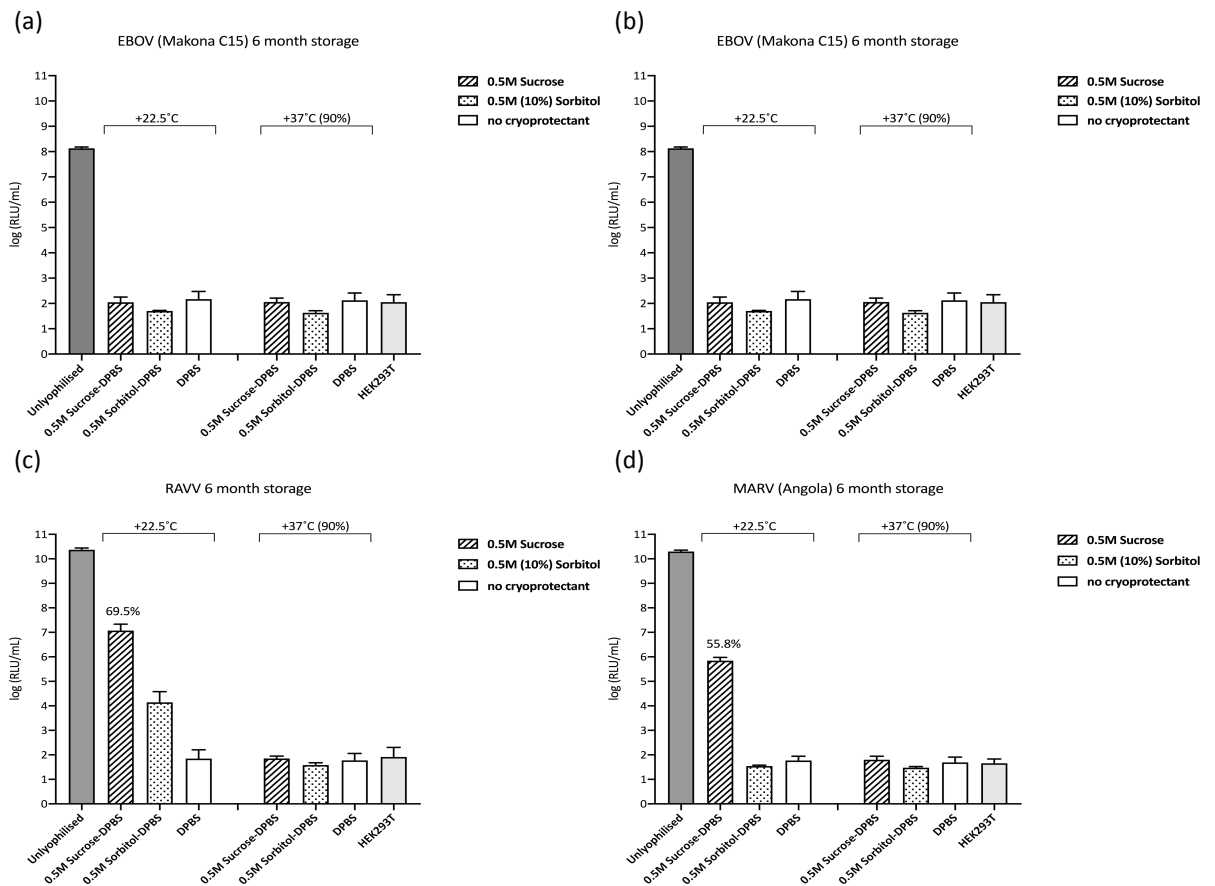


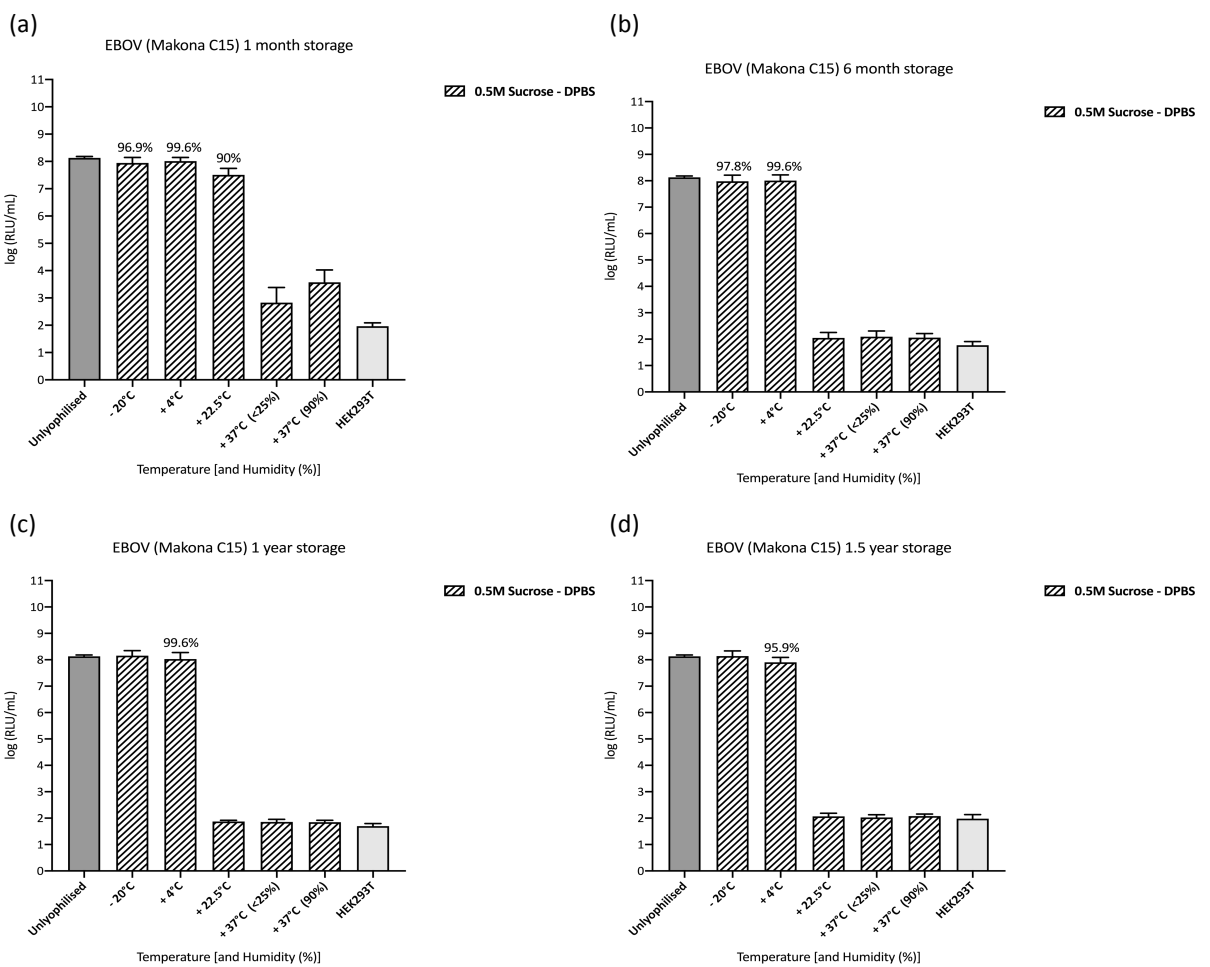
Figure 7.5. Infectivity assay following a six-month storage of lyophilised Filovirus PVs. (a) EBOV, (b) SUDV, (c) RAVV and (d) MARV (Angola). PVs were lyophilised at 0.5M Sucrose and 0.5M Sorbitol and kept at +22.5°C and +37°C (90% humidity). DPBS was used to prepare the cryoprotectant solutions. Unlyophilised PVs were positive controls for the assay, as well as a parameter for comparison to calculate titre retention after lyophilisation, storage and reconstitution. Transduction titres are expressed as the (log) mean RLU/mL \pm s.d from at least two independent experiments. Storage temperature [and (humidity)] is shown on top of each graph and % titre retention is displayed on top of each bar. Background luminescence in uninfected cells (HEK293T) is also shown. Graphs generated with Prism 8.

7.3.3 Long-term storage and stability of lyophilised *ebolavirus* PVs

EBOV PVs were lyophilised and stored for up to 2 years under various conditions.

EBOV PVs retained ~100% of their titre when reconstituted after being stored at -20°C and +4°C for 2 years (Figure 7.6e). At higher temperatures, titres decreased to cell only levels within 6 months (Figure 7.6b). As previously assessed (Figure 7.4), EBOV PVs retained 90% of their titre when reconstituted after being stored at +22.5°C for one month (Figure 7.6a), then titres decreased to cell only levels between one month and six months (Figure 7.6b).

EBOV PVs stored at +37°C in dry (<25% humidity) and humid (90% humidity) conditions for one month did not generate any functional titres (Figure 7.6).



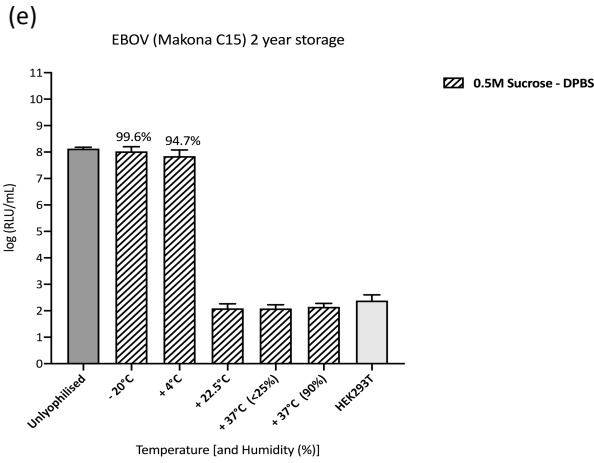
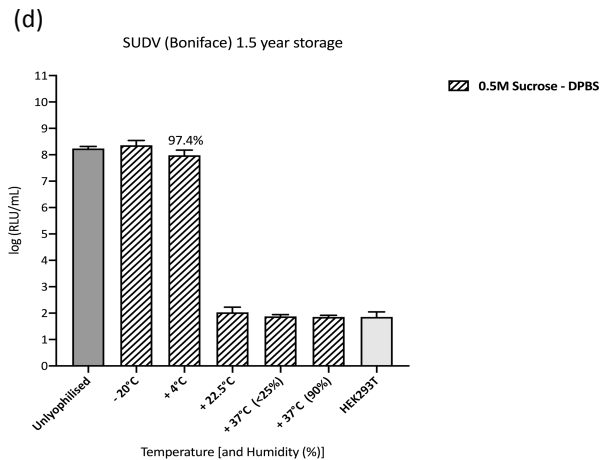
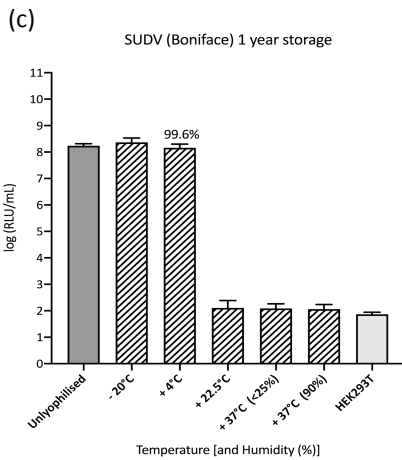
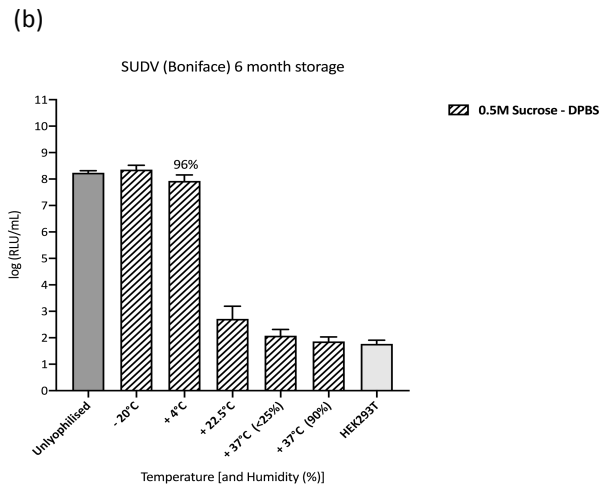
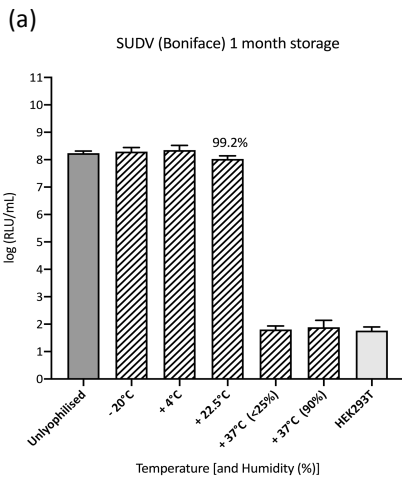


Figure 7.6. Infectivity assay following long-term storage of lyophilised EBOV PVs. PVs were lyophilised using 1M Sucrose in DPBS (final concentration 0.5M) and stored at different temperatures and humidity conditions (<25% or 90%) for (a) 1 month, (b) 6 months, (c) 1 year, (d) 1.5 years and (e) 2 years. Unlyophilised EBOV PVs were positive controls for the assay, as well as a parameter for comparison to calculate titre retention after lyophilisation, storage and reconstitution. Transduction titres are expressed as the (log) mean RLU/mL \pm s.d from at least two independent experiments and % titre retention for functional titres are displayed on top of each bar if less than 100%. Background luminescence in uninfected cells (HEK293T) is also shown. Graphs generated with Prism 8.



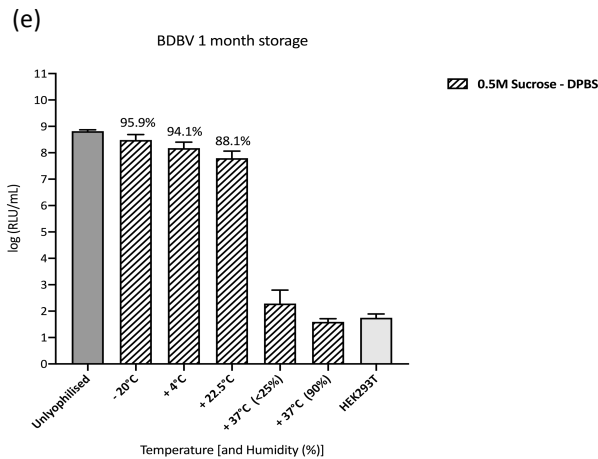


Figure 7.7. Infectivity assay following short and long-term storage of lyophilised BDBV and SUDV PVs. PVs were lyophilised 1M Sucrose in DPBS (final concentration 0.5M) and stored at different temperatures and humidity conditions (<25% or 90%). SUDV PVs were stored for (a) 1 month, (b) 6 months, (c) 1 year, (d) 1.5 years and BDBV PVs were stored for (e) 1 month. Unlyophilised PVs were a positive control for the assay as well as a parameter for comparison to calculate titre retention after lyophilisation, storage and reconstitution. Transduction titres are expressed as the (log) mean RLU/mL \pm s.d from at least two independent experiments. Background luminescence in uninfected cells (HEK293T) is also shown. Graphs generated with Prism 8.

SUDV PVs were lyophilised and stored for 1 month, 6 months, 1 year and 1.5 years and BDBV PVs were lyophilised and stored for 1 month. They followed a similar trend to EBOV when reconstituted to assess titre retention (Figure 7.7). SUDV PVs retained ~100% of their titre when reconstituted after being stored at -20°C and +4°C for 1.5 years (Figure 7.7d). At higher temperatures, titres decreased to background level within 6 months (Figure 7.7b). SUDV PVs retained 99.2% of their titre when reconstituted after being stored at +22.5°C for one month (Figure 7.7a), then titres decreased to background level between one month and six months (Figure 7.7b).

SUDV PVs stored at +37°C in dry (<25% humidity) and humid (90% humidity) conditions did not generate any functional titres after a month (Figure 7.7).

BDBV PVs retained high functional titres after a month's storage: 95.9%, 94.1% and 88.1% titre retention when stored at -20°C, +4°C and +22.5°C respectively (Figure 7.7e). At higher temperatures titres decreased to background level.

7.3.4 Long-term storage and stability of lyophilised *cuevavirus* PVs

LLOV PVs were lyophilised and stored for up to 1.5 years under different conditions.

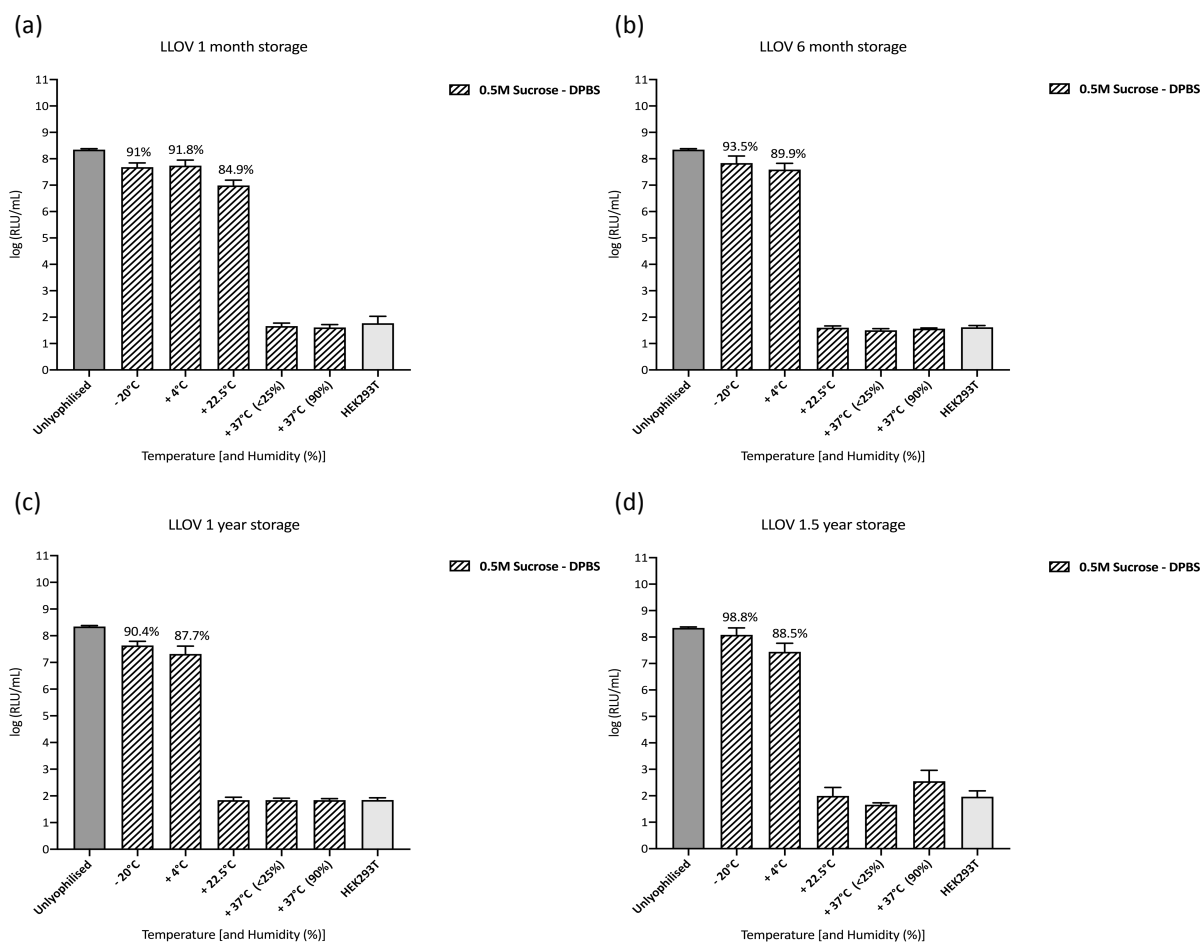


Figure 7.8. Infectivity assay following long-term storage of lyophilised LLOV PVs. PVs were lyophilised using 1M Sucrose in Dulbecco's Phosphate-Buffered Saline (final concentration 0.5M) and stored at different temperatures and humidity conditions (<25% or 90%) for (a) 1 month, (b) 6 months, (c) 1 year, (d) 1.5 years. Unlyophilised LLOV PVs were positive controls for the assay, as well as a parameter for comparison to calculate titre retention after lyophilisation, storage and reconstitution. Transduction titres are expressed as the (log) mean RLU/mL \pm s.d from at least two independent experiments. Background luminescence in uninfected cells (HEK293T) is also shown. Graphs generated with Prism 8.

LLOV PVs retained ~90% of their titre when reconstituted after being stored at -20°C and +4°C for up to 1.5 years (Figure 7.8). At higher temperatures titres decreased to background level within 6 months (Figure 7.8b). LLOV PVs retained 84.9% of their titre when reconstituted after being stored at +22.5°C for one month (Figure 7.8a), then titres decreased to background level between one month and six months (Figure 7.8b). PVs stored at +37°C in dry (<25% humidity) and humid (90% humidity) conditions did not generate any functional titres after storage (Figure 7.8).

7.3.5 Long-term storage and stability of lyophilised *marburgvirus* PVs

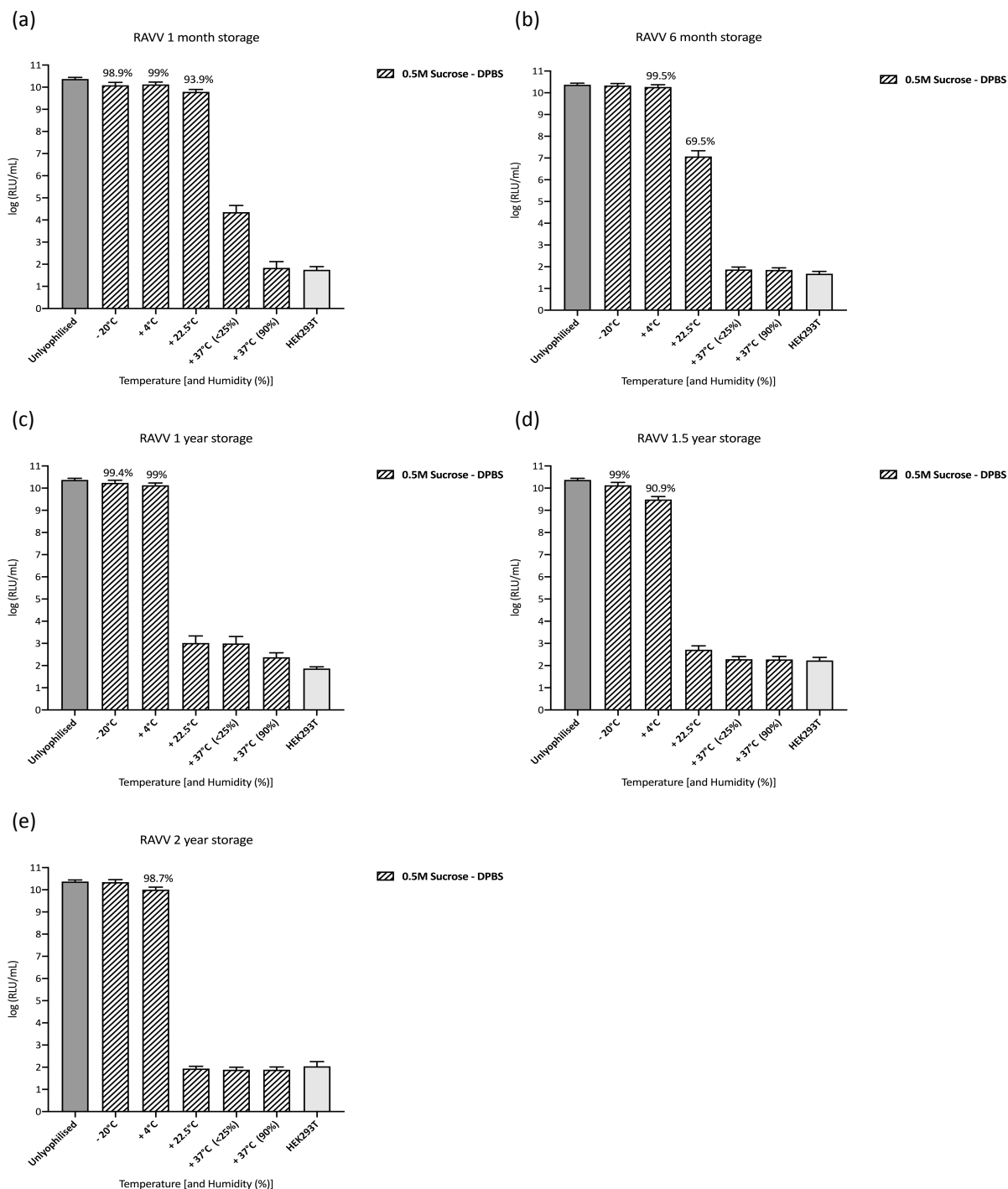


Figure 7.9. Infectivity assay following long-term storage of lyophilised RAVV PVs. PVs were lyophilised using 1M Sucrose in Dulbecco's Phosphate-Buffered Saline (final concentration 0.5M) and stored at different temperatures and humidity conditions (<25% or 90%) for (a) 1 month, (b) 6 months, (c) 1 year, (d) 1.5 years and (e) 2 years. Unlyophilised RAVV PVs were positive controls for the assay, as well as a parameter for comparison to calculate titre retention after lyophilisation, storage and reconstitution. Transduction titres are expressed as the (log) mean RLU/mL \pm s.d from at least two independent experiments. Background luminescence in uninfected cells (HEK293T) is also shown. Graphs generated with Prism 8.

RAVV PVs were lyophilised and stored for up to 2 years at different conditions, retaining >90% of their titre when reconstituted after being stored at -20°C and +4°C for up to 2 years (Figure 7.9). As previously assessed (Figure 7.4), RAVV PVs retained 93.9% of their titre when reconstituted after being stored at +22.5°C for one month (Figure 7.9a), then titre recovery decreased to 69.5% between one month and six months (Figure 7.9b). At higher temperatures titres decreased to background level within 6 months (Figure 7.9b). RAVV PVs stored at +37°C in dry (<25% humidity) and humid (90% humidity) conditions did not generate any functional titres (Figure 7.9), although titres were slightly higher (~10⁴ RLU/mL) than background level when stored for only one month at +37°C (<25% humidity) (Figure 7.9a).

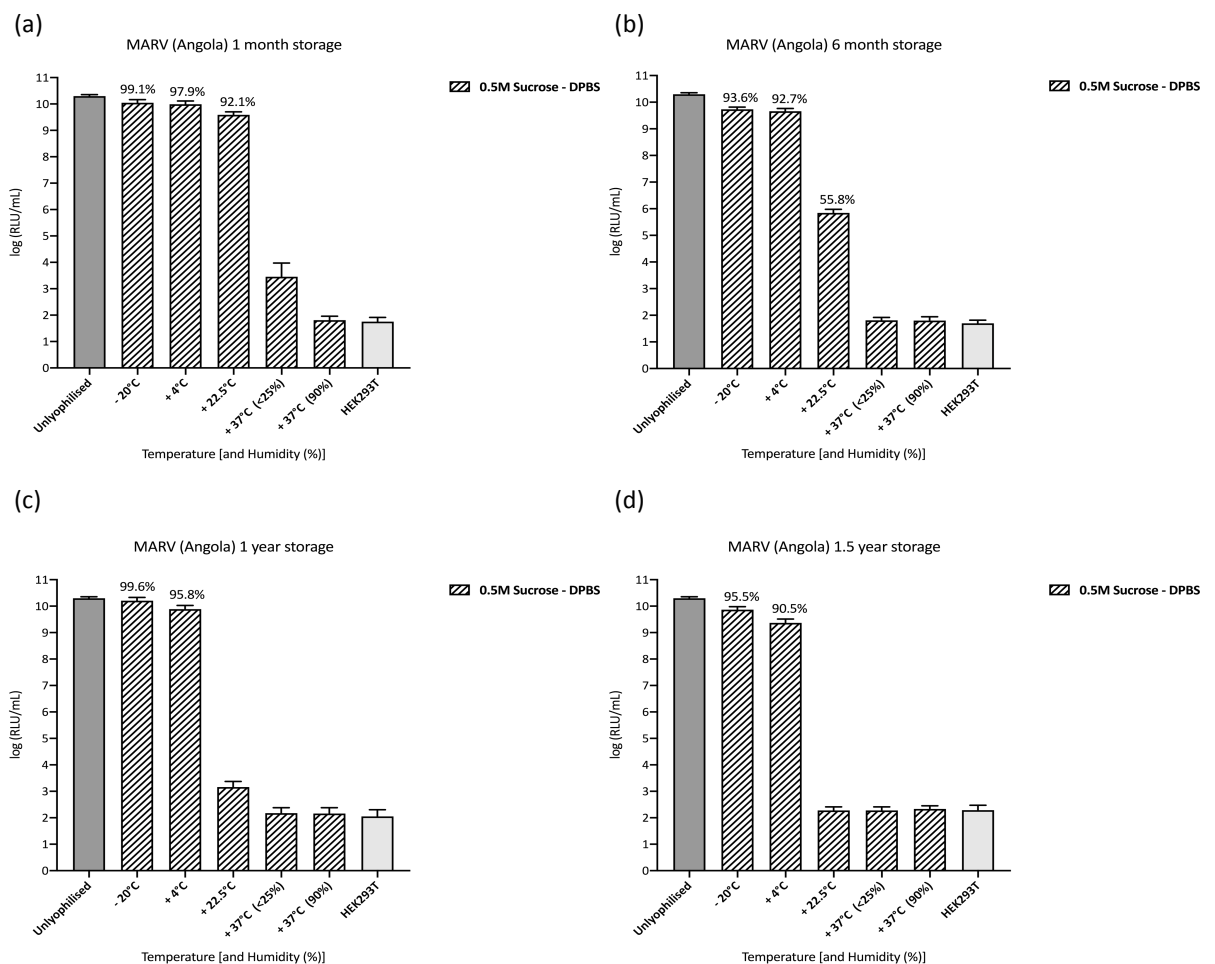


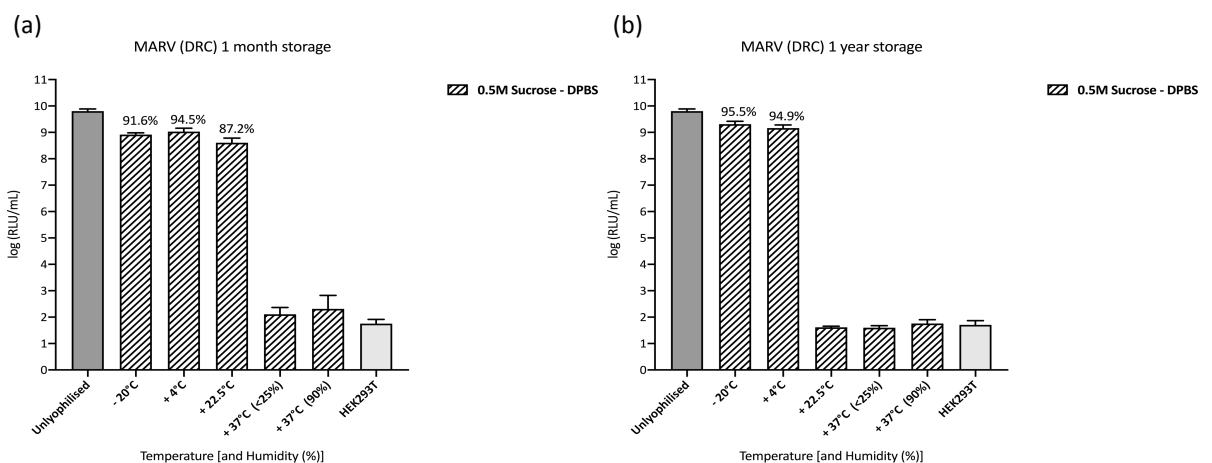
Figure 7.10. Infectivity assay following long-term storage of lyophilised MARV (Angola) PVs. PVs were lyophilised using 1M Sucrose in Dulbecco's Phosphate-Buffered Saline (final concentration 0.5M) and stored at different temperatures and humidity conditions (<25% or 90%) for (a) 1 month, (b) 6 months, (c) 1 year and (d) 1.5 years. Unlyophilised MARV (Angola) PVs were positive controls for the assay, as well as a parameter for comparison to calculate titre retention after lyophilisation, storage and reconstitution. Transduction titres are expressed as the (log) mean RLU/mL ± s.d from at least two independent experiments. Background luminescence in uninfected cells (HEK293T) is also shown. Graphs generated with Prism 8.

MARV (Angola) PVs retained >90% of their titre when reconstituted after being stored at -20°C and +4°C for up to 1.5 years (Figure 7.10); and retained 92.1% of their titre when reconstituted after being stored at +22.5°C for one month (Figure 7.10a), then titre recovery decreased to 55.8% between one month and six months (Figure 7.10b). At higher temperatures, PV titre decreased to background level within 6 months (Figure 7.10b).

MARV (Angola) PVs stored at +37°C in dry (<25% humidity) and humid (90% humidity) conditions did not generate any functional titres (Figure 7.10), although titres were slightly higher (~10³ RLU/mL) than background level (HEK293T) when stored for one month at +37°C (<25% humidity) (Figure 7.10a).

MARV (DRC) PVs retained >90% of their titre when reconstituted after being stored at -20°C, and >85.9% after being stored at +4°C for up to 1.5 years (Figure 7.11). An 87.2% titre retention was observed when reconstituted after being stored at +22.5°C for one month (Figure 7.11a), then PV titres decreased to background level during the period between one month and one year sampling (Figure 7.11b).

MARV (DRC) PVs stored at +37°C in dry (<25% humidity) and humid (90% humidity) conditions did not generate any functional titres after one month (Figure 7.11).



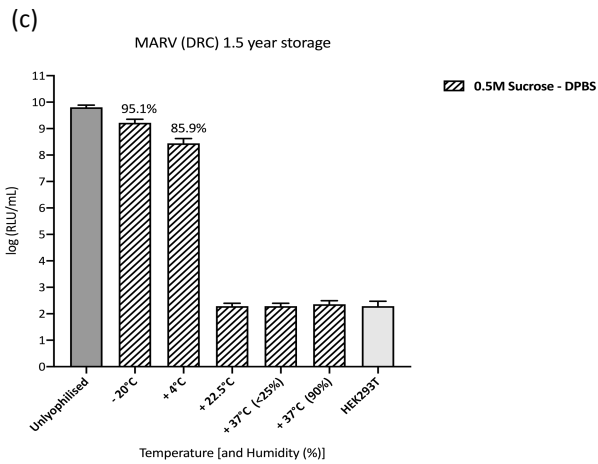
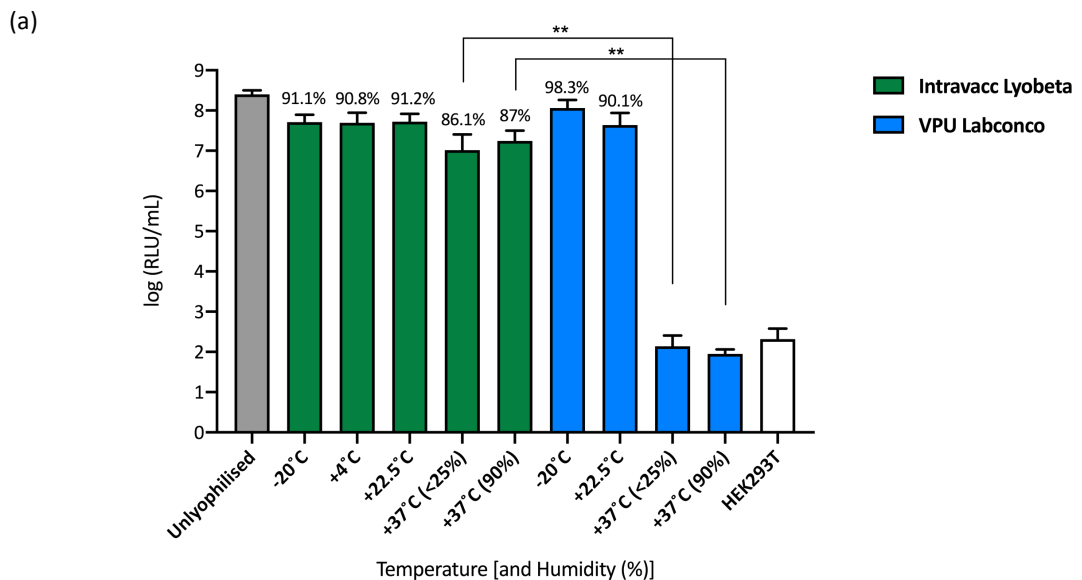


Figure 7.11. Infectivity following long-term storage of lyophilised MARV (DRC) PVs. PVs were lyophilised using 1M Sucrose in Dulbecco’s Phosphate-Buffered Saline (final concentration 0.5M) and stored at different temperatures and humidity conditions (<25% or 90%) for (a) 1 month, (b) 1 year and (c) 1.5 years. Six-month storage was not assessed. Unlyophilised MARV (DRC) PVs were positive controls for the assay, as well as a parameter for comparison to calculate titre retention after lyophilisation, storage and reconstitution. Transduction titres are expressed as the (log) mean RLU/mL \pm s.d from at least two independent experiments. Background luminescence in uninfected cells (HEK293T) is also shown. Graphs generated with Prism 8.

7.3.6 Short-term storage and stability EBOV PVs lyophilised at Intravacc



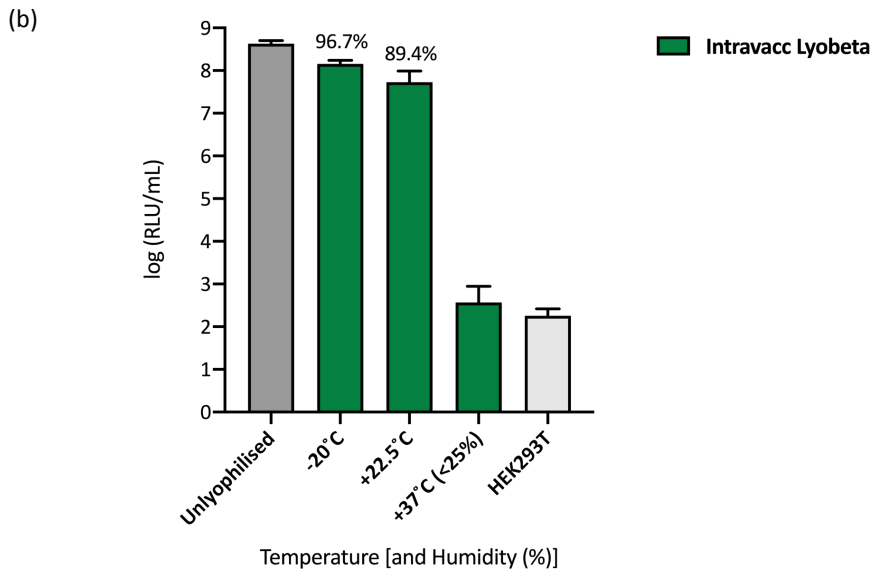


Figure 7.12. Infectivity assay following one-month and six-month storage of EBOV PVs lyophilised at Intravacc. PVs were lyophilised at Intravacc (green) or at the Viral Pseudotype Unit using 1M Sucrose in Dulbecco’s Phosphate-Buffered Saline (final concentration 0.5M) and stored at different temperatures and humidity conditions (<25% or 90%) for (a) 1 month and (b) 6 months. Unlyophilised EBOV PVs were positive controls for the assay, as well as a parameter for comparison to calculate titre retention after lyophilisation, storage and reconstitution. Transduction titres are expressed as the (log) mean RLU/mL \pm s.d from three independent experiments. Titre recovery (%) is expressed on top of each bar. ** $p < 0.01$ (Mann-Whitney test). Background luminescence in uninfected cells (HEK293T) is also shown. Graphs and statistical analysis calculated with Prism 8.

EBOV PVs generated and characterised at the VPU were mixed with 1M Sucrose – DPBS solution as described in section 7.2.3 and sent frozen (from -80°C freezer directly into dry ice for shipment) to Intravacc (Bilthoven, The Netherlands) to be lyophilised in their Telstar Lyobeta freeze-dryer. In addition, EBOV PVs were also lyophilised in the VPU’s Labconco freeze-dryer and sent along with rest of the samples to assess whether travel conditions (i.e., changes in temperature and pressure) would affect titre recovery.

EBOV PVs lyophilised at Intravacc were shipped back to the VPU on dry ice then stored at different temperatures and humidity conditions. These samples retained at least 86.1% of their original titres (Figure 7.12 – green bars). EBOV PVs lyophilised at VPU that were shipped to The Netherlands, kept refrigerated for 2 weeks then shipped back to the VPU, retained titres after a further one month’s storage at -20°C and $+22.5^{\circ}\text{C}$ above 90%, however at higher temperatures titres were similar to background level (Figure 7.12 – blue bars), as previously observed (Figure 7.6a). A temperature of $+4^{\circ}\text{C}$ was not tested, as retention at this temperature did not differ greatly from samples stored at -20°C in previous lyophilisation tests (Figures 7.6 – 7.11).

EBOV PV samples withstood storage at high temperatures of +37°C in dry or humid conditions for at least a month (Figure 7.12a – green bars), with 86.1% of titre recovered after being stored at +37°C (<25% humidity) and 87% of titre recovered after being stored at +37°C (90% humidity); a significant increase ($p < 0.01$) in recovery when compared to the EBOV PV samples lyophilised in the VPU Labconco freeze-dryer (Figure 7.12a).

Samples lyophilised at Intravacc stored at -20°C, ambient temperature (+22.5°C) and +37°C (<25% humidity) were further assessed after 6 months (Figure 7.12b). For PV samples stored at lower temperatures (-20°C and +22.5°C) titre retention was above 89.4%, however for samples stored at +37°C (<25% humidity) PV titres decreased to background levels (Figure 7.12b).

All lyophilised EBOV samples were then tested in neutralisation assays.

7.3.7 Neutralisation assays (PVNA) with lyophilised PVs

Lyophilised EBOV PVs from the Labconco 2.5L freeze-dryer (Figure 7.2) were stored for 1.5 years at +4°C then reconstituted and used as the PV input in PVNAs with two different target cells: HEK293T/17 (Figure 7.13a) and CHO-K1 (7.13b) cells, to assess a better cell target for PVNAs.

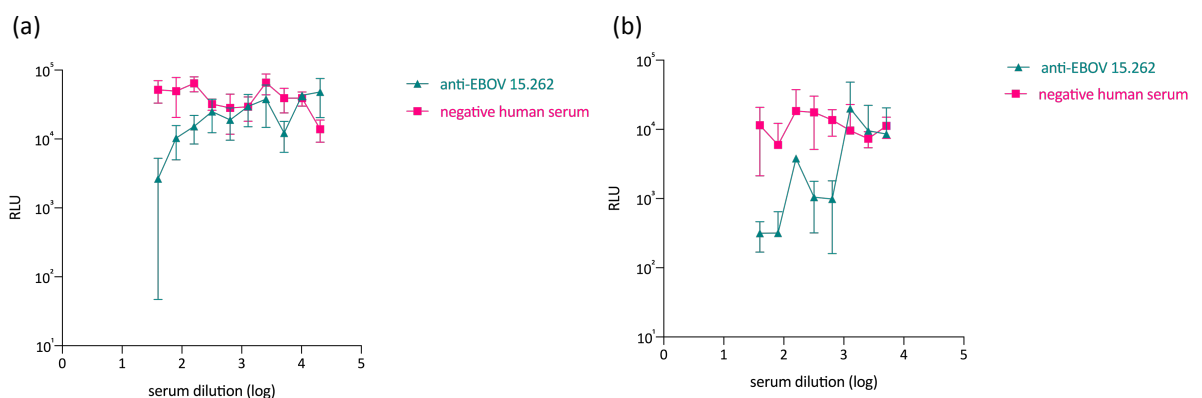


Figure 7.13. Neutralisation assay using reconstituted lyophilised EBOV PVs. WHO standard NIBSC 15.262 against EBOV PVs that had been stored for 1.5 years at +4°C and reconstituted with (a) HEK293T and (b) CHO-K1 target cells. Negative human serum (Sigma) was used as a negative control. Decrease in luminescence (mean \pm s.d) from triplicates in two independent experiments, calculated with Prism 8.

Neutralising titres were similar to PVNAs performed with unlyophilised PVs (Chapter 4): mean IC₅₀ values of 150 (HEK293T target) and 666 (CHO-K1 target) were observed.

Lyophilised EBOV PVs in Intravacc's Telstar Lyobeta freeze dryer stored at -20°C, +37°C (<25%) and +37°C (90%) were reconstituted to achieve approximately 10⁵ RLU (~100 TCID₅₀) per well (as above). They were utilised in PVNAs against pooled convalescent EBOV serum (NIBSC 15.262) to compare performance with unlyophilised PVs.

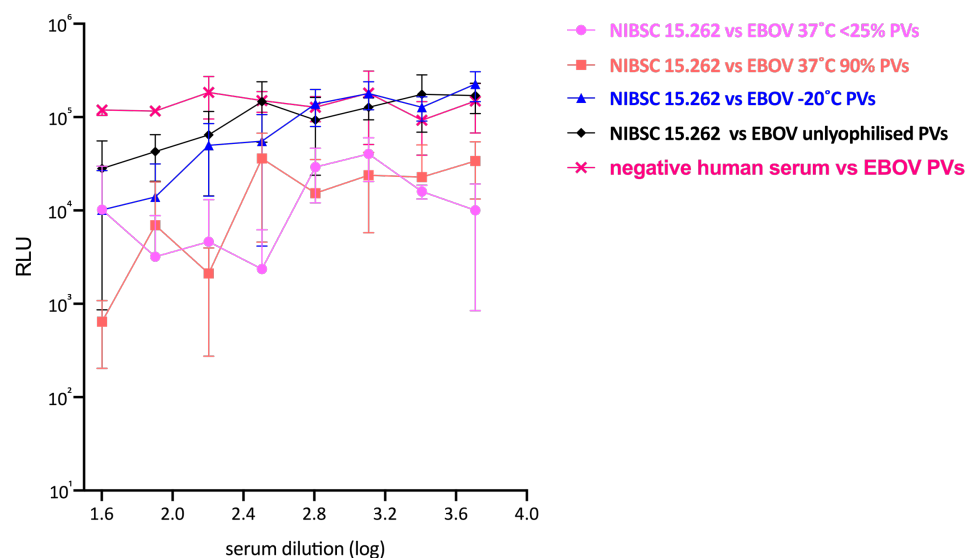


Figure 7.14. Neutralisation assay using reconstituted lyophilised EBOV PVs from Intravacc. WHO standard NIBSC 15.262 tested against EBOV PVs that had been stored for 1 month at -20°C, +37°C (<25% humidity), +37°C (90% humidity) and unlyophilised PVs, before being reconstituted. Negative human serum from a healthy donor (Sigma) was used as a negative control. Decrease in luminescence (mean ± s.d) from duplicates in two independent experiments, calculated with Prism 8.

Even though the neutralising response is variable between the samples, especially those that had been stored at higher temperatures (Table 7.5), they all detected neutralising antibodies in the serum, with PVs stored at -20°C more comparable to unlyophilised PVs (Figure 7.14, Table 7.5).

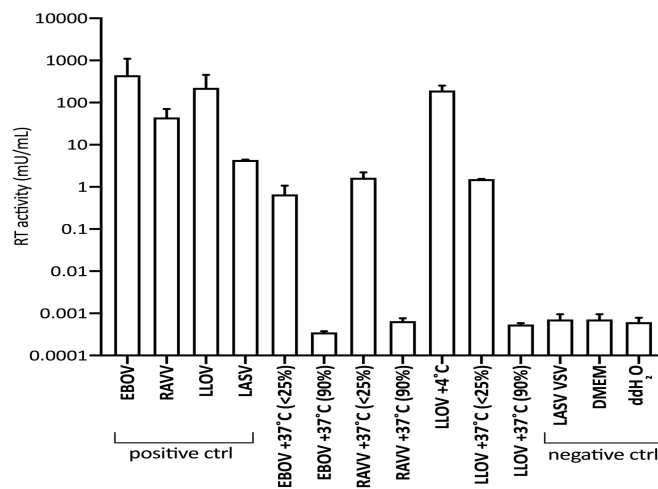
	Unlyophilised	-20°C	+37°C (<25%)	+37°C (90%)
mean IC ₅₀ (n=2)	320-640 (508)	320-640 (509)	640-1280 (1055)	160-320 (204)
mean IC ₉₀ (n=2)	40-80 (40)	80-160 (94)	80-160 (143)	80-160 (156)

Table 7.5. Mean half-maximum inhibitory concentration (IC₅₀) and 90% inhibitory concentration (IC₉₀) of Intravacc lyophilised samples in PVNAs. Antibody titres were calculated with Prism 8 and expressed as the reciprocal of the dilution (in brackets) where 50% or 90% inhibition of PVs was achieved within the dilution range.

7.3.8 Quality control of lentiviral particles present in samples stored at high temperatures – SG-PERT

To further investigate the drastic reduction in titre recovery of samples lyophilised with the Labconco freeze-dryer and stored at +37°C for one month, a reverse transcriptase assay (SG-PERT) was performed as described in Chapter 3, to detect reverse transcriptase activity from any remaining lentiviral particles. In EBOV, RAVV, LLOV and LASV unlyophilised lentiviral samples reverse transcriptase activity above 4 mU/mL was detected (Figure 7.15a).

(a)



(b)

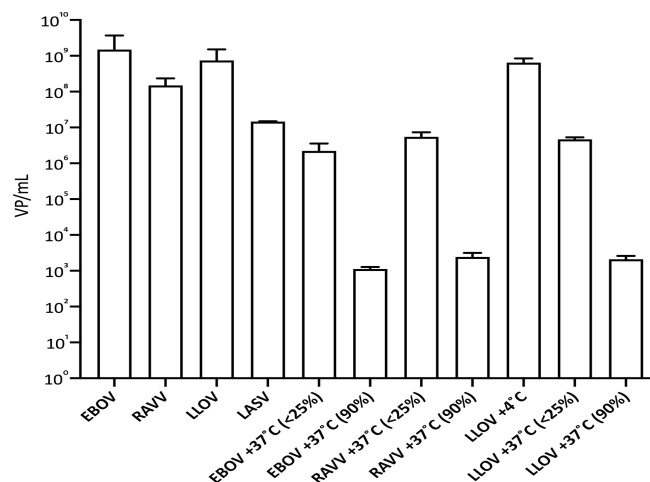


Figure 7.15. Reverse transcriptase assay (SG-PERT) of lyophilised samples. A standard curve is generated with recombinant HIV-1 RT and utilised to calculate (a) RT activity (mU/mL), which is then used to estimate (b) number of viral particles per mL (VP/mL). Unlyophilised EBOV, RAVV, LLOV and LASV were included as positive controls. A LASV VSV core PV, medium only (DMEM) and ddH₂O only were included as negative controls. Graphs were generated with Prism 8.

However, EBOV, RAVV and LLOV lyophilised samples had their RT activity decreased to negative control levels by storage at +37°C (90% humidity) for one month, but samples kept in dry conditions maintained a level of RT activity of approximately 1 mU/mL. LLOV PVs stored at +4°C had RT activity comparable to unlyophilised LLOV (Figure 7.15a). Other lyophilised PVs stored at +4°C were not tested for RT activity.

The number of viral particles per mL could then be estimated considering one lentiviral particle results in 300 pU/mL of RT activity (Vermeire *et al.* 2012). Unlyophilised PVs samples are estimated to contain approximately $1 \times 10^7 - 1 \times 10^9$ VP/mL (Figure 7.15b).

Estimation of lyophilised PVs kept in dry conditions was approximately 1×10^6 VP/mL (Figure 7.15b). However, none of them resulted in functional PVs (Figures 7.6 - 7.11).

7.4 Discussion

Improving diagnostics and serological tests for emerging diseases has been emphasised since the EBOV outbreak in West Africa in 2013-2016 (Gatherer 2014; Formella and Gatherer 2016; Murphy 2019), and more recently during the EBOV outbreak in the DRC with over 3000 people affected (WHO situation reports). Other emerging diseases such as measles in the DRC, concurrent with EBOV, and therefore increasing the burden on health services as well as the ongoing SARS-CoV-2 outbreak with over 84 million confirmed cases globally (WHO-05/01/2021) have also stressed the need for research in future emerging diseases.

Although RT-PCR based assays are the gold standard for diagnostic testing of filoviruses and other viruses such as SARS-CoV-2 (Clark *et al.* 2018; Osterdahl *et al.* 2020), PV based assays can be very useful for sero-epidemiological studies, including geographical distribution and zoonotic spillover. In addition, they can be used retrospectively to detect previous infections (Mather *et al.* 2013; Ewer *et al.* 2014; Kinsley, Scott and Daly 2016; Luczkowiak *et al.* 2016), especially in diseases with a large number of asymptomatic individuals.

A PV based serological assay that could differentiate between genera and species of filoviruses and complement ELISA would be highly desirable to help epidemiological studies, as well as monitoring outbreaks of novel viruses when cross-reactivity might be an issue and next generation sequencing is not available. In addition, it has the

advantages of only requiring low containment facilities (BSL 1-2) unlike assays utilising native viruses, and being amenable to multiplexing (Ewer *et al.* 2014; Carnell *et al.* 2015). Some limitations would be the need to wait for at least two days for results, requirement of expertise to perform the assay and cell culture facilities, in contrast to other serological methods such as ELISA.

Another issue is the need for refrigeration during transportation and storage of PVs, especially in low-resource countries where those assays are needed, as well as waiting times for customs clearance and transportation to the destination. Lyophilisation has been utilised as a means to avoid cold-chain transportation for certain reagents and vaccines (Kraan *et al.* 2014).

The possibility of using lyophilised PVs in a diagnostic kit has already been explored for influenza, rabies and Marburg viruses after short-term storage (Mather *et al.* 2014). Generally, PVs retained titres by storage at lower temperatures of -80°C up to ambient temperature when stored for up to one month. At +37°C in dry or humid conditions, PV titres decreased approximately 100-fold, but retained a functional titre. Reconstituted influenza and rabies PVs also performed well in PVNAs. Marburg PVs were not tested in PVNAs due to lack of available anti-sera, although they could be tested with monoclonal antibodies in the future.

The lyophilisation of mammalian cells has been explored but so far has proved elusive, although there has been some success in lyophilisation and reconstitution of platelets (Wolkers, Tablin and Crowe 2002), or somatic cells that have been lyophilised then used in nuclear transfer experiments (Loi *et al.* 2008). However, lyophilising mammalian cells for later propagation in culture has not been successful so far due to the integrity of the cell membrane being compromised and the resulting damage (Zhang *et al.* 2017). In that case, cells would have to be sent as a frozen stock for propagation.

In the current study, we undertook a more comprehensive analysis of storage and stability of lyophilised filovirus PVs for future development of a serological assay kit. We assessed short-term storage stability of lyophilised PVs in different excipients comprised of a cryoprotectant (Sucrose or Sorbitol) in two different buffers. After the best excipient was established, we kept samples stored for up to two years at different temperatures and humidity conditions before reconstitution for use in infectivity and neutralisation assays. We also compared our freeze-dryer, which does not perform a secondary drying step to remove residual moisture, with a freeze-dryer used for commercial purposes by

our collaborative partners based at Intravacc (Bilthoven, The Netherlands). All PVs were assessed in infectivity assays to calculate titre retention and recovery. In addition, the functionality of EBOV PVs was further assessed in PVNAs with available convalescent sera. Other filovirus genera or species were not assessed in PVNAs due to the lack of availability of specific anti-sera.

Filovirus PVs were generated in T75 flasks as described in Chapter 2. This ensured batch consistency, avoiding multiple transfection experiments. All PVs utilised in this study had a lentiviral core. Transduction titres in infectivity assays were consistent with previously generated PV (Chapter 3). For *ebolavirus* (EBOV, SUDV and BDBV) and *cuevavirus* (LLOV) PVs approximately 1×10^8 RLU/mL (or 1×10^4 TCID₅₀/mL) was observed (Figure 7.13). For *marburgvirus* (RAVV, MARV – Angola and MARV – DRC) PVs approximately 1×10^9 – 1×10^{10} RLU/mL (or 1×10^6 TCID₅₀/mL) was observed (Figure 7.13). RAVV titres were consistent with previously generated PVs (Mather *et al.* 2014). PV generation was also consistent with previously upscaled PV production in T75 flasks (Chapter 3).

Utilisation of disaccharides such as sucrose, or sugar alcohols such as sorbitol as cryoprotectants in freeze-drying excipients has already been established (Nireesha *et al.* 2013; Kraan *et al.* 2014; Mather *et al.* 2014). In a study designed to test conditions to lyophilise an inactivated polio vaccine, formulations containing sorbitol resulted in good recovery after being incubated for one week at +45°C (Kraan *et al.* 2014).

We tested whether sorbitol or sucrose would have an impact in titre recovery, especially at higher temperatures, as well as choice of buffer (DPBS or Tris). EBOV, SUDV, RAVV or MARV (Angola) PVs were lyophilised and stored at +22.5°C or +37°C (90% humidity) for one month. At +22.5°C, titre recovery was slightly higher (above 90%) in all species (Figure 7.4) when sucrose was used as a cryoprotectant, either in DPBS or Tris buffer, concurrent with previous results of RAVV PVs lyophilised in sucrose-DPBS (Mather *et al.* 2014). At +37°C (90%) all samples had lost their functional titre, decreasing to background (HEK293T) levels. The choice of DPBS or Tris buffer had no significant impact in titre recovery when samples were stored at +22.5°C (Figure 7.4).

For sorbitol, lower concentrations (0.25M) had better titre recovery than higher concentrations (0.5M), in contrast with the polio vaccine evaluation study. However, their formulation contained 10% sorbitol as well as 10% MgCl₂, 10% monosodium glutamate in McIlvaine buffer that contains citric acid and Na₂HPO₄ (Kraan *et al.* 2014).

In a previous short-term assessment storage and stability of lyophilised RAVV PVs, they retained a higher percentage of transduction titres after being stored at +37°C in dry and

humid conditions for one month (Mather *et al.* 2014), although it was reported then that titres at those temperatures were at the level of lentiviral particles devoid of GP (Δ env). Therefore, they were unsuitable for use in neutralisation assays, where a minimum functional titre is needed for the assay.

Samples lyophilised in 0.5M Sucrose-DPBS and 0.5M Sorbitol-DPBS were tested again after a 6-month storage. Most had no functional titre detected (Figure 7.5), however RAVV and MARV (Angola) retained approximately 60% of their titres (Figure 7.5c and 7.5d), but only testing these PVs in PVNAs would ensure they would be suitable for use in these assays.

For assessment of long-term storage and stability of lyophilised PVs, they were generated at a final concentration of 0.5M in Sucrose-DPBS as PVs lyophilised in this excipient had the highest percentage recovery (Figure 7.4). All three genera of lyophilised filovirus PVs followed a similar trend after long-term storage.

All lyophilised PVs had titre recovery above 85.9% when stored in a household fridge at +4°C for 1.5 years (Figure 7.6 to 7.11). Note that BDBV (Figure 7.7e) was only tested after a one-month storage. EBOV (Figure 7.6e) and RAVV (Figure 7.9e) PVs had titre recoveries of 94.7% and 98.7% respectively after being stored at +4°C for 2 years. These are particularly encouraging results as avoiding the need for high-powered freezers would extend the number of labs in low-resource countries being able to use such a kit, such as in the countries involved in the recent EBOV epidemics.

For samples stored at ambient temperature (+22.5°C), the decrease in titre recovery between one and six months was not investigated further. However, one month is a reasonable period of time for transport and delivery of such a reagent.

At higher temperatures, we observed a drop in transduction titres after one-month storage at +37°C in dry and humid conditions (Figure 7.4 – 7.11). We hypothesised that the decrease could be due to the residual moisture that remains after a lyophilisation procedure without the secondary drying step (Nireesha *et al.* 2013); therefore we sent EBOV PV samples in sucrose – DPBS (final concentration 0.5M) to be lyophilised at Intravacc (Bilthoven, The Netherlands) to include a secondary drying step. Samples were then transported back to us for analysis. Lyophilised EBOV PVs at Intravacc had titre recovery of 86.1% and 87% after being stored for a month at +37°C in dry and humid conditions, respectively (Figure 7.12a –green bars). We also sent samples that had been lyophilised at the VPU (University of Kent) for comparison (Figure 7.12a – blue bars). The return journey to The Netherlands did not affect titre recovery after storage at ambient

temperature or below in either lyophilisation protocols conducted at Intravacc or in the VPU, however samples not submitted to a secondary drying step had a drastic drop in titres after a month at +37°C. Samples lyophilised at Intravacc stored at +37°C (<25% humidity) lost titre retention between one and six months (Figure 7.12b). Overall, these are very encouraging results as PVs lyophilised using industrial equipment and a protocol used in vaccine production for instance, will retain a functional titre even when stored at harsher, warmer conditions. This will ensure lyophilised PVs could be transported at room temperature to warmer tropical countries.

To assess performance of lyophilised PVs in PVNAs, EBOV samples lyophilised at the VPU that had been stored at +4°C for 1.5 years were tested and performed well in PVNAs (Figure 7.13). EBOV PVs lyophilised at Intravacc also performed well in PVNAs, including samples stored at +37°C for one month (Figure 7.14). They all detected neutralising antibodies in the convalescent serum, even if with somewhat variable responses (Table 7.4).

A further assessment of samples lyophilised without a secondary drying step and stored at +37°C for one month was conducted to ascertain whether the lentiviral particles had been completely denatured by the heat, or whether it was the GP that was damaged and its structure compromised. We utilised a reverse transcriptase activity assay (SG-PERT) to detect any RT activity and estimate the number of lentiviral particles (Pizzato *et al.* 2009; Vermeire *et al.* 2012).

Samples stored in humid conditions had virtually undetectable levels of RT activity, similar to negative controls (Figure 7.15a); and samples stored in dry conditions (<25% humidity) had low level RT activity of approximately 1 mU/mL (Figure 7.15a), with an estimated number of lentiviral particles of approximately 1×10^6 VP/mL (Figure 7.15b). It is reasonable to speculate that the viral particles are present but the GP structure was compromised. This is because despite detection of approximately 1×10^6 VP/mL, samples stored at +37°C (<25% humidity) did not translate into functional titres (Figure 7.4 – 7.11). Having a functional titre is crucial for performing neutralisation assays. Utilising high titre PV stocks of $>1 \times 10^8$ RLU/mL (1×10^4 TCID₅₀/mL) will ensure any small decrease during transportation and storage would not affect performance in PVNAs.

Other filovirus genera were not assessed in PVNAs due to the lack of specific convalescent sera, however, they could be tested in PVNAs against monoclonal antibodies with neutralising activity in the future, as proof-of-principle.

It would also be useful to assess performance of filovirus VSV core PVs in lyophilisation studies as VSV is widely used as a PV core for filoviruses (Takada *et al.* 1997; Maruyama *et al.* 2014; Ilinykh *et al.* 2016; Ruedas *et al.* 2017; Salata *et al.* 2019).

Overall, these results are very promising for a future serological kit that could be transported at ambient temperature and would last at least two years in a household fridge. It would help us improve basic and translational research on these highly pathogenic viruses to better understand transmission dynamics.

CHAPTER 8: Final Conclusions and Future work

Filoviruses have been responsible for sporadic disease outbreaks since their discovery in 1967 (Table 1.2 & 1.3). Several species are associated with human infection with mortality rates of up to 90%. The need for improved therapeutics and diagnostics has become particularly apparent during the epidemic in West Africa (2013-2016), and the recent outbreaks in the DRC.

Research on these highly pathogenic viruses requires high containment facilities, hindering efforts. Pseudotype viruses (PV) allow entry, antiviral screening, vaccine delivery and evaluation studies to be conducted in low containment facilities. PVs contain the core of one virus (MLV, HIV, VSV) bearing the glycoprotein of virus to be studied.

The main objectives of this work were to improve filovirus PV titres, evaluate their use in pseudotype virus neutralisation assays, improve specificity in those assays and conduct lyophilisation studies evaluating long-term storage and stability of PVs for use in serological assays. In addition, PVs were used in a collaborative study to evaluate neutralising antibody response in bats captured in Hungary, following previous detection of filoviral RNA in similar bat populations (Kemenesi *et al.* 2018).

8.1 Chapter 3

The initial objective to improve titres of previously generated low titre *ebolavirus* lentiviral PVs was achieved through optimisation of previous protocols by varying the amount of envelope GP plasmid during PV production, and upscaling PV generation to larger cell culture flasks. A panel of lentiviral and VSV PVs were generated and optimised to display several filovirus GPs: *ebolavirus* (EBOV, SUDV, BDBV and RESTV), *cuevavirus* (LLOV) and *marburgvirus* (RAVV and MARV - Angola and DRC strains), as well as the *mammarenavirus* LASV.

Later in the project, VSV core filovirus PVs were generated to comparable titres to the lentiviral system, also through optimal envelope GP plasmid amount during PV production.

Marburgviruses had been previously generated to high titres (Mather *et al.* 2014). Infectivity assays for lentiviral core PVs resulted in high titres of approximately 1×10^8 RLU/mL for *ebolavirus* and *cuevavirus* PVs, whereas *marburgvirus* and *mamarenavirus* PVs exhibited even higher titres of 1×10^{10} RLU/mL and 1×10^{11} RLU/mL respectively.

Measuring tissue culture infectious dose (TCID₅₀), values of 1×10^4 TCID₅₀/mL for *ebolavirus* and *cuevavirus* PVs, and 1×10^6 TCID₅₀/mL for *marburgvirus* and *mamarenavirus* were obtained.

VSV core PVs yielded similar titres, however they were prone to input issues as evidenced by variable luminescence reading in control wells in PVNAs due to possible cytotoxicity in target cells. As they were generated at the end of the PhD project, there was not sufficient time available for optimisation attempts to address this issue.

Filovirus PVs, especially produced via the lentiviral platform, are easy to generate in HEK293T producer cells, and were shown to be amenable to upscaling for larger studies if necessary. Production takes approximately one week, and infectivity assays yield relatively quick results within 48h of set-up.

The difference in titres between genera was consistent within the several transfection experiments performed during the project, either with the lentiviral or VSV platforms. The differences in GP processing between *marburgviruses* and *ebolavirus* or *cuevaviruses* may partly explain those discrepancies. *Marburgviruses* do not require additional processing by endosomal proteases for instance; and have not been implicated in GP induced cytotoxicity (Gnirß *et al.* 2012).

This difference in titres has also been reported recently in a study utilising EBOV and MARV VSV PVs in two different infectivity assays (Takadate *et al.* 2020).

While the lentiviral system has yielded consistent and reproducible PV titres, the VSV core system needs further optimisation. Even though high titre VSV PVs were generated, there were issues with PV input in PVNAs, as mentioned above. It may be due to cytotoxicity observed in target cell lines; therefore finding a suitable target cell line could enable their use in PVNAs, as only HEK293T target cells were used in PVNAs with VSV core PVs. In addition, VSV PV optimization should include assessing shorter incubation in infectivity and neutralisation assays, as it might affect titres (Nie *et al.* 2020).

8.2 Chapter 4

EBOV PVs were used to detect neutralising antibodies in convalescent serum from patients that recovered from EVD, which was commercially available from the National Institute for Biological Standards and Control (NIBSC) in Potters Bar, UK. Three WHO standards were available: WHO NIBSC 15.220, a convalescent serum from one

healthcare worker who recovered from EVD; WHO NIBSC 15.262, a pooled serum from 6 patients from Sierra Leone and WHO NIBSC 16.344, a panel of sera from 4 patients (15.280, 15.282, 15.284 and 15.286) who recovered from EVD as well as a healthy donor (15.288).

The antibody neutralising response was weak and quite varied, in line with studies reported in the literature. WHO NIBSC 15.262 yielded higher antibody titres, probably because it is a pooled sera from 6 patients, and serum from some of them might have higher antibody titres.

The target cell line was important for detection of nAbs. The hamster cell line CHO-K1 produced clearer neutralising curves, even though PV titres were 10-fold lower in infectivity assays.

We tested our PVNA platform with monoclonal antibodies targetting EBOV (CA45, FVM04 and FVM09) and MARV GP (MR78). Strong neutralising responses were seen for CA45 and FVM04. MARV and RAVV PVs were neutralised by the MR78, albeit weakly. This could be because MR78 was isolated from a patient who recovered from an infection with the Uganda strain of *marburgvirus*, whereas in this study Angola and DRC strains, as well as RAVV were used.

ELISA utilising purified PVs as antigens was also able to detect antibodies in convalescent serum WHO NIBSC 15.262 (pooled serum) and 15.280 (single patient). However, background noise in serum from a healthy donor was high, therefore the assay would require further optimization, or utilisation of purified recombinant antigens for comparison.

In PVNAs, cross-reactivity was observed between EBOV convalescent serum and RAVV PVs, especially WHO NIBSC 15.220. Cross-reactivity was observed less with pooled serum WHO NIBSC 15.262 against RAVV PVs. No cross-reactivity was observed when LLOV or RESTV PVs were tested against these sera.

RAVV and EBOV GP have approximately 30% amino acid similarity (Liam B King *et al.* 2018). Considering the receptor-binding site (RBS) contains more conserved sequences between EBOV and RAVV than any other region of the GP (Sanchez *et al.* 1993; Kuhn *et al.* 2006; Manicassamy *et al.* 2007), that could partly explain cross-reactivity between RAVV and EBOV if enough nAbs target the RBS preventing entry, although it is not clear why cross-reactivity was not observed with other filovirus PVs from the same genus to the same extent. The issue of specificity should be a focus in future studies. Polyclonal sera from MARV/RAVV would be needed in future for use in reciprocal serum/PV studies.

8.3 Chapter 5

Chimeric GPs with LLOV and RESTV GPs as a scaffold to display EBOV epitopes were generated through site-directed mutagenesis, in order to improve specificity in PVNAs. LLOV and RESTV were chosen due to the earlier finding that convalescent serum did not cross-react against these PVs. Initial attempts were made with LLOV as a scaffold GP displaying EBOV epitopes. Two neutralising EBOV epitopes 4G7 and KZ52 were chosen, as well as the non-neutralising epitope 1H3. Murine monoclonal antibodies 4G7 and 1H3 target the GP₁ - GP₂ base interface and mucin-like domain whereas human KZ52 has overlapping regions with 4G7 mainly targetting the GP₂ base.

LLOV PVs displaying EBOV epitopes 4G7, 1H3 and KZ52 yielded functional PVs albeit to lower titres (10-fold) than wild-type LLOV PVs. However LLOV chimeric PVs were not neutralised by their corresponding mAbs. Antibody binding was not detected in ELISA either.

Attempts were then made with RESTV as a scaffold GP due to the size, the possibility of a better alignment and therefore having more chances of displaying the epitope correctly. PVs displaying RESTV GP containing KZ52 epitope (KZ52-RESTV) were successfully neutralised by the KZ52 mAb, using human HEK293T (n=3) or hamster CHO-K1 (n=2) target cell lines. Binding of KZ52 to KZ52-RESTV PVs was also detected in ELISA. However, RESTV-KZ52 PVs were not neutralised by EBOV polyclonal convalescent serum despite being neutralised by the KZ52 mAb, suggesting more neutralising epitopes would be necessary to induce neutralisation. KZ52 was isolated from a survivor of the 1995 Kikwit EBOV outbreak (Lee *et al.* 2008), whereas the convalescent serum tested (WHO NIBSC 15.262) is a pooled serum from six survivors of the 2013-2016 EBOV outbreak in West Africa. It was unlikely to have an antibody with exactly the same specificity within that particular pool.

The Marburg virus MR78 epitope had many scattered regions throughout the RBS. Two approaches were attempted to insert this epitope on another GP scaffold, gene synthesis or replacing the whole N-terminal region of LLOV or RESTV with RAVV. However, functional PVs were not produced. Mutations within the RBS probably resulted in an altered GP structure not conducive for binding with the NPC1 cell receptor. Changing the whole of the GP₁ could have yielded functional PVs however the desired improvement in specificity might not have been achieved.

For future studies, increasing the number of potent EBOV neutralising epitopes into the RESTV GP and avoiding any that may target the receptor-binding site, might make PVs displaying these chimeric GPs amenable to being neutralised by convalescent serum in PVNAs, potentially enabling use for differentiation between genera and species in antibody screening tests.

8.4 Chapter 6

One important aspect of research efforts is identifying the animal reservoir of filoviruses to help prevent future zoonotic spillovers. Of the three main genera, the reservoir for *marburgviruses* has been identified as fruit bats (Towner *et al.* 2009; Jones *et al.* 2015; Amman *et al.* 2020). The reservoir for *ebolaviruses* is likely to be bats but infectious virus has not been isolated from these animals yet (Leroy *et al.* 2005; Han *et al.* 2016; Kock *et al.* 2019). The *cuevavirus* genus (LLOV) was identified when filovirus RNA was detected in bats habiting caves in northern Spain (Negredo *et al.* 2011). The virus re-emerged in Hungary in 2016 after mortality events in bat populations were observed in caves in a region in Hungary (Kemenesi *et al.* 2018). In a collaborative study with the University of Pecs, we utilised LLOV PVs to detect neutralising antibodies in some of those animal samples. A strong neutralising response was detected in three bats that had tested positive in RT-PCR for LLOV infection, as well as one bat that had tested negative in RT-PCR, suggesting prior, but cleared, LLOV infection.

After this small successful pilot study, samples from 71 bats that had been caught alive were tested. A weak to moderate neutralising response was detected in 8 animals out of the 71. Due to the small amount of serum available, only 3 animals that were positive in PVNA could be tested in duplicate in a repeat experiment. However, the animal that tested negative in RT-PCR from the pilot study, as well as these live bats carrying neutralising antibodies against LLOV, indicates that these bats are able to sustain LLOV infection and recover, adding evidence that these bats could be the animal reservoir for *cuevaviruses*. Further efforts should be made to screen more bats in different regions of Europe to assess the distribution of this virus in the Continent.

Virus isolation from these animals will be crucial to establish the reservoir.

8.5 Chapter 7

Finally, long-term studies of storage and stability of PVs were performed with a panel of lentivirus PVs from three main filovirus genera, *ebolavirus*, *cuevavirus* and *marburgvirus*, including several species such as EBOV, SUDV, BDBV, LLOV, RAVV, MARV (Angola) and MARV (DRC), to assess their performance in infectivity and neutralisation assays following lyophilisation and storage in different temperature and humidity conditions. All these lyophilised PVs followed a similar trend regarding titre retention after storage.

EBOV PVs performed well in infectivity assays after being stored for even 2 years at +4°C and in neutralisation assays after being stored for 1.5 years at +4°C.

At temperatures higher than +4°C, PV titre retention was not as successful. At +22.5°C, PV titres dropped to background levels between 1 and 6 months, whereas lyophilised samples kept at +37°C in dry or humid conditions had no detectable titre within a month. Interestingly, when our PV supernatant was sent to our collaborators at Intravacc in The Netherlands to be lyophilised in industrial freeze-driers used for vaccine production, PV titres were retained when stored at +37°C for a month. This is very encouraging, as those PVs could be utilised, following shipping and potential exposure to such temperatures en-route, as a serological tool in a future diagnostic kit to be used in African countries where most filovirus outbreaks occur. Between one-month and six-month storage at +37°C, PV titres were reduced to background levels after reconstitution in infectivity assays. However titre retention for lyophilised PVs stored for one month at high temperatures (+37°C) should be adequate for transportation to warmer climates until a household fridge might be available.

It would be useful to assess titre retention on a monthly basis between one month and six month storage at high temperature (+37°C) in future investigations to determine exactly how long the PVs would be viable at those temperatures, as well as testing lyophilised PVs stored for 2 years in PVNAs.

In summary, an extensive panel of filovirus pseudotypes from different genera and species were generated to high titre for use in antibody assays such as ELISA and pseudotype virus neutralisation assays. Both lentiviral and VSV core generated functional PVs. Even though there were issues with PV input in PVNAs for VSV core PVs regarding luminescence readings, lentiviral PVs performed very well. However, specificity was an issue in some cases, as EBOV convalescent serum cross-reacted with RAVV PVs in our hands. To address that, chimeric GPs, as scaffolds bearing neutralising epitopes, were generated via mutagenesis to attempt to improve specificity in PVNAs. A proof-of-principle study with monoclonal antibodies was successful however further investigations are needed before using convalescent serum against PVs bearing those chimeric GPs. In addition, MARV convalescent serum would be useful for reciprocal testing.

A collaborative study was conducted to detect neutralising antibodies against LLOV in bats caught in Hungary. A small pilot study using sera from animals found dead in the wild, which were positive for LLOV by RT-PCR found high antibody titres. A further study of wild bats caught alive found a few animals with lower titres of antibodies against this virus, indicating these animals could have been previously infected, adding to the evidence of these animals as putative reservoirs for LLOV.

And finally, lyophilised filovirus PVs retained titres for up to two years in temperatures up to 4°C, and for up to a month at least in temperatures of 37°C, performing well in PVNAs, indicating they could be used in future serological studies and transported where they are needed avoiding the cold chain.

This work suggests PVs can be used extensively in filovirus research offering a safe and flexible platform that can be adapted for different investigations.

References:

- Alvarez, C.P. *et al.* (2002). C-Type Lectins DC-SIGN and L-SIGN Mediate Cellular Entry by Ebola Virus in cis and in trans. *Journal of Virology* **76**:6841–6844.
- Aman, M.J. *et al.* (2009). Development of a broad-spectrum antiviral with activity against Ebola virus. *Antiviral Research* **83**:245–251.
- Amarasinghe, G.K. *et al.* (2019). Taxonomy of the order Mononegavirales: update 2019. *Archives of Virology* **164**:1967–1980.
- Amman, B.R. *et al.* (2020). Isolation of Angola-like Marburg virus from Egyptian rousette bats from West Africa. *Nature Communications* [Online]:1–9.
- Amman, B.R. *et al.* (2015). Oral shedding of Marburg virus in experimentally infected Egyptian fruit bats (*Rousettus aegyptiacus*). *Journal of Wildlife Diseases* **51**:113–124.
- Andersen, K.G. *et al.* (2020). The proximal origin of SARS-CoV-2. *Nature Medicine* [Online] **26**:450–452.
- Ao, Z. *et al.* (2008). Characterization of a trypsin-dependent avian influenza H5N1-pseudotyped HIV vector system for high throughput screening of inhibitory molecules. *Antiviral Research* **79**:12–18.
- De Arellano, E.R. *et al.* (2019). First evidence of antibodies against Iloviu virus in schreiber's bent-winged insectivorous bats demonstrate a wide circulation of the virus in Spain. *Viruses* **11**.
- Atre, T. *et al.* (2019). Development and characterization of a Zaire Ebola (ZEBOV) specific IgM ELISA. *Journal of Immunological Methods* [Online] **468**:29–34.
- Audet, J. *et al.* (2015). Molecular Characterization of the Monoclonal Antibodies Composing ZMAb: A Protective Cocktail Against Ebola Virus. *Scientific Reports* **4**.
- Baer, A. and Kehn-Hall, K. (2014). Viral concentration determination through plaque assays: Using traditional and novel overlay systems. *Journal of Visualized Experiments*:1–10.
- Baize, S. *et al.* (1999). Defective humoral responses and extensive intravascular apoptosis are associated with fatal outcome in Ebola virus-infected patients. *Nature Medicine* **5**:423–426.
- Baker, M.L., Tachedjian, M. and Wang, L.F. (2010). Immunoglobulin heavy chain diversity in Pteropid bats: Evidence for a diverse and highly specific antigen binding repertoire. *Immunogenetics* **62**:173–184.
- Barrette, R.W. *et al.* (2009). Discovery of swine as a host for the reston ebolavirus. *Science*

325:204–206.

- Barrientos, L.G. *et al.* (2004). In Vitro Evaluation of Cyanovirin-N Antiviral Activity, by Use of Lentiviral Vectors Pseudotyped with Filovirus Envelope Glycoproteins. *The Journal of Infectious Diseases* **189**:1440–1443.
- Baseler, L. *et al.* (2017). The Pathogenesis of Ebola Virus Disease. *Annual Review of Pathology: Mechanisms of Disease* [Online] **12**:387–418.
- Basler, C.F. (2015). Innate immune evasion by filoviruses. *Virology* **479–480**:122–130.
- Basler, C.F. *et al.* (2003). The Ebola Virus VP35 Protein Inhibits Activation of Interferon Regulatory Factor 3. *Journal of Virology* **77**:7945–7956.
- Bausch, D.G. *et al.* (2006). Marburg Hemorrhagic Fever Associated with Multiple Genetic Lineages of Virus. *New England Journal of Medicine* [Online] **355**:909–919.
- Becker, S. *et al.* (1992). Evidence for occurrence of filovirus antibodies in humans and imported monkeys: do subclinical filovirus infections occur worldwide? *Medical Microbiology and Immunology* **181**:43–55.
- Becker, S., Spiess, M. and Klenk, H.D. (1995). The asialoglycoprotein receptor is a potential liver-specific receptor for Marburg virus. *Journal of General Virology* **76**:393–399.
- Becquart, P. *et al.* (2010). High prevalence of both humoral and cellular immunity to Zaire ebolavirus among rural populations in Gabon. *PLoS ONE* **5**.
- Bedford, T. and Malik, H.S. (2016). Did a Single Amino Acid Change Make Ebola Virus More Virulent? *Cell* [Online] **167**:892–894.
- Bengtsson, K.L. *et al.* (2016). Matrix-M adjuvant enhances antibody, cellular and protective immune responses of a Zaire Ebola/Makona virus glycoprotein (GP) nanoparticle vaccine in mice. *Vaccine* **34**.
- Beniac, D.R. and Timothy, B.F. (2017). Structure of the Ebola virus glycoprotein spike within the virion envelope at 11 angstrom resolution. *Scientific Reports* [Online] **7**:1–8.
- Bentley, E. *et al.* (2016). Ebolavirus pseudotypes as antigen surrogates for serological studies. *International Journal of Infectious Diseases* **53**:123.
- Biedenkopf, N. *et al.* (2016). RNA Binding of Ebola Virus VP30 Is Essential for Activating Viral Transcription. *Journal of Virology* **90**:7481–7496.
- Bixler, S.L. *et al.* (2018). Efficacy of favipiravir (T-705) in nonhuman primates infected with Ebola virus or Marburg virus. *Antiviral Research* **151**:97–104.
- Bornholdt, Z.A. *et al.* (2016). Host-primed Ebola virus GP exposes a hydrophobic NPC1

receptor-binding pocket, revealing a target for broadly neutralizing antibodies. *mBio* **7**.

- Bortz, R.H. *et al.* (2020). A virion-based assay for glycoprotein thermostability reveals key determinants of filovirus entry and its inhibition. *bioRxiv* [Online]:2020.02.25.965772.
- Bottcher-Friebertshauser, E. *et al.* (2010). Cleavage of Influenza Virus Hemagglutinin by Airway Proteases TMPRSS2 and HAT Differs in Subcellular Localization and Susceptibility to Protease Inhibitors. *Journal of Virology* **84**:5605–5614.
- Bower, H. and Glynn, J.R. (2017). A systematic review and meta-analysis of seroprevalence surveys of ebolavirus infection. *Scientific Data* **4**:1–9.
- Bramble, M.S. *et al.* (2018). Pan-Filovirus Serum Neutralizing Antibodies in a Subset of Congolese Ebola Virus Infection Survivors. *The Journal of Infectious Diseases* [Online]:1–8.
- Bray, M. (2001). The role of the type I interferon response in the resistance of mice of filovirus infection. *Journal of General Virology* **82**:1365–1373.
- Bray, M. and Geisbert, T.W. (2005). Ebola virus: The role of macrophages and dendritic cells in the pathogenesis of Ebola hemorrhagic fever. *The International Journal of Biochemistry & Cell Biology* [Online] **37**:1560–1566.
- Brecher, M. *et al.* (2012). Cathepsin Cleavage Potentiates the Ebola Virus Glycoprotein To Undergo a Subsequent Fusion-Relevant Conformational Change. *Journal of Virology* [Online] **86**:364–372.
- Brinkmann, C. *et al.* (2016). The Tetherin Antagonism of the Ebola Virus Glycoprotein Requires an Intact Receptor-Binding Domain and Can Be Blocked by GP1-Specific Antibodies. *Journal of Virology* [Online] **90**:11075–11086.
- Broadhurst, M.J. *et al.* (2015). ReEBOV Antigen Rapid Test kit for point-of-care and laboratory-based testing for Ebola virus disease: a field validation study. *The Lancet* **386**.
- Broadhurst, M.J., Brooks, T.J.G. and Pollock, R. (2016). Diagnosis of Ebola Virus Disease : Past , Present , and Future. **29**:773–793.
- Brook, C.E. *et al.* (2019). Disentangling serology to elucidate henipa- and filovirus transmission in Madagascar fruit bats. *Journal of Animal Ecology*:1–16.
- Brown, J.F. *et al.* (2018). Anti-ebola virus antibody levels in convalescent plasma and viral load after plasma infusion in patients with ebola virus disease. *Journal of Infectious Diseases* **218**:555–562.

- Brunton, B. *et al.* (2019). TIM-1 serves as a receptor for ebola virus in vivo, enhancing viremia and pathogenesis. *PLoS Neglected Tropical Diseases* **13**:1–20.
- Burk, R. *et al.* (2016). Neglected filoviruses. *FEMS Microbiology Reviews* **40**:494–519.
- Bwaka, M.A. *et al.* (1999). Ebola Hemorrhagic Fever in Kikwit, Democratic Republic of the Congo: Clinical Observations in 103 Patients. *The Journal of Infectious Diseases* **179**:S1–S7.
- Cantoni, D. *et al.* (2016). Risks Posed by Reston, the Forgotten Ebolavirus. *mSphere* **1**.
- Cantoni, D. and Rossman, J.S. (2018). Ebolaviruses: New roles for old proteins. *PLoS Neglected Tropical Diseases* **12**:1–17.
- Cardile, A.P. *et al.* (2016). Antiviral therapeutics for the treatment of Ebola virus infection. *Current Opinion in Pharmacology* **30**:138–143.
- Carette, J.E. *et al.* (2011). Ebola virus entry requires the cholesterol transporter Niemann–Pick C1. *Nature* [Online] **477**:340–343.
- Carnell, G.W. *et al.* (2015). Pseudotype-based neutralization assays for influenza: A systematic analysis. *Frontiers in Immunology* **6**:1–17.
- Carstea, E.D. *et al.* (1997). Niemann-Pick C1 Disease Gene: Homology to Mediators of Cholesterol Homeostasis. *Science* [Online] **277**:228 LP – 231.
- Cell Biolabs Inc. QuickTiter™ Lentivirus Titer Kit.
- Chan, S.Y. *et al.* (2000). Distinct Mechanisms of Entry by Envelope Glycoproteins of Marburg and Ebola (Zaire) Viruses. *Journal of Virology* **74**:4933–4937.
- Chan, S.Y. *et al.* (2001). Folate receptor- α is a cofactor for cellular entry by Marburg and Ebola viruses. *Cell* **106**:117–126.
- Chen, S. *et al.* (2013). Intestinal glucuronidation protects against chemotherapy-induced toxicity by irinotecan (CPT-11). *Proceedings of the National Academy of Sciences of the United States of America* **110**:19143–19148.
- Chernomordik, L. V and Zimmerberg, J. (1995). Bending membranes to the task: structural intermediates in bilayer fusion. *Current Opinion in Structural Biology* [Online] **5**:541–547.
- Cherpillod, P. *et al.* (2016). Ebola virus disease diagnosis by real-time RT-PCR: A comparative study of 11 different procedures. *Journal of Clinical Virology* [Online] **77**:9–14.
- Chertow, D.S. *et al.* (2014). Ebola Virus Disease in West Africa — Clinical Manifestations and Management. *New England Journal of Medicine* [Online] **371**:2054–2057.
- Chertow, D.S., Uyeki, T.M. and Dupont, H.L. (2015). Loperamide therapy for voluminous

- diarrhea in ebola virus disease. *Journal of Infectious Diseases* **211**:1036–1037.
- Clark, D.J. *et al.* (2018). The current landscape of nucleic acid tests for filovirus detection. *Journal of Clinical Virology* **103**:27–36.
- Coller, B.A.G. *et al.* (2017). Clinical development of a recombinant Ebola vaccine in the midst of an unprecedented epidemic. *Vaccine* **35**.
- Cook, J.D. and Lee, J.E. (2013). The Secret Life of Viral Entry Glycoproteins: Moonlighting in Immune Evasion. *PLOS Pathogens* [Online] **9**:e1003258.
- Corti, D. *et al.* (2016). Protective monotherapy against lethal Ebola virus infection by a potently neutralizing antibody. *Science* **351**:1339–1342.
- Cote, M. *et al.* (2012). Small molecule inhibitor reveal Niemann-Pick C1 is essential for Ebolavirus infection. *Nature* **477**:344–348.
- D.Simpson *et al.* (1978). Ebola haemorrhagic fever in Sudan, 1976. Report of a WHO/International Study Team. *Bulletin of the World Health Organization* [Online] **56**:247–270.
- Dahlmann, F. *et al.* (2015). Analysis of Ebola Virus Entry into Macrophages. *Journal of Infectious Diseases* **212**.
- Davey, R.T. *et al.* (2016). A randomized, controlled trial of ZMapp for ebola virus infection. *New England Journal of Medicine* **375**:1448–1456.
- Davidson, E. *et al.* (2015). Mechanism of Binding to Ebola Virus Glycoprotein by the ZMapp, ZMAb, and MB-003 Cocktail Antibodies. *Journal of Virology* [Online] **89**:10982–10992.
- Davis, C.W. *et al.* (2019). Longitudinal Analysis of the Human B Cell Response to Ebola Virus Infection. *Cell* **177**:1566-1582.e17.
- Dean, C.L. *et al.* (2020). Characterization of Ebola convalescent plasma donor immune response and psoralen treated plasma in the United States. *Transfusion*:1–8.
- Demaison, C. *et al.* (2002). High-level transduction and gene expression in hematopoietic repopulating cells using a human immunodeficiency virus type 1-based lentiviral vector containing an internal spleen focus forming virus promoter. *Human Gene Therapy* **13**:803–813.
- Deng, X. *et al.* (2020). Metagenomic sequencing with spiked primer enrichment for viral diagnostics and genomic surveillance. *Nature Microbiology*.
- Derveni, M. *et al.* (2019). Optimisation and characterisation of a VSV-core pseudotype system for the serological study of emerging viruses.
- Dhama, K. *et al.* (2018). Advances in Designing and Developing Vaccines, Drugs, and

- Therapies to Counter Ebola Virus. *Frontiers in Immunology* [Online] **9**.
- Diallo, B. *et al.* (2016). Resurgence of Ebola Virus Disease in Guinea Linked to a Survivor with Virus Persistence in Seminal Fluid for More Than 500 Days. *Clinical Infectious Diseases* **63**:1353–1356.
- Diamond, M.S. and Farzan, M. (2013). The broad-spectrum antiviral functions of IFIT and IFITM proteins. *Nature Reviews Immunology* **13**:46–57.
- Diehl, W.E. *et al.* (2016). Ebola Virus Glycoprotein with Increased Infectivity Dominated the 2013–2016 Epidemic. *Cell* **167**.
- Dolnik, O. *et al.* (2004). Ectodomain shedding of the glycoprotein GP of Ebola virus. *EMBO Journal* **23**:2175–2184.
- Dolnik, O., Kolesnikova, L. and Becker, S. (2008). Filoviruses: Interactions with the host cell. *Cellular and Molecular Life Sciences* **65**:756–776.
- Dormitzer, P.R., Grandi, G. and Rappuoli, R. (2012). Structural vaccinology starts to deliver. *Nature Reviews Microbiology* **10**:807–813.
- Dovih, P. *et al.* (2019). Filovirus-reactive antibodies in humans and bats in Northeast India imply zoonotic spillover Mossel, E. ed. *PLOS Neglected Tropical Diseases* [Online] **13**:e0007733.
- Edwards, J.K. *et al.* (2015). Interpretation of Negative Molecular Test Results in Patients With Suspected or Confirmed Ebola Virus Disease: Report of Two Cases. *Open Forum Infectious Diseases* [Online] **2**.
- Ehrhardt, S.A. *et al.* (2019). Polyclonal and convergent antibody response to Ebola virus vaccine rVSV-ZEBOV. *Nature Medicine* **25**:1589–1600.
- El-Duah, P. *et al.* (2019). Development of a whole-virus elisa for serological evaluation of domestic livestock as possible hosts of human coronavirus nl63. *Viruses* **11**.
- Elliott, L.H., Kiley, M.P. and McCormick, J.B. (1985). Descriptive analysis of Ebola virus proteins. *Virology* **147**:169–176.
- Escudero-Pérez, B. *et al.* (2016). Broadly neutralizing antibodies from human survivors target a conserved site in the ebola virus glycoprotein hr2-mper region. *Cell* [Online] **10**:1–11.
- Escudero-Pérez, B. *et al.* (2014). Shed GP of Ebola Virus Triggers Immune Activation and Increased Vascular Permeability. *PLoS Pathogens* **10**.
- Ewer, K. *et al.* (2016). A Monovalent Chimpanzee Adenovirus Ebola Vaccine Boosted with MVA. *New England Journal of Medicine* [Online] **374**:1635–1646.
- Ewer, K. *et al.* (2014). Multiplex evaluation of influenza neutralizing antibodies with

- potential applicability to in-field serological studies. *Expert review of molecular diagnostics* [Online] **212**:51–58.
- Falasca, L. *et al.* (2015). Molecular mechanisms of Ebola virus pathogenesis: focus on cell death. *Cell death and differentiation* **22**.
- Fan, J. *et al.* (2020). Proximity proteomics identifies novel function of Rab14 in trafficking of Ebola virus matrix protein VP40. *Biochemical and Biophysical Research Communications*:10–15.
- Faye, Oumar *et al.* (2015). Use of Viremia to Evaluate the Baseline Case Fatality Ratio of Ebola Virus Disease and Inform Treatment Studies: A Retrospective Cohort Study. *PLoS Medicine* **12**.
- Feldmann, H. *et al.* (1992). Marburg virus, a filovirus: messenger RNAs, gene order, and regulatory elements of the replication cycle. *Virus Research* [Online] **24**:1–19.
- Feldmann, H. *et al.* (1999). The glycoproteins of Marburg and Ebola virus and their potential roles in pathogenesis. *Archives of Virology, Supplement*:159–169.
- Feldmann, H., Klenk, H.-D. and Sanchez, A. (1993). Molecular biology and evolution of filoviruses. In: Kaaden, O.-R., Eichhorn, W. and Czerny, C.-P. eds. Vienna: Springer Vienna, pp. 81–100.
- Feldmann, H., Slenczka, W. and Klenk, H.-D. (1996). Emerging and reemerging of filoviruses. In: Schwarz, T. F. and Siegl, G. eds. Vienna: Springer Vienna, pp. 77–100.
- Ferrara, F. and Temperton, N. (2018). Pseudotype Neutralization Assays: From laboratory Bench to Data Analysis. *Methods and Protocols* [Online] **1**.
- Ferreira, C.B. *et al.* (2020). Lentiviral Vector Production Titer Is Not Limited in HEK293T by Induced Intracellular Innate Immunity. *Molecular Therapy - Methods and Clinical Development* **17**:209–219.
- Fields, B.N., Knipe, D.M. and Howley, P.M. (2013). *Fields Virology*. Philadelphia: Wolters Kluwer Health/Lippincott Williams & Wilkins.
- Fleming, T.H. (2019). Bat migration. *Encyclopedia of Animal Behavior*:605–610.
- Flyak, A.I. *et al.* (2016). Cross-Reactive and Potent Neutralizing Antibody Responses in Human Survivors of Natural Ebolavirus Infection. *Cell* **164**.
- Flyak, A.I. *et al.* (2015). Mechanism of Human Antibody-Mediated Neutralization of Marburg Virus. *Cell* [Online] **160**:893–903.
- Forbes, K.M. *et al.* (2019). Bombali virus in mops condylurus bat, kenya. *Emerging Infectious Diseases* **25**:955–957.
- Formella, M. and Gatherer, D. (2016). The serology of Ebolavirus - A wider geographical

- range, a wider genus of viruses or a wider range of virulence? *Journal of General Virology* **97**:3120–3130.
- Freedman, L.P. *et al.* (2015). Reproducibility: Changing the policies and culture of cell line authentication. *Nature Methods* **12**:493–497.
- Fuentes, S. *et al.* (2020). Human Antibody Repertoire following Ebola Virus Infection and Vaccination. *iScience* **23**.
- Furuyama, W. *et al.* (2016). Discovery of an antibody for pan-ebolavirus therapy. *Scientific reports* [Online] **6**:20514.
- Furuyama, W. and Marzi, A. (2019). Ebola Virus: Pathogenesis and Countermeasure Development. *Annual Review of Virology* **6**:435–458.
- Fusco, M.L. *et al.* (2015). Protective mAbs and Cross-Reactive mAbs Raised by Immunization with Engineered Marburg Virus GPs. *PLoS Pathogens* **11**.
- Gallaher, W.R. and Garry, R.F. (2015). Modeling of the ebola virus delta peptide reveals a potential lytic sequence motif. *Viruses* **7**:285–305.
- Garbutt, M. *et al.* (2004). Properties of Replication-Competent Vesicular Stomatitis Virus Vectors Expressing Glycoproteins of Filoviruses and Arenaviruses. *Journal of Virology* **78**:5458–5465.
- Gardy, J.L. and Loman, N.J. (2018). Towards a genomics-informed, real-time, global pathogen surveillance system. *Nature Reviews Genetics* [Online] **19**:9–20.
- Gatherer, D. (2014). The 2014 Ebola virus disease outbreak in West Africa. *Journal of General Virology* **95**:1619–1624.
- Gaudinski, M.R. *et al.* (2019). Safety, tolerability, pharmacokinetics, and immunogenicity of the therapeutic monoclonal antibody mAb114 targeting Ebola virus glycoprotein (VRC 608): an open-label phase 1 study. *The Lancet* **393**:889–898.
- Gear, J.S. *et al.* (1975). Outbreak of Marburg virus disease in Johannesburg. *British Medical Journal* [Online] **4**:489 LP – 493.
- Geisbert, T.W. *et al.* (2000). Apoptosis induced in vitro and in vivo during infection by Ebola and Marburg viruses. *Laboratory Investigation* **80**:171–186.
- Geisbert, Thomas W *et al.* (2003). Mechanisms Underlying Coagulation Abnormalities in Ebola Hemorrhagic Fever: Overexpression of Tissue Factor in Primate Monocytes/Macrophages Is a Key Event. *The Journal of Infectious Diseases* [Online] **188**:1618–1629.
- Geisbert, Thomas W., Hensley, L.E., Larsen, T., *et al.* (2003). Pathogenesis of Ebola Hemorrhagic Fever in *Cynomolgus* Macaques: Evidence that Dendritic Cells are Early

- and Sustained Targets of Infection. *American Journal of Pathology* [Online] **163**:2347–2370.
- Geisbert, Thomas W., Hensley, L.E., Jahrling, P.B., *et al.* (2003). Treatment of Ebola virus infection with a recombinant inhibitor of factor VIIa/tissue factor: A study in rhesus monkeys. *Lancet* **362**:1953–1958.
- Geisbert, T.W. *et al.* (2008). Vesicular stomatitis virus-based Ebola vaccine is well-tolerated and protects immunocompromised nonhuman primates. *PLoS Pathogens* **4**.
- Geisbert, T.W. and Jahrling, P.B. (1995). Differentiation of filoviruses by electron microscopy. *Virus Research* **39**:129–150.
- Geraerts, M. *et al.* (2006). Comparison of lentiviral vector titration methods. *BMC Biotechnology* **6**:1–10.
- Gilchuk, P. *et al.* (2020). Analysis of a Therapeutic Antibody Cocktail Reveals Determinants for Cooperative and Broad Ebolavirus Article Analysis of a Therapeutic Antibody Cocktail Reveals Determinants for Cooperative and Broad Ebolavirus Neutralization. :1–16.
- Gilchuk, P. *et al.* (2018). Multifunctional Pan-ebolavirus Antibody Recognizes a Site of Broad Vulnerability on the Ebolavirus Glycoprotein. *Immunity* **49**:363-374.e10.
- Giotis, E.S. *et al.* (2019). Entry of the bat influenza H17N10 virus into mammalian cells is enabled by the MHC class II HLA-DR receptor. *Nature Microbiology* [Online] **4**:2035–2038.
- Gire, S.K. *et al.* (2014). Genomic surveillance elucidates Ebola virus origin and transmission during the 2014 outbreak. *Science* **345**:1369–1372.
- Glynn, J.R. *et al.* (2017). Asymptomatic infection and unrecognised Ebola virus disease in Ebola-affected households in Sierra Leone: a cross-sectional study using a new non-invasive assay for antibodies to Ebola virus. *The Lancet Infectious Diseases* **17**:645–653.
- Gnirß, K. *et al.* (2012). Cathepsins B and L activate Ebola but not Marburg virus glycoproteins for efficient entry into cell lines and macrophages independent of TMPRSS2 expression. *Virology* [Online] **424**:3–10.
- Goldstein, T. *et al.* (2018). The discovery of Bombali virus adds further support for bats as hosts of ebolaviruses. *Nature Microbiology* [Online]:1.
- Gong, X. *et al.* (2016). Structural insights into the Niemann-Pick C1 (NPC1)-mediated cholesterol transfer and ebola infection. *Cell* [Online] **165**:1467–1478.

- González-Hernández, M. *et al.* (2018). A GXXXA Motif in the Transmembrane Domain of the Ebola Virus Glycoprotein Is Required for Tetherin Antagonism. *Journal of Virology* **92**:e00403-18.
- Gonzalez, J.P. *et al.* (2000). Ebola and Marburg virus antibody prevalence in selected populations of the Central African Republic. *Microbes and Infection* **2**:39–44.
- Gregory, S.M. *et al.* (2011). Structure and function of the complete internal fusion loop from Ebolavirus glycoprotein 2. *Proceedings of the National Academy of Sciences of the United States of America* **108**:11211–11216.
- van Griensven, J. *et al.* (2016). Evaluation of Convalescent Plasma for Ebola Virus Disease in Guinea. *New England Journal of Medicine* **374**.
- Grifoni, A. *et al.* (2016). Genetic diversity in Ebola virus: Phylogenetic and in silico structural studies of Ebola viral proteins. *Asian Pacific Journal of Tropical Medicine* [Online] **9**:337–343.
- Grimm, S.K. and Ackerman, M.E. (2013). Vaccine design: Emerging concepts and renewed optimism. *Current Opinion in Biotechnology* **24**:1078–1088.
- Groseth, A. *et al.* (2009). The Ebola virus ribonucleoprotein complex: A novel VP30-L interaction identified. *Virus Research* **140**:8–14.
- Guenno, B. Le *et al.* (1995). Isolation and virus partial characterisation of strain of Ebola. *The Lancet* **345**:1271–1274.
- Güven, E. *et al.* (2014). Non-specific binding in solid phase immunoassays for autoantibodies correlates with inflammation markers. *Journal of Immunological Methods* [Online] **403**:26–36.
- Haines, K.M. *et al.* (2012). Chinese hamster ovary cell lines selected for resistance to ebolavirus glycoprotein mediated infection are defective for NPC1 expression. *Virology* [Online] **432**:20–28.
- Halpin, K. *et al.* (2011). Pteropid bats are confirmed as the reservoir hosts of henipaviruses: A comprehensive experimental study of virus transmission. *American Journal of Tropical Medicine and Hygiene* **85**:946–951.
- Han, B.A. *et al.* (2016). Undiscovered Bat Hosts of Filoviruses. *PLoS Neglected Tropical Diseases* **10**:1–10.
- Han, Z., Ruthel, G., *et al.* (2020). Angiomotin Regulates Budding and Spread of Ebola Virus. *Journal of Biological Chemistry*:jbc.AC120.013171.
- Han, Z. *et al.* (2003). Biochemical and Functional Characterization of the Ebola Virus VP24 Protein: Implications for a Role in Virus Assembly and Budding. *Journal of Virology*

77:1793–1800.

- Han, Z., Dash, S., *et al.* (2020). Modular mimicry and engagement of the Hippo pathway by Marburg virus VP40: Implications for filovirus biology and budding. *PLOS Pathogens* [Online] **16**:e1008231.
- Harty, R.N. *et al.* (2000). A PPxY motif within the VP40 protein of Ebola virus interacts physically and functionally with a ubiquitin ligase: Implications for filovirus budding. *Proceedings of the National Academy of Sciences of the United States of America* **97**:13871–13876.
- Hashiguchi, T. *et al.* (2015). Structural Basis for Marburg Virus Neutralization by a Cross-Reactive Human Antibody. *Cell* **160**.
- Hausmann, S. *et al.* (1999). The Versatility of Paramyxovirus RNA Polymerase Stuttering. *Journal of Virology* **73**:5568–5576.
- Haydon, D.T. *et al.* (2002). Identifying reservoirs of infection: A conceptual and practical challenge. *Emerging Infectious Diseases* **8**:1468–1473.
- He, J. *et al.* (2017). Ebola Virus Delta Peptide Is a Viroporin. *Journal of Virology* **91**:1–14.
- Heckman, K.L. and Pease, L.R. (2007). Gene splicing and mutagenesis by PCR-driven overlap extension. *Nat Protoc* [Online] **2**:924–932.
- Henao-Restrepo, A.M. *et al.* (2015). Efficacy and effectiveness of an rVSV-vectored vaccine expressing Ebola surface glycoprotein: interim results from the Guinea ring vaccination cluster-randomised trial. *The Lancet* **386**.
- Henao-Restrepo, A.M. *et al.* (2017). Efficacy and effectiveness of an rVSV-vectored vaccine in preventing Ebola virus disease: final results from the Guinea ring vaccination, open-label, cluster-randomised trial (Ebola ça Suffit!). *The Lancet* **389**.
- Hensley, L.E. *et al.* (2002). Proinflammatory response during Ebola virus infection of primate models: Possible involvement of the tumor necrosis factor receptor superfamily. *Immunology Letters* **80**:169–179.
- Higashimoto, T. *et al.* (2007). The woodchuck hepatitis virus post-transcriptional regulatory element reduces readthrough transcription from retroviral vectors. *Gene Therapy* [Online] **14**:1298–1304.
- Hoenen, T. *et al.* (2012). Inclusion Bodies Are a Site of Ebolavirus Replication. *Journal of Virology* **86**:11779–11788.
- Hoenen, T. *et al.* (2010). Oligomerization of Ebola Virus VP40 Is Essential for Particle Morphogenesis and Regulation of Viral Transcription. *Journal of Virology* **84**:7053–7063.

- Hoenen, T., Groseth, A. and Feldmann, H. (2019). Therapeutic strategies to target the Ebola virus life cycle. *Nature Reviews Microbiology* [Online] **17**:593–606.
- Hoffmann, M. *et al.* (2019). Analysis of Resistance of Ebola Virus Glycoprotein-Driven Entry Against MDL28170, An Inhibitor of Cysteine Cathepsins. *Pathogens* **8**.
- Holmes, E.C. *et al.* (2016). The evolution of Ebola virus: Insights from the 2013-2016 epidemic. *Nature* **538**.
- Howell, K.A. *et al.* (2016). Antibody Treatment of Ebola and Sudan Virus Infection via a Uniquely Exposed Epitope within the Glycoprotein Receptor-Binding Site. *Cell Reports* **15**:1514–1526.
- Howell, K.A. *et al.* (2017). Cooperativity Enables Non-neutralizing Antibodies to Neutralize Ebolavirus. *Cell Reports* [Online] **19**:413–424.
- Huang, I.C. *et al.* (2011). Distinct patterns of IFITM-mediated restriction of filoviruses, SARS coronavirus, and influenza A virus. *PLoS Pathogens* **7**.
- Huang, Y. *et al.* (2002). The assembly of Ebola virus nucleocapsid requires virion-associated proteins 35 and 24 and posttranslational modification of nucleoprotein. *Molecular Cell* **10**:307–316.
- Hume, A.J. and Mühlberger, E. (2019). Distinct Genome Replication and Transcription Strategies within the Growing Filovirus Family. *Journal of Molecular Biology* [Online] **431**:4290–4320.
- Hunt, C.L., Lennemann, N.J. and Maury, W. (2012). Filovirus entry: A novelty in the viral fusion world. *Viruses* **4**:258–275.
- Illynykh, P.A. *et al.* (2016). Chimeric Filoviruses for Identification and Characterization of Monoclonal Antibodies. *Journal of Virology* **90**.
- Illynykh, P.A. *et al.* (2018). Ebolavirus Chimerization for the Development of a Mouse Model for Screening of Bundibugyo-Specific Antibodies. *Journal of Infectious Diseases* **218**:S418–S422.
- Ito, H. *et al.* (2001). Ebola Virus Glycoprotein: Proteolytic Processing, Acylation, Cell Tropism, and Detection of Neutralizing Antibodies. *Journal of Virology* **75**:1576–1580.
- Jacobson, R.H. (1998). *Validation of Serological Assays for Diagnosis of Infectious Diseases*. Vol. 17.
- Jae, L.T. and Brummelkamp, T.R. (2015). Emerging intracellular receptors for hemorrhagic fever viruses. *Trends in Microbiology* **23**.
- Jahrling, P.B. *et al.* (1990). Preliminary report: isolation of Ebola virus from monkeys

- imported to USA. *The Lancet* **335**:502–505.
- Jain, S. and Baranwal, M. (2019). Conserved peptide vaccine candidates containing multiple Ebola nucleoprotein epitopes display interactions with diverse HLA molecules. *Medical Microbiology and Immunology* [Online] **208**:227–238.
- Jasenosky, L.D. *et al.* (2019). The FDA-Approved Oral Drug Nitazoxanide Amplifies Host Antiviral Responses and Inhibits Ebola Virus. *iScience* **19**:1279–1290.
- Jasenosky, L.D. and Kawaoka, Y. (2004). Filovirus budding. *Virus Research* **106**:181–188.
- Jeffers, S. a, Sanders, D.A. and Sanchez, A. (2002). Covalent Modifications of the Ebola Virus Glycoprotein Covalent Modifications of the Ebola Virus Glycoprotein. *Journal of Virology* **76**:12463–12472.
- Ji, X. *et al.* (2005). Mannose-binding lectin binds to Ebola and Marburg envelope glycoproteins, resulting in blocking of virus interaction with DC-SIGN and complement-mediated virus neutralization. *Journal of General Virology* **86**:2535–2542.
- John, S.P. *et al.* (2007). Ebola Virus VP30 Is an RNA Binding Protein. *Journal of Virology* **81**:8967–8976.
- Johnson, E.D. *et al.* (1996). Characterization of a new Marburg virus isolated from a 1987 fatal case in Kenya BT - Imported Virus Infections. In: Schwarz, T. F. and Siegl, G. eds. Vienna: Springer Vienna, pp. 101–114.
- Johnson, K.M. *et al.* (1978). Ebola haemorrhagic fever in Zaire, 1976. *Bulletin of the World Health Organization* [Online] **56**:271–93.
- Jones, D.T. and Cozzetto, D. (2014). DISOPRED3: precise disordered region predictions with annotated protein-binding activity. *Bioinformatics* [Online] **31**:857–863.
- Jones, M.E.B. *et al.* (2015). Experimental inoculation of egyptian rousette bats (*Rousettus aegyptiacus*) with viruses of the ebolavirus and marburgvirus genera. *Viruses* **7**.
- Kalenga, O.I. *et al.* (2019). The ongoing Ebola epidemic in the Democratic Republic of Congo, 2018-2019. *New England Journal of Medicine* **381**:373–383.
- Kaletsky, R.L. *et al.* (2009). Tetherin-mediated restriction of filovirus budding is antagonized by the Ebola glycoprotein. **2008**.
- Kaletsky, R.L., Simmons, G. and Bates, P. (2007). Proteolysis of the Ebola Virus Glycoproteins Enhances Virus Binding and Infectivity. *Journal of Virology* [Online] **81**:13378–13384.
- Karan, L.S. *et al.* (2019). Bombali Virus in Mops condylurus Bats, Guinea. *Emerging infectious diseases* [Online] **25**:1774–1775.

- Kash, J.C. *et al.* (2006). Global Suppression of the Host Antiviral Response by Ebola- and Marburgviruses: Increased Antagonism of the Type I Interferon Response Is Associated with Enhanced Virulence. *Journal of Virology* **80**:3009–3020.
- Keck, Z.-Y. *et al.* (2016). Macaque Monoclonal Antibodies Targeting Novel Conserved Epitopes within Filovirus Glycoprotein. *Journal of Virology* **90**.
- Kelley, L.A. *et al.* (2015). The Phyre2 web portal for protein modeling, prediction and analysis. *Nature Protocols* [Online] **10**:845.
- Kemenesi, G. *et al.* (2015). Genetic characterization of a novel picornavirus detected in *miniopterus schreibersii* bats. *Journal of General Virology* **96**:815–821.
- Kemenesi, G. *et al.* (2018). Re-emergence of Lloviu virus in *Miniopterus schreibersii* bats, Hungary, 2016 correspondence. *Emerging Microbes and Infections* [Online] **7**:67–70.
- Khurana, S. *et al.* (2016). Human antibody repertoire after VSV-Ebola vaccination identifies novel targets and virus-neutralizing IgM antibodies. *Nature Medicine* **22**:1439–1447.
- King, B. *et al.* (2016). Troubleshooting methods for the generation of novel pseudotyped viruses. *Future Virology* **11**:47–59.
- King, Liam B *et al.* (2018). The Marburgvirus-Neutralizing Human Monoclonal Antibody MR191 Targets a Conserved Site to Block Virus Receptor Binding. *Cell Host & Microbe* [Online] **23**:101-109.e4.
- King, Liam B., West, B.R., *et al.* (2018). The structural basis for filovirus neutralization by monoclonal antibodies. *Current Opinion in Immunology* **53**:196–202.
- Kinsley, R., Scott, S.D. and Daly, J.M. (2016). Controlling equine influenza: Traditional to next generation serological assays. *Veterinary Microbiology* [Online] **187**:15–20.
- Kirchdoerfer, R.N. *et al.* (2016). The Ebola Virus VP30-NP Interaction Is a Regulator of Viral RNA Synthesis. *PLoS Pathogens* **12**:1–22.
- Kissling, R.E. *et al.* (1968). Agent of Disease Contracted from Green Monkeys. *Science* [Online] **160**:888 LP – 890.
- Klasse, P.J. and Sattentau, Q.J. (2002). Occupancy and mechanism in antibody-mediated neutralization of animal viruses. *Journal of General Virology* **83**:2091–2108.
- Ko, W.C. *et al.* (2020). Arguments in favour of remdesivir for treating SARS-CoV-2 infections. *International Journal of Antimicrobial Agents* **55**:10–12.
- Kock, R.A. *et al.* (2019). Searching for the source of Ebola: the elusive factors driving its spillover into humans during the West African outbreak of 2013-2016. *Revue scientifique et technique (International Office of Epizootics)* **38**:113–122.

- Koehler, A. *et al.* (2018). Analysis of the multifunctionality of Marburg virus VP40. *Journal of General Virology* **99**:1614–1620.
- Kondratowicz, A.S. *et al.* (2011). T-cell immunoglobulin and mucin domain 1 (TIM-1) is a receptor for Zaire Ebolavirus and Lake Victoria Marburgvirus. *Proceedings of the National Academy of Sciences* [Online] **108**:8426–8431.
- Konduru, K. *et al.* (2018). High degree of correlation between Ebola virus BSL-4 neutralization assays and pseudotyped VSV BSL-2 fluorescence reduction neutralization test. *Journal of Virological Methods* **254**:1–7.
- Kopecky, S.A. and Lyles, D.S. (2003). The Cell-Rounding Activity of the Vesicular Stomatitis Virus Matrix Protein Is due to the Induction of Cell Death. *Journal of Virology* [Online] **77**:5524 LP – 5528.
- Kraan, H. *et al.* (2014). Development of Thermostable Lyophilized Inactivated Polio Vaccine. :2618–2629.
- Krähling, V. *et al.* (2016). Development of an antibody capture ELISA using inactivated Ebola Zaire Makona virus. *Medical Microbiology and Immunology* **205**.
- Krammer, F. *et al.* (2013). Chimeric Hemagglutinin Influenza Virus Vaccine Constructs Elicit Broadly Protective Stalk-Specific Antibodies. *Journal of Virology* **87**:6542–6550.
- Kuhn, J.H. *et al.* (2006). Conserved receptor-binding domains of Lake Victoria marburgvirus and Zaire ebolavirus bind a common receptor. *Journal of Biological Chemistry* **281**:15951–15958.
- Kuhn, J.H. *et al.* (2019). New filovirus disease classification and nomenclature. *Nature Reviews Microbiology*.
- Kumar, S., Stecher, G. and Tamura, K. (2016). MEGA7: Molecular Evolutionary Genetics Analysis Version 7.0 for Bigger Datasets. *Molecular Biology and Evolution* [Online] **33**:1870–1874.
- Kuroda, M. *et al.* (2014). A polymorphism of the TIM-1 IgV domain: Implications for the susceptibility to filovirus infection. *Biochemical and Biophysical Research Communications* **455**.
- Kuroda, M. *et al.* (2015). Interaction between TIM-1 and NPC1 Is Important for Cellular Entry of Ebola Virus. *Journal of Virology* **89**.
- Kutner, R.H., Zhang, X.Y. and Reiser, J. (2009). Production, concentration and titration of pseudotyped HIV-1-based lentiviral vectors. *Nature Protocols* **4**:495–505.
- Kuzmina, N.A. *et al.* (2018). Antibody-Dependent Enhancement of Ebola Virus Infection by Human Antibodies Isolated from Survivors. *Cell Reports* [Online] **24**:1802-1815.e5.

- Laing, E.D. *et al.* (2018). Serologic Evidence of Fruit Bat Exposure to Filoviruses, Singapore, 2011–2016. *Emerging Infectious Disease journal* [Online] **24**.
- Lambe, T., Bowyer, G. and Ewer, K.J. (2017). A review of phase I trials of Ebola virus vaccines: What can we learn from the race to develop novel vaccines? *Philosophical Transactions of the Royal Society B: Biological Sciences* **372**.
- Landeras-Bueno, S. *et al.* (2019). Sudan ebolavirus VP35-NP crystal structure reveals a potential target for pan-filovirus treatment. *mBio* **10**:1–13.
- Languon, S. and Quaye, O. (2019). Filovirus Disease Outbreaks: A Chronological Overview. *Virology: Research and Treatment* **10**.
- Ledgerwood, J.E. *et al.* (2011). A replication defective recombinant Ad5 vaccine expressing Ebola virus GP is safe and immunogenic in healthy adults. **29**:304–313.
- Ledgerwood, J.E. *et al.* (2017). Chimpanzee Adenovirus Vector Ebola Vaccine. *New England Journal of Medicine* [Online] **376**:928–938.
- Lee, Jeffrey E. *et al.* (2008). Complex of a Protective Antibody with Its Ebola Virus GP Peptide Epitope: Unusual Features of a V λ x Light Chain. *Journal of Molecular Biology* **375**:202–216.
- Lee, Jeffrey E *et al.* (2008). Structure of the Ebola virus glycoprotein bound to an antibody from a human survivor. *Nature* [Online] **454**:177–82.
- Lee, J.E., Road, T.P. and Jolla, L. (2010). Ebolavirus glycoprotein structure and mechanism of entry Jeffrey. *North* **4**:621–635.
- Lee, S. *et al.* (2012). A virion-based assay for glycoprotein thermostability reveals key determinants of filovirus entry and its inhibition. *Journal of Chemical Information and Modeling* [Online] **53**:1689–1699.
- Leroy, E.M. *et al.* (2005). Fruit bats as reservoirs of Ebola virus. *Nature* [Online] **438**:575–576.
- Lester, S. *et al.* (2019). Middle East respiratory coronavirus (MERS-CoV) spike (S) protein vesicular stomatitis virus pseudoparticle neutralization assays offer a reliable alternative to the conventional neutralization assay in human seroepidemiological studies. *Access Microbiology* **1**.
- Leung, D.W. *et al.* (2010). Structural basis for dsRNA recognition and interferon antagonism by Ebola VP35. **17**.
- Li, Q. *et al.* (2018). Current status on the development of pseudoviruses for enveloped viruses. *Reviews in Medical Virology* **28**:1–10.
- Li, W. *et al.* (2005). Bats Are Natural Reservoirs of SARS-Like Coronaviruses. *Science*

- [Online] **310**:676 LP – 679.
- Lier, C., Becker, S. and Biedenkopf, N. (2017). Dynamic phosphorylation of Ebola virus VP30 in NP-induced inclusion bodies. *Virology* [Online] **512**:39–47.
- Liu, Y. and Harty, R.N. (2010). Viral and host proteins that modulate filovirus budding. *Future Virology* **5**:481–491.
- Lizée, G. *et al.* (2003). Real-time quantitative reverse transcriptase-polymerase chain reaction as a method for determining lentiviral vector titers and measuring transgene expression. *Human Gene Therapy* **14**:497–507.
- Loi, P. *et al.* (2008). Freeze-dried somatic cells direct embryonic development after nuclear transfer. *PLoS ONE* **3**:8–13.
- Long, J. *et al.* (2015). Antiviral therapies against Ebola and other emerging viral diseases using existing medicines that block virus entry. *F1000Research* [Online] **4**:30.
- Luczkowiak, J. *et al.* (2018). Broad Neutralizing Activity Against Ebolaviruses Lacking the Mucin-Like Domain in Convalescent Plasma Specimens from Patients with Ebola Virus Disease. *Journal of Infectious Diseases* **218**:S574–S581.
- Luczkowiak, J. *et al.* (2016). Specific neutralizing response in plasma from convalescent patients of Ebola Virus Disease against the West Africa Makona variant of Ebola virus. *Virus Research* **213**:224–229.
- Ma, Y.K. and Khan, A.S. (2009). Evaluation of different RT enzyme standards for quantitation of retroviruses using the single-tube fluorescent product-enhanced reverse transcriptase assay. *Journal of Virological Methods* **157**:133–140.
- MacNeil, A. *et al.* (2011). Filovirus outbreak detection and surveillance: Lessons from bundibugyo. *Journal of Infectious Diseases* **204**:761–767.
- MacNeil, A., Reed, Z. and Rollin, P.E. (2011). Serologic cross-reactivity of human IgM and IgG antibodies to five species of Ebola virus. *PLoS Neglected Tropical Diseases* **5**.
- Magro, L. *et al.* (2017). Paper-based RNA detection and multiplexed analysis for Ebola virus diagnostics. *Scientific Reports* **7**:1–9.
- Mahanty, S. *et al.* (2003). Cutting Edge: Impairment of Dendritic Cells and Adaptive Immunity by Ebola and Lassa Viruses. *The Journal of Immunology* **170**:2797–2801.
- Makiala, S. *et al.* (2019). Clinical evaluation of quicknavitm-ebola in the 2018 outbreak of ebola virus disease in the democratic republic of the congo. *Viruses* **11**.
- Malm, M. *et al.* (2020). Evolution from adherent to suspension – systems biology of HEK293 cell line development. :1–39.
- Malvy, D. *et al.* (2019). Ebola virus disease. *The Lancet* **393**:936–948.

- Manicassamy, B. *et al.* (2007). Characterization of Marburg virus glycoprotein in viral entry. *Virology* **358**:79–88.
- Marasco, W.A. and Sui, J. (2007). The growth and potential of human antiviral monoclonal antibody therapeutics. *Nature Biotechnology* **25**:1421–1434.
- Markosyan, R.M. *et al.* (2016). Induction of Cell-Cell Fusion by Ebola Virus Glycoprotein: Low pH Is Not a Trigger. *PLoS Pathogens* **12**.
- Markotter, W. *et al.* (2020). Bat-borne viruses in Africa: a critical review. *Journal of Zoology*:1–22.
- Martin, B. *et al.* (2016). Filovirus proteins for antiviral drug discovery: A structure/function analysis of surface glycoproteins and virus entry. *Antiviral Research* **135**.
- Martines, R.B., Ng, Dianna L., *et al.* (2015). Tissue and cellular tropism, pathology and pathogenesis of Ebola and Marburg viruses. *Journal of Pathology* **235**:153–174.
- Martinez, O. *et al.* (2011). Impact of Ebola mucin-like domain on antiglycoprotein antibody responses induced by Ebola virus-like particles. *Journal of Infectious Diseases* **204**:825–832.
- Martini, G.A. (1969). Marburg agent disease: In man. *Transactions of The Royal Society of Tropical Medicine and Hygiene* [Online] **63**:295–302.
- Maruyama, Junki *et al.* (2014). Characterization of the Envelope Glycoprotein of a Novel Filovirus, Lloviu Virus. *Journal of Virology* **88**:99–109.
- Maruyama, T. *et al.* (1999). Ebola Virus Can Be Effectively Neutralized by Antibody Produced in Natural Human Infection. *Journal of Virology* **73**:6024–6030.
- Marzi, A., Reinheckel, T. and Feldmann, H. (2012). Cathepsin B & L Are Not Required for Ebola Virus Replication. *PLoS Neglected Tropical Diseases* **6**.
- Mather, S. *et al.* (2013). Current progress with serological assays for exotic emerging/re-emerging viruses. *Future Virology* **8**:745–755.
- Mather, S.T. *et al.* (2014). Lyophilisation of influenza, rabies and Marburg lentiviral pseudotype viruses for the development and distribution of a neutralisation -assay-based diagnostic kit. *Journal of Virological Methods* [Online] **210**:51–58.
- Matsuno, K. *et al.* (2010). Different Potential of C-Type Lectin-Mediated Entry between Marburg Virus Strains. *Journal of Virology* **84**:5140–5147.
- Mbala-Kingebeni, P. *et al.* (2019). 2018 Ebola virus disease outbreak in Équateur Province, Democratic Republic of the Congo: a retrospective genomic characterisation. *The Lancet Infectious Diseases* [Online].
- McLellan, J.S. *et al.* (2011). Design and characterization of epitope-scaffold immunogens

- that present the motavizumab epitope from respiratory syncytial virus. *Journal of Molecular Biology* **409**:853–866.
- McMullan, L.K. *et al.* (2019). Characterisation of infectious Ebola virus from the ongoing outbreak to guide response activities in the Democratic Republic of the Congo: a phylogenetic and in vitro analysis. *The Lancet Infectious Diseases* **19**:1023–1032.
- Mehedi, M. *et al.* (2011). A New Ebola Virus Nonstructural Glycoprotein Expressed through RNA Editing. *Journal of Virology* **85**:5406–5414.
- Mehedi, M. *et al.* (2013). Ebola Virus RNA Editing Depends on the Primary Editing Site Sequence and an Upstream Secondary Structure. *PLoS Pathogens* **9**.
- Mendoza, E.J., Qiu, X. and Kobinger, G.P. (2016). Progression of Ebola therapeutics during the 2014-2015 outbreak. *Trends in Molecular Medicine* **22**.
- Mendoza, E.J., Racine, T. and Kobinger, G.P. (2017). The ongoing evolution of antibody-based treatments for Ebola virus infection. *Immunotherapy* **9**:435–450.
- Messaoudi, I., Amarasinghe, G.K. and Basler, C.F. (2015). Filovirus pathogenesis and immune evasion: insights from Ebola virus and Marburg virus. *Nature Reviews Microbiology* **13**.
- Metzger, W.G. and Vivas-Martínez, S. (2018). Questionable efficacy of the rVSV-ZEBOV Ebola vaccine. *The Lancet* [Online] **391**:1021.
- Meyer, M., Malherbe, D.C. and Bukreyev, A. (2019). Can Ebola Virus Vaccines Have Universal Immune Correlates of protection? *Trends in Microbiology* [Online] **27**:8–16.
- Miller, E.H. *et al.* (2012). Ebola virus entry requires the host-programmed recognition of an intracellular receptor. *The EMBO journal* [Online] **31**:1947–60.
- Millet, J.K. and Whittaker, G.R. (2015). Host cell proteases: Critical determinants of coronavirus tropism and pathogenesis. *Virus Research* [Online] **202**:120–134.
- Mingo, R.M. *et al.* (2015). Ebola Virus and Severe Acute Respiratory Syndrome Coronavirus Display Late Cell Entry Kinetics: Evidence that Transport to NPC1 + Endolysosomes Is a Rate-Defining Step. *Journal of Virology* **89**:2931–2943.
- Miranda, M. *et al.* (1987). Seroepidemiological study of filovirus related to Ebola in the Philippines. :425–426.
- Mire, C.E. *et al.* (2015). Single-dose attenuated Vesiculovax vaccines protect primates against Ebola Makona virus. *Nature* **520**.
- Mirza, M.U. *et al.* (2019). Perspectives towards antiviral drug discovery against Ebola virus. *Journal of Medical Virology* **91**:2029–2048.

- Misasi, J. *et al.* (2012). Filoviruses Require Endosomal Cysteine Proteases for Entry but Exhibit Distinct Protease Preferences. *Journal of Virology* **86**:3284–3292.
- Misasi, J. *et al.* (2016). Structural and molecular basis for Ebola virus neutralization by protective human antibodies. *Science* **351**:1343–1346.
- Misasi, J. and Sullivan, N.J. (2014). Camouflage and misdirection: The full-on assault of ebola virus disease. *Cell* **159**.
- Modrof, J., Becker, S. and Mühlberger, E. (2003). Ebola Virus Transcription Activator VP30 Is a Zinc-Binding Protein. *Journal of Virology* **77**:3334–3338.
- Mohan, G.S. *et al.* (2012). Antigenic Subversion: A Novel Mechanism of Host Immune Evasion by Ebola Virus. *PLoS Pathogens* **8**.
- Mohan, Gopi S. *et al.* (2015). Less Is More: Ebola Virus Surface Glycoprotein Expression Levels Regulate Virus Production and Infectivity. *Journal of Virology* **89**:1205–1217.
- Molesti, E. *et al.* (2014). Multiplex evaluation of influenza neutralizing antibodies with potential applicability to in-field serological studies. *Journal of Immunology Research* **2014**.
- Möller, P. *et al.* (2005). Homo-Oligomerization of Marburgvirus VP35 Is Essential for Its Function in Replication and Transcription. *Journal of Virology* **79**:14876–14886.
- Moritz, C.P. *et al.* (2019). Reducing the risk of misdiagnosis of indirect ELISA by normalizing serum-specific background noise: The example of detecting anti-FGFR3 autoantibodies. *Journal of Immunological Methods* [Online] **466**:52–56.
- Mühlberger, E. *et al.* (1999). Comparison of the Transcription and Replication Strategies of Marburg Virus and Ebola Virus by Using Artificial Replication Systems. *Journal of Virology* **73**:2333–2342.
- Mühlberger, E. (2007). Filovirus replication and transcription. *Future Virology* **2**:205–215.
- Mühlberger, E. *et al.* (1998). Three of the Four Nucleocapsid Proteins of Marburg Virus, NP, VP35, and L, Are Sufficient To Mediate Replication and Transcription of Marburg Virus-Specific Monocistronic Minigenomes. *Journal of Virology* **72**:8756–8764.
- Mulangu, S. *et al.* (2019). A Randomized, Controlled Trial of Ebola Virus Disease Therapeutics. *New England Journal of Medicine* [Online]:NEJMoa1910993.
- Mulangu, S., Alfonso, Vivian H, *et al.* (2018). Serologic Evidence of Ebolavirus Infection in a Population With No History of Outbreaks in the Democratic Republic of the Congo. *The Journal of Infectious Diseases* [Online] **217**:529–537.
- Munis, A.M. *et al.* (2018). Characterization of Antibody Interactions with the G Protein of Vesicular Stomatitis Virus Indiana Strain and Other Vesiculovirus G Proteins. *Journal*

of Virology **92**:1–14.

- Murin, C.D. *et al.* (2014). Structures of protective antibodies reveal sites of vulnerability on Ebola virus. *Proceedings of the National Academy of Sciences of the United States of America* [Online] **111**:17182–7.
- Murphy, C.N. (2019). Recent Advances in the Diagnosis and Management of Ebola Virus Disease. *Clinical Microbiology Newsletter* [Online] **41**:185–189.
- Nakayama, E. *et al.* (2011). Antibody-dependent enhancement of marburg virus infection. *Journal of Infectious Diseases* **204**.
- Nakayama, E. *et al.* (2010). Enzyme-linked immunosorbent assay for detection of filovirus species-specific antibodies. *Clinical and Vaccine Immunology* **17**:1723–1728.
- Naldini, L. *et al.* (1996). In vivo gene delivery and stable transduction of nondividing cells by a lentiviral vector. *Science* **272**:263–267.
- Ndungo, E. *et al.* (2016). A Single Residue in Ebola Virus Receptor NPC1 Influences Cellular Host Range in Reptiles Duprex, W. P. ed. *mSphere* [Online] **1**:e00007-16.
- Negredo, A. *et al.* (2011). Discovery of an ebolavirus-like filovirus in europe. *PLoS Pathogens* **7**:1–8.
- Neil, S.J.D., Zang, T. and Bieniasz, P.D. (2008). Tetherin inhibits retrovirus release and is antagonized by HIV-1 Vpu. *Nature* **451**:425–430.
- Nelson, C.D.S. *et al.* (2007). Different mechanisms of antibody-mediated neutralization of parvoviruses revealed using the Fab fragments of monoclonal antibodies. *Virology* [Online] **361**:283–293.
- Ng, M. *et al.* (2014). Cell entry by a novel European filovirus requires host endosomal cysteine proteases and Niemann-Pick C1. *Virology* **468**.
- Ng, M. *et al.* (2015). Filovirus receptor NPC1 contributes to species-specific patterns of ebolavirus susceptibility in bats. *eLife* **4**.
- Nie, J. *et al.* (2020). Establishment and validation of a pseudovirus neutralization assay for SARS-CoV-2. *Emerging Microbes and Infections* **9**:680–686.
- Nireesha, G. *et al.* (2013). Lyophilization/Freeze Drying -A Review. *Ijntps* **3**:87–98.
- Niwa, H., Yamamura, K. and Miyazaki, J. (1991). Efficient selection for high-expression transfectants with a novel eukaryotic vector. **108**:193–199.
- Noda, T. *et al.* (2002). Ebola Virus VP40 Drives the Formation of Virus-Like Filamentous Particles Along with GP. *Journal of Virology* **76**:4855–4865.
- Nys, H.M. De *et al.* (2018). Survey of Ebola Viruses in Frugivorous and Insectivorous Bats in Guinea, Cameroon, and the Democratic Republic of the Congo, 2015–2017.

- Emerging Infectious Disease journal* [Online] **24**.
- Oestereich, L. *et al.* (2014). Successful treatment of advanced Ebola virus infection with T-705 (favipiravir) in a small animal model. *Antiviral Research* **105**.
- Olejnik, J. *et al.* (2013). Ebola Virus Does Not Block Apoptotic Signaling Pathways. *Journal of Virology* **87**:5384–5396.
- Olinger, G.G. *et al.* (2012). Delayed treatment of Ebola virus infection with plant-derived monoclonal antibodies provides protection in rhesus macaques. *Proceedings of the National Academy of Sciences of the United States of America* **109**:18030–18035.
- Ooi, A. *et al.* (2016). A guide to transient expression of membrane proteins in HEK-293 cells for functional characterization. *Frontiers in Physiology* **7**:1–15.
- Osterdahl, M. *et al.* (2020). Detecting SARS-CoV-2 at Point of Care: Preliminary Data Comparing Loop-Mediated Isothermal Amplification (LAMP) to PCR. *SSRN Electronic Journal*.
- Oswald, W.B. *et al.* (2007). Neutralizing Antibody Fails to Impact the Course of Ebola Virus Infection in Monkeys. **3**:1–5.
- Pallesen, J. *et al.* (2016). Structures of Ebola virus GP and sGP in complex with therapeutic antibodies. *Nature Microbiology* **1**.
- Panchal, R.G. *et al.* (2003). In vivo oligomerization and raft localization of Ebola virus protein VP40 during vesicular budding. *Proceedings of the National Academy of Sciences of the United States of America* **100**:15936–15941.
- Di Paola, N. *et al.* (2020). Viral genomics in Ebola virus research. *Nature Reviews Microbiology* [Online] **18**.
- Pascal, K.E. *et al.* (2018). Development of Clinical-Stage Human Monoclonal Antibodies That Treat Advanced Ebola Virus Disease in Nonhuman Primates. *The Journal of Infectious Diseases* [Online] **218**:S612–S626.
- Paweska, J.T. *et al.* (2016). Experimental inoculation of Egyptian fruit bats (*Rousettus aegyptiacus*) with Ebola virus. *Viruses* **8**:1–11.
- Perry, D.L. *et al.* (2018). Ebola Virus Localization in the Macaque Reproductive Tract during Acute Ebola Virus Disease. *American Journal of Pathology* [Online] **188**:550–558.
- Pettini, F., Trezza, A. and Spiga, O. (2018). *A Focus on Ebola Virus Polymerase: Structure, Functions and Antiviral Therapies*. [Online]. Elsevier Inc.
- Phan, J.C. *et al.* (2016). Lateral Flow Immunoassays for Ebola Virus Disease Detection in Liberia. *Journal of Infectious Diseases* **214**:S222–S228.

- Pizzato, M. *et al.* (2009). A one-step SYBR Green I-based product-enhanced reverse transcriptase assay for the quantitation of retroviruses in cell culture supernatants. *Journal of Virological Methods* **156**:1–7.
- Powell, T.J. *et al.* (2012). Pseudotyped Influenza A Virus as a Vaccine for the Induction of Heterotypic Immunity. *Journal of Virology* [Online] **86**:13397–13406.
- Prins, K.C. *et al.* (2010). Basic Residues within the Ebolavirus VP35 Protein Are Required for Its Viral Polymerase Cofactor Function. *Journal of Virology* **84**:10581–10591.
- Prins, K.C., Cárdenas, W.B. and Basler, C.F. (2009). Ebola Virus Protein VP35 Impairs the Function of Interferon Regulatory Factor-Activating Kinases IKK ϵ and TBK-1. *Journal of Virology* **83**:3069–3077.
- Qiu, X. *et al.* (2011). Characterization of Zaire ebolavirus glycoprotein-specific monoclonal antibodies. *Clinical Immunology* [Online] **141**:218–227.
- Qiu, X. *et al.* (2014). Reversion of advanced Ebola virus disease in nonhuman primates with ZMapp. *Nature*.
- Qiu, X. *et al.* (2016). Two-mAb cocktail protects macaques against the Makona variant of Ebola virus. *Science Translational Medicine* **8**.
- Raftery, P. *et al.* (2018). Establishing Ebola Virus Disease (EVD) diagnostics using GeneXpert technology at a mobile laboratory in Liberia: Impact on outbreak response, case management and laboratory systems strengthening. *PLoS Neglected Tropical Diseases* **12**:1–20.
- Ram, E. *et al.* (2019). First Evidence of Antibodies Against Lloviu Virus in Schreiber ' s Bent-Winged Insectivorous Bats Demonstrate a Wide Circulation of the Virus in Spain.
- Ramanan, P. *et al.* (2012). Structural basis for Marburg virus VP35-mediated immune evasion mechanisms. *Proceedings of the National Academy of Sciences of the United States of America* **109**:20661–20666.
- Reed, D.S. *et al.* (2004). Depletion of Peripheral Blood T Lymphocytes and NK Cells During the Course of Ebola Hemorrhagic Fever in Cynomolgus Macaques. *Viral Immunology* [Online] **17**:390–400.
- Reed, L.J. and Muench, H. (1938). A Simple Method of Estimating Fifty Per Cent Endpoints. [Online]. Vol. 27.
- Reid, S.P. *et al.* (2006). Ebola Virus VP24 Binds Karyopherin α 1 and Blocks STAT1 Nuclear Accumulation. *Journal of Virology* **80**:5156–5167.
- Rijal, P. *et al.* (2019). Therapeutic Monoclonal Antibodies for Ebola Virus Infection Derived

- from Vaccinated Humans. *Cell Reports* **27**:172-186.e7.
- Rimoin, A.W. *et al.* (2018). Ebola Virus Neutralizing Antibodies Detectable in Survivors of the Yambuku, Zaire Outbreak 40 Years after Infection. *Journal of Infectious Diseases* **217**:223–231.
- Ristanovic, E. *et al.* (2020). A Forgotten Episode of Marburg Virus Disease: Belgrade, Yugoslavia, 1967. *Microbiology and Molecular Biology Reviews* [Online] **84**:e00095-19.
- Ruedas, J.B. *et al.* (2017). Spontaneous Mutation at Amino Acid 544 of the Ebola Virus Glycoprotein Potentiates Virus Entry and Selection in Tissue Culture. *Journal of Virology* **91**.
- Ruscic, J. *et al.* (2019). Lentiviral Vector Purification Using Nanofiber Ion-Exchange Chromatography. *Molecular Therapy - Methods and Clinical Development* [Online] **15**:52–62.
- Rutten, L. *et al.* (2020). Structure-Based Design of Prefusion-Stabilized Filovirus Glycoprotein Trimers. *Cell Reports* **30**:4540-4550.e3.
- S.Y., C. *et al.* (2000). Distinct mechanisms of entry by envelope glycoproteins of Marburg and Ebola (Zaire) viruses. *Journal of Virology* [Online] **74**:4933–4937.
- Saitou, N. and Nei, M. (1987). The neighbor-joining method: a new method for reconstructing phylogenetic trees. *Molecular Biology and Evolution* [Online] **4**:406–425.
- Sakurai, Y. *et al.* (2015). Two-pore channels control Ebola virus host cell entry and are drug targets for disease treatment. *Science* **347**.
- Salata, C. *et al.* (2019). Ebola Virus Entry: From Molecular Characterization to Drug Discovery. *Viruses* **11**.
- Sanchez, a *et al.* (1998). Biochemical analysis of the secreted and virion glycoproteins of Ebola virus. *Journal of virology* **72**:6442–6447.
- Sanchez, A. *et al.* (1993). Sequence analysis of the Ebola virus genome: organization, genetic elements, and comparison with the genome of Marburg virus. *Virus Research* **29**:215–240.
- Sanchez, A. *et al.* (1989). The nucleoprotein gene of ebola virus: Cloning, sequencing, and in vitro expression. *Virology* **170**:81–91.
- Saphire, E.O., Schendel, S.L., Gunn, B.M., *et al.* (2018). Antibody-mediated protection against Ebola virus. *Nature Immunology* **19**.
- Saphire, E.O., Schendel, S.L., Fusco, M.L., *et al.* (2018). Systematic Analysis of Monoclonal

- Antibodies against Ebola Virus GP Defines Features that Contribute to Protection. *Cell* **174**:938-952.e13.
- Schornerberg, K.L. *et al.* (2009). Alpha5beta1-integrin controls ebolavirus entry by regulating endosomal cathepsins. *Proceedings of the National Academy of Sciences of the United States of America* [Online] **106**:8003–8008.
- Schudt, G. *et al.* (2013). Live-cell imaging of Marburg virus-infected cells uncovers actin-dependent transport of nucleocapsids over long distances. *Proceedings of the National Academy of Sciences of the United States of America* **110**:14402–14407.
- Schuh, A.J. *et al.* (2019). Antibody-mediated virus neutralization is not a universal mechanism of Marburg, Ebola, or zika virus clearance in Egyptian rousette bats. *Journal of Infectious Diseases* **219**:1716–1721.
- Scianimanico, S. *et al.* (2000). Membrane association induces a conformational change in the Ebola virus matrix protein. *EMBO Journal* **19**:6732–6741.
- Scott, S. *et al.* (2012). The use of equine influenza pseudotypes for serological screening. *Journal of molecular and genetic medicine : an international journal of biomedical research* [Online] **6**:304–8.
- Sears, J.F., Repaske, R. and Khan, A.S. (1999). Improved Mg²⁺-based reverse transcriptase assay for detection of primate retroviruses. *Journal of Clinical Microbiology* **37**:1704–1708.
- Semper, A.E. *et al.* (2016). Performance of the GeneXpert Ebola Assay for Diagnosis of Ebola Virus Disease in Sierra Leone: A Field Evaluation Study. *PLoS Medicine* **13**:1–15.
- Shi, M. *et al.* (2018). The evolutionary history of vertebrate RNA viruses. *Nature* **556**.
- Shimajima, M., Ikeda, Y. and Kawaoka, Y. (2007). The Mechanism of Axl-Mediated Ebola Virus Infection. *The Journal of Infectious Diseases* **196**:S259–S263.
- Shin, S., Salvay, D.M. and Shea, L.D. (2010). Lentivirus delivery by adsorption to tissue engineering scaffolds. *Journal of Biomedical Materials Research - Part A* **93**:1252–1259.
- Shu, T. *et al.* (2019). Ebola virus VP35 has novel NTPase and helicase-like activities. *Nucleic Acids Research* **47**:5837–5851.
- Siegert, Rudolf (1972). Marburg Virus. In: Appel, M. J. G., Gillespie, J. H. and Siegert, R eds. Vienna: Springer Vienna, pp. 97–153.
- Simmons, J.A. *et al.* (2016). Ebolavirus Glycoprotein Directs Fusion through NPC1 + Endolysosomes. *Journal of Virology* [Online] **90**:605–610.
- Sinn, P.L. *et al.* (2003). Lentivirus Vectors Pseudotyped with Filoviral Envelope

- Glycoproteins Transduce Airway Epithelia from the Apical Surface Independently of Folate Receptor Alpha. *Journal of Virology* **77**:5902–5910.
- Sissoko, D. *et al.* (2016). Experimental Treatment with Favipiravir for Ebola Virus Disease (the JIKI Trial): A Historically Controlled, Single-Arm Proof-of-Concept Trial in Guinea. *PLoS Medicine* **13**.
- Smither, S.J. *et al.* (2014). Post-exposure efficacy of Oral T-705 (Favipiravir) against inhalational Ebola virus infection in a mouse model. *Antiviral Research* **104**.
- Sozhamannan, S. *et al.* (2015). Evaluation of signature erosion in ebola virus due to genomic drift and its impact on the performance of diagnostic assays. *Viruses* **7**:3130–3154.
- Spence, J.S. *et al.* (2016). Direct visualization of Ebola virus fusion triggering in the endocytic pathway. *mBio* **7**:1–12.
- Steffen, I. *et al.* (2019). Serologic Prevalence of Ebola Virus in Equatorial Africa. *Emerging Infectious Diseases* **25**:911–918.
- Steffen, I. *et al.* (2020). Seroreactivity against Marburg or related filoviruses in West and Central Africa. *Emerging Microbes and Infections* **9**:124–128.
- Ströher, U. *et al.* (2001). Infection and Activation of Monocytes by Marburg and Ebola Viruses. *Journal of Virology* **75**:11025–11033.
- Suder, E. *et al.* (2018). The vesicular stomatitis virus-based Ebola virus vaccine: From concept to clinical trials. *Human Vaccines and Immunotherapeutics* **14**:2107–2113.
- Suhrbier, A. and La Linn, M. (2003). Suppression of antiviral responses by antibody-dependent enhancement of macrophage infection. *Trends in Immunology* **24**:165–168.
- Sullivan, N.J. *et al.* (2005). Ebola Virus Glycoprotein Toxicity Is Mediated by a Dynamin-Dependent Protein-Trafficking Pathway. *Journal of Virology* **79**:547–553.
- Swanepoel, R. *et al.* (1996). Experimental Inoculation of Plants and Animals with Ebola Virus. *Emerging Infectious Diseases* **2**:321–325.
- Swanepoel, R. *et al.* (2007). Studies of reservoir hosts for Marburg virus. *Emerging Infectious Diseases* **13**:1847–1851.
- Takada, a *et al.* (1997). A system for functional analysis of Ebola virus glycoprotein. *Proceedings of the National Academy of Sciences of the United States of America* **94**:14764–14769.
- Takada, A. *et al.* (2003). Antibody-Dependent Enhancement of Ebola Virus Infection. **77**:7539–7544.

- Takada, A. *et al.* (2000). Downregulation of β 1 integrins by Ebola virus glycoprotein: Implication for virus entry. *Virology* **278**:20–26.
- Takada, A. *et al.* (2007). Epitopes Required for Antibody-Dependent Enhancement of Ebola Virus Infection. *The Journal of Infectious Diseases* **196**:S347–S356.
- Takada, A. (2012). Filovirus tropism: Cellular molecules for viral entry. *Frontiers in Microbiology* **3**:1–9.
- Takada, A. *et al.* (2001). Infectivity-Enhancing Antibodies to Ebola Virus Glycoprotein. *Journal of Virology* **75**:2324–2330.
- Takadate, Y. *et al.* (2020). Niemann-Pick C1 Heterogeneity of Bat Cells Controls Filovirus Tropism. *Cell reports* [Online] **30**:308-319.e5.
- Takahashi, K. *et al.* (2013). DNA Topoisomerase 1 Facilitates the Transcription and Replication of the Ebola Virus Genome. *Journal of Virology* [Online] **87**:8862 LP – 8869.
- Takamatsu, Y. *et al.* (2020). The Integrity of the YxxL Motif of Ebola Virus VP24 Is Important for the Transport of Nucleocapsid-Like Structures and for the Regulation of Viral RNA Synthesis. *Journal of Virology* **94**:1–19.
- Tamura, K., Nei, M. and Kumar, S. (2004). Prospects for inferring very large phylogenies by using the neighbor-joining method. *Proceedings of the National Academy of Sciences of the United States of America* [Online] **101**:11030 LP – 11035.
- Tchesnokov, E.P. *et al.* (2019). Mechanism of inhibition of ebola virus RNA-dependent RNA polymerase by remdesivir. *Viruses* **11**:1–16.
- Tchesnokov, E.P. *et al.* (2018). Recombinant RNA-Dependent RNA Polymerase Complex of Ebola Virus. *Scientific Reports* **8**:1–9.
- Temperton, N.J. *et al.* (2007). A sensitive retroviral pseudotype assay for influenza H5N1-neutralizing antibodies. *Influenza and Other Respiratory Viruses* [Online] **1**:105–112.
- Temperton, N.J., Wright, E. and Scott, S.D. (2015). Retroviral Pseudotypes – from scientific tools to clinical utility. *Encyclopedia of Life Sciences* [Online]:1–21.
- Terato, K. *et al.* (2016). Preventing further misuse of the ELISA technique and misinterpretation of serological antibody assay data. *Vaccine* [Online] **34**:4643–4644.
- Thiagarajah, J.R., Donowitz, M. and Verkman, A.S. (2015). Secretory diarrhoea: mechanisms and emerging therapies. *Nature Reviews Gastroenterology & Hepatology* [Online] **12**:446–457.
- Timmins, J. *et al.* (2003). Oligomerization and polymerization of the filovirus matrix protein VP40. *Virology* **312**:359–368.

- Timmins, J. *et al.* (2001). Vesicular release of Ebola virus matrix protein VP40. *Virology* **283**:1–6.
- Tong, S. *et al.* (2012). A distinct lineage of influenza A virus from bats. *Proceedings of the National Academy of Sciences of the United States of America* **109**:4269–4274.
- Tong, S. *et al.* (2013). New World Bats Harbor Diverse Influenza A Viruses. *PLoS Pathogens* **9**.
- Towner, J.S. *et al.* (2009). Isolation of genetically diverse Marburg viruses from Egyptian fruit bats. *PLoS Pathogens* **5**.
- Urbanowicz, R.A. *et al.* (2016). Human Adaptation of Ebola Virus during the West African Outbreak. *Cell* **167**:1079-1087.e5.
- Venkatraman, N. *et al.* (2018). Vaccines against Ebola virus. *Vaccine* [Online] **36**:5454–5459.
- Vermeire, J. *et al.* (2012). Quantification of Reverse Transcriptase Activity by Real-Time PCR as a Fast and Accurate Method for Titration of HIV, Lenti- and Retroviral Vectors. *PLoS ONE* **7**.
- Vidal, S. *et al.* (2019). Regulation of the Ebola Virus VP24 Protein by SUMO López, S. ed. *Journal of Virology* [Online] **94**:e01687-19.
- Volchkov, V E *et al.* (1998). Processing of the Ebola virus glycoprotein by the proprotein convertase furin. *Proceedings of the National Academy of Sciences of the United States of America* [Online] **95**:5762–7.
- Volchkov, V.E. *et al.* (2000). Proteolytic processing of Marburg virus glycoprotein. *Virology* **268**:1–6.
- Volchkov, V.E. *et al.* (2001). Recovery of Infectious Ebola Virus from Complementary DNA: RNA Editing of the GP Gene and Viral Cytotoxicity. *Science* [Online] **291**:1965 LP – 1969.
- Volchkov, Viktor E., Volchkova, V.A., *et al.* (1998). Release of viral glycoproteins during Ebola virus infection. *Virology* **245**:110–119.
- Volchkov, V.E. *et al.* (1995). GP mRNA of Ebola Virus Is Edited by the Ebola Virus Polymerase and by T7 and Vaccinia Virus Polymerases1. *Virology* **214**:421–430.
- Volchkova, V.A. *et al.* (1998). The nonstructural small glycoprotein sGP of ebola virus is secreted as an antiparallel-orientated homodimer. *Virology* **250**:408–414.
- Volchkova, V.A., Klenk, H.D. and Volchkov, V.E. (1999). Delta-peptide is the carboxy-terminal cleavage fragment of the nonstructural small glycoprotein sGP of Ebola virus. *Virology* **265**:164–171.

- Vuren, P.J. Van *et al.* (2016). Comparative Evaluation of the Diagnostic Performance of the Prototype Cepheid GeneXpert Ebola Assay Petrus. *Journal of Clinical Microbiology* **54**:359–367.
- Wahl-Jensen, V.M. *et al.* (2005). Effects of Ebola Virus Glycoproteins on Endothelial Cell Activation and Barrier Function. *Journal of Virology* [Online] **79**:10442 LP – 10450.
- Wan, Y. *et al.* (2020). Receptor Recognition by the Novel Coronavirus from Wuhan: an Analysis Based on Decade-Long Structural Studies of SARS Coronavirus Gallagher, T. ed. *Journal of Virology* [Online] **94**:e00127-20.
- Wang, Q. *et al.* (2015). Identification of an adeno-associated virus binding epitope for AVB sepharose affinity resin. *Molecular Therapy - Methods and Clinical Development* [Online] **2**:15040.
- Wang, W. (2000). *Lyophilization and Development of Solid Protein Pharmaceuticals*. Vol. 203.
- Wang, Yeming *et al.* (2020). Remdesivir in adults with severe COVID-19: a randomised, double-blind, placebo-controlled, multicentre trial. *The Lancet* [Online] **0**:1–10.
- Warren, T.K. *et al.* (2016). Therapeutic efficacy of the small molecule GS-5734 against Ebola virus in rhesus monkeys. *Nature* [Online] **531**:381–385.
- Watanabe, S. *et al.* (2007). Ebola Virus (EBOV) VP24 Inhibits Transcription and Replication of the EBOV Genome. *The Journal of Infectious Diseases* **196**:S284–S290.
- Watanabe, S. *et al.* (2000). Functional Importance of the Coiled-Coil of the Ebola Virus Glycoprotein. **74**:10194–10201.
- Watanabe, S., Noda, T. and Kawaoka, Y. (2006). Functional Mapping of the Nucleoprotein of Ebola Virus. *Journal of Virology* **80**:3743–3751.
- Watson, D.J. *et al.* (2002). Targeted transduction patterns in the mouse brain by lentivirus vectors pseudotyped with VSV, Ebola, Mokola, LCMV, or MuLV envelope proteins. *Molecular Therapy* **5**:528–537.
- Wec, A.Z. *et al.* (2017). Antibodies from a Human Survivor Define Sites of Vulnerability for Broad Protection against Ebolaviruses. *Cell* [Online] **169**:878-890.e15.
- Weidmann, M., Mühlberger, E. and Hufert, F.T. (2004). Rapid detection protocol for filoviruses. *Journal of Clinical Virology* **30**:94–99.
- Weik, M. *et al.* (2002). Ebola Virus VP30-Mediated Transcription Is Regulated by RNA Secondary Structure Formation. *Journal of Virology* **76**:8532–8539.
- Weissenhorn, W. *et al.* (1998). Crystal Structure of the Ebola Virus Membrane Fusion Subunit , GP2 , from the Envelope Glycoprotein Ectodomain. **2**:605–616.

- West, B.R. *et al.* (2019). Structural basis of broad ebolavirus neutralization by a human survivor antibody. *Nature Structural and Molecular Biology* [Online] **26**:204–212.
- Whitt, M.A. (2010). Generation of VSV pseudotypes using recombinant Δ G-VSV for studies on virus entry, identification of entry inhibitors, and immune responses to vaccines. *Journal of Virological Methods* [Online] **169**:365–374.
- Wijesinghe, K.J. *et al.* (2020). Mutation of Hydrophobic Residues in the C-terminal domain of the Marburg Virus matrix protein VP40 Disrupts Plasma Membrane Trafficking. *In transcript* **40**:1–15.
- Wilkinson, D.E. *et al.* (2017). Comparison of platform technologies for assaying antibody to Ebola virus. *Vaccine* **35**.
- Wilkinson, D.E. *et al.* (2015). Preliminary report WHO collaborative study to assess the suitability of interim standards for Ebola virus NAT assays. :1–47.
- Will, C. *et al.* (1993). Marburg virus gene 4 encodes the virion membrane protein, a type I transmembrane glycoprotein. *Journal of Virology* **67**:1203–1210.
- Wolkers, W.F., Tablin, F. and Crowe, J.H. (2002). From anhydrobiosis to freeze-drying of eukaryotic cells. *Comparative Biochemistry and Physiology - A Molecular and Integrative Physiology* **131**:535–543.
- Wonderly, B. *et al.* (2019). Comparative performance of four rapid Ebola antigen-detection lateral flow immunoassays during the 2014-2016 Ebola epidemic in West Africa. *PLoS ONE* **14**:1–14.
- Wong, G., Kobinger, G.P. and Qiu, X. (2014). Characterization of host immune responses in Ebola virus infections. *Expert Review of Clinical Immunology* [Online] **10**:781–790.
- Wool-Lewis, R.J. and Bates, P. (1998). Characterization of Ebola virus entry by using pseudotyped viruses: identification of receptor-deficient cell lines. *Journal of virology* [Online] **72**:3155–60.
- Wright, E. *et al.* (2009). A robust lentiviral pseudotype neutralisation assay for in-field serosurveillance of rabies and lyssaviruses in Africa. *Vaccine* [Online] **27**:7178–7186.
- Wright, E. *et al.* (2008). Investigating antibody neutralization of lyssaviruses using lentiviral pseudotypes: A cross-species comparison. *Journal of General Virology* **89**:2204–2213.
- Wright, E. *et al.* (2010). Virus neutralising activity of African fruit bat (*Eidolon helvum*) sera against emerging lyssaviruses. *Virology* [Online] **408**:183–189.
- Wu, Y. (2004). HIV-1 gene expression: Lessons from provirus and non-integrated DNA. *Retrovirology* **1**:1–10.

- Xiao, J.H. *et al.* (2018). Characterization of Influenza Virus Pseudotyped with Ebolavirus Glycoprotein García-Sastre, A. ed. *Journal of Virology* [Online] **92**:e00941-17.
- Xu, X. *et al.* (2020). Effective Treatment of Severe COVID-19 Patients with Tocilizumab. *chinaXiv*:1–12.
- Yamada, S. *et al.* (2006). Haemagglutinin mutations responsible for the binding of H5N1 influenza A viruses to human-type receptors. *Nature* **444**:378–382.
- Yang, X. Lou, Tan, C.W., Anderson, Danielle E., *et al.* (2019). Characterization of a filovirus (Měnglà virus) from Rousettus bats in China. *Nature Microbiology* **4**:390–395.
- Yang, X. Lou *et al.* (2017). Genetically diverse filoviruses in rousettus and eonycteris spp. Bats, China, 2009 and 2015. *Emerging Infectious Diseases* **23**:482–486.
- Yang, Z. *et al.* (1998). Distinct Cellular Interactions of Secreted and Transmembrane Ebola Virus Glycoproteins. *Science* [Online] **279**:1034 LP – 1037.
- Yang, Z.Y. *et al.* (2000). Identification of the Ebola virus glycoprotein as the main viral determinant of vascular cell cytotoxicity and injury. *Nature Medicine* **6**:886–889.
- Yeap, W.H. *et al.* (2016). CD16 is indispensable for antibody-dependent cellular cytotoxicity by human monocytes. *Scientific reports* [Online] **6**:34310.
- Yinda, C.K. *et al.* (2017). Highly diverse population of Picornaviridae and other members of the Picornavirales, in Cameroonian fruit bats. *BMC Genomics* [Online] **18**:249.
- Younan, P. *et al.* (2017). Ebola virus binding to Tim-1 on T lymphocytes induces a cytokine storm. *mBio* **8**:1–20.
- Yuan, J. *et al.* (2012). *Serological Evidence of Ebolavirus Infection in Bats, China*. [Online].
- Zampieri, C.A. *et al.* (2007). The ERK Mitogen-Activated Protein Kinase Pathway Contributes to Ebola Virus Glycoprotein-Induced Cytotoxicity. *Journal of Virology* **81**:1230–1240.
- Zapatero-Belinchón, F.J. *et al.* (2019). Characterization of the filovirus-resistant cell line SH-SY5Y reveals redundant role of cell surface entry factors. *Viruses* **11**.
- Zeitlin, L. *et al.* (2016). Antibody therapeutics for Ebola virus disease. *Current Opinion in Virology* [Online] **17**:45–49.
- Zhang, A.P.P. *et al.* (2012). The ebola virus interferon antagonist VP24 directly binds STAT1 and has a novel, pyramidal fold. *PLoS Pathogens* **8**.
- Zhang, C. *et al.* (2020). The cytokine release syndrome (CRS) of severe COVID-19 and Interleukin-6 receptor (IL-6R) antagonist Tocilizumab may be the key to reduce the mortality. *International Journal of Antimicrobial Agents* [Online]:105954.
- Zhang, M. *et al.* (2017). Freeze-drying of mammalian cells using trehalose: Preservation of

- DNA integrity. *Scientific Reports* **7**:1–10.
- Zhang, Q. *et al.* (2016). Potent neutralizing monoclonal antibodies against Ebola virus infection. *Scientific Reports* [Online] **6**:25856.
- Zhao, X. *et al.* (2017). Immunization-Elicited Broadly Protective Antibody Reveals Ebolavirus Fusion Loop as a Site of Vulnerability. *Cell* **169**.
- Zheng, H. and Yan, W. (2000). Epitope Swapping to Distinguish Transgenic from Endogenous Fibroblast Growth Factor Receptor Type 1. **28**:834–838.
- Zhu, L. *et al.* (2020). Ebola virus replication is regulated by the phosphorylation of viral protein VP35. *Biochemical and Biophysical Research Communications* **521**:687–692.
- Zhu, W. *et al.* (2019). The roles of ebola virus soluble glycoprotein in replication, pathogenesis, and countermeasure development. *Viruses* **11**.
- Ziegler, C.M. *et al.* (2019). *NEDD4 Family Ubiquitin Ligases Associate with LCMV Z's PPXY Domain and Are Required for Virus Budding, but Not via Direct Ubiquitination of Z*. Vol. 15.
- Zinzula, L. *et al.* (2019). Structures of Ebola and Reston Virus VP35 Oligomerization Domains and Comparative Biophysical Characterization in All Ebolavirus Species. *Structure* **27**:39-54.e6.
- Zufferey, R. *et al.* (1997). Multiply attenuated lentiviral vector achieves efficient gene delivery in vivo. *Nature Biotechnology* [Online] **15**:871–875.
- Zufferey, R. *et al.* (1998). Self-Inactivating Lentivirus Vector for Safe and Efficient In Vivo Gene Delivery. *Journal of Virology* [Online] **72**:9873 LP – 9880.

Appendix I - Envelope glycoprotein nucleotide sequences (5' – 3')

(virus abbreviation | species | virus isolate | accession number) *codon optimised

EBOV | *Zaire ebolavirus* | Ebola/Makona/GIN/2014/Kissidougou-C15 | KJ660346*

ATGGGCGTGACCGGAATCCTGCAGCTGCCAGAGACAGGTTCAAGCGGACCAGCTTCTTCCTGTGGGTGATCA
TCCTGTTCCAGCGGACCTTCAGCATCCCTCTGGGCGTGATCCACAACAGCACCTGCAGGTCTCCGACGTGGA
CAAGCTCGTGTGCCGGGACAAGCTGAGCAGCACCAACCAGCTGCGGAGCGTGGGCTGAACCTGGAAGGCAAC
GGCGTGGCCACCGATGTGCCAGCGCCACCAAGAGATGGGGCTTCAGATCCGGCGTGCCACCCAAGGTGGTGA
ACTACGAAGCCGGCGAGTGGGCCGAGAAGTGTACAACTGGAAAATCAAGAAGCCCGACGGCAGCGAGTGCCT
GCCTGCCGCTCCTGATGGCATCCGGGGCTTCCCAGATGCAGATACGTGCACAAGGTGTCCGGCACCAGGCCCC
TGTGCTGGCGACTTCGCCTTTCACAAAGAGGGCGCCTTTTCTGTACGACCGGCTCGCCAGCACCGTGATCT
ACCGGGGACCACCTTTGCCGAGGGCGTGGTGGCCTTCTGATCCTGCCCCAGGCCAAGAAGGACTTCTTCAG
CAGCCACCTCTGCGCGAGCCCGTGAACGCCACAGAAGATCCCAGCAGCGGCTACTACAGCACCCACATCAGA
TACCAGGCCACCGGCTTCGGCACCAACGAGACAGAGTACCTGTTCGAGGTGGACAACCTGACCTACGTGCAGC
TGGAAAGCCGGTTACCCCTCAGTTTCTGCTGCAGCTGAACGAGACAATCTACGCCAGCGGAAGCGGAGCAA
CACCACCGGCAAGCTGATCTGGAAAGTGAACCCGAGATCGACACCACAATCGGAGAGTGGGCCCTTCGGGAG
ACAAAGAAGAACCTGACCCGGAAGATCAGAAGCGAGGAAGTGAAGTTCACCGCCGTGTCCAACGGCCCCAAGA
ACATCAGCGCCAGAGCCCCCGCAGAACAGCAGCGCCATGGTGCAGGTCCACAGCAGGGCAGAAAGCCGCTGTCTCACCTG
CATGGCCAGCGAGAACAGCAGCGCCATGGTGCAGGTCCACAGCAGGGCAGAAAGCCGCTGTCTCACCTG
ACCACCTCGCCACCATCAGCACCAGCCCTCAGAGCCTGACCACCAAGCCTGGCCCCGACAACCTCCACCACA
ACACCCCTGTGTACAAGCTGGACATCAGCGAGGCCACCCAAGTGGGACAGCACACAGACGGGCCGACAACGA
CAGCACCGCCAGCGATACCCCTCCAGCCACAACAGCCGCCGAGCCCTGAAGGCCGAGAACACCAACACCAGC
AAGAGCGCCGACAGCCTGGATCTGGCCACCACAACCAGTCTCAGAATACTCCGAGACAGCCGGCAACAACA
ACACCCACCACCAGGACACCGGGCAGGAAAGCGCCAGCTCTGGCAAGTGGGCTGATCACCACAACAATCGC
CGGCGTGGCCGGACTGATCACCAGGAGCAGACGGACCAGACGGGAAGTATCGTGAACGCCAGCCAAAGTGC
AACCCCAACCTGCACTACTGGACCACCCAGGACGAGGGCGCTGCTATCGGCCCTGGCTGGATTCTTACTTCG
GCCCTGCCGCCGAGGGCATCTACACCGAGGGCTGATGCACAACCAGGACGGCCTGATCTGCGGCCCTGCGGCA
GCTGGCCAATGAGACAACCCAGGCCCTGCAGCTGTTCCTGCGGGCCACCACCAGCTGCGGACCTTCTCCATC
CTGAACAGAAAGGCCATCGACTTTCTGCTGCAGCGCTGGGGAGGCACCTGTACATCCTGGGCCCCGACTGCT
GCATCGAGCCCCACGACTGGACCAAGAATATCACCACAAGATCGACCAGATCATCCACGACTTCGTGGACAA
GACCTTGGCCGACCAGGGCGACAACGATAACTGGTGGACCGGCTGGCGGCAGTGGATTCCAGCCGGAATCGGA
GTGACCGGCGTGATCATTGCCGTGATCGCCCTGTTCCTGCATCTGCAAGTTTCGTGTTCTGA

SUDV | *Sudan ebolavirus* | Sudan/Boniface/SUD/1976 | FJ968794

ATGGAGGGTCTTAGCCTACTCCAATTGCCAGAGATAAATTCGAAAAAGCTTTCTTTGTTTTGGGTCAATCA
TCTTATTTCAAAGGCCCTTTCCATGCCTTTGGGTGTGTGACCAACAGCACTTTAGAAAGTAACAGAGATTGA
CCAGTATGCTGCAAGGATCATCTTGCATCCACTGACCAAGTGAATCAGTTGGTCTCAACCTCGAGGGGAGC
GGAGTATCTACTGATATCCCATCTGCGACAAAGCGTTGGGGCTTCAGATCTGGTGTGCCCTCCCAAGGTGGTCA
GCTATGAAGCAGGAGAATGGGCTGAAAATTGCTACAATCTTGAATAAAGAAGCCGGACGGGAGCGAATGCTT
ACCCACACCGCCGGATGGTGTGAGAGGCTTTCCAAGGTGCCGCTATGTTCAAAAAGCCCAAGGAACCGGGCC
TGCCCGGGTACTATGCCTTTACAAGGATGGAGCTTTCTTCTCTATGACAGGCTGGCTTCAACTGTAATTT
ACAGAGGAGTCAATTTTGTGAGGGGGTAATTGCATTCCTTGATATTGGCTAAACCAAAGGAAACGTTCCCTCA
ATCACCCCATTCGAGAGGCAGTAACTACTGAAAATACATCAAGTACTATGCCACATCCTACTTGGAG
TACGAAATCGAAAATTTTGGTGTCAACACTCCACGACCCCTTTTCAAATAAACAATAACTTTTGTTCCTTC
TGGACAGGCCCCACACGCTCAGTTCTTTTCCAGCTGAATGATACCATTACCTTACCACAGTTGAGCAA
CACAACCTGGGAAACTAATTTGGACACTAGATGCTAATATCAATGCTGATATTGGTGAATGGGCTTTTGGGAA
AATAAAAAAATCTCTCCGAACAACACTACGTGGAGAAGAGCTGTCTTTCGAACTTTATCGCTCAACGAGACAG
AAGACGATGATGCGACATCGTGCAGAACTACAAAGGGAAGAATCTCCGACCGGGCCACCAGGAAGTATTCGGA
CCTGGTTCCAAGGATTTCCCTGGGATGGTTTCAATTGCACGTACCAGAAGGGGAAACAACATTTGCCGTCTCAG
AATTCGACAGAAGGTGCAAGAGTAGATGTGAATACTCAGGAACTATCACAGAGACAACCTGCAACAATCATAG
GCACTAACGGTAACAACATGCAGATCTCCACCATCGGGACAGGACTGAGCTCCAGCCAAATCCTGAGTTCTTC
ACCGACCATGGACCAAGCCCTGAGACTCAGACCTCCACAACCTACACACCAAACTACCAGTGATGACCACC
GAGGAATCAACAACACCACCGAGAACTCTCCTGGCTCAACAACAGAAAGCACCCTCTCACCACCCAGAGA
ATATAACAACAGCGGTTAAAATGTTTTGCCACAAGAGTCCACAAGCAACGGTCTAATAACTTCAACAGTAAC
AGGATTCCTTTGGGAGCCTTTGGACTTCGAAAACGCAGCAGAAGACAAGTTAACACCAGGGCCACGGGTAAATGC
AATCCCAACTTACTACTGGACTGCACAAGAACAACATAATGCTGCTGGGATTGCCCTGGATCCCGTACTTTG
GACCGGGTGCAGAAGGCATATACACTGAAGGCCCTTATGCACAACCAAAATGCCCTTAGTCTGTGGACTCAGACA
ACTTGCAAAATGAAACAACCTCAAGCTCTGCAGCTTTTCTTAAAGGGCCACGACGGAGCTGCGGACATATACCATA
CTCAATAGGAAGGCCATAGATTTCTTCTGCGACGATGGGGCGGGACATGTAGGATCCTGGGACCAGATTGTT
GCATTGAGCCACATGATTGGACCAAAAACATCACTGATAAAATCAACCAATCATCCATGATTTTCATCGACAA
CCCTTTACCCAATCAGGATAATGATGATAATTGGTGGACGGGCTGGAGACAGTGGATCCCTGCAGGAATAGGC
ATTACTGGAATTATTATTGCAATCATTGCTCTTCTTTCGCTCTGCAAGCTGCTTTGTTGA

BDBV | *Bundibugyo ebolavirus* | Bundibugyo/UGA/2007 | FJ217161

ATGGTTACATCAGGAATTCTACAATTGCCCGTGAACGCTTCAGAAAAACATCATTTTTTGTGGTAATAA
TCCTATTTTACAAAAGTTTTCCCTATCCCATTTGGGCGTAGTTTCAACAACACTCTCCAGGTAAGTGATATAGA
TAAATTGGTGTGCCGGGATAAACTTTCCCTCCACAAGTCAGCTGAAATCGGTCGGGCTTAATCTAGAAGGTAAT
GGAGTTGCCACAGATGTACCAACAGCAACGAAGAGATGGGGATTCGAGCTGGTGTTCACCCAAAGTGGTGA
ACTACGAAGCTGGGGAGTGGGCTGAAAACCTGCTACAACCTGGACATCAAGAAAGCAGATGGTAGCGAATGCCT
ACCTGAAGCCCCTGAGGGTGTAAAGAGGCTTCCCTCGCTGCCGTTATGTGCACAAGGTTTCTGGAACAGGGCCG
TGCCCTGAAGGTTACGCTTTCCACAAAAGAGGCGCTTTCTTCTGTATGATCGACTGGCATCAACAATCATCT
ATCGAAGCACCACGTTTTTTCAGAAGGTGTTGTGGCTTTCTTGTATCCTCCCGAAAACAAAAAGGACTTTTTTCCA
ATCGCCACCCTACATGAACCGGCCAATATGACAACAGACCCATCCAGCTACTACCACACAGTCACACTTAAT
TATGTGGCTGACAATTTTGGGACCAATATGACTAACTTTCTGTTTCAAGTGGATCATCTAATTATGTGCAAC
TTGAACCAAGATTCACACCACAATTTCTTGTCCAACCTCAATGAGACCATTTATACTAATGGGCGTCGCAGCAA
CACCACAGGAACACTAATTTGGAAAAGTAAATCCTACTGTTGACACCGGCTAGGTGAATGGGCCCTTCTGGGAA
AATAAAAAAACTTCAAAAAACCTTTCAAGTGAAGAGCTGTCTGTCAATTTGTACCAAGAGCCAGGATC
CAGGCAGCAACCAGAAGACGAAGGTCACTCCACCAGCTTCGCCAACAAACCAACCTCCAAGAACCACGAAGA
CTTGGTTCAGAGGATCCCGCTTCAGTGGTCAAGTGCAGACCTCCAGAGGGAAAAACAGTGGCCGACCCCA
CCCCCAGACACAGTCCCCACAACCTCTGATCCCCGACACAATGGAGGAACAAACCACAGCCACTACGAACCAC
CAACATAATTTCCAGAAAACCATCAAGAGAGGAACAACACCGCACACCCCGAAAACCTTCGCCAACAAATCCCCCAGA
CAAACACACCCCGTCGACACCACCTCAAGACGGTACGCGGCAAGTTCACACACACACCTCCCCCGCCCA
GTCCCAACCAGCACAAATCCATCCACCACACGAGAGACTCACATTTCCACCACAATGACAACAAGCCATGACA
CCGACAGCAATCGACCCAACCAATGACATCAGCGAGTCTACAGAGCCAGGACCACTACCAACACCACAAG
AGGGGCTGCAAATCTGCTGACAGGCTCAAGAAGAACCAGAAGGAAATCACCTGAGAACACAAGCCAAATGC
AACCCAAACCTACACTATTGGACAACCCAAGATGAAGGGCTGCCATTGGTTTAGCTGGATACCTTACTTTCG
GGCCCGCAGCAGAGGGAATTTATACGGAAGGGATAATGCACAATCAAAATGGGCTAATTTGCGGGTTGAGGCA
GCTAGCAAATGAGACGACTCAAGCCCTACAGTTATTCTTTCGCTGCTACCACGGAATTGCGCATTTCCTCTATA
TTGAATCGAAAAGCCATCGACTTTTTACTCCAAAAGATGGGGAGGAACGTGCCACATCTTAGGCCCAGATTGCT
GTATTGAGCCCCATGATTGGACTAAGAACATTAAGTACAAAAATAGATCAAAATCATTCATGATTTCATTGATAA
ACCTCTACCAGATCAAAACAGATAATGACAATTTGGTGGACAGGGTGGAGGCAATGGGTTCCTGCCGGGATCGGG
ATCACGGGGTAATAATCGCAGTTATAGCACTGCTGTGATTTGCAAAATTTCTACTCTAA

RESTV | *Reston ebolavirus* | Reston/ Pennsylvania/USA/1989 | AY769362

ATGGGGTCAGGATATCAACTTCTCCAATTGCCTCGGGAACGTTTTTCGTAAAACCTCGTTCTTAGTATGGGTAA
TCATCCTCTTCCAGCGAGCAATCTCCATGCCGCTTGGTATAGTGACAAAATAGCACTCTCAAAGCAACAGAAAT
TGATCAATTGGTTTGTGCGGGACAAACTGTCAATCAACCAGTCAGCTCAAGTCTGTGGGGCTGAATCTGGAAGGA
AATGGAATTGCAACCGATGTCCCATCAGCAACAAAACGCTGGGGATTTTCGTTTCAGGTGTGCCATCCCAAGGTGG
TCAGCTATGAAGCCGGAGAATGGGCAGAAAATTTGCTACAATCTGGAGATCAAAAAGTCAGACGGAAGTGAATG
CCTCCCTCTCCCTCCCGACGGTGTACGAGGATTCCTTAGATGTGCTATGTCCACAAAAGTTCAAGGAACAGGT
CCTTGTCCCGGTGACTTAGCTTTCCATAAAAAATGGGGCTTTTTTCTTGTATGATAGATTGGCCCAACTGTCA
TCTACCGAGGGACAACTTTTGCTGAAGGTGTGCTAGCTTTTTTAATTTCTGTGTCAGAGCCCAAGAAGCATTTTTG
GAAGGCTACACCAGTCATGAACCGGTGAACACAACAGATGATTCACAAGCTACTACATGACCTGACACTGACAT
AGCTACGAGATGTCAAATTTTGGGGCAATGAAAGTAACACCTTTTTTAAGGTAGACAACCACACATATGTGC
AACTAGATCGTCCACACACTCCGAGTTTCTTGTTCAGCTCAATGAAACACTTCGAAGAAAATAATCGCCTTAG
CAACAGTACAGGGAGATTGACTTGGACATTTGGATCCTAAAAATGAACCAGATGTTGGTGAGTGGGCCCTTCTGG
GAACTAAAAAAACTTTTTCCCAACAACCTCATGGAGAAAACCTTGCATTTCCAAAATCTATCAACCCACACCA
ACAACCTCTCAGATCAGAGCCCGCGGGAACCTGTCCAAGGAAAAATTAGCTACCACCACCCGCCAACACTC
CGAGCTGGTTCCAACGGATTCCCCTCCAGTGGTTTCAGTGTCTACTGCAGGACGGACAGAGGAAATGTCGACC
CAAGGTCTAACCAACGGAGAGACAATCACAGTTTCCACCGCAACCAATGACAACCACCAATTGCCCAAGTC
CAACCATGACAAGCGAGGTTGATAACAATGTACCAAGTGAACAACCGAACAACACAGCATCCATTGAAGACTC
CCCCCATCGGCAAGCAACGAGACAATTTACCCTCCGAGATGGATCCGATCCAAGGCTCGAACAACTCCGCC
CAGAGCCACAGACCAAGACCACGCCAGCACCCACAACATCCCCGATGACCCAGGACCCGCAAGAGACGGCCA
ACAGCAGCAAAACCAGGAACCAGCCAGGAAGCGCAGCCGGACCAAGTCAGCCCGGACTCACTATAAATACAGT
AAGTAAGGTAGCTGATTCACTGAGTCCCACAGGAAACAAAGGCGATCGGTTTCGACAAAAACCCGCTAATAAA
TGTAAACCAGATCTTTACTATTGGACAGCTGTGTGAGGGGACAGAGTGGATGGCATGGATTCCATATTT
TCGGACCTGCAGCAGAAGGCATCTACATTTGAGGGTGTAAATGACATAATCAGAATGGGCTTATTTGCGGGCTACG
TCAGCTAGCCAATGAAACTACCCAGGCTCTTCAATTTATTTCTGCGGGCCACAACAGAATGAGGACTTACTCA
CTTCTTAACAGAAAAGCTATTGATTTTCTTCTTCAACGATGGGGAGGTACCTGTGCAATCCTAGGACCATCTT
GTTGCATTGAGCCACATGATTGGACAATAAATAATTAAGTATGAAATTAACCAATTAACATGACTTTATTTGA
CAATCCCCTACCAGACCACGGAGATGATCTTAATCTATGACAGGTTGGAGACAATGGATCCCGGCTGGAATTT
GGGATTATTGGAGTTATAATTGCTATAATAGCCCTACTTTGTATATGTAAGATTTTGTGTTGA

LLOV | *Lloviu cuevavirus* | Lloviu/ ESP/2003 | JF828358

ATGGTGCCACCTACCCGTACAGCAGCCTATTAGATTGGAGACCACCACCAAAACCCCTACCATGGATCCCTCA
ACCTTGTGGTCTTTTTATACCATAGCCTGGCTGCCCGGGGAGTCTCAGGAATTCCTACTCGGTTTTGTTGGGAAA
CAACAGCATCACCCAACTGTCGTGGACAATGTAGTGTGCAAGGAACACCTTGCCACAACAGATCAGCTACAG
GCTATTGGATTGGGACTAGAGGGGCTTGGTGAACATGCTGACCTCCCGACTGCCACCAAGCGATGGGGTTTTTC
GATCTGATGTCATCCCAAAAATCGTGGGATACACCGCTGGGGAATGGGTGGAAAACGCTACAATCTTGAAAT
CACCAAGAAAGATGGTCATCCTTGCCCTCCCCAGCCGCCAACTGGCTTACTTGGCTATCCCCGATGCCGCTAT
GTCCACAGAGCCAAAGGAGCAGGCCCTTGCCAGGTGGGAATGCTTTCACAAAACATGGTCTTTCTTTCTGT
ACCACGGTATGGCTTCTACAGTAATTTATCATGGTGTAACTTTACGGAAGGCACAATTGCTTTCTTAATTGT
CCCGAAGGATGCACCCCGTCTCAAGGCAGGGCTTGGAACAGGATTCAGTCATCAAGCAGAGAACCAAAACCA
AACACCAATTTGCAACAACAACCTTTAGATTATGATGTAATGAGTCTTGGATGGACAATGCTACCTTCTTCT
TTTCAGCGAGGGAAGACACATCAATGCTAATCCAAACAAGGTACCTCCAGCAAATCTAGAGCTTGTTCAGA
AAGATTGGCTAATCTTACCGGAGATCAAGCTGATCCATCAAAGATGGAAAGAGATTGTCGCTGAGGTTTTGACA
TTGGAGCTCGGTGATTGGTCCGGTTGGACAATAAAAAAACCGCAGTACAAAACCATACGGCTAAGAAACCCCT
TCACCAGCATCTGGTTCAACCAAGGACAAGACTGGCCAGAAGCCCATGACGGATCATCAGGAGTTCATCCTCC
AACCTCATTCTGCTGTTGGACAACCCCTGCCTCTGGAACATTTCTCGAACTCCGGGGCGGAACCCCTGCACGAAG
GCACCGGCGGGAACACCACCAACAATGTCCACTGCTGCTCCTGGGTGAGGATACAAGCCGTACATCCAG
GCAATACCTCTGGTGAAATTTTCGATGCCATTGGGAGGGTCTTCGGCATGTGTGCTCGTACCCCTCCTGGG
TTCAGTGAGCAACAATAGTTCAATACAGGAGCTTGAGACTTCATCTAAAAAGTGCAACAGAATTGACAACCTCC
ATCAATCACTCCCAATCACTACAGCTCGCATCCGTACAAAACACCCCCACACCGACAACACAGTCCAAGTCTT
GGACAGTTGACTACAACAACAACGCAACCATGGATCCCAACAATACTGACGACACCCGACACCGCAAC
CATTCCCCCTAACAACTCATCTGATCACAACGCCACAACAACAAGCAAAAACAAGCAGGAGACAGGTCAAC
CCAGTGGCCCCAACGATCACCCAACAACCTCTACAAGCATCAATACCTCCACCACCCCAATATGACAACAC
AGTTAGCAAGACATCCGAGTGTGCAACAAGGATGCAAAAACCCAGCTGTAATCCCAACCTTAGATACTGGAC
AAGCCGGGAGATGAGTAATGCTGGGGGGCTTGCATGGATTCCATGGATTGGACCAGGGATTGAGGGAGGGATC
ACAGACGGGATAATGGAGCATCAGAACACAATTGTCTGTGCTGAGTTACGGGAGCTCGCGAACACCCTACTAAAG
CCCTACAGCTTTTTCTCCGGGCTACCACTGAGCTCCGAACCTACTCTATCCTCAACCGCCATGCGATTGACTT
TCTACTACAGCGTTGGGGTGGTACCTGCAGAACTCTTGGCCAAACTGCTGTATCGAACCTCATGATTGGTCT
GCCAACATTACCGCTGAGATAAATCATATTAGAGAATAATCCTGAACCATCATGAGATCCAACCTTCTCAAG
ACCCCTCCTTTTGGACTGGATGGCAACAGTGGATCCCAACAGGAGCCAGTGTCTCGGAATCATCCTGGCAAT
ATTAGCCTTGATTTGTCTGTGCAGAATAACACGATGA

RAVV | *Marburg marburgvirus* | Ravn/KEN/1987/KitumCave | DQ447649

ATGAAGACCATATATTTTTCTGATTAGTCTCATTTTAATCCAAAGTATAAAAACTCTCCCTGTTTTAGAAATTG
CTAGTAACAGCCAACCTCAAGATGTAGATTCACTGTGCTCCGGAAACCTCCAAAAGACAGAAGATGTTTCATCT
GATGGGATTTACACTGAGTGGGCAAAAAGTTGCTGATTCCCTTTTGGAAAGCATCTAAACGATGGGCTTTTCAGG
ACAGGTGTTCTCCCAAGAAGCTTGAGTATACGGAAGGAGAAGGCCAAAACATGTTACAATATAAGTGTA
CAGACCCTTCTGGAAAATCCTTGCTGCTGGATCCTCCAGTAATATCCGCGATTACCCTAAATGTAAAACGT
TCATCATATTTCAAGTCAAAAACCTCATGCACAGGGATTGCCCTCATTGTGGGGGGCATTTTTCTTTGTAT
TACTCGCTTGCCTTACAACAATGTACCGAGGAGGTTTACTGAAAGGAAATATAGCAGCTATGATTGTTA
ATAAGACAGTTACAGAATGATTTTTTCTAGGCAAGGACAAGGTTATCGTCACATGAACTTGACCTCCACCAA
TAAATATTGGACAAGCAGCAATGAAACGCAGAGAAATGATACGGGATGTTTTGGCATCCTCCAAGAATACAAC
TCCACAACAATCAAACATGCCCTCCATCTCTTAAACCTCCATCCCTGCCACAGTAACCCGAGCATTCACT
CTACAATACTCAAATTAATACTGCTAAATCTGGAACATGAAACCAAGTAGCGACGATGAGGACCTTATGAT
TTCCGGCTCAGGATCTGGAGAACAGGGCCCCACAACTCTTAATGTAGTCACTGAACAGAAACAATCGTCA
ACAATATTGTCCACTCCTTCACTACATCCAAGCACCTCACAACATGAGCAAACAGTACGAATCCTTCCCGAC
ATGCTGTAACCTGAGCACAATGGAACCGACCCAACAACACAACCAGCAACGCTCCTCAACAATACTAATACAAC
TCCCACCTATAACTCTCAAGTACAACCTCAGTACTCCTTCCCTCCAACCCGCAACATCACCAATAATGAT
ACACAACGTGAACTAGCAGAAAGCGAACAAACCAATGCTCAGTTGAACACAACCTCTAGATCCAACAGAAAATC
CCACCACAGGACAAGACACCAACAGCACAACCAACATCATATGACGACATCAGATATAACAAGCAAACACCC
CACAATTTCTTCCGGATTCTAGTCCGACAACCCGCCCTCCTATATACTTTAGAAAAGAAACGAAGCATTTTT
TGGAAGAAGGTGATATATTTCCGTTTTAGATGGGTTAATAAAACTGAAATGATTTTTGATCCAATCCCAA
ACACAGAAACAATCTTTGATGAATCTCCAGCTTTAATACTTCAACTAATGAGGAACAACACACTCCCCGAA
TATCAGTTTTAACTTTCTTTATTTTCTGATAAAAAATGGAGATACTGCCTACTCTGGGGAAAACGAGAATGAT
TGTGATGCAGAGTTGAGGATTTGGAGTGTGCAGGAGGACGATTTGGCGGCAGGGCTTAGCTGGATACCATTTT
TTGGCCCTGGAATCGAAGGACTCTATACTGCCGGTTAATCAAAAATCAGAACAATTTAGTTTTGTAGTTGAG
GCGCTTAGCTAATCAAACCTGCTAAATCCTTGGAGCTCTTGTAAAGGTCACAACCGAGGAAAGGACATTTTCC
TTAATCAATAGGCATGCAATTGACTTTTTGCTTACGAGGTGGGGCGGAACATGCAAGGTGCTAGGACCTGATT
GTTGCATAGGAATAGAAGATCTATCTAAAAATATCTCAGAACAATCGACAAAATCAGAAAAGGATGAACAAAA
GGAGGAAACTGGCTGGGGTCTAGGTGGCAAAATGGTGGACATCTGACTGGGGTGTCTCACCAATTTGGGCATC
CTGCTACTATTATCTATAGCTGTTCTGATTGCTCTGTCTGTATCTGTCGATCTTCACTAAAATACATTTGGAT
GA

MARV | Marburg marburgvirus | Marburg/Ang0998/Angola/2005 | DQ447660

ATGAAAACCATGTCTCCTTATCAGTCTTATCTTAATCCAAGGGGTAAAACTCTCCCTATTTTLAGAGATAG
CCAGTAACATTCAACCCCAAAATGTGGATTGAGTATGCTCCGGGACTCTCCAGAAGACAGAAGACGTTTCATCT
GATGGGATTCACACTGAGCGGGCAAAAAGTTGCTGATTCCCCTTTAGAGGCATCCAAACGATGGGCCTTTCAGG
GCAGGTGTACCTCCCAAGAATGTTGAGTATACAGAAGGGGAGGAAGCTAAAACATGTTACAATATAAGTGTAA
CGGATCCCTCTGGAAAATCCTTGCTGTTAGATCCTCCTACCAACATCCGTGACTATCCTAAAATGCAAACTAT
CCATCATATTCAAGGTCAAAAACCTCATGCACAGGGGATCGCTCTCCATTTGTGGGGAGCATTTTTCTTGTAT
GATCGCATCGCCTCCACAACGATGTATCGAGGCAAAAGTCTTCACTGAAGGGAACATAGCAGCTATGATTGTCA
ATAAGACAGTGCACAAAATGATTTTTCTCGAGGCAAGGACAAGGGTACCGTCACATGAACCTAACCTTCTACTAA
TAAATATTGGACAAGTAGCAACGGAACGCAAACGAATGACACTGGATGCTTCGGTACTCTTCAAGAATATAAT
TCTACAAAGAACCACAAACATGTGCTCCGTCCAAAAAACCTTTACCCTGCCCACAGCCCATCCGGAGGTCAAGC
TCACTAGCACCTCAACTGATGCCACCAAACTCAATACCACAGACCCAAACAGTGATGATGAGGACCTCACAAAC
ATCTGGCTCAGGGTCTGGAGAACAGGAACCTTACACAACCTTCTGACGCAGCCACGAAGCAAGGGCTTTTCATCA
ACAATGCCGCCACTCCCTCACCACAACCAAGCACGCCACAGCAAGGAGGAAAACAACACGAACCATTTCCCAAG
GTGTTGTGACTGAACCCGGCAAAACCAACAACACTGCACAACCGTCCATGCCCCCTCACAACTACTACAAT
CTCTACTAACACACCTCCAAGCACAACCTCAGCACTCCCTCTGTACCAATACAAAATGCCACTAATTACAAC
ACACAGAGCACGGCCCTGAAAATGAGCAAACAGTGCACCACTCGAAAACAACCTGCTTCCAACAGAAAATC
CTACAACAGCAAAGAGCACCAATAGTACAAAAAGCCCCACTACAACAGTACCAATAACGACAAAATAAGTATTC
CACCAGTCCCTCCCCACCCCAACTCGACTGCACAACATCTTGTATATTTTCAGAAGGAAACGAAATATTTCTC
TGGAGGGAAGGCGACATGTTCCCTTTTCTGGATGGGTTAATAAATGCTCCGATTGATTTTGATCCGGTTCCAA
ATACAAAGACAATCTTTGATGAATCCTCTAGTCTGGTGCTTCAGCTGAGGAAGATCAGCATGCCCTCCCTAA
TATCAGTTTTAACTTTATCTTACTTTCTAAGGTAATGAAAACACTGCCACTCTGGAGAAAATGAAAATGAT
TGTGATGCAGAGTTAAGAATTTGGAGTGTTCAGGAGGACGACCTGGCAGCAGGACTCAGTTGGATACCGTTTT
TTGGCCCTGGAATCGAAGGACTTTATACTGCTGGTTTAATTAATAAATCAAAAATAATTTGGTTTGCAGGTTGAG
GCGTCTAGCCAATCAGACTGCCAAATCCTTGGAACTCTTATTAAGAGTCACAACCGAGGAAAGAACATTTTCC
TTAATCAATAGACATGCCATTGATTTTTTACTCGCAAGGTGGGGAGGAAACATGCAAAGTGCCTGGACCTGATT
GTTGCATCGGAATAGAAGACTTGTCCAGAAAATTTTCAGAACAAATGATCAAAATCAAAAAGGACGAACAAAA
AGAGGGGACTGGTTGGGGTCTGGGTGGTAAATGGTGGACATCAGACTGGGGTGTCTTACTAACCTGGGCATC
TTGCTACTACTGTCCATAGCTGTCTTAATTGCTCTGTCTGTATTTGTCTGATTTTACTAAAATATATTGGAT
AA

MARV | Marburg marburgvirus | Marburg/07DRC099/DRC/1999 | DQ447650

ATGAGGACTACATGCTTCTTTATCAGTCTCATCTTAATCCAAGGGATAAAAACTCTCCCTATTTTGGAGATAG
CCAGTAACGATCAACCCCAAAATGTGGATTCCGGTATGCTCCGGAACCTCTCCAGAAAACAGAAGACGTCATCT
GATGGGATTTACACTGAGCGGGCAGAAAAGTTGCTGATTCCCCTTTGGAGGCATCCAAAGCGATGGGCCTTTCAGG
ACAGGTGTACCTCCTAAGAATGTTGAGTATACGGAAGGGGAGGAAGCCAAAAACATGCTACAATATAAGTGTAA
CAGATCCCTCTGGAAAATCCTTGCTGTTAGATCCTCCACCAACGTCCGTGACTATCCTAAAATGCAAACTAT
CCATCACATTTCAAGGTCAAAAACCTCATGCGCAGGGGATCGCCCTCCATTTGTGGGGAGCATTTTTCTTATAT
ATAAGACAGTGCACAAAATGATTTTTCTCGAGGCAAGGACAAGGGTACCGTCACATGAATCTGACTTCTACTAA
TAAATATTGGACAAGTAGCAACGGAACGCAAACAAATGACACTGGATGCTTTGGTACTCTTCAAGAATACAAT
TCTACGAAGAACCACAAACATGTGCTCCATCTAAAAACCCCCACCACCGCCACAGCCCGTCCGGAGATCAAAC
CCACAAGCACTCCAACCGATGCCACTAGACTCAACACCACAAAACCAACAGTGATGATGAGGATCTCACAAAC
ATCCGGCTCGGGGTCTGGGGAACAGGAACCTTATACGACTTCTGATGCGGTCACTAAGCAAGGGCTTTTCATCA
ACAATGCCACCCACTCCCTCACCACAACAGGACGCCACAGCAAGGAGGAAAACAACACAAACCACTCCCAAG
ACGCTGCAACTGAACTTGACAACACCAATACAACACTGCACAACCTGCCACGCCCTCCCAACACCACCACAAT
CTCCACCAACAACACCTCCAAACACAACCTCAGCACCTCTCCGAACCACCACAAAACACCACCAATCCCAAC
ACACAAAGCATGGCCACTGAAAATGAGAAAACCTAGTGCCCCCGAAAAACAACCTGCCCTCCAATAGAAAGTC
CAACCACAGAAAAGAGCACCAACAATACAAAAAGCCCCACCACAATGGAACCAAAATACAACAAATGGACATTT
CACTAGCCCTCTCCACCCCAACTCGACTACTCAACACTTATATATTTTCAGGAGGAAACGAAGTATCCCTC
TGGAGGGAAGGCGACATGTTCCCTTTTCTAGATGGGTTAATAAATGCTCCAATGATTTTGATCCAGTTCCAA
ATACAAAGACAATCTTTGATGAATCTTCTAGTCTGGTGTCTCAGCTGAGGAAGATCAACATGCATCTCCAA
TATCAGTTTTAACTTTATCTTATCTTCTCATACAAGTAAAAACACTGCCCTACTCTGGAGAAAATGAAAATGAT
TGTGATGCAGAGCTAAGAATTTGGAGCGTTTCAGGAGGACGACCTGGCAGCAGGGCTCAGTTGGATACCATTTT
TTGGCCCTGGAATCGAAGGACTTTATACCGCTGGTTTAATTAATAAATCAAAAACAATTTGGTCTGCAGGTTGAG
GCGTCTAGCCAATCAAACCTGCAAAAATCTTTGAACTCTTACTAAGGGTCACAACCGAGGAAAGAACATTTTCC
TTAATCAATAGACACGCTATTGACTTTCTACTACAAGGTGGGGAGGAAACATGCAAAGTGCCTGGACCTGATT
GTTGCATAGGAATAGAGGACTTGTCCAGAAAATTTTCAGAACAGATTGACCAATCAAGAAGGACGAACAAAA
AGAGGGGACTGGTTGGGGTCTGGGTGGTAAATGGTGGACATCCGACTGGGGTGTCTTACCAACTTGGGCATC
TTACTACTATTGTCCATAGCTGTCTTATTGCTCTATCTGTATTTGTCTGATTTTACTAAAATATATTGGAT
AG

LASV | *Lassa marmarenavirus* | Lassa/Sierra Leone/Josiah/1976 | M15076*

ATGGGCCAGATCGTGACCTTCTTCCAGGAGGTGCCCCACGTGATCGAGGAGGTGATGAACATCGTGCTGATCG
CCCTGAGCGTGCTGGCCGTGCTGAAGGGCCTGTACAACCTTCGCCACCTGCGGCCTGGTGGGCCCTGGTGACCTT
CCTGCTGCTGTGCGGCAGAAGCTGCACCACCAGCCTGTACAAGGGCGTGTACGAGCTGCAGACCCCTGGAGCTG
AACATGGAGACCCTGAACATGACCATGCCCTGAGCTGCACCAAGAACAACAGCCACCCTACATCATGGTGG
GCAACGAGACCCGGCCTGGAGCTGACCCTGACCAACACCAGCATCATCAACCACAAGTTCTGCAACCTGAGCGA
CGCCACAAGAAGAACCTGTACGACCACGCCCTGATGAGCATCATCAGCACCTTCCACCTGAGCATCCCCAAC
TTCAACCAGTACGAGGCCATGAGCTGCGACTTCAACGGCGGCAAGATCAGCGTGCAGTACAACCTGAGCCACA
GCTACGCCGGCGACGCCGCCAACCCTGCGGCACCGTGGCCAACGGCGTGTGCGAGACCTTCATGAGAAATGGC
CTGGGGCGGCAGCTACATCGCCCTGGACAGCGGCAGAGGCAACTGGGACTGCATCATGACCAGCTACCAGTAC
CTGATCATCCAGAACCACCCTGGGAGGACCCTGCCAGTTCAGCAGACCCAGCCCCATCGGCTACCTGGGCC
TGCTGAGCCAGAGAACCAGAGACATCTACATCAGCAGAAGACTGCTGGGCACCTTCACCTGGACCCTGAGCGA
CAGCGAGGGCAAGGACACCCCCGGCGGCTACTGCTGACCAGATGGATGCTGATCGAGGCCGAGCTGAAGTAC
TTTCGGCAACACCGCCGTGGCCAAGTGAACGAGAAGCAGCAGAGGAGTTCTGCCACATGCTGAGACTGTTTCG
ACTTCAACAAGCAGGCCATCCAGAGACTGAAGGCCGAGGCCAGATGAGCATCCAGCTGATCAACAAGGCCGT
GAACGCCCTGATCAACGACCAGCTGATCATGAAGAACCCTGAGAGACATCATGGGCATCCCCTACTGCAAC
TACAGCAAGTACTGGTACCTGAACCACACCACCACCGGCAGAACCAGCTGCCAAGTGTGGCTGGTGAGCA
ACGGCAGCTACCTGAACGAGACCCACTTCAGCGACGACATCGAGCAGCAGGCCGACAACATGATCACCAGAT
GCTGCAGAAGGAGTACATGGAGAGACAGGGCAAGACCCCCCTGGGCCCTGGTGGACCTGTTTCGTGTTTCAGCACC
AGCTTCTACCTGATCAGCATCTTCTGCACTGGTGAAGATCCCCACCCACAGACACATCGTGGGCAAGAGCT
GCCCCAAGCCCCACAGACTGAACCACATGGGCATCTGCAGCTGCGGCCTGTACAAGCAGCCCGGCCTGCCCGT
GAAGTGAAGAGATAA

H3N8 | *Influenza A virus* | A/canine/Colorado/30604/2006 (H3N8) | AB537183
Haemagglutinin sequence:

ATGAAGACAACCATTATTTTAATACTACTGACCCATTGGGCCTACAGTCAAAACCCAATCAGTGCGCAATAACA
CAGCCACACTGTGTCTGGGACACCATGCAGTAGCAAATGGAACATTGGTAAAAACAATGAGTGATGATCAAAT
TGAGGTGACAAATGCTACAGAATTAGTTTCAGAGCATTTCAAATGGGGAAAATATGCAACAAATCATATAGAATT
CTAGATGGAAGAAATTGCACATTAATAGATGCAATGCTAGGAGACCCCCACTGTGACGCCCTTTCAGTATGAGA
GTTGGGACCTCTTTATAGAAAAGCAACGCTTTCAGCAATTGCTACCCATATGACATCCCTGACTATGCATC
GCTCCGATCCATTGTAGCATCCTCAGGAACAGTGAATTCACAGCAGAGGGATTACATGGACAGGTGTCACCT
CAAAACGGAAGAAGTGGAGCCTGCAAAAGGGGATCAGCCGATAGTTTCTTTAGCCGACTGAATTGGCTAACAA
AATCTGGAAGCTCTTACCCACATTGAATGTGACAATGCCTAACAAATAAAAATTTTCGACAAGCTATACATCTG
GGGGATTTCATCACCCAAGCTCAAATCAAGAGCAGACAAAATTTGATACATCCAAGAAATCAGGACGAGTAACAGTC
TCAACAAAAAGAAGTCAACAAAATAATCCCTAACATCGGATCTAGACCGTTGGTCAGAGGTCAATCAGGCA
GGATAAGCATATACTGGACCATTGTAACAACTGGAGATATCCTAATGATAAACAGTAATGGCAACTTAGTTGC
ACCTCGGGGATATTTTAAATTGAACACAGGGAAAAGCTCTGTAATGAGATCCGATGTACCCATAGACATTTGT
GTGTCTGAATGTATTACACCAAATGGAAGCATCTCCAACGACAAGCCATTCAAAAATGTGAACAAAGTTACAT
ATGGAAAATGCCCCAAGTATATCAGGCAAAACACTTTAAAGCTGGCCACTGGGATGAGGAATGTACCAGAAAA
GCAAAACAGAGGAATCTTTGGAGCAATAGCGGGATTTCATCGAAAACGGCTGGGAAGGAATGGTTGATGGGTGG
TATGGGTTCCGATATCAAAAATCTGAAGGAACAGGGCAAGCTGCAGATCTAAAAGCACTCAAGCAGCCATCG
ACCAGATTAATGGAAAGTTAAACAGAGTGATTGAAAAGAACCAATGAGAAAATTCATCAAAATAGAGAAGGAATT
CTCAGAAGTAGAAGGAAGAATTCAGGACTTGGAGAAAATATGTAGAAGACACCAAAATAGACCTATGGTCCAC
AATGCAGAATTGCTGGTGGCTCTAGAAAATCAACATACAATTGACTTAACAGATGCAGAAAATGAATAAATTTAT
TTGAGAAGACTAGACGCCAGTTAAGAGAAAACCGCAGACGACATGGGAGATGGATGTTTCAAGATTTACCACAA
ATGTGATAATGCATGCATTGAATCAATAAAGAACTGGAACATATGACCATTACATATACAGAGATGAAGCATTA
ACAACCGATTTTCAGATCAAAGGTGTAGAGTTGAAATCAGGCTACAAAAGATTTGGATACTGTGGATTTTCATTCC
CCATATCATGCTTCTTAATTTGCGTTGTTCTATTGGGTTTCATTTATGTGGGCTTGCCAAAAGGCAACATCAG
ATGCAACATTTGCATTTGA

H7N9 | Influenza A virus | A/avian/Shanghai/2/2013 (H7N9) | KF021599

Neuraminidase sequence:

ATGAATCCAAATCAGAAGATTCTATGCACTTCAGCCACTGCTATCATAATAGGCGCAATCGCAGTACTCATTG
GAATGGCAAACCTAGGATTGAACATAGGACTGCATCTAAAACCGGGCTGCAATTGCTCACACTCACAACTGA
AACAAACCAACAAGCCAAACAATAATAAACAACATTTATAATGAAACAAACATCACCAAYATCCAAATGGAA
GAGAGAACAAGCAGGAATTTCAATAACTTAATAAAGGGCTCTGTACTATAAATTCATGGCACATATATGGGA
AAGACAATGCAGTAAGAATTGGAGAGAGCTCGGATGTTTTAGTCACAAGAGAACCCTATGTTTCATGCGACCC
AGATGAATGCAGGTTCTATGCTCTCAGCCAAGGAAACAACATCAGAGGGAAACACTCAAACGGAACAATACAC
GATAGGTCCCAGTATCGCGCCCTGATAAGCTGGCCACTATCATCACCGCCACAGTGTACAACAGCAGGGTGG
AATGCATTGGGTGGTCAAGTACTAGTTGCCATGATGGCAAATCCAGGATGTCAATATGTATATCAGGACCAAA
CAACAATGCATCTGCAGTAGTATGGTACAACAGAAGGCCCTGTTGCAGAAATTAACACATGGGCCCGAAACATA
CTAAGAACACAGGAATCTGAATGTGTATGCCACAACGGCGTATGCCAGTAGTGTTCACCGATGGGTCTGCCA
CTGGACCTGCAGACACAAGAATATACTATTTTAAAGAGGGGAAAATATTGAAATGGGAGTCTCTGACTGGAAC
TGCTAAGCATATTGAAGAATGCTCATGTTACGGGGAACGAACAGGAATTACCTGCACATGCAGGGACAATTGG
CAGGGCTCAAATAGACCAGTGATTTCAGATAGACCCAGTAGCAATGACACACACTAGTCAATATATATGCAGTC
CTGTTCTTACAGACAATCCCCGACCGAATGACCCAAATATAGGTAAGTGTAAATGACCCCTTATCCAGGTAATAA
TAACAATGGAGTCAAGGGATTCTCATACTGGATGGGGCTAACACTTGGCTAGGGAGGACAATAAGCACAGCC
TCGAGGTCTGGATACAGAGATGTTAAAGTGCACAAATGCATTGACAGATGATAGATCAAAGCCCATTCAGGTC
AGACAATTTGATTAAACGCTGACTGGAGTGGTTACAGTGGATGTTTCATGGACTTTGGGCTGAAGGGGACTG
CTATCGAGCGTGTTTTTATGTGGAGTTGATACGTGGAAAGACCCAAAGGAGGATAAAGTGTGGTGGACCAGCAAT
AGTATAGTATCGATGTGTTCCAGTACAGAATTCCTGGGACAATGGAACCTGGCCTGATGGGGCTAAAATAGAGT
ACTTCCTCTAA

Chimeric glycoproteins:

LLOV | Lloviu cuevavirus | Lloviu/ ESP/2003 | JF828358 + EBOV 4G7 epitope

ATGGTGCCACCTACCCGTACAGCAGCCTATTAGATTGGAGACCACCACCAACACCCTACCATGGATCCTCA
ACCTTGTGGTCTTTTATAACCATAGCCTGGCTGCCCGGGGAGTCTCAGGAATTCCTCGGTTTGTGGGAAA
CAGTACAATCACCCAAACTGTCTGGACAATGTAGTGTGCAAGGAACACCTTGCCACAACAGATCAGCTACAG
GCTATTGGATTGGGACTAGAGGGGCTTGGTGAACATGCTGACCTCCCGACTGCCACCAAGCGATGGGGTTTTTC
GATCTGATGTCATCCAAAAATCGTGGGATACACCGCTGGGGAAATGGGTGGAAAACCTGCTACAATCTTGAAT
CACCAAGAAAGATGGTCATCCTTGCCCTCCCCAGCCCGCAACTGGCTTACTTGGCTATCCCCGATGCCGCTAT
GTCCACAGAGCCAAAGGAGCAGGCCCTTGCCAGGTGGGAATGCTTTCCACAAACATGGTTCCTTCTTCTGT
ACCACGGTATGGCTTCTACAGTAATTTATCATGGTGTAACTTTACGGAAGGCACAATGCTTTCCCTAATTTGT
CCCCAAGGATGCACCCCGTCTCAAGGCAGGGCTTGGAAACAGGATTCAGTCATCAAGCAGAGAACCAAAACCCA
ACCAACCAATTTCAACAACAACCTTTAGATTATGATGTAATGAGTCCCTTGGATGGACAATGCTACCTTCTCT
TTTCGAGCGAGGGAAGACACATCAATGCTAATCCAAACAAGGTACCCCTCCACAGAATCTAGACTTTGTTCAAGA
AAGATTGGCTAATCTTACCGGAGATCAAGCTGATCCATCAAAAGATGGAAGAGATTGTCGCTGAGGTTTTGACA
TTGGAGCTCGGTGATTGGTCCGGTTGGACAACATAAAAAAACCGCAGTACAAAACCATACGGCTAAGAAACCCCT
TCACCAGCATCTGGTTCAACCAAGGACAAGACTGGCCAGAAGCCCATGACGGATCATCAGGAGTTCATCCTCC
AACCTCATTCTGCTGTTGGACAACCCCTGCCTCTGGAACATTTCTCGAACTCCGGGGCGGAACCCCTGCACGAAG
GCACCGGCGGGAAACACCACCAACAATGTCCATCACTGCTGCTCCTGGGTGAGGATACAAGCCGTACATCCAG
GCAATACCTCTGGTGAATTTTCGATGCCATTGGGAGGGTCTTCGGCATGTGTGTCGTCGATACCCCTCCTGGG
TTCAGTGAGCAACAATAGTTCAATACAGGAGCTTGAGACTTCATCTAAAAGTGCAACAGAATTGACAACCTCCC
ATCAATCACTCCCAATCACTACAGCTCGCATCCGTCAAAAACACCCCCACACCGACAACACAGTCCAAGTCTT
GGACAGTTGACTACAACAACAACGCAACCATGGATCCCACAACAATACTGACGACACCCGACACCCGCAAC
CATTCCCCCTAACAACTCATCTGATCACAACGCCACAACAACAAGCAAAACAAGACGAAGGAGACAGGTCAAC
CCAGTGCCCCCAACAGATCACCACAACAACCTCTACAAGCATCAATACCTCCCACCCCAATATGACAACAC
AGTTAGCAAGACATCCGAGTGTGGCAATTGTCAATGCTAACCCCAATGTAATCCCAACCTTCATTACTGGAC
AAGCCGGGAGATGAGTAATGCTGGGGGGCTTGCATGGATTCCATGGATTGGACCAGGGATTGAGGGAGGGATC
ACAGACGAGGGGCTAATGGAGCATCAAGATACAATTTGCTGTGGGTACGGGAGCTCGCGAACACCCTACTA
AAGCCCTACAGCTTTTCTCCGGGCTACCACTGAGCTCCGAACCTACTCTATCCTCAACCGCCATGCGATTGA
CTTTCTACTACAGCGTTGGGGTGGTACCTGCAGAATCCTTGGCCAAACTGCTGTATCGAACCTCATGATTGG
TCTGCCAACATTACGGCTGAGATAAATCATATTAGAGAAGATATCCTGAACCATCATGAGATCCAACCTTCTC
AAGACCCCTCCTTTTGGACTGGATGGCAACAGTGGATCCCAACAGGAGCCAGTGTCTCGGAATCATCCTGGC
AATATTAGCCTTGATTTGTCTGTGCAGAATAACACGATGA

LLOV | *Lloviu cuevavirus* | Lloviu/ ESP/2003 | JF828358 + EBOV 1H3 epitope

ATGGTGCCACCTACCCGTACAGCAGCCTATTAGATTGGAGACCACCACCAAACACCCTACCATGGATCCTCA
ACCTTGTGGTCTTTTATACCATAGCCTGGCTGCCCGGGGAGTCTCAGGAATTCACCTCGGTTTGTGGGAAA
CAACAGCATCACCCAAACTGTCGTGGACAATGTAGTGTGCAAGGAACACCTTGCCACAACAGATCAGCTACAG
GCTATTGGATTGGGACTAGAGGGGCTTGGTGAACATGCTGACCTCCCGACTGCCACCAAGCGATGGGGTTTTTC
GATCTGATGTCATCCCAAAAATCGTGGGATACACCGCTGGGGAATGGGTGGAAAACCTGCTACAATCTTGAAT
CACCAAGAAAGATGGTCATCCTTGCCTCCCCAGCCGCAACTGGCTTACTTGGCTATCCCCGATGCCGCTAT
GTCCACAGAGCCAAAGGAGCAGGCCCTTGCCAGGTGGGAATGCTTTCACAAAACATGGTTCTTTCTTTCTGT
ACCACGGTATGGCTTCTACAGTAATTTATCATGGTGTAACTTTACGGAAGGCACAATGCTTTCCTAATTTGT
CCCGAAGGATGCACCCCGTCTCAAGGCAGGGCTTGGAAACAGGATTCAGTCATCAAGCAGAGAACCAAACCCA
AACAACCAATTTGCAACAACAACCTTTAGATTATGATGTAATGAGTCTTGGATGGACAATGCTACCTTCTTCT
TTTCGAGCGAGGGAAGACACATCAATGCTAATCCAAAACAAGGTACCCCTCCAGCAAACTAGAGCTTGTTCAGA
AAGATTGGCTAATCTTACCGGAGATAGCAACACCACCGGCAAGCTGATCTGGAAAAGTGAACCCCGAGATCACA
TTGGAGCTCGGTGATTGGTCCGGTTGGACAACATAAAAAAACCGCAGTACAAAACCATACGGCTAAGAAACCC
TCACCAGCATCTGGTTCAACCAAGGACAAGACTGGCCAGAAGCCATGACGGATCATCAGGATTCATCCTCC
AACCTCATTCTGCTGTTGGACAACCCCTGCCTCTGGAAACATCTTCGAACTCCGGGGCGGAACCTGCACGAAG
GCACCGGCGGGAACACCACCAACAATGTCCATCACTGCTGCTCCTGGGTGAGGATACAAGCCGTACATCCAG
GCAATACCTCTGGTGAATTTTCGATGCCATTGGGAGGGTCTTCGGCATGTGTGTCGTCGATACCCCTCCTGGG
TTCAGTGAGCAACAATAGTTCAATACAGGAGCTTGGAGCTTTCATCTAAAAGTGCAACAGAAATGACAACCTCC
ATCAATCACTCCCAATCACTACAGCTCGCATCCGTACAAAACACCCCCACACCGACAACACAGTCCAAGTCT
GGACAGTTGACTACAACAACACAACGCCAACCATGGATCCCAACAATACTGACGACACCCGACACCGCAAC
CATTCCCCCTAACAACCTCATCTGATCACAACGCCACAACAACAAGCAAAACAAGACGAAGGAGACAGGTCAAC
CCAGTGCCCCAACGATCACCCAACAACCTCTACAAGCATCAATACCTCCACCACCCCAATATGACAACAC
AGTTAGCAAGACATCCGAGTGTGCAAAAAGGATGCAAAAACCCAGCTGTAATCCCAACCTTAGATACTGGAC
AAGCCGGGAGATGAGTAATGCTGGGGGGCTTGCATGGATTCCATGGATTGGACCAGGGATTGAGGGAGGGATC
ACAGACGGGATAATGGAGCATCAGAACAATTTGTCTGTGAGTTACGGGAGCTCGCGAACACCCTACTAAAG
CCCTACAGCTTTTCTCCGGGCTACCACTGAGCTCCGAACCTACTCTATCTCAACCGCCATGCGATTGACTT
TCTACTACAGCTTGGGGTGGTACCTGCAGAATCTTGGCCAAAACCTGCTGTATCGAACCTCATGATTTGGTCT
GCCAACATTACGGCTGAGATAAATCATATTAGAGAAGATATCTGAACCATCATGAGATCCAACCTTCTCAAG
ACCCCTCCTTTTGGACTGGATGGCAACAGTGGATCCCAACAGGAGCCAGTGCTCTCGGAATCATCTGGCAAT
ATTAGCCTTGATTTGTCTGTGCAGAATAACACGATGA

LLOV | *Lloviu cuevavirus* | Lloviu/ ESP/2003 | JF828358 + EBOV 4G7/1H3 epitopes

ATGGTGCCACCTACCCGTACAGCAGCCTATTAGATTGGAGACCACCACCAAACACCCTACCATGGATCCTCA
ACCTTGTGGTCTTTTATACCATAGCCTGGCTGCCCGGGGAGTCTCAGGAATTCACCTCGGTTTGTGGGAAA
CAGTACAATCACCCAAACTGTCGTGGACAATGTAGTGTGCAAGGAACACCTTGCCACAACAGATCAGCTACAG
GCTATTGGATTGGGACTAGAGGGGCTTGGTGAACATGCTGACCTCCCGACTGCCACCAAGCGATGGGGTTTTTC
GATCTGATGTCATCCCAAAAATCGTGGGATACACCGCTGGGGAATGGGTGGAAAACCTGCTACAATCTTGAAT
CACCAAGAAAGATGGTCATCCTTGCCTCCCCAGCCGCAACTGGCTTACTTGGCTATCCCCGATGCCGCTAT
GTCCACAGAGCCAAAGGAGCAGGCCCTTGCCAGGTGGGAATGCTTTCACAAAACATGGTTCTTTCTTTCTGT
ACCACGGTATGGCTTCTACAGTAATTTATCATGGTGTAACTTTACGGAAGGCACAATGCTTTCCTAATTTGT
CCCGAAGGATGCACCCCGTCTCAAGGCAGGGCTTGGAAACAGGATTCAGTCATCAAGCAGAGAACCAAACCCA
AACAACCAATTTGCAACAACAACCTTTAGATTATGATGTAATGAGTCTTGGATGGACAATGCTACCTTCTTCT
TTCGAGCAGGGGAAGACACATCAATGCTAATCCAAAACAAGTACCTCCACAGAATCAGAGCTTGTTCAGA
AAGATTGGCTAATCTTACCGGAGATAGCAACACCACCGGCAAGCTGATCTGGAAAAGTGAACCCCGAGATCACA
TTGGAGCTCGGTGATTGGTCCGGTTGGACAACATAAAAAAACCGCAGTACAAAACCATACGGCTAAGAAACCC
TCACCAGCATCTGGTTCAACCAAGGACAAGACTGGCCAGAAGCCATGACGGATCATCAGGAGTTCATCCTCC
AACCTCATTCTGCTGTTGGACAACCCCTGCCTCTGGAACATCTTTCGAACTCCGGGGCGGAACCCCTGCACGAAG
GCACCGGCGGGAACACCACCAACAATGTCCATCACTGCTGCTCCTGGGTGAGGATACAAGCCGTACATCCAG
GCAATACCTCTGGTGAATTTTCGATGCCATTGGGAGGGTCTTCGGCATGTGTGTCGTCGATACCCCTCCTGGG
TTCAGTGAGCAACAATAGTTCAATACAGGAGCTTGGAGCTTTCATCTAAAAGTGCAACAGAAATGACAACCTCC
ATCAATCACTCCCAATCACTACAGCTCGCATCCGTACAAAACACCCCCACACCGACAACACAGTCCAAGTCT
GGACAGTTGACTACAACAACACAACGCCAACCATGGATCCCAACAATACTGACGACACCCGACACCGCAAC
CATTCCCCCTAACAACCTCATCTGATCACAACGCCACAACAACAAGCAAAACAAGACGAAGGAGACAGGTCAAC
CCAGTTGCCCAACAGATCACCCAACAACCTCTACAAGCATCAATACCTCCACCACCCCAATATGACAACAC
AGTTAGCAAGACATCCGAGTGTGGCAATTTGCTAATGCTAATCCCAAAATGTAATCCCAACCTTCAATGAGGAC
AAGCCGGGAGATGAGTAATGCTGGGGGGCTTGCATGGATTCCATGGATTGGACCAGGGATTGAGGGAGGGATC
ACAGACGAGGGGCTAATGGAGCATCAAGATACAATTTGTCTGTGGGTTACGGGAGCTCGCGAACACCCTACTA
AAGCCCTACAGCTTTTCTCCGGGCTACCACTGAGCTCCGAACCTACTCTATCTCAACCGCCATGCGATTGA
CTTTCTACTACAGCGTTGGGGTGGTACCTGCAGAATCCTTGGCCAAAACCTGCTGTATCGAACCTCATGATTGG
TCTGCCAACATTACGGCTGAGATAAATCATATTAGAGAAGATATCTGAACCATCATGAGATCCAACCTTCTC
AAGACCCCTCCTTTTGGACTGGATGGCAACAGTGGATCCCAACAGGAGCCAGTGCTCTCGGAATCATCTGGCAAT
AATATTAGCCTTGATTTGTCTGTGCAGAATAACACGATGA

LLOV | *Lloviu cuevavirus* | Lloviu/ ESP/2003 | JF828358 + EBOV KZ52 epitope

ATGGTGCCACCTACCCGTACAGCAGCCTATTAGATTGGAGACCACCACCAAACACCCTACCATGGATCCTCA
ACCTTGTGGTCTTTTATAACCATAGCCTGGCTGCCCGGGGGAGTCTCAGGAATTCCACTCGGTTTGTGGGAAA
CAACACCCTGACCCAAACTGTCTGGACAATGTAGTGTGCAAGGAACACCTTGCCACAACAGATCAGCTACAG
GCTATTGGATTGGGACTAGAGGGGCTTGGTGAACATGCTGACCTCCCGACTGCCACCAAGCGATGGGGTTTTTC
GATCTGATGTTCATCCCAAAAATCGTGGGATACACCGCTGGGGAATGGGTGGAAAACCTGCTACAATCTTGAAT
CACCAAGAAAGATGGTCATCCTTGCCCTCCCCAGCCCGCAACTGGCTTACTTGGCTATCCCCGATGCCGCTAT
GTCCACAGAGCCAAAGGAGCAGGCCCTTGCCAGGTGGGAATGCTTTCCACAACATGGTTCTTTCTTTCTGT
ACCACGGTATGGCTTCTACAGTAATTTATCATGGTGTAACTTTACGGGAAGGCACAATTTGCTTTCCCTAATTGT
CCCGAAGGATGCACCCCGTCTCAAGGCAGGGCTTGGAAACAGGATTCAGTCATCAAGCAGAGAACCAAACCCA
AACAACCAATTTGCAACAACAACCTTTAGATTATGATGTAATGAGTCTTGGATGGACAATGCTACCTTCTTCT
TTGAGAGAGGGGAAGACACATCAATGCTAATCCAAACAAGGTACCTCCAGCAATCTAGAGCTTGTTCAGA
AAGATTGGCTAATCTTACCGGAGATCAAGCTGATCCATCAAAGATGGAAGAGATTGTCTGCTGAGGTTTTGACA
TTGGAGCTCGGTGATTGGTCCGGTTGGACAACCTAAAAAAAACCGCAGTACAAACCATAACGGCTAAGAAAACCT
TCACCAGCATCTGGTTCAACCAAGGACAAGACTGGCCAGAAGCCCATGACGGATCATCAGGAGTTCATCCTCC
AACCTCATTCTGCTGTTGGACAACCCCTGCCTCTGGAACATTTCTTCGAACTCCGGGGCGGAACCCCTGCACGAAG
GCACCGGGCGGAAACACCACCAACAATGTCCATCACTGCTGCTCCTGGGTCAGGATACAAGCCGTACATCCAG
GCAATACCTCTGGTGAATTTTCGATGCCATTGGGAGGGTCTTCGGCATGTGTGTCGTCGATACCCCTCCTGGG
TTCAGTGAGCAACAATAGTTCAATACAGGAGCTTGAGACTTCATCTAAAAGTGCAACAGAAATGACAACCTCC
ATCAATCACTCCCAATCACTACAGCTCGCATCCGTACAAAACACCCCCACACCGACAACACAGTCCAAGTCTT
GGACAGTTGACTACAACAACAACGCAACCATGGATCCCACAACAATACTGACGACACCCGACACCGCAAC
CATTCCCCCTAACAACCTCATCTGATCACAACGCCACAACAACAAGCAAAAACAAGCAGGAGACAGGTCAAC
CCAGTGCCCCAACGATCACCAACAACCTCTACAAGCATCAATACCTCCACCACCCCAATATGACAACAC
AGTTAGCAAGACATCCGCGGGAAGTGATCGTGAACGCCAGCCCAAGTGAATCCAACCTTAGATACTGGAC
AAGCCGGGAGATGAGTAATGCTGGGGGCTTGCATGGATTCCATGGATTGGACCAGGGATTGAGGGAGGGATC
ACAGACGGGATAATGCACAACCAGGACGGCCTGATCTGCCAGTTACGGGAGCTCGCGAACACCCTACTTAAAG
CCCTACAGCTTTTTCTCCGGGCTACCACTGAGCTCCGAACCTACTCTATCCTCAACCGCCATGCGATTGACTT
TCTACTACAGCGTTGGGGTGGTACCTGCAGAATCCTTGGCCAAAACCTGCTGTATCGAACCTCATGATTGGTCT
GCCAACATTACGGCTGAGATAAATCATATTAGAGAAGATATCCTGAACCATCATGAGATCCAACCTTCTCAAG
ACCCCTCCTTTTGGACTGGATGGCAACAGTGGATCCCAACAGGAGCCAGTGCTCTCGGAATCATCTGGCAAT
ATTAGCCTTGATTTGTCTGTGCAGAATAACACGATGA

LLOV | *Lloviu cuevavirus* | Lloviu/ ESP/2003 | JF828358 + EBOV KZ52/1H3 epitopes

ATGGTGCCACCTACCCGTACAGCAGCCTATTAGATTGGAGACCACCACCAAACACCCTACCATGGATCCTCA
ACCTTGTGGTCTTTTATAACCATAGCCTGGCTGCCCGGGGGAGTCTCAGGAATTCCACTCGGTTTGTGGGAAA
CAACACCCTGACCCAAACTGTCTGGACAATGTAGTGTGCAAGGAACACCTTGCCACAACAGATCAGCTACAG
GCTATTGGATTGGGACTAGAGGGGCTTGGTGAACATGCTGACCTCCCGACTGCCACCAAGCGATGGGGTTTTTC
GATCTGATGTTCATCCCAAAAATCGTGGGATACACCGCTGGGGAATGGGTGGAAAACCTGCTACAATCTTGAAT
CACCAAGAAAGATGGTCATCCTTGCCCTCCCCAGCCCGCAACTGGCTTACTTGGCTATCCCCGATGCCGCTAT
GTCCACAGAGCCAAAGGAGCAGGCCCTTGCCAGGTGGGAATGCTTTCCACAACATGGTTCTTTCTTTCTGT
ACCACGGTATGGCTTCTACAGTAATTTATCATGGTGTAACTTTACGGGAAGGCACAATTTGCTTTCCCTAATTGT
CCCGAAGGATGCACCCCGTCTCAAGGCAGGGCTTGGAAACAGGATTCAGTCATCAAGCAGAGAACCAAACCCA
AACAACCAATTTGCAACAACAACCTTTAGATTATGATGTAATGAGTCTTGGATGGACAATGCTACCTTCTTCT
TTGAGAGAGGGGAAGACACATCAATGCTAATCCAAACAAGGTACCTCCAGCAATCTAGAGCTTGTTCAGA
AAGATTGGCTAATCTTACCGGAGATAGCAACACAACCGCAAGCTGATCTGGAAAGTGAACCCCGAGATACACA
TTGGAGCTCGGTGATTGGTCCGGTTGGACAACCTAAAAAAAACCGCAGTACAAACCATAACGGCTAAGAAAACCT
TCACCAGCATCTGGTTCAACCAAGGACAAGACTGGCCAGAAGCCCATGACGGATCATCAGGAGTTCATCCTCC
AACCTCATTCTGCTGTTGGACAACCCCTGCCTCTGGAACATTTCTTCGAACTCCGGGGCGGAACCCCTGCACGAAG
GCACCGGGCGGAAACACCACCAACAATGTCCATCACTGCTGCTCCTGGGTCAGGATACAAGCCGTACATCCAG
GCAATACCTCTGGTGAATTTTCGATGCCATTGGGAGGGTCTTCGGCATGTGTGTCGTCGATACCCCTCCTGGG
TTCAGTGAGCAACAATAGTTCAATACAGGAGCTTGAGACTTCATCTAAAAGTGCAACAGAAATGACAACCTCC
ATCAATCACTCCCAATCACTACAGCTCGCATCCGTACAAAACACCCCCACACCGACAACACAGTCCAAGTCTT
GGACAGTTGACTACAACAACAACGCAACCATGGATCCCACAACAATACTGACGACACCCGACACCGCAAC
CATTCCCCCTAACAACCTCATCTGATCACAACGCCACAACAACAAGCAAAAACAAGCAGGAGACAGGTCAAC
CCAGTGCCCCAACGATCACCAACAACCTCTACAAGCATCAATACCTCCACCACCCCAATATGACAACAC
AGTTAGCAAGACATCCGCGGGAAGTGATCGTGAACGCCAGCCCAAGTGAATCCAACCTTAGATACTGGAC
AAGCCGGGAGATGAGTAATGCTGGGGGCTTGCATGGATTCCATGGATTGGACCAGGGATTGAGGGAGGGATC
ACAGACGGGATAATGCACAACCAGGACGGCCTGATCTGCCAGTTACGGGAGCTCGCGAACACCCTACTTAAAG
CCCTACAGCTTTTTCTCCGGGCTACCACTGAGCTCCGAACCTACTCTATCCTCAACCGCCATGCGATTGACTT
TCTACTACAGCGTTGGGGTGGTACCTGCAGAATCCTTGGCCAAAACCTGCTGTATCGAACCTCATGATTGGTCT
GCCAACATTACGGCTGAGATAAATCATATTAGAGAAGATATCCTGAACCATCATGAGATCCAACCTTCTCAAG
ACCCCTCCTTTTGGACTGGATGGCAACAGTGGATCCCAACAGGAGCCAGTGCTCTCGGAATCATCTGGCAAT
ATTAGCCTTGATTTGTCTGTGCAGAATAACACGATGA

ATGGTGCCACCTACCCGTACAGCAGCCTATTAGATTGGAGACCACCACCAAACACCTACCATGGATCCTCA
ACCTTGTGGTCTTTTATACCATAGCCTGGCTGCCCGGGGAGTCTCAGGAATCCACTCGTTTTGTTGGGAAA
CAACAGCATCACCCAAACTGTCGTGGACAATGTAGTGTGCAAGGAACACCTTGCCACAACAGATCAGCTACAG
GCTATTGGATTGGGACTAGAGGGCTTGGTGAACATGCTGACCCCTTTGACTGCCCTCAAACGATGGGCTTTCC
GATCTGATGTCATCCAAAAATCGTGGGATACACCGCTGGGGAATGGGTGGAAAACTGCTACAATATAGAAGT
AACCAAGCCTGATGGTCATCCTTGCCTGCCAGCCGCAACTGGCTTACTTGGCTATCCCCGATGCCGCTAT
GTCCATAGAATTCAAGGTCAAAACCCCTCATCCAGGTGGGAATGCTTCCACAAAACATGGTTCTTTCTTTCTGT
ACCACGGTATGGCTTCTACAGTAATGTATCATGGTGTAACTTTACGGAAGGCACAATGCTTTCCTAATTGT
CCCGAAGGATGCACCCCGTCTCAAGGCAGGGCTTGGAAACAGGATTCAGTCATCAAGCAGAGAACCAAAACCCA
AACAAACAAATTTGCAACAACAACCTTTAGATTATGATGTAATGAGTCCCTTGATGGACAATGCTACCTTCTTCT
TTTCGAGCGAGGGAAAGACACATCAATGCTAATCCAAAACAAGGTACCCCTCCAGCAAACTAGAGCTTGTTCAGA
AAGATTGGCTAATCTTACCGGAGATCAAGCTGATCCATCAAAGATGGAAAGAGATTGTCGCTGAGGTTTTGACA
TTGGAGCTCGGTGATTGGTCCGGTTGGACAACATAAAAAAACCGCAGTACAAAACATACGGCTAAGAAAACCT
TCACCAGCATCTGGTTCAACCAAGGACAAGACTGGCCAGAAGCCATGACGGATCATCAGGATTCATCCTTCT
AACCTCATTCTGTGTTGGACAACCCCTGCCTCTGGAACATCTTTCGAACTCCGGGGCGGAACCTGCACGAAG
GCACCGCGGGAAACACCACCAACAATGTCCATCACTGCTGCTCCTGGGTACAGGATACAAGCCGTACATCCAG
GCAATACCTCTGGTGAATTTTCGATGCCATTGGGAGGGTCTTCGGCATGTGTGTCGTCGATACCCCTCCTGGG
TTCAGTGAGCAACAATAGTTCAATACAGGAGCTTGGAGCTTCACTTAAAAAGTGCAACAGAATTGACAACCTCC
ATCAATCACTCCCAATCACTACAGCTCGCATCCGTCAAAAACACCCCCACACCGACAACACAGTCCAAGTCT
GGACAGTTGACTACAACAACACAACGCCAACCATGGATCCACAACAATACTGACGACACCCGACACCGCAAC
CATTCCCCCTAACAACTCATCTGATCACAACGCCACAACAACAAGCAAAACAAGACGAAGGAGACAGGTCAAC
CCAGTGCCCCAACGATCACCCAACAACCTCTACAAGCATCAATACCTCCACCACCCCAATATGACAACAC
AGTTAGCAAGACATCCGAGTGTGCAAAAAGGATGCAAAAACCCAGCTGTAATCCCAACCTTAGATACTGGAC
AAGCCGGGAGATGAGTAATGCTGGGGGGCTTGCATGGATTCCATGGATTGGACCAGGGATTGAGGGAGGGATC
ACAGACGGGATAATGGAGCATCAGAACACAATTGTCTGTGAGTTACGGGAGCTCGCGAACACCCTACTAAAG
CCCTACAGCTTTTCTCCGGGCTACCACTGAGCTCGAAGCTTACTTATCTCAACCGCCATGCGATTGACTT
TCTACTACAGCTTGGGGTGGTACCTGCAGAATCTTGGCCCAAACTGCTGTATCGAACCTCATGATTGGTCT
GCCAACATTACGGCTGAGATAAATCATATTAGAGAAGATATCCTGAACCATGAGATCCAACCTTCTCAAG
ACCCCTCCTTTTGGACTGGATGGCAACAGTGGATCCCAACAGGAGCCAGTGCTCTCGGAATCATCTGGCAAT
ATTAGCCTTGATTTGTCTGTGCAGAATAACACGATGA

Chimeric RAVV GP₁ – LLOV GP₁ - GP₂

ATGAAGACCATATATTTTTCTGATTAGTCTCATTTTTAATCCAAAGTATAAAAACTCTCCCTGTTTTAGAAATTG
CTAGTAACAGCCAACCTCAAGATGTAGATTCAAGTGTGCTCCGGAACCTCCAAAAGACAGAAGATGTTTCATCT
GATGGGATTTTACACTGAGTGGGCAAAAAGTTGCTGATTCCCTTTTGGAAAGCATCTAAACGATGGGCTTTTCAGG
ACAGGTGTTCTCCCAAGAAGCTTGGAGTATACGGAAGGAGAAGAACCAAAACATGTTACAATATAAGTGTA
CAGACCCTTCTGGAAAATCCTTGTGCTGGATCCTCCAGTAATATCCGCGATTACCTAAATGTAAAACGT
TCATCATATTTCAAGGTCAAAACCCCTCATGCACAGGGGATTGCCCTCCATTTGTGGGGGGCATTTTTCTTGTAT
GATCGCGTTGCCTCTACAACAATGTACCGAGGCAAGGTCTTCACTGAAGGAAATATAGCAGCTATGATTGTTA
ATAAGACAGTTCACAGAATGATTTTTTCTAGGCAAGGACAAGGTTATCGTCACATGAACTTGACCTCCACCA
TAAATATTGGACAAGCAGCAATGAAACGCAGAGAAATGATACGGGATGTTTTGGCATCCTCCAAGAATACAAC
TCCACAACAATCAAAACATGCCCTCCATCTTCTCCAGCAAACTTAGAGCTTGTTCAGAAAGATTGGCTA
ATCTTACCGGAGATCAAGCTGATCCATCAAAGATGGAAGAGATTGTCGCTGAGGTTTTGACATTGGAGCTCGG
TGATTGGTCCGGTTGGACAACATAAAAAAACCGCAGTACAAACCATACGGCTAAGAAAACCTTCACCAGCATC
TGGTTCAACCAAGGACAAGACTGGCCAGAAGCCATGACGGATCATCAGGAGTTCATCTCCAACCTCATTTCT
GCTGTTGGACAACCCCTGCCTCTGGAACATTTCTCGAACTCCGGGGCGGAACCTGCACGAAGGCACCGCGGG
AAACACCACCAACAATGTCCATCACTGCTGCTCCTGGGTACAGGATACAAGCCGTACATCCAGGCAATACCTCT
GGTGAATTTTCGATGCCATTGGGAGGGTCTTCGGCATGTGTGTCGTCGATACCCCTCCTGGGTTTCAGTGAGCA
ACAATAGTTCAATACAGGAGCTTGGAGCTTCACTTAAAAAGTGCAACAGAATTGACAACCTCCCATCAATCACTC
CCAATCACTACAGCTCGCATCCGTCAAAAACACCCCCACACCGACAACACAGTCCAAGTCTTGACAGTTGAC
TACAACAACACAACGCCAACCATGGATCCCAACAACAATACTGACGACACCCGACACCGCAACCATTCCCCCTA
ACAACCTCATCTGATCACAACGCCACAACAACAAGCAAAAACAAGACGAAGGAGACAGGTCAACCAGTGCCCC
AACGATCACCCAACAACCTCTACAAGCATCAATACCTCCACCACCCCAATATGACAACACAGTTAGCAAGA
CATCCGAGTGTGCAAAAAGGATGCAAAAACCCAGCTGTAATCCCAACCTTAGATACTGGACAAGCCGGGAGA
TGAGTAATGCTGGGGGGCTTGCATGGATTCCATGGATTGGACCAGGGATTGAGGGAGGGATCACAGACGGGAT
AATGGAGCATCAGAACACAATTTGTCTGTGAGTTACGGGAGCTCGCGAACACCCTACTTAAAGCCCTACAGCTT
TTCTCCGGGCTACCCTGAGCTCCGAACCTACTTATCTCAACCGCCATGCGATTGACTTTCTACTACAG
GTTGGGGTGGTACCTGCAGAATCTTGGCCCAAACTGATCTGATCGAACCTCATGATTGGTCTGCCAACATTAC
GGCTGAGATAAATCATATTAGAGAAGATATCCTGAACCATGAGATCCAACCTTCTCAAGACCCCTCCTTT
TGGACTGGATGGCAACAGTGGATCCCAACAGGAGCCAGTGCTCTCGGAATCATCTGGCAATATTAGCCTTGA
TTTGTCTGTGCAGAATAACACGATGA

RESTV | *Reston ebolavirus* | Reston/ Pennsylvania/USA/1989 | AY769362 + EBOV 4G7 epitope

ATGGGGTCAGGATATCAACTTCTCCAATTGCCTCGGGAACGTTTTTCGTAAAACTTCGTTCTTAGTATGGGTAA
TCATCCTCTTCCAGCGAGCAATCTCCATGCCGCTTGGTATAGTGACAAAATAGCACTCTCAAAGCAACAGAAAT
TGATCAATTGGTTTGTCTGGGACAACTGTCATCAACCAGTCAGCTCAAGTCTGTGGGGCTGAATCTGGAAGGA
AATGGAATTGCAACCGATGTCCCATCAGCAACAAAAACGCTGGGGATTTTCGTTTCAGGTGTGCCTCCCAAGGTGG
TCAGCTATGAAGCCGGAGAATGGGCAGAAAAATTGCTACAATCTGGAGATCAAAAAGTCAGACGGAAGTGAATG
CCTCCCTCTCCCTCCCGACGGTGTACGAGGATTCCCTAGATGTCTGCTATGTCCACAAAGTTCAAGGAACAGGT
CCTTGTCCCGGTGACTTAGCTTTCCATAAAAAATGGGGCTTTTTTCTTGTATGATAGATTGGCCTCAACTGTCA
TCTACCGAGGGACAACTTTTGCTGAAGGTGTCTGACTTTTTTAATTCTGTTCAGAGCCCAAGAAGCATTTTTTG
GAAGGCTACACCAGCTCATGAACCGGTGAACACAACAGATGATTCACAAGCTACTACATGACCCGTGACACTC
AGCTACGAGATGTCAAATTTTTGGGGCAATGAAAGTAACACCCTTTTTAAGGTAGACAACCACACATATGTGC
AACTAGATCGTCCACACACTCCGCAGTTCCCTTGTTCAGCTCAATGAAACACTTCGAAGAAAATAATCGCCTTAG
CAACAGTACAGGGAGATTGACTTGGACATTGGATCCTAAAAATTGAACCAGATGTTGGTGAGTGGGCCTTCTGG
GAAACTAAAAAACTTTTTCCCAACAACCTTCATGGAGAAAACTTGCATTTCCAAATCTATCAACCCACACCA
ACAACCTCCTCAGATCAGAGCCCGGGGAACTGTCCAAGGAAAAATAGCTACCACCCACCCGCCAACAACCTC
CGAGCTGGTTCCAACGGATTCCCCTCCAGTGGTTTTAGTGTCTACTGCAGGACGGACAGAGGAAATGTCGACC
CAAGGTCTAACCAACGGAGAGACAATCACAGTTTTACCAGTCCGAGATGGATCCGATCCAAGGCTCGAACAACCTCCGCC
CCCCCATCGGCAAGCAACGAGACAATTTACCAGTCCGAGATGGATCCGATCCAAGGCTCGAACAACCTCCGCC
CAGAGCCACAGACCAAGACCACGCCAGCACCACAACATCCCCGATGACCCAGGACCCGCAAGAGACGGCCA
ACAGCAGCAAACCAGGAACCAGCCAGGAAGCGCAGCCGGACCAAGTCAGCCCGGACTCACTATAAATACAGT
AAGTAAGGTAGCTGATTCACTGAGTCCACCAGGAAAACAAAGGCGATCGGTTATTGTCAATGCTCAACCCAAA
TGCAACCCCAATCTTCATTATTGGACAGCTGTTGATGAGGGGGCAGCAGTAGGATTGGCATGGATTCCATATT
TCGGACCTGCAGCAGAAGGCATCTACATTGAGGGTCTAATGCATAATCAGGATGGGCTTATTTGCGGGCTACG
TCAGCTAGCCAATGAAACTACCCAGGCTCTTCAATTATTTCTGCGGGCCACAACAGAACTGAGGACTTACTCA
CTTCTTAACAGAAAAGCTATTGATTTTTCTTCTTCAACGATGGGGAGGTACCTGTGCAATCCTAGGACCATCTT
GTTGCATTGAGCCACATGATTGGACAAAAAATATTACTGATGAAAATTAACCAAATTAACATGACTTTTATTGA
CAATCCCCTACCAGACCACGGAGATGATCTTAATCTATGGACAGGTTGGAGACAATGGATCCCGGCTGGAAT
GGGATTATTGGAGTTATAATTGCTATAATAGCCCTACTTTGTATATGTAAGATTTTGTGTTGA

RESTV | *Reston ebolavirus* | Reston/ Pennsylvania/USA/1989 | AY769362 + EBOV 1H3 epitope

ATGGGGTCAGGATATCAACTTCTCCAATTGCCTCGGGAACGTTTTTCGTAAAACTTCGTTCTTAGTATGGGTAA
TCATCCTCTTCCAGCGAGCAATCTCCATGCCGCTTGGTATAGTGACAAAATAGCACTCTCAAAGCAACAGAAAT
TGATCAATTGGTTTGTCTGGGACAACTGTCATCAACCAGTCAGCTCAAGTCTGTGGGGCTGAATCTGGAAGGA
AATGGAATTGCAACCGATGTCCCATCAGCAACAAAAACGCTGGGGATTTTCGTTTCAGGTGTGCCTCCCAAGGTGG
TCAGCTATGAAGCCGGAGAATGGGCAGAAAAATTGCTACAATCTGGAGATCAAAAAGTCAGACGGAAGTGAATG
CCTCCCTCTCCCTCCCGACGGTGTACGAGGATTCCCTAGATGTCTGCTATGTCCACAAAGTTCAAGGAACAGGT
CCTTGTCCCGGTGACTTAGCTTTCCATAAAAAATGGGGCTTTTTTCTTGTATGATAGATTGGCCTCAACTGTCA
TCTACCGAGGGACAACTTTTGCTGAAGGTGTCTGACTTTTTTAATTCTGTTCAGAGCCCAAGAAGCATTTTTTG
GAAGGCTACACCAGCTCATGAACCGGTGAACACAACAGATGATTCACAAGCTACTACATGACCCGTGACACTC
AGCTACGAGATGTCAAATTTTTGGGGCAATGAAAGTAACACCCTTTTTAAGGTAGACAACCACACATATGTGC
AACTAGATCGTCCACACACTCCGCAGTTCCCTTGTTCAGCTCAATGAAACACTTCGAAGAAAATAATCGCCTTAG
CAACACCACGGGAAAACCTAATTTGGAAGGTCAACCCCGAAAATTGAACCAGATGTTGGTGAGTGGGCCTTCTGG
GAAACTAAAAAACTTTTTCCCAACAACCTTCATGGAGAAAACTTGCATTTCCAAATCTATCAACCCACACCA
ACAACCTCCTCAGATCAGAGCCCGGGGAACTGTCCAAGGAAAAATAGCTACCACCCACCCGCCAACAACCTC
CGAGCTGGTTCCAACGGATTCCCCTCCAGTGGTTTTAGTGTCTACTGCAGGACGGACAGAGGAAATGTCGACC
CAAGGTCTAACCAACGGAGAGACAATCACAGTTTTACCAGTCCGAGATGGATCCGATCCAAGGCTCGAACAACCTCCGCC
CAACCATGACAAGCGAGGTTGATAACAATGTACCAAGTGAACAACCGAACAACACAGCATCCATTGAAGACTC
CCCCCATCGGCAAGCAACGAGACAATTTACCAGTCCGAGATGGATCCGATCCAAGGCTCGAACAACCTCCGCC
CAGAGCCACAGACCAAGACCACGCCAGCACCACAACATCCCCGATGACCCAGGACCCGCAAGAGACGGCCA
ACAGCAGCAAACCAGGAACCAGCCAGGAAGCGCAGCCGGACCAAGTCAGCCCGGACTCACTATAAATACAGT
AAGTAAGGTAGCTGATTCACTGAGTCCACCAGGAAAACAAAGGCGATCGGTTTCGACAAAACACCGCTAATAAA
TGTAACCCAGATCTTTACTATTGGACAGCTGTTGATGAGGGGGCAGCAGTAGGATTGGCATGGATTCCATATT
TCGGACCTGCAGCAGAAGGCATCTACATTGAGGGTGTAAATGCATAATCAGAATGGGCTTATTTGCGGGCTACG
TCAGCTAGCCAATGAAACTACCCAGGCTCTTCAATTATTTCTGCGGGCCACAACAGAACTGAGGACTTACTCA
CTTCTTAACAGAAAAGCTATTGATTTTTCTTCTTCAACGATGGGGAGGTACCTGTGCAATCCTAGGACCATCTT
GTTGCATTGAGCCACATGATTGGACAAAAAATATTACTGATGAAAATTAACCAAATTAACATGACTTTTATTGA
CAATCCCCTACCAGACCACGGAGATGATCTTAATCTATGGACAGGTTGGAGACAATGGATCCCGGCTGGAAT
GGGATTATTGGAGTTATAATTGCTATAATAGCCCTACTTTGTATATGTAAGATTTTGTGTTGA

RESTV | *Reston ebolavirus* | Reston/ Pennsylvania/USA/1989 | AY769362 + EBOV 4G7/1H3 epitopes

ATGGGGTCAGGATATCAACTTCTCCAATTGCCTCGGGAAACGTTTTTCGTAAAACCTCGTTCTTAGTATGGGTAA
TCATCCTCTTCCAGCGAGCAATCTCCATGCCGCTTGGTATAGTGACAAAATAGCACTCTCAAAGCAACAGAAAT
TGATCAATTGGTTTGTTCGGGACAAACTGTCATCAACCAGTCAGCTCAAGTCTGTGGGGTGAATCTGGAAGGA
AATGGAATTGCAACCGATGTCCCATCAGCAACAAAACGCTGGGGATTTTCGTTTCAGGTGTGCCGCCAAGGTGG
TCAGCTATGAAGCCGGAGAATGGGCAGAAAATTTGCTACAATCTGGAGATCAAAAAGTCAGACGGAAGTGAATG
CCTCCCTCTCCCTCCCGACGGTGTACGAGGATTCCTAGATGTGCTATGTCCACAAAAGTTCAAGGAACAGGT
CCTTGTCCCGGTGACTTAGCTTTCCATAAAAAATGGGGCTTTTTTCTTGTATGATAGATTGGCCCAACTGTCA
TCTACCGAGGGACAACTTTTGCTGAAGGTGTCGTAGCTTTTTTAATTTCTGTTCAGAGCCCAAGAAGCATTTTTG
GAAGGCTACACCAGCTCATGAACCGGTGAACACAACAGATGATTCACAAGCTACTACATGACCCAGACACTC
AGCTACGAGATGTCAAATTTTTGGGGCAATGAAAAGTAACACCCCTTTTTAAGGTAGACAACCACACATATGTGC
AACTAGATCGTCCACACACTCCGAGTTTCTTGTTCAGCTCAATGAAACACTTCGAAGAAAATAATCGCCTTAG
CAACACCACGGGAAAATAATTTGGAAGGTCAACCCCGAAAATGAAACAGATGTTGGTGAGTGGGCCCTTCTGG
GAACTAAAAAAAACTTTTCCCAACAACCTCATGGAGAAAACCTGCATTTCCAAAATCTATCAACCCACACCA
ACAACCTCCTCAGATCAGAGCCCGGCGGGAACGTCCAAGGAAAAATAGCTACCACCCACCCGCCAACAACTC
CGAGCTGGTTCCAACGGATTCCTCCAGTGGTTTCAGTGTCTACTGCAGGACGGACAGAGGAAAATGTCGACC
CAAGGTCTAACCAACGGAGAGACAATCACAGTTTTACCGCGAACCCTAATGACAACACCACCAATGCCCCAAGTC
CAACCATGACAAGCGAGGTTGATAACAATGTACCAAGTGAACAACCGAACAACACAGCATCCATTGAAGACTC
CCCCCATCGGCAAGCAACGAGACAATTTACCCTCCGAGATGGATCCGATCCAAGGCTCGAACAACCTCCGCC
CAGAGCCACAGACCAAGACCACGCCAGCACCCACAACATCCCCGATGACCCAGGACCCGCAAGAGACGGCCA
ACAGCAGCAAACAGGAACAGCCAGCCAGGAAGCGCAGCCGGACCAAGTCAGCCCGGACTCACTATAAATACAGT
AAGTAAGGTAGCTGATTCAGTACTGAGTCCACCAGGAAACAAAGGCGATCGTTTATTGTCAATGCTCAACCCAAA
TGCAACCCCAATCTTCATTATTGGACAGCTGTTGATGAGGGGGCAGCAGTAGGATTTGGCATGGATTTCCATATT
TCGGACCTGCAGCAGAAGGCATCTACATTTAGGGTCTAATGCATAATCAGGATGGGCTTATTTGCGGGCTACG
TCAGCTAGCCAATGAAACTACCCAGGCTCTTCAATTTCTGCGGGCCACAACAGAAGTGAAGGACTTACTCA
CTTCTTAACAGAAAAGCTATTGATTTTTCTTCTTCAACGATGGGGAGGTACCTGTGCAATCCTAGGACCATCTT
GTTGCATTGAGCCACATGATTGGACAAAAAATATTACTGATGAAATTAACCAAATTAACATGACTTTATTGA
CAATCCCCTACCAGACCACGGAGATGATCTTAATCTATGGACAGGTTGGAGACAATGGATCCCGGCTGGAATT
GGGATTATTGGAGTTATAATTGCTATAATAGCCCTACTTTGTATATGTAAGATTTTGTGTTGA

RESTV | *Reston ebolavirus* | Reston/ Pennsylvania/USA/1989 | AY769362 + EBOV KZ52 epitope

ATGGGGTCAGGATATCAACTTCTCCAATTGCCTCGGGAAACGTTTTTCGTAAAACCTCGTTCTTAGTATGGGTAA
TCATCCTCTTCCAGCGAGCAATCTCCATGCCGCTTGGTATAGTGACAAAATAGCACTCTCAAAGCAACAGAAAT
TGATCAATTGGTTTGTTCGGGACAAACTGTCATCAACCAGTCAGCTCAAGTCTGTGGGGTGAATCTGGAAGGA
AATGGAATTGCAACCGATGTCCCATCAGCAACAAAACGCTGGGGATTTTCGTTTCAGGTGTGCCGCCAAGGTGG
TCAGCTATGAAGCCGGAGAATGGGCAGAAAATTTGCTACAATCTGGAGATCAAAAAGTCAGACGGAAGTGAATG
CCTCCCTCTCCCTCCCGACGGTGTACGAGGATTCCTAGATGTGCTATGTCCACAAAAGTTCAAGGAACAGGT
CCTTGTCCCGGTGACTTAGCTTTCCATAAAAAATGGGGCTTTTTTCTTGTATGATAGATTGGCCCAACTGTCA
TCTACCGAGGGACAACTTTTGCTGAAGGTGTCGTAGCTTTTTTAATTTCTGTTCAGAGCCCAAGAAGCATTTTTG
GAAGGCTACACCAGCTCATGAACCGGTGAACACAACAGATGATTCACAAGCTACTACATGACCCAGACACTC
AGTACGAGATGTCAAATTTTTGGGGCAATGAAAAGTAACACCCCTTTTTAAGGTAGACAACCACACATATGTGC
AACTAGATCGTCCACACACTCCGAGTTTCTTGTTCAGCTCAATGAAACACTTCGAAGAAAATAATCGCCTTAG
CAACAGTACAGGGAGATTGACTTGGACATTGGATCCTAAAAATGAAACAGATGTTGGTGAGTGGGCCCTTCTGG
GAACTAAAAAAAACTTTTCCCAACAACCTCATGGAGAAAACCTGCATTTCCAAAATCTATCAACCCACACCA
ACAACCTCCTCAGATCAGAGCCCGGCGGGAACGTCCAAGGAAAAATAGCTACCACCCACCCGCCAACAACTC
CGAGCTGGTTCCAACGGATTCCTCCAGTGGTTTCAGTGTCTACTGCAGGACGGACAGAGGAAAATGTCGACC
CAAGGTCTAACCAACGGAGAGACAATCACAGTTTTACCGCGAACCCTAATGACAACACCACCAATGCCCCAAGTC
CAACCATGACAAGCGAGGTTGATAACAATGTACCAAGTGAACAACCGAACAACACAGCATCCATTGAAGACTC
CCCCCATCGGCAAGCAACGAGACAATTTACCCTCCGAGATGGATCCGATCCAAGGCTCGAACAACCTCCGCC
CAGAGCCACAGACCAAGACCACGCCAGCACCCACAACATCCCCGATGACCCAGGACCCGCAAGAGACGGCCA
ACAGCAGCAAACAGGAACAGCCAGCCAGGAAGCGCAGCCGGACCAAGTCAGCCCGGACTCACTATAAATACAGT
AAGTAAGGTAGCTGATTCAGTACTGAGTCCACCAGGAAACAAAGGCGATCGTTTATTGTCAATGCTCAACCCAAA
TGCAACCCCAATCTTTACTATTGGACAGCTGTTGATGAGGGGGCAGCAGTAGGATTTGGCATGGATTTCCATATT
TCGGACCTGCAGCAGAAGGCATCTACATTTAGGGTGTAAATGCATAATCAGGATGGGCTTATTTGCGGGCTACG
TCAGCTAGCCAATGAAACTACCCAGGCTCTTCAATTTCTGCGGGCCACAACAGAAGTGAAGGACTTACTCA
CTTCTTAACAGAAAAGCTATTGATTTTTCTTCTTCAACGATGGGGAGGTACCTGTGCAATCCTAGGACCATCTT
GTTGCATTGAGCCACATGATTGGACAAAAAATATTACTGATGAAATTAACCAAATTAACATGACTTTATTGA
CAATCCCCTACCAGACCACGGAGATGATCTTAATCTATGGACAGGTTGGAGACAATGGATCCCGGCTGGAATT
GGGATTATTGGAGTTATAATTGCTATAATAGCCCTACTTTGTATATGTAAGATTTTGTGTTGA

Chimeric RAVV GP₁ – RESTV GP₁ - GP₂

ATGAAGACCATATATTTTTCTGATTAGTCTCATTTTAATCCAAAGTATAAAAACTCTCCCTGTTTTAGAAATTG
CTAGTAACAGCCAACCTCAAGATGTAGATTTCAGTGTGCTCCGGAACCTCCAAAAGACAGAAGATGTTTCATCT
GATGGGATTTACACTGAGTGGGCAAAAAGTTGCTGATTCCCTTTGGAAGCATCTAAACGATGGGC'TTTCAGG
ACAGGTGTTCTCCCAAGAACGTTGAGTATACGGAAGGAGAAGGCCAAAACATGTTACAATATAAGTGTA
CAGACCCTTCTGGAAAATCCTTGCTGCTGGATCCTCCAGTAATATCCGCGATTACCCTAAATGTAAAACGTG
TCATCATATTCAAGGTCAAAACCTCATGCACAGGGGATTGCCCTCCATTTGTGGGGGGCATT'TTCTTGAT
GATCGCGTTGCCTCTACAACAATGTACCGAGGCAAGGTCTTCACTGAAGGAAATATAGCAGCTATGATTGTTA
ATAAGACAGTTCACAGAATGATTTTTTCTAGGCAAGGACAAGGTTATCGTCACATGAACTTGACCTCCACCAA
TAAATATTGGACAAGCAGCAATGAAACGCAGAGAAATGATACGGGATGTTTTGGCATCCTCCAAGAATACAAC
TCCACAAACAATCAAACATGCCCTCCATCTCTTGATCGTCCACACACTCCGCGATTCCCTGTTTCAGCTCAATG
AAACACTTCCGAAGAAATAATCGCCTTAGCAACAGTACAGGGAGATTGACTTGGACATTGGATCCTAAAAATTGA
ACCAGATGTTGGTGAGTGGGCCTTCTGGGAAACTAAAAAAAAC'TTTCCCAACAAC'TTCATGGAGAAAACTTG
CATTTCCAAATTCTATCAACCCACACCAACAAC'TCCTCAGATCAGAGCCCGGCGGGAAC'TGTCCAAGGAAAA
TTAGTACCACCCACCCGCAACAAC'TCCGAGCTGGT'TCCAACGGAT'TCCCTCCAGTGGT'TTCAGTGCAC
TGCAGGACGGACAGAGGAAATGTCGACCCAAGGCTTAACCAACGGAGAGACAATCACAGG'TTTCACCGCAAC
CCAATGACAACCACCATTGCCCAAGTCCAACCATGACAAGCGAGGTTGATAACAATGTACCAAGTGAACAAC
CGAACAACACAGCATCCATTGAAGACTCCCCCCATCGGCAAGCAACGAGACAATTTACCACTCCGAGATGGA
TCCGATCCAAGGCTCGAACAAC'TCCGCCAGAGCCACAGACCAAGACCACGCCAGCACCCACAACATCCCCG
ATGACCCAGGACCCGCAAGAGACGGCCAACAGCAGCAAACCAGGAACCAGCCAGGAAGCGCAGCCGGACCAA
GTCAGCCCGGACTCACTATAAATACAGTAAGTAAGGTAGCTGATTCACTGAGTCCACCAGGAAACAAAGGCG
ATCGGTTTCGACAAAACACCGCTAATAAATGTAACCCAGATCTTTACTATTGGACAGCTGTTGATGAGGGGGCA
GCAGTAGGATTGGCATGGATTCCATATTTTCGGACCTGCAGCAGAAGGCATCTACATTGAGGGTGTAAATGCATA
ATCAGAATGGGCTTATTTGCGGGCTACGTCAGCTAGCCAATGAAACTACCCAGGCTCTTCAATTAATTTCTGCG
GGCCACAACAGAACTGAGGACTTACTCACTTCTTAACAGAAAAGCTATTGATTTTCTTCTTCAACGATGGGGA
GGTACCTGTCGAATCCTAGGACCATCTTGTGTCATTGAGCCACATGATTGGACAAAAAATATTACTGATGAAA
TTAACCAAATTAACATGACTTTATTGACAATCCCCTACCAGACCACGGAGATGATCTTAATCTATGGACAGG
TTGGAGACAATGGATCCCAGCTGGAATTGGGATTATTGGAGTTATAATTGCTATAATAGCCCTACTTTGTATA
TGTAAGATTTTGTGTTGA

CLUSTAL O(1.2.4) multiple sequence alignment

```

RESTV      MGSYQLLQLPRERFRKTSFLVWVILFQRAISMPLGIVTNSLTKATEIDQLVCRDKLSS 60
EBOV       -MGVTGILQLPRDRFKRTSFLLWVILFQRTFSIPLGVIHNSLQVSDVDKLVCRDKLSS 59
           . :*****:*:*:*:*:*:*:*:*:*:*:*:*:*:*:*:*:*:*:*:*:*:*
RESTV      TSQKLSVGLNLENGIATDVPSATKRWGFRRSGVPPKVVSYEAGEWAENCYNLEIKKSDGS 120
EBOV      TNQLRSVGLNLENGVATDVPSATKRWGFRRSGVPPKVVNYEAGEWAENCYNLEIKKPDGS 119
           *.*:*:*:*:*:*:*:*:*:*:*:*:*:*:*:*:*:*:*:*:*:*.*

RESTV      ECLPLPPDGVRGFRPCRYVHKVQGTGPCPGDLAFHKNGAFFLYDRLASTVIYRGTTFAEG 180
EBOV      ECLPAAPDGIRGFPCRYVHKVSGTGPCAGDFAFHKEGAFFLYDRLASTVIYRGTTFAEG 179
           **** *:*:*:*:*:*:*.*.*.*:*:*:*:*:*:*:*:*:*:*

RESTV      VVAFILSEPKKHFWKATPAHEPVNTDSTSYMTLTLSEMSNFGGNESENTLFKVDNH 240
EBOV      VVAFILPQAKKDFSSHPLREPVNATEDPSSGYSTTIRYQATGFGTNETEYLFEVDNL 239
           ***** :*:*:*:*:*:*:*:*:*:*:*:*:*:*:*:*:*:*:*

RESTV      TYVQLDRPHTPQFLVQLNETLRRNRLSNSTGRLTWTLPKIEPDVGEWAFWETKKNFSQ 300
EBOV      TYVQLESRFTPQFLQLNETIYASGKRSNTTGKLIWKNPEIDTTIGEWAFWETKKNLTR 299
           ***** :*****:*:*:*:*:*:*:*:*:*:*:*:*:*:*:*:*

RESTV      QLHGENLHFQIPSTHTNNSDQSPAGTVQGKISYHPPANNSELVPTDSPPVSVLTAAGRT 360
EBOV      KIRSEELSFTAVSNGPKNISGQSPARTSSDPETNTTNEHDHKIMASENSAMVQVHSQGRK 359
           :::*:* * * . :* *.*.* * .. : : : . . : * :* * : * .

RESTV      EEMSTQGLTNGETITGFTANPMTTIIASPMTMS-----EVDNNV----PSEQPNNT 408
EBOV      AAVSHL-----TTLATISTSPQSLTTKPGPDNSTHNTPVYKLDISEATQVQGHRRADND 414
           :* : : : : * : * *.* : : : : . . : *

RESTV      ASIEDSPPSASNETIYHSEMDPIQGSNNSAQSPTKTTAPTTSPMTQDPQETANSKPG 468
EBOV      STASDTPPATTA-----AGPLKAENTNTSKSADSLDLATTTSPQNYSETAGNNNTHHQ 467
           ::.*:*:*:: :*:*:*.*.*.*.*.*.*.*.*.*.*.*.*.*.*.*.*.*.*

RESTV      TSPGSAAGPSQPGLTINTVSKVADSLSPTRKQKRSVRQNTANKCNPDLIYWTAVDEGA 528
EBOV      DTGEESASSGKGLITNTIAGVAGLITGRRTRREVI VNAQPKCNPNIHYWTTQDEGAAI 527
           : .:* . : * * *:*:* * . : * :*.* * : * * * : * * * :

RESTV      GLAWIPYFGPAAEGIYIEGVMHNQNGLICGLRQLANETTQALQLFLRATTELRTYLLNR 588
EBOV      GLAWIPYFGPAAEGIYTEGLMHNQDGLICGLRQLANETTQALQLFLRATTELRTFSILNR 587
           ***** *:*:*:*:*:*:*:*:*:*:*:*:*:*:*:*:*:*:*:*:*:*

RESTV      KAIDFLLQRWGGTTCRILGPSCCIEPHDWTKNITDEINQIKHDFIDNPLPDHDDLNLWTG 648
EBOV      KAIDFLLQRWGGTCHILGPDCCIEPHDWTKNITDKIDQI IHDFVDKTLPDQGDNDNWWTG 647
           *****:*:*.*.*.*.*.*.*.*.*.*:*:* * * * : * * * : * * *

RESTV      WRQWIPAGIGIIGVIIAIIALLCICKILC- 677
EBOV      WRQWIPAGIGVTGVIIAVIALFCICKFVFZ 677
           ***** : * * * : * * * : * * * :
    
```

Figure II.5. Position of epitope KZ52 within the RESTV GP. Alignment of RESTV and EBOV GP amino acid sequence with Clustal omega. Primers were designed to substitute RESTV sequence with EBOV (red boxes), except where sequence was conserved.

CLUSTAL O(1.2.4) multiple sequence alignment

```

RESTV      MGSYQLLQLPRERFRKTSFLVWVILFQRAISMPLGIVTNSTLKATEIDQLVCRDKLSS 60
EBOV       -MGVTGILQLPRDRFRKTSFLLWVILFQRTFSIPLGVIHNSTLQVSDVDKLVCRDKLSS 59
           .      :*****:***:***:*****:***:***:  *****:..:***:*****

RESTV      TSQLKSVGLNLENGIATDVPSATKRWGFRRSGVPPKVVSYEAGEWAENCYNLEIKKSDGS 120
EBOV       TNQLRSVGLNLENGVATDVPSATKRWGFRRSGVPPKVVNYEAGEWAENCYNLEIKKPDGS 119
           * .***:*****:*****:*****:*****:*****:*****:***** **

RESTV      ECLPLPDGVRGFRPCRYVHKVQGTGPCPGDLAFHKGAFFLYDRLASTVIYRGTTFAEG 180
EBOV       ECLPAAPDGIRGFRPCRYVHKVSGTGPCAGDFAFHKEGAFFLYDRLASTVIYRGTTFAEG 179
           ****  ***:*****:***** **:***:*****:*****:*****

RESTV      VVAFILSEPKKHFWKATPAHEPVNTDSTSYMTLTLSEMSNFGGNETLTKVDNH 240
EBOV       VVAFILPQAKKDFSSHPLREPVNATEDPSSGYSTTIRYQATGFGTNETEYLFEVDNL 239
           ***** : **.*:.*: * :****:***: * * : * : * : .** **:*: **:*

RESTV      TYVQLDRPHTPQFLVQLNETLRRNRLSNSTGRLTWTLDPKIEPDVGEWAFWETKKNFSQ 300
EBOV       TYVQLESRFTPQFLQLNETIYASGKRSNTTGKLIWKVNPETITIGEWAFWETKKNLNR 299
           *****: .*****:*****: ..: [***:** * ..:**:] :*****:***:

RESTV      QLHGENLHFQIPSTHTNNSDQSPAGTVQKISYHPPANNSELVPTDSPPVSVLTAGRT 360
EBOV       KIRSEELSFTAVSNGPKNISGQSPARTSSDPETNTTNEDEHKIMASENSAMVQVHSQGRK 359
           :::**:* * * . :* *.**** * .. : : : . . : * :* * : **

RESTV      EEMSTQGLTNGETITGFTANPMTTIIAPSPMTS-----EVDNNV----PSEQPNNT 408
EBOV       AAVSHL----TTLATISTSPQSLTTKPGPDNSTHNTPVYKLDISEATQVGHRRADND 414
           :*          *:: :..* : * *. * : : : : . . : *

RESTV      ASIEDSPPSASNETIYHSEMDPIQGSNNSAQSPQTKTTPAPTSPMTQDPQETANSKPG 468
EBOV       STASDTPPATTA-----AGPLKAENTNTSKSADSLDLATTSPOQNYSETAGNNNTHHQ 467
           :: .**:*::: .*:::..*::: . * **** . . *:::

RESTV      TSPGSAAGPSQPGLTINTVSKVADSLSPTRKQKRSVRQNTANKCNPDLYWTAVDEGAAV 528
EBOV       DTGEESASSGKGLITNTIAGVAGLITGRRTRREVIIVNAQPKCNPNLHYWTTQDEGAAI 527
           : .:* . : ** **:: ** . : : * : : * * : *****:*****: *****:

RESTV      GLAWIPYFGPAAEGIYIEGVMHNQGLICGLRQLANETTQALQLFLRATTELRTYLLNR 588
EBOV       GLAWIPYFGPAAEGIYTEGLMHNQDGLICGLRQLANETTQALQLFLRATTELRTFSILNR 587
           *****:*****:*****:*****:*****:*****:*****:*****:

RESTV      KAIDFLLQRWGGTTCRILGPSCCIEPHDWTKNITDEINQIKHDFIDNPLPDHGDDLNLWTG 648
EBOV       KAIDFLLQRWGGTCHILGPDCCIEPHDWTKNITDKIDQI IHDFVDKTLPDQGDNDNWWTG 647
           *****:*****:*****:*****:*****:*****:*****:*****:

RESTV      WRQWIPAGIGIIGVIIAIIALLCICKILC- 677
EBOV       WRQWIPAGIGVTGVIIAIVIALFCICKFVZ 677
           *****: *****:*****:*****:

```

Figure II.6. Position of epitope 1H3 within the RESTV GP. Alignment of RESTV and EBOV GP amino acid sequence with Clustal omega. Primers were designed to substitute RESTV sequence with EBOV 1H3 epitope (blue box).

CLUSTAL O(1.2.4) multiple sequence alignment

```

RESTV  MGSYQLLQLPRERFRKTSFLVWVILFQRAISMPGIVTNSLTKATEIDQLVCRDKLSS 60
RAVV   -----MKTIIYFLISLILIQSIKTLPLVLEIA--SNSQPQDVDSVCSGTLQK 43
          ** :: : ** * : : : : : : : : * * . . . .

RESTV  TSQKSVGLNLENGIATDVPSATKRWGFVPPKVVSYEAGEWAENCYNLEIKKSDGS 120
RAVV  TEDVHLMGFTLSGQKVADSPLEASKRWAFRTGVPPKNVEYTEGEEAKTCYNISVTDPSGK 103
          * . : : : * . * : * . . : * * * * * * * * * * * * * * * * * * * * * * * *

RESTV  ECLPLPDGVRGFPRCRYVHKVQGTGPCDGLAFHKNGAFFLYDRLASTVIYRGTTFAEG 180
RAVV  SLLLDPPSNIRDYPKCKTVHHIQGQNPAAQGIALLHGWGAFFLYDRVASTTMYRKGKVFTEG 163
          . * * * . . * . : * : * * * * * * * * * * * * * * * * * * * * * * * *

RESTV  VVAFILILSEPKKHFWKATPAHEPVNTDDSTSYMTLTLTSY---EMSNFNGNESNTLFKV 237
RAVV  NIAAMIVNKTVHRMIFSRQGGYRHMNLTSTNKYWTSSNETQRNDTGCFCILQ---EYNS 220
          : * : * : : : : : : . : : . * * . * * : : : . * * : : :

RESTV  -DNHT-YVQIDRPHTPQFLVQLNETLRRNRLSNSTGRLTWTLDPKIEPDVGEWAFWETK 295
RAVV  TNNQTCPPSIIKPPSLPTVTPSIHSTNTQINT--AKSG---TMNP---SSDDELMFTEG 270
          : * * * . * . * * . . : : * * : * . : * * * * * . : : : : :

RESTV  KNFSQQLHGENLHFQILSTHTNNSDQSPAGTVQGKISYHPPANNSEL----- 343
RAVV  SG--SGEQPHHTLNVV-----TEQKQSTILSTPLHPSTSQHESTNPSRHAVTE 321
          . . . * : : : : : : : * . : * * : . . * * * : . : *

RESTV  ----V-----P-TDSPVVSVLTAGRTEEMSTQGLTNGETI 374
RAVV  HNGTDPPTQPATLLNNTNTPYNTLKYNLSTPSPPTRNITNNDTQRELAESEQTNA--- 378
          * * * . . : . . * : : . * *

RESTV  TGFTANPMTTTIAPSPMTSEVDN-----NVPSEQPNTASIEDSPSPASNETI 423
RAVV  -----QLNTTLDPTENPTTGQDTNSTNIIMTSDITSKHPNNS--SPDSSPTR-PP 429
          : . * * : * . * : * . : : : * * * * * : * * * : *

RESTV  YHSEMDPIQGSN-----NSAQSPQTKTTPAPTTSPMTQDPQETANSKPGTSPGSA-A 475
RAVV  YFRKRSIFWKEGDIFFLDGLINTEIDFDPIPNTEIFDE-----SPSNTSTNEE 481
          * . : * . : : . . : . * * . : : : . * . . :

RESTV  GPSQPGLTINTVSKVADSLSPTRKQRRSVRQNTANKCNPDLYYWTAVDEGAAVGLAWIPY 535
RAVV  QHTPPNI-----SLTFSYFPDKNGDTAYSGENENDCAELRIWSVQEDDLAAGLSWIPF 535
          : * . : : : * * : : : : . * * : * * . : . * * * * * :

RESTV  FGPAIEGIYIEGVMMHNQGLICGLRQLANETTQALQLFLRATTELRTYSLNRAIDFLL 595
RAVV  FGPGIEGLYTAGLIKNQNNLVCLRLRLANQAKSLELLLRVTTEERTFSLINRHAIIDFLL 595
          * * * . * * * : : : * * * * * * * * * * * * * * * * * * * * * * * * * * * *

RESTV  QRWGGTCRILGPSCCIEPHDWTKNITDEINQIKHDFIDNPLPDHGDDLNLW-TGWRQWIP 654
RAVV  TRWGGTCVKLGPDCIGIEDLSKNISEQIDKIRKDEQKEET-GWGLGGKWWTSDWGVLTN 654
          * * * * * : * * * * * * * * * * * * * * * : . * . : * . : *

RESTV  AGIGIIGVIAIALLCICKILC---- 677
RAVV  LGILLLSIAVLIALLSCICRIFTKYIG 681
          * * : : * . : * * * * * * * * :

```

Figure II.7. Strategy to generate chimeric RAVV-RESTV GP. Primers were designed to ligate the N-terminal region of RAVV (blue boxes) containing the RBS and the remainder of the RESTV GP (red boxes). Alignment of RESTV and RAVV GP amino acid sequence with Clustal omega.

Table II.1. PCR #1 generation of fragments AB and CD for mutating epitope 1H3 into LLOV GP:

	Fragment #1 (AB)	Fragment #2 (CD)	Neg ctrl #1	Neg ctrl #2
Green Taq (2X)	12.5 µL	12.5 µL	12.5 µL	12.5 µL
LLOV-pCAGGS	0.3 µL	0.3 µL	-	-
LLOV_ClaI_FWD_A	2 µL	-	2 µL	-
1H3LLOV_REV_B	2 µL	-	2 µL	-
1H3LLOV_FWD_C	-	2 µL	-	2 µL
LLOV_XhoI_REV_D	-	2 µL	-	2 µL
ddH ₂ O	to 25 µL	to 25 µL	to 25 µL	to 25 µL

Table II.2. PCR #2 generation of final gene fragment AD containing 1H3 epitope:

	fragment AD (complete gene)	negative control
Green Taq (2X)	12.5 µL	12.5 µL
fragment #1	(50 – 125 ng)	-
fragment #2	(50 – 125 ng)	-
LLOV_ClaI_FWD_A	2 µL	2 µL
LLOV_XhoI_REV_D	2 µL	2 µL
ddH ₂ O	to 25 µL	to 25 µL

Table II.3. PCR #1 generation fragments 1,2 and 3 for mutating epitope KZ52 into RESTV GP:

	Fragment #1	Fragment #2	Fragment #3	Neg ctrl #1	Neg ctrl #2	Neg ctrl #3
Green Taq (2X)	12.5 µL					
RESTV-pCAGGS	0.3 µL	0.3 µL	0.3 µL	-	-	-
RESTV_EcoRI_FWD_A	2 µL	-	-	2 µL	-	-
KZ52RESTV_504-14_REV_B	2 µL	-	-	2 µL	-	-
KZ52RESTV_504-14_FWD_C	-	2 µL	-	-	2 µL	-
KZ52RESTV_N553D_REV_B	-	2 µL	-	-	2 µL	-
KZ52RESTV_N553D_FWD_C	-	-	2 µL	-	-	2 µL
RESTV_XhoI_REV_D	-	-	2 µL	-	-	2 µL
ddH₂O	to 25 µL					

Table II.4. PCR #2 generation of final gene fragment AD containing KZ52 epitope in RESTV GP:

	fragment AD (complete gene)	negative control
Green Taq (2X)	12.5 µL	12.5 µL
fragment #1	(50 – 125 ng)	-
fragment #2	(50 – 125 ng)	-
fragment #3	(50 – 125 ng)	-
RESTV_EcoRI_FWD_A	2 µL	2 µL
RESTV_XhoI_REV_D	2 µL	2 µL
ddH₂O	to 25 µL	to 25 µL